STUTZMAN

1991 NORTH AMERICAN RADIO SCIENCE MEETING

PROGRAM AND ABSTRACTS

International Union of Radio Science

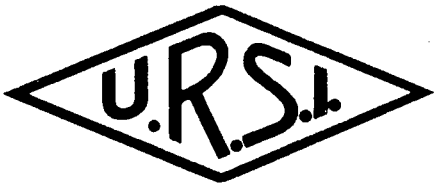

Union Radio-Scientifique Internationale

RÉUNION RADIO-SCIENTIFIQUE NORD-AMÉRICAINE 1991

PROGRAMME ET RÉSUMÉS

June 24–28 juin 1991

THE UNIVERSITY OF WESTERN ONTARIO
LONDON, ONTARIO, CANADA

Canada

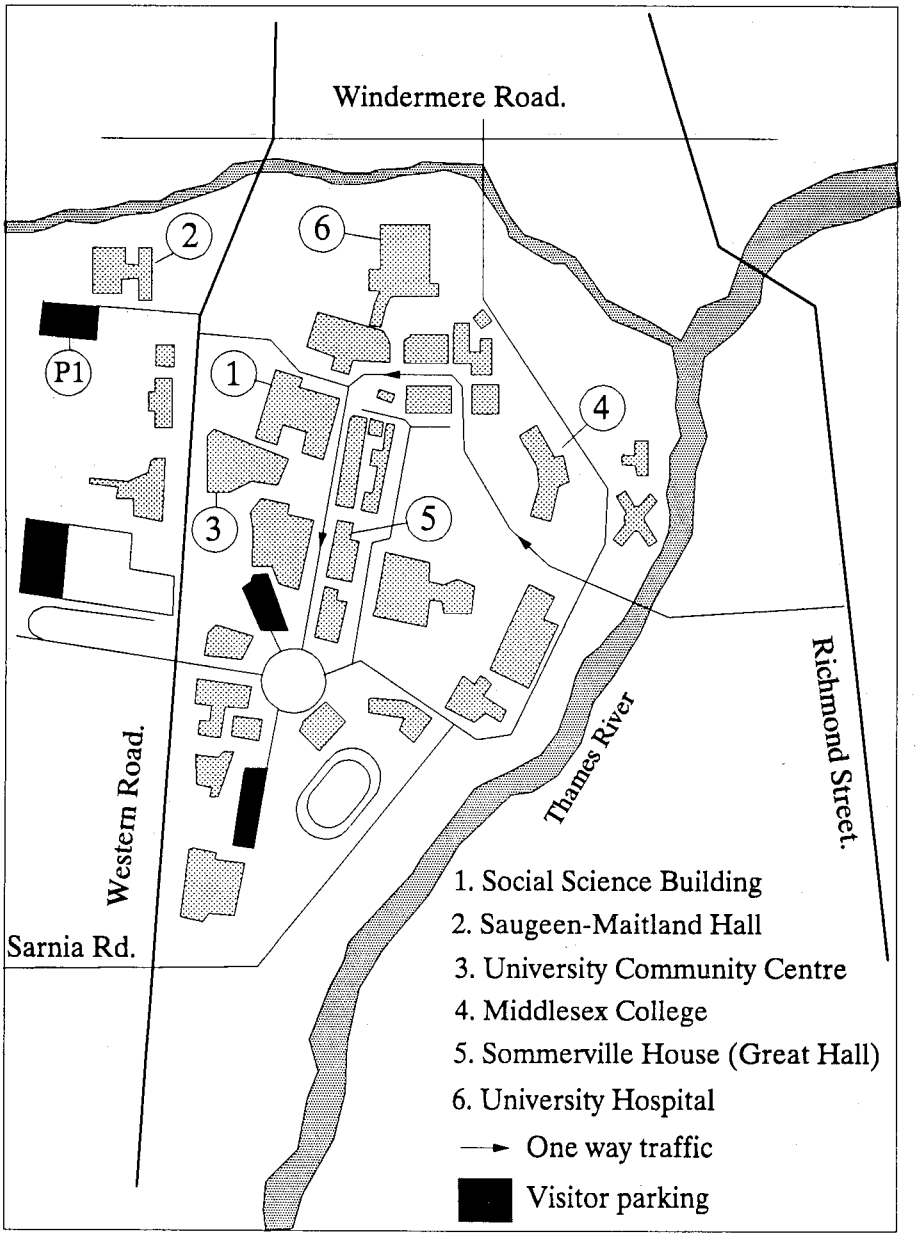

U.W.O. Campus - general layout.

PROGRAM AND ABSTRACTS
for the
1991 NORTH AMERICAN
RADIO SCIENCE MEETING

PROGRAMME ET RÉSUMÉS
pour la
RÉUNION RADIO-SCIENTIFIQUE
NORD-AMÉRICAINE 1991

Sponsored by/Parrainée par:

the United States National Committee for URSI
and/et
the Canadian National Committee for URSI/
le comité national canadien de l'URSI

Organized by/organisée par:

the National Research Council of Canada/
le Conseil national de recherches Canada
and/et
The University of Western Ontario

Printed in Canada/Imprimé au Canada

437

647

Organizing Committee/Comité de Direction

Chairman/Président.
A. R. Webster
The University of Western Ontario,
London, Ontario.

Vice-Chairman/
Vice-Président.
J. W. MacDougall.

Secretary/Secrétaire.
R. F. Clark.

Technical Program/Programme Technique
H. G. James (U.R.S.I.)
S. J. Kubina (AP-S)

Advisers/Conseillers.
C. M. Butler
E. V. Jull
S. A. Long
K. S. McCormick
L. Shafai
W. K. Stutzman
P. H. Wittke
J. Y. Wong

Coordinator/Coordonnatrice
(Mrs/Mme) D. Ruest.
National Research Council/Conseil national de recherches,
Ottawa, Ontario

Technical Program/Programme Technique

U.R.S.I. Chairman.
H. G. James
Communications Research Centre,
Ottawa, Ontario.

AP-S Chairman.
S. J. Kubina
Concordia University,
Montreal, Quebec.

Y.M.M. Antar, P. Bhartia, I.F. Blake, W.M. Boerner, P.K. Bondyopadhyay, C.M. Butler, K.K. Chan, Y.L.Chow, R.F. Clark, G. Costache, G-Y Delisle, J Gower, M.F. Iskander, S. Kashyap, K. Kagoshima, M. Kanda, O.B. Kesler, R.E.Kleinman, T.L. Landecker, J. Litva, R. Luebbers, S. Mishra, J.M. Moran, M. Ney, T.J.F. Pavlasek, L.W. Pearson, A.S. Podgorski, J. Qian, J.H. Richter, C.A.T. Salama, T.K. Sarkar, L. Shafai, M. Shur, B.P.Sinha, E. Soderberg, G.J. Sofko, H. Soicher, M A. Stuchly, W.W.L. Taylor, C.W. Trueman, K. Umashankar, P.L.E. Uslenghi, A.R. Webster, A.I. Zaghloul.

Local Arrangements/Organisation Locale

G.F. Chess, J.F. Eggleston , J. W. MacDougall, D. R. Moorcroft, A. R. Webster

TABLE OF CONTENTS

TABLE DES MATIÈRES

ROOM	MONDAY AM	MONDAY PM	TUESDAY AM	TUESDAY PM		WEDNESDAY PM	THURSDAY AM	THURSDAY PM	FRIDAY AM
2020	1 URSI J Radio Techniques for Geodesy	16 URSI J VLBI & Aperture Synthesis Techniques	31 URSI J Millimetre & Sub-millimetre Instrumentation	47 URSI J New Radio Telescopes & Signal Processing	WEDNESDAY AM	64 URSI B Scattering I	81 URSI B Rough Surfaces	97 URSI B Microstrip Antennas	
2024	2 APS Scattering & Diffraction I - High Frequency Techniques	17 APS Scattering & Diffraction II - Gratings	32 APS Scattering & Diffraction III - Media Interface	48 APS Scattering & Diffraction IV		65 APS Scattering & Diffraction V - Cavities & Complex Objects	82 APS Antenna Theory II	98 APS Electromagnetic Theory III	114 URSI B Antennas II
2028	3 APS Microstrip Antenna Elements	18 APS Printed Circuit & Microstrip Antennas	33 APS Microstrip Antenna Arrays	49 APS Microstrip Antenna on a Curved Surface	PLENARY SESSION ROOM 2050	66 APS Aperture Coupled Microstrip Antennas	83 APS Multilayer Microstrip Antennas ..... 84 APS Electromagnetic Theory II	99 APS Microwave materials in Antenna Applications ..... 100 APS Multiple Beam Antennas	115 URSI B Guided Waves
2032	4 APS Adaptive & Signal Processing Antennas I	19 APS Adaptive & Signal Processing Antennas II	34 APS Antenna Theory I	50 APS Electromagnetic Theory I		67 APS Phased Arrays	85 APS Array Analysis	101 APS Antenna Pattern Synthesis	116 URSI B Complex Media
2036	5 APS Monolithic Active Array Techniques	20 APS PDE-Based Methods in the Time Domain	35 URSI B Gratings ..... 36 URSI B Inverse Scattering	51 APS Numerical Methods I		68 APS Compact Ranges & Specialized Antenna Measurements	86 APS Near-field Theory & Measurement	102 URSI B Radar Cross Section ..... 103 URSI B Physical - Optics Based Asymptotics	117 APS Frequency Selective Surfaces II
2050	6 APS Reflector Antenna Design	21 APS Dual & Offset Reflector Antennas	37 APS Spacecraft Reflector Antennas	52 URSI B Role of Electromagnetic Modeling in Electronic Packaging		69 APS Numerical Methods II	87 APS Moment Method	104 APS FDTD/ Boundary Conditions	
2110	7A URSI B Transients I ..... 7B APS Frequency Selective Surfaces I	22 URSI B Numerical Methods - Computational Efficiency	38 URSI B Numerical Methods - Finite Element	53 APS Special Purpose Antennas ..... 54 APS Mobile Communication Antennas		70 APS Numerical Aspects ..... 71 APS Slot Antennas	88 APS Mobile/ Satellite Communications	105 APS Propagation - General	
3006	8 URSI A Time Domain Measurements	23 URSI A Electromagnetics in Environment & Medicine	39 URSI A Antenna/ Microwave Measurements	55 URSI B Asymptotic Representations of Waves		72 URSI A Measurements of Materials I	89 URSI A Measurements of Materials II	106 URSI A Noise	

ROOM	MONDAY AM	MONDAY PM	TUESDAY AM	TUESDAY PM		WEDNESDAY PM	THURSDAY AM	THURSDAY PM	FRIDAY AM
3010	9 URSI C Signal Processing in Communications	24 URSI D Chiral Materials	40 URSI E Natural Impulsive & Spectral Noise & Propagation Effects	56 URSI E Man made EM Environment ..... 57 URSI B Arrays		73 URSI D Optical Devices & Circuits	90 URSI D Microwave Circuits & MMIC 's	107 URSI D High Frequency Devices, Waveguides & Interconnections	
3014	10 APS Microwave Systems & Component Design	25 APS Analysis of Microwave Components & Systems	41 APS Broadband & Multifrequency Antennas	58 APS Millimeter Wave Antennas		74 URSI B Radiation	91 URSI B Scattering II	108 URSI B Antennas I	
3018	11 URSI B Electromagnetic Theory I	26 APS Imaging Radars	42 Joint APS/URSI Polarimetric Metrology	59 Joint APS/URSI Polarimetric Imaging Radars		75 Joint APS/URSI Inverse Methods	92 Joint APS/URSI Memorial Session R.H.T. Bates I	109 Joint APS/URSI Memorial Session R.H.T. Bates II	
3022	12 APS Innovative Applications of Computers to Undergraduate Education in Electromagnetics	27 URSI B Special Shapes	43 URSI B Electromagnetic Theory II	60 URSI B Finite Difference Time Domain		76 URSI J Magellan Mission to Venus ..... 77 URSI J Natural & Man- made Disturbances & their Effects on Radio Telescopes	93 URSI B On-Surface & Absorbing Boundary Conditions	110 URSI B Scattering III	
3024	13 URSI F Mobile & Indoor Radio Channel Modelling	28 URSI F Microwave Propagation	44 URSI F Rain Effects on Propagation	61 URSI F Rain Effects on Propagation & Observations of the Atmosphere		78 URSI F Microwave Scattering Signatures for Remote Sensing	94 URSI F Remote Sensing Concepts & Instruments for Telesonde	111 URSI F HF and Microwave Radar for Observations of Land & Sea	
3026	14 URSI G & H Extremely High Latitude Observatories & Observations I	29 URSI G & H Extremely High Latitude Observatories & Observations II	45 URSI G High Latitude F & E Region Observations	62 URSI G High Latitude & Low Latitude E & F Region Observations		79 URSI G Ionosonde Results & Atmospheric Gravity Waves	95 URSI G Recent Advances in Ionospheric Tomography I	112 URSI G Recent Advances in Ionospheric Tomography II	
3028	15 URSI E/F/H Recording & Interpretation of ULF/ELF/VLF Signatures	30 URSI B Transients II	46 URSI H Ionospheric Heating & Modification	63 URSI H Waves in Laboratory & Ionospheric Plasmas		80 URSI H Waves in Plasmas: Applications	96 APS Satellite Antennas	113 APS Radiating Elements	

Plenary Session — Séance plénière

Wednesday — Mercredi

Room 2050 Salle

08:30	Introductory Remarks
08:45	URSI Student Paper Competition
10:00	**COFFEE/CAFÉ**
10:20	Optical Transmission and Switching Technologies for Broadband Telecommunication Networks, **A. JAVED**, *Bell Northern Research Ltd., Ottawa, Ontario.*
11:10	Magellan, A Mission to Map Venus, **R.L. HORTTER**, *Jet Propulsion Laboratory, California Institute of Technology, Pasadena, CA.*

PL1

OPTICAL TRANSMISSION AND SWITCHING TECHNOLOGIES FOR BROADBAND TELECOMMUNICATION NETWORKS

A. Javed

Bell Northern Research Limited
P.O. Box 3511, Station C
Ottawa, Ontario
K1Y 4H7

In the last decade, a great deal of progress has been made in optical devices which has made broadband telecommunication networks feasible. In the first part of this paper, we will present an overview of the advances in the optical devices for applications in broadband telecommunication networks. Starting with basic optical fibers, semi conductor lasers and photo detectors, it will cover optical devices for coherent optical communications, optical amplifiers and optical switching as well as optical passive devices.

In the second part we will present an overview of advances in optical transmission and switching systems made possible by the evolving optical technologies as well as their impact on the viability of broadband telecommunication network.

MAGELLAN, A MISSION TO MAP VENUS

Richard L. Hortter
Jet Propulsion Laboratory,
California Institute of Technology
Pasadena, CA, U.S.A. 91125

For centuries, astronomers amateur and professional alike have wondered about the surface features of the Earth's nearest celestial neighbor. A Soviet lander gave a brief look at one local surface area and an Orbiter provided limited imaging at 1 km resolution. A NASA mission provided altimetric profiles which together with Earth based observation yielded excellent large scale geographical knowledge. Not until Magellan has there been sufficient resolution to begin defining surface evolution processes.

The Magellan Mission will cover at least 70% of the surface with resolution as good as 120 meters, or an order of magnitude better than the best previous results. The mission provides an excellent example of economic and technical trade-offs, involving radar system design, Spacecraft design, mission design and operational complexity.

While showing a broad range of publicly released imaging and science results, this talk will provide an interesting view of a mission from conception to operation.

Time Domain Measurements | **Room 3006 Salle URSI A Session 8** | **Mesures dans le domaine temporel**

Chairs/présidents: M. KANDA, USA; G.L. YIP, Canada

08:30 (8.1) Phase Distortion When Using Casual Deconvolution Filters, A. BENNIA[1], **S.M. RIAD**[1], N.S. NAHMAN[2], [1]*Virginia Polytechnic Institute and State University, Blacksburg, VA, and* [2]*Boulder, CO, USA*

08:50 (8.2) A Novel Way to Make TDR Measurements at the Middle of a Transmission Line, **Z.-Y. SHEN**, *DuPont Company, Wilmington, DE, USA*

09:10 (8.3) Modeling of Ultrafast Time-Domain Experiments, **K.M. CONNOLLY**[1], S.M. EL-GHAZALY[1], R.O. GRONDIN[1], R.P. JOSHI[2], [1]*Arizona State University, Tempe, AZ, and* [2]*Old Dominion University, Norfolk, VA, USA*

09:30 (8.4) An Automated Time Domain Synthesis Technique for Microwave Devices, K.M. FIDANBOYLU, **S.M. RIAD**, A. ELSHABINI-RIAD, *Virginia Polytechnic Institute and State University, Blacksburg, VA, USA*

09:50 (8.5) Time-Domain Measurements with Hewlett-Packard Network Analyzer HP8510 Using Matrix Pencil Method, Z.A. MARICEVIC[1], **T.K. SARKAR**[1], Y. HUA[2], A.R. DJORDJEVIC[3], [1]*Syracuse University, Syracuse, NY, USA;* [2]*Melbourne University, Melbourne, Australia;* [3]*University of Belgrade, Yugoslavia*

10:10 **COFFEE/CAFÉ**

10:30 (8.6) Modeling and Simulation of Crosstalk in Tab Packages Using Time Domain Techniques, W. SU[1], **S.M. RIAD**[1], T. POULIN[2], [1]*Virginia Polytechnic State University, Blacksburg, VA, and* [2]*DuPont Electronics, Research Triangle Park, NC, USA*

10:50 (8.7) Transient Performance of Parabolic-Dish Transmitting Antennas, **J.F. AURAND**, *Sandia National Laboratories, Albuquerque, NM, USA*

11:10 (8.8) Sensitivity Predictions for an Impulse Radar, **D. LAMENSDORF**, D.P. ALLEN, N.M. TOMLJANOVICH, *The MITRE Corporation, Bedford, MA, USA*

11:30 (8.9) Design and Development of a Wideband/High-Power TEM-Horn Transmitting Antenna for Impulse Radar, **J.F. AURAND**, *Sandia National Laboratories, Albuquerque, NM, USA*

11:50 (8.10) Solution to the Radiation Characteristics of a Microstrip Antenna by the FD-TD Technique, **S. MIN**, K.M. CHEN, *Michigan State University, East Lansing, MI, USA*

A8.1

PHASE DISTORTION WHEN USING CAUSAL DECONVOLUTION FILTERS

Abdelhak Bennia[#], S. M. Riad[#*]
and Norris S. Nahman[##]
[#]Electrical Engineering Department
Virginia Polytechnic Institute and State University
Blacksburg, VA 24061
[##]Consulting Electrical Engineer
375 Erie drive, Boulder, Colorado 80303
(formerly with Picosecond Pulse Labs, Inc.,
P.O. Box 44, Boulder, Colorado 80306)

In an earlier paper (A. Bennia & N.S. Nahman, IMTC Conf., 1990), the effects of the use of non-casual deconvolution methods on the deconvolved result were discussed. A method for eliminating such non-casual effects from the deconvolved result was also discussed. The method suggests the addition of a phase component to the magnitude of the deconvolution filter. It was shown that the effects of the use of deconvolution methods on casual pulse and transient data were eliminated when causal deconvolution methods were used. However, the use of such causal methods introduces a certain phase distortion (delay) in the deconvolved result. In this paper, the phase distortion introduced by causal methods is discussed and means to eliminate it are suggested.

A NOVEL WAY TO MAKE TDR MEASUREMENTS AT THE MIDDLE OF A TRANSMISSION LINE

Zhi-Yuan Shen
DuPont Co.
Experimental Station 304/C127
P.O. Box 80304
Wilmington, DE 19880-0304

Usually TDR measurements are only carried out at either the input or the output of a transmission line. This limitation is a problem for devices under test (DUT) with long and lossy lines, or for DUT behind a large discontinuity. It is desirable to make TDR measurements anywhere in the line close to the DUT. This paper provides a way to do so. Theory, formulas, and error analysis are presented.

A8.3

MODELING OF ULTRAFAST TIME-DOMAIN EXPERIMENTS

K.M. Connolly, S.M. El-Ghazaly, R.O. Grondin, and R.P. Joshi†

Center for Solid State Electronic Research
Arizona State University
Tempe, AZ 85287, USA

† Elect. and Comp. Eng. Dept.
Old Dominion University
Norfolk, VA 23529, USA

Photoconductivity and electrooptic sampling are used to generate and study electrical phenomena on a subpicosecond scale (D.H. Auston, *IEEE J. Quantum Electronics,* **QE-19**, pp. 639-648, April 1983.). In general, these experiments use femtosecond laser pulses to photoconductively generate and electrooptically sample electric waveforms. Quantitative modeling of these experiments requires retention of all electrodynamic effects and all dynamic conduction processes as well. Both Poisson's equation and drift-diffusion conduction model are not valid in the dynamic limit (S. El-Ghazaly, R.P. Joshi and R.O. Grondin, *IEEE Trans. Microwave Theory Tech,* **38**,pp. 629-637, 1990).

When modeling such experiments, the high frequency and large switching fields of the device have to be considered carefully. When using numerical semiconductor models one must consider the relatively large switching fields associated with the introduction and motion of free carriers, which may reshape the device's response. Moreover, due to the subpicosecond risetimes involved, higher order modes may be excited along the microstrip lines thus complicating the electromagnetic solution. We shall describe how one can improve the modeling of such problems by embedding a bipolar ensemble Monte-Carlo model of a photoconductive gap in a microstrip line into a time-domain solution of Maxwell's equations for the field structures present on the line.

In the experiments, electron velocities are not directly measured. The polarization shift of the probe beam is measured instead (K.E. Meyer and G.A. Mourou, Picosecond Electronics and Optoelectronics, Edited by G.A. Mourou, D.M. Bloom and C.-H. Lee, Springer-Verlag, Berlin, 1985). In this paper, we will present a technique for calculating the polarization shift. Also, we will present the correlation between the polarization shift and accurately calculated electron velocity curves in the transient state.

AN AUTOMATED TIME DOMAIN SYNTHESIS TECHNIQUE FOR MICROWAVE DEVICES

K. M. Fidanboylu, S. M. Riad*
and A. Elshabini-Riad
Electrical Engineering Department
Virginia Polytechnic Institute and State University
Blacksburg, VA 24061

A new time domain synthesis technique which has several applications in microwave measurements and material characterization has been developed. The technique uses a general (lossy) transmission line synthesis approach to obtain an equivalent network model for a microwave device under test excited with a time domain step waveform. The response waveform acquired from a time domain network analyzer is divided into N equal time intervals. Each interval is synthesized by a lossy transmission line segment. The parameters of each line are determined by using an iterative least squares optimization technique to fit its simulated response to the measured waveform. The optimization is performed in the time domain by minimizing the error function due to the difference between the two waveforms.

A8.5

TIME-DOMAIN MEASUREMENTS WITH HEWLETT-PACKARD NETWORK ANALYZER HP8510 USING MATRIX PENCIL METHOD

Zoran A. Maricevic and Tapan K. Sarkar
Department of Electrical and Computer Engineering
Syracuse University, Syracuse, NY 13244-1240

Yingbo Hua
Department of Electrical Engineering
Melbourne University, Victoria, Australia

Antonije R. Djordjevic
Department of Electrical Engineering
University of Belgrade, P. O. Box 816
11001 Belgrade, Yugoslavia

The HP8510 Time-Domain Network Measurements are frequency-domain measurements transformed to time domain using Inverse Fourier Transform, with the objective being to discriminate various scattering centers. This computational technique benefits from the wide dynamic range and the error correction of the frequency-domain data, but requires frequency-domain response measured over wide frequency range to give useful resolution in time-domain. The Generalized Pencil-of-Function (GPOF) method, also known as Matrix Pencil method, provides for much higher resolution than the Fourier techniques. A comparison of two methods is given for example of Beatty Standard.

MODELING AND SIMULATION OF CROSSTALK IN TAB PACKAGES USING TIME DOMAIN TECHNIQUES

*Wansheng Su and Sedki M. Riad**
The Bradley Department of Electrical Engineering
Virginia Polytechnic Institute and State University
Blacksburg, VA 24061-0111

Thomas Poulin
DuPont Electronics
Research Triangle Park, NC 27709

A time domain method for the characterization of crosstalk in TAB packages is developed. Noticing the features of the tiny and quasi-periodic geometric structures of the TAB package, directly measuring the crosstalk between all the package lines is almost impossible and unnecessary. An alternative approach to characterize the performance of a TAB is presented.

In this method, first, a physically based model for a section of the TAB is established by using field analysis package applied to the specific geometric structure. The time domain measurement is then used to refine and verify the model. The Hypres PSP-1000 superconducting sampling TDR system has been used to do the time domain measurements and a time domain simulation package, MTCAP(S. M. Riad and K. M. Fidanboylu, MTCAP users manual, 1988), is used to simulate the experiment. The obtained model is finally used to predict the crosstalk performance of the TAB package.

A8.7

TRANSIENT PERFORMANCE OF PARABOLIC-DISH TRANSMITTING ANTENNAS

Dr. John F. Aurand, Sr. Member of Technical Staff
Microwave Physics Division 1244
Sandia National Laboratories
P.O. Box 5800, Albuquerque, NM 87185

Transmitting antennas for impulse radars typically require wide bandwidth, low dispersion, and as much directivity as possible for a given system application. Parabolic dishes offer a simple and inexpensive way of achieving greater directivity for time-domain radiation, just as they do for narrowband frequency-domain signals, but transient operation is very different than sinusoidal operation and can be more difficult to analyze or predict.

This oral presentation will include both a simple theoretical analysis and also an empirical investigation of a transmitting antenna consisting of a parabolic dish fed by a TEM horn. Simple equations will be proposed for predicting the boresight radiated electric field of a prime-focus-fed dish when used with a TEM-horn feed. These equations can be used in systems analyses of potential impulse radar configurations.

The TEM-horn feed radiates a boresight electric field proportional to the time-derivative of the driving voltage waveform, and the dish reradiates (on boresight) the negative time-derivative of that feed radiation. This results in a negative, second-derivative time-domain response for the combination. For example, given a step input voltage to the TEM horn, an impulse (monopolar) field will radiate toward the dish, and then a negative-going bipolar field waveform (resembling a single-cycle doublet) will be reflected off the dish into the far-field.

This second-derivative operation has a significant impact on the waveforms used in an impulse radar, and strongly affects the spectral content of the transmitted wave. The presented equations will characterize the scaling factors involved in predicting the radiated electric field from knowledge of the TEM-horn driving voltage waveform. It is apparent that CW frequency-domain conditions for steady-state dish illumination are never achieved for short-duration transient electromagnetic fields, so that design methods for dish antennas based on traditional sinusoidal analysis are inappropriate for this problem.

SENSITIVITY PREDICTIONS FOR AN IMPULSE RADAR

D. Lamensdorf*, D. P. Allen, N. M. Tomljanovich
The MITRE Corporation
Bedford, MA 01730

Impulse radar uses an ultra-wideband signal (50 to 100% instantaneous bandwidth) to achieve very short pulses with a baseband (unmodulated) waveform. The most significant characteristic of this type of radar is its very narrow range resolution. Until now, application of impulse radar has been limited to short range sensing in which the low cost of the components and the low level of interference with narrowband receivers are also advantageous. In order to determine the viability of this type of radar for the detection of targets that have a low radar cross section, an evaluation of sensitivity is required that extends the radar range equation to the time domain for this ultra wideband waveform.

The basic radar equation can be described as the product of three frequency filters: the generator signal spectrum, the antenna transfer function, and the target scattering response. The generated pulse is typically a low pass filter since the high frequency content of its spectrum is limited by the rise time and pulsewidth. The combined response of the transmitting and receiving antennas is a high pass filter. This is evident from the antenna reciprocity relationship in which the transmitting pattern is proportional to the receiving pattern times frequency. The scattering from a finite size target is typically a band pass filter with its maximum in the resonance scattering band where the characteristic length is 0.5 to one wavelength. The overlap of these three filters determines the system sensitivity. The time domain signal (pulse response) at the input to the detector of the radar is the Fourier transform of the product of these filters.

An example of these sensitivity calculations is provided for small airborne targets. Emphasis is placed upon an implementation based upon an array of N synchronized pulse generators, each feeding one element of a transmitting array antenna with an equal sized receiving array antenna. This antenna configuration was chosen to maximize the potential sensitivity of the radar while allowing it to be scanned for surveillance.

An estimate has also been made of the clutter suppression needed to detect these types of targets. This is based upon the use of velocity filters for suppressing clutter within the main beam and the sidelobe level needed for suppressing clutter outside of the main beam.

A8.9

DESIGN & DEVELOPMENT OF A WIDEBAND/HIGH-POWER TEM-HORN TRANSMITTING ANTENNA FOR IMPULSE RADAR

Dr. John F. Aurand, Sr. Member of Technical Staff
Microwave Physics Division 1244
Sandia National Laboratories
P.O. Box 5800, Albuquerque, NM 87185

A high-power TEM-horn transmitting antenna has been developed for use with an experimental impulse radar. It has moderate directivity, high radiation efficiency, very low dispersion for good time fidelity, and very wideband input match. It was designed for monopolar high-voltage pulses with appreciable low frequency content (from below 100 MHz up to several GHz).

The TEM-horn antenna is a traveling-wave endfire type for very wideband operation (and nonresonant behavior), low dispersion, and moderate directivity. It consists of an end-fed long triangular flat plate mounted with a constant flare angle above a flat ground plane. The antenna, including feed, is 3 m long and 1 m wide (at the aperture). Features are included to suppress higher-order TE or TM modes.

The antenna feed is a unique inline coax-to-microstrip transition designed to provide a very wideband, high-power input to the TEM horn from an RG-220 50-Ω coaxial cable. The antenna can be operated with or without carbon-loaded lossy-foam loading of the aperture; this is used to minimize ringing (and the resulting late-time residual radiation) due to multiply-reflected transient antenna currents.

This antenna has been evaluated with a vector network analyzer, and has impressive performance. The input return loss is greater than 10 dB from less than 130 MHz to above 13 GHz (the frequency range of the analyzer); this is a bandwidth of greater than 100:1. The synthesized time-domain impulse transmitting response indicates the expected time-derivative and low dispersion as well.

The antenna has been successfully used with two different pulsed-power drivers, each providing high-voltage output pulses having a fast risetime of about 200 ps, a duration of several ns, and operation from single-shot to 1-kHz PRF.

The oral presentation will include design guidelines, construction details, vector measurements, and performance in high-power operation.

SOLUTION TO THE RADIATION CHARACTERISTICS OF A MICROSTRIP ANTENNA BY THE FD-TD TECHNIQUE

Shirley Min*, K.M. Chen
Michigan State University

The FD-TD technique is applied to model a probe-fed or aperture coupled microstrip patch antenna. The analysis with the FD-TD method includes all effects of the coupling, radiation and surface waves. In addition, the FD-TD modeling treats the higher order modes due to the discontinuities of the feed with greater simplicity than other techniques. Further, the FD-TD modeling can easily take into account various types of sub/superstrates such as magnetic, anisotropic material and multi-layered structures which raise tough difficulties for an integral equation technique in dealing with Green's functions. A microstrip antenna CAD tool can be developed based on the computer code of a FD-TD scheme with most flexibilities on antenna design parameters. This effort investigates into two types of microstrip antennas, probe-fed and aperture coupled. The numerical results with an FD-TD scheme are compared to existing results with spectrum domain Green's function techniques.

a. PROBE-FED MICROSTRIP ANTENNA

The radiation boundary condition is applied to the truncated outer surface upon the infinite ground screen enclosing the patch, and also across the aperture of the coaxial. One of the advantages for treating the feed in this way is that all the waves reflected from the discontinuities are counted, and consequently the matching of the input impedance, as in the case of diaphragm presented at the aperture of coaxial feed, can be analyzed. While applying Radiation boundary condition to the truncated outer surfaces above the ground plane and inside the coaxial cable, image theory is utilized here for the components of electric fields perpendicular to the ground plane. The parameters which characterize the material of either substrate or superstar can be directly incorporated into Maxwell's equations.

b. APERTURE COUPLED MICROSTRIP ANTENNA

The development of an FD-TD scheme here is similar to the case of a probe fed microstrip antenna with the only exception of the feed. In the case of rectangular waveguide feeding, artificial boundary condition is placed on a transverse cross section, and the incident wave is assumed to be the TE_{10} mode. If a microstrip line is used, artificial boundary condition is placed on the surface enclosing the aperture, and the incident wave along the feeding microstrip line is assumed to be a quasi-transverse electromagnetic (TEM) wave.

Numerical results will be shown, and the effects of aperture/probe position, parameters of substrates on the radiation patterns will be disscussed in details at the presentation.

Electromagnetics in Environment and Medicine | **Room 3006 Salle URSI A Session 23** | **L'électromagnétisme dans l'environnement et la médecine**

Chairs/présidents: E.K. MILLER, USA; K.P. ESSELLE, Canada

13:30 (23.1) A Near-Field, Three-Loop Antenna Method for Determining the Radiation Characteristics of an Electrically Small Radiation Source, **M. KANDA**, D. HILL, *National Institute of Standards and Technology, Boulder, CO, USA*

13:50 (23.2) Measurement of Low Voltage Power Line Properties at Frequencies 1 MHz - 1 GHz, **P.J. KWASNIOK**, M.D. BUI, A.J. KOZLOWSKI, S.S. STUCHLY, *University of Ottawa, ON, Canada*

14:10 (23.3) Measurements of EM Fields with Arbitrary Wave Impedances Generated Inside a TEM Cell, **M.T. MA**, *National Institute of Standards and Technology, Boulder, CO, USA*

14:30 (23.4) Experimental Study of Electric and Magnetic Fields Produced by Household Appliances, **Z. PANTIC-TANNER**, *San Francisco State University, San Francisco, CA, USA*

14:50 (23.5) Quasi-Static Induced Electric Field Due to a Coil Above Tissue Half-Space, **K.P. ESSELLE**, M.A. STUCHLY, *Health and Welfare Canada, Ottawa, ON, Canada*

15:10 **COFFEE/CAFÉ**

15:30 (23.6) Computer Simulation of RF B_1 Field in a Human Head, **W.L. KO**, L. XU, D.T. GLENNON, H.R. BROOKER, R.P. VELTHVIZEN, L.P. CLARKE, *University of South Florida, Tampa, FL, USA*

15:50 (23.7) Experimental and Numerical Characterization of Cardiac Current Density During Defibrillation, **K.T. NG**[1], S. GAO[1], O.C. DEALE[2], B.B. LERMAN[2], [1] *New Mexico State University, Las Cruces, NM, and* [2] *Cornell University Medical College, New York, NY, USA*

16:10 (23.8) Analysis of Electromagnetic Anechoic Chamber Performance Using Finite Difference Time Domain Methods, R. LUEBBERS, D. STEICH, **D. RYAN**, K. KUNZ, *Pennsylvania State University, University Park, PA, USA*

16:30 (23.9) Swept-Frequency Measurement of the Permittivities of Saline Water, **H. JIANG**, J. HAO, *Sichuan University, Sichuan, China*

16:50 (23.10) Combined Method of Treatment of Venous Pathology of Lower Extremeties, **B.N. ZHUKOV**, V.E. KOSTYAEV, *Kuibyshev Medical Institute, Institute, Kuibyshev, USSR*

A23.1

A NEAR-FIELD, THREE-LOOP ANTENNA METHOD FOR DETERMINING THE RADIATION CHARACTERISTICS OF AN ELECTRICALLY SMALL RADIATION SOURCE

M. Kanda and D. Hill
Fields and Interference Metrology Group
Electromagnetic Fields Divison
National Institute of Standards and Technology
Boulder, Colorado 80303

Electronic equipment can emit unintentional electromagnetic radiation that can interfere with other electronic equipment. If the radiating source is electrically small, then it can be characterized by equivalent electric and magnetic dipole moments at the near-field region. A previous method for determining the equivalent dipole moments involved the use of a TEM cell. (M. T. Ma and G. H. Koepke, "A Method to quantify the radiation characteristics of an unknown interference source," Nat. Bur. Stand., Boulder, CO, NBS Technical Note 1059, 1982.)

In this paper we describe a new method that involves locating the radiator at the center of three orthogonal loop antennas. Each loop is terminated with identical loads located at two diametrically opposite points. This type of loop loading has been used in a sensor for simultaneous measurements of electric and magnetic fields. (M. Kanda, "An electromagnetic near-field sensor for simultaneous electric and magnetic-field measurements," IEEE Trans. Electromag. Compat., vol. EMC-26, pp. 102-110, 1984.)

We have also found it to be useful for simultaneous determination of electric and magnetic dipole moments. Once the dipole moments are determined, the total radiated power of the source can be computed.

MEASUREMENT OF LOW VOLTAGE POWER LINE PROPERTIES AT FREQUENCIES 1 MHz - 1 GHz

P. J. Kwasniok *, M. D. Bui, A. J. Kozlowski, S. S. Stuchly

Laboratory for Electromagnetics and Microwaves
Department of Electrical Engineering
University of Ottawa
770 King Edward Avenue,
Ottawa, Ontario, Canada K1N 6N5

Power line cables can act as receiving antennas within most electronic systems and can be inclined to having interfering voltages and/or currents induced in them by radiated fields due to fast transients, e.g. electrostatic discharges, or due to strong monochromatic fields caused by nearby paging transmitters, land mobile transmitters and even hand-held transceivers.

Knowledge of the electrical properties of power lines over a wide frequency range plays an important role in investigating and eliminating such undesirable phenomena. So far power line impedance and product input impedance in the frequency range up to 30 MHz and power line transmission losses up to 500 MHz have been reported. In practice, parasitic signals of much higher frequencies have been observed in power line cables.

We have designed two different types of special couplers (current and voltage) for use in conjunction with HP 3577A and HP 8510B network analyzers to measure impedances under normal operating conditions. The first coupler utilizes two Tektronix current probes (CT-1 and CT-2) and is sufficient for measurements up to 200 MHz. In the second coupler, an RC first-order high-pass filter with diode protection is employed to extend the frequency range of measurements up to 1 GHz and beyond.

The measurements of power line impedances at several outlets and input impedances of various electronic equipment under normal active conditions were performed in differential mode (phase and neutral) and common mode (phase and ground) from 1 MHz to 1 GHz. The results of these measurements will be very useful in modeling, predicting and eliminating parasitic EMI coupling to electronic equipment through power line wiring.

A23.3

MEASUREMENTS OF EM FIELDS WITH ARBITRARY WAVE IMPEDANCES GENERATED INSIDE A TEM CELL

M. T Ma
National Institute of Standards and Technology
Boulder, CO 80303, U. S. A.

Transverse electromagnetic (TEM) cells have been used widely in the electromagnetic compatibility (EMC) community for performing EM susceptibility and vulnerability tests. Conventionally, one of the two ports is connected to an rf source, and the other port is terminated with a matched load so that a far-field environment is created inside the cell for testing. The wave propagation direction is from source to load, and the wave impedance (defined as the ratio of electric field to magnetic field) has the free-space value of 377 Ω. Such TEM cells offer many advantages [M. T. Ma & M. Kanda, NBS TN 1099, 1986].

In the real world, however, the EM environment may not be close to such an ideal condition (free space). Most often, a practical environment may be arbitrary and complex due to combinations of multiple interference sources at various locations, with multiple reflections and several frequencies. In addition, the interference signal may be predominantly electric field (high impedance) or predominantly magnetic field (low impedance). Yet, many electronic devices or components are required to be tested under these practical conditions. Thus, a standard testing method based on EM fields with arbitrary wave impedances is needed.

To meet this need, this paper suggests two methods for generating EM fields having arbitrary wave impedances inside a TEM cell by: 1) exciting both ports of a TEM cell simultaneously with different amplitudes and phases, or 2) exciting the cell at one port as usual and then terminating the other port with an intentionally mismatched load. Both theoretical derivations and measurement results (electric field, magnetic field, and wave impedance) with specific instrumentations will be presented.

EXPERIMENTAL STUDY OF ELECTRIC AND MAGNETIC FIELDS PRODUCED BY HOUSEHOLD APPLIANCES

Dr. Zorica Pantic-Tanner
Division of Engineering
San Francisco State University
1600 Holloway Ave, San Francisco, CA 94132

Household appliances generate electromagnetic fields in broad frequency range starting from extremely-low to radio and microwave frequencies. Radio interference produced by these fields has been a subject of permanent concern according to the expansion of radio services during the last 50 years and the growth and proliferation of noise generating household appliances. Protection of the radio spectrum users has been provided through national and international standards that limit radio interference and that have been developed by FCC and CISPR. However, just recently, public concern has focused on possible human health effects from exposure to nonionizing radiation in residential and industrial settings. Standards have been set for radio- and microwave-frequency radiation, but for ELF electromagnetic fields there are no standards or unique guidelines. In order to develop these standards various epidemiological studies are being performed, especially in residential areas. They require electromagnetic characterization of residential radiation sources, i.e. theoretical prediction and/or accurate measurements of electromagnetic fields produced by them. Household appliances comprise a big class of these residential radiation sources. Even though electromagnetic fields produced by appliances have been studied in the past most of the measurements have been performed either at one point in space or along one (maximum-field) direction (Gauger,PAS-104, 2436-2444, 1985). Hence, there is a need for more complete characterization of EM fields spatial and temporal variations. To fulfil this need a new study is proposed. It has a few tasks:

First, to develop a protocol for measurement of electric and magnetic fields produced by household appliances (point-in-space, point-in-time, frequency content and personal exposure).

Second, to measure and record spatial and temporal variation of electromagnetic fields for a certain number of samples for each type of selected appliances. Measurements are performed separately for ELF range (60 Hz and content of higher-order harmonics) and for HF, VHF and MWF range. Commercially available and specifically designed instruments are used.

Third, on the basis of experimental results, to develop a relatively simple model that could be used to predict the radiation from the selected type of household appliances.

Some of the representative results will be presented.

A23.5

QUASI-STATIC INDUCED ELECTRIC FIELD DUE TO A COIL ABOVE TISSUE HALF-SPACE

KARU P. ESSELLE* AND MARIA A. STUCHLY
Bureau of Radiation and Medical Devices
Health and Welfare Canada
Tunney's Pasture, Ottawa, ON, Canada K1A 0L2

Electromagnetic stimulation of neurons in the cerebral cortex has been used to diagnose various neurological disorders. When a magnetic field is used rather than surface electrodes, the procedure is painless. In magnetic stimulation, a coil carrying a current pulse is placed closed to a biological body. The time-varying magnetic field produced by the coil penetrates into the body and induces an electric field. A nuron inside the body may be stimulated by this electric field, depending on its strength, temporal variation and spatial distribution in the vicinity of the nerve (B.J. Roth *et al.*, IEEE Trans. Biomed. Eng. 37, 588-597, 1990). For a theoretical evaluation of the stimulation process, one therefore needs to know the electric field in the body due to various current-carrying coils. Since the current pulses used in nerve stimulation are of the order of 100 μs, the frequencies encountered are usually limited to the kilohertz range. At these frequencies, quasi-static conditions can be assumed, and therefore, the Laplace's equation can be used instead of the diffusion equation. As the displacement current both inside and outside the body is negligible when compared with the conduction current inside the biological body, the normal component of the electric field inside the body should be zero at the body surface. The electric field inside a biological body can be obtained by solving the Laplace's equation subjected to the above boundary condition (B.J. Roth *et al.*, Muscle & Nerve 13, 734-741, 1990).

In this paper, the biological body is modelled by a semi-infinite tissue (tissue half-space). A semi-analytical method is used for the calculation of the induced electric field in tissue half-space. An analytical solution is obtained for the electric field produced by an elementary section of the current-carrying coil. The total electric field is obtained by numerically integrating the analytical solution, along the length of the coil. Since the numerical part is limited to a simple one-dimensional integration, this method is expected to be significantly more efficient when compared with previous methods. The analytical solution for the elementary section also provides a better physical insight. It was found that the electric field is parallel to the air/tissue boundary everywhere in the tissue half-space. The electric field is insensitive to conductivity-variations perpendicular to the boundary.

Due to minimal computing requirements, this method is useful in the design and optimization of coils with various shapes and orientations. Final evaluation of the coil design can be made using sophisticated numerical methods based on more realistic models of biological bodies (M. Guidi *et al.*, IEEE Eng. in Med. & Biol. Society Annual Int. Conf. 12, 2252-53, 1990).

COMPUTER SIMULATION OF RF B_1 FIELD IN A HUMAN HEAD

W.L. Ko*[1], L. Xu[1], D.T. Glennon[1], H.R. Brooker[2], R.P. Velthvizen[3], and L.P. Clarke[3]
Departments of Electrical Engineering[1], Physics[2], and Radiology[3]
University of South Florida
Tampa, FL 33620

ABSTRACT

An attempt is being made on this campus and other research sites to automate tissue classification of images obtained by magnetic resonance imaging (MRI). The technique employed is similar to that used by NASA for "multi-spectral" analysis of the earth's surface. MRI images are obtained using several different pulse sequences that emphasize different aspects of the tissue. Sophisticated algorithms are employed to combine information from all the images for computerized tissue classification. The images obtained by MRI always contain some variation in amplitude due to the non-uniform radio-frequency field produced by the imaging coils. The experienced radiologist is usually able to compensate for this effect. The computerized method of image segmentation, however, requires that the amplitude of each part of the image have a consistent relationship to tissue characteristics. The initial purpose of this project is to develop methods to calculate the radio-frequency field in the subject being imaged and use this information to correct for the amplitude variation across the image. The program developed for mapping radio-frequency fields is also used to calculate the power deposited in the subject and to study theoretically the problems that develop as the high field limits of MRI are extended.

The success of intensity based MRI image segmentation depends on how accurate the radio frequency magnetic field (the B_1 field) within the imaging volume inside the RF coils is computed. Recently a number of MRI groups have been investigating various computational methods for the realistic prediction of the B_1 field. Some of these methods are based on a quasi-static approach which is not accurate at the frequency employed, e.g., 63 MHz. To remedy this weakness, Maxwell's full equation must be used. In addition, no model of the human head has been included in the imaging volume where the B_1 field is computed. The mutual coupling effects between the human head inside the imaging volume and the RF coils must be taken into consideration.

A computational technique expressly suited for this purpose is the FD-TD (Finite-Difference Time-Domain) technique, which is based on the direct discretization of Maxwell's curl equations and the enforcement of proper boundary conditions entailed by the physical structure under investigation. This approach is attractive because complex structures such as the human head can be incorporated in the computational space. The computational time depends on the degree of realism of the human head model.

To implement the computation of B_1 field distribution in the RF coils with the human head present, a model of the human head as well as the dimensions of the RF coils are needed. To model the human head, the conductivity, the permitivity, and the permeability of the various soft tissues are specified. Once these structures are described to the computer program, the field distribution can be computed. The quantities of interest, including non-uniformity correction, specific absorption or local heating effects, and high frequency/high field effects, can be extracted from the field distribution in a straightforward manner. The methodology and results of this computer simulation will be presented.

A23.7

EXPERIMENTAL AND NUMERICAL CHARACTERIZATION OF CARDIAC CURRENT DENSITY DURING DEFIBRILLATION

K.T. Ng* and S. Gao
New Mexico State University
Las Cruces, NM 88003

O.C. Deale and B.B. Lerman
Cornell University Medical College
New York, NY 10021

The single most effective means to defibrillate patients who develop cardiac arrest (ventricular fibrillation) is by application of high voltage electric shocks to the chest wall. Unfortunately the mechanisms for defibrillation are not fully understood, and it is therefore difficult to formulate guidelines for optimal delivery of the shock. To better delineate these mechanisms, Cornell University Medical College and New Mexico State University have recently begun to analyze the current density in the canine heart during defibrillation.

Due to limitations of both experimental and numerical approaches to this type of problem, the investigation will integrate both methods in a complementary fashion. A numerical torso model is being developed to predict current distribution under multiple conditions. In parallel with this work is the development of a multichannel measurement system for mapping current density in the canine heart. The two methods will be combined to test hypotheses and determine the current density required for defibrillation.

In this paper the methodology for combining the numerical and experimental approach will be described. The measurement system consists of 1) a new kind of bipolar electrode for measuring difference voltages, and 2) a multichannel data acquisition system based on a Masscomp MC 5450 computer for processing the signals from the electrode pairs. Design of the measurement system will be presented together with preliminary results. Numerical torso models based on the finite-element analysis and implemented on both the conventional and massively-parallel Connection machine will be presented. Application of these models in calibrating the electrodes in the measurement system will be discussed.

ANALYSIS OF ELECTROMAGNETIC ANECHOIC CHAMBER PERFORMANCE USING FINITE DIFFERENCE TIME DOMAIN METHODS

R. Luebbers, D. Steich, D. Ryan*, and K. Kunz
Department of Electrical and Computer Engineering
The Pennsylvania State University
University Park, PA 16802

Prediction of anechoic chamber performance is a very difficult challenge. In order to be applicable, an analytical technique must be capable of dealing with widely different shapes and materials, from the smooth conducting reflector to penetrable absorber materials. In addition, transient methods to reduce undesired reflections, such as time gating, may be difficult to include in frequency domain analyses. While methods suitable for analysis of chamber sub-systems exist, few analytical techniques are capable of including the diversity of shapes and materials encountered in the analysis of a complete compact range system.

One approach which can accommodate this diversity is the Finite Difference Time Domain technique. Visual and numerical analysis results which can be used to evaluate the performance of compact ranges will be presented. These results include the effects of the reflector shape, including edge treatments, and the electromagnetic properties, shapes, and locations of the absorber materials. While three dimensional modeling is possible at lower frequencies with current computers, this presentation considers two dimensions only. Nevertheless, significant insight into compact range design and performance can be obtained from the results.

A23.9

SWEPT-FREQUENCY MEASUREMENT OF THE PERMITTIVITIES OF SALINE WATER

Hanbao Jiang* and Jin Hao
Department of Radio-Electronics
Sichuan University, Chengdu, Sichuan, P. R. of China

The permittivities of 0.45 and 0.9% saline water were determined using a coaxial slotted line filled with the liquid under test and a network analyzer system (HP8410C, HP8350B, etc) controlled by a computer. The slotted line has a length of 70cm with 50cm-long slot and terminated with a load. A untuned probe is fit onto the slotted line. The RF fields along the slotted section are basically travelling waves due to lossy water. The phases and attenuations of selected frequencies can be measured and shown as following.

$$\Delta\varphi_{ij} = \varphi_{ij} - \varphi_{i0} = \beta_i(Z_j - Z_0); \quad \Delta A_{ij} = A_{ij} - A_{i0} = \alpha_i(Z_j - Z_0)$$

where i = 1, 2, ···, n, for frequencies interested in, j = 0, 1, 2, ···, m, for distances along the slotted section. These measured data treated by the compute using linear regression. The relative permettivity can be calculated by

$$\varepsilon' = (\beta^2 - \alpha^2)/k_0^2, \quad \varepsilon'' = 2\beta\alpha/k_0^2, \quad k_0 = \omega\sqrt{\varepsilon_0\mu_0}$$

The measured and theoretic relative permittivities of 0.45% saline water as list below (T = 14℃)

frequency (MH_2)	500	750	1000	1250	1500	2000	2450
β(rad / cm)	−0.957	−1.431	−1.904	−2.375	−2.836	−3.727	−4.558
$\delta\beta$(rad / cm)	0.006	0.005	0.006	0.015	0.011	0.024	0.066
α(dB / cm)	−1.292	−1.492	−1.677	−2.037	−2.498	−3.664	−4.791
$\delta\alpha$(dB / cm)	0.007	0.013	0.016	0.016	0.023	0.035	0.209
measured							
ε'	81.4	81.8	81.0	81.4	80.7	78.2	77.7
ε''	25.9	19.9	16.7	16.0	16.5	17.9	19.1
theoretic*							
ε'	81.4	81.2	81.1	80.8	80.5	79.8	79.0
ε''	24.3	18.6	16.4	15.6	15.6	16.5	17.8

* A. stogryn. IEEE Trans. Microwave Theory Tech. Vol. MTT-19

The results show this measurement system is suitable for liquid or paste-like material with 0.25~5dB / cm attenuations.

COMBINED METHOD OF TREATMENT OF VENOUS PATHOLOGY OF LOWER EXTREMETIES

*

B.N.Zhukov, V.E.Kostyaev
Kuibyshev medical institute, USSR

Problems in the treatment of complicated forms of varicose and posttrombophlebitical diseases are still actual. Varicose disease of lower extremeties is one of the most widespread surgical diseases, nearly 14,7% (V.S. Savelyev, 1978, Steinbrukk, 1981).

Posttrombophlebitical disease of lower extremeties is also widely spread among the diseases of blood vessels and achieves 28% of all the pathology of venous system.

Taking into consideration the significance of the fact of the wide spreadness of the disease, as well as the hihg percentage of disablement and invalidity (10-48%), the treatment of patients with these pathologies is very important and actual.

Since 1987, we use the new physiotherapeutic device in the treatment of patients with trophic ulcers of lower extremeties. We examed and treated 84 patients with different forms of chronic venous insufficiency of lower extremeties, complicated by trophic ulcers.

The essence of the method with using of the system is concluded in the following: joint application of therapeutic properties of He-Ne laser and of local application of various medicines. Besides, in the device there is an opportunity of pneumomassage of the trophic ulcer's surface by the modification of temperature and frecuency of air flow.

As the results of treatment, the following things were received: shortening of the time of preparation for surgical intervention and of the whole time of treatment, decreasing of the percentage of complications and invalidity.

Antenna/Microwave Measurements | Room 3006 Salle URSI A Session 39 | Antennes/mesures micro-ondes

Chairs/présidents: D.A. HILL, USA

08:30 (39.1) Superconducting Microstrip Patch Antennas, R.L. SMITH, T.E. HARRINGTON, **J.T. WILLIAMS**, S.A. LONG, *University of Houston, TX, USA*

08:50 (39.2) A Half-Loop 500-MHz Antenna Made from High Temperature Superconducting YBCO, **D.R. BOWLING**[1], R.J. DINGER[1], A.M. MARTIN[1], J. TALVACCHIO[2], [1] *Naval Weapons Center, China Lake, CA, and* [2] *Westinghouse Science and Technology Center, Pittsburgh, PA, USA*

09:10 (39.3) μm-Resolution Field Probe for Non-Invasive MMIC Measurement, **G.E. BRIDGES**, D.J. THOMSON, C. SHAFAI, T. FORZLEY, *University of Manitoba, Winnipeg, MB, Canada*

09:30 (39.4) A Method to Determine the Phase Centres of the Field in the Aperture on a Horn Antenna, **J.W. ODENDAAL**, C.W.I. PISTORIUS, *University of Pretoria, South Africa*

09:50 (39.5) Near Field and Fresnel Zone Measurement Using Plane Wave Synthesis, **M. BAQUERO**, M. FERRANDO, D. GALDAMEZ, *Universidad Politécnica de Valencia, Spain*

10:10 **COFFEE/CAFÉ**

10:30 (39.6) The Effect of Temperature and Time on the Pointing Angle of an MLS Azimuth Antenna, **M.Z. EL-GAMAL**, *Transport Canada, Ottawa, ON, Canada*

10:50 (39.7) Loss Measurements of Microstrip with Controlled Surface Roughness, **T. NICHOLS**, *University of Colorado, Boulder, CO, USA*

11:10 (39.8) Airy Function Solutions to Eigenvalue Problems with Applications to Schrodinger's Equation and Non-Uniform Optical Waveguides, **R.L. GALLAWA**, A.K. GHATAK, I.C. GOYAL, *National Institute for Standards and Technology, Boulder, CO, USA*

11:30 (39.9) Spread Spectrum Microwave Level Meter, **A. NAGAMUNE**, K. TEZUKA, *NKK Corporation, Kawasaki, Japan*

11:50 (39.10) Equipment for Precise Microwave Holography Measurements at 22 GHz, **V. KHAIKIN**, *USSR Academy of Sciences, Stavropol Territory, USSR*

A39.1

SUPERCONDUCTING MICROSTRIP PATCH ANTENNAS

Richard L. Smith, Timothy E. Harrington,
Jeffery T. Williams*, and Stuart A. Long
Applied Electromagnetics Laboratory
Department of Electrical Engineering
University of Houston
Houston, TX 77204-4793

The primary advantage of using superconducting materials in antenna systems is the reduction of the loss associated with the transmission-line feeds, where the ohmic losses of normal conductors are often prohibitive. For large, high frequency arrays, the result is a substantial increase in the gain of the antenna. Constructing the radiating elements with superconductors will also reduce the ohmic losses associated with the element; however, for most antenna designs only modest increases in the efficiency and gain are obtained since the ohmic resistance of the element is generally much smaller than the radiation resistance. For antennas in which the ohmic resistance is not small, relative to the radiation resistance, the increased efficiency is usually offset by a corresponding increase in the Q of the antenna. However, these common generalizations are not true for thin microstrip patch antennas.

Microstrip antennas are generally characterized as efficient radiators, with typical designs having efficiencies of approximately 85% to 95%. For these designs, the inefficiency is due, primarily, to the power radiated into surface waves, which is a function of the substrate thickness t. Over a wide range of thickness, the efficiency varies as the inverse of t. In order to achieve maximum efficiency t must be made small. But, for very thin dielectrics (typically, less than $t \sim 0.02\lambda_o$) the efficiency begins to fall off due to conductor and dielectric losses. Constructing the microstrip patches and ground planes from superconducting material will significantly reduce the effects of conductor loss, resulting in increases in the efficiency for cases where t is less than $\sim 0.01\lambda_o$. In addition, the Q of the antenna will not increase substantially since it is, generally, limited by the dielectric losses of the substrate material. These results will be demonstrated for a superconducting rectangular microstrip patch antenna fed by a superconducting coplanar waveguide. The antenna and ground plane will be constructed with the high temperature $YBa_2Cu_3O_7$ superconductor on an $LaAl_2O_3$ substrate. Examples of the efficiency and impedance, for antennas constructed of normal conductors and superconductors, will be presented.

A HALF-LOOP 500-MHZ ANTENNA MADE FROM HIGH TEMPERATURE SUPERCONDUCTING Y-BA-CU-O

Donald R. Bowling,*[1] Robert J. Dinger,[1] Anna M. Martin[1]
John Talvacchio[2]

[1] Code 3814, Naval Weapons Center, China Lake, CA 93555
[2]Westinghouse Science and Technology Center
1310 Beulah Rd, Pittsburgh, PA 15235

Radiating elements, matching circuits, and feed networks fabricated from high-temperature superconductors are particularly attractive in the frequency range from 100 MHz to 1 GHz because of the large decrease in the surface resistance relative to copper. Very small and compact radiating elements (a few centimeters or less in size) are possible that have radiation efficiencies approaching 100%. We report the design, fabrication, and test of a 500-MHz half-loop antenna with integral matching network made from a sputtered Y-Ba-Cu-O thin film. The antenna, formed on one side of the lanthanum aluminate substrate, protrudes through a slot in a normal metal sheet to form a rectangular half-loop-over-a-groundplane antenna. A microstrip matching network is formed on the same substrate on the portion behind the antenna groundplane; the matching network is a novel microstrip coupled-line section that provides the proper impedance match from the antenna (Z_a = 0.1 + j80 Ω) to the feedline (Z_0 = 50 Ω) in a small planar area. The complete antenna and matching network fits on a 2-by-2 cm substrate and is enclosed in a compact shroud and Teflon radome cooled by a closed-cycle refrigerator. The antenna was measured over a temperature range of 20°K to 150°K. The Y-Ba-Cu-O antenna has a radiation efficiency of 17%, compared to 6% for a copper version of the antenna. Recent preliminary measurements, to be described in more detail in the presented paper, have been made on a Th-Ba-Ca-Cu-O version of the antenna and have yielded a radiation efficiency of 30%.

A39.3

μm-RESOLUTION FIELD PROBE FOR NON-INVASIVE MMIC MEASUREMENT

G.E. Bridges*, D.J. Thomson, C. Shafai and T. Forzley
Department of Electrical and Computer Engineering
University of Manitoba
Winnipeg, Canada R3T 2N2

The use of high-frequency planar integrated circuit components in both hybrid and monolithic form has become a common place technology. While the advantages of miniaturization and integration are obvious, the experimental measurement of such circuits has become a difficult task. Since conventional network analyzer multi-port techniques can only be applied to device ports, they can not easily be used to characterize the operation of the internal components in an integrated planar circuit. Further, the use of external connections to contact points inside the circuit under test would disturb the normal operation of the circuit. To overcome this problem, electro-optic and photoelectron based measurement techniques have been developed, but have some serious disadvantages such as being complex and expensive. Recently a simple microwave magnetic field probe with a 200μm resolution has been tested (S.S. Osofsky and S.E. Schwarz, Intl. IEEE MTT Symp., p. 823, 1989), but this resolution is still insufficient to examine some of the desired features of integrated circuits.

As an alternative method for measuring the internal operation of planar microwave integrated circuits, a non-contacting electric field probe with a μm resolution has been developed. The high resolution capability is obtained by utilizing a scanning force microscope as the positioner. The field probe consists of a 100μm long, 10μm wide and 0.3μm thick Si_3N_4 insulating beam with a small inverted pyramidal tip at its end. A gold conducting layer is deposited on one side of the beam for coupling to the circuit under test. Piezoelectric actuators are used to scan the probe over the test circuit surface. The probe structure measures the surface charge density in the localized region of the probe tip. The developed technique has the advantage that both the topological as well as the electrical characteristics of the circuit surface can be measured with the same instrument. Experimental results of measurements done on MMIC test structures will be presented and a numerical model, developed for optimizing the probe design will be discussed.

A METHOD TO DETERMINE THE PHASE CENTRES OF THE FIELD IN THE APERTURE OF A HORN ANTENNA

J.W. Odendaal and C.W.I. Pistorius*
Dept. Electronics and Computer Engineering
University of Pretoria
0002 Pretoria, South Africa

A method to determine the phase centre of the field in the aperture of a horn antenna will be described in this paper. By measuring the field in the aperture of a horn it is possible to determine an approximation for the field distribution in the aperture. The phase centres in the *E*- and *H*-plane are calculated from the phase information of the measured field in the aperture of the horn antenna.

The phase of the field in the plane of the aperture are measured at different known positions. A position for the phase centre is assumed on the axis of the horn due to the symmetry of the aperture. The field in the aperture due to a line source at the phase centre is calculated at each point where the measured phase is known. This is done for different positions of the assumed phase centre on the axis of the horn. A convolution between the measured and calculated phase in the aperture will yield a maximum value for the position of the phase centre that will best fit the measured phase in the aperture of the horn. A line source positioned at the phase centre will generate an incident field in the aperture of the horn whose phase will correspond with the phase of the measured field. It is thus possible to determine the position of the phase centre of the field in the aperture of a horn from the measured phase in the aperture.

The tangential fields over the aperture of a horn antenna exitated by the TE_{10} waveguide mode can be approximated by a cosinusoidal amplitude distribution in the *H*-plane and a uniform amplitude distribution in the *E*-plane. The phase information of the field is incorporated into the approximation by assuming that the field in the aperture is exitated by two line sources one in the *E*-plane and the other in the *H*-plane at the positions of the phase centres computed from the measured phase of the field.

NEAR FIELD AND FRESNEL ZONE MEASUREMENT USING PLANE WAVE SYNTHESIS

*M. Baquero *, M. Ferrando, D. Galdamez*
Dpto. Comunicaciones. UNIVERSIDAD POLITECNICA
46071-Valencia, Spain

In antenna measurements there are two limits, the far field $2D^2/\lambda$ and the near field spacing $\lambda/2$. This paper will present a method of plane wave synthesis with reduced number of sources avoiding this limits. The 2D problem can be solved using the modal solution of cylindrical modes.

$$e^{-jk\rho\cos\phi} = \sum_{n=-\infty}^{\infty} j^{-n} J_n(k\rho) e^{jn\phi}$$

and the translation theorem for Bessel functions:

$$a_m H_o^{(2)}(k|\vec{\rho} - \vec{\rho}'|) = a_m \sum_{n=-\infty}^{\infty} J_n(k\rho) H_n^{(2)}(k\rho') e^{jn(\phi-\phi')}$$

The array element currents, a_m, can be obtained solving a linear equations system.

The theory can be extended to 3D problems using spherical modes.

The figure 1 shows a phase representation of a plane wave generated with 3 sources spaced λ, at D^2/λ ; the same result can be obtained with 7 sources spaced $\lambda/2$ in near field, and with 1 source at $4D^2/\lambda$. The same formulation can be used to extend the validity of angular region in near field measurements as it is shown in figure 2.

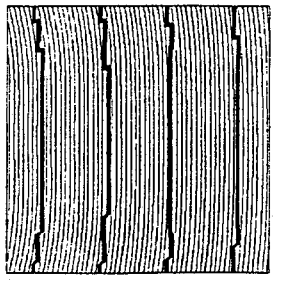

Figure 1

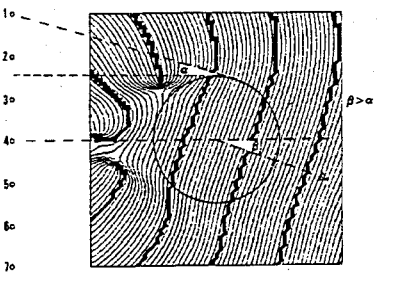

Figure 2

THE EFFECT OF TEMPERATURE AND TIME ON THE POINTING ANGLE OF AN MLS AZIMUTH ANTENNA

M.Z. EL-GAMAL
Microwave Landing System Project
Transport Canada, 110 O'Connor St., Ottawa, Ontario K1A 0N8

The analysis of the performance of Microwave Landing System (MLS) antennas must take into account the effect of manufacturing errors inherent in the system as well as the effect of thermal expansion or contraction of the antenna frame. In this work, the effect of simulated and actual variations in element positioning due to temperature in the -55° to 60°C range is investigated. The effect of these errors on the pointing angle, sidelobe levels and beam width is analyzed and presented for a 56 element phased array MLS antenna. The actual pointing angle error is measured over a three year period and is compared with the simulated error.

A39.7

LOSS MEASUREMENTS OF MICROSTRIP WITH CONTROLLED SURFACE ROUGHNESS

Todd Nichols
Department of Electrical and Computer Engineering
University of Colorado at Boulder
Boulder, CO 80309-0425

The subject of the author's PhD research at the University of Colorado is loss calculations and measurements in planar conductors, specifically microstrip. The goal is to improve CAD modeling of loss due to finite conductivity, edge shape, and surface roughness.

This paper discusses a Au-on-GaAs wafer designed for measuring loss, especially that due to a known surface roughness. In this case the canonical problems of a rectangular cross section of 50Ω line with no grooves, grooves parallel to the direction of propagation, and grooves transverse to the direction of propagation were chosen. Several wafers with both microstrip lines and gap-coupled two-port resonators were fabricated at Wright-Patterson Air Force Base in Dayton, Ohio, last summer with continuing fabrication at the University of Colorado. The main experimental objective is accurate measurement of γ, specifically α, of the microstrips with known roughness profile. To this end TRL calibration standards with the ability to use the statistical procedure introduced by NIST were put on the wafer. As a part of this project, an accurate 40 GHz wafer-probing station is now operational at the university; measurements were made with this unit and an HP8510 VNA. Validation of the probe station and calibration, experimental results, and comparison with commercial CAD models with be presented.

AIRY FUNCTION SOLUTIONS TO EIGENVALUE PROBLEMS WITH APPLICATIONS TO SCHRODINGER'S EQUATION AND NON-UNIFORM OPTICAL WAVEGUIDES

R.L. Gallawa*, A.K. Ghatak, I.C. Goyal
Electromagnetic Technology Division
National Institute for Standards and Technology
Boulder, Colorado 80303

A formalism that utilizes Airy functions is applied to equations of mathematical and quantum physics. We show that the computational procedure is very simple and allows a very accurate description of the guided modes of optical waveguides (waveguide problems) and the wave function for bound states (Schrodinger's equation). The method is much more useful than the conventional WKB method inasmuch as it is valid even in the vicinity of the turning point, where the WKB procedure fails. The method yields the eigenvalues to about the same accuracy as the WKB method. We then show a new perturbation equation, based on the same Airy function solutions, which yields extremely accurate eigenvalues. Problems that are amenable to exact analysis, one from quantum mechanics and one from optical waveguide theory, are used to illustrate the method and to demonstrate the accuracy. We also discuss a new formalism that is a direct corollary to the WKB quantization condition, but this new one is cast in terms of the Airy functions. This corollary quantization condition holds (for now, we believe) only for the antisymmetric mode when the profile is symmetric.

A39.9

SPREAD SPECTRUM MICROWAVE LEVEL METER

Akio Nagamune* and Kouichi Tezuka
Electronics Research Center, NKK Corp.
Kawasaki, Japan 210

An extremely sensitive, accurate and simple microwave level meter has been developed for the iron and steel making industry applications. This level meter consists of a continuous wave radar in which the carrier is modulated by the M-sequence (Maximal-length-sequence). Employing two M-seq. which are the same in code but generated by the slightly different clock frequencies, the implementation of the cross-correlation between the received and the reference signals can be simple and this radar successfully gains the sensitivity and suppresses the noise. Moreover, the quantization error of this radar can be designed smaller than the conventional FMCW (Frequency Modulated Continuous Wave) microwave radar. The principle of this microwave level meter is studied and its design criteria are described.

This spread spectrum microwave level meter is useful in the case that exclusive performance in terms of sensitivity and accuracy is required for the crucial measurement conditions in the environment such as the iron and steel making process where dust and flare may make it difficult to employ the laser beam or supersonic as sensing waves. The application of the microwave level meter is discussed in the experiments measuring the metallurgical slag and the molten metal levels.

In the prototype of the spread spectrum microwave level meter, the carrier frequency is 10GHz, the output power 60mW, the clock frequencies driving the two M-seq. generators about 220MHz, the difference of the two clock frequencies 5.4kHz or 10kHz, and the lengths of the M-seq. 127bit or 1023bit. The water-cooled horn antennas with the gain of 17db are used. The metallurgical slag level in a mini-converter was continuously measured with the accuracy of 88mm. The sensitivity was high enough to detect the weak reflected wave from the slag surface whose reflection coefficient was -40dB. The molten metal level in a tandish of a continuous casting process was measured with the good accuracy of 20mm. Some practical models of this radar are to be under operation in our works.

Equipment for precise microwave holography measurements at 22 GHz

V. Khaikin

We should have a phase decorrelation of main and reference holography channels only several degrees to measure 100 mkm antenna surface distortions. To solve this problem the two-channel parametric amplifire with common pumping and noise temperature Tn1 =Tn2=210 K was developed as Front end of the holography receiver at 22 GHz(V. Khaikin, A. Yaremenko-Proceedins of International Workshop on Holography in N. Arkhyz, USSR, 1990/1/). The mutual phase instability of two channels measured by the special very precise method(G. Dvoyan, G. Birumyan, V. Khaikin-/1/) is equal 0.12° for 5 min and 1.2° for 6 hr. After Front end the reference signal obtains a linear phase shift to form the effective "off-axis" reference wave and avoid output holography image distortions; the main signal obtains $0^{\circ}/180^{\circ}$ phase modulation to remove a power component from the microwave holography signal(MHS) and expand dynamic range of recording. The Regia-Spenser linear phase shifter has <0.05 DB modulation of inserted losses and 1-2 % nonlinearity or -36 DB level of undesirable components in the spectrum of the phase-modulated signal. The $0^{\circ}/180^{\circ}$ phase modulator developed on the basis of flat ferrit in azimuth magnetic field guarantees 1% accuracy and a high stability of phase-swiching due to magnetic ferrit memory(G. Romanov, O. Trehovitskij, V. Khaikin- /1/). Then holography channels are combined together and MHS is amplified by common 8-stage FET down video detector.

The highly stabilized Gunn oscillator at 22 GHz with 10^{-7} short-time frequency instability(V. Makarenko, G. Pinchuk, V. Khaikin. -Equipment and techniques of experiment in USSR, 3, 1990) was developed as a MHS source to guarantee coherence of the main and reference holography channels if the difference between their length in good atmospheric conditions is equal to more than 100 m

The described equipment was succesfuly tried in the holography measurements of RATAN-600 radio telescope.

Measurements of Materials I

Room 3006 Salle
URSI A Session 72

Mesures des matériaux I

Chairs/présidents: R.F. CLARK, Canada; C.M. WEIL, USA

13:30 (72.1) Dielectric Properties of the Colorado Potato Beetle and Its Environment, **B.G. COLPITTS**, *University of New Brunswick, Fredericton, NB, Canada*

13:50 (72.2) T-Pattern Resonator Method of Determining Material Dielectric Constant, **J.P. CURILLA**, D.I. AMEY, *E.I. Du Pont de Nemours & Company Inc., Wilmington, DE, USA*

14:10 (72.3) Dielectric Characterization of Substrate Materials Using Stripline Resonators, W. SU, **S.M. RIAD**, A. ELSHABINI-RIAD, *Virginia Polytechnic Institute and State University, Blacksburg, VA, USA*

14:30 (72.4) Accurate Measurement of the Complex Permittivity of Low Loss Dielectric Materials at Microwave Frequencies Using Rectangular Microstrip Resonators, **M.A. SAED**, *State University of New York, New Paltz, NY, USA*

14:50 (72.5) Time Domain Dielectric Characterization Using Stripline Geometry, K.M. FIDANBOYLU, **S.M. RIAD**, A. ELSHABINI-RIAD, *Virginia Polytechnic Institute and State University, Blacksburg, VA, USA*

15:10 **COFFEE/CAFÉ**

15:30 (72.6) Transmission Line Modeling for Material Characterization: Including Dielectric/Conductor Losses and Interfacial Effects, W.A. DAVIS, **S.E. BUCCA**, C.F. BUNTING, *Virginia Polytechnic Institute and State University, Blacksburg, VA, USA*

15:50 (72.7) Radial Air Gap Corrections for Precision High Dielectric Constant Measurements, **R. GEYER**, C. WEIL, J. BAKER-JARVIS, *National Institute of Standards and Technology, Boulder, CO, USA*

16:10 (72.8) Constrained Nonlinear Estimation of Scattering Parameters for Transmission/Reflection Permittivity and Permeability Measurement Methods, **J. BAKER-JARVIS**, R. GEYER, P. DOMICH, *National Institute of Standards and Technology, Boulder, CO, USA*

16:30 (72.9) Free Space ϵ, μ Measurements Variable Impedance Load Method, **V. SAAVEDRA**, *Commissariat à l'Énergie Atomique, Le Barp, France*

16:50 (72.10) Validity of the Theories for the Measurement of Electric Fields and Electric Conductivity in the Stratosphere, **R. GODARD**[1], D. TREPANIER[1], J.S. CHANG[2], [1]*Royal Military College of Canada, Kingston, ON, and* [2]*McMaster University, Hamilton, ON, Canada*

A72.1

DIELECTRIC PROPERTIES OF THE COLORADO POTATO BEETLE AND ITS ENVIRONMENT

Bruce G. Colpitts
Department of Electrical Engineering
University of New Brunswick,
Fredericton, New Brunswick, Canada

The results of measurement of the complex dielectric properties of the Colorado Potato Beetle (Leptinotarsa decemlineata) and its habitat are presented. Measurements were performed over a frequency range from 2.6 GHz to 12.4 GHz using a series of waveguide sample holders and the transmission reflection technique of James Baker-Jarvis et.al. (J. Baker-Jarvis, et.al., IEEE MTT vol. 38, no. 8, pp.1096-1103, August 1990) implemented on an automatic vector network analyzer. The purpose of these measurements was to determine the properties of the beetle and its surroundings which serve as the first step in evaluating the feasibility of using microwave energy as a means to control beetle populations other than by the insecticide presently being used.

Results are presented for several sample types associated with the beetle and its surroundings including: 1. Entire beetle, 2. Head and prothorax, 3. Mesothorax, metathorax and abdomen, 4. Leaf of the potato plant, 5. Stem of the potato plant, 6. Soil. In cases 1-3 involving the beetle the measured samples were homogenized into a paste or crushed to fit the sample holders. Since sample deterioration begins upon breaking cell walls it was necessary to prepare the insect samples immediately before measurement. In the case of potato plants the leaves and stems were cut and layered in the sample holders for either vertical or horizontal polarization. In cases where large volumes of material were available several sample thicknesses were measured but in specimens 2 and 3 only a very short sample holder could be used and then only at the higher frequencies where less sample is required.

The problem of using a single sample holder for broadband measurements is overcome in the technique of Baker-Jarvis in that his technique is stable over frequencies corresponding to integer multiples of one-half wavelength in the sample. Although this technique is very stable one must exercise caution in that the solution may have multiple roots which can go undetected if the results are not carefully examined.

The results indicate that in general the plant has the highest permittivity both real and imaginary while the beetle is slightly lower followed by the soil.

T-PATTERN RESONATOR METHOD OF DETERMINING MATERIAL DIELECTRIC CONSTANT

J.P. Curilla* and D.I. Amey
E.I. du Pont de Nemours & Co., Inc.
Wilmington, DE 19898

A method of measuring substrate material dielectric constant in the microwave frequency range is presented. The method, which requires the fabrication of microstrip transmission line parts, utilizes a computer-controlled network analyzer measuring system. Measurements are typically from 1 to 15 GHz. Measurement precision is typically less than 1%, and accuracy is estimated to be less than 5% for dielectric constant values less than 10.

A72.3

DIELECTRIC CHARACTERIZATION OF SUBSTRATE MATERIALS USING STRIPLINE RESONATORS

Wansheng Su, Sedki M. Riad and Aicha Elshabini-Riad*
The Bradley Department of Electrical Engineering
Virginia Polytechnic Institute and State University
Blacksburg, VA 24061-0111

Two stripline methods, line resonator and ring resonator, are described to characterize dielectric materials. Since the property of the material is only related to the resonator frequency and the quality factor, it is relatively easier to obtain accurate results for both the dielectric constant and loss tangent of the material undertest. To improve the accuracy of the method, the fringing effects at the gap discontinuities and curvature in ring resonator are also accounted for.

In the stripline resonator design, a critical design parameter is the width of the coupling gap. If the gap is too large, the coupling is too weak to yield a measurable resonance. If the gap is too small, the external loading effect degrades the quality factor, Q, of the resonant circuit and affect the loss tangent analysis. In order to optimally design the width of the gap, a 3-D static field analysis program has been developed and used to calculate an estimate to the coupling capacitance. A computer simulation of the resonant circuit is then used to optimize the gap width.

Some experimental results are presented. All measurements are done using HP 8510B network analyzer. The Cascade Microtech EL-18 Eisenhart Launchers are used to provide connections between the system and the stripline samples. The measurement uncertainty for dielectric constant is less than 1% and for loss tangent is less than 5%.

ACCURATE MEASUREMENT OF THE COMPLEX PERMITTIVITY OF LOW LOSS DIELECTRIC MATERIALS AT MICROWAVE FREQUENCIES USING RECTANGULAR MICROSTRIP RESONATORS

Mohammad A. Saed
Electrical Engineering Department
State University of New York
College at New Paltz
New Paltz, New York 12561

In this paper, a method for accurate measurement of the complex permittivity of low loss dielectric materials is presented. The method uses a resonant rectangular microstrip patch with the material under test forming the dielectric separating the patch and the ground plane. The microstrip patch can be fed using aperture coupling or a probe feed. The reflection coefficient, measured using a network analyzer, will be used to determine the complex permittivity, ϵ^*, at the resonance frequency of the TM_{10} mode.

The structure is analyzed based on a cavity model taking into account higher order modes. The analysis also takes into account radiation as well as conductor losses. The measured resonance frequency of the TM_{10} mode is used to determine the dielectric constant (real part of ϵ^*) while the magnitude of the reflection coefficient or the quality factor is used to compute the dielectric loss (imaginary part of ϵ^*). These computations are carried out iteratively using an optimization procedure.

The concept, method of analysis, as well as results of experiments using dielectric materials with known properties to verify this technique will be presented.

A72.5

TIME DOMAIN DIELECTRIC CHARACTERIZATION USING STRIPLINE GEOMETRY

K. M. Fidanboylu, S. M. Riad*
and A. Elshabini-Riad
Electrical Engineering Department
Virginia Polytechnic Institute and State University
Blacksburg, VA 24061

In an earlier paper (K.M. Fidanboylu, S.M. Riad & A. Elshabini-Riad, IMTC Conf., 1990), a new time domain approach for the determination of the complex permittivity of a dielectric material in a stripline geometry was discussed. In this paper, an extension to the earlier work is presented. The new technique uses both Time Domain Reflectometry (TDR) and Time Domain Transmission (TDT) measurements for determining an optimum frequency dependent lossy transmission line model for the stripline under test. The optimization is done in the time domain by comparing the experimental TDR and TDT response waveforms with the simulated ones using a non-linear least squares fit. The conventional optimization algorithms have shown to be inefficient in this specific application. In this paper an efficient optimization algorithm which has been developed to suit this application is also presented.

In general, the material properties in a stripline under test are related with the geometrical parameters of the line through complicated integral expressions. Using the approach explained in this paper, the use of complicated integral expression are avoided. The material properties such as the complex permittivity of the dielectric material is determined from the optimum lossy transmission line model.

Transmission Line Modeling for Material Characterization: Including Dielectric/Conductor Losses and Interfacial Effects

W. A. Davis, S. E. Bucca*, and C. F. Bunting
Virginia Polytechnic Institute and State University
Blacksburg, VA 24061-0111

This paper considers the problem of modeling for the characterization of the materials used in transmission line type structures. The modeling of materials in transmission lines requires a fundamental understanding of the lines themselves. This is particularly the case when the lines are used in the measurement process itself. This paper reviews the basics of transmission line modeling as derived for the exact coax problem and extends this analysis to other geometries. The extensions include the effects of conductor loss (as commonly found in the literature), dielectric loss, and the effects of the dielectric–conductor interface. We will emphasize the propagation constant γ of the line which is of primary importance in relating to measured data. The frequency behavior of the propagation constant may be used to separate the behavior of the dielectric material from the properties of the conductor used to construct the line, except for the dielectric–conductor interface effects. The conductor properties will be found to be directly related to the line geometry while the dielectric properties appear without the dependence on the geometry. Thus, we will be able to extract the dielectric properties without full knowledge of the cross-section of the line. The resultant material properties may be considered to be effective parameters. To separate the dielectric–conductor interface effects, additional measurements involving the variation of the cross-sectional geometry must be performed and related to the model. Though the model does not account for the amplitude of conductor effects, it does define a proper behavior and relates to the interface effects in the same proportion.

To support some of the concepts of the development for rough surfaces, a one-dimensional model of a rough surface is also considered for analysis. This model demonstrates the interface effects being described in the above model. Some discussion will be made concerning the extension of the rough surface model to two dimensions and the additional aspects of a truly rough surface rather than a periodic surface. A few measurements will also be presented in support of the modeling approach.

A72.7

RADIAL AIR GAP CORRECTIONS FOR PRECISION HIGH DIELECTRIC CONSTANT MEASUREMENTS

*R. Geyer, C. Weil, J. Baker-Jarvis
National Institute of Standards and Technology
Electromagnetic Fields Division
325 Broadway
Boulder, CO 80303

A large potential source of error in dielectric property measurements at microwave frequencies is that due to the air gap between the sample under test and the wall of the waveguide or resonator fixture. This is particularly true for materials having high dielectric constants or in situations where appreciable air gaps exist. Limitations of first-order perturbation correction relations are discussed, and comparisons with mode-matching and variational methods are shown.

CONSTRAINED NONLINEAR ESTIMATION OF SCATTERING PARAMETERS FOR TRANSMISSION/REFLECTION PERMITTIVITY AND PERMEABILITY MEASUREMENT METHODS

*J. Baker-Jarvis, R. Geyer, P. Domich, NIST
National Institute of Standards and Technology
Electromagnetic Fields Division
325 Broadway
Boulder, CO 80303

Constrained nonlinear optimization of 2-port transmission/reflection scattering parameters is used to determine the complex permittivity and permeability of various materials. The approach allows the weighting of scattering equation relations with respect to their corresponding uncertainties. This technique also enables accurate determinations of complex permittivity and permeability of low- and high- loss materials that have large effective real permittivities and permeabilities.

A72.9

FREE SPACE ε,μ MEASUREMENTS VARIABLE IMPEDANCE LOAD METHOD

V. SAAVEDRA - Commissariat à l'Energie Atomique - 33114 - LE BARP - FRANCE

The Electromagnetic characterization of materials is usually performed using waveguides.

For the SHF measurements, the samples are about one centimeter large. When the materials include one millimeter-scale heterogeneities, the aboved mentioned methods are not appropriate.

Then the evaluation of both effective permittivity and permeability can be performed in free space, using square plane plates which have approximately a side of 30 cm and a thickness between 1 millimeter and several centimeters (for measurements on the frequency range : 1-18 GHz)

When the target is illuminated by an electromagnetic field, it backscatters a fraction of the incident energy. The Radar Cross Section represents this backscattered energy.

The Reflexion Coefficient is computed by comparing the RCS of a sample to the one of a metal plate.

The method which is described here is based on the measurements of the reflexion coefficients when loading the material plate with two different impedances.

These load impedances are easily adjusted by inserting a layer of a dielectric between the material and the metal plate .

The Reflexion Coefficient is a function of the unknown permittivity and permeability, of the material thickness, frequency and load.

If the sample is large enough in regard to the wavelength, then the dependance is explicit. This condition is verified for 300 X 300 mm2 plates in the SHF range.

In order to inverse the problem, two different loads are needed to calculate ε and μ.

If some uncertainties still remain in these computations, the correct choice of thickness enables us to reduce them and additional tests provide a solution to the remaining ambiguities.

The measurements have been made in an anechoïc chamber (12 x 6 x 6 m3)

The distance between the sources and the target is 8 meters, which in practice means that the target is located in the far field for the considered frequency range.

Microwaves are transmitted and received by a bank of usual horns (frequency range : 1.7. - 18 GHz) and analysed by an HP 8510 Network Analyser. In order to obtain a good accuracy, the target position and its flatness must be checked to be better than 1 millimeter.

This method has been tested with various types of dielectric, ferrite, foam...

Finally, a good agreement with the guided wave measurements is obtained.

VALIDITY OF THE THEORIES FOR THE MEASUREMENT OF ELECTRIC FIELDS AND ELECTRIC CONDUCTIVITY IN THE STRATOSPHERE

R. Godard[1], D. Trepanier[1], J.S. Chang[2]

1. Department of Mathematics and Computer Science, Royal Military College of Canada, Kingston, Ontario, Canada K7K 5L0.
2. Department of Engineering Physics, McMaster University, Hamilton, Ontario, Canada

The theories and the techniques for the measurement of ionospheric and atmospheric electric fields in the stratosphere and the measurement of the electric conductivity by on board balloon experiments are re-examined. The theory is directly linked to the theory of electrostatic probes and double probes in a continuum plasma and exact numerical results for the collected current by an electrode are given. We emphasize the fact that the electrodes are immersed in a medium of relatively high pressure and that their surfaces are covered by an irregular layer of adsorbed gases. This adsorbed layer may trap charged particles and the relaxation profiles for the measurement of the conductivity may be convoluted with surface relaxation effects. If we represent the surface relaxation phenomena by an equivalent classical R_sC_s network, we indicate how the time constant of this latter effect can be estimated and removed from the data.

Measurements of Materials II

Room 3006 Salle
URSI A Session 89

Mesures des matériaux II

Chairs/présidents: S.M. RIAD, USA; J. BAKER-JARVIS, USA

08:30 (89.1) A Millimeter-Wave Open Resonator with Application in Measurement of Surface Resistance of Conducting Materials, S. ADITYA[1], **R.K. ARORA[2]**, [1]*Indian Institute of Technology Delhi, New Dehli, India;* [2]*Florida State University, Tallahassee, FL, USA*

08:50 (89.2) Accuracy Improvements in Resonant Cavity Measurement Techniques for Dielectric Materials, E.J. VANZURA[1], J. ROGERS[1], **C.M. WEIL[1]**, A.J. ESTIN[2], [1]*National Institute of Standards and Technology, Boulder, CO, and* [2]*Cyberlink Corporation, Boulder, CO, USA*

09:10 (89.3) Dielectric Loss Determination Using a Wideband Dielectric Filled Cavity, M.Y. ANDRAWIS, W.A. DAVIS, **S.M. RIAD**, A. ELSHABINI-RIAD, *Virginia Polytechnic Institute and State University, Blacksburg, VA, USA*

09:30 (89.4) Modeling of Open-Ended Coaxial Line Dielectric Sensors, **C.L. SIBBALD**, S.S. STUCHLY, *University of Ottawa, ON, Canada*

09:50 (89.5) A Generalized Aperture Admittance Model for the Open-Ended Dielectric Sensors: Experimental Method, **A. NYSHADHAM**, C.L. SIBBALD, S.S. STUCHLY, *University of Ottawa, ON, Canada*

10:10 **COFFEE/CAFÉ**

10:30 (89.6) A New Technique for Measuring the Permittivity of Planar Materials, **W.R. SCOTT JR.**, *Georgia Institute of Technology, Atlanta, GA, USA*

10:50 (89.7) A Study of Error Sensitivities in Dielectric Spectroscopy for the Open Circuit Coaxial Sample Holder, R.B. STAFFORD[1], **J. BAKER-JARVIS[2]**, [1]*Virginia Polytechnic Institute and State University, Blacksburg, VA, and* [2]*National Institute of Standards and Technology, Boulder, CO, USA*

11:10 (89.8) Time Domain Reflectometry Measurements on Liquid Crystals, R. NOZAKI, **T.K. BOSE**, *Université du Québec, Trois-Rivières, PQ, Canada*

11:30 (89.9) A Dual Resonator Technique for the Characterization of High T_C Superconductors, R.D. BYNUM, **J.T. WILLIAMS**, *University of Houston, TX, USA*

11:50 (89.10) Characterization of Conduction Losses in High-T_C Films, **N.J. KOLIAS[1]**, R.A. YORK[1], R.C. COMPTON[1], P.J. KIRLIN[2], [1]*Cornell University, Ithaca, NY, and* [2]*ATM Corporation, New Milford, CT, USA*

A89.1

A MILLIMETER-WAVE OPEN RESONATOR WITH APPLICATION IN MEASUREMENT OF SURFACE RESISTANCE OF CONDUCTING MATERIALS

Sheel Aditya
Department of Electrical Engineering
Indian Institute of Technology Delhi
Hauz Khas, New Delhi 110016, India

and

Rajendra K. Arora*
FAMU/FSU College of Engineering
Department of Electrical Engineering
Tallahassee, Florida 32316

Closed cavity resonators are frequently employed for measurements on dielectric and conducting materials. In this paper is proposed a millimeter-wave "open" resonator comprising a concave mirror and a plane reflector. The whole assembly is shielded inside a cylindrical metallic enclosure. The input and output coupling holes are offset from the axis of the reflector and both holes are located on the same (concave) reflector. This configuration allows one to substitute one plane reflector by another constructed out of a different conducting material with least dimensional change. Measurement of surface resistance is performed by the method of substitution in which the Q-factor of the resonator is accurately measured with the plane reflector made of different conducting materials. The design and performance of the resonator in the frequency range 80-100 GHz are presented. Also included are measurement results to demonstrate the application of this resonator in the measurement of surface resistance of low-loss conducting materials.

ACCURACY IMPROVEMENTS IN RESONANT CAVITY MEASUREMENT TECHNIQUES FOR DIELECTRIC MATERIALS.

Eric J. Vanzura, Janet Rogers, Claude M. Weil*
National Institute of Standards and Technology,
325 Broadway, Boulder, CO 80303, USA

and Arthur J. Estin
Cyberlink Corporation, P.O. Box 12180, Boulder, Co

The resonant cavity perturbation technique is considered to be the most accurate technique available for characterizing the microwave properties of low-loss dielectric materials. Determination of the material loss-tangent requires an accurate measurement of the cavity resonance quality factor, Q when the cavity is first empty and subsequently with the material sample in place. The textbook procedures for determining the cavity Q, which involves measuring the frequency half-power points, are of limited accuracy. Furthermore, a correct application of the theory requires the use of the unloaded Q factor whereas measurements yield a value for the loaded Q; i.e. the reduced Q created by the loading of the input and output coupling ports. This is another significant source of error.

The advent of the automatic network analyzer has created opportunities for considerably improving the accuracy of cavity Q measurements. This talk will discuss some new techniques and measurement procedures developed at NIST that have more than halved the existing uncertainities in loss-tangent measurements. These techniques involve the use of statistical curve fitting routines for measured reflection and transmission data. Such techniques have the advantage that all of the data available in a typical resonance scan are utilized, not just the two half-power data points. They also allow for the determination of the port coupling factors from which the unloaded Q can be subsequently computed. The new techniques currently in use are based on a first-order cavity circuit model, that may not be of sufficient accuracy. The possible need for a second or third order order theory is currently being investigated. Different measurement options will also be discussed. These involve measuring only the input scattering parameters following a simple 1-port response calibration of the detuned cavity or measuring both input and transfer parameters following a full 2-port TRL calibration.

A89.3

DIELECTRIC LOSS DETERMINATION USING A WIDEBAND DIELECTRIC FILLED CAVITY

M. Y. Andrawis, W. Davis, S. Riad, and A. Elshabini-Riad

Virginia Polytechnic Institute and State University

Bradley Department of Electrical Engineering

Blacksburg, VA 24061-0111

A wideband dielectric filled cavity (WDFC) structure is currently being used to estimate the dielectric constant and loss factor of dielectric materials which fill the cavity structure. The method has previously been used successfully to measure the dielectric constant of materials [M. A. Saed, "Dielectric Characterization Using a Wideband Dielectric Filled Cavity", Ph.D. Dissertation, Virginia Polytechnic Institute and State University, November 1987], but limitations in the method have created difficulties in accurate measurement of the dielectric loss factor. The loss in this method yields a measure of the total cavity loss, including both the dielectric loss and that of the conductor walls. However, the electromagnetic field analysis used in the method is restricted to perfectly conducting walls leading to the inability to separate the dielectric loss estimate from the conductor loss.

In this paper the separation of conductor loss from the total loss is presented using a perturbational method. The loss free full analysis solution is used to determine the electric current at the conductor boundaries, and thus the current flow in the conductor. This current distribution is then used to evaluate the power dissipated in the conductor walls based on known conductor properties. By subtracting the loss due to the conductor walls from the total loss measured in the system, the dielectric loss, and thus the dielectric loss factor, may be estimated.

Modeling of Open-Ended Coaxial Line Dielectric Sensors

C.L. Sibbald* and S.S. Stuchly
Department of Electrical Engineering
University of Ottawa, Ottawa, Ontario, Canada

In order to achieve accurate broadband measurements of the permittivity of materials using open-ended coaxial line probes, an accurate aperture admittance model of the probe is required. This paper presents a novel technique for determining simple, accurate, broadband admittance models for apertures radiating into homogeneous, lossy dielectrics.

This technique exploits the analytic properties of the mapping from the permittivity plane to the admittance plane in order to determine polynomial expressions for the aperture conductance and susceptance. These expressions are explicit functions of the dielectric constant and loss factor of the medium whereas the coefficients are functions of frequency and probe geometry. The coefficients, or model parameters, are easily determined from the computed admittance of the probe as a function of the dielectric constant alone. This computed data is obtained via a full-wave moment method solution, and hence, includes the effects of radiation and energy storage in the evanescent modes and the near-field.

The new method has several advantages. The conductance and susceptance are real functions of the dielectric constant and loss factor, and the model parameters are determined from a relatively small number of computed points. Furthermore, the resulting closed-form expressions simplify uncertainty analysis.

In order to illustrate the technique, an aperture admittance model for a 3.6mm semirigid coaxial line is compared with experimental results. The suitability and limitations of the method for other structures, such as waveguide and stripline apertures, is discussed.

A89.5

A GENERALIZED APERTURE ADMITTANCE MODEL FOR THE OPEN-ENDED DIELECTRIC SENSORS: EXPERIMENTAL METHOD

A. Nyshadham*, C. L. Sibbald and S. S. Stuchly
Dept. of Electrical Engineering,
University of Ottawa
Ottawa, Ontario, Canada

An accurate aperture admittance representation of the open-ended dielectric sensor is necessary to estimate the permittivity of the materials from the measurements. A wide range of admittance models reported in the literature differ.

Hence, a unified treatment of the majority of the existing admittance models is discussed in this presentation. The aperture admittance of the open-ended coaxial line is represented by a parallel combination of a capacitance and a conductance which are functions of frequency and are explicit functions of the permittivity of the test material. The aperture admittance is then given by

$$Y(f,\hat{\epsilon}) = G(f)\hat{\epsilon}^n + j\omega C(f)\hat{\epsilon}$$

where n depends on the coaxial line dimensions and frequency of the measurement only.

An experimental technique including time domain gating is used to determine the equivalent circuit parameters of aperture admittance model. The measurements are performed using HP8510B network analyzer and three reference liquids, water, methanol and saline. The experimental results for these materials are compared with those reported in the literature.

A New Technique for Measuring the Permittivity of Planar Materials

Waymond R. Scott, Jr.
School of Electrical Engineering
Georgia Institute of Technology
Atlanta, Georgia 30332-0250

A technique which is specifically designed for measuring the permittivity of planar samples is investigated in this work. Figure 1 is a sketch of the fixture that is used in the technique. The material to be measured is placed between the two conducting plates which are attached to the coaxial lines. A planar material can be placed in the fixture without any preparation; this is a big advantage over techniques which require the sample to be machined to fit into a waveguide, coaxial line, or other measurement fixture. In many of these techniques, the preparation of the sample is the most difficult part of the measurement procedure.

In the technique, the reflection and transmission coefficients of the fixture are measured, and the permittivity is determined from these measurements. This step requires a very accurate relationship between the material parameters and the reflection and transmission coefficients. Such a relationship cannot be determined analytically and must be determined numerically. The finite element method is used to determine the relationship in this work. The technique is verified experimentally by measuring the permittivity of materials with known properties.

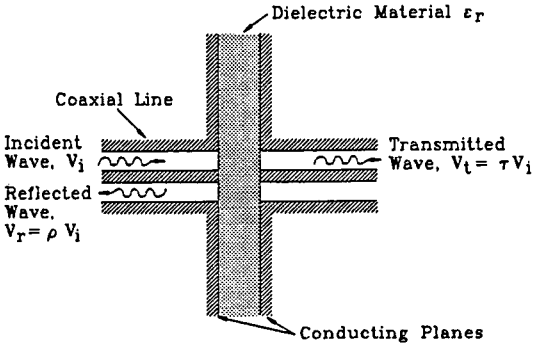

Figure 1. Fixture Used to Measure the Permittivity.

A89.7

A STUDY OF ERROR SENSITIVITIES IN DIELECTRIC SPECTROSCOPY FOR THE OPEN CIRCUIT COAXIAL SAMPLE HOLDER

Robert B. Stafford
Virginia Polytechnic Institute
Blacksburg, VA 24061-0111

*James Baker-Jarvis
National Institute of Standards and Technology
325 Broadway
Boulder, CO 80303

The shielded open circuit coaxial sample holder is often used in materials characterization. In this talk we develop the permittivity equations for this device from first principles and identify a number of error contributing factors. Numerical expressions for these errors will be presented and procedures for reducing some of these error contributions will be discussed.

TIME DOMAIN REFLECTOMETRY MEASUREMENTS ON LIQUID CRYSTALS

Ryusuke Nozaki and Tapan K. Bose*
Groupe de Recherche sur les Dielectriques
Departement de Physique
Universite du Quebec a Trois-Rivieres
C.P.500 Trois-Rivieres, Quebec, G9A 5H7, Canada

Time domain reflectometry technique (TDR) can be used to measure the complex permittivity of materials, both for liquids and solids, over a wide frequency range between 100KHz and 25GHz (R.Nozaki & T.K.Bose, IEEE Trans. IM39-6, 1990). The instrumentation is simple, easy to use and inexpensive.

In this paper, we shall report the complex permittivity measurements of liquid crystals using TDR technique. It is well known that the complex permittivity of a liquid crystal has two components, parallel to the direction of the molecular long axis ($\epsilon_{//}$) and perpendicular to the axis ($\epsilon_{\perp}$). A sufficiently strong magnetic field is used to control the direction of the molecular axis.

Normally, in the case of TDR measurement, a coaxial sample cell is used because of the ease of using basic transmission line theory. However, some modifications in the cell configurations are necessary for producing an uniform magnetic field. Possible cell configurations and corrections in use are discussed.

As an example for a wide frequency measurement, the complex permittivity measurements are performed on a reentrant nematic liquid crystal mixture (8OCB/6OCB) in the frequency range between 100KHz and 1GHz. In the nematic, smectic A and reentrant nematic phases, the parallel components show the dielectric relaxation to be in the megahertz range and the perpendicular components are in the subgigahertz range. Comparisons between high and low temperature nematic phases are discussed.

On the other hand, for a high frequency measurement, we conducted experiment on a ferroelectric liquid crystal (4-[(S,S)-2,3-Epoxyhexyloxy]phenyl 4-(decyloxy) benzoate) in the frequency range between 10MHz and 10GHz. In this case, both of the components of the dielectric relaxation are in the gigahertz range. These relaxations are considered to be due to a rotational motion around the molecular long axis.

A89.9

A DUAL RESONATOR TECHNIQUE FOR THE CHARACTERIZATION OF HIGH T_C SUPERCONDUCTORS

R. Dale Bynum and Jeffery T. Williams*
Applied Electromagnetics Laboratory
Department of Electrical Engineering
University of Houston
Houston, TX 77204-4793

Microstrip and stripline resonator based characterization techniques used to determine the surface resistance of high T_c superconducting thin films require an accurate knowledge of the dielectric constant and loss tangent of the substrate at the temperature and frequency of interest. Presently, these electrical parameters are determined from either specifications given by the manufacturer or extrapolated from measurements made at very low temperatures, where it is assumed that the dielectric losses dominate the Q of the structure. We have developed a new measurement technique using two resonators of different strip width to measure the average surface resistance of the superconducting strip and ground plane(s), and to determine the dielectric properties of the substrate at the measurement temperature and frequency. This method also has the advantage that the an absolute determination of the surface resistance is obtained from the measured Q's of the *dual* resonators, as opposed to techniques which yield surface resistances which are related to a known standard, such as niobium, copper, or gold. As with all microstrip and stripline resonator techniques, the minimum value of the surface resistance that can be measured (the sensitivity of the measurement) is limited by the loss of the dielectric substrate and radiation losses. We will present results which shows the sensitivity limitations of resonator based techniques, and will demonstrate the capabilities of the dual resonator technique by presenting results of characterization studies for $YBa_2Cu_3O_7$ superconducting thin films on $LaAl_2O_3$ substrates. We will also show the temperature and frequency dependence of the dielectric constant and loss tangent of $LaAl_2O_3$.

CHARACTERIZATION OF CONDUCTION LOSSES IN HIGH-Tc FILMS

N. J. Kolias, R. A. York, and R. C. Compton*
School of Electrical Engineering
Cornell University, Ithaca, NY 14853

P. J. Kirlin
ATM Corporation
New Milford, CT 06776

Before high-Tc superconductors can receive widespread use more work must be done in understanding their properties. Especially important, for microwave applications, is to understand and quantify the conduction losses in these superconductors. To this end, a resonator technique which accurately calculates the attenuation of superconducting films via reflection measurements has been implemented.

The technique works as follows: The superconducting film is patterned as an open-circuited microstrip resonator and placed in a test fixture. The fixture is immersed in liquid nitrogen and the magnitude and phase of the reflection coefficient (s_{11}) is measured using a network analyzer. From a least squares fit of the data the loss is calculated.

This technique yields accurate measurements for frequencies from 1 to 20 GHz. The technique has been used to measure the attenuation in MOCVD grown high-Tc thallium films. Promising results were obtained for these films at 77 K and 8 GHz.

Noise — Bruit

Room 3006 Salle
URSI A Session 106

Chairs/présidents: W. KESSEL, Germany; D.F. WAIT, USA

13:30 (106.1) Millimeter Wave Noise Applied for the Investigation of the Earth Atmosphere, **G.K. HARTMANN**, P. HARTOGH, *Max-Planck-Institüt für Aeronomie, Katlenburg-Lindau, Germany*

13:50 (106.2) Noise Standards and Calibration Techniques in Europe: Recent Developments and Future Trends, G. GENEVÈS[1], **F.-Im. BUCHHOLZ**[2], M.W. SINCLAIR[3], [1]*Laboratoire Central des Industries Electriques, Fontenay-aux-Roses, France;* [2]*Physikalisch-Technische Bundesanstalt, Braunschweig, Germany;* [3]*National Physical Laboratory, Malvern, UK*

14:10 (106.3) Noise Power Measurements and Measurement Uncertainties, **F.-Im. BUCHHOLZ**, W. KESSEL, F. MELCHERT, *Physikalisch-Technische Bundesanstalt, Braunschweig, Germany*

14:30 (106.4) Correction Factor in Broadband Heterodyne Systems, **S. PERERA**, *National Institute of Standards and Technology, Boulder, CO, USA*

14:50 (106.5) A "Terminal Invariant" Description of Amplifier Noise, **G.F. ENGEN**, D.F. WAIT, *National Institute of Standards and Technology, Boulder, CO, USA*

15:10 **COFFEE/CAFÉ**

15:30 (106.6) Noise Parameter Accuracy and Repeatability Considerations, **V. ADAMIAN**, *ATN Microwave Inc., Billerica, MA, USA*

15:50 (106.7) The Use of a Mismatched Attenuator to Validate the Performance of a Four Parameter Amplifier Noise Test Set, **D.F. WAIT**, *National Institute of Standards and Technology, Boulder, CO, USA*

16:10 (106.8) Avoiding Adapter Measurements, **W.C. DAYWITT**, *National Institute of Standards and Technology, Boulder, CO, USA*

16:30 (106.9) W-Band Noise Measurement Technique, **T.V. MAI**, J.J. O'NEILL, J.A. MOLNAR, *Naval Research Laboratory, Washington, DC, USA*

16:50 (106.10) A New Formula for Calculating High Voltage Standing Wave Ratio from Slotted Line Measurements, **D. ZHANG**, H. JIANG, *Sichuan University, Sichuan, China*

A106.1

MILLIMETER WAVE NOISE APPLIED FOR THE INVESTIGATION OF THE EARTH ATMOSPHERE

G.K. Hartmann and P. Hartogh
Max-Planck-Institut fur Aeronomie
P.O. Box 20, W-3411 Katlenburg-Lindau
Federal Republic of Germany

Constituents of the Earth atmosphere such as O_2, O_3, H_2O, ClO, and others like CO, N_2O, HNO_3, NO_2, etc. exhibit resonances in the frequency range below 300 GHz (wave lengths larger than 1 mm). The rapid progress made in recent years in solid state technology now allows the construction of low noise, high resolution millimeter wave receivers and spectrometers which can be used to measure the small radiation - millimeter wave noise - emitted by those resonances. The measurement process of these remotely sensed spectral lines might be briefly described as the extraction of the "coloured noise", originating from the atmosphere from the white noise produced by the receiving equipment. This is a new situation in radio science, since now the normally unwanted noise - with regard to the (deterministic) radio signal - carries the information and is therefore highly wanted. The shapes of the information and is therefore highly wanted. The shapes of the measured spectral lines allow after the application of so called inversion algorithms the calculation of temperature, pressure, and volume mixing ratio profiles of the above mentioned constituents in the atmosphere. This is very important information for recent environmental studies.

NOISE STANDARDS AND CALIBRATION TECHNIQUES IN EUROPE: RECENT DEVELOPMENTS AND FUTURE TRENDS

G. Genevès
Laboratoire Central des Industries Electriques
33, avenue du Général Leclerc
92260 Fontenay-aux-Roses, France

F.-Im. Buchholz
Physikalisch-Technische Bundesanstalt (PTB)
Bundesalle 100, W-3300 Braunschweig
Federal Republic of Germany

M. W. Sinclair
National Physical Laboratory
c/o Royal Signals and Radar Establishment
St. Andrews Road, Malvern, Worcs., WR14 3 PS, UK

During the last few years, needs for noise standards and noise calibration systems have developed for frequencies where no standard was available. In order to satisfy users, different national laboratories developed primary standards and measurement systems either at low frequencies or at millimeter wavelengths.

A review of the recent works of the different European national laboratories will be presented. This includes coaxial noise standards developed with European cooperation, a waveguide standard set up in UK (waveguide R 900), and a waveguide standard developed in Germany and France (waveguide R 100). Improvemented wide band radiometers use an in situ vector network analyzer to determine mismatches.

The needs of industrial users will be discussed. Important demands at millimeter wavelength will set the future trends in noise metrology.

A106.3

NOISE POWER MEASUREMENTS AND MEASUREMENT UNCERTAINTIES

*F.-Im. Buchholz, W. Kessel, and F. Melchert
Physikalisch-Technische Bundesanstalt (PTB)
Bundesallee 100, W-3300 Braunschweig
Federal Republic of Germany

The accuracy of noise power intercomparisons between unknown noise generators and reference noise standards is stipulated by parameters as low signal levels, long detector integration constants, and small numbers of individual measurements. The present paper is concerned with the aspect in RF metrology of evaluating the uncertainties in noise power calibrations.

At present the realization of the unit Watt of noise power in the GHz-frequency range is based on thermal noise generators. In order to guarantee traceability in the distribution from the primary national standards to the noise sources under test many countries have established national calibration services.

There exist different demands for measurement uncertainties on the single levels of the calibration chains. On the one hand lowest values of uncertainties are required on echelon A for calibrations of noise sources against primary standards. Measurements at this level are generally performed at distinct standard calibration frequencies. On the other hand the requirement of a broadband frequency coverage must be satisfied at the echelon levels B and C which are more directly connected to applications. The problem arises how to transform the uncertainties at distinct measurement frequencies to broad frequency intervals.

The main sources and components of uncertainties of RF noise power measurements will be discussed in relation to the recommendation INC-1 (1980) of the Comité International des Poids et Mesures (CIPM) and to the "Guidelines for the Expression of the Uncertainty of Measurement in Calibrations" (Doc. 19-1990 of the Western European Calibration Cooperation (WECC)).

The paper gives specific advice for the treatment of measurement uncertainties of the RF noise power field to make the information more readily applicable. The state of the art in RF noise power metrology is illustrated with examples of the calibration data of noise sources on different levels of the calibration chains.

CORRECTION FACTOR IN BROADBAND HETERODYNE SYSTEMS

Sunchana Perera
Electromagnetic Fields Division
National Institute of Standards and Technology
Boulder, Colorado 80303

Many radiometers are based on the heterodyning principle and utilize both sidebands in order to increase the system sensitivity. The noise power is therefore measured not at the local oscillator (LO) frequency, but within the two symmetrical bandwidths, centered at LO$\pm$IF, where IF stands for the intermediate frequency, typically selected to be in the low - to - middle MHz region.

In order to correctly calculate the incoming signal power, a mismatch factor at the input of the radiometer must be determined. This is done at the LO frequency. However, the derivation of the system equation assumes that the mismatch factor is measured in the plane of the front–end isolator, or negligibly close to it. This is often not quite true, especially if there are lengths of cable, switches or directional couplers positioned between the isolator and the input port. If that distance l is electrically long, the results need to be corrected by a factor which is proportional to a product of $\sinh(\frac{2\pi lB}{c}) \cdot \cos(\frac{4\pi l f_{IF}}{c})$, where B stands for the limiting system bandwidth and c for the speed of light.

In a noise calibration system recently developed at NIST, having a bandwidth of 3 MHz, the IF frequency of 30 MHz, and the electrical line length of 0.35 m, the above product was 0.9, resulting in the second largest error in the noise temperature, of almost 0.5%. However, treated as a correction, with only a small uncertainty in the electrical length determination, the contribution of the error becomes negligible.

A106.5

A "Terminal Invariant" Description of Amplifier Noise

Glenn F. Engen (Ret)* & David F. Wait

National Institute of Standards and Technology

Although the use of scattering parameters in the analysis of microwave circuits is well nigh universal, the treatment of amplifier noise represents an exception. Here the most common practice is to revert to the lower frequency description which is based on voltage, current, etc. Over the years a number of alternative formulations, which are more in keeping with the scattering description, have been proposed by different authors, but these have attracted only a limited amount of interest. Perhaps a major reason for this has been the lack of a well defined statement of the relationships among the parameters upon which the different descriptions are based. This issue has been addressed in a recent paper by the authors, (D. F. Wait & G. F. Engen, "Application of Radiometry to the Accurate Measurement of Amplifier Noise," *IEEE Trans. Instru. & Meas.*, April, 1991) and given the set of problems associated with the MMIC environment, the interest in the scattering formulation is growing.

Among the problems, in the MMIC environment, is that of defining the *characteristic impedance*. For this reason, the potential advantages of the *terminal invariant* formulation (which is *independent* of the characteristic impedance) becomes of increasing practical importance. A review of the prior practice reveals that while these considerations do emerge upon occasion, their potential value has perhaps not yet been fully realized or exploited. The formulation contained in the authors' prior paper, for example, provides a substantial amount of terminal invariance at the amplifier input terminals, (where it is obviously the most useful) but little or none at the output. As a consequence, the measurement techniques, which are based on this description, include implied references to a "matched" termination at the amplifier output.

It is the purpose of this paper to review the potential advantages of the *terminal invariant* description, and present an alternative scattering formulation of amplifier noise which eliminates these implied references, and more fully exploits the concept.

NOISE PARAMETER ACCURACY AND REPEATABILITY CONSIDERATIONS

Vahe' Adamian
ATN Microwave, Inc.

A noise parameter measuring system, suitable for on-wafer or fixtured devices, is presented. The accuracy and repeatability of the four noise parameters in terms of published noise source, noise figure meter, and network analyzer uncertainties along with the quantity and location of the source states is analyzed using the measurement simultation method described by Hewlett Packard (HP AP Note 57-2).

Accurate and repeatable noise parameter measurements are essential not only for the design of low noise microwave circuits and systems but also to speed low noise device development. Previous noise parameter measurement accuracy studies have either dealt with the location of the source reflection coefficient states alone (A.J. McCamant, Microwaves and RF, June 1989), or analyzed theoretical instrument source reflection coefficient states and instrumentation errors independently (A. Davidson, B. Leake, and E. Strid, IEEE MTT-S, June 1989). This work presents the accuracy and repeatability as a function of the number and location of the actual source reflection coefficient states and the published instrumentation uncertainties as they are encountered during actual system calibration and measurement.

The noise parameter system under study is based on the Adamian and Uhlir (IEEE, Instrumentation and Measurement, June 1973) concept which states the knowledge of the total hot output noise power of a standard noise source plus the total output noise power of several passive one port terminations is sufficient for complete noise parameter characterization of a linear receiver. For better understanding of the procedure, one may regard the noisy receiver as having noise emergent from its input port. This noise is reflected by the source reflection coefficient so that it eventually adds in a partially coherent fashion to the noise emerging from the output port by a direct path. From this viewpoint, it is easy to see how useful information on the noise characterization can be obtained by varying the source reflection coefficient without varying the source temperature. Measurement of tuner loss as extensively analyzed by previous work (E. Strid, IEEE MTT, March 1981) is not necessary anymore for noise parameter characterization. This fundamental receiver concept can be extended to characterization of a linear two-port by simply using the correlation matrix to deembed the linear two-port from the overall and receiver noise parameters (H. Hillbrand and Russir P., IEEE CAS, April 1976).

THE USE OF A MISMATCHED ATTENUATOR TO VALIDATE THE PERFORMANCE OF A FOUR PARAMETER AMPLIFIER NOISE TEST SET

David F. Wait
National Institute of Standards and Technology, Boulder, CO 80303

This paper discusses the usefulness of measuring a mismatched attenuator as part of a process to validate whether an amplifier noise parameter test set is working properly. A particularly interesting challenge is the automated measurement system with software that cannot be examined.

The mismatched attenuator presents an unusual challenge to the amplifier measurement system. Obtaining correct results demands careful corrections for the noise originating in the measurement system. If these corrections are done well, then the measurement results can verify, within limits, that the measurement system is functioning properly.

When treated as an amplifier, the amplifier noise parameters are known in terms of the physical temperature of the attenuator, and its scattering coefficients. For example, for a 3 dB attenuator with the physical temperature T_{amb} = 296 K, $S_{12} = S_{21} = 0.7$, $S_{11} = S_{22} = 0.11$, the effective input noise temperature, T_e, with a reflectionless input termination is 301 K. The dependence of T_e versus the reflection coefficient of the source on its input Γ_1 may be written as

$$T_e = \frac{T_a + T_{rev}\,|\Gamma_1' - \beta|^2}{(1 - |\Gamma_1'|^2)} ,$$

where

$$\Gamma_1' = \frac{\Gamma_1 - S_{11}^*}{1 - S_{11}\Gamma_1} ,$$

T_a = 269 K, T_{rev} = 149 K, β = 0.33 + 0 j. In our laboratories, we estimate the accuracy of measuring the parameters should be $T_{e,0} \pm 7\%$, $T_a \pm 7\%$, $T_{rev} \pm 6\%$, $\beta \pm 0.03$. If it differs from the predicted value by a greater amount, something is wrong. If it differs by more than the random errors from previous measurements, something has changed.

There are several potential problems posed by a system using inaccessible software that are easy to detect using a passive device, and difficult without. However, there remain many potential difficulties that passive circuits cannot catch, so there still exists a need for calibrated amplifiers.

AVOIDING ADAPTER MEASUREMENTS

W. C. Daywitt *
National Institute of Standards and Technology
Electromagnetic Fields Division
Department of Commerce, Boulder Laboratories
Boulder, Colorado 80303. U.S.A.

There are numerous examples where adapters must be used to compare devices with dissimilar connectors, usually in a standard-versus-DUT context: a waveguide noise source is calibrated against a coaxial noise standard; a waveguide standard-gain pyramidal horn must be compared to a coaxial cavity-backed spiral antenna to determine the latter's gain; or the efficiencies of two bolometer mounts with different flanges need to be compared. Concomitant with these requirements, it is often convenient or necessary to make the comparisons through a switch or through two extended measurement paths. For example, the gain measurement of a 60' dish antenna using a standard gain horn involves comparing the response of each antenna to a distant radio source through two lengthy and different transmission lines. The technique to be described in the talk solves both these problems, different connectors and distinct paths, is one step by utilizing a vector reflectometer at the input of the system with which the comparison is to be made.

To be specific, suppose a waveguide noise source is to be calibrated with a coaxial noise standard through a switch by attaching each source to one of the input ports of the switch, the output port leading to a coaxial radiometer/reflectometer. A waveguide-to-coax adapter is attached to one of the ports to accomodate the waveguide noise source. The reflectometer can be characterized at each of the source input ports to determine the system constants abc and a'b'c' (G. F. Engen, IEEE/MTT-22, No.12, 1255-1260, 1974). The ratio of the efficiencies from the DUT and standard ports to the radiometer detector can then be expressed in the form

$$\frac{\eta'}{\eta} = \left|\frac{S'_{41}}{S_{41}}\right|^2 \left(\frac{1-|c|^2}{1-|c'|^2}\right) \left|\frac{a'-b'c'}{a-bc}\right|$$

where the constants and the derivation of the equation will be explained in the talk. The S_{41}-ratio is not determined by the reflectometer calibration as are the final two ratios, but it is very close to unity in most applications. Thus, the first ratio can be dropped, leaving an expression for the efficiency ratio that is completely determined from the reflectometer characterization, and allowing the noise calibration to be effected without the need for a separate efficiency measurement of the waveguide-to-coax adapter.

A106.9

W-band Noise Measurement Technique

Trang V. Mai, J.J. O'Neill and J.A. Molnar
Naval Research Laboratory
Code 5524
4555 Overlook Ave.
Washington, DC 20375

The generation of broadband noise power provides an efficient method of evaluating receiver sensitivity. The accuracy of the resulting sensitivity analysis depends upon the stability of the noise source and the precision of noise source calibration. A W-band noise measurement receiver was developed to characterize a solid state noise source in this frequency band. The noise measurement receiver was characterized with a gas discharge tube that provided a stable noise output throughout the band. The gas discharge tube was calibrated at 93 GHz and provided an output ENR of 14.2 dB ± 0.5 dB. To ensure the accuracy of the receiver characterization the results were correlated with the results of noise temperature measurements obtained from loads maintained at liquid nitrogen and elevated temperatures. A frequency stabilized local oscillator was used in both sets of measurements to ensure the accuracy with respect to frequency. The background principles of noise measurement and the methods and limitations of each measurement technique are discussed. Results of the measurement system receiver characterization are described. The results of the receiver characterization are applied to the evaluation of the solid state noise source.

While the techniques used to characterize the receiver are acceptable for laboratory conditions, they lack the simplicity required for evaluating receiver systems in operational environments. The solid state noise source provides the necessary simplicity and possesses additional advantages of low drive voltage and abrupt transitions from on to off state. Both of these features have made the solid state noise source desirable for automated field tests of receiver systems. For a field measurement system both the noise source and measurement receiver must be characterized to provide accurate measures of system performance. This results in the requirement for calibration and transfer standards.

Two W-band noise sources were developed on separate Naval Research Laboratory (NRL) contracts. The contractors were Marconi and NoiseCom. These noise sources were evaluated with the noise measurement system characterized at NRL. The specified performance for the devices were an ENR of 15 dB ±1dB and full waveguide coverage, 75-110 GHz. The actual performance results presented indicate that ENR values in excess of 15 dB are available, but the device lacked a flat output over the band.

The results of this study are discussed in the context of providing an automated procedure for W-band receiver measurements. The central feature is the assessment of the accuracy and stability of the respective W-band solid state noise sources.

A NEW FORMULA FOR CALCULATING HIGH VOLTAGE STANDING WAVE RATIO FROM SLOTTED LINE MEASUREMENTS

Daiyuan Zhang* and Hanbao Jiang
Department of Radio–Electronics
Sichuan University, Chengdu, Sichuan, P. R. of China

The slotted line is still widely used in China. With high voltage standing wave ratio (VSWR), it is a customary to employ equal–levels (usually twice–minimum levels) method to caculate the VSWR as following,

$$S=\left[\left(R/R_{min}\right)^{2/n}-\cos^2\left(\frac{\pi W}{\lambda g}\right)\right]^{1/2}/\sin\left(\frac{\pi W}{\lambda g}\right)$$

where R_{min} is the minimum level reading and R is the reading corresponding to the level selected in measuring the node width W, n is the detector law.

It is well known that the minimum level is difficult to measure accurately when VSWR is very high. A new formula has been derived in which two levels instead of the minimum level are employed to calculate high VSWR as following.

$$S=\left[\frac{\left(R_1/R_2\right)^{2/n}\cos^2(\pi W_2/\lambda g)-\cos^2(\pi W_1/\lambda g)}{1-\left(R_1/R_2\right)^{2/n}+\left(R_1/R_2\right)^{2/n}\cos^2(\pi W_2/\lambda g)-\cos^2(\pi W_1/\lambda g)}\right]^{1/2}$$

where R_1, R_2, W_1 and W_2 are the selected level readings and the corresponding node widthes respectively.

Since R_1, R_2, W_1 and W_2 can be measured as accurately as possible, the new formula for calculating high VSWR is more accurate than the former. The errors caused by the node width measurements are as following

$$\frac{|\Delta S|}{S}=\left|\frac{1-\left(R_1/R_2\right)^{2/n}}{2F\left[1-\left(R_1/R_2\right)^{2/n}+F\right]}\left(\frac{\pi W_1}{\lambda g}\right)\sin\left(\frac{2\pi W_1}{\lambda g}\right)\right|\cdot\left|\frac{\Delta W_1}{W_1}\right|$$

$$+\left|\frac{1-\left(R_1/R_2\right)^{2/n}}{2F\left[1-\left(R_1/R_2\right)^{2/n}+F\right]}\left(\frac{R_1}{R_2}\right)^{2/n}\left(\frac{\pi W_2}{\lambda g}\right)\sin\left(\frac{2\pi W_2}{\lambda g}\right)\right|\cdot\left|\frac{\Delta W_2}{W_2}\right|$$

where

$$F=\left(R_1/R_2\right)^{2/n}\cos^2(\pi W_2/\lambda g\ )-\cos^2(\pi W_1/\lambda g\ )$$

Transients I **Room 2110 Salle** **Transitoires I**
URSI B Session 7A

Chairs/présidents: S.M. RAO, USA; A.S. PODGORSKI, Canada

08:30 (7.1) Development of a Frequency-Dependent TLM, **F.H. BELLAMINE**, E.F. KUESTER, *University of Colorado, Boulder, CO, USA*

08:50 (7.2) Time Dependent Surface Fields, **R.K. RITT**, *Illinois State University, Normal, IL, USA*

09:10 (7.3) Periodic Signal Electromagnetic Missiles, **C. WAN**, C. RUAN, *University of Electronic Science and Technology of China, Chengdu, China*

09:30 (7.4) Time-Domain Edge-Element Method and Its Application for Electromagnetic Problems with Non-Rectangular Geometry, D.C. CHANG, **R.C. BOOTON JR.**, *University of Colorado, Boulder, CO, USA*

09:50 (7.5) Studies of Lightning Radiated-Field Propagation Over Lossy Ground, **W.A. CHISHOLM**[1], N. HERODOTOU[2], W. JANISCHEWSKYJ[2], [1] *Ontario Hydro, Toronto, ON, and* [2] *University of Toronto, ON, Canada*

10:10 **COFFEE/CAFÉ**

B7.1

DEVELOPMENT OF A FREQUENCY-DEPENDENT TLM

Fethi H. Bellamine* and Edward F. Kuester
Department of Electrical and Computer Engineering
Electromagnetics Laboratory: Campus Box 425
University of Colorado, Boulder 80309

The transmission line matrix (TLM) method is an iterative numerical technique of simulating transient electromagnetic propagation phenomena. In most previous work, the frequency dependence of the constitutive parameters has only been accounted for indirectly in the TLM method; that is, the TLM program should be executed repeatedly using frequency-independent ϵ and σ, one frequency at a time until the band of interest is covered. This repetitive procedure causes a serious limitation to the efficient use of TLM compared to frequency domain methods. This paper presents a TLM formulation which is capable of efficient treatment of a wide variety of dispersive media for a wide range of frequencies with a single computer run.

The basic idea is to load conductance-capacitance blocks at the elementary nodes. Similar models have been used in power systems when approximating the transmission line frequency-dependent characteristic impedance by resistance-capacitance combinations (J. Marti, *IEEE Trans. Power Apparatus and systems*, **101**, 147-157, 1982), and in the semiconductor area when representing an n-layer dielectric by a cascade of n-parallel resistance-capacitance circuits (J. Volger, *Prog. Semicond.*, 4, 209, 1960). A direct comparison between Maxwell's and transmission line equations yields expressions for the frequency-dependent constitutive parameters of the dispersive media. In the case of measured frequency dependences of permittivity and conductivity, selection of the conductance and capacitance parameters is done through optimisation. The newly developed frequency-dependent node can be employed in two or three dimensional problems. Typical numerical results to demonstrate the validity and accuracy of the formulation will be presented, including the cutoff frequency of a homogeneous rectangular waveguide loaded with a dispersive medium.

TIME DEPENDENT SURFACE FIELDS

R.K.Ritt
Department of Mathematics
Illinois State University

The time dependent electromagnetic field $\begin{bmatrix} \mathbf{E}(x,t) \\ \mathbf{H}(x,t) \end{bmatrix}$, exterior to a perfectly conducting scatterer, caused by a current, $\mathbf{J}(\mathbf{x})\,\delta(t)$, has the formal representation $\exp(At)\begin{bmatrix} -\mathbf{J} \\ 0 \end{bmatrix}$, in which A is the differential operator $\begin{pmatrix} 0 & \nabla\times \\ -\nabla\times & 0 \end{pmatrix}$, subject, of course, to appropriate boundary conditions on the surface of the scatterer and at infinity. As we have previously observed (NRS Meeting, Boulder, Jan.,1990), this formal representation can be expressed, rigorously, as a spectral integral $\int_{-\infty}^{\infty} \exp(i\omega t)\, dP(\omega)$, corresponding to the self-adjoint -iA.

In the present paper, we find an approximate solution for the surface field $\mathbf{n} \times \mathbf{H}$, in the time interval which starts at t_0, when the free-space wave generated by $\mathbf{J}$ reaches the scatterer, and which ends some time before the diffraction effects give rise to damped oscillations.

The approximation is based upon both using a finite part of the formal expansion of the differential operator $\exp(A(t-t_0))$, and using the spectral integral to obtain error estimates. Even if the source $\mathbf{J}$ is not differentiable, the formally derived representation for $\mathbf{n} \times \mathbf{H}$ can be applied, as a distribution, to calculate the scattered field..

Periodic Signal Electromagnetic Missiles

Changhua Wan and Chengli Ruan
Institute of Applied Physics
University of Electronic Science and Technology of China
Chengdu, Sichuan 610054, P. R. China

Rencently, the study of electromagnetic (EM) missiles has been very active because the energy transfer by an EM missile in a certain direction involves a low loss in free space. Such a property is of great benefit to many applications, such as Radar and communications. But so far, various EM missiles can be generated only by transient signals. The possible applications of EM missiles are hindered by a series of difficulties of transmitting and receving them. Can a periodic signal also yield an EM missile? If possible, periodic signal EM missiles will find a wide use in the above mentioned area without additional difficulties. This paper gives a definite answer to the question which is of practical interest.

Consider a circular disk of radius a with uniform periodic current excitation.

$$J(r,t)\begin{cases} xf(t)\delta(z); & \text{for } \rho \leqslant a \\ 0; & \text{for } \rho > a \end{cases}$$

where f(t) is a periodic rectangular signal. According to Fourier's expansion theorem, f(t) is written as follows

$$f(t)=\tau/T+\sum_{n=-\infty(n\neq 0)}^{\infty} \sin(n\pi\,\tau/T)\exp(-jn\omega t)/n\pi;\ \omega=2\pi/T$$

Following Wu's way similarly (T. T. Wu, J. Appl. Phys. 7, 2370—2373, 1985), one can obtain the radiated electric field at large distances z for frequency nω

$$E(z,\ n\omega t)=A_n\exp[jn(kz-\omega t)]\{\exp[jnk(R-z)]-1\}$$

where $R=\sqrt{z^2+a^2}$; $A_0=\tau/T$; $A_n=\sin(n\pi\tau/T)/n\pi$; $k=\omega/c$

and c is the velocity of light in free space.

The associated time average energy flux is

$$G(z,\ n\omega)=|E|^2/2=|A_n|^2\{1-\cos[nk(R-z)]\}$$

The total average energy flux is then

$$G(z)=\sum_{n=-\infty}^{\infty}G(z,n\omega)=2\sum_{n=1}^{\infty}G(z,n\omega)=(R-z)/T\approx a^2/2cTz$$

for $z\geqslant[a^2-(\tau c)^2]/2c\tau$; $T\geqslant 2\tau$ or $z\geqslant\{a^2-[(T-\tau)c]^2\}/2c(T-\tau)$; $T<2\tau$

This is an EM missile with energy decay as 1/z.

TIME-DOMAIN EDGE-ELEMENT METHOD AND ITS APPLICATION FOR ELECTROMAGNETIC PROBLEMS WITH NON-RECTANGULAR GEOMETRY

David C. Chang and Richard C. Booton, Jr.*
Center for Microwave and Millimeter-Wave
Computer-Aided Design (MIMICAD)
University of Colorado, Boulder, Colorado 80309-0425

The time-domain, finite difference (TDFD) method and other related methods such as the transmission-line matrix (TLM) method, have been actively investigated in recent years. Ease in implementing the algorithm as well as elimination of the need to invert large matrices make them particularly attractive as general solvers for structures with complex geometries. However, because they are based upon converting differential equations to finite-difference equations in rectangular coordinate, only element cells of rectangular or cubic shape can naturally fit into the prescribed computational scheme; as a result, accuracy of this method often depends upon how well the actual geometry of a physical problem can be approximated.

In this paper, we shall first describe how one can devise an edge-element expansion in which the electric or magnetic field components in a tetrahedral cell are expressed by a linear combination of *constant tangential field components* along its six edges, and vary linearly inside the cell. Use of the Maxwell curl equations relates the time derivative of the edge element for the electric field at one edge to the edge elements for the magnetic field in those cells sharing the same edge, and vice versa. A central difference approximation then allows us to proceed in half time steps to alternately solve for the electric and magnetic fields without requiring a matrix inversion for each time step. Because the edge elements are tangential to its cell face, boundary conditions for both the tangential electric and magnetic fields are satisfied automatically. Thus, the method not only allow us to fit tetrahedral cells of varying sizes and shapes onto a physical boundary, it also eliminate the cause for spurious modes encountered in a finite-element method where the field components are expressed in term of its nodal fields.

Numerical examples using this method and comparison with other more established ones will be presented.

B7.5

STUDIES OF LIGHTNING RADIATED-FIELD PROPAGATION OVER LOSSY GROUND

William A. Chisholm *
Ontario Hydro
Research Division
(416)231-4111

Nicos Herodotou and Wasyl Janischewskyj
University of Toronto
Dept. of Electrical Engineering
(416)978-3116

Measurements of radiated magnetic fields from lightning at known locations can be used to infer source currents. Theoretical calculations for propagation over lossy ground show attenuation rates and waveshape changes for the distance range 50-500 km. An experimental investigation using synchronized multiple-source measurements of gated wideband receivers verifies the theoretical attenuation rate in this distance range. The use of an attenuation model has a significant effect on the stroke current distribution inferred from the remote measurements.

Automatic lightning location equipment using magnetic-field sferics from return strokes has been installed in many areas of North America. Triangulation of sine and cosine signal components provides estimates of source location. Sixteen specialized receivers form a network within the province of Ontario. Peak radiated fields also measured by the Ontario system provide a data base of over 10^6 flashes per year for estimating peak stroke current distributions via field-source inversion.

Several factors influence the signals from lightning return strokes. Close to the flash, the induction field contributes to the total magnetic field. However, the radiated component dominates at distances as close as 10 km. Reflections from the ionosphere are unimportant since the automatic peak-detection reports only the magnitude of the first peak, thereby discriminating against all subsequent peaks. The lightning channel is tortuous, but measurements based on the peak field use information only from the bottom 100-500 m of the stroke channel. The peak of a lightning current can be represented by sine-wave frequencies in the range of 80-120 kHz. For these frequencies, the Sommerfeld-Norton ground wave attenuation model predicts significant decay of lightning signals as a function of distance, ground conductivity and permittivity.

Observations from Ontario were used to compute lightning locations and to provide multi-source amplitude measurements of the same lightning flash. Distance normalization established experimental decay rates of 1.1 to 1.5 dB per 100 km. These agree with attenuation rates from the Sommerfeld-Norton ground-wave attenuation model, using median soil and water characteristics in Ontario.

The fixed attenuation rate of 1.5 dB/100 km will bias the current distribution inferred from readings that do not correct for the attenuation. A lower number of large-current flashes would be found if no attenuation model was used. Using a uniform inverse-distance model [Uman 1975], the median current for the observation period is found to be 30 kA. When the exponential attenuation model corrects the readings, the median shifts upward to 44 kA. More significant changes are found at the high-current end of the distribution.

Studies of attenuation in the Ontario lightning detection network have pointed that signal attenuation leads to significant changes in the radiated fields before they are received. Both theoretical and experimental investigations confirm the effects of attenuation over lossy ground. Any inference of peak stroke current from remote measurements should take these factors into account, either through selection of data in limited distance ranges or by use of a suitable correction.

Electromagnetic Theory I | **Room 3018 Salle URSI B Session 11** | **Théorie électromagnétique I**

Chairs/présidents: D.R. WILTON, USA; J.R. WAIT, USA

08:30 (11.1) Coupling to a Discrete Body of Revolution, **R.M. SHARPE**, D.R. WILTON, *University of Houston, TX, USA*

08:50 (11.2) Scattering by Large, Coated Bodies of Revolution, P. BONNEMASON, **R. LE MARTRET**, B. SCHEURER, B. STUPFEL, *C.E.A., Villeneuve St. Georges, France*

09:10 (11.3) On the Equivalence of the Lorentz and Coulomb Gauge Green's Functions, **R.D. NEVELS**, Z. WU, C. HUANG, *Texas A&M University, College Station, TX, USA*

09:30 (11.4) Treatment of Scalar Potential Field with Lorentz Gauge Condition in Time Domain, **N. YOSHIDA**, *Hokkaido University, Sapporo, Japan*

09:50 (11.5) Numerical Computation of Hertz Potentials for Helical Structures, **R.J. POGORZELSKI**, *General Research Corporation, Santa Barbara, CA, USA*

10:10 **COFFEE/CAFÉ**

10:30 (11.6) Single Series of the Green's Function for the Elliptic Patch, **F.A. ALHARGAN**, S.R. JUDAH, *University of Hull, UK*

10:50 (11.7) Direct Integration of the Maxwell Equations, **R. DONNELLY**, J. WALSH, *Memorial University of Newfoundland, St. John's, NF, Canada*

11:10 (11.8) Image Principle for the Electrostatic Problem Involving a Dielectric Sphere, **I.V. LINDELL**, *Helsinki University of Technology, Espoo, Finland*

11:30 (11.9) Advantages and Limitations of the Path Integral Method in Electromagnetic Scattering, **R.D. NEVELS**, C. HUANG, Z. WU, *Texas A&M University, College Station, TX, USA*

11:50 (11.10) To the Problem on Simulation of the Electromagnetic Fields Arising in the Cavity of Conducting Envelope Under the Influence of Penetrating Radiation Flow, **A.E. VYVOLOKIN**, *Ukrainian Academy of Sciences, Kharkov, USSR*

COUPLING TO A DISCRETE BODY OF REVOLUTION

Robert M. Sharpe*
and
Donald R. Wilton

Department of Electrical Engineering
University of Houston, Houston, TX 77204-4793

Previously, theoretical and numerical results were presented which take advantage of a common type of rotational symmetry in which the geometrical surface of a scatterer or radiator may be rotated about an axis through an angle of $2\pi/K$ into coincidence with itself. We used the term *discrete body of revolution* (DBOR) to describe such a surface. As K becomes large the body approaches a continuous BOR; however, there are objects such as spiral antennas, which exhibit rotational symmetry that is inherently discrete in nature. In order to exploit the symmetry in a moment method solution, both the current and the excitation are expanded in symmetrical components, which reduces the moment matrix to a block-diagonal form due to the orthogonality between the components. Solution of the linear system can be computed on a block at a time basis to obtain the individual modal responses, though the desired excitation occasionally happens to be one of the symmetrical components, in which case only a single mode needs to be calculated. Transformation from the original moment matrix to the reduced block-diagonal form can be efficiently performed via the DFT, and similarly recombining the modal responses back to find the actual currents can be performed via an inverse DFT.

In this work we review the theory and present numerical results for efficiently treating a problem involving a DBOR which is coupled to an object without any symmetry. The procedure is general so that the asymetrical object can either be disjoint from or attached to the DBOR. The approach retains the advantages of subsectional modeling and does not require any special basis function to be developed if the asymetrical object is attached to the DBOR. This appears to be an improvement over coupling an object to a continuous BOR where extensive work is required to treat the attachment point. An algorithm is presented which takes advantage of the block diagonal nature of the DBOR moment matrix and efficiently solves the coupled system of equations by substituting the solution of linear systems for matrix inversion. Numerical results will be presented for several canonical objects, as well as for more practical geometries.

SCATTERING BY LARGE, COATED BODIES OF REVOLUTION

P. BONNEMASON, R. LE MARTRET*
B. SCHEURER, B. STUPFEL
CEA - Centre de Limeil Valenton - 94195 VILLENEUVE St GEORGES
Cedex, FRANCE

In this paper, we consider the problem of computing the surface currents and the Radar Cross Section (RCS) of bodies of revolution (BOR) that may be imperfectly conducting and of general shape. For instance, the bodies under consideration may be open or closed surfaces and, furthermore, they may be connected or disjointed. Our emphasis in this paper is to consider bodies that are large compared to the wavelength and to investigate the reliability of the Leontovich boundary condition for modeling imperfect conductors. In addition, our objective in this work is to achieve a high degree of numerical accuracy even in the angular range where the RCS is low. This is an important issue in the design of low observable targets.

Our approach to solving the RCS problem is to combine the finite element method with the integral equation formulation. The finite element formulation is used to solve Maxwell's equations within the axisymmetrical inhomogeneous domain defined by the imperfectly conducting body. The integral equation formulation, applied to the outer boundary of the body, ensures that the Sommerfeld's radiation condition is fulfilled, once the appropriate Green's function is employed for the external region. An important problem that must be successfully resolved in the process of deriving the high frequency solution of the scattering problem is the suppression of the spurious internal resonances. An approach to circumventing this problem is described in the paper.

A fully-vectorized computer program has been developed for the CRAY YMP 8128 using the formulation described above. This paper presents typical numerical results for a variety of large BOR geometries including two coated spheres, a torus and a hollow cone coated with low and high index materials. These results are then interpreted in terms of edge and creeping wave contributions. We also compare the above results with those obtained with an integral equation program using the Leontovich boundary condition and demonstrate, when the later is legitimate, the excellent agreement between the two. On the other hand, we exemplify cases where the Leontovich boundary condition is inappropriate.

ON THE EQUIVALENCE OF THE LORENTZ AND COULOMB GAUGE GREEN'S FUNCTIONS

R.D. Nevels,* Z. Wu, and C. Huang
Department of Electrical Engineering
Texas A&M University
College Station, Texas 77843

Often Maxwell's equations are solved by expressing the electric and magnetic fields in terms of a set of potentials. Although the fields are unique it is well known that the potentials, both vector and scalar, depend upon the choice of gauge, of which the Lorentz and Coulomb are the most common. Complete expressions for the free space Coulomb gauge frequency domain vector and scalar potential Green's functions have only recently been derived (R.D. Nevels & K. Crowell, IEE Trans. ~ H, Dec., 1990).

In this paper we show how the frequency domain Green's functions can be transformed into proper and complete time domain forms by a method which avoids the pitfalls encountered by some previous researchers. It has often been observed that the time domain Coulomb gauge scalar potential is non-causal. Here it is shown that the Coulomb gauge vector potential also contains non-causal terms which have the effect of canceling those of the scalar potential.

Finally, we demonstrate that the Lorentz and Coulomb gauge potentials are mathematically equivalent. Our proof is different from that in a commonly referenced paper (O.L. Brill & B. Goodman, Am. J. Phys. 35, 832-837, 1967), in that our Green's function expressions are complete and therefore no reliance on the solenoidal or lamellar properties of the associated current is required.

TREATMENT OF SCALAR POTENTIAL FIELD WITH LORENTZ GAUGE CONDITION IN TIME DOMAIN

Norinobu Yoshida
Department of Electrical Engineering
Hokkaido University, Sapporo 060 Japan

In the analysis of electromagnetic fields, the vector potential has important roles especially when sources exist. But the formulation by the vector potential brings about the problems of selecting the gauge conditions, that is, the Coulomb's gauge condition and the Lorentz gauge condition. For the Coulomb's gauge condition, since the relation between the scalar and vector potentials does not exist, both potentials can be calculated independently. On the other hand, for the Lorentz gauge condition, the scalar and the vector potentials have effects on each other. Therefore, the formulation including the gauge condition is necessary.

I have already proposed the treatment of the vector potential in the three-dimensional space and time domain (N. Yoshida, Radio Sci. 1 1991; to be published). In the treatment, both the magnetic vector potential and the electric vector potential are used, and each component of the vector potential variables is arranged at each lattice point in the three-dimensional lattice network. The time-dependent analysis of electromagnetic fields has shown its utility not only in clarifying the variation of the fields in time but also in gaining information on mechanisms by which the distribution of an electromagnetic field at the stationary state are brought about.

In this paper, I proposed the time-dependent formulation of the scalar potential with the Lorentz gauge condition. The Lorentz gauge condition is given as follows.

$$\mathrm{div}\ \mathbf{A} = -\varepsilon_0\mu_0\frac{\partial \phi}{\partial t} - \mu_0\sigma\phi \qquad (1)$$

The new variable "F" and the electric field "E" are defined as follows by using the analogy to the relation among the velocity potential and the pressure and the particle velocity in the sound field.

$$\mathbf{F} = \mu_0\frac{\partial \phi}{\partial t} + \frac{\mu_0\sigma}{\varepsilon_0}\phi \qquad (2a)$$

$$\mathbf{E} = -\frac{\partial \phi}{\partial \xi} \qquad (2b)$$

where ξ ia an arbitrary spatial coordinate and

$$\mathrm{div}\ \mathbf{A} = -\varepsilon_0\mathbf{F} \qquad (3)$$

By these definitions, next wave equation for the scalar field variables is given.

$$\frac{\partial^2}{\partial \xi^2}\begin{bmatrix}\phi\\ \mathbf{F}\\ \mathbf{E}\end{bmatrix} + \varepsilon_0\mu_0\frac{\partial^2}{\partial t^2}\begin{bmatrix}\phi\\ \mathbf{F}\\ \mathbf{E}\end{bmatrix} + \mu_0\sigma\frac{\partial}{\partial t}\begin{bmatrix}\phi\\ \mathbf{F}\\ \mathbf{E}\end{bmatrix} = 0 \qquad (4)$$

NUMERICAL COMPUTATION OF HERTZ POTENTIALS FOR HELICAL STRUCTURES

R. J. Pogorzelski
General Research Corporation
5383 Hollister Avenue
Santa Barbara, CA. 93111

Recently some work was reported concerning the computation of the electric and magnetic fields of helically disposed filamentary distributions of current [R. J. Pogorzelski, National Radio Science Meeting Digest, May 1989, p. 78]. These fields constitute a dyadic Green's function which may be used to formulate integral equations for arbitrary helical structures. These Green's functions are, as may be expected, highly singular and require that, in the solution of the resulting integral equations by the method of moments, one use basis functions possessing a high degree of smoothness. The less singular alternative of formulation in terms of potentials was rejected because the series acceleration technique used did not readily generalize to the potential expressions. The present work employs a new acceleration approach which is applicable to the potential series and thus forms the basis of a moment method formulation involving at most logarithmically singular integrands. It is the purpose of this paper to present the details of the acceleration method and to thereby illustrate the utility of symbolic manipulation software in an electromagnetics context.

The acceleration is accomplished by the well known Kummer method wherein one subtracts a series of analytically known sum from the given sum term by term and then adds to the result the analytical sum. One selects the series of known sum so as to maximize the convergence rate of the difference series. In the present case, the subtracted series is of the form,

$$\sum_{n=1}^{\infty} \sum_{m=0}^{M} A_{mn} \frac{e^{-n\alpha}}{n+m}$$

wherein the n series for each fixed m can be summed in closed form. The coefficients of the series are obtained in terms of the geometrical parameters of the helix by means of symbolic manipulation software which directly provides the results in FORTRAN form. As a result, the expansion can easily be carried out to many more terms than would be practical by hand. Armed with the required potentials, one may formulate moment method solutions for the behavior of helical structures encountering only integrable singularities.

Single Series of the Green's function for the Elliptic Patch

Fayez A. Alhargan and Sunil R. Judah
Department of Electronics Engineering University of Hull

The Green's function for the elliptic microstrip patch is obtained in two different forms, double series form and single series form. The single series form is much simpler to compute and is independent of parameter changes. A new method of calculating the eigenvalues, hence the resonant frequencies is developed.
The elliptic microstrip antenna presents high design flexibility over other shapes such as the circular disk. However this flexibility is coupled with numerical difficulties of determining the dimensions, for the desired response. This is mainly due to Mathieu function calculations. For the present, the Green's function will be simplified to a single series summation, which eliminates the need for the eigenvalues [3]. Which makes the design process far easier since the eigenvalues are very difficult to calculate, varying with eccentricity and boundary condition in a nonlinear fashion. The eigenvalues for the Mathieu functions involve simultaneous equations in Mathieu functions. This has lead to erroneous results for which only recently has there been any corrections, where numerical integration was used to evaluate the eigenvalues. In this paper an algorithm is presented, for evaluating the eigenvalues, which does not involve numerical integration.
The double series even Green's function is given by

$$G^e(u,v\,|\,u_0,v_0)=\sum_{n=0}^{\infty}\sum_{m=1}^{\infty}\frac{Je_n(he_{nm},\cosh u)Se_n(he_{nm},\cos v)Je_n(he_{nm},\cosh u_0)Se_n(he_{nm},\cos v_0)}{(he_{nm}^2-h^2)T_{nm}^e} \qquad 1$$

Which can be simplified to

$$G^e(u,v\,|\,u_0,v_0)=\sum_{n=0}^{\infty}\frac{Je_n(h,\cosh u)fe_n(h,\cosh u_0,\cosh u_1)Se_n(h,\cos v)Se_n(h,\cos v_0)}{Je_n'(h,\cosh u_1)} \qquad 2$$

Where Je_n, Jo_n, Se_n and So_n are Mathieu functions and he_{nm} are the eigenvalues

References

[1] T.M. Habashy, J. A. Kong and W.C. Chew, "Resonance and Radiation of the Elliptic Disk Microstrip Structure, Part I: Forumlation," IEEE Trans. Antennas Propagation, vol AP-35, August 1987.
[2] P.M. Morse and H. Feshback, Methods of Theortical Physics, McGraw-Hill, 1953.
[3] F.A. Alhargan and S.R. Judah, "Reduced Form of the Green's Functions for Disk and Annular Rings," To be published in IEEE Trans. Microwave Theory Tech., March 1991.

B11.7

DIRECT INTEGRATION OF THE MAXWELL EQUATIONS

Rod Donnelly* & John Walsh
Faculty of Engineering & Applied Science
Memorial University of Newfoundland
St. John's, Newfoundland, CANADA, A1B 3X5

In order to solve electromagnetic boundary value problems (BVPs) it is not necessary to use intermediate potentials. Rather, the Maxwell equations can be directly integrated to give the electric and magnetic field vectors, E&H, in terms of sources and the limiting values of the fields and their normal derivatives on any surfaces present. This approach is recognized, for example, in the well known methods of Stratton & Chu, and Huygen's principle for electromagnetic waves. However, these classical approaches have not been as widely used, to solve specific BVPs, as has the method of potentials.

The authors have, for some years, been solving electromagnetic BVPs by an alternate approach, one that expresses the fields directly, without the use of potentails, but that is different from the existing direct integration methods mentioned above. Our method, which has been detailed elsewhere in the open literature, involves decomposing all quantities in terms of sums of their [possibly discontinuous] regional values, and then applying the Maxwell equation operators, in the sense of generalized functions, to these quantities. The boundary conditions follow automatically from this approach. Moreover, we cannot directly model fictitious "idealized" scattering problems involving infinitesimally thin surfaces; rather, we must consider physically realizable situations in the limit.

In this paper we shall compare out method, for directly integrating the Maxwell equations, with the classical approaches mentioned above. We shall demonstrate how the important aspects of the classical approaches are actually contained in our method, and then explain its advantages.

IMAGE PRINCIPLE FOR THE ELECTROSTATIC PROBLEM INVOLVING A DIELECTRIC SPHERE

I.V. Lindell
Electromagnetics Laboratory
Helsinki University of Technology
Otakaari 5A, Espoo SF-02150 FINLAND

It is well documented in almost all elementary textbooks on electromagnetics that the problem of a conducting sphere in front of a static point charge Q can be solved for the potential outside the sphere by replacing the sphere by two image point charges. One of them is located at the Kelvin image point $d_K = a^2/d$, if a is the radius of the sphere and d the distance of the charge from the center of the sphere and it has the charge $Q_K = -aQ/d$. At the center of the sphere there is another point charge which is determined by the total charge or the potential of the sphere. If the potential of the sphere is null, the centered charge is also null. If the total charge of the sphere is null, the centered charge must equal $-Q_K$. This solution was probably first found by Sir William Thomson, later Lord Kelvin, in 1848.

No obvious generalization to Kelvin's theory for dielectric spheres seems to have been published, even if occasional attempts have been made. Expressions for the potential both inside and outside the dielectric sphere are well known, so the question remains how to present them as arising from a simple source. Since the solutions are in terms of spherical harmonics whose sources are multipoles of different order, it is not difficult to form the image corresponding to the reflection field outside the sphere as an infinite set of multipoles residing at the center of the dielectric sphere. However, such an image is not very convenient since it converges slowly in many cases. Also, it is not very obvious to see the limit case of the conducting sphere when $\epsilon_r \to \infty$.

In the present paper, solutions for the outside and inside potential problems with the original point source residing outside of the sphere, in terms of simple image charges, are given for the dielectric sphere. The images consist of a point source and a line source extending from the Kelvin point to the center of the sphere (the exterior problem) or from the original source point to infinity (the interior problem), with surprisingly simple analytic expressions. The image functions are seen to satisfy all the asymptotic tests with known results ($\epsilon \to 0$, $\epsilon \to \epsilon_o$, $\epsilon \to \infty$, $d \to \infty$, $a \to \infty$) in a very natural manner. Extensions and applications of the theory are finally discussed in the paper.

ADVANTAGES AND LIMITATIONS OF THE PATH INTEGRAL METHOD IN ELECTROMAGNETIC SCATTERING

R.D. Nevels,* C. Huang and Z. Wu
Department of Electrical Engineering
Texas A&M University
College Station, Texas 77843

Electromagnetics and quantum mechanics both describe the wave nature of the physical world. From a mathematical point of view, the Helmholtz equation for the electromagnetic field and the stationary Schrödinger equation for a quantum mechanical system can both be classified as elliptical equations. In this paper we exploit this similarity in order to demonstrate that electromagnetic scattering analysis can be formulated by adopting and extending the path integral method which originated in quantum mechanics.

A mathematical representation for a quantum mechanical system is most often obtained by an eigenfunction expansion solution to Schrödiger's equation. In those cases where the geometry is such that Schrödinger's equation is not separable, the task of finding the system wave function can be alternatively fulfulled by the technique of path integration, which was developed by Feynman. There have only been few attempts to apply the path integral method to solve electromagnetic scattering problems. Our general impression of this previous work is that, although the classical result can be recovered in some cases, the analytical details are often not mathematically rigorous in the sense that the result has not been derived purely by evaluating the path integral expression.

A formulation which leads to the path integral Green's function that satisfies the scalar Helmholtz equation for the electromagnetic field in an inhomogeneous region is summarized and completed. The scalar Helmholtz equation is first transformed into its equivalent 'time'-domain Schrödinger equation. The solution to the latter is given in terms of Feynman's path integral expression and then transformed back to the frequency domain. An explicit Green's function, including the constants of proportionally, is found through this set of transformations.

We demonstrate the utility of the path integral method for boundary value problems by deriving the Green's function for a source in the presence of a perfectly conducting half-space. The method presented here is different from the solution to the quantum mechanical analogue described elsewhere because here the boundary condition is incorporated in the initial unevaluated path integral expression.

In conclusion we describe a stationary phase Monte-Carlo numerical technique for evaluating the path integral. Limitations of the numerical method are presented along with our attempts to circumvent the numerical difficulties.

TO THE PROBLEM ON SIMULATION OF THE ELECTROMAGNETIC FIELDS ARISING IN THE CAVITY OF CONDUCTING ENVELOPE UNDER THE INFLUENCE OF PENETRATING RADIATION FLOW.

A.E.VYVOLOKIN
Research and project-design institute "MOLNIYA" under Kharkov Politechnical Institute,47,Shevchenko St.,310013 Kharkov,The Ukrain,USSR.

In paper [1] the problem of excitation of non-stationary electromagnetic fields in the cavity of conducting cylindric envelope filled with air by the flow of penetrating radiation varying in time has been considered.The resulting solutions of electrodynamic equations,wich establish the relationship between the intrinsic currents induced by the radiation flow in the envelope cavity,non-stationary conductivity of medium filling the envelope and other parameters of this medium with the values of fields arising in the cavity were compared to the solutions of electrodynamic equations for the coaxial cylinder,excited by the current carrying thread.The general view of the solutions is concretized for case of longitudinal radiation of the cylindric envelope.

The results of the comparable analysis of the mathematical models show,that for the most adequate process simulation the observance of several conditions imposed on the exciting pulse parameters, longitudinal and transversal dimension ratio of cylinder as well as on the areas of the objects locations is required.

The experimental results confirming the main aspects of the developed theory have been obtained.

LITERATURE

1.Mangan D.L.,Scrivner G.J.,EMP Response of a Cavity:Field Generation Within a Lossy Dielectric Pulse. IEEE Transactions on Nuclear Science Dec.,1972., vol. NS-19,Number 6.

Numerical Methods – Computational Efficiency | **Room 2110 Salle URSI B Session 22** | **Méthodes numériques – éfficacité des calculs**

Chairs/présidents: Y.L. CHOW, Canada; A.W. GLISSON, USA

13:30 (22.1) The Solution and Numerical Accuracy of Large MoM Problems, **T. CWIK**, J. PATTERSON, *California Institute of Technology, Pasadena, CA, USA*

13:50 (22.2) A Multilevel Moment Method Technique for Large Scatterers, K. KALBASI, **K.R. DEMAREST**, *University of Kansas, Lawrence, KS, USA*

14:10 (22.3) Reduced Source Distributions for Calculating the Mutual Impedances of Complex Structures, **G.E. HOWARD**, Y.L. CHOW, *University of Waterloo, ON, Canada*

14:30 (22.4) Removal of Source Fringe Effects in the Diakoptic Theory, **G.E. HOWARD**, Y.L. CHOW, *University of Waterloo, ON, Canada*

14:50 (22.5) Quadratic Basis Functions for the Modeling of Thin, Arbitrarily Shaped Wire Structures, N.J. CHAMPAGNE II, **J.T. WILLIAMS**, D.R. WILTON, *University of Houston, TX, USA*

15:10 **COFFEE/CAFÉ**

15:30 (22.6) The Fast Multipole Method for Scattering from Electrically Large Objects, N. ENGHETA[1], **W.D. MURPHY**[2], V. ROKHLIN[3], M.S. VASSILOU[2], [1] *University of Pennsylvania, Philadelphia, PA,* [2] *Rockwell International Science Center, Thousand Oaks, CA, and* [3] *Yale University, New Haven, CT, USA*

15:50 (22.7) MMP Solutions of Scattering at Large Bodies, **CH. HAFNER**, *Swiss Federal Institute of Technology, Zurich, Switzerland*

16:10 (22.8) Reducing the CPU of EMF for Slot Antennas: Combining the Babinet Theorem with the GMT, F. BOMHOLT, **S. KIENER**, *ETH-Zurich, Switzerland*

16:30 (22.9) On the Convergence of Matrix Elements in Planar and Waveguide Problems, **R. KASTNER**, *Tel Aviv University, Tel Aviv, Israel*

16:50 (22.10) A New Hybrid Diakoptic/Spatial Decomposition Method to EM Scattering and Antenna Problems, **D.G. FANG**[1], P.K. LIANG[1], K.L. WU[2], [1] *East China Institute of Technology, Nanjing, China;* [2] *McMaster University, Hamilton, ON, Canada*

THE SOLUTION AND NUMERICAL ACCURACY OF LARGE MoM PROBLEMS

Tom Cwik and Jean Patterson*
Jet Propulsion Laboratory
California Institute of Technology
Pasadena CA 91109

The continuing advancement of computing hardware and software technology has allowed the solution of electromagnetic problems of ever increasing electrical size. This advancement has been a stimulus to the evolution of partial differential techniques such as finite difference or finite element methods, as well as permitting the use of existing integral equation solution techniques to solve larger problems in shorter amounts of time. Existing supercomputers such as the Cray 2 may have 256 Megawords of memory, allowing the in-core storage of a 128 bit, complex, dense matrix of rank ten thousand. The Intel Delta parallel supercomputer, to become operational in Spring 1991, has over 1 Gigaword of memory, allowing the in-core solution of a matrix of rank twenty thousand. Magnetic disk drives attached to these machines enable the use of specially written out-of-core matrix solvers to extend the size of problems practically solvable to as great as forty thousand. Indeed, benchmark factorization and solutions of matrices of rank twenty thousand have been reported to be under two hours. In this paper, the study of the solution and numerical accuracy of scattering from electrically large objects using a method of moments (MoM) formulation, and using these in-core and out-of-core matrix solution algorithms, will be presented.

A thorough study of the numerical solution and its accuracy must include the application of numerical analysis (e.g., Wilkinson, *The Algebraic Eigenvalue Problem*, Oxford, 1965) to the large systems developed in the MoM formulation. This includes the knowledge of the number of significant digits in the calculation of the matrix elements, an estimate of the condition number of the system, and the word size of the machine used. The use of pivoting over some or all of the matrix, and any approximations inherent in 'fast multiplication' algorithms, must also be understood. This study uses the *PATCH* MoM code to solve for scattered fields from large, perfectly conducting scatterers. The accuracy of the matrix elements is determined, and the condition number of the system depending on the number of basis functions per wavelength, and the overall size of the problem is examined. The solution for the current induced on large canonical objects is examined, as well as far-field results, which are compared to existing measurements and to asymptotic calculations.

A MULTILEVEL MOMENT METHOD TECHNIQUE FOR LARGE SCATTERERS

Khalil Kalbasi, *Kenneth R. Demarest

Radar Systems and Remote Sensing Laboratory
Department of Electrical and Computer Engineering
The University of Kansas
Lawrence, KS 66045

The method of moments (MoM) continues to be a robust technique for modeling the scattering and radiation of the time harmonic fields. Its advantages are many and well known. Unfortunately, it is not practical for electrically large problems. This arises from the high cost associated with solving large, and dense systems of equations via direct methods.

Iterative techniques have long offered the promise of significant solution time reductions for MoM formulations, but this promise has often proved illusive. While some successful iterative formulations have been reported, they tend to either converge slowly or lack robustness. Such techniques can be used confidently when it is known in advance that a particular scatterer falls within the capabilities of the method. In this paper we present a very efficient, yet robust iterative technique that models a scatterer using several levels of discretization, capitalizing on the unique perspective that each level offers.

Multilevel schemes are well established with PDE formulations, but are somewhat new in integral equation modeling. The central idea of multilevel modeling is that most iterative methods exhibit unique convergence characteristics when applied to the system of equations associated with different sampling densities. Thus, different aspects of a particular solution can be identified at different levels. By cycling between these levels, the desired solution can be constructed much more quickly than through direct solution methods, with comparable accuracy.

We have shown this technique to be very robust for 2-dimensional scatterers, and it holds significant promise for 3-dimensional problems. Example calculations from several multilevel schemes will be presented, and their performances compared with the standard (i.e., single level) MoM. Suggestions for future developments also will be presented.

B22.3

REDUCED SOURCE DISTRIBUTIONS FOR CALCULATING THE MUTUAL IMPEDANCES OF COMPLEX STRUCTURES

G.E. Howard* and Y.L. Chow
Department of Electrical and Computer Engineering
University of Waterloo
Waterloo, Ontario, Canada N2L 3G1

The reduction of computer time in the calculation of large electromagnetic problems has generated significant interest which is indicated by the special session on reducing the operation count in EM modeling in the 1990 AP Symposium. This paper presents a technique whereby a complex structure is replaced by a simpler structure which is equivalent to the complex structure where the external field and therefore the mutual coupling is concerned.

The technique involves the choice of a reduced source distribution with variable parameters such as source strength, size and location. The parameters are chosen through an optimization procedure which minimizes the error in the field at an appropriate external boundary. The error in the reduced source distribution field is obtained by comparing to the field of a full moment method solution of the original complex structure at the external boundary.

Once the reduced source distribution is obtained, it can then be used to calculate the mutual coupling between this complex structure and other structures external to it. Because the number of parameters required to describe the complex structure has been significantly reduced, the operation count required for the computation of the mutual impedances is also significantly reduced.

Some examples of the application of this technique, including the representation of an MMIC spiral inductor by a magnetic multipole, will be given in the presentation.

REMOVAL OF SOURCE FRINGE EFFECTS IN THE DIAKOPTIC THEORY

G.E. Howard* and Y.L. Chow
Department of Electrical and Computer Engineering
University of Waterloo
Waterloo, Ontario, Canada N2L 3G1

The use of diakoptic theory reduces the operation count in the computation of large electromagnetic problems with complex structures by a factor of 10 or more. The procedure is to divide the structure into smaller substructures which are then solved separately. The resulting current distribution in each substructure is a *generalized basis function* in the diakoptic theory.

When a smaller substructure is solved separately, a source must be used to excite it. A source excitation inevitably creates undesired fringe fields. This paper describes a technique which removes these fringe fields.

The technique involves the addition of extra line lengths to the substructure beyond its defined ports. Typically this involves the addition of two or three current segments for each defined port in a 40 or 50 segment substructure. The extended substructure is then solved by the moment method. By removing the extended line currents and thus the fringe fields from the solution of the extended substructure, a *filtered* generalized basis function for that substructure is obtained. These generalized basis functions are then combined using the diakoptic theory to obtain an overall solution for the structure.

Results indicate that at higher frequencies fringe fields can cause errors of 2 to 5 percent in the overall structure solution without this technique. Utilization of this technique makes these errors negligible. Several examples of the application of this technique will be presented.

B22.5

QUADRATIC BASIS FUNCTIONS FOR THE MODELING OF THIN, ARBITRARILY SHAPED WIRE STRUCTURES

Nathan J. Champagne II, Jeffery T. Williams*,
and Donald R. Wilton

Applied Electromagnetics Laboratory
Department of Electrical Engineering
University of Houston
Houston, TX 77204-4793

Previous algorithms developed for the analysis of scattering and radiation from thin, arbitrarily shaped wire structures are based upon a method of moments solution of an appropriate integral equation for the current along the wire. In these formulations, the current is expanded in a series of basis functions, usually piecewise-linear or piecewise-sinusoidal functions, supported by piecewise-linear wire segments used to approximate the structure. For intricate or complicated wires, the required number of expansion functions and segments (thus, the number of unknowns) is often dictated by that needed to accurately model the actual structure, not the current variations. To reduce the number of unknowns, it is necessary to develop basis functions and supporting wire segments that more closely represent the actual structure. We will present a new wire basis function which has support on a curved wire segment. The curved segment is described by a quadratic which is parametrically defined by 3 points along the actual wire. The current is assumed to vary linearly along the length of the segment. These *curved* basis functions are incorporated into a mixed potential integral equation formulation for the current along thin wire scatterers and antennas, which is solved using a Galerkin method of moments procedure. To handle the kernel singularity, we will discuss an extraction technique where the kernel singularity for an associated linear wire segment is used to remove that of the curve segment. The example of a free-space Archimedian spiral antenna will be used to demonstrate the utility of these new basis functions.

THE FAST MULTIPOLE METHOD FOR SCATTERING FROM ELECTRICALLY LARGE OBJECTS

N. Engheta‡,W.D. Murphy†, V. Rokhlin*, and M. S. Vassiliou†
‡Dept. of Electrical Engineering, University of Pennsylvania, Philadelphia, PA 19104
†Rockwell International Science Center, 1049 Camino Dos Rios, Thousand Oaks, CA 91360
*Dept. of Computer Science, Yale University, New Haven CT 06520

The Fast Multipole Method (FMM) was developed by Rokhlin (*J. Comp. Phys.* 60, 187-207, 1985; *Yale Univ. Research Report* YALEU/DCS/RR-440, 1985) to solve acoustic scattering problems very efficiently. We have modified and adapted it to electromagnetic scattering problems in two dimensions.

Consider a 2-D closed conducting scatterer with n nodes on its boundary. Divide the boundary into p segments, each containing n/p nodes. Instead of calculating n^2 interactions among n current sources on the boundary, consider each segment to be a cluster of n/p sources. For segments that are close together, the exact interactions must be calculated. For segments sufficiently far apart, however, we may do the following: we combine the sources in each segment, approximating their radiation fields by the first N multipoles. We describe each segment via an equivalent source located at the segment's center. We can calculate the contribution of each such equivalent source to the field at the center of any sufficiently separated receiver segment, and in that receiver segment we can use a Taylor expansion to obtain the field at all the individual n/p nodes. The radiation field at any particular node on the scatterer boundary is the sum of contributions of N multipoles of each of the far-away segments, and the direct contribution of very close segments.

The method reduces the operation count for solving the Magnetic-Field Integral Equation (MFIE) from $O(n^3)$ for Gaussian elimination to $O(n^{4/3})$ per conjugate-gradient iteration. It has proven useful in calculating the scattering from electrically large objects difficult to compute by many other methods.

[1]*This work was supported by Air Force Office of Scientific Research Contract Number F49620-89-C-0048*

B22.7

MMP SOLUTIONS OF SCATTERING AT LARGE BODIES

Ch.Hafner, Inst.f.Feldtheorie, Swiss Federal Institute of Technology,
ETH Zentrum, CH-8092 Zürich, Switzerland

The MMP code is based on the Generalized Multipole Technique (GMT). In this technique, analytic solutions of Maxwell's equations inside homogeneous domains are used as basis functions. On one hand, Maxwell's sight of light as an electromagnetic wave is believed to be better than older theories like Geometrical Optics (GO). On the other hand, codes based more or less directly on Maxwell's theory show tremendous numerical problems if large bodies (compared with the wavelength) are involved because the discretization of the model has to be fine with respect to the wavelength.

It is well known that concepts based on geometry like the GO are especially well suited for large scatterers. Thus, codes based on the Geometric Theory of Diffractions (GTD) and similar extensions of GO are preferable. These codes show difficulties if relatively small details of the scatterers are of interest. Such difficulties can be overcome with more complicated formalisms that lead to a more complicated modelling and to an increasing numerical effort.

Of course, one expects that a combination of both GO and Maxwell's concepts might be fruitful. Unfortunately, a complete combination is extremely difficult because of the incompatibility of the ray and the wave concept. Thus, one has to look for partial combinations. For example, the field near a detail of the surface can be computed with the MMP code or another code based on Maxwell's equations. After a "translation" into the language of GO or GTD, these results can be used in a GTD code. Instead of this, the MMP code offers the inverse approach. First, one can start with a simplified model that can be handled by GO. If the results are translated into terms of Maxwell's theory, they can be introduced into the MMP code. This can be done using two different MMP features: "special expansions", i.e. user-definable basis functions and "connections". The latter allows to read in fields of previous computations and to use them as new basis functions. Incidentally, these features are helpful not only for combining the MMP code with other concepts but also to simplify MMP computations of complicated structures with "step-by-step" or iterative procedures.

In many cases, the built-in "special functions" in combination with "fictitious boundaries" allow a direct MMP computation of large or even infinite bodies. In such computations, the consideration of GO constructions can be very helpful to find an appropriate numerical model. For example, in the case of an ideally conducting infinite half plane of finite thickness, one can subdivide the space outside the conductor into four domains that can be characterized as follows: 1) incident and reflected waves, 2) incident wave only, 3) shadow, 4) near field around the edge. To approximate the field, MMP expansions with origins near the edge are applied in all domains. In addition to that, the known field of the incident wave is applied to domain 1) and 2). Finally, the reflected wave in domain 1) is computed by simple symmetry operations in such a way that the boundary conditions far away from the edge are fulfilled exactly.

Reducing the CPU of EMF for Slot Antennas: Combining the Babinet Theorem with the GMT

F. Bomholt & S. Kiener*,
Institut für Feldtheorie und HFT,
ETH-Zurich, CH-8092 Switzerland

The theorem of Babinet is used to reduce the amount of discretization work as well as computation time for a slot antenna ("cylindrical" aperture, length 1 λ, thickness and width $\lambda/5$). The principles of the GMT which are now well known will not be presented.

The aim of this paper is to show the amazing accuracy of the use of the Babinet theorem for 3D structures. The problem of calculating slot antennas with the MMP codes is that a "fictitious" domain (domain which has the same electrical characteristics than his neighbor) must be introduced to separate the side of the slot which receives the illumination from the other one. Furthermore, the discretization must be performed around the slot for at least one wavelength. Finally, geometry does not make the localization of the multipoles very convenient. Still, an accurate result can be achieved [1].

On the other side, the complementary geometry demands a looser discretization as only the object has to be constructed with the full use of three symmetry planes. There is a factor bigger than 10 in the reduction of the CPU for the same accuracy.

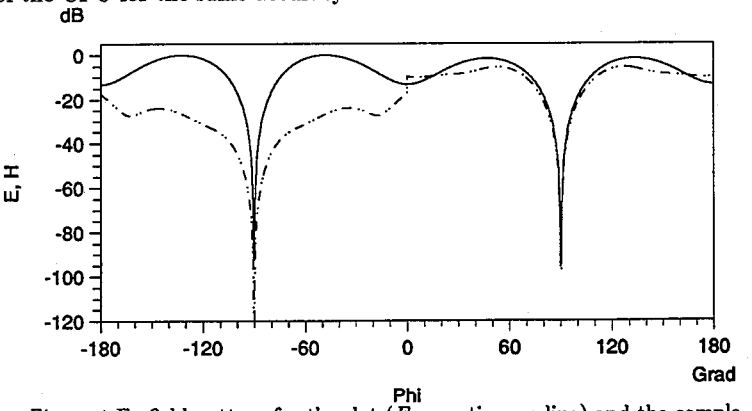

Figure 1 Farfield pattern for the slot (E_ϕ, continuous line) and the complementary geometry ($H_\phi * Z$, dashed line)

[1] S. Kiener & F. Bomholt, "The GMT and the MM-Codes: Applications to EMC, the Babinet Theorem", *Proc. 9th int. Zurich Symp. on EMC*, Zurich, 1991

B22.9

On the Convergence of Matrix Elements in Planar and Waveguide Problems

Raphael Kastner

Department of Electrical Engineering, Physical Electronics
Tel Aviv University, Tel Aviv 69978, Israel

For a number of integral operators solved by the Moment Method scheme, the choice of the basis and testing function designed to solve the integral equation is crucial for the convergence of the matrix elements. As an example, for the infinite cylinder subject to TE illumination case, when solved with the EFIE, it has been shown that pulse type basis functions with point matching lead to divergence, and that a more elaborate choice of basis and testing function is needed. The use of the EFIE may be required when the cylindrical cross section becomes elongated, and is mandatory at the limiting case when the cylinder degenerates into a strip. The alternative of solving the aperture problems with the dual magnetic source - magnetic field formulation also leads to the same operator. Slots and apertures in waveguide walls also involve similar operators and exhibit similar convergence problems. In this work, it is shown that the spectral content of the basis functions may fail to offset the divergent behavior of the spectral Green's dyad component, leading to divergent matrix elements when a point matching formulation is used. This analysis leads to the choice of a smoother testing function with a higher decay rate in the spectral domain, e.g. the Galerkin choice. Indeed, the Galerkin choice for the standard formulation can be viewed as another spectral filter which can alleviate convergence problems encountered in the context of point matching. However, non divergence also depends on the choice of basis functions with the proper spectral content. Given a proper choice of the basis functions, the Galerkin choice has the well known advantage of ensuring power conservation. In fact, one can use the Poynting theorem to formulate an integral equation where only the basis function need to be specified. In such a formulation, the apparent non linear equation indeed reduces to the (linear) Galerkin system of equation. The Galerkin choice, utilizing twice the spectral decay of the basis functions, leads to convergent expressions in most cases, although it may require some extra work in computing the matrix elements compared with point matching. This approach is applied to the problematic transversal slot in the broad wall of a rectangular waveguide where divergence has been observed in the past. Convergent results are obtained.

A NEW HYBRID DIAKOPTIC / SPATIAL DECOMPOSITION METHOD TO EM SCATTERING AND ANTENNA PROBLEMS

D.G.Fang P.K.Liang
Department of Electrical Engineering
East China Institute of Technology
Nanjing, China, 210014
K.L.Wu
Communication Research Laboratory
McMaster University.
Hamilton, Ontario, Canada, L8S 4K1

The quest for more effficient ways of analyzing electrically large structures has resulted in a number of recent publications (for example G.Goubau, N.N.Puri & F.K.Schwering, IEEE Trans. Antennas Propagat., 30, 15–26, 1982; K.R.Umashankar, Wave Motion, 10, 493–525, 1988). A comparative study of several methods for reducing the operation count in EM modeling has been made (P.K.Liang, D.G.Fang, K.Sha & J.J.Yang, submitted for publication in AP–S, 1991). The diakoptic method and spatial decomposition method appear to be very attractive. Both methods possess their advantages and limitations. This fact suggests the hybrid of diakoptic method and spatial decomposition method. The new method takes the advantages of each method. Compared to the moment method, both the computer time and the storage are reduced significantly. Numerical examples to EM scattering and antenna array problems confirm the validity of this new method and will be presented at the meeting.

Special Shapes | **Room 3022 Salle URSI B Session 27** | **Formes spéciales**

Chairs/présidents: R. HARRINGTON, USA; S.R. MISHRA, Canada

13:30 (27.1) Approximations to Beam Diffraction by a Half Plane, G.A. SUEDAN, **E.V. JULL**, *University of British Columbia, Vancouver, BC, Canada*

13:50 (27.2) Scattering from an Array of Large Dielectric Cylinders, **X. SHEN**, E. ARVAS, R.F. HARRINGTON, *Syracuse University, Syracuse, NY, USA*

14:10 (27.3) Electromagnetic Scattering by Two Dielectric Elliptic Cylinders, **A. SEBAK**, *University of Manitoba, Winnipeg, MB, Canada*

14:30 (27.4) Electromagnetic Backscattering by a Two-Dimensional Ogive, **H. SHAMANSKY**, A. DOMINEK, N. WANG, *Ohio State University, Columbus, OH, USA*

14:50 (27.5) Double Diffraction by Two Skewed Edges, L.P. IVRISSIMTZIS[1], **R.J. MARHEFKA**[2], [1]*Radix Ltd., Thessaloniki, Greece;* [2]*Ohio State University, Columbus, OH, USA*

15:10 **COFFEE/CAFÉ**

15:30 (27.6) Scattering from a Non-Metallic Sphere Imbedded in an Infinite Disapative Material, **S.S. SANDLER**[1,3], R.W.P. KING[2,3], [1]*Northeastern University, Boston, MA,* [2]*Harvard University, Cambridge, MA, and* [3]*GEO-CENTERS, Inc., Newton Centre, MA, USA*

15:50 (27.7) Scattering by a Coated Thin Wire and a Finite Rectangular Groove Using a Physical Basis Model, **A. CHATTERJEE**[1], J.L. VOLAKIS[1], W.J. KENT[2], [1]*University of Michigan, Ann Arbor, MI, and* [2]*Mission Research Corporation, Dayton, OH, USA*

16:30 (27.8) The Electromagnetic Scattering by a Material Loaded Step with a Lip in a Ground Plane and by a Pair of Material Loaded Partially Overlapping Semi-Infinite Ground Planes, **G.A. SOMERS**, P.H. PATHAK, *Ohio State University, Columbus, OH, USA*

16:50 (27.9) TLM Solution of a Dipole Over a Half-Space, **N.R.S. SIMONS**, A. SEBAK, *University of Manitoba, Winnipeg, MB, Canada*

B27.1

APPROXIMATIONS TO BEAM DIFFRACTION BY A HALF PLANE

G.A. Suedan and E.V. Jull*
Department of Electrical Engineering
University of British Columbia
Vancouver, B.C. V6T 1W5

An omnidirectional source solution to a diffraction problem becomes a beam source solution by replacing the real source coordinates with appropriate complex coordinates. This gives the exact solution for a simple Gaussian beam. Diffraction by more general beams, which can be synthesized from arrays of omnidirectional sources, may in principle be treated similarly, but numerical evaluation of the diffraction integrals with complex arguments is required. Attempts to circumvent this numerical hurdle are investigated here.

One approximate method is based on the observation that the exact beam source solution for the half plane diffracted field is well approximated by the product of the isotropic source diffracted field and the ratio of the beam and isotropic source fields at the edge. Agreement with the exact solution improves as the distance of the source from the edges and the beamwidth increase. Also if the beam is directed at the edge the Fresnel integral arguments for the beam and isotropic cases are exactly proportional to the ratio beam to isotropic source fields at the edge. Asymptotic expressions for the Fresnel integral are then easily evaluated. The approach is approximate if the beam is not directed at the edge. These results will be discussed with numerical examples shown.

SCATTERING FROM AN ARRAY OF LARGE DIELECTRIC CYLINDERS

X. Shen*, E. Arvas, R. F. Harrington
Department of Electrical & Computer Engineering
Syracuse University
Syracuse, N.Y. 13244, U.S.A.

In order to design a more efficient Xerox color copy machine we have investigated electromagnetic phenomena inside the machine. We want to find out how to determine the reflectance, transmittance, and radar coss section of an array of dielectric cylinders illuminated by a CW laser beam with a wavelength of 700 nm.

Consider the problem of electromagnetic scattering from a two dimensional system consisting of 20 identical dielectric cylinders with arbitary cross section excited by a linerly polarized plane wave. Assume the radius of each cylinder is ten wavelengths. A direct application of the method of moments to this problem is not pratical, because it will result in a moment matrix of order more than twenty thousand. To overcome this obstacle, at first we decomposed the system into several smaller systems. Second, we made use of various symmetric properties of the moment matrix so that the computer memory and CPU time requirements are reduced to a reasonable level. We can then solve the problem on a regular mainframe computer.

A general computer program is written to compute the reflectance, transmittance, and radar cross section of the system. Both TM and TE excitation are considered. To test the accuracy of our approach, we compare our results for a small system to the computed result obtained by a conventional moment method and observe excellent agreement.

B27.3

ELECTROMAGNETIC SCATTERING BY TWO DIELECTRIC ELLIPTIC CYLINDERS

A. Sebak

Department of Electrical and Computer Engineering, University of Manitoba
Winnipeg, Manitoba, Canada, R3T 2N2

The problems of multiple electromagnetic scattering by many objects have received intensive interest because of their presence in many practical applications. Both exact and approximate formulations have been devised to treat such a class of problems. Exact solutions are obtained by using translational-addition theorems for 3D problems and addition theorems for 2D problems. In this paper, a boundary-value solution for the problem of multiple scattering by two dielectric elliptic cylinders is derived. The cylinders are of arbitrary size, material, orientation, location, but non-overlapping. The solution is exact and based on the separation of variable technique in the elliptic cylindrical coordinate system. It is obtained by expanding the incident, transmitted and scattered fields in terms of Mathieu and modified Mathieu functions. The addition theorem for Mathieu functions is then used to express the scattered fields of each individual cylinder in terms of the local coordinates of the other cylinder. Applications of the boundary conditions on the surface of each cylinder result in an infinite system of linear equations for the unknown expansion coefficients of the scattered and transmitted fields. In order to obtain numerical results, the series solution must be truncated in a suitable fashion to obtain a finite matrix. This procedure has been successfully applied to scattering by parallel dielectric circular cylinders (G.O. Olaofe, Radio Sci. 5, 1351-1360, 1970).

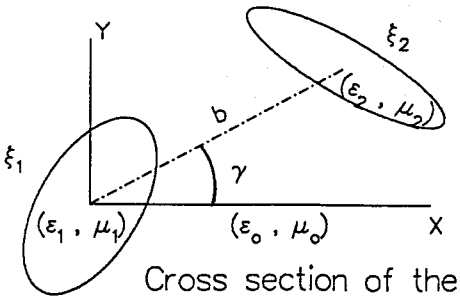

Cross section of the elliptic cylindrical geometry under consideration.

The formulation is applied to many configurations to investigate the scattered field dependence on the geometrical shape, material, and orientation of the cylinders. Numerical results for some selected objects will be presented.

Electromagnetic Backscattering by a Two-Dimensional Ogive

H. Shamansky* A. Dominek N. Wang
The ElectroScience Laboratory
Department of Electrical Engineering
The Ohio State University
Columbus, OH 43212

Abstract

The electromagnetic backscattering from a two-dimensional ogive is examined, including a mechanism by mechanism account for the scattered field. The Uniform Theory of Diffraction is used in conjunction with a creeping wave representation to yield a solution which provides an accurate and continuous backscattering result (echo width) for a wide range of ogive geometry parameters. This solution provides insight into the relative contributions of the various creeping waves which are generated and propagate around the two-dimensional ogive. Comparisons with moment method calculations are used to demonstrate the range of applicability of this high frequency asymptotic solution.

B27.5

DOUBLE DIFFRACTION BY TWO SKEWED EDGES

Leonidas P. Ivrissimtzis
Radix Ltd., Thessaloniki, Greece
and
Ronald J. Marhefka
ElectroScience Lab., The Ohio State University, Columbus, OH

The double diffraction by a pair of arbitrarily oriented edges is investigated via an extended Spectral Theory of Diffraction [*Tiberio and Kouyoumjian;* 1979]. Incorporation of doubly diffracted rays in high frequency approximations of the scattered field may be essential for accurate field predictions within the transition regions, that surround the shadow boundaries of singly diffracted and diffracted reflected rays, or for electrically smaller flat plate scatterers.

In the case of two co-planar skewed edges illuminated by a plane wave, the diffraction is formulated by expressing the edge diffracted field in terms of a spectrum of inhomogeneous plane waves. Such elementary inhomogeneous waves impinge on the second edge from complex angles of incidence. Hence, the doubly diffracted wave is canonically represented by an integral on a double complex angle domain.

A uniform stationary phase procedure is implemented for the asymptotic reduction of the diffraction integral. A similar process was employed by *Jones* [1971] in the study of an integral appearing in the canonical problem of diffraction from a pair of parallel knife edges. The asymptotic analysis leads to the definition of a dyadic double edge diffraction coefficient that involves an edge transition function, which compensates for the discontinuities of the singly diffracted rays at their shadow boundaries [*Ivrissimtzis and Marhefka;* 1990] It is expressed in terms of the generalized Fresnel integral, a single integral of two parameters, that can be easily computed and tabulated. Numerical computations show that the suggested transition function exhibits the correct behavior within the transitional domains. On the other hand the solution asymptotically reduces to Keller's double diffraction outside those regions.

A similar canonical formulation for a pair of non-coplanar skewed edges is not feasible. Therefore, a rather heuristic UTD procedure is adopted. Once the double edge transition function is defined, its parameters can be determined in such a way that continuity across the shadow boundary of the singly edge diffracted rays is warranted. A similar implementation applies to the study of the double edge diffraction for an arbitrary astigmatic illumination of the two wedges.

SCATTERING FROM A NON-METALLIC SPHERE IMBEDDED IN AN INFINITE DISAPATIVE MATERIAL

Sheldon S. Sandler*, Visiting Scholar, Harvard University, Cambridge, MA 02138
Prof. of ECE, Northeastern University, Boston, MA 02115
and Technical Advisor, GEO-CENTERS, INC.
Newton Centre, MA 02159

Ronald W.P. King, Professor Emeritus, Harvard University, Cambridge, MA 02138 and Consultant, GEO-CENTERS, INC., Newton Centre, MA 02159

Using previously published work (Aden, A.L., Cruft Lab. Tech Rpt. No. 106, Harvard University, 1950) as a guide, the backscattered fields from non-metallic spheres embedded in a disaptive material are calculated. Aden dealt with a problem that is essentially the inverse of ours. He computed the backscattering cross-section of water spheres in air. The problem of interest here is roughly equivalent to air spheres in water. The formulation is sufficiently general to allow it to include materials with complex electrical properties. In this study backscattering cross-sections are computed as a function of material parameter and electrical size. Particular attention is given to the parameters characteristic of plastic spheres embedded in salt water.

Applications based on this work can be made to the detection of non-metallic bodies in human tissue. Using the results for the backscattering cross-sections of dielectric spheres, received signals can be computed to determine the range of parameters which allow remote detection of the sphere.

B27.7

SCATTERING BY A COATED THIN WIRE AND A FINITE RECTANGULAR GROOVE USING A PHYSICAL BASIS MODEL

Arindam Chatterjee*, John L. Volakis
Radiation Laboratory
Department of Electrical Engineering and Computer Science
University of Michigan
Ann Arbor, MI 48109-2122
and
William J. Kent
Mission Research Corporation
4220 Executive Drive
Dayton, OH 45430.

The problem of scattering and diffraction by thin wires has been investigated by many authors primarily because the wire is one of the very few practical geometries amenable to an analytic solution. Similar analyses, though, for the coated wire or related geometries such as the finite length narrow groove have not been considered. In this paper, we employ the travelling wave model in conjunction with a Galerkin's solution of the exact integral equation to solve for the scattering by a thin perfectly conducting wire, a thin dielectrically coated wire and a finite length narrow groove in a ground plane. As usual, the proposed current model consists of three weighted travelling wave components. One is associated with the current on the finite wire whereas the other two describe the reflected travelling waves from the wire terminations. For the coated wire, their coefficients are evaluated analytically through a convenient variable transformation. In the case of the finite length narrow groove, an approximate impedance boundary condition is employed at the surface of the groove for constructing the integral equation involving a surface magnetic current which is then represented by the weighted sum of the three travelling wave components. The associated travelling wave coefficients are found in terms of single integrals which are reduced from the original quadruple integrals by employing certain variable transformations. Several current distributions and scattering patterns are presented which serve to validate the accuracy of the model and the derived analytical formulae.

THE ELECTROMAGNETIC SCATTERING BY A MATERIAL LOADED STEP WITH A LIP IN A GROUND PLANE AND BY A PAIR OF MATERIAL LOADED PARTIALLY OVERLAPPING SEMI-INFINITE GROUND PLANES

G.A. Somers* and P.H. Pathak
The Ohio State University ElectroScience Laboratory
Department of Electrical Engineering
Columbus, Ohio 43212

Often, the electromagnetic scattering by a metallic step in a ground plane needs to be controlled or minimized especially in the backscatter direction. This can be accomplished by introducing a lip to the step and by loading the cavity formed by the ground plane and the lip with a dielectric and/or a magnetic material (Fig. 1). By using optimization techniques to adjust the length and/or the material parameters of the filler material, the scattering pattern can be controlled. In this paper, an analytical solution is presented for the scattering by a 2-D step with a lip via the generalized scattering matrix technique used in conjunction with the Wiener-Hopf procedure.

Planar structures with overlapping sections (Fig. 2) are commonly found in fluid guiding structures in which the electromagnetic scattering and transmission may be a concern. Using a procedure similar to the one used by the authors for analyzing the diffraction by just the step, the scattering by the loaded step is calulated and the reflection and the transmission characteristics are controlled by material loading the space between the two conductors in the lip region.

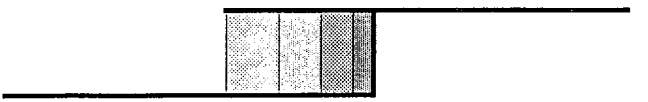

Figure 1: Loaded step with a lip.

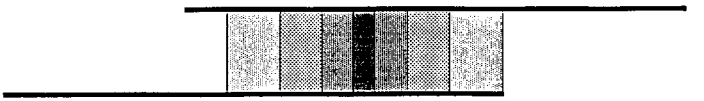

Figure 2: Loaded partially overlapping semi-infinite metallic plates.

The present solutions obtained for analyzing the scattering by 3-D rectangular perturbations also has applications in RCS prediction if they exist on otherwise low cross-section platforms.

B27.9

TLM SOLUTION OF A DIPOLE OVER A HALF-SPACE

N.R.S. Simons and A.A. Sebak*
Department of Electrical and Computer Engineering
University of Manitoba
Winnipeg, Manitoba, Canada, R3T 2N2

The problem of electromagnetic scattering and radiation in the presence of a half space has many applications. We consider the Transmission-Line Matrix (TLM) method as a possible candidate for the solution of this class of problem. The three dimensional symmetric-condensed TLM node is used (P.B. Johns, IEEE Trans MTT, 368-374, 1986). To establish the accuracy of the method, the problem of an infinitesimal dipole radiating in the presence of a half space is examined. A general technique based on the equivalence principle is presented for exciting a TLM mesh with arbitrary field distributions. The procedure allows the excitation of the numerical mesh with the fields of the dipole without the need for modelling an infinitesimal wire antenna. An unperturbed current distribution is assumed. The dipole moment is specified in the time domain and analytical expressions for the time domain fields are used. Both time and frequency domain field distributions are compared to analytical (when convenient) or other numerical solutions. The change in input impedance is also examined as a method of validation.

Transients II

Room 3028 Salle
URSI B Session 30

Transitoires II

Chairs/présidents: R.K. RITT, USA

13:30 (30.1) Time-Domain Synthesis Options for Pulsed-Source and Pulsed-Beam Dyadic Green's Functions in Cylindrically Layered Environments, **L.B. FELSEN**, F. NIU, *Polytechnic University, Farmingdale, NY, USA*

13:50 (30.2) Pulse Propagation on a Semi-Infinite Horizontal Wire Above Ground: Near-Zone Radiated Fields, **S.L. DVORAK**, D.G. DUDLEY, *University of Arizona, Tucson, AZ, USA*

14:10 (30.3) On the Transient Response of a Conducting Cylinder to an Electromagnetic Pulse, **J. MA**, I.R. CIRIC, *University of Manitoba, Winnipeg, MB, Canada*

14:30 (30.4) Short-Pulse Plane Wave Scattering by an Infinite Plane Periodic Array of Perfectly Conducting Strips Above a Perfectly Conducting Ground Plane, **P. BORDERIES**, L.B. FELSEN, L. CARIN, *Polytechnic University, Farmingdale, NY, USA*

14:50 (30.5) Transient Response of Radar Targets Using Wide-Band Stepped-Frequency Measurements, **J. ROSS**, E. ROTHWELL, D. NYQUIST, K.M. CHEN, *Michigan State University, East Lansing, MI, USA*

15:10 **COFFEE/CAFÉ**

15:30 (30.6) A Relaxation Method to Stabilize the Late-Time Oscillations in the Marching-on-in-Time Method, **D.A. VECHINSKI**, S.M. RAO, *Auburn University, Auburn, AL, USA*

15:50 (30.7) Transient Scattering Analysis for a Circular Disk, **A. DOMINEK**, *Ohio State University, Columbus, OH, USA*

16:10 (30.8) The Transient Response of a Pyramidal Horn Antenna, **A.W. BIGGS**, H. POHLE, B.K. SINGARAJU, *Phillips Laboratory, Kirtland AFB, NM, USA*

16:30 (30.9) Transient Responses by Dielectric Cylinders and Spheres Excited by Sources at their Center, **H. SHIRAI**, *Chuo University, Tokyo, Japan*

16:50 (30.10) Pulsed Dipole Inside a Spherical Dielectric Cavity, **R.W. SCHARSTEIN**, *University of Alabama, Tuscaloosa, AL, USA*

B30.1

TIME-DOMAIN SYNTHESIS OPTIONS FOR PULSED-SOURCE AND PULSED-BEAM DYADIC GREEN'S FUNCTIONS IN CYLINDRICALLY LAYERED ENVIRONMENTS

L. B. Felsen* and F. Niu
Department of Electrical Engineering / Weber Research Institute
Polytechnic University
Route 110, Farmingdale, NY 11735

Increased attention is now being given to pulsed, and even short-pulsed, excitation of printed element configuration on layered material substrates, and on the scattering of short-pulse, nonfocused and focused (pulsed beam), incident fields by these structures. Furthermore, printed element configurations have been placed on cylindrically layered substrates to accommodate azimuthal coverage and, more generally, the effect of conformal geometries as on an airplane wing. The systematic treatment of these wideband time-domain operating conditions requires knowledge of the three-dimensional dyadic electromagnetic Green's functions for cylindrically stratified environments. While alternative options for the time-harmonic regime have received some attention, though limited, any excursion into the time domain have proceeded by frequency synthesis over time-harmonic solutions. This becomes impractical and nonphysical for the ultrawideband conditions generated by very short pulses. Utilizing the theory of analytic signals and complex-space-time source techniques for pulsed beams, the present investigation explores all possible options for spectral analysis and synthesis by employing alternative combinations and sequencing of basis fields described by the spectral spatial and temporal wavenumbers $(k_\rho, k_\phi, k_z, \omega)$ corresponding to the space-time coordinates (ρ, ϕ, z, t) in cylindrical coordinates. These alternative formulations, conducted in an infinitely extended multisheeted ϕ-domain, are categorized, with special attention to nonconventional forms that perform ω-inversion before (k_ρ, ϕ, z) inversion. This results in direct time domain synthesis over transient basis fields, and provides new perspectives, especially on the physical behavior of time-domain trapped and leaky modes. Exact hybrid combinations are derived that combine wavefronts, traveling modes and resonant modes self-consistently, and asymptotic approximations highlight the physical wave phenomena.

PULSE PROPAGATION ON A SEMI-INFINITE HORIZONTAL WIRE ABOVE GROUND: NEAR-ZONE RADIATED FIELDS

Steven L. Dvorak* and Donald G. Dudley
Department of Electrical and Computer Engineering
University of Arizona
Tucson, AZ 85721

The near-zone electric field distribution due to a transient current pulse propagating on a semi-infinite wire above the ground is investigated. A quasi-transverse electromagnetic approximation to the modal equation for the propagation wave number is used to obtain the time history of the pulse on the wire. Spectral domain techniques are then used to obtain an expression for the electric field. D.G. Dudley and K.F. Casey (*Radio Sci.* 2, 224-234, 1989) used a saddle point integration to obtain a closed form expression for the far-zone electric field due to an infinitesimal horizontal current element over ground. The far-zone fields of the wire, at polar angles away from grazing, were then obtained in closed form by integrating over the length of the wire. A numerical inverse Fourier transform provided the transient response.

In this paper, we extend the work of D.G. Dudley and K.F. Casey to the near-zone. The computation of the near-zone electric fields usually involves a two-dimensional numerical integration. When the spectral domain representation for the field is employed, as in this paper, the integrand of the angular integral oscillates rapidly for observation points which are located at large transverse distances from the origin of the wire. We handle this difficulty by representing the angular integral in terms of incomplete Lipschitz-Hankel integrals (S.L. Dvorak & E.F. Kuester, 1987 National Radio Science Meeting, 72). A further numerical problem occurs in the integrand of the outer semi-infinite integral. The integrand oscillates rapidly when the observation point is a large distance above the line source. This problem is handled using the transformation in W.A. Johnson and D.G. Dudley (*Radio Sci.* 2, 175-186, 1983). The method which is discussed in this paper allows for the computation of the electric field in the near- and intermediate-zones.

Representative results for the near- and intermediate-zone fields in the frequency and time domains will be presented. A comparison will also be made between the intermediate-zone fields and the far-zone fields which were obtained by D.G. Dudley and K.F. Casey.

B30.3

ON THE TRANSIENT RESPONSE OF A CONDUCTING CYLINDER TO AN ELECTROMAGNETIC PULSE

J. Ma* and I.R. Ciric
Department of Electrical and Computer Engineering
University of Manitoba
Winnipeg, Manitoba, Canada R3T 2N2

An analytical expression has been derived for the transient current density on a perfectly conducting circular cylinder illuminated by an electromagnetic pulse of a double exponential type. The analysis is based on the frequency domain eigenfunction solution of the induced surface current density. The inverse Laplace transform is computed by adding the branch cut contributions and the contributions due to the poles. Since the two exponential functions in the incident plane wave have introduced two poles on the branch cut, the integrals involved are not convergent in a general sense. A careful study shows that the branch cut integrals are convergent in the sense of the principal value. In order to calculate the corresponding principal values, the integration interval is divided into three regions and the integration limits have to be appropriately selected.

The analytical expression obtained in this paper is valid for both the shadow and illuminated regions and for all the time ranges. Numerical results show that for larger time values only the first few terms in the series expression are needed to give a satisfactory accuracy.

Short-Pulse Plane Wave Scattering by an Infinite Plane Periodic Array of Perfectly Conducting Strips Above a Perfectly Conducting Ground Plane

by

P. Borderies*, L.B. Felsen, and L. Carin
Dept. of Electrical Engineering/Weber Research Institute
Polytechnic University, Farmingdale N.Y. 11735

There is currently a trend toward interrogation of propagation environments and targets by wideband signals.. When the targets or environments adjust multiple scattering that renders them structurally dispersive, the time domain response is synthesized conventionally via Fourier inversion from the frequency domain. For ultrawideband signals, i.e. very short pulses, (VSP), this inversion is not only computationally intensive but it fails to match the synthesis to the physical features actually seen in the response. A feature-oriented synthesis, which we call observable-based-parametrization (OBP), proceeds directly in the time domain, thereby allowing resolution, via propagating wavefronts, of the visible individual multiple scatter events at early observation times, and the monitoring, via resonances, of the buildup of collective dispersive effects at later times. This strategy is pursued here for VSP plane wave scattering from a plane infinite periodic array of perfectly conducting strips above a perfectly conducting ground plane. This canonical model has been adopted to gain basic physical and quantitative insight, via OBP, into the wave processes that are operative under these environmental conditions. Such understanding is expected to be helpful for future study of VSP returns from irregularities and clutter. The reference solution is constructed analytically and numerically by the conventional route that involves CW Floquet mode scattering and subsequent frequency inversion. The analytic solution is then converted into OBP via a self-consistent hybrid wavefront-resonance scheme that homes in on distinctive features, of the synthesized response directly in the time domain. The physical content of the OBP synthesis is stressed in the presentation. Also considered is illumination of a finite portion of the array by a pulsed beam.

* On leave from ONERA-CERT, 2-Ave. E. Belin, 31055-Toulouse-Cedesc, France

B30.5

TRANSIENT RESPONSE OF RADAR TARGETS USING WIDE-BAND STEPPED-FREQUENCY MEASUREMENTS

J. Ross*, E. Rothwell, D. Nyquist and K.M. Chen
Department of Electrical Engineering
Michigan State University
E. Lansing, MI 48824

There has been considerable interest in the transient response of radar targets in recent years. Successful target discrimination schemes based on the E-Pulse/K-Pulse methods have employed the late time portion of the transient response. The early time portion of the response, though not used as extensively, is receiving more attention for use in discrimination and detection.

The early time is inherently more difficult to study than late time. Typical late time applications require the natural resonance frequencies of the target be measured. Usually, the natural frequencies can be extracted from the measured response without the need to deconvolve the system response from the measurement. This is possible since for conducting targets the late time response has been shown to be composed of only a sum of damped sinusoids. When a sum of damped sinusoids is convolved with any system impulse response the result is still a sum of damped sinusoids. Thus, direct measurement of natural resonances frequencies is possible without deconvolution. For the early time response, there are no simplifying assumptions possible and the measurement must be corrected for the system impulse response.

For direct time domain measurements the deconvolution of the system response is difficult due to the limited dynamic range, stability, and power output of most measurement systems. A possible way around these difficulties is to make use of frequency domain measurements. The recent introduction of automated frequency-stepping network analyzers has provided a means of measuring the target response over a wide band of frequencies. The transient response of the target can be synthesized via the Inverse Fourier Transform. The resulting transient response is equivalent to the direct time domain measurement provided the system and target are linear and time invariant. However, frequency domain measurements using modern network analyzers provide much greater dynamic range, power, and stability than current time domain systems. The network analyzer also provides automatic correction for known system response errors as well as flexibility in measurement configuration and frequency range.

This paper will demonstrate the utility of frequency domain measurements in the study of the early time response from canonical targets and in the investigation of coupling between wire targets. Theoretical results and direct time domain measurements will be presented to substantiate the synthesized transient responses where possible.

A RELAXATION METHOD TO STABILIZE THE LATE-TIME OSCILLATIONS IN THE MARCHING-ON-IN-TIME METHOD

D. A. Vechinski* and S. M. Rao, Department of EE, Auburn University, Auburn, Alabama, USA.

Traditionally, the transient scattering from a conducting object illuminated by an electromagnetic pulse is obtained using the marching-on-time method. In this procedure, the current distribution induced on the scatterer at each time-step is calculated by using the currents at previous instants. The obvious disadvantage of this procedure is the accumulation of the round-off errors as the solution progresses which shows up as uncontrolled oscillations in the late-time.

In this paper, we present a numerical method known as the relaxation method originally proposed by Tijhuis (A.G. Tijhuis, *Electromagnetic Inverse Profiling: Theory and Numerical Implementation,* VNU Science Press, 1987). In the present work, this technique, with some modifications, is applied to the electric field integral equation solution for the two-dimensional TE and TM transient scattering problems. Numerical procedures highlighting the important steps along with the results for the case of a strip and cylinder will be presented.

TRANSIENT SCATTERING ANALYSIS FOR A CIRCULAR DISK

Allen Dominek
ElectroScience Laboratory
Department of Electrical Engineering
The Ohio State University
Columbus, OH 43212

Far field transient signatures are presented for the backscattered fields from a perfectly conducting circular disk. These signatures are generated from broadband frequency domain solutions which are numerically transformed into the time domain using standard techniques. Two solutions are computed and compared. One solution is calculated using an eigenfunction solution and serves as a reference solution to the second solution which is based upon the geometrical theory of diffraction (GTD). This GTD solution includes first, second and third order edge diffractions as well as a very accurate representation for the edge wave. The use of transient signatures provides an excellent diagnostic capability to confirm the presence of various GTD mechanisms and a validation of their analytical representation.

THE TRANSIENT RESPONSE OF A PYRAMIDAL HORN ANTENNA

A. W. Biggs*, Hugh Pohle, and B. K. Singaraju

Phillips Laboratory, Kirtland Air Force Base, New Mexico

The transmitting and receiving responses of a pyramidal horn antenna are studied analytically and experimentally using the fast Fourier transform (FFT).

A pulse with a pulse width inversely proportional to the center frequency of the pyramidal horn antenna is introduced into the transmitting antenna and is observed at the receiving antenna, a standard gain horn, which is also dispersive. A TEM horn, which is relatively non-dispersive, will also be used as a receiving antenna.

The dispersive properties of the pyramidal horn antennas appear with both transmitting and receiving responses.

TRANSIENT RESPONSES BY DIELECTRIC CYLINDERS AND SPHERES EXCITED BY SOURCES AT THEIR CENTER

Hiroshi SHIRAI

Department of Electrical and Electronic Engineering
Faculty of Science and Engineering, Chuo University
1-13-27 Kasuga, Bunkyo-ku, Tokyo 112 Japan.

Analyses of transient scattering responses have become more important and can be applied to various area, such as target identification and inverse scattering techniques. Comparing with the corresponding time harmonic counterpart, there are many interesting features in it.

In this paper, time transient responses have been calculated for dielectric cylinders and spheres. By setting a line source and a dipole source at the center of an infinitely long dielectric cylinder and a dielectric sphere, respectively, the configuration of each becomes axially symmetric. Under these circumstances, one doesn't have to be bothered by angularly propagating wave constituents, such as creeping waves and whispering gallery modes, and the analyses become very simple accordingly. In the analysis, the corresponding time harmonic result has been formulated first rigorously, then high frequency asymptotic expansion result has been derived. Thus obtained results are found to coincide with those constructed directly by ray approximation.

Fourier inversion for an impulsive response has been done by two methods, namely The Singularity Expansion Method (SEM) and wavefront expansion method. While the former method collects the contribution around the singularities in the complex frequency domain, the latter gives us a result which is a summation of each successive wavefront arrivals. A finite Hilbert transform technique has been introduced to recover the causal responses of odd-time caustic passing wavefronts for the scattering case of the dielectric cylinder. Also derived are results of numerical inversion by Fast Fourier Transform (FFT) method for the band limited incident pulses. Gaussian pulse has been introduced to simulate an impulse response result, and raised cosine pulse which de-emphasizes the low frequency defects of asymptotically constructed frequency spectrum confirms the usefulness of ray solution.

Pulsed Dipole Inside a Spherical Dielectric Cavity

ROBERT W. SCHARSTEIN

The University of Alabama
Department of Electrical Engineering
317 Houser Hall, Box 870286
Tuscaloosa, Alabama 35487-0286
205-348-1761

ABSTRACT. The fields radiated by a Hertzian dipole at the center of a spherical cavity in a homogeneous dielectric of infinite extent are studied for several exciting waveforms. Transient response is obtained by the inverse Fourier transform of the closed-form time harmonic solution. The inverse Fourier transform is evaluated using a combination of numerical quadrature and Cauchy's integral theorem, taking advantage of a high frequency asymptotic approximation. Computational details and analytic approximations are addressed and compared with respect to accuracy and energy for both the early and late-time response to impulsive excitations.

Gratings | Room 2036 Salle URSI B Session 35 | Réseaux

Chairs/présidents: R. HALL, USA; A.A. OLINER, USA

08:30 (35.1) Grating Lobe Suppression in Wideband Radars, **W. WASYLKIWSKYJ**, W.K. KAHN, *George Washington University, Washington, DC, USA*

08:50 (35.2) Antenna Lens Design Based upon Flat Periodic Structures, R.P. TORRES, M.T. LÓPEZ, **M.F. CÁTEDRA**, *Universidad de Cantabria, Santander, Spain*

09:10 (35.3) Conductor Losses in Metallic Gratings, **H.A. KALHOR**, *State University of New York, New Paltz, NY, USA*

09:30 (35.4) Diffraction by Inhomogeneous Gratings of Arbitrary Cross-Section, **S.D. GEDNEY**, R. MITTRA, *University of Illinois, Urbana, IL, USA*

09:50 (35.5) Analysis of Electromagnetic Scattering from Doubly-Periodic Perfectly Conducting Surfaces Using a Patch Current Model, Am. BOAG[1], **Y. LEVIATAN**[2], Al. BOAG[1], [1] *Technion-Israel Institute of Technology, Haifa, Israel;* [2] *George Washington University, Washington, DC, USA*

10:10 **COFFEE/CAFÉ**

GRATING LOBE SUPPRESSION IN WIDEBAND RADARS

W. Wasylkiwskyj and W. K. Kahn
Department of Electrical Engineering & Computer Science
The George Washington University
Washington, DC 20052

The grating lobes of array antennas are due to both spatial and temporal periodicity. Generally only the former is explicitly recognized as contributing to the effect. The latter is implicit in narrow band systems. Suppression of grating lobes should be possible by destroying either the spatial or the temporal periodicity; the latter condition is attained in a wide band system. In this paper we investigate the degree of suppression attained for systems employing pulses. Representative results are presented. Fig. 1 shows the relative level of the first grating lobe as a function of the number of elements in a strictly periodic linear array for a chirp pulse.

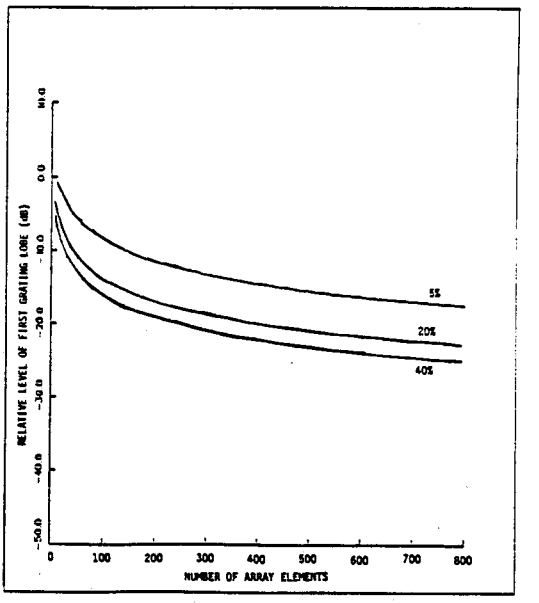

Fig. 1: Level of first grating lobe relative to main beam as a function of the number of array elements. (Single-chirp pulse; bandwidths 5%, 20%, and 40%.)

ANTENNA LENS DESIGN BASED UPON FLAT PERIODIC STRUCTURES

R. P. Torres, M. T. López, M. F. Cátedra.

Departamento de Electrónica.
Universidad de Cantabria.
Avda. los Castros, s/n.
39005-Santander. SPAIN.

Periodic structures have been used succesfully in the design of many devices of interest in the field of microwave engineering: frequency selective subreflectors , radomes, polarizers, etc. This communication presents the design of a plane lens based on slowly varying periodic structures (SVPS)

In (R. Milne,"Dipole Array Lens Antenna", IEEE Trans. AP-30, July, 1982) the idea of a plane lens based on flat periodic surfaces (FPS) is developed. In this case the main idea lies in the usage of zoning, where each zone is formed by regular periodic structures of different parameters.

The classical lens give a phase difference changing the geometrical and electrical characteristics of the device. The same idea can be applied to SVPS which changes locally its transmission coefficient.

For a structure of slowly varying periodicity it can be assumed that behaves locally as an infinite periodic structure. Taking into account the relationship between frequency and electrical size of the scattering structure, it can be assumed that a slight change in the frequency response can be reproduced spatially. Using structures that advance or delay the phase it is possible to design a lens with different zones capable of reproducing the ideal distribution of the phase on the lens.

A pre-design of a lens with six zones, nine layers, and 30% bandwidth have been developed. Good results for a final design are expected.

B35.3

CONDUCTOR LOSSES IN METALLIC GRATINGS

Hassan A. Kalhor
Electrical Engineering Department
State University of New York
New Paltz, NY 12561

Metallic gratings of different groove shapes have many applications in the areas of optics and microwaves, because of their strong frequency dependent behavior. Many ingenious numerical methods have been developed for the analysis of such problems. Almost all of these analysis methods assume that the gratings are made of perfectly conducting materials. In practice, all scatterers are made of finitely conducting materials and in some applications the knowledge of losses becomes very important. The effects of finite conductivity in gratings with triangular groove shape have been previously calculated (H.A. Kalhor & A.R. Neureuther, JOSA, 63, 11, 1973) by using a surface impedance model.

In the present work, conductor losses are calculated by a pertubation method similar to that used in calculating the wall losses in waveguides. To demonstrate the method, a grating with rectangular grooves is considered, and it is assumed that the metal has infinite conductivity. This structure is easily amenable to solution by a mode matching technique. The scattered fields due to an incident plane wave are calculated inside and outside the grooves. The current distribution on the walls is then computed and conductor losses are determined. The impact of these losses on the scattered orders is then evaluated, and compared against results we have obtained by a rigorous method based on solution of the wave equation in the lossy medium. It is concluded that the simple method gives accurate results and that the more complex rigorous method is not needed.

DIFFRACTION BY INHOMOGENEOUS GRATINGS OF ARBITRARY CROSS-SECTION

Stephen D. Gedney and Raj Mittra*
Electromagnetic Communication Laboratory
University of Illinois at Urbana-Champaign
Urbana, IL 61801

The study of diffraction by gratings in the microwave and optical regions finds a plethora of applications in diverse areas such as microwave antennas, integrated optics, and holography. Many analytical and numerical techniques have been successfully applied to this problem (R. Petit, Ed., *Electromagnetic Theory of Gratings*. New York: Springer-Verlag, 1980). In this paper a new method for analyzing a general grating, with an inhomogeneous profile and an arbitrary cross-section, is introduced. The material in the grating cell can be assumed to have an arbitrary spatial variation and may contain conductors, either lossy or lossless, as illustrated in the figure below. This method, which is based on the generalized network formulation, combines the method of moments and the finite element method by matching tangential fields across an artificial boundary. Finite elements are used to model the electromagnetic fields within the unit cell region where the material profile is inhomogeneous. With the use of a periodic boundary condition, the finite element solution is computed in the interior region. The tangential fields on the artificial boundary, computed via the FEM, are weighted by unknown coefficients and matched to the exterior region. In this region, the field problem is formulated in terms of an integral equation and the effect of periodicity is taken into accounted via the use of the periodic Green's function. The unknown coefficients are then solved for and the scattering parameters are subsequently computed. In this paper the properties of a variety of gratings are presented and it is demonstrated that the diffraction properties of a gratings can be greatly manipulated by introducing various cross-sections, profiles and conductors.

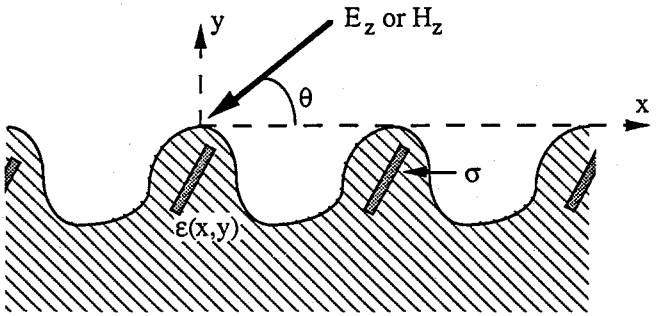

B35.5

ANALYSIS OF ELECTROMAGNETIC SCATTERING FROM DOUBLY-PERIODIC PERFECTLY CONDUCTING SURFACES USING A PATCH CURRENT MODEL

Amir Boag[1], Yehuda Leviatan*[2], and Alona Boag[1]

[1]Department of Electrical Engineering, Technion-Israel Institute of Technology, Haifa 32000, Israel.

[2]Department of Electrical Engineering and Computer Science, The George Washington University, Washington, D.C. 20052, on sabbatical leave from the Department of Electrical Engineering, Technion- Israel Institute of Technology, Haifa 32000, Israel.

Effective computational techniques for analyzing electromagnetic scattering from periodic structures facilitate the designing of diffraction gratings often used as filters, broadband absorbers, and polarizers. In this paper, we describe a novel solution for the scattering problem of a time-harmonic plane wave from a nonplanar perfectly conducting surface. The surface is of arbitrary smooth shape periodic along two directions. The directions of periodicity need not be constrained to be orthogonal.

In this technique, rather than employing a surface integral equation to solve for a surface current, we solve for fictitious currents that lie at some distance away from the surface. First, we set up a simulated equivalence for the homogeneous half space above the surface. In this step, the reflected field is simulated by a linear combination of the fields of a set of spatially doubly-periodic and properly modulated fictitious patch currents. These fictitious sources lie outside the considered half-space at some distance from the boundary, and they are assumed to radiate in an unbounded homogeneous space filled with the same medium as that filling the half space above the conducting surface in the original problem. Usually, the centers of the fictitious sources are placed on a surface of shape similar to that of the actual boundary. Each of the doubly-periodic patch sources lies in a plane parallel with the plane spanned by the directions of the periodicity. They all are characterized by the same current density profile multiplied by a unit direction vector, but their complex amplitudes are yet to be determined. The fields radiated by these patch sources are computed by summing a discrete spectrum of outgoing and decaying evanescent waves known as Floquet modes. It is worth pointing out that when the patch currents lie at some distance away from the boundary surfaces, their fields constitute a basis of smooth field functions on the boundaries. In addition to the formation of a smooth field, the freedom in the choice of source locations also permits fitting of the actual fields on the boundaries as per requirement. The main advantage, however, is that the periodic patch currents have analytically derivable fields. This quality is appealing as one can avoid the computationally intensive surface integrations routinely used for evaluating the fields at the various stages of the solution. Finally, since we are using, though indirectly, a basis of field functions smooth on the boundary, the simulated fields can be forced to obey the zero tangential electric field condition in some simple sense. Here, the solution is effected by adjusting the amplitudes of the fictitious sources for the continuity conditions at a discrete set of points.

The suggested procedure is simple to implement. It has been applied to doubly-periodic sinusoidal surfaces, but it is by no means restricted to this special case. The results have been shown to satisfy the boundary condition and energy conservation consistency checks within a very low error.

Inverse Scattering **Room 2036 Salle URSI B Session 36** **Diffusion inverse**

Chairs/présidents: W.R. STONE, USA; G.E. BRIDGES, Canada

10:30 (36.1) Using Doppler-Induced Phase Shift to "Cohere" An Imaging Phased Array, **W.R. STONE**, *Expersoft Corporation, La Jolla, CA, USA*

10:50 (36.2) Microwave Holographic Imaging with Partial Spectrum Knowledge, **A. ALBIOL**, M. FERRANDO, N. CABALLERO, *Universidad Politécnica de Valencia, Spain*

11:10 (36.3) Non-Destructive Measurement of Electromagnetic Properties of Materials, **C.-L. LI**, K.-M. CHEN, *Michigan State University, East Lansing, MI, USA*

11:30 (36.4) Radar Target Discrimination Using S-Pulse Waveforms, **P. ILAVARASAN**, E. ROTHWELL, J. ROSS, D. NYQUIST, K.M. CHEN, *Michigan State University, East Lansing, MI, USA*

11:50 (36.5) Target Identification in Non-Interactive Clutter Using the Bispectrum, I. JOUNY, **E.K. WALTON**, *Ohio State University, Columbus, OH, USA*

Using Doppler-Induced Phase Shift to "Cohere" An Imaging Phased Array

W. Ross Stone
Expersoft Corporation
1446 Vista Claridad
La Jolla, CA 92037

Large phased arrays are used in many applications where the phase of the signal recorded at each antenna in the array needs to be known with respect to a common reference. In many applications, involving both real and synthetic apertures, the size of the array is so great and/or the position of each element of the array is known or varies with sufficient uncertainty that correcting the phase at each element (e.g., so that a point scatter is recorded as producing an undistorted spherical wavefront across the array) is difficult. This problem has been studied, and elegant solutions obtained, using the "self-cohering" techniques developed by the Valley Forge Radio Camera project. When at least one dimension of the array is synthesized by relative motion of the object being imaged and the array, or by relative motion between the source of the illumination and the array, there is a different approach possible for "cohering" the array. It should be noted that this approach is probably only applicable when the phase "error" at each antenna is less than a wavelength.

Consider the situation in which an array of antennas, with an aperture very large compared to the wavelength, is fixed along an east-west line on the earth, and the north-south dimension of a two-dimensional array is synthesized by using a beacon on a satellite in a north-south circular, polar orbit. The signal recorded by one of the antennas, with respect to a local oscillator, can be shown to contain two contributions to the variation in phase as a function of time: the Doppler shift due to the motion of the source, and the fluctuations due to any target within the field of view of the array. The phase variation due to the Doppler shift can be shown to be adequately approximated by a quadratic function, with an accuracy of better than 10^{-5} of a wavelength. Furthermore, if the distance from the array to the beacon is sufficiently greater than the distance to any target, it can be shown that every antenna in the array should see the same phase shift due to the Doppler shift, to within a similar accuracy. Adjusting the phase at each antenna to remove the inter-antenna variations due to the Doppler can thus be used to "cohere" the array. It is shown that a similar, but somewhat more complicated, procedure can be derived based on the relative motion of a target and the array. Experimental results from the Holographic Radio Camera demonstration experiment, in which a correction to better than 10^{-3} of the two-meter wavelength across a one-kilometer array was achieved, are shown.

MICROWAVE HOLOGRAPHIC IMAGING WITH PARTIAL SPECTRUM KNOWLEDGE

* Antonio Albiol, Miguel Ferrando, Narciso Caballero

Departamento de Comunicaciones
Escuela Tecnica Superior de Ingenieros de Telecomunicación
Universidad Politecnica de Valencia
Camino de Vera s/n
46022 VALENCIA
SPAIN

It is well known that reflectivity or transmittance images of an object can be obtained by illuminating the object with plane waves from all directions, and with a certain range of wavelengths. When using non-diffracting radiation like X-rays, the information obtained from each measurement with a certain incident direction fills one line of data in the spectral domain. Repeating the measurement from ideally all directions, one can fill the spectral domain, obtaining a transmittance image by Fourier inversion. In practice however, one only measures at certain directions, and interpolates at the spectral domain to fill a rectangular grid of spectrum points to apply fast Fourier algorithms. With diffracting radiation, like microwaves or ultrasounds, the process is the same, being the only difference the way one fills the spectral domain. In the case of diffracting radiation the information obtained from each measurement fills one semicircle of the spectral domain. By changing the angle of the incident wave and line of measurement, one can again ideally fill all the spectral domain. In practical cases however, only a few measurements are made and interpolation from measured data is again required.

One problem that appears in radar, microwave and ultrasounds tomography, is that one can not illuminate-measure from all spatial directions. These leads to limited spectral filling possibilities. One possibility is to take Fourier inverse considering the unavailable data to be zero. However, since the spectral knowledge available is not a low-pass one may get strange reconstruction images by using this procedure with no further assumption.

In this paper, we see that if the phase of the reflectivity function of the object can be assumed to vary much more rapidly than the modulus, then it is still possible to get good reconstructions from the available data (DAVID C. MUNSON, JORGE L. C. SANZ, Image reconstruction from Frequency-Offset data, Proc. IEEE June 1984). We have found the conditions required for good image reconstructions. These are, to have an available data bandwith comparable to the modulus bandwith, to have a phase bandwith comparable to the centre frequency of the available spectral data. Failure in the first condition causes an overblurred reconstruction image to be recovered, but still similar to the expected image. Failure in the second condition causes strange reconstructed images to be recovered, very similar to the zero-phase case.

Apart from the considerations above, to get good reconstructions, one must consider questions as the spectral interpolation method, windowing of spectral data to avoid ringing reconstructions, and multiplicative noise reduction techniques to improve the quality of the obtained images.

Sample results will be presented at URSI.

NON-DESTRUCTIVE MEASUREMENT OF ELECTROMAGNETIC PROPERTIES OF MATERIALS

Ching-Lieh Li* and Kun-Mu Chen
Department of Electrical Engineering
Michigan State University
East Lansing, MI 48824

The purpose of this study is to develop a non-destructive and accurate method for measuring EM properties of materials over a wideband of frequency.

A probe consisting of an open-ended coaxial line with a large flange placed against a sample of material has been developed. By measuring the short-circuit input impedance (material shortened by a metallic plate) and the open-circuit input impedance (material open to the air) of the probe, EM parameters, including the complex permittivity and permeability, of the material can be inversely determined, because the EM parameters of the material are implicitly related to the input impedances of the dominant (TEM) mode of the probe. Since a coaxial line does not suffer a cut-off phenomenon, this probe can be operated over a wideband of frequency. Previous works on this type of probe either used approximate analyses or assumed simplified material geometries. Our study provides accurate theoretical analysis and considers general material geometries.

Theoretical analysis of this probe placed against a material is mainly based on an integral equation for the electric field on the probe aperture. This aperture field was determined by solving the integral equation numerically with the point-matching method or the Galerkin's method. After that the input impedances of the probe can be expressed implicitly as functions of EM parameters of the material. Finally, EM parameters of the material are determined inversely from the measured input impedances of the probe through a Broyden's numerically algorithm.

Experimentally, the input impedances of the probe placed against various materials are measured using a Network Analyzer or a Vector Voltmeter. The EM parameters of these materials are then determined through the numerical algorithm over a wideband of frequency.

RADAR TARGET DISCRIMINATION USING S-PULSE WAVEFORMS

P. Ilavarasan*, E. Rothwell, J. Ross, D. Nyquist and K. M. Chen
Department of Electrical Engineering
Michigan State University
E. Lansing, MI 48824

The E-pulse radar target identification scheme uses an aspect-independent waveform (E-pulse) which when convolved with the late-time scattered signal of an expected radar target eliminates the natural resonance spectrum of the target. An S-pulse, or single mode extraction waveform, eliminates all but one mode, leaving behind a single damped sinusoid. Interaction of an E-pulse or S-pulse with an unexpected target results in the excitation of the entire target modal spectrum, thus allowing discrimination between expected and unexpected targets. The theory of S-pulse waveforms is well developed but its application has been hampered by lack of an efficient means of interpreting the convolved signal. This paper suggests a simple means of quantifying S-pulse discrimination.

Consider the convolution of sine and cosine S-pulses with a return from the expected target. During a finite time period between the onset of late-time and the end of the measured return the convolved outputs will be single damped sinusoids of unknown amplitudes and unknown phases (differing by 90^0), but known complex frequency. These outputs are analyzed for expected single-mode content in an approach inspired by the matched filtering concept. Define DSR, the "S-Pulse discrimination ratio", as

$$DSR = \frac{\left[\int_{-\infty}^{\infty} |C(\omega)||F(\omega)|\,d\omega\right]^2}{\int_{-\infty}^{\infty} |C(\omega)|^2\,d\omega \int_{-\infty}^{\infty} |F(\omega)|^2 d\omega}$$

where $C(\omega)$ is the Fourier spectrum (obtained via the FFT) of the sine and cosine single mode outputs combined to form a complex exponential, and $F(\omega)$ is the analytic spectrum of the expected complex exponential, taken over the same finite time interval. It is apparent that the DSR takes on a maximum of unity when the convolved output matches the expected signal. Note that the unknown phase of the convolved output is inconsequential since only the spectral magnitude is involved.

S-pulse discrimination will be demonstrated using measurements made from scale-model targets. It will be shown that by using several S-pulse waveforms, designed to extract different modes from each target, discrimination can be enhanced markedly over that allowed using only E-pulses.

B36.5

TARGET IDENTIFICATION IN NON-INTERACTIVE CLUTTER USING THE BISPECTRUM

I. Jouny and E. K. Walton*
The Ohio State University ElectroScience Laboratory
1320 Kinnear Road, Columbus, Ohio 43212

This paper uses features extracted from the bispectrum of radar signals for classification of unknown radar targets in clutter. The classification performance is compared with the performance of other classifiers that are not based on higher order processing of the measured radar data. The radar signals used in this study are experimental measurements that correspond to scattering from real radar targets. The data is corrupted with different types of disturbances that are likely to occur in a real radar system.

There are three reasons for using bispectral features of radar targets in clutter for classification purposes. First, the bispectrum suppresses additive disturbances that are zero mean with symmetric probability density functions. Second, bispectral processing detects implicit correlations between spectral components that may be present in the data and that are not recovered using spectral processing; this property has been investigated by E. K. Walton and I. Jouny, (Radio Sci. 25, 101-113, 1990), where it is shown that the bispectrum of radar signals can be used to detect multiple interactions between scatterers. Third, the bispectral features of radar targets include, in addition to the spectral features, responses that are due to strong multiple interactions along the target and are relatively independent of clutter (particularly non-interactive clutter).

Classification performance using bispectral features is compared with that obtained using spectral features and time-domain scattering features. The classifiers used in this study are non-parametric in the sense that no prior information is needed about the underlying distribution of radar measurements or the probability of occurrence of each target. These classifiers either measure the distance between the signal of the unknown target and that of the catalog or use cross-correlation between features of the unknown target and that of the catalog. The case where the azimuth position of the target is not exactly known will be also investigated.

Numerical Methods – Finite Element

Room 2110 Salle URSI B Session 38

Méthodes numériques – élément finis

Chairs/présidents: C.M. BUTLER, USA

08:30 (38.1) A Study of Discretization Errors in the Finite Element Method, **R. LEE**, *Ohio State University, Columbus, OH, USA*

08:50 (38.2) Accurate Full Wave Analysis of Generalized Waveguiding Structures Employing a Finite Element Self-Adaptive Mesh Technique, **M. SALAZAR-PALMA**[1], F. HERNÁNDEZ-GIL[2], [1] *Universidad Politécnica de Madrid, and Telefónica Investigación y Desarrollo, Madrid, Spain*

09:10 (38.3) Parallel Mesh Generation for Electromagnetic Finite Element Computations, **R.D. FERRARO**, J. PARKER, J.E. PATTERSON, *California Institute of Technology, Pasadena, CA, USA*

09:30 (38.4) A Hybrid Finite Element/Boundary Element Method for Solving Three-Dimensional Electromagnetic Coupling Problems, **R.P. JEDLICKA**, S.P. CASTILLO, *New Mexico State University, Las Cruces, NM, USA*

09:50 (38.5) Analysis of Passive Microwave Structures by a Combined Finite Element Generalized Scattering Matrix Method, **J. ZAPATA**, J. GARCÍA, *Universidad Politécnico de Madrid, Spain*

10:10 **COFFEE/CAFÉ**

10:30 (38.6) Finite Element Analysis of Inhomogeneous, Axisymmetric Scatterers and Radomes, **R. GORDON**[1], R. MITTRA[2], [1] *University of Mississippi, University, MS, and* [2] *University of Illinois, Urbana, IL, USA*

10:50 (38.7) Finite Element Analysis for an Obliquely Incident Plane Wave Incident on Cylinders Near a Planar Media Interface, **R. LEE**, A.C. CANGELLARIS, *Ohio State University, Columbus, OH, USA*

11:10 (38.8) Numerical Modeling of Axisymmetric Coaxial Waveguide Discontinuities Using the Finite Element and Mode Matching Techniques, G.M. WILKINS, J.-F. LEE, **R. MITTRA**, *University of Illinois, Urbana, IL, USA*

11:30 (38.9) Microwave Directional Coupler Design Using Spectral Domain and Finite Element Technique, **L. KALIOUBY**, Y. CASSIVI, R.G. BOSISIO, *École Polytechnique de Montréal, PQ, Canada*

11:50 (38.10) Finite Element Modeling on the Desktop Using the i860 Microprocessor, **G.T. SHOEMAKER**, *Pennsylvania State University, Erie, PA, USA*

A STUDY OF DISCRETIZATION ERRORS IN THE FINITE ELEMENT METHOD

R. Lee
Department of Electrical Engineering
Ohio State University
2015 Neil Avenue
Columbus, OH 43210-1272, USA

The finite element method has been used by numerous researchers to solve electromagnetic problems. As the size of the geometries grows , the number of unknowns can become very large. Obviously, the number of unknowns depends upon the discretization of the grid. Therefore, it is important to obtain an estimate of the solution error based on the nodal density in the grid.

We performed a numerical experiment using the problem of a plane wave propagating through free space since the analytical solution is known and the magnitude of the solution is constant. It was found that many factors influence the size of the solution error. The error depends on wavelength, the direction of the incident field, the type of element, the type of boundary condition, and the size of the grid in terms of wavelength.

The cause of the solution error can be shown to come from the numerical wave number which propagates through the grid. Since we use a finite element approximation for the field, the numerical wave number is different from the actual wave number. Thus, if the boundary condition depends on the wave number, an error will occur in the solution. For the problem of a plane wave propagating through free space, it is interesting to note that a Dirichlet boundary condition produces both a magnitude and phase error in the form of a standing wave, whereas an absorbing boundary condition only produces a phase error which increases linearly as the plane wave propagates from one end of the grid to the other.

ACCURATE FULL WAVE ANALYSIS OF GENERALIZED WAVEGUIDING STRUCTURES EMPLOYING A FINITE ELEMENT SELF-ADAPTIVE MESH TECHNIQUE

Magdalena Salazar-Palma*, Félix Hernández-Gil**

*Dpto. Señales, Sistemas y Radiocomunicaciones. E.T.S.I. Telecomunicación. U. Politécnica de Madrid. c/ Ciudad Universitaria s/n. Madrid 28040.Spain.

**Telefónica Investigación y Desarrollo. c/ Emilio Vargas,6. Madrid 28043.Spain.

The Finite Element Method is a flexible numerical procedure capable of analysing different geometries without the need of new analytical developments. Nevertheless, the accuracy of the results depends strongly on the mesh selection.

In a previous paper (M.Salazar-Palma & F.Hernández-Gil, MTT-S Symposium Digest, pp. 507-510, June 12-16,1989, Long-Beach, CA) a self-adaptive mesh algorithm for the FEM quasi-static analysis of general inhomogeneous anisotropic transmission-lines was presented. The self-adaptive technique has proved to be an efficient tool leading to an easy-to-use accurate FEM analysis program, in which the mesh is automatically well adapted not only to the structure geometry but to field behaviour.

The extension of the self-adaptive algorithm to full-wave analysis of generalized arbitrarily shaped waveguiding structures (including inhomogeneous, anisotropic, multiconductor ones) is presented in this paper. A formulation employing the longitudinal components of the electric and magnetic field has been selected. The FEM is applied using a coarse initial mesh. A postprocess of the solution provides local error indicators; a new mesh, refined according to them, is automatically generated and the FEM is applied to it. The process will continue until a given criterion is achieved. The full-wave adaptive algorithm has provided a complete automatic program for accurate analysis of any type of guiding structure: metallic, dielectrically filled, dielectric and optical waveguides and multiconductor structures. Results have been compared with those obtained by other authors and methods. In the figure an example of a vaned waveguide is given; results for the cutoff wavelength are compared with that obtained by P.Silvester (IEEE Trans. MTT, vol. 17, April 1969, pp.204-210).

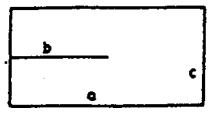

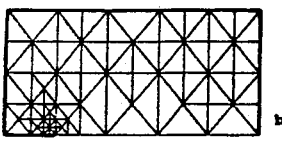

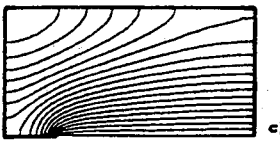

Vaned waveguide.
a) Structure
b) One half of the fourth mesh for the first TE mode with odd symmetry, $_b$=0.2a, c=a
c) Hz equipotential contours

Mesh	λ_c (mm)
1	1.998
2	2.053
3	2.093
4	2.121
5	2.130
6	2.137
7	2.147
8	2.149
9	2.152
10	2.153
11	2.155
12	2.156
Silvester	2.2

B38.3

Parallel Mesh Generation for Electromagnetic Finite Element Computations

R.D.Ferraro, J.Parker, J.E.Patterson*

Jet Propulsion Laboratory / California Institute of Technology
4800 Oak Grove Drive
Pasadena, CA 91109

The availability of parallel computers with hundreds of processors, tens of megabytes of memory per processor, and tens of gigaflops of total computing power has made it possible to run electromagnetic computations using finite element meshes with tens of thousands to almost a million elements. Running electromagnetic finite element codes on parallel computers requires some means of generating and partitioning an unstructured mesh so that load balance is maintained and solver communication is minimized. A finite element mesh may contain several different types of finite elements, each with a different computational requirement for the stiffness matrix setup and for the solver. Solution of electromagnetic problems require a certain minimum mesh density, on the order of 5 to 10 quadratic elements per linear wavelength, to support the wave behavior properly. To maintain load balance in a finite element code, these varying element loads must be considered when partitioning the mesh among processors. The unstructured nature of the mesh requires more sophistication than a simple bisection algorithm allows.

Our most pressing problem with finite elements on distributed memory computers has to do with the limited I/O bandwidth to the machine from other computers. Currently, we generate finite element meshes with a commercial solids modeling package, and transfer the mesh information to the parallel computer. The amount of information required to describe a finite element mesh is enormous. Our codes spend a large fraction for their execute time simply reading the mesh information. To avoid this problem, we have begun to look at parallel mesh generation in the context of finite element meshes for electromagnetic problems. As a first approach, we are doing parallel mesh refinement. The model of the scattering object is translated into a coarse mesh with just enough elements to correctly describe the geometry. Our partitioning code then breaks up the mesh, possibly splitting elements into pieces, for assignment to processors. Then each processor does a mesh refinement to the mesh density required for supporting electromagnetic waves.

We are refining the partitioning algorithm we currently use to handle geometric solids descriptions. Previously, we partitioned the finite element mesh which was generated elsewhere, taking into account the shapes of the individual elements in the mesh, as well as their computational requirements. The algorithm, called Recursive Inertial Partitioning (RIP), is based upon the physics of rotation of solid bodies. In order to generate a mesh in parallel which will be load balanced and have minimal communication, we need to partition the solid model itself among processors, using the mesh density requirements for each section as a guide to the computational load. We will discuss some of the issues which are shaping our approach to complete parallel mesh generation.

A HYBRID FINITE ELEMENT/BOUNDARY ELEMENT METHOD FOR SOLVING THREE-DIMENSIONAL ELECTROMAGNETIC COUPLING PROBLEMS

R.P. Jedlicka* and S.P. Castillo
Department of Electrical and Computer Engineering
New Mexico State University
Las Cruces, New Mexico

Electromagnetic penetration of shielded enclosures can couple energy into interior electronic components. This can cause a degradation in performance, or in some instances malfunction, of the electronic systems contained within. The coupling from the exterior to the interior can be in many forms. Entry may be via straightforward routes such as antennas designed to operate in conjunction with the interior electronic systems or inadvertent paths such as gaps or cracks created by warping or bowing at mechanical interfaces. Significant fields can be coupled through these gaps. These seams may be modeled as narrow slot apertures. This paper addresses the problem of electromagnetic coupling through narrow slot apertures into cavities of moderate complexity. That is, cavities which may be irregularly shaped and filled with inhomogeneous, lossy dielectrics.

An equivalent antenna/local transmission line model has been developed for narrow slot apertures with depth and losses (L.K. Warne & K.C. Chen, IEEE Trans. EMC-32, pp185-196, Aug. 1990). This model takes into account not only the slot depth but also the finite conductivity of the walls as well as lossy gaskets within the aperture. This model may be applied to tortuous paths which is more realistic in the practical case. In this model a magnetic antenna is used to characterize the coupling from the exterior to the interior through a narrow slot aperture. An equivalent antenna radius for the slot is used to account for depth and losses.

To facilitate modeling of the inhomogeneous, irregular interior region the finite-element method (FEM) is utilized to solve the 3-D vector wave equation subject to the boundary conditions. In this case, an impedance boundary condition is used to account for wall loss in the imperfect conductors bounding the cavity. An H-field formulation is used with the forcing function being the magnetic current along the equivalent antenna. For the slot, the method of moments (MOM) is used to discretize the operator. The resulting linear system of equations relate the unknown equivalent magnetic current to the magnetic field incident upon the aperture from the exterior region as well as the total short-circuit magnetic field in the cavity. The coupled slot/cavity equations are then solved in a two-step elimination process.

Results will be presented for coupling through a variety of cavity-backed narrow slot apertures. Narrow slots with depth fabricated from several different conductors will be considered. Comparison will be made to experimental results.

B38.5

ANALYSIS OF PASIVE MICROWAVE STRUCTURES BY A COMBINED FINITE ELEMENT GENERALIZED SCATTERING MATRIX METHOD

* J. Zapata, J. García
Grupo de Electromagnetismo Aplicado y Microondas
E.T.S.I. de Telecomunicación. U.P.M.
E28040 Madrid. Spain

This work extends the Generalized Scattering Matrix Method to the analysis multistep homogeneous arbitrary shaped waveguide circuits. The method, is useful also for arbitrary shaped planar transmision line discontinuities or dielectric-loaded multistep waveguide discontinuities.

In the present work the Helmholtz equation solution for the axial field is obtained by the Finite Element Method. When the axial field is known, the transversal components of the field can be obtained by numerical derivation in the element's Barlow point. Numerical integration of the internal products of the fields of a number of modes gives the GSM of the discontinuity.

The precedent calculus can be made frecuency independent, and then the band response of a multistep structure can be obtained in an eficient straighforward manner.

A structure involving ridge-waveguides and another involving truncated circle waveguides circuits have been analized with a very good agreement between computer and measured, or reported, data.

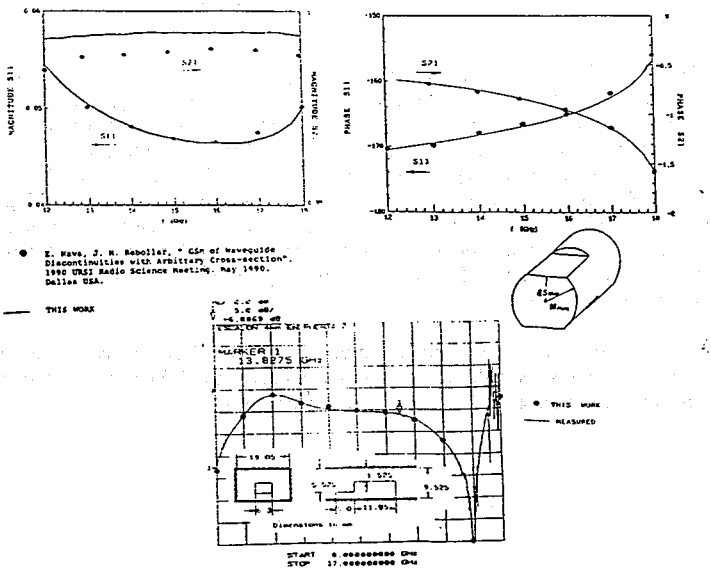

FINITE ELEMENT ANALYSIS OF INHOMOGENEOUS, AXISYMMETRIC SCATTERERS AND RADOMES

*R. Gordon**
Department of Electrical Engineering
University of Mississippi
University, MS 38655

R. Mittra
Electromagnetic Communication Lab
University of Illinois
Urbana, IL 61801

The problem of electromagnetic scattering by a p.e.c. body of revolution (BOR) has been investigated by Gordon & Mittra(1990 URSI Digest) by using the finite element technique applied to the coupled differential equations satisfied by the scalar azimuthal potentials introduced by Morgan and Mei. The Bayliss-Turkel type of absorbing boundary condition, typically used for FEM mesh truncation at the outer boundary, does not lend itself to generalization to these potentials. However, it was shown in the Gordon & Mittra paper that an asymptotic boundary condition, obtained from Wilcox's expansion for the scattered field in terms of powers of r^{-1}, could be used for truncating a finite element mesh with a *cylindrical* outer boundary.

The objectives of the present paper are threefold. First, we apply the asymptotic boundary condition *a la* Wilcox for a finite element mesh with a *spherical* outer boundary. By comparing the results for the two different outer boundary shapes, we find a somewhat unexpected result that, even in those cases where the spherical outer boundary is, at some points, less than a wavelength from the surface of the scatterer, the results for a spherical boundary can be considerably more accurate than when this boundry is cylindrical. Second, we extend the previous work to the important practical problem of radar scattering by a p.e.c body coated with an arbitrarily inhomogeneous dielectric material(see Fig.1) and validate the p.d.e. approach by comparing its results with those derived from the Method of Moments. Third, by invoking the principles of reciprocity, we enlarge the scope of application of the previous analysis to the problem of axis-symmetric antenna radomes(Fig.2) which may contain both an inhomogeneous dielectric and a conducting material, a problem that has not been previously treated in the literature using a similar method.

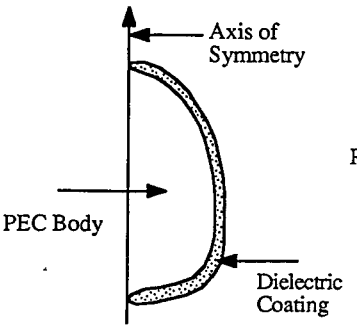

Fig. 1

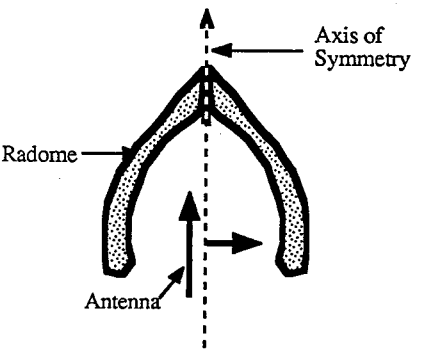

Fig. 2

FINITE ELEMENT ANALYSIS FOR AN OBLIQUELY INCIDENT PLANE WAVE INCIDENT ON CYLINDERS NEAR A PLANAR MEDIA INTERFACE

*R. Lee**
A.C. Cangellaris
Department of Electrical Engineering
Ohio State University
2015 Neil Avenue
Columbus OH, USA

The problem of electromagnetic scattering from cylinders near a media interface can be used to study scattering problem near the air-earth interface. In addition, it has applications to microelectronics where light is used to measure the line widths of interconnects. Several researchers have considered the case of a plane wave normally incident on a cylinder near a media interface, but the general case of oblique incidence was never considered. A finite element formulation in conjunction with the bymoment method is presented which considers the general case. The shape along the cross section of the cylinders is arbitrary. The material properties of the cylinders are isotropic and in general inhomogeneous along the cross section but constant along the length of the cylinder.

Because the incident field is obliquely incident, the TE and TM polarizations are coupled through both the cylinder and the interface. A formulation is presented in which the coupling due to the cylinder is embedded in the finite element solution, and the coupling due to the interface is embedded in the bymoment method. Numerical results for several geometries are presented.

Numerical Modeling of Axisymmetric Coaxial Waveguide Discontinuities Using the Finite Element and Mode Matching Techniques

Gregory M. Wilkins*, Jin-Fa Lee, and Raj Mittra
Electromagnetic Communication Laboratory
University of Illinois

Electromagnetic energy is frequently transported within an electrical network by way of coaxial transmission lines. However, the dimensions of the individual components included in the network tend to vary. These differences in dimension are most prevalent at the interfaces between the respective regions containing the components. The focus of our investigation is the field behavior in the presence of these coaxial-to-coaxial interfaces. Specifically, we are interested in junctions which occur between a system of cascaded coaxial lines as encountered, for example, in high-frequency connectors. At such junctions problems such as dispersion, loss, non-fundamental mode propagation, and impedance discontinuities are commonplace and thus warrant special attention.

The axial symmetry of the geometry of concern prompts us to formulate the problems in terms of the cylindrical coordinate system. The method of formulation employed enables us to analyze many configurations repeatedly and consistently without major modifications to the approach. We are also able to predict the field distribution throughout all regions and the corresponding energy reflection and transmission at the interfaces, from which we may develop an equivalent circuit model for the transmission line network. This information may be used to optimize the design procedure.

One approach, the Finite Element Method (FEM), provides a means of designing high-frequency connectors without tedious trial and error experimentation. It is also very general in that it enables us to solve problems with irregular geometries that cannot be conveniently handled using conventional approaches. In this presentation, the use of FEM is outlined for the axisymmetric geometries of interest. A bilinear functional is formulated as a first step, and the field solutions are obtained by solving a matrix equation derived from this functional. An absorbing boundary condition is applied at the input and output port boundaries for mesh truncation. A second approach, using the mode-matching method, is also employed to solve some representative discontinuity problems (see figure) and the numerical results obtained from this method are used to compare with those derived from FEM.

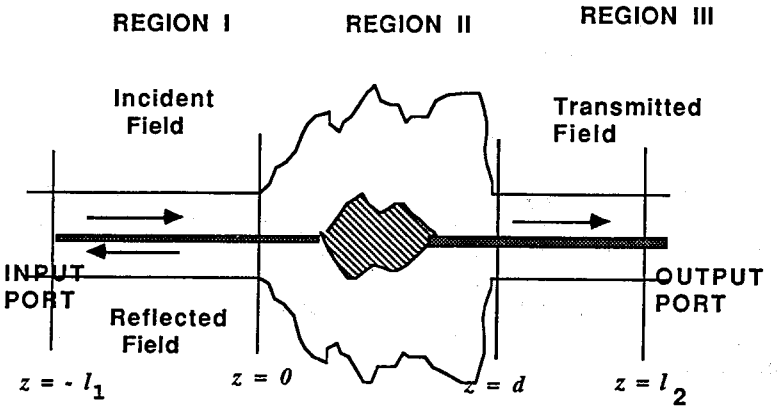

B38.9

MICROWAVE DIRECTIONAL COUPLER DESIGN USING SPECTRAL DOMAIN AND FINITE ELEMENT TECHNIQUE

L. KALIOUBY, Y. CASSIVI, R.G. BOSISIO
Electrical Engineering Department
Ecole Polytechnique of Montreal
P.O. Box 6079, Station A
Montreal, Quebec, CANADA
H3C 3A7

Directional couplers were conventionally done in waveguide technology. However, for low power applications, microwave integrated circuits are increasingly used for that purpose. The first microwave integrated circuits used microstrip (unilayer) technology. Computations for such configurations are relatively simple, well documented and already available on some commercial software packages (e.g. Touchsotne, Super Compacts, etc.). However, single layer microstrip technology suffers too much dispersion and losses at millimeter wave frequencies. In order to circumvent this difficulty, multilayer microstrip technology is now being used. However, computation for such configuration becomes more complex due to the many boundary differential equations involved.

The most efficient known method for the analysis of multilayer configuration is the spectral domain technique. This technique consists in making a Fourier transform of the boundary conditions, and then applying Galerkin's optimization technique in order to determine the charge distribution. The technique is very efficient due to the fact that the solution of the problem can be obtained by simply solving a linear system of equations with a $n_t x n_b$ matrix, where n_t = number of layers, n_b = number of basis functions. The choice of basis functions determines the convergence and precision of results.

Presently, the choice of these basis functions is commonly done on intuitive basis, which may results in imprecision of the impedance value.

Since no technique has yet been developped for the optimization of these basis functions, we are computing them explicitly, using a numerical technique, namely the finite element method.

These results are presently used to develop precise design curves for the multilayer broadside coupler; experimental verification of these curves is also planned.

The present methodology can equally by applied to other multilayer circuit.

FINITE ELEMENT MODELING ON THE DESKTOP USING THE i860 MICROPROCESSOR

George T. Shoemaker
Division of Science Engineering and Technology
The Pennsylvania State University, Erie
The Behrend College
Station Road
Erie, PA 16563-0203

Finite element modeling of electromagnetic scattering has been a popular technique for evaluating complex problems for a number of years. Finite elements have received a great deal of research attention recently as well. This technique has not however been widely applied to three dimensional problems however due to the relatively large finite element meshes required for even simple problems. Due to these large mesh sizes most realistic three dimensional problems solved using finite elements have been solved on super computers since solution on other systems results in excessive solution times. With the introduction of single chip microprocessors capable of near super computer performance it is now possible to carry out three dimensional finite element studies on microprocessor based systems. This should significantly reduce the cost of such studies as well as significantly improve the acceptance of the finite element method as a practical solution technique.

This paper reports early results of a study to determine the performance of the i860 microprocessor when used to solve practical scattering problems using the finite element method. This study when completed should give a realistic view of the performance which can be expected from this new category of system.

Electromagnetic Theory II | **Room 3022 Salle URSI B Session 43** | **Théorie électromagnétique II**

Chairs/présidents: P.L.E. USLENGHI, USA; Z. CSENDES, USA

08:30 (43.1) A Unified Theory of Thin Material Wires, **E.H. NEWMAN**, *Ohio State University, Columbus, OH, USA*

08:50 (43.2) Specialized Formulations for Complex Surface and Material Intersections: A Unified Approach, **J.M. PUTNAM**, L.N. MEDGYESI-MITSCHANG, *McDonnell Douglas Research Laboratories, St. Louis, MO, USA*

09:10 (43.3) Comparison of the Unified Perturbation Method with the Two Scale Expansion, **Y. KIM**, E. RODRIGUEZ, *California Institute of Technology, Pasadena, CA, USA*

09:30 (43.4) Linear Representations of the Microwave Characteristics of Soft Ferrite in Time-Domain Simulation, **J.F. DeFORD**[1], G. KAMIN[1], G.D. CRAIG[1], P. ALLISON[2], M. BURNS[2], L. WALLING[2], [1]*Lawrence Livermore National Laboratory, Livermore, CA, and* [2]*Los Alamos National Laboratory, Los Alamos, NM, USA*

09:50 (43.5) Efficient Evaluation of Integrals with Oscillatory Integrands, **S. SINGH**, R. SINGH, *University of Tulsa, OK, USA*

10:10 **COFFEE/CAFÉ**

10:30 (43.6) Electromagnetic Diffraction by Periodic Wire Grids Experimental and Numerical Results, **C. TESSIERAS**, S. VERMERSCH, *Commissariat à l'Énergie Atomique, Le Barp, France*

10:50 (43.7) Short-Pulse Plane Wave Scattering by a Collection of Flat Strips in the Presence of an Infinite Perfectly Conducting Ground Plane, **L. CARIN**, L.B. FELSEN, *Polytechnic University, Farmingdale, NY, USA*

11:10 (43.8) Analyse fréquentielle de structures multicouches, **Y. CASSIVI**, L. KALIOUBY, R.G. BOSISIO, *École Polytechnique de Montréal, PQ, Canada*

11:30 (43.9) Wire-Grid Modeling Near a Delta-Gap Source in the NEC Code, J. CHOI, **J. PENG**, C.A. BALANIS, *Arizona State University, Tempe, AZ, USA*

11:50 (43.10) On the Numerical Solutions of Eigenvalue Problems, **CH. HAFNER**, *Swiss Federal Institute of Technology, Zurich, Switzerland*

A UNIFIED THEORY OF THIN MATERIAL WIRES

E.H. Newman
Ohio State University
Department of Electrical Engineering
ElectroScience Laboratory
1320 Kinnear Rd. Columbus, Ohio 43212

This paper will present an integral equation and method of moments (MM) solution to the problem of scattering by a thin material wire of circular cross section. In general the material wire has permittivity and permeability different from that of free space. The wire of radius a must be sufficiently thin that $k_0 a \ll 1$, where k_0 is the free space wavenumber. However, there is no restriction on $|k|a$, where k is the wavenumber in the material wire. The method is referred to as *unified* in that it applies to thin material wires of arbitrary complex permittivity and permeability. Thus, a single or unified formulation applies to a low density dielectric/ferrite wire or to a highly conducting metallic wire.

The method is based upon the MM solution of a pair of coupled integral equations for equivalent electric and magnetic volume polarization currents representing the material wire. The unified formulation is obtained by employing piecewise sinusoidal expansion functions which incorporate the proper radial variation of the current density. The expansions include both the longitudinal and radial components of the current, however, the radial component is treated as a dependendent unknown. Numerical results will illustrate the ability of the formulation to treat thin wires with high and low conductivity and/or permittivity.

Specialized Formulations for Complex Surface and Material Intersections: A Unified Approach

J. M. Putnam and L. N. Medgyesi-Mitschang
McDonnell Douglas Research Laboratories
P.O. Box 516, MC 1111041
St. Louis, MO 63166

The method of moments (MM) has been used extensively over the past two decades to solve a variety of scattering/radiation problems involving penetrable bodies. Recently, a class of such problems has been analyzed where the complex intersections of multiple surfaces and material regions require new, more accurate modeling of the surface currents near these intersections and junctions. In these problems, different expansion functions, optimized for the specific surfaces and regions, are used. Specific cases examined include conducting or partially penetrable surfaces with embedded, attached, or partially embedded appendages. The discussion will focus on the current representation at the surface intersections. The intersections may be formed by two-dimensional bodies-of-translation (2D-BOT) and bodies-of-revolution (BOR) with partially embedded infinitesimally thin conducting surfaces of the same or different type penetrating the dielectric region (i.e., BOR-wire, BOR-patch, BOT-plane, etc.). It will be shown that a unified approach to these problems based on integral equation formulations solved by the MM Galerkin technique is computationally attractive. Numerical results are presented to validate the proposed approach and demonstrate its overall utility. A tabulation of optimum expansion functions for the various cases is given.

B43.3

Comparison of the Unified Perturbation Method with the Two Scale Expansion

Yunjin Kim* and Ernesto Rodriguez
Jet Propulsion Laboratory
California Institute of Technology
Pasadena, Ca 91109

We present the Unified Perturbation Method (UPM) which converges over a wider domain of surface roughness than other perturbations such as the small perturbation method, the phase perturbation expansion, and the momentum transfer expansion. It can be shown that UPM possesses the two scale characteristic intrinsically. Even though the conventional two scale theory requires the artificial split of the surface spectrum, the UPM does not require any artificial split.

In order to compare the UPM and the two scale expansion, we expand the induced surface current in the two scale manner using the extinction theorem. The expansion is carried out such that the UPM can be recovered as a limit of this two scale expansion. A similar expansion is developed for the conventional two scale expansion. The scattering cross sections for various surfaces are evaluated for various spectral split. By doing this, we show that the UPM is an optimum expansion theory.

The research described in this abstract was carried out by the Jet Propulsion Laboratory, California Institute of Technology, and was sponsored by Office of Naval Research.

Linear Representations of the Microwave Characteristics of Soft Ferrite in Time-Domain Simulation†

J. F. DeFord*, G. Kamin, and G. D. Craig
Lawrence Livermore National Laboratory
L-626, Livermore, CA, 94550

P. Allison, M. Burns and L. Walling
Los Alamos National Laboratory
MSP-940, Los Alamos, NM 87545

Ferrite plays an important role in many microwave devices, including circulators, phase shifters, inductor cores, etc. In accelerators, ferrite is used to lower the Qs of cavities which are open to the beamline, its field-dependent properties are used to tune RF booster cavities, and in induction machines large quantities of ferrite are used for inductive isolation in the accelerating modules (see Fig. 1).

In order to understand quantitatively the effect that ferrite has on the RF properties of induction accelerator modules, two different material models have been developed and tested for the 2-D, finite-difference, time-domain (FDTD) code AMOS. The simplest model is non-dispersive, and consists of adding the term $\sigma_m \vec{H}$ to Faraday's Law. The value of σ_m is determined experimentally for a given ferrite, and a description of the experimental setup will be given. Results for the calculated induction cavity interaction impedances using this model compare reasonably well with the measured values, and these comparisons will be presented.

To enhance the validity of the model for the broad range of frequencies of interest to the induction module designer, we have incorporated the dispersive nature of the material into a second material model. This model uses the experimentally measured data to compute coefficients in the complex exponential expansion of the permeability $\mu(t)$. Comparisons of the calculated and experimentally measured interaction impedances using this model will be presented.

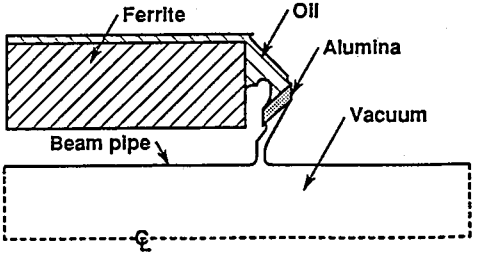

Fig. 1. Cross-sectional diagram of induction cell for Experimental Test Accelerator - II at LLNL.

† Work was performed by the Lawrence Livermore National Laboratory under the auspices of the U. S. Department of Energy under contract No. W-7405-ENG-48.

B43.5

EFFICIENT EVALUATION OF INTEGRALS WITH OSCILLATORY INTEGRANDS

Surendra Singh* and Ritu Singh
Department of Electrical Engineering
The University of Tulsa
Tulsa, OK 74104

In the numerical solution to electromagnetic radiation or scattering problems, one is often faced with the problem of evaluating integrals to a given accuracy. If the integrand is a well behaved function, standard techniques such as Gaussian quadrature, or Simpson's rule would yield a satisfactory result within a reasonably small computer time. In case the integrand exhibits an oscillatory behaviour over an infinite range, simple integration routines yield inaccurate results and moreover the process becomes computationally expensive.

One way to overcome this problem is to employ transform methods to efficiently evaluate such integrals. These transforms, which have previously been used to accelerate the summation of slowly converging series, can be employed to evaluate the integrals. If the integral over a finite range $[a, b]$ is denoted by I, then approximation to I can be obtained by an n point Gaussian quadrature. The approximation denoted by I_n, can be obtained for various values of n, thus arriving at a sequence $\{I_n\}$. From this sequence $\{I_n\}$, another sequence $\{k_n\}$ can be obtained via the use of transform which enables the $\{k_n\}$ sequence to converge faster than the original sequence $\{I_n\}$. The application of two transforms, namely, ρ-algorithm and ϵ- algorithm will be presented. Numerical results will include evaluation of integrals with sinusoidal and Bessel function as integrands.

ELECTROMAGNETIC DIFFRACTION BY PERIODIC WIRE GRIDS EXPERIMENTAL AND NUMERICAL RESULTS

C. TESSIERAS*
S. VERMERSCH
CEA/CESTA - BP2 - 33114 - LE BARP - FRANCE

We compared experimental and numerical results for the reflection coefficient from resistive wire grids. We used two different numerical methods.
- The first is a FDTD method in which we use the YEE scheme and a classical thin wire approximation.
- The other is an Integral Equation method based on a variationnal formulation of the 3D problem and computation of the periodic Green function.
Measurement has been done between 1.7 and 18 GHz on planar grids (30 x 30 cm) parallel to a conducting plane. A typical example is as follows : a grid of resistive wires with spacing 0.5 cm as placed at 0.75 cm above the conducting plane. Conductivity of the wires is 32 Ω^{-1} m^{-1} and diameter is 450 µm. The following figure shows calculated and measured reflection coefficients.

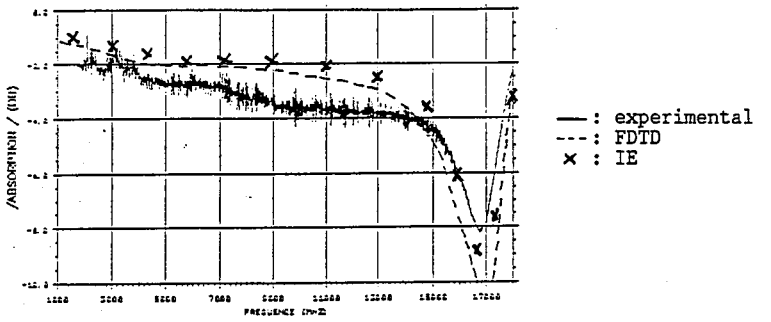

Other examples including different grids, or multilayered structures have shown a very good agreement between theory and experiment.

B43.7

Short-Pulse Plane Wave Scattering by a Collection of Flat Strips in the Presence of an Infinite Perfectly Conducting Ground Plane

Lawrence Carin and Leopold B. Felsen
Weber Research Institute/ Electrical Engineering Department
Polytechnic University
Farmingdale, NY 11735

In remote sensing applications pertaining to clutter environments, and especially for detection of targets in clutter, methods of wideband illumination are receiving increased attention. For very short pulses (VSP), the conventional route, which proceeds via inversion from the frequency domain, becomes computationally impractical and does not furnish insight into the physically observed events. A better suited approach, via an observable-based parameterization (OBP) directly in the time domain, permits resolution of early time multiple scatter as well as later time buildup of spectra by collective reording of multiple (hybrid wavefront-resonance scheme). OBP analysis of VSP plane wave scattering from an infinite periodic array of perfectly conducting flat strips above an infinite perfectly conducting ground plane has been carried out in a companion paper I (P. Borderies, L. B. Felsen, and L. Carin, this meeting). The present study considers finite arrangements of parallel but not necessarily coplanar or identical strips to allow systematic investigation of truncated periodic and nonperiodic arrays, disordered arrays, and "strip targets" in the presence of a strip clutter background. As in paper I, the analytic and numerical reference solution is obtained by CW synthesis from the frequency domain, and it is then converted into direct-time-domain OBP. The problem is analyzed at each frequency by taking a Fourier transform in the transverse spatial direction of the two-dimensional problem. A spectral dyadic Green's function is derived and used in a Galerkin Moment Method procedure from which the induced currents on the strips are calculated. These currents are then used in conjunction with the dyadic Green's function to find the scattered fields. The time domain results are calculated via Fourier inversion of the frequency-domain results. The presentation includes numerical data for various examples and their OBP analysis and interpretation.

ANALYSE FRÉQUENTIELLE DE STRUCTURES MULTICOUCHES

Yves Cassivi*, L. Kaliouby, R. G. Bosisio
Département de génie électrique et informatique
École Polytechnique de Montréal
Montréal (Québec) H3C 3A7

Les structures multicouches se retrouvent dans les technologies MIC, MHMIC et MMIC. Ces structures donnent une dispersion faible. Cet avantage permet d'utiliser la structure à des fréquences plus élevées.

L'analyse de structures multicouches peut s'effectuer de deux façons. La première est l'approximation quasi-statique. Cette méthode est rapide mais ne donne pas la fréquence limite à laquelle les résultats sont encore valables. La seconde méthode est d'utiliser les équations de Maxwell directement. On obtient alors le comportement fréquentiel de la structure. Pour garder les manipulations analytiques à un niveau faible, on résoud ces équations différentielles par la méthode des éléments finis. Et pour illustrer le bon fonctionnement de la méthode, nous analysons un coupleur à lignes superposées (*'broadside coupler'*). Le comportement fréquentiel de ce dispositif n'a pas encore été étudié.

Sachant que le milieu analysé est linéaire, non-homogène, sans charge d'espace et sans perte, on utilise les relations $\nabla \times \vec{H} = w\epsilon_o\epsilon_r\vec{E}$, $\nabla \times \vec{E} = -w\mu_o\mu_r\vec{H}$ et $\nabla \cdot \vec{H} = 0$. Après plusieurs manipulations, nous obtenons la fonctionnelle suivante : $F(\vec{H}) = \int\int_\Omega \left[(\nabla \times \vec{H})^* \epsilon_r^{-1}(\nabla \times \vec{H}) + (\nabla \cdot \vec{H})^* \mu_r (\nabla \cdot \vec{H}) - k_o^2 \vec{H}^* \cdot \vec{H}\right] d\Omega$. Cette équation représente l'énergie dans la structure. En appliquant la méthode des éléments finis et en minimisant l'énergie dans la structure, on obtient un système d'équations que l'on résoud pour obtenir les modes de propagation possible dans la structure. Pour l'analyse du coupleur, on calcule les caractéristiques des modes pair et impair , en utilisant les murs de symétrie appropriés pour diminuer le temps de calcul.

Nous montrons que pour un coupleur formé d'un substrat de permittivité relative $\epsilon_r = 4.0$, d'une épaisseur de $9mm$, et de deux conducteurs de largeur de $10mm$ (épaisseur négligeable), tous placés dans un boitier de $55mm$ de hauteur et de $100mm$ de largeur, les caractéristiques des modes pair et impair sont :

f GHz	ϵ_{effp}	Z_p Ω	ϵ_{effi}	Z_i Ω	Z_o Ω	C dB
0	1.3	180	1.7	46	91	4.5
2.0	1.38	200	1.8	50	96	4.4
2.55	1.46	255	1.83	52	115	3.59

Ce tableau montre qu'avec les calculs quasi-statique ($f = 0Hz$), le coupleur devrait avoir un couplage C de 4.5 dB à une fréquence d'opération de 2.0 GHz ou 2.55 GHz. Cependant, avec les calculs fréquentiels, nous obtenons C = 4.4 dB à $f_o = 2.0GHz$ et C = 3.59 dB à $f_o = 2.55GHz$. Donc à $2GHz$, les calculs quasi-statique sont encore valable, mais à $2.55GHz$, nous obtenons une erreur de 25 % sur le couplage.

B43.9

WIRE-GRID MODELING NEAR A DELTA-GAP SOURCE IN THE NEC CODE

Jaehoon Choi, Jian Peng*, and Constantine A. Balanis
Department of Electrical Engineering
Telecommunications Research Center
Arizona State University
Tempe, AZ 85287-7206

In this paper, we are investigating how the wire-grid geometry modeling of the NEC code near a delta gap voltage source is affecting the radiation characteristics of antennas. Three different aspects of geometry modeling are considered to see how the electromagnetic quantities, such as input impedance and far field amplitude patterns, are affected. First, the effects of the segment size are examined using different segment lengths. Since the basis functions (pulse plus sine plus cosine) used in the NEC code are dependent not only on the individual segment size but also upon the length of neighboring segments, the segmentation scheme, especially near a delta-gap generator, is very important to predict the correct radiation characteristics. Second, the effects of the radii of the wire segments are explored. Finally, the wire-grid scheme near the junction of the antenna element and the ground plane is examined for antenna characteristics variation and stability.

As numerical examples, the antenna patterns of a center-fed dipole and a monopole mounted on a finite size PEC ground plane are predicted using the NEC code. The results are compared to measured data. Also radiation patterns of a monopole mounted on a helicopter structure are evaluated using different modeling schemes. Based on our extensive applications of the NEC code to various geometries, guidelines for the geometry modeling near a delta gap source are suggested.

ON THE NUMERICAL SOLUTIONS OF EIGENVALUE PROBLEMS

Ch.Hafner, Inst.f.Feldtheorie, Swiss Federal Institute of Technology,
ETH Zentrum, CH-8092 Zürich, Switzerland

To compute the electromagnetic fields in resonators and waves on cylindrical structures, the solution of a nonlinear eigenvalue problem is required. Usually, the eigenvalues are derived from a transcendent equation that has to be solved iteratively. Afterwards, the eigenfunctions can be determined. In most codes, the transcendent equation is written as the determinant of a square matrix that has to be zero. Since the elements of the matrix are functions of the eigenvalue, the determinant is a complicated function of the eigenvalue as well. Nonetheless, the numerical computation of the zeros of the determinant is not a severe problem and the eigenvalues can be obtained with a very high accuracy. Difficulties arise because the order of the matrix is infinite in most cases. Thus, one has to select the "most important" part of the matrix and to omit an infinite number of rows and columns. The zeros of the determinant of the resulting finite matrix can still be computed very accurately, but the accuracy of the zeros does not give any idea about the accuracy of the results. Beside inaccurate solutions, physically wrong (spurious) modes can be obtained. Although inaccurate results can be improved by increasing the order of the matrix, obtaining reliable values of the eigenfunctions and of the eigenvalues turns out to be difficult.

The procedure of handling eigenvalue problems in the MMP code is different from the procedure outlined above and can bring some more insight. In the MMP code overdetermined systems of equations, i.e., rectangular matrices are solved directly. The determinant of rectangular matrices is not defined. Thus, one is forced to find another technique for solving eigenvalue problems. The most simple idea of searching minima of the sum of the squares of the residuals instead of zeros of the determinant leads to completely wrong results, even if one is aware of the importance of a correct scaling of overdetermined systems of equations. Analyzing the situation, one finds that the procedure usually tends to results that can be considered to be a numerical approximation of the trivial but not interesting zero-field solutions. To avoid such solutions, one has to define and to fix the amplitude of the eigenfunction to be computed. As a consequence, the eigenvalue cannot be computed without a simultaneous computation of the eigenfunction. In each iteration, an approximation of the eigenvalue is estimated first. In a second step the parameters P0 that determine the eigenfunction and the residuals R0 are evaluated under the assumption that one of the parameters is equal to one. From this, one computes the amplitude A0 and divides P0 and R0 by A0 in order to get the set P=P0/A0, R=R0/A0 with fixed amplitude A=1. The sum S of the squares of the residuals R is a function of the eigenvalue. The search for its minima usually leads to useful results. Moreover, the value and shape of S around the minima gives some important information on the accuracy of the results: Low values of S mean that the eigenfunction has been computed accurately, whereas the eigenvalue is obtained accurately if S has a sharp minimum.

Especially at low frequencies, the function S can be very flat. This means that the eigenvalues cannot be determined accurately even if the eigenfunctions can be computed with a high precision. In such cases, the eigenvalues are obtained much easier - without an iterative procedure - from integral conditions that are derived from energy conservation and similar theorems.

Role of Electromagnetic Modeling in Electronic Packaging

Room 2050 Salle URSI B Session 52

Le rôle de la modélisation électromagnétique dans la mise sous boîtier de circuits électroniques

Chairs/présidents: R. MITTRA, USA; B.J. RUBIN, USA

13:50 (52.1) Full-Wave Modeling of Signal Propagation and Radiation in Electronic Packages, **B.J. RUBIN**, *IBM T.J. Watson Research Center, Yorktown Heights, NY, USA*

14:30 (52.2) Electromagnetic Modeling in VLSI Interchip Packaging, **C.C. GORDON**, S.Y. POH, *Digital Equipment Corporation, Andover, MA, USA*

15:10 **COFFEE/CAFÉ**

15:30 (52.3) Electrical Issues in Design, Characterization and Optimization of Digital VLSI Packages, **U.A. SHRIVASTAVA**, *Motorola Inc., Phoenix, AZ, USA*

16:10 (52.4) Computational Techniques for Electromagnetic Modeling of Electronic Packages – A Review, **R. MITTRA**, *University of Illinois, Urbana, IL, USA*

B52.1

FULL-WAVE MODELING OF SIGNAL PROPAGATION AND RADIATION IN ELECTRONIC PACKAGES

B. J. Rubin, IBM T. J. Watson Research Center, Yorktown Heights, NY 10598

The electrical characteristics of arbitrarily shaped, 3D electronic packages are calculated using two complementary frequency-based, moment-method approaches. In each approach, the conduction currents are represented using two-dimensional rooftop expansion functions; finite-size dielectric regions are first replaced by a three-dimensional array of interlocking thin-wall sections having appropriate surface impedance so that the volume polarization can be also represented by rooftop functions. Application of the electric field boundary condition through the use of line function testing yields a matrix equation that may be solved for the current distribution and propagation characteristics.

In the first approach (B. Rubin, IBM J. Res. Develop, 34, 585-600, July 1990 and B. Rubin, IEEE Trans. Microwave Theory Tech., MTT-38, 807-812, June 1990), the structure of interest is considered to be a unit cell of a periodic structure. From the propagation constants, resultant currents, and line integrals of electric field, equivalent circuit parameters are then determined. Though the inherent periodicity, from experience, does not significantly limit the types or geometries of structures that can be analyzed, this approach is well-suited for determining signal propagation and crosstalk but is not appropriate for determining such quantities as radiation. The second approach (B. Rubin and S. Daijavad, IEEE Trans. Antennas Propagat., AP-38, 1863-1873, Nov. 1990) deals with finite-sized structures, and gives the radiated fields and input impedance. Equivalent circuits may be inferred from the input impedance, which may be calculated as a function of frequency. For instance, the static capacitance and inductance may be obtained from the low frequency input impedance of appropriate open- and closed-loop structures.

These approaches have been proven to work over a wide range of geometries and frequencies. They consistently give results that agree with previously known solutions and experimental measurements; and the results consistently display numerical convergence as the subsection grid is made finer. This consistency is essential for accurate package characterization. For example, as the geometrical parameters of a via and its surrounding environment are varied, the structure may become indistinguishable from a connector or signal line structure. Package analysis must provide results that smoothly vary as geometries and material compositions change, otherwise confidence in the results is lost. This consistency would not be possible if a number of widely differing approaches were used, in piecemeal fashion, to characterize the package.

Each package element, such as signal line or connector, is first determined to be most suitable for analysis by the first or second approach. Examples of the former are the signal line structures in multi-chip modules and some connector structures. Examples of the latter are other connector structures, T03-type packages, and finite-size microstrip structures. In the paper, the basic concerns in electrical analysis of packages are briefly reviewed and the moment-method approaches are discussed. A number of structures are analyzed, including signal lines, vias, connectors, microstrips, patch antennas, and shielding enclosures. Comparisons between calculated and measured results are given where possible.

ELECTROMAGNETIC MODELING IN VLSI INTERCHIP PACKAGING

Colin C. Gordon* and Soon Y. Poh
Physical Technology Group
Digital Equipment Corporation
Andover, Massachusetts 01810

As the complexity, density, and operating speed of computer systems continue to increase, greater emphasis is placed on accurate prediction of the electrical performance of the VLSI interchip interconnect. Offchip signals have frequency bandwidths extending into the microwave region, and require interconnect models founded on appropriate electromagnetic theory.

This paper will describe the manner in which electromagnetic modeling and analysis is integrated into the development of VLSI interchip packaging for advanced digital computer systems. First, electrical models for the component parts of the interconnect system are developed from their physical geometries using boundary element parameter estimation tools. The validity of the quasistatic approximations upon which these tools are based must be verified for the system frequency bandwidth. These interconnect component models, which may consist of either distributed (transmission line) or lumped parameters, are then used with appropriate models for the onchip active devices in conventional time domain simulators to predict system performance. As prototypes of the interconnect system components become available, broadband S-parameter measurements are taken, from which electrical model parameters are extracted and used to refine the system simulation models.

Electromagnetic modeling is also employed to assess the levels of electromagnetic emissions emanating from the interconnect system. The potential for electromagnetic interference (EMI) is enhanced when the electrical dimensions of the chip package conductors become sizable. Radiation models are developed for key components in the chip packaging environment which provide a means of addressing EMI concerns during the initial design phase, rather than relying on increasingly inefficient and cost-prohibitive corrective measures at the system level to meet regulatory emissions limits.

B52.3

ELECTRICAL ISSUES IN DESIGN, CHARACTERIZATION AND OPTIMIZATION OF DIGITAL VLSI PACKAGES

U. A. Shrivastava
Motorola, Inc. Mail Stop B136
5005 E McDowell Road
Phoenix, Az, 85008

High performance IC packages require careful electrical design to minimize speed and noise penalties. Fortunately, analysis and design techniques developed for analog microwave circuits can be used in digital package design, such as the use of the results of an S parameter analysis in subsequent transient analysis. Some of the differences between analog microwave and digital systems, however, must be considered before efficient implementation of microwave techniques in digital package design. Also, presently available tools have their limitations. For example, accurate modeling of coupled noise in pin grid array packages is very difficult and time consuming. Further, most of the package analysis tools limit the designer to analyze each response individually, and lack facilities for optimization, and design centering.

In this paper, the above issues are addressed. A list of IC, component package and board parameters which affect speed and noise performance of a digital system are identified, along with competing electrical response parameters of single chip (level 1) packages and multichip (level 2) packages. Software tools and measurement methodologies used to analyze these package issues are discussed. The role of electromagnetics, in those areas where it applies, will be highlighted.

In this paper, a number of desirable directions for package electrical analysis are then suggested. For instance, the integration of digital and analog design software and the use of statistical methods when accurate mechanistic models are not available. Since higher device densities and speed increase power dissipation of electronic systems and thus further complicate package design, it may be desirable to tightly couple electrical design with thermo-mechanical design. Response surface methodology based tools can be integrated with electrical (and, eventually with thermo-mechanical) software to develop optimum and robust designs. Examples of design tools of varying levels of complexity, speed, accuracy and ease of use that are needed to facilitate electrical system designs will be presented.

Computational Techniques for Electromagnetic Modeling of Electronic Packages- A Review

Raj Mittra
Electromagnetic Communication Laboratory
University of Illinois, Urbana, IL 61801

In this review paper, we present a brief summary of the computational techniques for electromagnetic modeling of electronic packages for digital and communication circuit applications. We consider the problems of simulating the crosstalk and edge degradation of digital signals propagating in multiconductor transmission lines terminated by nonlinear devices. We discuss both the quasi-static and full-wave approaches to deriving the equivalent circuits of microstrip discontinuities, such as bends, tapers and vias, in a form that can be directly utilized in SPICE-like simulation programs. We address the issue of estimating the upper frequency limit of the validity of the quasi-TEM models of transmission lines and discontinuities. We review the developmental status of some general purpose computer algorithms, e.g., the transmission line matrix(TLM) and the Finite Difference Time Domain(FDTD) methods, that are useful for EM modeling problem of arbitrary three-dimensional configurations of interest to the package designer. We include some numerical results for signal propagation through a variety of microstrip discontinuities, obtained through the use of these algorithms. We also address the problem of estimating the delta-I noise in power planes that can cause undesirable fluctuations in the voltage levels of the power supply of electronic packages. Finally, we examine the problem of spurious radiation from these packages and present techniques for estimating the level of untoward radiation from arbitrarily-oriented microstrip etches on a circuit board, as well as from slits in enclosures or reference planes.

Asymptotic Representations of Waves | **Room 3006 Salle URSI B Session 55** | **Représentations asymptotiques des ondes**

Chairs/présidents: E.V. JULL, Canada

13:30 (55.1) The Caustic Phase Anomaly Revisited, **P.O. IVERSEN**[1], Y. RAHMAT-SAMII[2], [1] *LJR Inc., Torrance, CA, and* [2] *University of California, Los Angeles, CA, USA*

13:50 (55.2) Modified WKB Method by Correcting the Phase Shift at the Turning Point, **F. XIANG**, G.L. YIP, *McGill University, Montreal, PQ, Canada*

14:10 (55.3) Asymptotic Evaluation of the Field Radiated by a Dipole on a Cylindrical Dielectric Substrate, **K. NAISHADHAM**[1], L.B. FELSEN[2], [1] *Wright State University, Dayton, OH, and* [2] *Polytechnic University, Farmingdale, NY, USA*

14:30 (55.4) An Equivalent Edge Current Formulation Including Edge Interaction Effects for Flat Plate Structures, **O. BREINBJERG**, *Technical University of Denmark, Lyngby, Denmark*

14:50 (55.5) A New Asymptotic Feature of the Field Scattered by a Polygonal Plate, M.V. VESNIK[1], **P.Y. UFIMTSEV**[2], [1] *USSR Academy of Sciences, Moscow, USSR;* [2] *University of California, Los Angeles, CA, USA*

15:10 (55.6) On the Backscatter Caused by Waves Traveling Along a Finite Length Body of Constant Section, **K.M. MITZNER**, *Northrop Corporation, Pico Rivera, CA, USA*

15:30 (55.7) High Frequency Scattering by Complex Open Cavity Structures, **R.-C. CHOU**, R.J. BURKHOLDER, P.H. PATHAK, *Ohio State University, Columbus, OH, USA*

15:50 (55.8) An Improved Method of Calculating Numerical Diffraction Coefficients, **M.P. HURST**, *McDonnell Douglas Research Laboratories, St. Louis, MO, USA*

16:10 (55.9) Uniform Asymptotic Solution for the Diffraction by a Discontinuity in Curvature at Grazing Incidence with Creeping Wave Launching, **F.A. MOLINET**, *Societé MOTHESIM, Le Plessis-Robinson, France*

16:30 (55.10) GTD and Reciprocity, **D. BOUCHE**, *Commissariat à l'Énergie Atomique, Le Barp, France*

16:50 (55.11) On the Asymptotic Frequency Behavior of Uniform GTD in the Shadow Region of a Smooth Convex Surface, **P. HUSSAR**, R. ALBUS, *IIT Research Institute, Annapolis, MD, USA*

THE CAUSTIC PHASE ANOMALY REVISITED

P. O. Iversen*
LJR, Inc.,
A Subsidiary of EMS, Inc.
3051 Fujita St., Torrance, CA90805

Y. Rahmat-Samii
Department of Electrical Engineering
University of California, Los Angeles
Los Angeles, CA 90024-1594

One century ago Frenchman Gouy predicted that a wave traveling through a focal point experiences a rapid 180° phase change. This phase shift has been treated repeatedly in the optics field and has become known as the Phase Anomaly. A more general treatment reveals that there is a 90 degree phase shift as a wavefront passes through a single caustic.

In this paper attention is given to the phase characteristics near the focal point of an offset ellipsoidal reflector. It is shown that the phase shift is predicted by Geometrical Optics (GO), Gaussian Beam, and Physical Optics (PO) techniques. The phase shift appears in the divergence factor of the GO solution, in the form of an arctangent in the exponent for the Gaussian beam solution, and as a result of a sign change in the kernel of the radiation integral for the PO solution. For systems with a small subtended angle α, the phase changes slowly, while when α is large the phase change is abrupt. Figs. 1 and 2 show a plot of the phase of a wave traveling through a focal point normalized to the distance traveled for two different geoemetries.

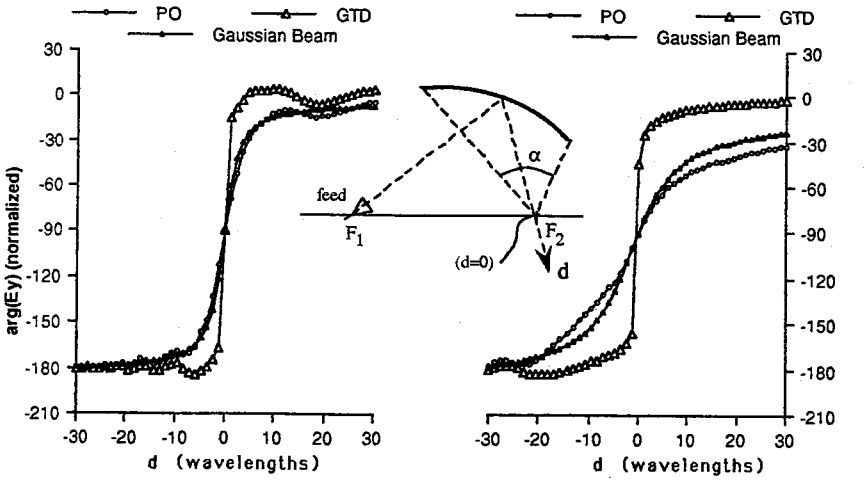

Fig. 1 $\alpha = 50°$

Fig. 2 $\alpha = 25°$

MODIFIED WKB METHOD BY CORRECTING THE PHASE SHIFT AT THE TURNING POINT

F. XIANG* and G.L. Yip
Guided Wave Optics Laboratory
McGill University, Dept. of Electrical Eng.
3480 University Street
Montreal, Quebec, Canada H3A 2A7

The WKB method has been widely used to obtain approximate solutions of the guided mode propagation constants for optical waveguides with slowly varying graded-index profiles. One of the key features of this method is the assumption of a constant phase shift ($\pi/4$) at the turning point. However, with the presence of index discontinuity near the turning point, the phase shift is no longer a constant. Here, we present analytical closed form expressions of this phase shift, where both the index discontinuity and the index slope discontinuity have been taken into account.

The principle of this phase shift modification is based upon two main points. The first consists of using Airy functions as the field solutions at the discontinuity. The second point is that the introduction of virtual turning points makes the modification suitable for many types of discontinuities. The expressions of the modified phase shift can be easily computed numerically. The figure below shows an example of a given index profile with a significant improvement over the conventional WKB method, especially near the mode cutoffs. At cutoffs, our result of the phase shift is $\pi/12$ instead of $\pi/4$ or zero for a waveguide with a truncated index profile. We also found the phase shift expression of a total internal reflection at an index discontinuity where the index slopes on both sides of the discontinuity have been considered.

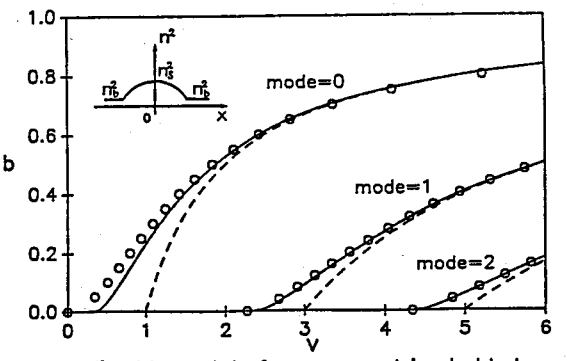

Fig. Normalized b–v plots for a symmetric cladded–parabolic profile: o exact (staircase method), - - WKB, —— modified WKB.

B55.3

ASYMPTOTIC EVALUATION OF THE FIELD RADIATED BY A DIPOLE ON A CYLINDRICAL DIELECTRIC SUBSTRATE

Krishna Naishadham
Department of Electrical Engineering
Wright State University
Dayton, OH 45429

L. B. Felsen
Department of Electrical Engineering
Polytechnic University
Farmingdale, NY 11735

The circular cylindrical dielectric multilayer is an important prototype for the study of conformal antennas on a nonplanar substrate. A detailed analysis of the dyadic Green's functions of the layered environment is necessary to determine the radiation by elements embedded in the multilayer. In this paper we determine asymptotically by the saddle point method, complex integration and residue calculus the field radiated by an axial dipole located on or outside a conductor–backed dielectric substrate. Similar considerations apply to an azimuthally oriented dipole; the total field due to an arbitrarily shaped element on the substrate can be synthesized from these two contributions.

The Green's functions for the multilayer are best expressed in terms of a double integral representation over continuous spectra of the complex azimuthal wavenumber (ν) (with the azimuthal spatial (ϕ) domain extended to infinity), and the axial wavenumber (β) (L.B. Felsen and K. Naishadham, Radio Science, 26, 1991). For large $\kappa_0 b$, where "b" is the radius of the substrate and κ_0 is the radial wavenumber in the outermost layer, the cylinder functions in the ν–integrand may be reduced by Debye approximations to trigonometric or exponential functions. The integral is evaluated by saddle point asymptotics along steepest descent paths for extraction of the direct and specularly reflected fields, and by contour deformation around the ν–plane simple poles of the integrand for contributions from multiple circumnavigations of surface–guided leaky, creeping and trapped modes (L.B. Felsen, J.M. Ho and I.T. Lu, J. Acoust. Soc. Am., 87, 543–569, 1990). To simplify the ν–plane root search, the exact dispersion equation is solved by asymptotic approximations for the cylinder functions and subsequent quasiplanar approximations. The range of validity of this simple model is established by comparison with exact solutions. Results are obtained first for the two–dimensional case of phased line source excitation, which does not involve the β–integral, and they are then generalized to synthesize the dipole excitation. The numerical data reveals the influence of the various substrate parameters (dielectric constant, thickness, radius, etc.) on the radiation characteristics of the dipole.

An Equivalent Edge Current Formulation Including Edge Interaction Effects For Flat Plate Structures

Olav Breinbjerg
Electromagnetics Institute,
Technical University of Denmark
DK-2800 Lyngby, Denmark

The high-frequency approximation for the bistatic radar cross section of flat plate structures is significantly improved when the edge interaction effects are taken into account. The present approach is formulated in terms of equivalent edge currents (EEC) because, for polygonal structures, the conventional ray-optical techniques fail due to the lack of isolated stationary edge points. Three constituent parts of the surface current induced on the scattering structure are taken into account here. First, the physical optics (PO) current, the field of which can be exactly represented by a set of POEEC's. Secondly, the fringe wave (FW) current excited at the leading edge by the incident plane wave and, thirdly, the FW current excited at the trailing edge by the incident leading edge current. Consequently, the first-, the second-, and part of the third-order edge effects are included. The leading edge current is approximated by the FW current excited on a half plane conforming to the actual structure at the leading edge point and illuminated by the plane wave. In order to approximate the trailing edge current, it is noted that for a half plane illuminated at grazing incidence, the excited FW current can be expressed in terms of the incident PO current at the edge. By way of analogy, the two components of the trailing edge current are given the same functional dependence on the value of the incident leading edge current at the trailing edge point :

$$J_{T,\perp}(u) = J_{L,\perp}\frac{-2e^{j\pi/4}}{\sqrt{\pi}}F(\sqrt{2ku}\sin\beta')\exp(-jku\cos 2\beta')$$

$$J_{T,\parallel}(u) = J_{L,\parallel}\frac{-2e^{j\pi/4}}{\sqrt{\pi}}\left(F(\sqrt{2ku}\sin\beta') - \frac{e^{-j2ku\sin^2\beta'}}{j\sqrt{2ku}\sin\beta'}\right)\exp(-jku\cos 2\beta')$$

J_T is the trailing edge current, J_L the value of the leading edge current at the trailing edge point, u is the distance along the trailing edge Keller cone, β' the cone half angle, and F denotes a Fresnel function. For both the leading and trailing edge currents, the directions of propagation along the respective Keller cones are taken into account. The approximate FW currents are subsequently cast into one set of PTDEEC's to be placed at the leading edge.

The scattered field is found by performing one single integration over the POEEC's and the PTDEEC's along the edge of the structure. Numerical results for the disc and the square plate are presented and compared to an exact and a moment method solution, respectively.

B55.5

A NEW ASYMPTOTIC FEATURE OF THE FIELD SCATTERED BY A POLYGONAL PLATE

Michail V. Vesnik
Institute of Radioengineering and Electronics
USSR Academy of Sciences, K. Marx Avenue 18,
Moscow, 103907, USSR
and
Peter Y. Ufimtsev *
Department of Electrical Engineering
University of California, Los Angeles
Los Angeles, CA90024

Plane wave scattering from a polygonal plate is investigated in the framework of Physical Optics. Reflection and transmission coefficients are used to describe the scattering behaviour of various plates, including perfectly absorbing, perfectly reflecting, and semi-transparent lossy plates. As is known, the scattered far field is the sum of waves scattered by the vertices.

A new asymptotic feature of this solution has been established. The algebraic sum of all the vertex diffraction coefficients is zero for any direction of scattering. Thus the scattering is due to relative phase shifts between waves from individual vertices. The nature of this phenomenon is discussed.

ON THE BACKSCATTER CAUSED BY WAVES TRAVELING ALONG A FINITE LENGTH BODY OF CONSTANT SECTION

K. M. Mitzner
MS W944/AP B-2 Division Northrop Corporation
8900 Washington Blvd., Pico Rivera, California 90660

In a recent paper ("How End Effects Alter the Backscatter Pattern for a Body of Constant Section," 1990 URSI Meeting, Dallas, Texas) we applied Ufimtsev's Physical Theory of Diffraction (PTD) to far-field backscatter of a plane wave from a finite length body of constant section with end terminations, and we obtained a general form solution for the case in which the traveling waves induced at each end damp out to negligible amplitude before reaching the other end.

This paper extends the theory to the case in which the traveling waves do not damp out in less than one transit. Each traveling wave then gives rise to a backscatter amplitude pattern with lobe structure set by the sinc function

$$\frac{\sin\,[(k\,\sin\,\theta - \alpha k)L/2]}{(k\,\sin\,\theta - \alpha k)L/2}\,.$$

Here L is the effective length of the constant section, θ is the obliquity angle of incidence and backscatter as measured from the plane normal to the axis of length L, k is the free space wave number, and αk is the wave number of the traveling wave. The relative phase velocity α can be complex, with the sign of the real part indicating the direction of phase propagation along the axis and with the magnitude close to unity for a large class of problems.

Both the scattering caused by the traveling waves and the direct edge scattering can be described by rays emanating from the two ends of the body. These effects are blended together smoothly in a typical backscatter pattern so that direct scattering dominates near normal incidence to the axis and traveling wave scattering dominates near grazing.

B55.7

HIGH FREQUENCY SCATTERING BY COMPLEX OPEN CAVITY STRUCTURES

Ri-Chee Chou*, Robert J. Burkholder, and Prabhakar H. Pathak
The Ohio State University ElectroScience Laboratory
1320 Kinnear Road, Columbus, Ohio 43212

There has been considerable recent interest in the electromagnetic scattering from the interior of open-ended cavity structures. Ray shooting approaches such as the shooting and bouncing ray (SBR) method (H. Ling, R. Chou, & S.W. Lee, *IEEE Trans. Antennas and Prop.* 37, 194-205, 1989) and the generalized ray expansion (GRE) method (P.H. Pathak & R.J. Burkholder, *Radio Science* 37, Jan-Feb 1991), have been developed that, within the high frequency limitations, place virtually no restrictions on the shape of the cavity and allows more realistic modeling of inlets and ducts. But while these methods can, in principle, be used to compute the scattering by relatively arbitrarily shaped cavities, published works have been generally restricted to fairly simple analytically described surfaces for computational and other reasons. This paper will discuss the modeling aspects as well theoretical and computational issues in the application of SBR and GRE methods to increasingly complex analytically describable cavity models.

One very versatile analytically described model used for duct modeling is the generalized super-ellipse (S.W. Lee, R. Chou, H. Ling, *SBRI: Computer Code for Calculating RCS of an S-Inlet*, University of Illinois Technical Report, Aug. 1988). By letting every parameter of the super-ellipse be a function of the the cavity axial coordinate as well as including axial "lofting" functions, S-bend or other shaped ducts with non-uniform cross sections, e.g. an S-bend duct with a rectangular aperture that transitions smoothly to an circular termination, can be described using a single equation. Several super-elliptical sections can be combined to model more complex duct shapes. Results shown will include the modeling of and scattering from multi-sectioned super-ellipses and bifurcated duct geomeries, neither of which have been previously treated.

In the GRE, the cavity aperture is divided into smaller subapertures, and the incident field in the aperture is replaced by equivalent surface currents which radiate the desired fields from each subaperture into the cavity. Previous implementations of the GRE have been restricted to the use of rectangular subapertures. Thus GRE was limited to cavities with rectangular apertures. The generalization of the GRE method to non-rectangular apertures will be also discussed.

AN IMPROVED METHOD OF CALCULATING NUMERICAL DIFFRACTION COEFFICIENTS

M.P. Hurst
McDonnell Douglas Research Laboratories
P.O. Box 516
St. Louis, MO 63166

Diffraction coefficients in analytic form are known only for a small number of canonical geometries. Ray-optics techniques can, however, be applied to a much broader class of geometries if one uses diffraction coefficients in numerical form, as shown by Herrmann (G.F. Herrmann, *IEEE Trans. Antennas Propagat.*, vol. AP-35, pp. 53–61, 1987). In the method given by Herrmann diffraction coefficients are obtained by first analyzing finite bodies using the method of moments and isolating the contribution of a single scattering center by applying windowing functions to the calculated current. The radiated field is then computed and an appropriate shadow boundary singularity is grafted on to yield the desired diffraction coefficient. This method gives imperfect results for geometries which support wave propagation along the surface (such as the conducting half-plane, H-polarization case), and fails for diffraction angles near grazing.

In this paper a new method will be described which yields numerical diffraction coefficients near grazing angles and provides improved accuracy at other angles. As in Herrmann's method, a finite body having a scattering center of the type of interest is analyzed using the method of moments. In this method, however, no attempt is made to suppress diffraction from other scattering centers. Rather, the scattered field contributions from different mechanisms are separated through the solution of low-order simultaneous equations. These equations are obtained by assuming the total scattered field from a finite body can be described in terms of scattering centers and fitting the unknown diffraction coefficients to the moment method data. Multiple bodies must be analyzed (one for each unknown diffraction coefficient). For near-grazing diffraction angles the near fields of the finite bodies are used in conjunction with Uniform Theory of Diffraction (UTD) 'correction factors,' while for other angles far fields are used to obtain the far-field diffraction coefficients directly, including the correct shadow boundary singularity. Because the unknown coefficients are extracted from total scattered field data, the present method can also be applied in the context of measured data.

The accuracy of the method will be established by comparing calculated and exact diffraction coefficients for the conducting half-plane. Frequency selective surfaces will be shown to be amenable to UTD analysis through several two-dimensional examples. Both near- and far-field examples will be given in the paper with comparisons to direct moment method calculations.

B55.9

UNIFORM ASYMPTOTIC SOLUTION FOR THE DIFFRACTION BY A DISCONTINUITY IN CURVATURE AT GRAZING INCIDENCE WITH CREEPING WAVE LAUNCHING

Frédéric A. MOLINET

Société MOTHESIM, La Boursidière

RN 186 - 92357 LE PLESSIS-ROBINSON, France

The existing Geometrical Theory of diffraction solution for the diffraction by a discontinuity in curvature on a perfectly conducting cylindrical surface including the effect of the creeping wave launched by the discontinuity, is extended to grazing incidence. The extended solution is continuous when the observation direction crosses the boundary at $\phi = 0$ between the discontinuity diffracted and surface diffracted rays and when the direction of incidence approaches $\pi - \phi$.

The solution is given in the form of a difference of two Fock type functions involving incomplete Airy functions. It has been established by approaching the currents on both sides of the curvature discontinuity by Fock currents and by using an extended Ufimtsev's correction in order to take into account the contribution of the fringe currents.

GTD AND RECIPROCITY

D. BOUCHE CEA CESTA
BP N°2 33114 LE BARP FRANCE

In this paper, we examine the question of the satisfaction of the reciprocity theorem in the context of GTD, by considering the problems of scattering and radiation involving a perfectly conducting body. Let us first consider a perfectly conducting obstacle illuminated by an electromagnetic plane wave (RCS handbook, Chapter 1). The currents at a point M in the shadow zone are given, to a leading order in k, by Fock fuctions multiplied by a convergence factor for the surface rays. This convergence factor is the ratio of the width of an infinitesimal pencil of surface rays, at the shadow boundary (d y) and at the point where the current is computed (d y'), as shown in the following figure

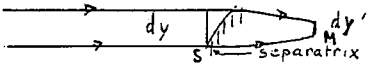

Next, let a magnetic current source be situated on a perfectly conducting surface (Pathak IEEE AP, 1981). The radiation of this source at infinity is given by Fock functions multiplied by a convergence factor $\sqrt{\frac{d\Psi}{d\Psi'}}$. This convergence factor is the ratio of the angular width of an infinitesimal pencil of surface rays at the position of the source (d Ψ) and at the detachment point (d Ψ'), as depicted in the following figure.

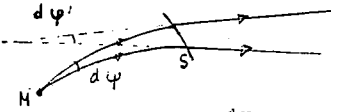

The convergence factors $\sqrt{\frac{dv}{dy'}}$, and $\sqrt{\frac{d\Psi}{d\Psi'}}$ can be computed by introducing a semi geodesic coordinate system. It is shown that these factors depend only of the value of the gaussian curvature along the geodesic line SM. However, the two precedings problems are related by reciprocity, and this implies the equality of the convergence factors $\sqrt{\frac{dy}{dy'}}$, and $\sqrt{\frac{d\Psi}{d\Psi'}}$. We show that this equality occurs only if the gaussian curvature along the geodesic SM is constant .

For the case of two dipole sources (1) and (2) separated by a perfectly conducting smooth convex surface Ω, we show by the same technique that reciprocity is satisfied if and only if the gaussian curvature of Ω along each creeping rays between (1) and (2) is constant.

B55.11

ON THE ASYMPTOTIC FREQUENCY BEHAVIOR OF UNIFORM GTD IN THE SHADOW REGION OF A SMOOTH CONVEX SURFACE†

P. Hussar* and R. Albus
IIT Research Institute
185 Admiral Cochrane Drive
Annapolis, MD 21401

A number of canonical plane-wave and line-source solutions involving circular cylinders have led to a widely accepted uniform Geometrical Theory of Diffraction (GTD) formulation for the scattered electromagnetic field in the shadow region of a smooth convex surface. The uniform GTD formulation consists of the linear combination of a transition function in the form of a Fresnel integral and a Pekeris caret function that reproduces the original GTD result in the deep shadow region. The current uniform GTD shadow region solution does not constitute a properly formulated asymptotic high-frequency theory in the sense that it becomes increasingly inaccurate with increasing frequency. This inaccuracy results from transition-function dominance over the Pekeris caret function in the deep shadow region. An improved formulation that circumvents this difficulty by avoiding use of a transition function is derived via a straightforward extension of Jones' canonical line-source solution. This new solution takes the form of Keller-type modes with modified diffraction coefficients that result in convergence at the shadow boundary provided that the source and observation point are not both located at asymptotic distances from the scatterer.

†This work was supported by the Electromagnetic Compatibility Analysis Center, Electronic Systems Division, Air Force Systems Command, under contract #F19628-85-C-0071

Arrays

Room 3010 Salle
URSI B Session 57

Réseaux

Chairs/présidents: **G.Y. DELISLE, Canada**

15:30 (57.1) Termination Effects in Low Profile Skin Embedded Arrays, **L.N. MEDGYESI-MITSCHANG**, J.M. PUTNAM, *McDonnell Douglas Research Laboratories, St. Louis, MO, USA*

15:50 (57.2) Infinite Phased Arrays of Dipoles Printed on Ferrite Substrates, **N.E. BURIS**, T. FUNK, *University of Massachusetts, Amherst, MA, USA*

16:10 (57.3) Analysis of a Tapered Stripline Element in an Infinite Array Environment, **P.S. SIMON**, K. McINTURFF, *Raytheon Company, Goleta, CA, USA*

16:30 (57.4) Analysis of a Wideband Array of Flared Notch Elements, E.J. KUSTER, **J.J.H. WANG**, T.E. GIBBS, V.K. TRIPP, *Georgia Institute of Technology, Atlanta, GA, USA*

16:50 (57.5) Synthesis of Wave Guide Slot Antenna Arrays with Low Side Lobes, **S.N. BORODIN**, *Moscow Power Engineering Institute, Moscow, USSR*

B57.1

TERMINATION EFFECTS IN LOW PROFILE SKIN EMBEDDED ARRAYS

L. N. Medgyesi-Mitschang* and J. M. Putnam
McDonnell Douglas Research Laboratories
P. O. Box 516, MC 1111041
St. Louis, MO 63166

Effective performance of linear phased arrays operating over wide scan angles, from broadside to end-fire, requires special consideration of the array termination. This is a function of many interrelated parameters including the excitation taper, the element spacing (uniform/nonuniform), the curvature and/or the finiteness of the ground plane as well as its conductivity. Because of the analytical complexities, earlier studies dealt mostly with linear phased arrays on infinite conducting or penetrable planar interfaces. In such problems a modified Green's function, deduced from image theory for the conducting case or the Sommerfeld formulation for the penetrable case, is generally used. When the interface is nonplanar or discretely penetrable, as is the case with many low profile, skin embedded arrays, the foregoing approaches are inappropriate. With embedded elements, the characteristics of the embedding superstrates and substrates have an increasingly critical impact as the array is scanned to end-fire. If the superstrate is multi-layered as is the case with integral radomes, the form of its termination into the ground plane strongly influences array directivity and side lobe levels at given scan angles.

The foregoing issues are illustrated for arrays consisting of two classes of antennas: short monopoles and patch antennas. The analysis is based on two integral formulations solved by the method of moments using the Floquet-Galerkin expansion. Detailed results are derived for the two classes of elements, varying superstrate/substrate thickness and composition, array excitation tapers and element spacing. Comparisons are made with available published data.

INFINITE PHASED ARRAYS OF DIPOLES PRINTED ON FERRITE SUBSTRATES

N. E. Buris* and T. Funk
Dept. of Electrical & Computer Engineering, Univ. of Massachusetts, Amherst, MA 01003

When a ferrite material is biased by a dc magnetic field it becomes anisotropic of the gyrotropic type. Biased ferrites have several properties including frequency tunability. Although ferrite properties have been exploited in microwave devices, relatively little research has been dedicated to ferrites as substrates of printed antennas. In this paper we investigate infinite arrays of dipoles printed on ferrite substrates. We have derived the Green's function for a source on a grounded ferrite substrate and we have employed the method of moments to solve for the input impedance of the dipoles of an infinite phased array. Our computer codes have been checked at the unbiased ferrite (dielectric) limit with published results (D. M. Pozar and D. H. Schaubert, IEEE Trans. Antennas and Propagat., Vol. AP-32, pp. 602-611, 1984) and excellent agreement has been found. In this paper we discuss the scan blindness as a function of bias field. Conditions under which a waveguide simulator can be used to experimentally verify some of the theoretical results are also discussed. In the following figure the H-plane scan performance of an infinite dipole array printed on an unbiased and biased ferrite substrate is shown.

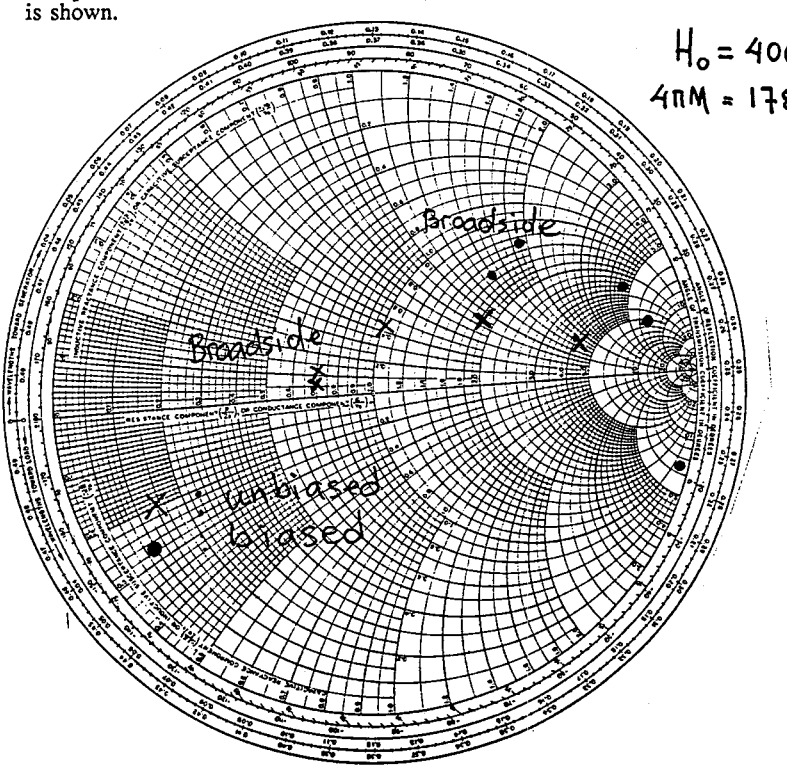

B57.3

ANALYSIS OF A TAPERED STRIPLINE ELEMENT IN AN INFINITE ARRAY ENVIRONMENT

Peter S. Simon* and Kim McInturff

Raytheon Electromagnetic Systems Division
6380 Hollister Avenue
Goleta, CA 93117

This paper describes the analysis of an infinite periodic array of striplines all of which feed into a semi-infinite parallel-plate region. This structure is of interest in the design of parallel plate lenses (e.g. Rotman lenses) which are used as beam forming networks for microwave scanning antennas. The periodicity of the structure allows one to focus attention on only a single unit cell, subject to periodic (Floquet) boundary conditions at the edges of the cell. The unit cell consists of a uniform-width stripline joined to the parallel-plate region via a tapered-width section which models a Rotman lens feed port.

The analysis is formulated as an electromagnetic boundary value problem with the stripline center conductor current determined using the method of moments. The basis functions selected for use here are the triangle subdomain functions of Rao, Wilton, and Glisson, suitable for treating arbitrary polygonal geometries. A key feature of this analysis is the use of a wide-band cavity Green's function, which allows the generalized impedance matrix to be written as a four-term rational function of frequency: $\mathbf{Z}(f) = \sum_{q=0}^{3} \mathbf{Z}_{2q-1} f^{2q-1}$. The coefficient matrices in this expression are determined only once for a given geometry and phasing, regardless of the number of frequencies to be analyzed. Since matrix fill time far exceeds matrix equation solution time for the number of unknowns used, a large savings in computation time is realized.

To verify the predictions of the theory, several back-to-back rectangular waveguide simulators were built, each consisting of two identical transitions connected by a length of rectangular waveguide. Measurement of two such fixtures, identical except for differing connecting lengths, allows determination of the individual transition S-parameters. An advantage of this type of simulator is that it avoids the problem of terminating a nominally semi-infinite region. Additionally, both amplitude and phase information are obtained for *all* S-parameters S_{11}, S_{22}, and $S_{12} = S_{21}$. This is in contrast to the usual looking-in or looking-out simulator technique, which provides reflection information for only a single port of the device.

ANALYSIS OF A WIDEBAND ARRAY OF FLARED NOTCH ELEMENTS

E. J. Kuster, J. J. H. Wang*, T. E. Gibbs, and V. K. Tripp
Georgia Tech Research Institute
Georgia Institute of Technology
Atlanta, Georgia 30332

The flared notch, or flared slot, is an antenna which has a multioctave bandwidth and is used both as a stand-alone antenna and as elements in phased arrays. Although several arrays of flared notch elements have been designed, fabricated and tested successfully, there appears to be little analytical work in this array.

A moment method algoritm has been developed to discretize an infinite planar periodic structure; and its application to array elements of simple plates has been presented (E. Kuster and J. Wang, 1990 URSI Symp.; J. Wang, *Generalized Moment Methods in Electromagnetics*, Wiley, 1991). In this presentation, the application of this algorithm to flared notch arrays will be discussed.

Because the computer program had been developed with applications to general problems in mind, it is rather inefficient in compuation time. As a result, only a limited amount of computation was made.

The computed data were then compared with measured data obtained by element mutual coupling data measured from a small array and by waveguide simulation.

B57.5

Synthesis of wave guide slot antenna arrays with low side lobes

S.N.Borodin, Moscow Power Engineering Institute

Plane wave guide slot antenna arrays (WSA) are wide used on practice for realization pattern with low side lobes (SL). Usual this antenna consists of linear traveling-wave arrays with inclined alter-phase slots situated in the narrow wall of rectangular wave guide. All linear arrays are excited from general demultiplier. This antenna allows to realize electronic wide-angle scanning of beam in the plane of demultiplier and mechanical scanning in the plane of linear arrays.

However the important defect of this antenna is the cross-polarization beams that are stable present in the field of antennas vision. The level of cross-polarization beams is near to -(14...15) dB, that doesn't allow to save low side lobes in a wide sector of scanning beam in the plane of demultiplier.

The construction of linear WSA with equiphase exciting slots is known from literature. The term "equiphase exciting slots" determines alternative mode to "alter-phase exciting slots". Usual this antenna is used in the mode of radiation -" end-on", but the author has suggested to use it in the mode near to the " broad-side".

Slots in this antenna are spaced with counting $d < 0{,}5\ \lambda$, where λ-wavelength in a free-space.In reality IT was used nonequidistant counting $d=(0{,}2...0{,}3)\ \lambda$.

The main direction of polarization is determined by the middle angle slots elevation, weighted with amplitude coefficients.

The author has suggested combined method of WSA synthesis on the basis of:

- method of successive approximations for determine amplitudes distribution of exciting slots,
- method of cross-resonant for determining: phases distribution,distortions along antennas aperture and dispersional characteristics of the WSA .

We make the following conclusions in accordance to the results of investigation:

1.The new construction of plane array allows to arrive the better division "signal-to-jam" at the entRY of antenna by means of: realization of necessary tapered amplitudes distribution (for different angles slots elevation) and linear phases characteristics (for nonequidistant spacing of a slots), deleting of cross- polarization beams.

2.The level of SL field pattern of this antenna is determined only by SL of the main polarization . SL may be constructed less than -(30...40) dB.

3.Natural experiments have confirmed rightness of suggested mathematical method.

Finite Difference Time Domain | **Room 3022 Salle URSI B Session 60** | **Différences finies dans le domaine temporel**

Chairs/présidents: R. MacPHIE, Canada; K. KUNZ, USA

13:30 (60.1) FD-TD Computational Modeling of Nonlinear Electromagnetic Phenomena Using a Nonlinear Convolution Approach, P.M. GOORJIAN[1], **A. TAFLOVE[2]**, [1] *NASA Ames Research Center, Moffett Field, CA, and* [2] *Northwestern University, Evanston, IL, USA*

13:50 (60.2) Modeling Waveguide Coupling through Apertures with the Finite Difference Time Domain Technique, P. ALINIKULA, **K. KUNZ**, R. LUEBBERS, *Pennsylvania State University, University Park, PA, USA*

14:10 (60.3) FD-TD Analysis of Vivaldi Flared Horn Antennas, E.T. THIELE, **M. PIKET-MAY**, A. TAFLOVE, *Northwestern University, Evanston, IL, USA*

14:30 (60.4) A Study of the Characteristics of Microstrip Line on Grounded Semiconductor Slab by FD-TD Method, **C. WU**, Z. BI, K. WU, R. FRALICH, J. LITVA, *McMaster University, Hamilton, ON, Canada*

14:50 (60.5) Investigation of RF Absorbers Through FDTD Techniques, **B.G. COLPITTS**, J.S. PLOYER, *University of New Brunswick, Fredericton, NB, Canada*

15:10 **COFFEE/CAFÉ**

15:30 (60.6) Calculation of Beam-Cavity Interaction Impedances Using FDTD Technique, **C.C. SHANG**, J.F. DeFORD, G.D. CRAIG, *Lawrence Livermore National Laboratory, Livermore, CA, USA*

15:50 (60.7) Analysis of the Numerical Error Caused by the Stair-Stepped Approximation of Material Boundaries in FD-TD Simulations of Electromagnetic Phenomena, A.C. CANGELLARIS, **D.B. WRIGHT**, *University of Arizona, Tucson, AZ, USA*

16:10 (60.8) Effects of Finite-Difference Time-Domain Second Order Radiation Boundary Condition on the Convergence and Accuracy of Electromagnetic Fields, S. GONZALEZ[1], B. GARCIA[1], R. GOMEZ[1], **K. UMASHANKAR[2]**, [1] *Universidad de Granada, Spain;* [2] *University of Illinois, Chicago, IL, USA*

16:30 (60.9) An Investigation of the Effects of Numerical Dispersion in the FD-TD Method, **T.G. MOORE**, J.G. BLASCHAK, *Massachusetts Institute of Technology, Lexington, MA, USA*

16:50 (60.10) The Inclusion of Wall Loss in Electromagnetic Finite-Difference Time-Domain Thin-Slot Algorithms, **D.J. RILEY**, C.D. TURNER, *Sandia National Laboratories, Albuquerque, NM, USA*

B60.1

FD-TD COMPUTATIONAL MODELING OF NONLINEAR ELECTROMAGNETIC PHENOMENA USING A NONLINEAR CONVOLUTION APPROACH

Peter M. Goorjian
NASA Ames Research Center
Moffett Field, California 94035 USA
and
Allen Taflove *
Department of Electrical Engineering
and Computer Science
McCormack School of Engineering
Northwestern University
Evanston, IL 60208 USA

There is a substantial effort in solving Maxwell's equations by finite-differences in the time-domain (FD-TD) for applications to linear electromagnetic fields in aeronautics and electronics (A. Taflove, Wave Motion, 10, 1988, North-Holland). Nonlinear fields become important in the generation of very short, fast rise-time pulses. Such pulses are important in Ultra-Wideband technology in aeronautics (W. Scott, Aviation Week and Space Technology, Nov. 19, 1990). Experimental researchers have achieved the switching of short (100 femtoseconds) optical pulses in nonlinear directional couplers (S. Friberg et al, Optics Letters, vol. 13, No. 10, Oct. 1988). Theoretical work has included the solution of nonlinear scalar equations for the slowly varying envelope of the optical pulses. This class of equations, known as the nonlinear Schrodinger equations (NLSE), has been solved by the split-step Fourier method (G. Agrawal, Nonlinear Fiber Optics, Ch. 2, Academic Press, 1990) and by the Propagating beam method (PBM), (M. Feit and J. Fleck, IEEE J. Quantum Electronics, vol.24, No. 10, Oct. 1988). However certain effects are neglected when Maxwell's equations are approximated by the nonlinear Schrodinger equation, including scattering and diffraction effects and short pulse effects in the 10 femtosecond regime.

In this paper, a new approach will be presented that solves the nonlinear Maxwell's equations with no approximations. The equations will be solved by finite-differences in the time domain (FD-TD). The nonlinear relation between the polarization and the electric field will be modeled by a nonlinear convolution relation (K. Blow and D. Wood, IEEE J. Quantum Electronics, vol. 25, No. 12, Dec. 1989). The effects that were not accounted for in the NLSE approach are included here. Also, unlike the split-step Fourier method, the effects of nonlinearity and dispersion are not treated separately in this approach. The inclusion of the nonlinear terms in the algorithm for Maxwell's equations employs techniques that were developed in computational fluid dynamics for the solution of nonlinear equations (P. Goorjian and S. Obayashi, p. 169, vol. 29, Notes on Numerical Fluid Dynamics, Pub. Vieweg, 1990).

MODELING WAVEGUIDE COUPLING THROUGH APERTURES WITH THE FINITE DIFFERENCE TIME DOMAIN TECHNIQUE

P. Alinikula, K. Kunz*, and R. Luebbers
Department of Electrical and Computer Engineering
The Pennsylvania State University
University Park, PA 16802

The finite difference time domain (FDTD) technique is used to model coupled waveguides. A TE_{01} pulse with a sinusoidal carrier above cutoff and a Gaussian envelope is injected into the end of one of the waveguides. Single and double circular aperture coupling is treated and the results validated using existing experimental measurements of the double aperture geometry. Sensitivity to the number of cells used in the FDTD model and to the predicted response duration is examined. The response converges reasonably well with the aperture sixteen cells across and for run times of 4096 time steps. Agreement in the predicted forward and backward coupling with the experimentally measured coupling is typically within one or two dB or better over a roughly 2:1 frequency band using these model parameters. FDTD has therefore shown itself to be a very promising technique for broad band analysis of waveguide and waveguide-like structures. The modeling is not restricted to any particular geometry or material because of the generality of the FDTD technique.

B60.3

FD-TD ANALYSIS OF VIVALDI FLARED HORN ANTENNAS

Eric T. Thiele, Melinda Piket-May*, and Allen Taflove
Department of Electrical Engineering and Computer Science
McCormick School of Engineering
Northwestern University
Evanston, IL 602028

In this paper we report the use of the finite-difference time-domain (FD-TD) method to computationally model tapered slot antennas. FD-TD, which numerically solves Maxwell's time dependent curl equations, can account for the complex geometrical and electrical characteristics associated with this type of antenna.

We compare FD-TD to measured data for the co-pol and cross-pol radiation patterns of a stripline-fed, electrically small Vivaldi tapered slot antenna, and an electrically large linearly tapered slot antenna. In all cases, there is good agreement between computed and measured data. Subtle ripples in the co-pol pattern of the Vivaldi flare were first seen in the computations, and later verified by additional measured data. We have also computationally shown the sensitivity of the Vivaldi's cross-pol fields to slight construction perturbations. Any kind of feed asymmetry or alignment error due to non-machine construction of the antenna causes a dramatic enhancement of the cross-pol. The co-pol pattern exhibits no distortion for any of these perturbations.

Our results indicate that the basic Vivaldi design itself is good. If manufacturing tolerances are high enough, this antenna should perform to specifications. We are also satisfied that FD-TD modeling yields useful engineering design guidance for this entire class of slot antennas, including arrays.

A STUDY OF THE CHARACTERISTICS OF MICROSTRIP LINE ON GROUNDED SEMICONDUCTOR SLAB BY FD-TD METHOD

Chen Wu, Zhiqiang Bi, Keli Wu, Russell Fralich and John Litva

Communications Research Laboratory

McMaster University, Hamilton, Ontario, Canada

The finite difference time domain method, proposed by Yee, is the direct solution of the time dependent Maxwell's curl equations. The central difference approximations are used in both space and time derivatives in Maxwell's equations. By invoking the boundary and source conditions and using Yee's scheme (Fig. 1), the equations are solved in a leap-frog time-marching procedure. Due to the simplicity of the method, Yee's algorithm has been widely used in electromagnetic problems.

In this paper, the FD-TD method is applied to analyze the characteristics of a microstrip line on grounded semiconductor slab (Fig. 2). Parameters of interest, such as the effective dielectric constant, characteristic impedance and loss factor due to the conductivity of semiconductor are obtained by a simulation of Gauss pulse propagation. The effects of the thickness of the metal strip can be easily taken into account. The FD-TD method can provide a wide frequency range response and simultaneously give the field distribution along the transmission line. Comparison of the results with the quasi-static method results shows good agreement in the low frequency range. the details will be presented at the symposium.

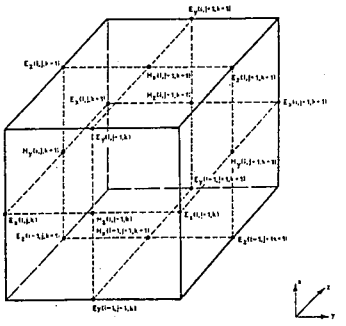

Figure 1 Node distribution on Yee's scheme

Figure 2 Microstrip line on grounded semiconductor slab

B60.5

INVESTIGATION OF RF ABSORBERS THROUGH FDTD TECHNIQUES

*Bruce G. Colpitts and J. Scott Ployer

Department of Electrical Engineering
University of New Brunswick,
Fredericton, New Brunswick, Canada

In this work RF absorbing materials used in lining anechoic chambers are evaluated through Finite Difference Time Domain (FDTD) techniques. This is the first step in an objective of modelling anechoic and semi-anechoic chambers for use in electromagnetic interference measurements such as are used in performing MIL STD 461/2 and other related measurements. With the large variations in chamber size, shape and absorber type and location as well as the diversity of equipment to be tested it is difficult to generalize anechoic chamber performance. The usefulness of a modelling package would be in evaluating chamber performance given specific equipment to be tested or in the converse to make optimum use of absorber material in a semi-anechoic configuration.

This work deals with a two dimensional analysis of a conducting wall lined with infinite rows of absorbing material. The testing involves an examination of the standing wave patterns for a number of cases of absorber dielectric properties and dimensions as well a range of frequencies and incident angles. The model is verified through measurement of standing waves in a shielded anechoic chamber where a directional antenna is used to illuminate only a portion of one wall.

Although this two-dimensional analysis demonstrates the applicability of the technique it is the three-dimensional extension of this work that will provide the tool necessary for anechoic and semi-anechoic chamber evaluation.

Calculation of Beam-Cavity Interaction Impedances Using FDTD Technique†

C. C. Shang*, J. F. DeFord and G. D. Craig
Lawrence Livermore National Laboratory
L-626, Livermore, CA, 94550

The nature of the electromagnetic interaction of a charged particle beam in an accelerator beampipe with imperfections or perturbations in the beampipe wall is of fundamental importance to the design of the accelerator. These interactions can be characterized by an interaction impedance, which relates moments of the beam current to the work done on the beam by the beam-induced electromagnetic fields.

In this paper we present the application of the finite-difference, time-domain (FDTD) technique to the computation of interaction impedances in accelerator components. The impedance quantities of interest may all be derived from the characteristic wake potential w_c, defined by the expression

$$\frac{dw_c(s)}{ds} = \frac{1}{Q}\int_{-\infty}^{\infty} E_z(z,t)\Big|_{t=\frac{z+s}{c}} dz,$$

where E_z is the electric field induced by the source charge Q, and it is evaluated at the test charge position (see Fig. 1).

The calculation of w_c is stressing to time-domain codes for several reasons. The cavities of interest are often geometrically complicated, with considerable structure on scales smaller than the minimum wavelength of interest. The bandwidth over which information is sought is large, often ranging from D.C. to several GHz. This bandwidth requirement has serious consequences for both mesh density and material models. The structures of interest often contain ferrite, and also may have several different dielectrics, such as solid and fluid insulators. In addition, highly efficient absorbing boundary conditions are required, and they must work well even when in contact with the object being simulated.

We will discuss FDTD tools used to compute w_c for a variety of accelerator components. In some cases experimental validation of simulation results has been obtained, and these data will be presented. Some simple problems yield to analytic analysis, and comparisons with these solutions will also be shown. Future development objectives will be discussed.

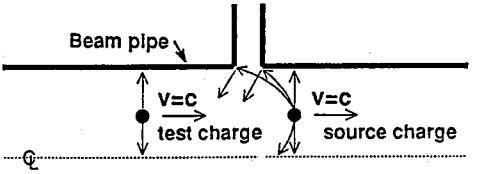

Fig. 1. Canonical beampipe geometry showing configuration of charges in calculation of w_c.

† Work was performed by the Lawrence Livermore National Laboratory under the auspices of the U. S. Department of Energy under contract No. W-7405-ENG-48.

B60.7

ANALYSIS OF THE NUMERICAL ERROR CAUSED BY THE STAIR-STEPPED APPROXIMATION OF MATERIAL BOUNDARIES IN FD-TD SIMULATIONS OF ELECTROMAGNETIC PHENOMENA

A.C. Cangellaris
*D.B. Wright**
Department of Electrical and Computer Engineering
University of Arizona
Tucson, AZ 85721, USA

The Finite-Difference Time-Domain (FD-TD) method of solving Maxwell's equations with general time dependence is considered by many to be the most versatile and efficient approach to current and future simulations of very complex electromagnetic wave interactions. As the applications of the FD-TD method to the simulation of electromagnetic wave interactions with more complex, anisotropic, non-linear media are becoming reality, a good understanding of the various sources of numerical error, introduced by the spatial and temporal discretization and the integration algorithm, becomes mandatory. Indeed, the rigorous quantification of artificial wave phenomena, such as the numerically-induced dispersion and anisotropy of the velocity of propagation, becomes invaluable when studying wave propagation in dispersive media.

One source of error in FD-TD simulations is associated with the stair-stepped (saw-tooth) surfaces used to approximate media interfaces that are not parallel to one of the coordinate planes in an orthogonal coordinate system. Despite the fact that methods have been proposed for treating such boundaries, thus avoiding the stair-stepped approximation, the simplicity of the latter justifies a more careful analysis of the numerical error introduced by it and its rigorous quantification.

This paper presents a rigorous analysis of the effects of such stair-stepped boundaries on the numerical solution. First, a dispersion analysis in two dimensions is performed to obtain the numerical reflection coefficient for a plane wave scattered by a perfectly conducting wall, tilted with respect to the axes of the finite difference grid, under both transverse electric and transverse magnetic polarizations. From this reflection coefficient it is then possible to derive the characteristic equation for surface waves that can be supported by such saw-tooth conducting surfaces for both polarizations. These equations lead naturally to expressions that show the dependence of the velocity of propagation along the boundary and the attenuation constant perpendicular to it on cell size and wavelength. Finally, numerical simulations of pulse propagation in non-uniform waveguides are used to demonstrate the effects predicted by this dispersion analysis.

EFFECTS OF FINITE-DIFFERENCE TIME-DOMAIN SECOND ORDER RADIATION BOUNDARY CONDITION ON THE CONVERGENCE AND ACCURACY OF ELECTROMAGNETIC FIELDS

S.Gonzalez, B.Garcia, R.Gomez
Departamento de Fisica Aplicada
Facultad de Ciencias
Universidad de Granada, Granada, Spain

and

K.Umashankar
Department of Electrical Engineering and Computer Science
University of Illinois at Chicago
Chicago, Illinois 60680, U.S.A

Extensive applications based on the Finite-Difference Time-Domain (FD-TD) technique have been reported previously in the study of radar cross section of complex structures and field penetration into complex cavity backed apertures. In the FD-TD field interaction and penetration studies, the complete geometry is generally embedded in the total field region of the FD-TD total field/scattered field volume in order to numerically simulate a wide dynamic range electric and magnetic field distributions. The outer boundary of the scattered field region is utilized to simulate the near field radiation boundary condition (RBC) in order to limit the composite FD-TD numerical field volume to a minimum. Number of modeling parameters including the electrical distance between the radiation boundary and the surface of interacting object play a critical role both in the scattering and also in the penetration studies. Numerical region having as small as eight FD-TD cells has been previously utilized and validated for the monostatic radar cross section of electrically large conducting objects with second order RBC. In many applications involving bistatic radar cross section as well as field penetration studies to evaluate complicated field coupling to the cavity backed apertures, the second order RBC is not just enough to obtain good convergence and accuracy requirements. Further, the RBC cannot just be simulated very close to the interacting object, in which case higher order RBC is required.

In this paper, detailed FD-TD studies are reported involving bistatic radar cross section and field penetration into cavity behind aperture. Detailed validation of the accuracy and convergence studies are also reported to evaluate location and order of the FD-TD radiation boundary condition.

AN INVESTIGATION OF THE EFFECTS OF NUMERICAL DISPERSION IN THE FD-TD METHOD

Thomas G. Moore
Jeffrey G. Blaschak

Lincoln Laboratory
Massachusetts Institute of Technology
Lexington, MA 02173

It is well known that finite difference approximations to Maxwell's equations exhibit anisotropic propagation characteristics, which lead to artificial dispersive effects. What has not been clearly demonstrated is whether this numerical artifact leads to significant errors in computed solutions. In this paper, we review the basic theory of numerical dispersion in finite difference schemes and conclude with several examples to asses the practical effect of numerical dispersion.

The first example considered is the interaction of two time harmonic point sources in a large two-dimensional FD-TD grid. This problem could be considered a prototype that models the scattering from a large target that posses two distinct, interacting scattering centers many wavelengths apart. In order for the finite difference scheme to successfully model this problem it must accurately propagate cylindrical wavefronts over a large distance.

The second example is the demonstration of propagation in a parallel-plate waveguide, 100 λ_g wavelengths in length. Since this is a canonical problem with a well known solution, the phase characteristics of the computed solution can be compared to the exact solution. The waveguide is positioned in the grid to provide propagation in the direction yielding maximum numerical dispersion.

The third example addressed is the computation of the scattered field from a large, perfectly conducting strip illuminated by a plane wave. The incident field polarization and strip size are chosen to maximize the multiple diffraction between the ends of the strip. The finite difference solution to this problem is compared to the classic GTD solution for a large strip. This problem was selected to investigate the practical effects of grid dispersion in the computation of far field results.

THE INCLUSION OF WALL LOSS IN ELECTROMAGNETIC FINITE–DIFFERENCE TIME–DOMAIN THIN–SLOT ALGORITHMS

Douglas J. Riley* and C. David Turner
Radiation and Electromagnetic Analysis Division
Sandia National Laboratories
Albuquerque, NM 87185 USA

The resolution of apertures that are much narrower than the spatial cell is an important problem in finite-difference time-domain (FDTD) electromagnetics codes. Previous thin-slot methods have assumed that the slot walls are perfectly conducting. As the slot depth-to-width ratio becomes large, interior wall losses for realistic materials can significantly affect the coupling through the slot, and therefore these loss effects should not be neglected. This paper presents two methods for incorporating loss for walls with good, but not perfect conductivity, into the FDTD calculations. The first method modifies an FDTD equation internal to the slot to include a surface-impedance contribution. This method is appropriate for the usual FDTD thin-slot formalisms. The second method includes the losses into a "half-space" integral equation that can be used by the recently introduced Hybrid Thin-Slot Algorithm (D.J.Riley & C.D.Turner,*IEEE Trans. Ant. Prop.*,AP–38, Dec. 1990). Results based on the two methods are compared for a variety of slot parameters and wall conductivities.

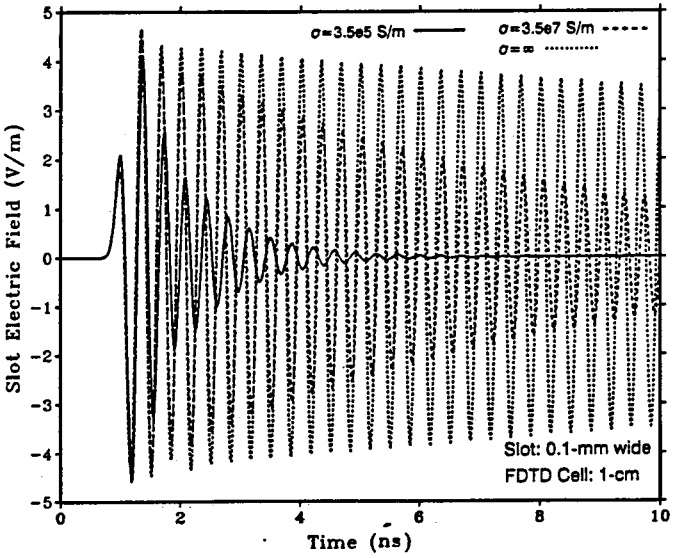

Fig. 1: **Effect of interior wall conductivity (σ) on the gap electric field. The slot is 5-cm long, 1-cm deep, 0.1-mm wide and couples into a cavity. Gaussian-pulse excitation with a bandwidth of about 3 GHz.**

Scattering I

Room 2020 Salle
URSI B Session 64

Diffusion I

Chairs/présidents: T.K. SARKAR, USA

13:30 (64.1) Higher Order Modeling of Geometry and Surface Currents in Integral Equation Approaches to the Computation of Three-Dimensional Scattering, **R.D. GRAGLIA**[1], D.R. WILTON[2], [1]*Politecnico di Torino, Italy;* [2]*University of Houston, TX, USA*

13:50 (64.2) Correcting Currents on Two-Dimensional Structures at Resonance, **R.E. JORGENSON**, L.A. ROMERO, *Sandia National Laboratories, Albuquerque, NM, USA*

14:10 (64.3) On the Uniqueness of Two Integral Equations Used in Electromagnetic Scattering Problems, **A. TAAGHOL**, E. ARVAS, *Syracuse University, Syracuse, NY, USA*

14:30 (64.4) Uniqueness of Numerical Solution to EFIE, MFIE and CFIE for Scattering Problems, Y. ZHANG, **Y.-M. XIAO**, *Xi'an Jiaotong University, Xi'an, China*

14:50 (64.5) On the Non-Huygens Principles of the Scattered Field's Appearance in the Diffraction Problems, **V.F. APELT'CIN**, *Moscow State University, Moscow, USSR*

15:10 **COFFEE/CAFÉ**

15:30 (64.6) Scattering from a Lossy Straight Wire Resonator, **P.Y. UFIMTSEV**[1], A.P. KRASNOZHEN[2], [1]*University of California, Los Angeles, CA, USA;* [2]*USSR Academy of Sciences, Moscow, USSR*

15:50 (64.7) Electromagnetic Backscatter from Slots Conformal to the Surface of a Cylinder, **J.A.G. MALHERBE**, K. CLOETE, *University of Pretoria, South Africa*

16:10 (64.8) Scattering by Periodic Non Planar Wire Grids whose Cell Size is Small Compared to the Wavelength, **E. MICHIELSSEN**, R. MITTRA, *University of Illinois, Urbana, IL, USA*

16:30 (64.9) EM Scattering by Arrays of Dielectric Bars, **H.A. KALHOR**, *State University of New York, New Paltz, NY, USA*

16:50 (64.10) Electromagnetic Modeling of Arbitrarily Shaped Inhomogeneous Thin Shells, **S.U. HWU**[1], D.R. WILTON[2], *Lockheed Engineering and Sciences Company, Houston, TX, and* [2]*University of Houston, TX, USA*

Higher Order Modeling of Geometry and Surface Currents in Integral Equation Approaches to the Computation of Three-Dimensional Scattering

R. D. Graglia*
Dipartimento Elettronica, Polytecnico di Torino
10129 Torino, ITALY
D. R. Wilton
Dept. of Electrical Engineering, University of Houston
Houston, TX 77204-4793, USA

Most integral equation approaches to computing the scattering characteristics of three-dimensional objects employ planar-faceted models for the surfaces which support equivalent surface currents. The limitations of such models frequently pose problems for the modeler, however, and more sophisticated schemes for geometry modeling are needed; the difficulty is in finding suitable representations for the tangential equivalent surface current quantities. In this paper, a scheme is proposed for improving the modeling of both surfaces and surface currents using higher order schemes.

Surface representation by bicubic splines is chosen to obtain, if desired, continuity through the second derivative of the surface position vector. A point $\boldsymbol{\rho} = u\hat{\boldsymbol{u}} + v\hat{\boldsymbol{v}}$ in the rectangle $0 < u < 1,\ 0 < v < 1$ of the parameter space is mapped through the spline representation to the point $\boldsymbol{r}(\boldsymbol{\rho})$ on a surface *patch*. One or more spline patches are then pieced together to form an object, and each patch is tesselated into triangles in the spline parameter space. Local normalized area coordinates ξ_1, ξ_2 are in turn used to parameterize each triangle, and thus a double mapping takes the point $\boldsymbol{\xi} = \xi_1\hat{\boldsymbol{\xi}}_1 + \xi_2\hat{\boldsymbol{\xi}}_2$ into the point $\boldsymbol{r}(\boldsymbol{\rho}(\boldsymbol{\xi}))$ in a (curved) triangle on the patch. The tangent vectors $\boldsymbol{r}_u$ and $\boldsymbol{r}_v$ are then used as non-orthogonal basis vectors for the surface current, while the vector component amplitudes are modeled via a quadratic representation in $\boldsymbol{\xi}$. If a contra-variant vector representation for the surface current is chosen, then the intervening non-linear Jacobians involved in transforming from $\boldsymbol{r}$ to $\boldsymbol{\xi}$ are canceled and all potential integral calculations may be conveniently performed in the $\boldsymbol{\xi}$ domain.

CORRECTING CURRENTS ON TWO-DIMENSIONAL STRUCTURES AT RESONANCE

Roy E. Jorgenson * and Louis A. Romero
Sandia National Laboratories
P.O. Box 5800
Albuquerque, NM 87185

The surface currents on a closed, perfectly conducting scatterer may be found by discretizing and solving an electric field integral equation (EFIE) or magnetic field integral equation (MFIE). When the frequency of the incident field is close to a resonant frequency of the structure, however, the condition number of the impedance matrix increases and the currents are incorrect.

Many numerical methods have been developed to correct this situation. A few examples are the combined field, combined source and augmented field integral equations, and specifying boundary conditions at points within the scatterer. Because of the additional complexity involved in using the above techniques, they are usually applied only in the vicinity of resonance. Unfortunately, for a general body, the resonant frequencies cannot be predicted, so the analyst first realizes that the solution is wrong is after the impedance matrix has been filled and decomposed and the condition number has been examined. The impedance matrix must then be regenerated using the above techniques and re-solved.

In this paper, the currents found by the EFIE are corrected without regenerating the matrix. The corrupted current (J_{tot}) is composed of a series of eigenvectors of the impedance matrix weighted by coefficients. Most of the eigenvectors have proper weighting (J_{ok}), but a few (J_n) associated with the small eigenvalues are weighted improperly. The goal, which is accomplished in two steps, is to correct these weighting coefficients. The first step is to find the eigenvectors J_n using the decomposed impedance matrix and inverse iteration. This requires an order of N^2 operations. The second step is to find the proper weighting for J_n by taking the inner product of J_n with the MFIE. At resonance, certain orthogonality properties can be exploited to eliminate the necessity of calculating the scattered H field. These properties continue to hold approximately for frequencies slightly off resonance. This step requires an order of N operations.

This correction method can be easily implemented in existing codes based on the EFIE and is computationally efficient. The method will be demonstrated for TE and TM scattering from combinations of two-dimensional cylinders and strips. Results will be compared to those from the combined field integral equation and from analytical solutions.

B64.3

ON THE UNIQUENESS OF TWO INTEGRAL EQUATIONS USED IN ELECTROMAGNETIC SCATTERING PROBLEMS

*Ardalan Taaghol** and *Ercument Arvas*
Department of Electrical and Computer Engineering
Syracuse University, Syracuse, NY 13244

A numerical experiment is performed to investigate the uniqueness properties of two integral equations used in the electromagnetic scattering problems involving dielectric scatterers. Both of the integral equations are in terms of a single unknown; an electric surface current. Both of the equations are obtained from the application of the surface equivalence principle. One of them (IEEE Trans. AP-32, pp.173-175, Feb.84) uses only an electric current as the unknown, whereas the second one (IEEE Trans. AP-37, pp.1070-1071, Aug. 89) introduces an additional magnetic surface current which is not a new unknown, but is linearly related to the electric surface current. It is shown that the first of these integral equations fails to have a unique solution at certain frequencies whereas the second one has a unique solution at all frequencies. Both equations are applied to the problem of TM scattering from a dielectric cylinder of arbitrary cross section. The method of moments is used to solve the equations approximately. The figure below shows the condition number of the moment matrix for the case of a circular cylinder. The smooth curve corresponds to the second equation.

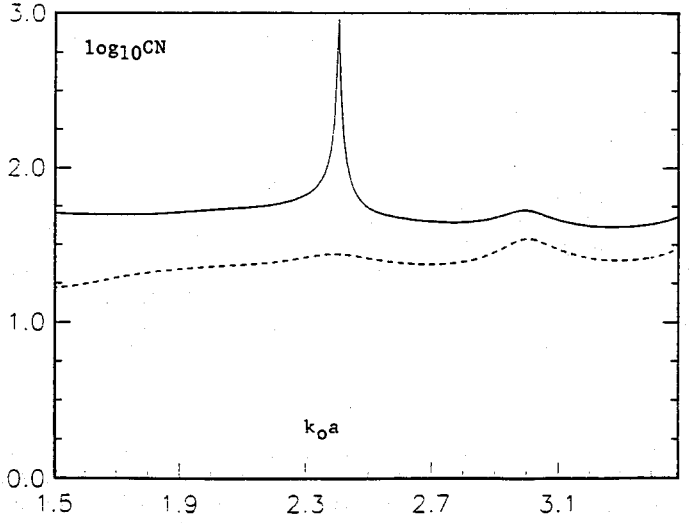

UNIQUENESS OF NUMERICAL SOLUTION TO EFIE, MFIE AND CFIE FOR SCATTERING PROBLEMS

YING ZHANG YAN-MING XIAO

Department of Information & Control Engineering
Xi'an Jiaotong University, Xi'an, P. R. China

This paper presents a new explanation for the nonuniqueness of integral equations in solving scattering problems.
Considering an infinite square cylindrical scatterer illuminated by TM plane wave, EFIE has nonunique solutions at discrete frequencies, which are frequencies of $TM_{2n+1,m}$ waveguide modes of the region enclosed by the conducting surface; but MFIE fails to have unique solutions at frequencies of $TE_{m,2n}$ waveguide modes. It seems that the nonunique solutions of EFIE and MFIE occur at different frequencies. It can be proved that the matrix of MFIE for the exterior region for the TM excitation is the transposition to the matrix of MFIE for the interior problem for the TE case. Hence the resonance we experience solving the exterior problem for the TM case must have the same variation at the resonance for the interior for the TE case. This paper also shows theoretically that the MFIE does not have a correct solution for the far field at these resonant frequencies, but the EFIE and the CFIE do have unique solutions. Condition number is also used to demonstrate the behavior of the equations.
The moment method is used to solve the EFIE, the MFIE and the CFIE of 2-D,TM illumination. Pulse expansion and point matching are used. Our numerical solutions accurately proved the above conclusions.

B64.5

ON THE NON-HUYGENS PRINCIPLES OF THE SCATTERED FIELD'S APPEARANCE IN THE DIFFRACTION PROBLEMS.

V.F. Apelt'cin
Faculty V.M.K of Moscow St.University.

The Huygens - Poincare principle of scattered field's forming in the wave's diffraction problems for the finite bodies supposes the bodie's surface being a support of the scattered field's sources (currents) and absence of the field in the interior of a perfect conductor (H.Honl, A.W.Maue, K. Westpfahl, Theorie der Beugung , Springer- verlag, Berlin, 1961). From the mathematical point of view it corresponds to the Fredholm integral equation methods due to the potential theory (D.Kolton, R.Kress, Integral equation methods in scattering theory, New-York, 1983) Nevertheless there exists another model of the scattered field's forming which corresponds to the image method's generalization when the scattered field is synthesized by the sources distributed in the interior of the bodie's geometric boundary.

It's demonstrated that an analytic continuation of the solutions of external two-dimension wave's diffraction problems due to the Dirichlet or Neumann's boundary value conditions into the domain's interior with a smooth closed boundary leads to the appearance not only of point source's singularities in the points of an external source's images (as for the most simple boundary value problems in the semi-plane, semi-space or strip) but also of some singular linear set corresponding to the system of cuts on a Riemann surface due to the analytic function induced by the domain's boundary. The Riemann surface has a finite-sheet structure if the domain's boundary is algebraic (may be described by polynomial). Solutions of the initial boundary value problems may be expressed by means of the fundamental solutions of the Helmholtz equation on the Riemann surface mentioned above. According to the Sommerfeld's branched solutions method these fundamental solutions may be constructed by means of the solutions of Dirichlet and Neumann's boundary value problems for the singular set which is a simple connected starlike system of the linear segments.

SCATTERING FROM A LOSSY STRAIGHT WIRE RESONATOR

Peter Y. Ufimtsev *
Department of Electrical Engineering
University of California, Los Angeles
Los Angeles, CA90024
and
Alexander P. Krasnozhen
Institute of Radioengineering and Electronics
USSR Academy of Sciences, K. Marx Avenue 18,
Moscow, 103907, USSR

A new analytical solution is given for the problem of plane wave scattering from a lossy straight wire resonator. The method of parabolic equations and modal boundary conditions are used. The total surface current is given as the sum of fast space waves and slow surface waves. The scattered field is found via integration of the surface current. The customary method of using vector potentials leads to an equation which does not satisfy the reciprocity principle. The degree of violation of this principle is evaluated by numerical calculations, and it proves to be quite small. In addition, we present a new closed-form solution for the scattered field which exactly satisfies the reciprocity principle.

The scattered field and losses are investigated for this wire resonator. The results are compared with known data. Possible generalizations of this technique to other diffraction problems are discussed.

B64.7

ELECTROMAGNETIC BACKSCATTER FROM SLOTS CONFORMAL TO THE SURFACE OF A CYLINDER

J.A.G. Malherbe, Faculty of Engineering*
and
K. Cloete, Department of Electronics
and Computer Engineering
University of Pretoria, South Africa

The problem of predicting the external contribution to the backscatter from an antenna consisting of slots cut into the surface of a cylinder, is addressed.

The internal contribution of an antenna to the RCS is a function of the antenna radiation pattern, as well as the quality of the antenna match over the frequency bandwidth of interest. In the case of planar arrays with broadside radiation patterns, the external and internal backscatter patterns would usually have the same generic shape. In the case of a cylindrical array, the phases for the internal and external backscatter patterns are dissimilar.

Previously, a planar array of slots in a metal plate was evaluated, and it was found that a simple physical optics approximation to the current on the surface between the slots gave results that compared well with measurements. In this paper, the principle is extended to the case of slots on a conducting cylinder. The dependence of the backscatter on the current distribution in the immediate vicinity of the slots is discussed.

Scattering by Periodic Non Planar Wire Grids whose Cell Size is Small Compared to the Wavelength.

Eric Michielssen and Raj Mittra*
Electromagnetic Communication Laboratory
University of Illinois at Urbana-Champaign
Urbana, IL 61801.

It is well-known, that the accuracy of most Electric Field Integral Equation (EFIE) techniques deteriorates when the dimensions of the scatterer become very small compared to the wavelength. This effect is due to the inaccuracies that arise when calculating the electric charge from the divergence of the electric current at low frequencies. This paper presents a technique for analyzing the scattering by double periodic wire grids for which the unit cell size can be arbitrarily small, e.g., less than 10^{-3} wavelengths. The wire grids can consist of a complex layout of arbitrarily interconnected wires, arranged in a rectangular or skewed grid. In addition, the structure can be non-planar, i.e. the wires need not be parallel to the plane of periodicity. Such structures find useful applications as artificial dielectrics and the ability to model them accurately is important for the design of radar absorbing materials.

To analyze these grating structures, an EFIE is formulated in terms of the current on the wires by forcing the tangential component of the electric field along the wire axis to vanish. The formulation is implemented in the spatial domain using a periodic scalar Green's function. As proposed by Mautz and Harrington ("An E-Field Solution for a Conducting Surface Small or Comparable to the Wavelength", Trans. Ant. & *Prop,* vol. AP-32, no. 4, April 1984), the current on the wires is expanded using two different sets of basis functions. The basis functions in the first category describe divergence free currents in the closed wire loops formed by the wire grid. This first set of basis functions is therefore suitable for expanding the magnetostatic currents on the structure. The basis functions of the second category are piecewise triangular functions and are employed on the entire wire structure, except on a number of nodes that cut open the closed wire loops on which the first set of basis functions is active. After appropriately scaling the latter type of basis functions, and computing their divergences, we generate a set of functions that are well-suited for expanding the electrostatic charges on the wires. Combined, both families of basis functions make up a complete set, suitable for expanding the current on the wires and, when used in conjunction with the Galerkin testing procedure, they guarantee a well-behaved moment method matrix.

Most wire meshes exhibit a very small transmission coefficient at low frequencies. It is shown in the paper that using this technique, transmission coefficients as low as -40 to -50 dB can be reliably predicted. The method of analysis described herein can also be applied to the problem of scattering from wire grids that contain helical elements. Depending on the inductance of the helical elements in the unit cell, these structures may exhibit significant transmission of the impinging signal even for a very small unit cell. In analyzing these structures one finds that the traditional E-field formulations fail to provide accurate results. However, with the technique presented in this paper, stable results have been obtained for grids with a unit cell size much smaller than 10^{-6} square wavelengths.

B64.9

EM SCATTERING BY ARRAYS OF DIELECTRIC BARS

Hassan A. Kalhor
Electrical Engineering Department
State University of New York
New Paltz, NY 12561

Scattering of electromagnetic waves from periodic structures are of interest in many applications in optics and electromagnetics because of their strong frequency dependent behavior. Arrays made of perfectly conducting materials have received a lot of attention whereas arrays of dielectric materials have not been widely studied.

The objective of this presentation is to calculate scattering of electromagnetic waves from a periodic array of dielectric bars of rectangular cross section when a uniform plane wave is incident on the array. A combined modal expansion and finite difference method is employed in the analysis. The scattered fields above and below the array are expanded in terms of outgoing modes. Within the bars and in the air spaces between the bars, finite difference is employed. The three sets of representations are then coupled through the application of the boundary conditions and solved. This simple method can treat lossy, lossless, and inhomogeneous dielectrics with ease.

ELECTROMAGNETIC MODELING OF ARBITRARILY SHAPED INHOMOGENEOUS THIN SHELLS

Shian U. Hwu*
Lockheed Engineering & Sciences Company
Houston, TX 77258

Donald R. Wilton
Department of Electrical Engineering
University of Houston, Houston TX 77204-4793

In this study the problem of determining the scattering characteristics of a thin dielectric shell of inhomogeneous material with arbitrary shape illuminated by a time-harmonic field is considered. For such geometries, numerical solution methods are usually needed, but they may be compared to analytical solutions available for homogeneous material shells of planar, circular, or spherical geometries.

In this numerical approach, an arbitrary thin shell is modeled by a collection of *triangular slabs* which are sufficiently small and thin that the electric field intensity may be assumed linear in the transverse dimension and constant across the normal dimension of each slab. The transverse polarization current directed across the edge of each adjacent slab and the polarization current normal to the thin dimension of each slab are the unknown quantities of interest. A system of linear equations is obtained by enforcing the condition that the total electric field in each slab, expressed in terms of the polarization current density, equals the sum of the incident and scattered fields. The latter quantity is also related to the polarization current through the potential integral representation. The resulting system of linear equations is solved by computer for the unknown polarization currents. It is then a simple procedure to calculate the scattered field at any point in space. Numerical results are obtained using codes developed based on the formulation and are presented for a variety of material properties. The computational results and comparisons illustrate the versatility, accuracy, and efficiency of the method.

Radiation Room 3014 Salle Rayonnement
URSI B Session 74

Chairs/présidents: R. SHARPE, USA

13:30 (74.1) Radiation Due to a Convex Curvature Discontinuity of a Dielectric Coated Perfect Conductor, **D.H. MONTEITH**, R.G. OLSEN, *Washington State University, Pullman, WA, USA*

13:50 (74.2) TM Surface-Wave Scattering by Vertical Wires in a Layered MM-Wave/Optical IC Environment, **B. KZADRI**, D.P. NYQUIST, *Michigan State University, East Lansing, MI, USA*

14:10 (74.3) Compact Representation of Radiation Patterns Using Spherical Mode Expansions, **T.L. SIMPSON**, J.C. LOGAN, *University of South Carolina, Columbia, SC, USA*

14:30 (74.4) Asymptotic Expansions of Antenna Currents, **K.C. CHEN**, L.K. WARNE, *Sandia National Laboratories, Albuquerque, NM, USA*

14:50 (74.5) Analytical Technique for Determining Backscattering from Cylindrical Screens of Arbitrary Cross Section, M. MARTÍNEZ, **A. MARTÍN**, R. VILLAR, *Consejo Superior de Investigaciones Científicas, Madrid, Spain*

15:10 **COFFEE/CAFÈ**

15:30 (74.6) Cavity-Fed Slots Excited by Narrow Wires, **S. HASHEMI-YEGANEH**, *Arizona State University, Tempe, AZ, USA*

15:50 (74.7) A Conjecture on the Polarizabilities of a Planar Aperture, **K.S.H. LEE**, *Kaman Sciences Corporation, Santa Monica, CA, USA*

16:10 (74.8) Synthesis and Analysis of HPM Reflector Antenna Systems: A Generalized Optimization Approach, D.-W. DUAN, **Y. RAHMAT-SAMII**, *University of California, Los Angeles, CA, USA*

16:30 (74.9) Source Field Studies for a Spherical Dielectric Antenna Excited by TE_{11} Mode, **S. PAL**[1], A. KUMAR[2], R. CHATERJEE[2], [1]*ISRO Satellite Centre, Bangalore, and* [2]*Indian Institute of Science, Bangalore, India*

16:50 (74.10) Discrete Radiating Systems Phase Synthesis from Given Radiation Characteristics, **A.S. KONDRATJEV**, *Moscow Power Engineering Institute, Moscow, USSR*

B74.1

RADIATION DUE TO A CONVEX CURVATURE DISCONTINUITY OF A DIELECTRIC COATED PERFECT CONDUCTOR

D. H. Monteith* and R. G. Olsen
Electrical and Computer Engineering Department
Washington State University
Pullman, WA. 99164-2752

It is known that surface waves radiate energy at curvature discontinuities. By reciprocity, surface waves will be excited by plane waves incident upon such a discontinuity. Here, the problem of the radiation of a surface wave on a flat dielectric coated perfect conductor which changes abruptly into a convex cylindrical dielectric coated perfect conductor is considered. The dielectric is assumed to be homogeneous, isotropic and linear. The problem is formulated as an integral equation over the discontinuity aperture in terms of Green's functions of flat and cylindrical coated conductors. This integral equation can be simplified by the use of regular perturbation theory in the case for large radius of curvature. Thus, perturbation forms of the Green's functions are determined and from these an iterative approximate solution to the integral equation is obtained. These results are compared to a numerical solution of the integral equation and in the case of a thin coating to known results for an impedance surface.

TM SURFACE-WAVE SCATTERING BY VERTICAL WIRES IN A LAYERED MM-WAVE/OPTICAL IC ENVIRONMENT

Boutheina Kzadri* and Dennis P. Nyquist
Department of Electrical Engineering
Michigan State University
East Lansing, MI 48824

The background environment surrounding planar integrated circuits for mm/optical wavelengths consists typically of a tri-layered substrate/film/cover configuration. The film layer of refractive index n_f and thickness "t" is deposited upon a semi-infinite substrate of index n_s and covered by a semi-infinite layer of index n_c. Such a planar environment supports surface waves, which are scattered by conducting IC devices. The scattering of incident TM surface waves by vertical wires located in the cover layer (a canonical problem) is studied here.

A coordinate system is chosen with y normal and x,z tangential to the planar interfaces; the origin is at the film/cover interface. The current I induced in a thin wire of radius "a" and length l which lies along the y-axis and is illuminated by TM surface-wave field E_y^i satisfies the integral equation

$$\left[\frac{\partial^2}{\partial y^2} + k_c^2\right] \int_d^{d+l} G(\vec{\rho},y|\vec{\rho}',y')I(y')\,dy' = -j\,\frac{k_c}{\eta_c}\,E_y^i(y) \quad \text{... all } d<y<(d+l)$$

for $|\vec{\rho}-\vec{\rho}'| = a$, where k_c,η_c are the wavenumber and intrinsic impedance of the cover while d is the spacing between wire and film/cover interface. Green's function $G = G^p + G^r$ decomposes into primary and reflected components having the Sommerfeld-integral representations

$$G^{p,r}(\vec{\rho},y|\vec{\rho}',y') = \int_0^{\infty} \frac{\lambda F(\lambda;y|y')}{4\pi p_c}\,J_0(\lambda|\vec{\rho}-\vec{\rho}'|)\,d\lambda$$

where $p_c = \sqrt{\lambda^2 - k_c^2}$ and $F = \exp(-p_c|y-y'|)$ for the principal term while $F = R\exp(-p_c[y+y'])$ for the reflected term ($R(\lambda)$ a reflection coefficient). The above integral equation is converted to Hallen form to accelerate the convergence of necessary Sommerfeld integrals.

Solutions to the Hallen-type integral equation for I(y) are obtained by MoM numerical methods. The scattered surface waves are obtained as residue contributions arising from TM surface-wave poles of $R(\lambda)$ in the reflected Green's function component. Scattering coefficients are defined and computed to describe the dependence of TM wave scattering upon configuration parameters.

B74.3

COMPACT REPRESENTATION OF RADIATION PATTERNS USING SPHERICAL MODE EXPANSIONS

T. L. Simpson* and J. C. Logan
Electrical and Computer Engineering Department
University of South Carolina
Columbia, SC 29210

Compact representations of the time-harmonic radiation patterns of wire antennas were obtained. Spatially band-limited spherical mode expansions of the magnetic vector potential, **A**, were obtained using a vector spherical mode expansion for the free space Green's function, e^{-jkR}/R:

$$e^{-jkR}/R = -j\,k\,h_0^{(2)}(kR)$$

$$= -j\,k \sum_{n=0}^{\infty} (2n+1)\, j_n(kr')\, h_n^{(2)}(kr)\, P_n(\cos\xi), \qquad (1)$$

The contribution of each segment to each Cartesian component was computed separately and summed to produce the vector series:

$$A(r,\theta,\varphi) = \frac{-j\mu_0\, e^{-jkr}}{2r} \sum_{n=0}^{\infty} \sum_{m=0}^{n} \left[a_{nm}\, Y_{nm}^{e}(\theta,\varphi) + b_{nm}\, Y_{nm}^{o}(\theta,\varphi) \right], \qquad (2)$$

where a_{nm} and b_{nm}, the coefficients, are given by

$$a_{nm} = \sum_{i=1}^{P} I_i \int_{\Delta s_i} j^{n+1}\, j_n(kr')\, Y_{nm}^{e}(\theta',\varphi')\, ds', \qquad (3a)$$

and

$$b_{nm} = \sum_{i=1}^{P} I_i \int_{\Delta s_i} j^{n+1}\, j_n(kr')\, Y_{nm}^{o}(\theta',\varphi')\, ds', \qquad (3b)$$

where Δs_i is the i^{th} segment, $i = 1, 2, \ldots, P$, and the normalized even and odd spherical modes, Y_{nm}^{e} and Y_{nm}^{o}, are given by

$$Y_{nm}^{\substack{e \\ o}}(\theta,\varphi) = \left[\epsilon_m \frac{(2n+1)}{2\pi} \frac{(n-m)!}{(n+m)!} \right]^{1/2} P_n^m(\cos\theta) \begin{matrix} \cos \\ \sin \end{matrix} m\varphi. \qquad (4)$$

Since $j_n(kr)$ decays rapidly as n exceeds kr, the coefficients a_{nm} and b_{nm} decay similarly. For antennas of modest electrical size, $kR < M$, this suggests that the pattern series can be truncated with $n \le N \approx M$. Confirmation was obtained by comparison with MININEC patterns. For $N < 2M$, the observed rms discrepancy was typically more than 60 dB below the maximum.

ASYMPTOTIC EXPANSIONS OF ANTENNA CURRENTS

K. C. Chen* and L. K. Warne
Sandia National Laboratories
P. O. Box 5800
Albuquerque, New Mexico, 87185–5800

An asymptotic technique for approximating time–domain and time–harmonic antenna currents on an infinite cylindrical antenna is discussed. The time–domain solution is expressed in terms of one parameter: the ratio of transverse–wavefront–to–wire distance to wire radius, and this solution is valid to near the wavefront. The time–harmonic solution is based on a faithful evaluation of the Hallén filament integral. The solution is uniform with respect to kz but for a large parameter $\ell n \frac{2kz}{(ka)^2}$. The restriction is the usual condition $z >> a$. These newly derived formulas are shown to reduce to known existing results. Inconsistencies in the literature on the subject are discussed.

B74.5

ANALYTICAL TECHNIQUE FOR DETERMINING BACKSCATTERING FROM CYLINDRICAL SCREENS OF ARBITRARY CROSS SECTION

M. Martínez, A. Martín *, R. Villar
Instituto de Electrónica de Comunicaciones
Consejo Superior de Investigaciones Científicas
C./ Serrano 144. 28006 - MADRID. SPAIN

The aim of this work is to present an analytical and uniform solution for the backscattering of an arbitrary plane wave by a screen which is a rectangular section of a cylinder of arbitrary cross section.

In a recent work (The Fourth Biennal IEEE Conference on Electromagnetic Field Computation, Toronto, October 1990), the authors have presented analytical solution for the backscattering from a screen which is part of a circular cylinder. In this paper we consider screens of arbitrary cross section.

The solution is derived from an asymptotic evaluation by the stationary phase approximation of the physical optics integral for the incidence of an arbitrary plane wave on the screen. The solution includes separated contributions from the specular line and from the edges. These contributions are easily evaluated knowing the variation of the radius of curvature in the transversal section. The amelioration of that solution with an analytical result from the Physical Theory of Diffraction is also shown.

Applications for calculating the RCS monostatic of screens of circular and elliptical cross section and ogival cylinders are presented.

CAVITY-FED SLOTS EXCITED BY NARROW WIRES

Shahrokh Hashemi-Yeganeh
Department of Electrical Engineering
Arizona State University
Tempe, Arizona, USA 85287-7206

Cavity-fed slot radiators are most useful in airborne applications. They are light weight, and they can be flush mounted easily on the body of an aircraft. This presentation deals with the theoretical modeling and analysis of a single cavity-fed slot, excited by a narrow strip conductor, which is attached to the inner conductor of a coaxial cable feeding the cavity. Coupled integral equations are derived and solved, using the method of moments, to obtain the slot aperture electric field and the current distribution on the strip. Assumed equivalent magnetic current (magnetic frill), infinitesimally close to aperture of the coaxial line with the cavity wall, is used as the forcing function in the moment-method solution. Computed current on the strip is used to determine the input impedance of the cavity-fed slot. The input impedance data can be used to construct a planar array of these slots, including mutual interaction between them.

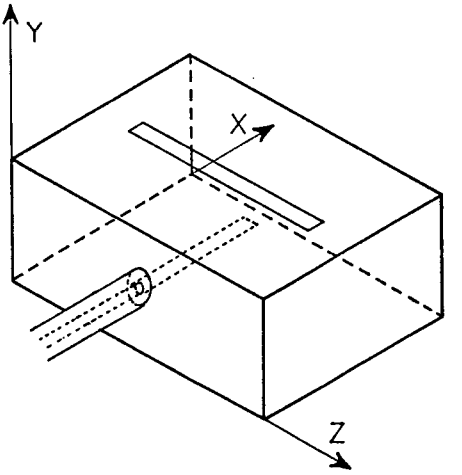

B74.7

A CONJECTURE ON THE POLARIZABILITIES OF A PLANAR APERTURE

K.S.H. Lee

Kaman Sciences Corporation, Dikewood Division
Santa Monica, CA 90405, USA

This paper first reviews the background that has led to the conjecture regarding a relationship among the electric and magnetic polarizabilities of an arbitrary aperture in an infinite plane. The conjecture is, the inverse of the electric polarizability is equal to or greater than the sum of the inverses of the two prinicpal magnetic polarizabiities [1]. The equality sign is shown to hold for elliptic and circular apertures. With the aid of the variational principle the conjecture is proved for apertures with two axes of symmetry [2]. Finally, by an application of the causality principle and the optical theorem a weaker conjecture is proved.

References

[1] K.S.H. Lee, "Relations Between Electric and Magnetic Polarizabilities and Other Related Quantities," Radio Sci., vol. 22, no. 7, pp. 1235-1238, Dec. 1987.

[2] R.L. Gluckstern, R. Li, and R.K. Cooper, "Correction to Electric Polarizability and Magnetic Susceptibility of Small Holes in a Thin Screen, " IEEE Trans. Microwave Theory Tech., vol. 38, no. 10, pp. 1529-1530, October 1990.

SYNTHESIS AND ANALYSIS OF HPM REFLECTOR ANTENNA SYSTEMS: A GENERALIZED OPTIMIZATION APPROACH

Dah-Weih Duan and Yahya Rahmat-Samii*
Department of Electrical Engineering
University of California, Los Angeles
Los Angeles, CA 90024-1594

Reflector antennas can be effectively used to produce directive High Power Microwave (HPM) radiations. In order to fulfill various HPM requirements, a general reflector antenna configuration which consists of a single- or dual-shaped reflectors and an array feed may have to be used. In this paper, diffraction analysis and synthesis of such reflector antennas will be discussed and results presented.

Carrying the power generated by HPM sources, the antenna feeding system may consist of a cluster of feeds that are distributed three dimensionally with different orientation, polarization and excitations. A computer program for feed analysis must be capable of (a) handling such general array configurations, (b) utilizing various models for each feed type, and (c) calculating the vector E-field and H-field at near- and far-field points. Various HPM issues can be discussed based on the results of feed analysis. To analyze the radiation from the reflectors, diffraction analysis techniques such as physical optics (PO) and physical theory of diffraction (PTD) will be applied. PO can accurately predict the field in the main beam region and near side lobes. In the far-angle or cross-polarized field predictions, however, the reflector edge diffraction may become important and demand the inclusion of PTD fringe field. The observation points can be in the near- or the far-field of the reflectors. Near-field analysis is important for HPM antennas not only because of the near-field effect of the feeds, but also for air breakdown considerations.

Optimization (mathematical programming) techniques provide a general and more flexible approach to antenna design problems. For HPM applications, the reflector(s) will be shaped to focus the HPM energy at various distances using an array feed (instead of a single feed). To do so, one may parameterize the reflector surfaces, and search for a set of parameters that produces the desired radiation characteristics. Using this method, no more approximations than those assumed in the analysis is necessary, and the analysis of the resultant antenna is performed simultaneously in the course of synthesis. There are many other interesting design problems that can be solved effectively using optimization techniques. For example, one can (a) restore a mislocated feed by maximizing the antenna gain, (b) compensate a distorted reflector surface by adjusting the excitations of an array feed, and (c) produce a specific field pattern (e.g. contoured beam designs) over a frequency band by shaping the reflector(s) and/or adjusting feed excitations.

B74.9

SOURCE FIELD STUDIES FOR A SPHERICAL DIELECTRIC ANTENNA EXCITED BY TE_{11} MODE

* S.PAL ** A.KUMAR ** R.CHATERJEE

In the paper boundary value problems have been formulated and solved for a Spherical Dielectrie Antenna excited by a cylindrical waveguide operating in TE_{11} mode. It is shown that for such a case infinite number of hybrid modes are excited over the surface of the sphere but only a few are of importanee. The calculated and measured source field results over a sphere at X-Band are also presented.

* Communication Systems Division
ISRO SATELLITE CENTRE
Airport Road
BANGALORE-560 017.

** EC Department
Indian Institute of Science
IISc Post;
BANGALORE-560 012.

DISCRETE RADIATING SYSTEMS PHASE SYNTHESIS FROM GIVEN RADIATION CHARACTERISTICS

A.S. Kondratjev,
Moscow Power Engineering Institute,
105250, Moscow, E-250, Krasnokazarmennaya, 14

Some problems of discrete radiating systems (e.g. antenna array) radiation characteristics synthesis by excitation phases selection with fixed excitation amplitudes are considered. Named problems are schematically classified into three main groups:

1) complex pattern synthesis;
2) amplitude pattern synthesis;
3) array gain maximization in selected direction.

Numerical iterative method is proposed for solution of first problem. This method may be a cause for development of specific solution methods for remaining problems.

Phase synthesis problem is solved in r.m.s. approximation and reduced to quadratic form constrained minimization with quadratic constraints. Mutual coupling of array elements is taken into consideration. When additional constraints are considered (e.g. fixation of pattern shape for given directions and/or element input impedances correction), additional linear and/or quadratic constraints are arised.

Solution of these problems may be given by means of synthesis method based on Lagrange multipliers method and penalty functions method combination. Modification of this method is presented for planar array phase synthesis with phase control by row and column.

Efficiency comparison is performed for this method and pure penalty functions phase synthesis method. Results obtained shows that method proposed produces more stable solutions with less r.m.s. synthesis error.

This method application to linear equispaced (space = $\lambda/2$, λ - wavelength) array of 33 isotropic radiators synthesis for a given flat-top pattern (width = 6.4°) with null direction $\vartheta_o=5^\circ$ is presented in table below. First column presents initial pattern value for ϑ_o direction; following - synthesized pattern values with different allowed phase discretisation $\Delta\varphi$.

$\Delta\varphi$	0	0	$\pi/32$	$\pi/8$
$F(\vartheta_o)$, dB	-15,0	-101,0	-59,0	-48,0

Rough Surfaces | Room 2020 Salle URSI B Session 81 | Surfaces rugueuses

Chairs/présidents: G.S. BROWN, USA; A. ISHIMARU, USA

08:30 (81.1) Electromagnetic Scattering of Waves by Random Rough Surface: Finite-Difference Time-Domain Approach, **C.H. CHAN**[1], S.H. LOU[1], L. TSANG[1], J.A. KONG[2], [1] *University of Washington, Seattle, WA, and* [2] *Massachusetts Institute of Technology, Cambridge, MA, USA*

08:50 (81.2) Comparison of Conductor Loss for Rough and Smooth Surfaces, **C.L. HOLLOWAY**, E.F. KUESTER, *University of Colorado, Boulder, CO, USA*

09:10 (81.3) Insight into the Normalized First Order Smoothing Method for the Analysis of Rough Surface Scattering, **G.S. BROWN**, *Virginia Polytechnic Institute and State University, Blacksburg, VA, USA*

09:30 (81.4) Electromagnetic Scattering from Perfectly Conducting Rough Surfaces (A New Full Wave Method), **R.E. COLLIN**, *Case Western Reserve University, Cleveland, OH, USA*

09:50 (81.5) The Condition for Distribution of Many Scatterers to be Purely Random in View of Expressions of the Coherent Field, **M. TATEIBA**, Y. NANBU, *Kyushu University, Fukuoka, Japan*

10:10 **COFFEE/CAFÉ**

10:30 (81.6) A New Method and Its Validity for the Analysis of Mean Scattered Power on a Gaussian-Distributed-Type Rough Surface, **Y. KOTSUKA**, K. ENOMOTO, *Tokai University, Hiratsuka City, Japan*

10:50 (81.7) Backscattering Enhancement from Random Media and Rough Surfaces, **A. ISHIMARU**[1], J.S. CHEN[1], P. PHU[1], K. YOSHITOMI[2], [1] *University of Washington, Seattle, WA, and* [2] *Kyushu University, Fukuoka, Japan*

11:10 (81.8) A Numerical Comparison of Scattering Model Results for 2-D Randomly-Rough Dirichlet Surfaces, **T.Q. YANG**, S.L. BROSCHAT, *Washington State University, Pullman, WA, USA*

11:30 (81.9) Scattering of Electromagnetic Wave from a Random Cylindrical Surface, **H. OGURA**, N. TAKAHASHI, M. KUWAHARA, *Kyoto University, Kyoto, Japan*

11:50 (81.10) A Numerical Assessment of Rough Surface Scattering Theories, E. RODRIGUEZ, **Y. KIM**, *California Institute of Technology, Pasadena, CA, USA*

ELECTROMAGNETIC SCATTERING OF WAVES BY RANDOM ROUGH SURFACE: FINITE-DIFFERENCE TIME-DOMAIN APPROACH

C. H. Chan*, S. H. Lou and L. Tsang
University of Washington, Seattle, WA 98195

J. A. Kong
Massachusetts Institute of Technology, Cambridge, MA 02139

Numerical analysis of scattering of waves by random rough surfaces has been studied extensively using the integral equation approach. The disadvantage of the integral equation approach is that it requires to solve a full matrix of the order of 10 times the surface length. Recently, finite difference and finite elements methods have been reported for the Monte Carlo simulation of the random rough surface. In both of these methods, one requires to solve large sparse matrices and a full matrix of the order of only twice the surface length size. Both of these methods require less computer memory and computation time than that of the integral equation method. In this paper, we present a finite-difference time-domain (FDTD) approach to the analysis of rough surface scattering. The advantage of the FDTD approach is that matrix inversion of any kind has been completely eliminated.

For an one-dimensional perfect electric conducting rough surface, the Gaussian surface profile is replaced by a stair-case approximation. FDTD is then applied to the scattered field instead of the total field. Boundary condition is enforced on the rough surface by setting the sum of the scattered field and that of the incident one equal to zero. Although the incident field is known explicitly, we calculate the incident field using the FDTD to offset discretization errors. The calculation domain of the FDTD is bounded by the rough surface at the bottom, a periodic boundary condition on the two sides and an absorbing boundary condition (ABC) on the top. The particular absorbing boundary condition chosen here is the second order Liao's ABC for its accuracy as well as its simplicity in implementation.

For the source excitation, plane waves with either sinusoidal or Gaussian distribution in time can be used. Figure 1 shows the spatial distributions of the reflected electric field in the frequency domain calculated by the FDTD and the finite element method at normal incidence, excellent agreement is obtained.

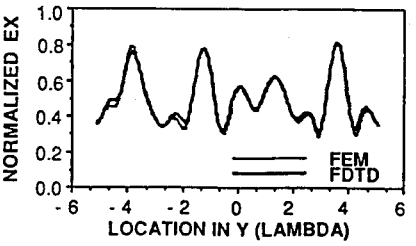

Figure 1. Comparison of reflected fields calculated by FDTD and FEM. Surface length L=10.2λ, rms height = 0.1λ and correlation length l = 1λ.

COMPARISON OF CONDUCTOR LOSS FOR ROUGH AND SMOOTH SURFACES

Christopher L. Holloway* and Edward F. Kuester
Dept. of Electrical and Computer Engineering
MIMICAD CENTER: Campus Box 425
University of Colorado, Boulder, CO 80309

The problem of determining the amount of the power loss that is associated with a rough conducting interface has been analyzed by a number of authors, beginning with the work of Morgan in the late 1940's (S.P.Morgan, *J. App. Phys.*, **vol. 20**, 352-362, 1949). Morgan analyzed two-dimensional periodic rough conducting interfaces, and was able to obtain the dependence of power loss on skin depth for various roughness profiles for current flowing transverse to the grooves. It wasn't until the mid 1980's (the work by Mende on superconductors (F.F.Mende, *Cryogenics*, **vol. 25**, 10-12, 1985)) that similar results were obtained for current flowing parallel to the roughness.

In this paper a model of the surface roughness is developed that will handle both polarizations and is general enough to handle two-dimensional as well as three-dimensional rough periodic conducting surfaces. The model is based on the method of *homogenization*. In this technique an expansion of the fields as a function of the period of the roughness in obtained. From this expansion it is then possible to determine impedance boundary conditions for the *average* fields at a reference plane near the actual rough surface.

Parameters that appear in the impedance boundary condition that are associated with the roughness profile must be determined numerically. A variational functional has been developed that is proportional to these parameters. The non-standard boundary conditions that arise in this problem are natural for this functional. As a result, ordinary finite-element basic functions can be used with no special constraints. Numerical results for two-dimensional roughness for both non-perfectly conducting and super-conducting surfaces will be presented. Comparisons will be made with results found in the literature for the periodic profiles.

By analyzing periodic roughness it is possible to examine what effect different roughness profiles will have on power loss. Research by Sanderson (A.E.Sanderson, *Advances in Microwaves*, **vol. 7**, 1-55, 1971) shows that Rayleigh-Rice perturbation techniques give good results for periodic surface roughness whose slope is small to moderate. We speculate that this may also be true for random or non-periodic roughness. It is then possible to use Rayleigh-Rice theory to obtain an impedance boundary condition for such randomly rough profiles.

B81.3

INSIGHT INTO THE NORMALIZED FIRST ORDER SMOOTHING METHOD FOR THE ANALYSIS OF ROUGH SURFACE SCATTERING

Gary S. Brown
Bradley Department of Electrical Engineering
Virginia Polytechnic Institute & State University
Blacksburg, Virginia 24061-0111

A great deal of effort is presently being put into the analysis of rough surface scattering via the solution of the fundamental integral equations by means of numerical methods. Unfortunately, such solutions are presently limited to one-dimensionally rough surfaces (corduroy surfaces) because of the computer storage and time required to solve the integral equations. This limitation does not appear to be a short term delay.

One particular means of circumventing this problem to a degree is to develop more robust approximations than are presently available. Such an approach may not permit the analysis of all rough surfaces, but it might enable us to obtain results for most surfaces of interest. Such is the long range goal of this research.

The normalized first order smoothing (NFOS) method is a technique which appears to have the capability of providing a tractable analytical/numerical tool for dealing with two-dimensionally rough surfaces which support small to moderate multiple scattering. The primary technique is first order smoothing which provides a compact approximation for surfaces having very small heights relative to a wavelength but arbitrary surfaces slopes. Such surfaces give rise to non-localized diffraction as opposed to the localized diffraction that is associated with surfaces having small heights and slopes. This method works because the average field scattered by the surface is much more dominant than the fluctuating field. The second component of the technique is the normalization of the basic integral equation by a surface height dependent phase factor. This nornaliza- tion is done prior to the application of the first order smoothing; after the application of smoothing, the phase factor is reintroduced via a convolution than the current.

The purpose of this paper is to report on the reasons why this particular technique appears to be so robust. First, we show that the normalization maximizes the mean "normalized" Born current and this is a key ingredient in extending the method to moderate/large height surfaces. However, this maximization, while necessary, is not obviously sufficient to guarantee the need for the integral term in the integral equation. Recent investigations have shown, however, that what this normalization appears to be doing is to give rise to an effective suppression of the multiple scattering that occurs in the immediate vicinity of any point on the surface. That is, the normalized equation seems to support only very long range multiple scattering for surfaces with moderate to large slopes. As the surface slopes become very large or grazing incidence is approached, very long range multiple scattering is the dominant mechanism and this is where the technique fails. The results will be discussed in detail.

Electromagnetic Scattering from Perfectly Conducting Rough Surfaces (A New Full Wave Method).

R. E. Collin
Electrical Engineering and Applied Physics Dept.
Case Western Reserve University
Cleveland, OH 44106

In this paper a relatively simple full wave solution for scattering from a perfectly conducting rough surface is developed. The surface profile is described by $y = \zeta(x,z)$. For applied electric and magnetic sources J and J_m Maxwell's equations are

$$\nabla XE = - j\omega\mu_o H - J_m \ , \quad \nabla XH = j\omega\varepsilon_o E + J$$

The three dimensional problem is reduced to a two dimensional one by assuming that each rectangular component of the field has an expansion of the form

$$E_x(x,y,z) = \int_o^\infty e_x(x,z,k_y)\, \psi_o(k_y,y)\, dk_y$$

$$E_y(x,y,z) = \int_o^\infty e_y(x,z,k_y)\, \psi_e(k_y,y)\, dk_y$$

etc., where ψ_e and ψ_o are local basis functions that are even and odd about the point $y = \zeta(x,z)$. The transformed field equations have equivalent sources that are given by coupling integrals proportional to the slopes ζ_x and ζ_z. These equations are functions of x and z only and are solved using Fourier transforms. The equivalent source terms are evaluated by approximating the fields in the coupling integrals by the unperturbed incident and specular reflected plane wave. The scattered field is found by eliminating the slopes through integration by parts over x and z and inverting the Fourier transforms by the method of stationary phase. By this means scattering coefficients are derived for the co-and cross-polarized fields when a vertical or horizontal polarized plane wave is incident.

Bahar and Rajan (IEEE Trans., AP-27, 214-225, 1979) obtained scattering coefficients for a surface that was rough along the x direction only. Their method was based on the use of telegraphist's equations which are not applicable to surfaces with two dimensional roughness. In spite of this limitation in the derivation Bahar assumes that their scattering coefficients are applicable to surfaces with two dimensional roughness (E. Bahar, IEEE Trans., AP-29, 443-454, 1981). Our more rigorous derivation shows that indeed Bahar's scattering coefficients are correct for a perfectly conducting surface with two dimensional roughness.

B81.5

THE CONDITION FOR DISTRIBUTION OF MANY SCATTERERS TO BE PURELY RANDOM IN VIEW OF EXPRESSIONS OF THE COHERENT FIELD

Mitsuo Tateiba and Yukihisa Nanbu

Department of Computer Science and Communication Engineering
Fuculty of Engineering, Kyusyu University
6-10-1 Hakozaki, Higashi-ku, Fukuoka 812, Japan

In a previous paper(M. Tateiba, Radio Sci.,22,881-884,1987), we presented a new approach to the problem of wave scattering by many particles. According to the paper, the coherent field is generally expressed by using two parameters P and Q, where P denotes the periodicity of the distribution of scatterers and Q denotes the dislocation from the periodicity. Under the condition for the coherent field to be expressed by using only the Q, the distribution of scatterers may be regarded as pure-random one.

In order to calculate the condition, it is assumed that each scatterer is a dielectric cylinder of infinite length and that only the position of the cylinder is expressed as a random vector. We derive the mean Green function which becomes a propagator in the integral equation for the coherent field, in both cases of random and slightly periodic distributions. The condition can readily calculated from the mean Green function, if we assume the wavenumber in free space, the mean length between cylinders, the dielectric constant and the size of the cylinder, and the observation point.

Some numerical results for the condition to be satisfied are shown graphically. The results presented here is useful for the precise calculation of the equivalent dielectric constant of the medium composed of many dieleric cylinders. As an illustrative example, the position distributions are shown in Figs. 1 and 2, where they are described by computer on the assumption that the dislocation from the periodic distribution is Gaussian random. Figure 1 shows a non pure-random distribution which becomes more periodic as the frequency of the wave increases, although Fig. 2 shows an almost pure-random distribution even for a high freqency.

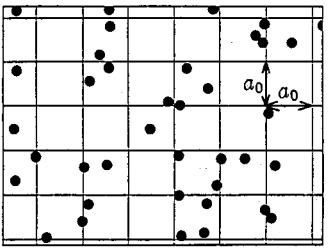

Fig. 1 The distribution of cylinders for $\sigma_0 = 0.45a_0$.

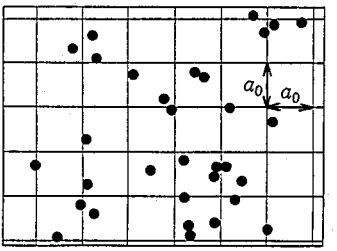

Fig. 2 The distribution of cylinders for $\sigma_0 = 0.9a_0$.

In above figures, a_0 is the mean length between cylinders, σ_0 is the standerd deviation of the dislocation from the periodicity, the wavelength in free space is assumed to be $0.1a_0$.

A NEW METHOD AND ITS VALIDITY FOR THE ANALYSIS OF MEAN SCATTERED POWER ON A GAUSSIAN-DISTRIBUTED-TYPE ROUGH SURFACE

Youji Kotsuka*, Kazuo Enomoto

Faculty of Engineering, Tokai University
1117, Kitakaname, Hiratsuka City, JAPAN

A new method is introduced for the analysis of mean scattered power on a slightly deformed Gaussian-distributed random rough surface, validating the prior method.

It is very important to regard Gaussian distribution which is slightly deformed (quasi-Gaussian distribution) as a different kind of statistical geometry from that of "pure Gaussian distribution," especially from the viewpoint of microwave remote sensing. This is because the difference in magnitude of the scattering coefficients between quasi-Gaussian and Gaussian distribution increases as the incident wave becomes perpendicular to the random rough surface.

The author has presented these problems in the previous paper on the general analysis of mean scattered power (Y. Kotsuka, Proc. of URSI Int. Symp. on Electromagnetic Theory, pp. 521-523, 1989).

The method of analysis was based upon the introduction of a general Gram-Charlier expansion and a general Hermite function to calculate the expression of the scattering coefficient. In the previous paper, from this expression the scattering patterns for a pure random case were calculated. However, Gram-Charlier expansion has a problem in that the convergence characteristics are not generally stable.

In this paper, instead of Gram-Charlier expansion, a new probability density function which approximates Gram-Charlier expansion is introduced. This new probability density function is derived from the non-monotonic transformation of random variables. Unknown coefficients which appear in the new probability density function are determined by the method of Taylor series successive approximation.

Using the new probability density function, the characteristic function, which is related to the expression of the scattering coefficient, is calculated with the same distributions as the Gram-Charlier distributions. On the basis of this new function, a detailed investigation of the convergence problem for Gram-Charlier expansion is also examined by taking variance, skewness and so on as the parameters. As to the caclulation of the scattering pattern in terms of the new probability density function, it has become clear that the value of mean scattered power closely approximates that of mean scattered power using Gram-Charlier expansion. At the same time, from the investigations mentioned above, the validity for the analysis of the mean scattered power in the previous paper has been clarified.

B81.7

BACKSCATTERING ENHANCEMENT FROM RANDOM MEDIA AND ROUGH SURFACES

Akira Ishimaru,* Jei S. Chen and Phillip Phu
Department of Electrical Engineering
University of Washington
Seattle, Washington 98195

Kuniaki Yoshitomi
Department of Computer Science and Communication Engineering
Kyushu University
6-10-1 Hakozaki, Higashi-ku
Fukuoka 812, Japan

This paper gives recent work on the backscattering enhancement from rough surfaces and discrete scatterers. Enhanced backscattering has been observed for many years and has been sometimes called retroreflectance or opposition effect. Recently, more quantitative experimental and theoretical studies have been reported. Enhanced backscattering by discrete scatterers has been observed experimentally and explained theoretically by noting the constructive interference of two waves traversing through the same particles in opposite directions. This has been recognized as weak Anderson localization caused by the coherent backscattering. The enhanced peak is close to 2, and the angular width is governed by the diffusion length in the medium. Recently, experimental and numerical studies have been reported on backscattering enhancement from rough surfaces. There are two distinct enhancement phenomena. One is when the rms height is close to a wavelength and the slope is also close to unity. We present an analytical theory making use of the second-order Kirchhoff approximation with shadowing functions. The second is when the rms height is small, but the surface supports a surface wave mode. This occurs when the incident wave is polarized parallel to the plane of incidence and the dielectric constant of the second medium has a negative real part. Numerical and experimental results are presented and compared with theoretical predictions. Intensity correlations of the scattered wave as the surface is moved are investigated using millimeter wave experiments and compared with numerical Monte Carlo simulations. The possibility of using this technique for remote sensing of the surface characteristics is discussed.

A NUMERICAL COMPARISON OF SCATTERING MODEL RESULTS FOR 2-D RANDOMLY-ROUGH DIRICHLET SURFACES

T.Q. Yang*
S.L. Broschat
Electrical Engineering & Computer Science Department
Washington State University
Pullman, WA 99164-2752
(509) 335-6470
FAX: 509 335-3818

Wave scattering from random rough surfaces is important in a variety of scientific and engineering applications, including radio communications, microwave remote sensing, underwater acoustics, and integrated optics. Unfortunately, the two classical methods, the field perturbation and Kirchhoff approximations, have been shown to be limited in their range of validity (E.I. Thorsos, JASA 83(1), Jan. 1988, 78-92; E.I. Thorsos & D.R. Jackson, JASA 86(1), Jul. 1989, 261-277).

New scattering models have recently been introduced: the phase perturbation technique by Winebrenner and Ishimaru and the small slope approximation by Voronovich. The phase perturbation technique has been shown to have a much wider range of validity than the classical methods (Broschat *et al.*, JEWA, 3(3), 237-256, 1989), and the second-order small slope approximation has been shown to give good results for a Pierson-Moskowitz spectrum using a Monte Carlo method (D.H. Berman, private communication). In this paper we present numerical results for these two models for the bistatic scattering cross section for two-dimensional randomly-rough surfaces with a Gaussian spectrum for the Dirichlet problem. Results are compared with those of the classical techniques. It is shown that both the phase perturbation and small slope approximation results reduce to those of the classical perturbation method in the appropriate limits. In addition, results for both models reduce to those of the Kirchhoff approximation over certain ranges of scattering angles.

B81.9

SCATTERING OF ELECTROMAGNETIC WAVE FROM A RANDOM CYLINDRICAL SURFACE

H.OGURA*, N.TAKAHASHI and M.KUWAHARA
Dept. Electronics, Kyoto University, Yoshida, Kyoto, 606 Japan

The scattering from a random cylindrical surface is studied for a plane-wave injection with s (TE) polarization by means of Wiener-Ito's stochastic functional calculus combined with the group-theoretic consideration concerning the homogeneity of the random surface. The analysis is made on the basis of a stochastic scattering theory developed by the authors (Nakayama,Ogura et.al: Radio Sci.,**16**, 831, 847, 1981; Ogura, Nakayama: J. Math. Phys. **29**, 851, 1988; Ogura, Takahashi: J. Math. Phys. **31**, 61, 1990) The random surface is assumed to be a homogeneous Gaussian random field on the cylinder C, that is, its probability measure is invariant with respect to the group of motions on C, called the cylindrical group: translations along the axis and rotations around the cylinder; both additive and mutually commutative. An operator D, operating on a random field on C, is introduced in such a way that it keeps invariant the homogeneous random surface, and that it gives a representation of the cylindrical group. Since D commutes with the boundary condition and the Maxwell equation, a stochastic electromagnetic wave field can be given by an irreducible representation, i.e., an eigenfunction of D. If the incident wave is a m-th cylindrical vector-function of TE or TM wave, a vector eigenfunctions of D operator, the scattered random wave field should be an eigenfunction with the same eigenvalue. The scattered stochastic wave field, which satisfies the Maxwell equation and at the same time is an eigenfunction of D as well as a stochstic functional of the Gaussian random surface, can be represented as a vector form of Wiener-Ito expansion in terms of TE and TM modes as well as the Gaussian random measures generating the random cylindrical surface. The vector boundary condition on the random cylinder is cast into a hierarchy of equations for the Wiener kernels, which can be solved approximately. The random wave field for a plane-wave injection can be obtained by summing the above fields over m. From the stochastic representation of scattered electromagnetic wave so obtained, various statistical characteristics can be calculated. From the asymptotic form we obtain the coherent scattering amplitude and the total coherent power flow. The incoherent power flow can be obtained from the Wiener kernels. The power conservation law is derived, especially, a stochstic electromagnetic version of the optical theorem stating that the total scattering cross-section is given by the imaginary part of the forward coherent scattering amplitude. We also obtain the differential cross-sections of the coherent scattering and the incoherent scattering. Numerical calculations are made in the case of plane wave injection with s (TE) polarization. The case of p (TM) polarization can be treated in a similar manner.

A Numerical Assessment of Rough Surface Scattering Theories

Ernesto Rodriguez and Yunjin Kim*
Jet Propulsion Laboratory
California Institute of Technology
Pasadena, Ca 91109

We present a numerical evaluation of the regime of the validity for various rough surface scattering theories against numerical results obtained by the Method of Moments (MOM). The theories under consideration are the SPM (Small Perturbation Method), the MTE (Momentum Transfer Expansion), the TSE (Two Scale Expansion), and a new theory, which we call the UPM (Unified Perturbational Method). All these theories are derived in a unified manner starting with the extinction theorem. The rough surfaces that we consider are ocean-like surfaces, which exhibit height power law spectra.

The scattering cross sections are evaluated for both horizontal and vertical polarizations. Differences in the methods are summarized for the different roughness, incidence angles, and polarizations. For the vertical polarization, we will discuss the singularities occurred in both SPM and UPM. For both polarizations, UPM provides best results among all theories examined.

The research described in this abstract was carried out by the Jet Propulsion Laboratory, California Institute of Technology, and was sponsored by Office of Naval Research.

Scattering II Room 3014 Salle Diffusion II
URSI B Session 91

Chairs/présidents: R.E. KLEINMAN, USA; G.Y. DELISLE, Canada

08:30 (91.1) Coupling Finite Element and Integral Equation Solutions for Modeling a Class of Scattering and Radiating Structures, **T. CWIK**, L. EPP, *California Institute of Technology, Pasadena, CA, USA*

08:50 (91.2) Efficient Coupling of Finite Methods and Method of Moments in Electromagnetics Modeling, **D.-S. WANG**, R.A. WHITAKER, L.J. BAHRMASEL, *McDonnell Douglas Research Laboratories, St. Louis, MO, USA*

09:10 (91.3) A Second-Order Accurate Method on a Non-Uniform Mesh in the Finite Difference Frequency Domain Approach to EM Scattering Problems, **R. GORDON**[1], J.-F. LEE[2], R. MITTRA[2], [1]*University of Mississippi, University, MS, and* [2]*University of Illinois, Urbana, IL, USA*

09:30 (91.4) Finite-Volume Time-Domain (FVTD) Techniques for Scattering Calculation, **R. HOLLAND**[1], V.P. CABLE[2], L. WILSON[2], [1]*Albuquerque, NM, and* [2]*Lockheed Advanced Development Company, Burbank, CA, USA*

09:50 (91.5) Application of ABC-FEM-ICBCG to 2-D EM Scattering Problems, B. OUYANG, X.P. CAO, **Y.-M. XIAO**, *Xi'an Jiaotong University, Xi'an, China*

10:10 **COFFEE/CAFÉ**

10:30 (91.6) Hybrid Analysis (MM-UTD) of EM Scattering from Complex Structures, **M. HSU**, R.-C. CHOU, P.H. PATHAK, *Ohio State University, Columbus, OH, USA*

10:50 (91.7) Comparison of Maxwell-Garnett and Coherent Potential Theories for Layered Scatterers, **A.H. SIHVOLA**, *Helsinki University of Technology, Espoo, Finland*

11:10 (91.8) Electromagnetic Scattering by General Two-Dimensional Anisotropic Bodies, **J.C. MONZON**, N.J. DAMASKOS, *Damaskos Inc., Concordville, PA, USA*

11:30 (91.9) Scattering of Electromagnetic Waves by Charging Cloud of Particles, **N.I. PETROV**, I.N. SISAKIAN, *USSR Academy of Sciences, Moscow, USSR*

11:50 (91.10) The Phase Function Approximation to the Radiative Transfer Equation in Discrete Random Media with Large Particles, **S. ITO**, *Toyo University, Saitama, Japan*

B91.1

Coupling Finite Element and Integral Equation Solutions for Modeling a Class of Scattering and Radiating Structures

Tom Cwik and Larry Epp*
Jet Propulsion Laboratory
California Institute of Technology
Pasadena CA 91109

The use of surface integral equations to truncate the computational mesh used in finite element modeling is proving to be a useful method to model electrically large and inhomogeneous objects. The finite element model is used in inhomogeneous or irregular regions to provide a local description of the fields and material parameters. The surface integral equation is used to model fields in the homogenous region exterior to the object and incorporates the radiation condition exactly. The surface is taken to reside directly on the object, and the surface tangential fields are the unknown quantities in the integral equation. By matching field boundary conditions through the surface, fields are coupled from the interior to exterior regions, and a system of equations is formed which can be solved by various means. Using the integral equation to truncate the computational mesh is an alternative to using local boundary conditions which, though approximate, provides a more computationally efficient means of generating a solution for the fields.

This method is applicable to a wide range of radiating and scattering structures. In this paper, the class of periodic and non-periodic structures containing apertures in metallic groundplanes or combinations of metallic and dielectric regions is considered. Specifically, the following models will be considered: 1) Infinitely periodic screen models consisting of thick apertures in a conducting screen. Finite element modeling is used in the aperture which can be filled with dielectric and have a non-standard cross-section and depth profile. The integral equation reduces to a standard Floquet expansion in the exterior regions where reflection and transmission coefficients are calculated. 2) Finite-sized periodic screens similar to the above model, but with the surface surrounding the entire screen where an integral equation for the tangential surface fields is used. This screen may be planar or curved. Radar cross-sections are calculated. 3) A feedhorn or array of feedhorns radiating from a groundplane. In this structure a feed model is incorporated and radiated fields and VSWR are computed. 4) Aperture antennas fed by an integrated network.

EFFICIENT COUPLING OF FINITE METHODS AND METHOD OF MOMENTS IN ELECTROMAGNETICS MODELING

D. -S. Wang*, R. A. Whitaker, and L. J. Bahrmasel
McDonnell Douglas Research Laboratories
P.O. Box 516
St. Louis, MO 63166

The computation of electromagnetic (EM) scattering and radiation from large complex objects with embedded cavities such as gaps, inlets, and apertures is difficult because of (a)the coupling effects between the cavities and the remaining portion of the object, and (b)the electrical size of the object. The geometric and material complexities of the embedded cavities restrict the application of any numerical methods that are based on the surface integral equation (SIE) formulation. The fine details inside gaps and apertures require the application of volume-differential or volume-integral equation formulations. It has been shown that the finite-element/finite-difference (FE/FD) methods are computationally efficient for treating inhomogeneous, but bounded, problems in comparison with the volume-integral formulation. However, an application of the FE/FD methods for unbounded problems, such as the exterior problem of a scatterer, requires the incorporation of approximate radiation boundary conditions and the extension of the solution region (mesh domain) beyond the physical boundary of the scatterer. The FE/FD methods can be computationally prohibitive for electrically large scatterers. Recently, we have developed a method of moments (MM) based surface-wave hybrid analysis incorporating a new basis set that combines the subdomain basis functions with a surface-wave basis set. The surface-wave basis set substantially reduces the number of unknowns required on large smooth surfaces, and consequently, electrically large objects can be treated. However, this technique does not circumvent the inherent problem for SIE-based analyses in treating EM scattering and radiation problems from objects with embedded cavities.

In this presentation, we effectively combine the FE/FD methods with the MM formulation. Schelkunoff's equivalence principle is used to divide the original problem into an exterior and interior problem separated by perfectly electrical conducting boundaries (R. F. Harrington, IEEE Antennas Propagat., vol. AP-30, pp. 205, 1982). We use the surface-wave hybrid analysis for the exterior problem and the FE/FD methods for the embedded cavities. The present approach emphasizes computational efficiency for electrically large objects and an application of the present approach is demonstrated for objects with complex surface-conformal antennas embedded in dielectric layers. The effectiveness of this approach is illustrated using previously published data.

B91.3

A SECOND-ORDER ACCURATE METHOD ON A NON-UNIFORM MESH IN THE FINITE DIFFERENCE FREQUENCY DOMAIN APPROACH TO EM SCATTERING PROBLEMS

*R. Gordon**
Department of Electrical Engineering
University of Mississippi
University, MS 38655

J. F. Lee, and R. Mittra
Electromagnetic Communication Lab
University of Illinois
Urbana, IL 61801

In a recent paper (R. Gordon & R. Mittra, 1988 URSI Digest), a finite difference technique for solving the problem of electromagnetic scattering by a p.e.c. body of revolution (BOR) was presented. This technique employed the coupled azimuthal potentials (CAPs) introduced by Morgan and Mei and an asymptotic boundary condition obtained from Wilcox's expansion for the scattered field in terms of powers of r^{-1}. In the interior of the meshed region, the partial differential equations governing the CAPs were enforced using the conventional central difference formulas for all the derivatives appearing in these equations. On those parts of the boundary where it was necessary to enforce the Neumann boundary condition, a one-sided, first-order accurate derivative formula was used. In the present paper, two major improvements are presented. First, we derive second-order accurate formulas for the first and second derivatives that can be used with either uniform or non-uniform meshes. Second, we show how these formulas can be used to find a one-sided, second-order accurate formulas for the derivatives that are needed to enforce the Neumann boundary condition on the mesh boundaries. By comparing with the numerical results obtained using uniform meshes, we demonstrate that noticeable improvements can be achieved by using the one-sided, second order accurate derivative formula in applying the Neumann boundary condition. Then, with results generated using non-uniform meshes, we illustrate the kind of improvement that can be obtained by using the modified formulas for the derivative in discretizing the partial differential equations in the interior of the meshed region.

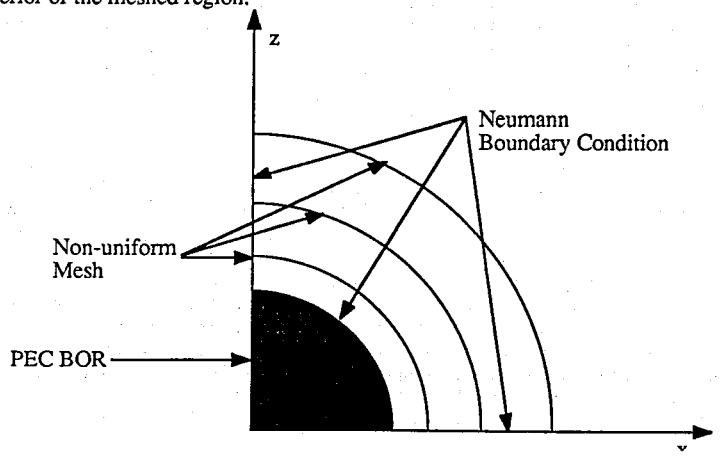

FINITE-VOLUME TIME-DOMAIN (FVTD) TECHNIQUES FOR SCATTERING CALCULATION

Richard Holland, 1625 Roma NE, Albuquerque, NM 87106, USA
Vaughn P. Cable and Louis Wilson, Lockheed Advanced Development Company, Burbank, CA 91520, USA

This paper describes our efforts to compute electromagnetic scattering using a generalization of the FDTD Yee algorithm in which a nonorthogonal, conforming mesh may be applied. Both 2D and 3D formulations are developed, although at present, we have extensive results only in 2D. Problems presented include a PEC circular cylinder, an S-shaped duct, and a PEC ojive. The circular cylinder, while seemingly simple, is actually a somewhat stressing case of the meshing algorithm which stretches a cartesian grid to fit a curved geometry.

The primary goal of this work is to model oblique or curved surfaces without the use of staircasing. We demonstrate that edge-on illumination of an ojive requires 120 cells per wavelength for 1 dB accuracy when staircasing is used, but only 15 cells per wavelength when conformal meshing is used. The conformal-mesh S-duct model shown below accurately precicts the first 12 depth resonances and first two width resonances in the monostatic scatter versus frequency when illumination is directly into the aperture. This S-duct model retains some fidelity with as few as four cells per wavelength, while staircased models require at least 20 cells per wavelength.

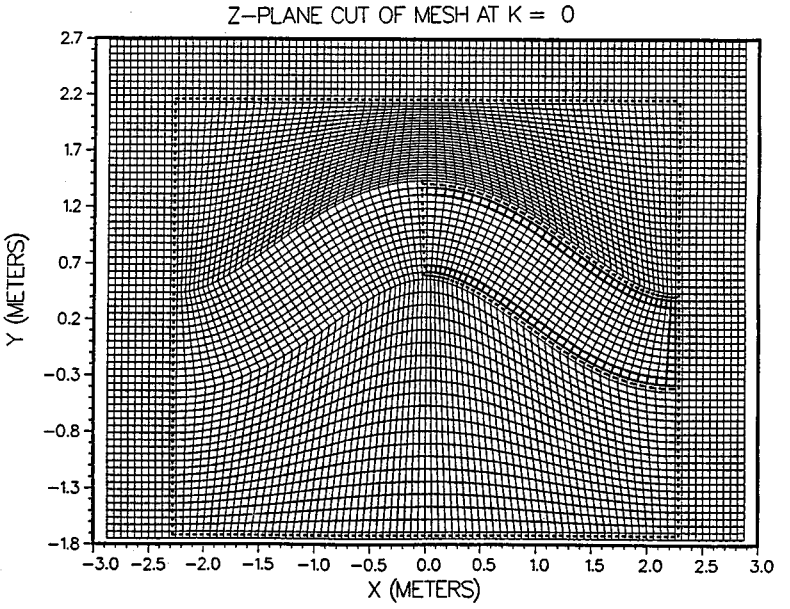

B91.5

APPLICATION OF ABC-FEM-ICBCG TO 2-D EM SCATTERING PROBLEMS

BING OUYANG, XIAO PING CAO, YAN-MING XIAO

Department of Information & Control Engineering
Xi'an Jiaotong University, Xi'an, P. R. China

SUMMARY

In many cases, OSRC seems not practicable because it is too sensitive to the geometry shapes of the scattering objects. Another feasible method, Combination of ABC and FEM (hereafter refer as ABC-FEM), hence was proposed by Ramahi and Mittra[1] in 1989. They truncated the region surrounding the scatterer with an artificial boundary on which an ABC was imposed, and inside which FEM was used. And it was shown that the results was in well agreement with those of MOM.

In present work, firstly, we introduced the ABC-FEM method to the analysis of various scatterers, such as conducting cylinders coated with dielectric material and multi-layer dielectric cylinders. Numerical results was carefully studied. And comparison indicated well agreement with the results of other method. Secondly, we evaluated several iterative methods of solving highly sparse large complex matrix equations which was resulted from ABC-FEM. ICBCG seems the best method because it requires much fewer iterations to produce the solution. A computer program based on ICBCG formulae was successfully used in our work. Thirdly, using regular artificial boundary and the treatments of OSRC to simplify the formation of ABC, and the results are promising.

REFERENCE

[1] M. Ramahi & R. Mittra, " Finite-Element Analysis of Dielectric Scatterers Using the Absorbing Boundary Condition, " IEEE Trans. Vol.MAG-25, No.4, 1989

HYBRID ANALYSIS (MM-UTD) OF EM SCATTERING FROM COMPLEX STRUCTURES

Mimi Hsu* , Ri-Chee Chou, Prabhakar H. Pathak
The Electroscience Laboratory
Department of Electrical Engineering
The Ohio State University
Columbus, Ohio

Hybrid methods, the combination of two or more analytical or numerical methods, are used for analyzing problems more accurately or efficiently than is generally possible using a single method alone. This paper presents a hybrid combination of the method of moments (MM) and the uniform theory of diffraction (UTD) to analyze the electromagnetic scattering from electrically large complex structures containing electrically small perturbations.

The MM converts an integral equation, in this case based on the reaction principle, into a set of matrix equations by expanding the unknown currents in terms of a set of basis functions and testing the integral equation with weighting functions. The size of the coefficent matrix which is dependent on the number of basis functions increases as the electrical size of the object increases. Therefore, at high frequencies this method usually requires the computation, storage, and inversion of an extremely large matrix. This is a very accurate method but usually is only viable at low frequencies.

The UTD, on the other hand, is an asympototic high frequency method. However, there are a limited number of canonical geometries for which UTD solutions currently exist. Therefore, if the radiating object or any part of it cannot be locally approximated by such canonical geometries, then the formulas cannot be applied.

The MM-UTD uses the UTD to deal with the electrically large parts of the radiating object since it is a highly efficient method while the MM is used on the electrically small, irregular parts for which the UTD is not applicable or for parts of the geometry for which UTD solutions are not available. The use of the hybrid MM-UTD in electromagnetic scattering problems will be discussed, and results will be presented for the scattering from a finned PEC convex cylinder and other geometries.

COMPARISON OF MAXWELL-GARNETT AND COHERENT POTENTIAL THEORIES FOR LAYERED SCATTERERS

Ari H. Sihvola
Helsinki University of Technology, Electromagnetics Laboratory
Otakaari 5 A, SF-02150 Espoo, Finland

In this presentation electromagnetic effects in heterogeneous media are considered. Examples of such media are encountered in remote sensing problems and composite material research, where the electric properties of the components comprising the medium are known but not those of the mixture itself. Especially dense mixtures have been a problem with no unique solution, i.e. media in which the scatterers form a considerable part of the total volume of the material. This transition region where single-scatterer solutions start to fail may be even as low as 10–20 % in the volume fraction of the scatterer phase.

It is not only the volume fraction of the scatterers that matters to the validity of the theories but also the dielectric contrast of the scatterer and the background medium. If this is large, like is the case for water in mixtures where the background can be modeled as air, the mixture is called nontenuous and also needs special attention. The formulas valid for tenuous cases, like the so called Maxwell-Garnett formula in the dielectric mixing theories, have to replaced by other approaches.

One of these theories is the coherent potential approach. In this presentation it is shown how this approach can be included in formulas that are valid for mixtures where there are spherical layered scatterers embedded in a background medium. The number of layers in the scatterers is not limited. The formulas derived form a family from which also other mixing rules emanate.

ELECTROMAGNETIC SCATTERING BY GENERAL TWO-DIMENSIONAL ANISOTROPIC BODIES

J. Cesar Monzon and Nick J. Damaskos
Damaskos, Inc.
P.O. Box 469
Concordville, PA 19331

In this paper we describe KRSTL, a unified numerical approach to the study of scattering by anisotropic bodies. The formulation is based on a surface integral approach (J.C. Monzon, IEEE Trans. Ant. Propagat., Vol. 36, No. 10, October 1988) originally developed for homogeneous regions, which has been extended via inclusion of a variety of algorithms to handle two dimensional geometries of arbitrary complexity. The result of this extensive work is KRSTL, a powerful tool in frequency domain RCS calculations which can analyze not only anisotropic regions in contact, not in contact, embedded in others, layered, coated and/or in the presence of resistive sheets, on top of a ground plane, and other possible combinations, but can also handle the case of bodies with parasitic resonances and any or all of the previous bodies in the presence of recessed openings in a ground plane, the cavities being of arbitrary anisotropic material composition as well. The figure shows a typical application of KRSTL in edge design.

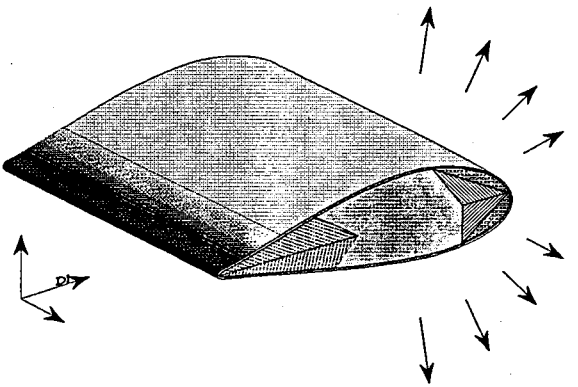

B91.9

SCATTERING OF ELECTROMAGNETIC WAVES BY CHARGING CLOUD OF PARTICLES

N.I.Petrov, I.N.Sisakian
Central Designer's Office of Unique Instrument Building of the USSR Academy of Sciences, Butlerova str.15, 117342 Moscow, USSR

In the last years a scattering of electromagnetic waves by charging clouds of particles is of great interest. First of all this is connected with the observing of anomalous strong reflection of radiowaves by charging clouds.

In this paper the physical mechanisms of that anomalous scattering are suggested. It is known that the strong scattering of electromagnetic waves by the metallic surface is caused by the conduction electrons. A top concentration of a free charges in the charging cloud is determined by the maximum possible potential of cloud at which the breakdown in air still absent. A breakdown neutralize the charge of cloud. However the stationary microdischarges or corona discharges in the cloud also to be possible. Corona discharge in avalanche-type and streamer forms may be exist. The streamer discharge in air are the plasma thread-like formations with a length of few centimeters at atmospheric pressure. The charge density in the streamer equal to 10^{13}-10^{14} cm^{-3}. The scattering section of one streamer equal approximately to 10^{-2} cm^2. When the conditions for the beginning of corona to be fulfilment the charging cloud is covered by the "net" of streamers or conducting needles. Anomalous reflection of radiowaves may be caused by interference effects leading to localization of waves in that physical system. As a rule two types of localization to be distinguished. These are the weak localization and Andersons strong localization. The parameter determining the localization is the $\gamma = \lambda/2\pi\ell_{el}$, where λ is the wavelength, ℓ_{el} is the elastic mean-free-path. At $\gamma \ll 1$ a weak localization is realized, and at $\gamma \sim 1$ a strong localization take place. At the weak localization the peak in the scattering on the angle 180° is appeared. At the strong localization the standing electromagnetic wave on the random placed centres is formated. The localization effects become strongly if the sizes of inhomogeneities $a \sim \lambda$ and the inelastic mean-free-path $\ell_{in} >> \ell_{el}$. If as the inhomogeneities to consider the streamers with a length of few centimeters then the strong localization will take place for the radiowaves GHz range.

THE PHASE FUNCTION APPROXIMATION TO THE RADIATIVE TRANSFER EQUATION IN DISCRETE RANDOM MEDIA WITH LARGE PARTICLES

Shigeo Ito
Department of Electrical Engineering, Toyo University
Kawagoe-shi, Saitama, 350 Japan

Multiple scattering problems of optical waves propagating in discrete random media have been extensively studied in the past. For random media with large particles the radiative transfer equation under the small-angle approximation has been used to analyze the propagation characteristics.

Although theoretical studies have been reported on the small-angle solution which is known to be generally valid for optical propagation in actual rain, fog, and clouds, the validity of the solution has not been clearly confirmed in comparison with experiments. This may be because the phase function is approximated to satisfy the energy conservation as in turbulence case and therefore the optical irradiance has no attenuation even when the optical distance increases. However, for the scattering by the above single particle, which is contrast to that by turbulence, the scattered energy confined within a small angle in the forward direction is at most half of the incident energy. This fact has not been incorporated in the analysis of the radiative transfer equation under the small-angle approximation.

In this paper we discuss the propagation characteristics of optical waves in discrete random media with large particles and obtain small-angle solutions of the scalar radiative transfer equation with a modified phase function. When we employ the small-angle approximation, the phase function is modified to include the large-angle scattering effects for optical wave propagation through fog and rain. The use of the usual phase function similar to that in turbulence is shown to exceedingly overestimate the scattered intensity.

The solution obtained is compared with both numerical solutions and simultaneously measured data [J. Awaka et al., ISAP '89, Vol.4, 1041, 1989] on millimeter and optical wave propagation in rain. The present theory indicates that the attenuation of optical waves is about half of that of millimeter waves due to multiple scattering effects, which is consistent with the experimental results.

On-Surface and Absorbing Boundary Conditions | **Room 3022 Salle URSI B Session 93** | **Conditions aux limites absorbantes**

Chairs/présidents: L.W. PEARSON, USA; A. PETERSON, USA

08:30 (93.1) New Methods for Developing Higher Order Impedance Boundary Conditions on Curved Surfaces, B. ENGQUIST[1], **W.D. MURPHY**[2], V. ROKHLIN[3], M.S. VASSILOU[2], [1] *University of California, Los Angeles, CA,* [2] *Rockwell International Science Center, Thousand Oaks, CA, and* [3] *Yale University, New Haven, CT, USA*

08:50 (93.2) Use of Three-Dimensional Vector Absorbing Boundary Conditions for RF Radiation and Scattering Problems, A. KHEBIR, **J. D'ANGELO**, *General Electric Company, Schenectady, NY, USA*

09:10 (93.3) Numerical Simulation of Three Dimensional Coatings and Cavities Using Higher Order Impedance Boundary Conditions, **K. BARKESHLI**, J.L. VOLAKIS, *University of Michigan, Ann Arbor, MI, USA*

09:30 (93.4) Scattering from Two Dimensional Composite Objects Using a Mixture of Boundary Conditions, P.M. GOGGANS, **A.A. KISHK**, *University of Mississippi, University, MS, USA*

09:50 (93.5) Solving 3-D Scattering Problems with Finite Elements Using a Second-Order Local Absorbing Boundary Condition, **J.W. PARKER**, R.D. FERRARO, P.C. LIEWER, *California Institute of Technology, Pasadena, CA, USA*

10:10 **COFFEE/CAFÉ**

10:30 (93.6) A New Look at the Absorbing Boundary Conditions for PDE Solution of Electromagnetic Scattering Problems in Time and Frequency Domains, **R. MITTRA**, J.-F. LEE, *University of Illinois, Urbana, IL, USA*

10:50 (93.7) A Study of Wave Interaction with a Slit Cylindrical Cavity Using the On-Surface Radiation Condition Method, P.D. SMITH[1], **G.A. KRIEGSMANN**[2], [1] *Dundee University, Dundee, UK;* [2] *New Jersey Institute of Technology, Newark, NJ, USA*

11:10 (93.8) Scattering by Homogeneous Cylinders Using Surface Radiation Conditions, **R. JANASWAMY**, *Naval Postgraduate School, Monterey, CA, USA*

11:30 (93.9) Evaluation of OSRC Higher Order Operators for Electromagnetic Scattering, **W. CHUN**[1], K. UMASHANKAR[1], A. TAFLOVE[2], [1] *University of Illinois, Chicago, IL, and* [2] *Northwestern University, Evanston, IL, USA*

B93.1

NEW METHODS FOR DEVELOPING HIGHER ORDER IMPEDANCE BOUNDARY CONDITIONS ON CURVED SURFACES[1]

B. Engquist‡W.D. Murphy†, V. Rokhlin*, and M. S. Vassiliou†
‡Dept. of Mathematics, University of California at Los Angeles, Los Angeles, CA 90024
†Rockwell International Science Center, 1049 Camino Dos Rios, Thousand Oaks, CA 91360
*Dept. of Computer Science, Yale University, New Haven CT 06520

We have developed techniques for computing electromagnetic scattering from closed 2-D conductors coated with multiple thin layers of possibly lossy dielectric and/or magnetic material. Using Fourier integral techniques, we derive higher-order impedance boundary conditions of $O(\delta^2)$ and $O(\delta^4)$ in the thickness parameter δ. We develop second-kind, weakly singular integral equations. These integral equations are discretized and solved using Nyström's method and approximately fourth-order-convergent quadrature formulas. Solutions compare favor'ably with analytical results. We have used our techniques to study the effects of layer thickness, body geometry, and incidence angle on the scattered fields.

[1]*This work was partially supported by Air Force Office of Scientific Research Contract Number F49620-89-C-0048*

USE OF THREE-DIMENSIONAL VECTOR ABSORBING BOUNDARY CONDITIONS FOR RF RADIATION AND SCATTERING PROBLEMS

*A. Khebir and J. D'Angelo**
General Electric Corporate Research and Development
Schenectady, NY 12301

Partial differential equation methods are well-suited for solving RF problems for objects of realistic complexity. However, one has to deal with the error introduced by the truncation of the unbounded domain. One way is to impose an operator, called the absorbing boundary condition (ABC), on the exterior boundary to make it as transparent as possible and minimize the nonphysical reflection from it. There has been considerable amount of research on ABC's for two-dimensional problems. Although the three-dimensional vector ABC has been around for few years (Peterson, Microwave Opt. Technol. lett., 1988, Gordon and Mittra, Electromagnetics, 1990) to the best of our knowledge, it has not been used to date to solve full three-dimensional RF problems. A family of absorbing boundary conditions based on the Wilcox expansion theorem was derived by Peterson. In particular, the second order condition reads as

$$\hat{r} \times (\nabla \times \mathbf{H}) \equiv \alpha(r)\, \mathbf{H}_s^{tan} + \beta(r) \nabla \times [\, \hat{r} (\hat{r} \cdot \nabla \times \mathbf{H})]$$

$$- \frac{\alpha(r)\gamma(r)}{k^2} \nabla^{tan} (\nabla \cdot \mathbf{H}_s^{tan}) \qquad (1)$$

where

$$\alpha(r) = jk \qquad (2)$$

$$\beta(r) = \frac{1}{2jk + \frac{2}{r}} \qquad (3)$$

$$\gamma(r) = \frac{jk}{2jk + \frac{2}{r}} \qquad (4)$$

The ABC shown in (1) was applied on a spherical outer boundary to truncate the unbounded domain for three dimensional problems. Results will be presented for various radiation and scattering problems.

NUMERICAL SIMULATION OF THREE DIMENSIONAL COATINGS AND CAVITIES USING HIGHER ORDER IMPEDANCE BOUNDARY CONDITIONS

K. Barkeshli* and J. L. Volakis
Department of Electrical Engineering and Computer Science
University of Michigan
Ann Arbor, MI 48109-2122

Applications of the generalized impedance boundary conditions (GIBCs) to two problems of interest, namely, scattering from filled cavities recessed in infinite ground planes and dielectric coatings on infinite ground planes are considered. The dielectric media may be layered and include losses. The study of electromagnetic scattering from these targets is important in modeling the radar response to various man-made structures.

GIBCs are higher order boundary conditions which involve derivatives of the fields beyond the first. They have been found to be effective in modeling thick dielectric coatings and layers. A convenient form of these conditions is expressed in terms of the normal derivatives of the normal field components

$$\sum_{m=0}^{M} \frac{a_m}{(-jk_o)^m} \frac{\partial^m E_n}{\partial n^m} = 0 \quad , \quad \sum_{m=1}^{M'} \frac{a'_m}{(-jk_o)^m} \frac{\partial^m H_n}{\partial n^m} = 0$$

where a_m and a'_m are constants of the impedance sheet chosen to reproduce the desired scattering behavior of the surface, layer or coating under consideration. When $M = M' = 1$, the conditions are equivalent to the traditional first order (standard) conditions (SIBC).

It is shown that the formulations based on the GIBCs render the problems amenable to a conjugate gradient FFT solution, thus making them attractive in modeling electrically large targets.

SCATTERING FROM TWO DIMENSIONAL COMPOSITE OBJECTS USING A MIXTURE OF BOUNDARY CONDITIONS

Paul M. Goggans
Ahmed A. Kishk*

Department of Electrical Engineering
University of Mississippi
University, MS 38677

Numerical techniques for solving scattering problems often require the use and solution of large matrices. Use of these matrices can be a problem because of the amount of memory required for storage and the CPU time required for filling and solving. The problem of matrix size usually becomes severe when the scattering object contains dielectric material. For a dielectric object, the number of unknowns required for a numerical solution is more than twice the number of unknowns required in the case of a perfectly conducting object of the same shape and size. However, if the dielectric is lossy, the problem of excessive matrix size can be mitigated by use of the Impedance Boundary Condition (IBC) in place of the actual boundary conditions on the dielectric surface. The IBC relates the tangential electric field to the tangential the magnetic field via a known impedance factor. Surfaces for which the IBC is applicable are here referred to as impedance surfaces. Use of the IBC results in a significant reduction in the number of unknowns and therefore of the matrix size. If the object is composed of both lossy and lossless materials, the IBC cannot be used on all the object boundaries. One way to efficiently solve this problem is to use different boundary conditions on different parts of the object. For example, the IBC can be imposed on the impedance surfaces while continuity of the tangent electric and magnetic fields can be enforced on the lossless dielectric surfaces. Because of its efficient use of unknowns, this method minimizes matrix size.

In this paper, mixed boundary conditions are used in conjunction with the equivalence principle to yield efficient surface integral-equation formulations. Solutions are obtained for two dimensional scatterers in both the TE and TM polarized incident wave cases. The solution of the integral equations is carried out numerically using a point matching technique. Verification of the numerical solution is achieved through comparison with the series solution of an impedance circular cylinder coated with uniform homogeneous dielectric layer. Also, the solution of partially coated objects is verified numerically by comparison of results obtained from different formulations.

B93.5

SOLVING 3-D SCATTERING PROBLEMS WITH FINITE ELEMENTS USING A SECOND-ORDER LOCAL ABSORBING BOUNDARY CONDITION

J. W. Parker, R. D. Ferraro, P. C. Liewer*

Jet Propulsion Laboratory / California Institute of Technology
4800 Oak Grove Drive
Pasadena, CA 91109

Near-field solutions are calculated for 3-D electromagnetic scattering from dielectric and conducting spheres and other objects with radii of order of one wavelength using the finite element method to solve the weak-form vector Helmholtz equations for the electric (or magnetic) field. The near field domain is truncated by a spherical outer boundary, where a new local boundary condition is implemented. The local boundary condition is of the form

$$\hat{r}\times\nabla\times\vec{E^s} = \alpha(r)\,\vec{E^s_{tan}} + \beta(r)\left\{\nabla\times\left[\hat{r}(\hat{r}\cdot\nabla\times\vec{E^s})\right] + \nabla^{tan}\left(\nabla\cdot\vec{E^s_{tan}}\right)\right\},$$

where

$$\alpha(r) = ik$$
$$\beta(r) = \frac{1}{2ik + \frac{2}{r}}.$$

When applied to the Galerkin form of the scattering problem, this condition results in a symmetric complex sparse matrix system which is solved by direct or iterative methods. The Galerkin form of this condition uses only tangential components of the field, and the first tangential derivatives of these components; thus it may be termed second-order by analogy to the 2-D scalar Bayliss-Turkel condition used elsewhere. The truncation error vanishes asymptotically as $O(r^{-5})$.

The finite elements used are quadratic Lagrangean tetrahedra, which are said to be subject to "spurious modes" in eigenvalue problems and possibly lead to problems for scattering problems as well. However, the quality of results obtained is sufficient to verify the new absorbing boundary condition. For a production code, alternative finite element schemes may be more reliable.

A New Look at the Absorbing Boundary Conditions for PDE Solution of Electromagnetic Scattering Problems in Time and Frequency Domains

R. Mittra and Jin-Fa Lee
Electromagnetic Communication Laboratory
University of Illinois, Urbana, IL 61801

Recent surge of activity in the solution of electromagnetic scattering problems using the partial differential equation(PDE) techniques has sparked considerable interest in the development of accurate absorbing boundary conditions(ABCs) that permit the truncation of the PDE mesh in the Fresnel field region of the scatterer. A plethora of ABCs have been reported in the literature, including those developed by Mur, Enguist and Majda, Bayliss and Turkel, Peterson, Mittra and Ramahi, etc., to name just a few. All of the above authors have presented ABCs that trade the normal derivative of the wave function on the boundary with their tangential derivatives, also on the boundary, enabling one to truncate the mesh and exclude the nodes that fall outside the truncation boundary. A typical boundary condition of this type, say the one derived by Enguist and Majda, reads:

$$\left[\frac{1}{c}\partial_{zt}^2+\frac{1}{c^2}\partial_{tt}^2-\frac{1}{2}\left(\partial_{xx}^2+\partial_{yy}^2\right)\right]w\equiv 0 \tag{1}$$

In a recent paper(1990 AP-S Symposium, Dallas), Deveze et al. have suggested a different type of boundary condition, suitable for the Finite Difference Time Domain(FDTD) algorithm, that involves both the transverse and longitudinal components of the field. Their proposed boundary condition generates reflectionless behavior for plane waves incident upon the boundary both at the normal incidence as well as at a previously specified incident angle θ_0. It takes the form:

$$\left(\frac{1}{c}\partial_t+\partial_z\right)E_x-\frac{\cos\theta_0}{1+\cos\theta_0}\partial_x E_z+\frac{\mu_0 c}{1+\cos\theta_0}\partial_y H_z\equiv 0$$
$$\left(\frac{1}{c}\partial_t+\partial_z\right)E_y-\frac{\cos\theta_0}{1+\cos\theta_0}\partial_y E_z-\frac{\mu_0 c}{1+\cos\theta_0}\partial_x H_z\equiv 0 \tag{2}$$

The steps involved in the development of this boundary condition, as described in the 1990 AP-S Symposium digest, are somewhat abstruse. The purpose of this paper is to present a new derivation of the Deveze boundary condition, based upon a totally different approach. The advantages of following the new approach to deriving this ABC are threefold. First, it allows us to put the derivation on a firm and rigorous footing. Second, it opens up the possibility of generalizing it to cases where the angles of incidences for which the boundary condition satisfies the zero reflection condition can be different from those chosen in the original derivation, Third, it suggests a way to derive a new boundary condition in the frequency domain which does retain some of the desirable features of the boundary condition in (2), and yet does not involve the longitudinal components E_z and H_z(for z=constant boundary) that are awkward and inconveneient to use in the finite element(FEM) formulation.

The boundary conditions of the form in (2) have been tested and compared against the conventional ABCs and the results of this comparative study will be reported in the paper.

B93.7

A STUDY OF WAVE INTERACTION WITH A SLIT CYLINDRICAL CAVITY USING THE ON-SURFACE RADIATION CONDITION METHOD.

Paul D. Smith
Dept. of Mathematics & Computer Science,
Dundee University, Dundee DD1 4HN, Scotland. UK.

Gregory A. Kriegsmann
Department of Mathematics,
New Jersey Institute of Technology,
University Heights, Newark NJ 07102. USA.

The approximate solution of electromagnetic scattering problems by applying the radiation condition (at various levels of accuracy) on the surface of convex perfectly conducting scatterers was introduced by Kriegsmann et al. (*IEEE Trans. Antennas Propagat. AP-* **35** ,153-161, 1987.) Subsequently its applicability for penetrable dielectric obstacles was demonstrated. More recently the method was successfully modified to study the simplest open resonator, a flanged rectangular short-circuited waveguide, by applying the radiation condition to the aperture of the cavity (Blaschak, Kriegsmann and Taflove, *Wave Motion* **11** , 65-76, 1989).

To assess the efficacy of the method for electromagnetic configurations involving cavity backed apertures another geometry was considered: a perfectly conducting cylinder with a slit cut parallel to its axis. The scattering of a plane wave from this open resonator is then approximately solved by using the on surface radiation condition method on the aperture to convert the original problem, in which the exterior and interior fields are coupled, into a form in which the fields in these regions decouple. Basically the interior problem requires the solution of the Helmholtz equation inside the cylindrical cavity subject to mixed boundary conditions. Simple formulae can then be derived for the field within the cavity as well as the bistatic cross-section. For narrow slits the frequencies at which "near resonance" occurs are related, as expected, at the resonant frequencies of the *closed* cylinder. These results are compared to those obtained by an "exact" method such as that described by Ziolkowski and Grant(*IEEE Trans. Antennas Propagat. AP-* **35** ,504-528, 1987). This method, designed to incorporate the singular behaviour of the fields at the edges, requires substantially more computation (including matrix inversions).

SCATTERING BY HOMOGENEOUS CYLINDERS USING SURFACE RADIATION CONDITIONS

R. Janaswamy
Code EC/Js
Department of Electrical and Computer Engineering
Naval Postgraduate School
Monterey, CA 93943, U.S.A.

The method of On-Surface Radiation Condition (OSRC) was recently introduced for formulating electromagnetic scattering problems (G. A. Kreigsmann, A. Taflove and K. Umashankar, *IEEE Trans. Antennas Propagat.*, vol. AP-35, pp. 153-161, February 1987). The method was shown to yield remarkable results for convex, two-dimensional perfectly conducting bodies at medium and medium-high frequencies. More recently, the method was applied to scattering by homogeneous cylinders (S. Arendt, K. R. Umashankar, A. Taflove and G. A. Kriegsmann, *IEEE Trans. Antennas Propagat.*, vol. AP-38, no. 10, pp. 1551–1558, October 1990). In the above reference, the authors concluded that the method predicted good results for convex shaped objects. However, a closer look at the problem reveals that even for the simplest case of a circular cylinder, the method could yield incorrect results.

In the present work, the second order radiation boundary condition of Kriegsmann and Morawetz is applied to two-dimensional scattering by a homogeneous cylinder. Specific case of a circular cylinder of radius R_a is considered. Approximate fields are obtained by imposing the radiation boundary condition on a conformal outer cylinder, S_b, of radius R_b. Error functions based on comparison of surface currents and complex scattered power are established. Results are presented for low frequency ($R_a = 2.5$) and high frequency ($R_a = 10$) cylinders. It is shown that the OSRC method does not always yield accurate results for the scattered fields for all values of material constants (ϵ_r, μ_r). Accurate results are achieved for some values of material constants, but highly erroneous results are produced for others. The accuracy of the surface radiation condition method is shown to improve considerably by moving the outer surface S_b sufficiently far away form the object surface. Numerical results are presented for the TM as well as the TE polarizations.

B93.9

EVALUATION OF OSRC HIGHER ORDER OPERATORS FOR ELECTROMAGNETIC SCATTERING

Wan Chun
Korada Umashankar
Department of Electrical Engineering and Computer Science
University of Illinois at Chicago, Chicago, Illinois 60680

Allen Taflove
Department of Electrical Engineering and Computer Science
Northwestern University, Evanston, Illinois 60208

The on-surface radiation condition theory (OSRC) has been reported recently as a viable technique for the analysis of electromagnetic scattering by both perfectly conducting and homogeneous dielectric objects. Earlier studies, in fact, are limited to the application of the second order boundary operator. Based on the second order operator, preliminary OSRC results are reported in the literature for the electromagnetic scattering by a two dimensional conducting circular cylinder, a thin strip and a square cylinder with TM polarization. Further, a differential equation solution is reported for the scattering by a circular cylinder with TE polarization. Some validation data are also reported for the induced surface current and the radar cross section of dielectric circular and elliptic scatterers. Using the second order operator, validations of the OSRC analysis can be obtained for TM polarization except for minor differences in the shadow region where the field levels are very small. But, for the case of TE excitation, validations of the OSRC analysis can be obtained for the illuminated region. In the shadow region of the scatterer, the OSRC does not pick up completely the magnitude and phase of the creeping wave effects.

In the present study, a detailed OSRC analysis is reported based on the higher order operators. To examine the limitations, the OSRC operators B_m, m = 1, 2, 3 and 4 are analyzed in detail to check the field distributions and the corresponding field levels obtained in the application of the on surface boundary conditions. The operators B_3 and B_4 are examined by applying to a circular cylinder with both TM and TE plane wave excitations. The results of this study show that there exists remarkable improvement over the B_2 operator solution. Validation data for the induced surface electric current distribution and the monostatic radar cross section are reported here. It is observed for TM polarization, particularly in the shadow region, most of the low level field differences completely vanish. Similarly, for the case of TE polarization, the higher order OSRC operators pick up completely the magnitude and phase of the creeping wave distributions.

Microstrip Antennas

Room 2020 Salle
URSI B Session 97

Antennes microrubans

Chairs/présidents: P. BHARTIA, Canada; N.G. ALEXOPOULOS, USA

13:30 (97.1) Analysis of Microstrip Resonators of Arbitrary Shape, **K.A. MICHALSKI**, D. ZHENG, *Texas A&M University, College Station, TX, USA*

13:50 (97.2) Analysis of Series Fed Microstrip Arrays, **K.V.S. RAO**[1], I. TCHAPLIA[1], P. BHARTIA[2], [1]*I.T.S. Electronics Inc., Concord, ON, and* [2]*Defence Research Establishment, Dartmouth, NS, Canada*

14:10 (97.3) Electric Field Distributions in the Substrate of Microstrip Antennas, **R.C. HALL**[1], W.R. HARADER[1], J.R. MOSIG[2], [1]*Ball Communication Systems Division, Broomfield, CO, USA;* [2]*École Polytechnique Fédérale de Lausanne, Switzerland*

14:30 (97.4) Experimental Study of Mutual Coupling on Triangular Microstrip Antennas, **P.S. BHATNAGAR**[1], C. TERRET[2], K. MOHODJOUBI[2], [1]*Central Electronics Engineering Research Institute, Pilani, India;* [2]*Université de Rennes I, Rennes, France*

14:50 (97.5) An Edge Coupled Microstrip Patch Antenna for Array Applications, **D.C. CHANG**, J.-X. ZHENG, *University of Colorado, Boulder, CO, USA*

15:10 **COFFEE/CAFÉ**

15:30 (97.6) Quasi-TEM Characteristics of a Class of Cylindrical Microstrip Lines, **A.Z. ELSHERBENI**[1], H.A. AUDA[2], M.A. KOLBEHDARI[1], [1]*University of Mississippi, University, MS, USA;* [2]*Kato Group, Cairo, Egypt*

15:50 (97.7) Unusual Transition-Region Behavior Between Bound and Leaky Ranges on Microstrip Lines with Anisotropic Substrates, **H. SHIGESAWA**[1], M. TSUJI[1], A.A. OLINER[2], [1]*Doshisha University, Kyoto, Japan;* [2]*Polytechnic University, Brooklyn, NY, USA*

16:10 (97.8) Characteristics of a Shielded Microstrip Loop Antenna, **H.A.N. HEJASE**[1], W. SMITH[1], K. NAISHADHAM[2], [1]*University of Kentucky, Lexington, KY, and* [2]*Wright State University, Dayton, OH, USA*

16:30 (97.9) Numerically Efficient Analysis of the Generalized Microstrip Line Problem, **F. MEDINA**, M. HORNO, *University of Seville, Spain*

16:50 (97.10) A Full-Wave Solution for the RCS of a Microstrip Array Antenna, W.J. BOW, **A.S. KING**, *Sandia National Laboratories, Albuquerque, NM, USA*

B97.1

ANALYSIS OF MICROSTRIP RESONATORS OF ARBITRARY SHAPE

Krzysztof A. Michalski* and Dalian Zheng

Electromagnetics & Microwave Laboratory
Department of Electrical Engineering
Texas A&M University
College Station, Texas 77843 USA

A space-domain approach based on a mixed-potential integral equation formulation is developed for efficient computation of complex resonance frequencies of laterally open microstrip-patch resonators of arbitrary shape. The effects of the substrate—which may consist of any number of planar, possibly uniaxially anisotropic, dielectric layers—are rigorously incorporated in the formulation by means of the vector and scalar potential Green's functions. The current distribution on the conducting patch is approximated in terms of vector basis functions defined over triangular elements. Computed resonance frequencies, quality factors, modal currents, and far-field radiation patterns are presented for several microstrip resonators. For patches of simple, regular shapes, the results are in agreement with published data obtained by specialized techniques, which—unlike the method presented here—are not extendable to arbitrary shapes.

ANALYSIS OF SERIES FED MICROSTRIP ARRAYS

K.V.S.RAO[†] and ILYA TCHAPLIA
I.T.S.Electronics Inc
200 Edgeley Blvd, Unit 24
CONCORD, ONT, L4K 3Y8

PRAKASH BHARTIA
Defence Research
Establishment Atlantic
DARTMOUTH, N.S., B2Y 3Z7

Series fed microstrip arrays are most useful configurations for large planar arrays (see Figure). When high gain and narrow beamwidth are necessary, the corporate feed arrangement becomes bulky and contributes for more cross polarization level due to interference from the feed lines. Hence series fed arrays are best alternatives to corporately fed microstrip arrays when low side lobe ratio and better cross polarization are required. In the present communications, analysis of a series fed travelling wave linear array chain will be presented. The loaded cavity analysis of single microstrip antenna with two ports is used here for calculating the overall input impedance of the chain. Various tapered distributions can be realized when the width of each element in the series fed chain is varied in a specified manner. Results on the input impedance for different configurations like uniform width array and width modulated array will be presented. The radiation characteristics for these cases will also be discussed for the above arrays.

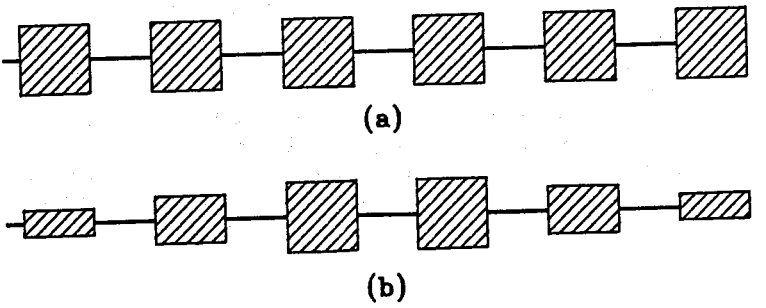

Fig. Configurations of Series fed Microstrip Chain.

B97.3

ELECTRIC FIELD DISTRIBUTIONS IN THE SUBSTRATE OF MICROSTRIP ANTENNAS

R. C. Hall* and W. R. Harader
Ball Communication Systems Division
P.O. Box 1235
Broomfield, CO 80038-1235 USA

J. R. Mosig
Laboratoire d'Electromagnétisme et d'Acoustique
Ecole Polytechnique Fédérale de Lausanne
Lausanne, Switzerland

Integral equation models of microstrip patch antennas are capable of computing approximate field distributions in the near field region of the antenna. The study of these field distributions can lead to a better understanding of the antenna's operation and to theoretical limits on the maximum power handling capabilities of the antenna.

The analytical technique used here to model the antenna and compute the near fields begins with a mixed potential integral equation that describes the currents on the metallic surfaces of the antenna, i.e. the patch and probe (R. C. Hall and J. R. Mosig, *Electromagnetics*, vol. 4, 367-384, 1989). The method of moments is then used to solve the integral equation for the approximate induced current and charge distributions. There are no thin substrate approximations, however, the substrate and ground plane are assumed to be infinite in extent. Once the current and charge distributions are known, typical antenna performance parameters such as input impedance and far field radiation patterns are easily calculated. In this paper, however, the main topic of interest will be the electric field distribution in the substrate region electrically close to the antenna. These fields are found from the vector and scalar potentials that are calculated by convolving the current and charge distributions on the antenna with the appropriate Green's functions. The gradient of the scalar potential is approximated using central-difference formula.

The methods used to calculate the approximate current distribution on the antenna will be briefly outlined and various plots will be presented of the electric field magnitude in the substrate region for a variety of patch antenna structures. Approximate power dissipation in typical substrate materials will also be discussed.

EXPERIMENTAL STUDY OF MUTUAL COUPLING ON TRIANGULAR MICROSTRIP ANTENNAS

P.S. Bhatnagar*
Central Electronics Engineering Research Institute,
Pilani (Rajasthan) 333 031, INDIA

and

C. Terret, K. Mohodjoubi,
Universite de Rennes I, 35042, Rennes, FRANCE

To achieve high gain and low side lobe performance, a large number of microstrip elements have to be aligned in an array. The effects of mutual coupling between the array elements, especially on matching, side lobe level and limitation of scanning angle, are most important for the array design. These coupling effects have been investigated for rectangular and circular microstrip antennas by many workers. In this communication, the results of an experimental investigation of mutual coupling are presented; in order to establish typical coupling levels in triangular microstrip arrays. Series of S parameter measurements were conducted at 3.0 GHz to 3.6 GHz for two element arrays of equilateral triangular elements, where pairs were oriented in different E plane and H plane configurations (5 possible configurations). The mutual coupling level decreases monotonically with increasing the separation between the elements, with the E plane coupling down to 30 dB (at distance between adjacent edges $d = 0.5\lambda$) and the H plane coupling down to 28 dB ($d = 0.5\lambda$) at $f_0 = 3.245$ GHz. The measured phase of S_{12} also decreases with increasing the elements separation 'd', with the E plane phase of S_{12} down to 100° ($d = 0.1\lambda$) and about 180° ($d = 0.5\lambda$), while the H plane S_{12} phase down to 90° ($d = 0.1\lambda$) and 180° ($d = 0.5\lambda$). Measured values of $|S_{11}|^2$ and S_{11} phase versus edge spacing are also presented. The measured mutual coupling results are also compared with rectangular and circular patch antennas (Carver, 1981) and observed better results for triangular arrays at certain separation gaps. For two elements array design, the measured E pland and H plane patterns shown very small differences (In Beam width, cross polar levels) between the desired pattern and the coupling effected pattern.

B97.5

AN EDGE COUPLED MICROSTRIP PATCH ANTENNA FOR ARRAY APPLICATION

D. C. Chang* and J. X. Zheng
MIMICAD Center, University of Colorado at Boulder
Boulder, CO 80309-0425

An edge coupled microstrip patch antenna as shown in the figure is investigated for the purpose of designing a linear series-fed microstrip antenna array. It is expected that an array composed of such elements has the advantage of: (1) much less metallic loss compared to the corporate feed scheme at millimeter-wave frequency range; (2) the phase center is always located at the center of the coupling region so that it is easy to control the phase of each element; (3) the size of the patches are the same, and the width of the gap is used to control the amplitude of each element so that the beam pointing bandwidth can be improved from a conventional design of a direct series-fed microstrip patch array. The antenna element is simulated using an accurate and efficient full-wave microstrip solver developed earlier (D.C.Chang & J.X.Zheng, IEEE T-MTT, to be published). It is found that the width of the gap between the patch and the feed-line can be used to control the radiation power effectively when the coupled edge of the patch is a radiating edge. It is predicted that as much as 60% of the incident power can be radiated out so that the antenna can be used as the elements, except the last one, of an array. It is also found that the power reflected back can be significant when the gap width is very small. A new CAD procedure to design a series-fed array taking into account of the reflected waves will be addressed in this talk as well.

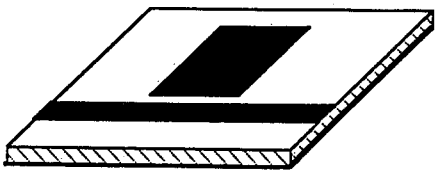

QUASI-TEM CHARACTERISTICS OF A CLASS OF CYLINDRICAL MICROSTRIP LINES

ATEF Z. ELSHERBENI*
DEPARTMENT OF ELECTRICAL ENGINEERING
UNIVERSITY OF MISSISSIPPI
UNIVERSITY, MISSISSIPPI 38677. USA

HESHAM A. AUDA
KATO GROUP
4 BEHLER PASSAGE, KASR EL NIL STREET
CAIRO, EGYPT

MOHAMMED A. KOLBEHDARI
DEPARTMENT OF ELECTRICAL ENGINEERING
UNIVERSITY OF MISSISSIPPI
UNIVERSITY, MISSISSIPPI 38677. USA

Perfectly conducting wedges and cylindrically-capped wedges are widely utilized in the design of cylindrical radiating structures for aircraft and missiles. A typical radiating element in such application would consist of a cylindrical-rectangular patch fed with a microstrip line. Here, the quasi-TEM characteristics of a class of cylindrical microstrip lines are rigorously determined. Specifically, single and multiple microstrip lines on a multilayered dielectric substrate on wedge and/or cylindrically-capped wedge are analyzed.

The analysis is based on deriving exact potential distributions for the regions outside and inside the dielectric substrate. The potentials are constructed in such a way that the continuity of the potential, and, hence, the continuity of the tangential component of the electric field, across the various dielectric interfaces are automatically enforced. The equations of the problem are obtained from enforcing the potential to have specified constant values on the strips and satisfying the jump discontinuity in the normal derivatives of the potential across the dielectric interfaces. The boundary condition equations are subsequently combined and solved using Galerkin's method. Expressions for the charge distributions on the strips and elements of the capacitance matrix of the microstrip lines are then obtained. Numerical results are also given and discussed.

B97.7

UNUSUAL TRANSITION-REGION BEHAVIOR BETWEEN BOUND AND LEAKY RANGES ON MICROSTRIP LINES WITH ANISOTROPIC SUBSTRATES

H. Shigesawa* and M. Tsuji
Doshisha University, Kyoto, Japan

and

A. A. Oliner
Polytechnic University, Brooklyn, New York

Two years ago we showed that, contrary to customary belief, the dominant mode on microstrip line with an anisotropic substrate can leak power in the form of a surface wave on the surrounding substrate, instead of remaining purely bound. Such leakage occurs above a particular critical frequency when the anisotropy is appropriate. We then investigated the transition region between the bound-wave (real, proper) solutions at lower frequencies and the leaky-wave (complex, improper) solutions at higher frequencies, and we observed that the behavior followed the expected pattern in which a real but improper solution exists over a narrow frequency range; the solution in this narrow range is also not captured in a steepest-descent-plane plot. These calculations, which were made for Epsilam 10 substrates, were presented at last year's URSI Meeting.

We then repeated these calculations for a more-anisotropic substrate, pyrolytic boron nitride, and we were surprised to find quite different behavior. In fact, several different types of behavior were obtained, depending on the aspect ratio of the microstrip line. When the strip width w is small relative to the substrate height h, for example when w/h=0.6 or so, a short range of improper real solutions is again found, as in the Epsilam 10 case, but there also exists an ***additional leaky-wave solution*** that occurs at ***lower*** frequencies. When w/h is greater than about 0.8, however, the bound and leaky solutions do not even cross each other; they are separated by a small gap in wavenumber, where the bound-wave proper solution at lower frequencies continues into a bound-wave improper solution, and the leaky-wave solution at higher frequencies continues as a leaky-wave solution at the ***lower*** frequencies. As the frequency is lowered, the new leaky-wave solution ***is captured*** in the steepest-descent plane, indicating that an ***additional mode*** is present that has until now not been discovered.

On the usual normalized wavenumber (β/k_0) *vs.* frequency plots, it is difficult to follow these solutions and to understand their nature. When the data are transferred to the steepest-descent plane, the picture clarifies substantially and we can understand in a systematic way the change in behavior as the aspect ratio w/h varies. The talk will discuss the behavior of these unusual transition regions, and will address the physical significance of the additional mode mentioned above.

CHARACTRISTICS OF A SHIELDED MICROSTRIP LOOP ANTENNA

Hassan A. N. Hejase*, William Smith
Department of Electrical Engineering
University of Kentucky
Lexington, KY 40506–0046

and

Krishna Naishadham
Department of Electrical Engineering
Wright State University
Dayton, OH 45435

The analysis of a printed wire–loop antenna with a conducting cover is presented. A mixed potential integral equation for the loop current is derived by first determining the Green's function. Using complex Fourier series expansions for the loop current, Galerkin's moment method is applied to transform the integral equation into a matrix equation. The impedance matrix elements are Sommerfeld type integrals which need to be evaluated numerically using special techniques. The input impedance and current are computed and compared with results available in the literature. When the conducting shield or cover recedes to infinity, the structure approximates that of a printed loop antenna. The radiation pattern and gain will then be compared to those available from literature. This formulation will be useful to study coupling between printed loops with and without a conducting cover. Comparisons will be also be made with results obtained from a previous work on a loop in a parallel–plate region by letting the dielectric permittivity approach that of air in the present study.

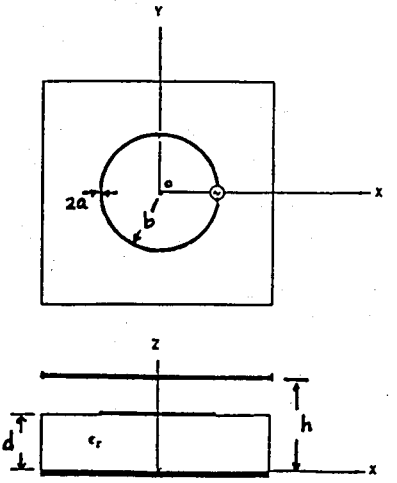

B97.9

NUMERICALLY EFFICIENT ANALYSIS OF THE GENERALIZED MICROSTRIP LINE PROBLEM

F. Medina*, M. Horno
Microwave Group. Electronics and Electromagnetics Department
UNIVERSITY OF SEVILLE
Avda. Reina Mercedes s/n. 41012 SEVILLA (Spain)

Microstrip is the most popular transmission line in modern microwave technology. Quasi-TEM and full-wave models have been used to study the propagation characteristics of this structure over more than 30 years. However, although the literature on this subject is extensive, analytical or quasi-analytical solutions have been provided just for a few cases. Recent important advances in this sense have been reported in (B.E. Kretch et al., IEEE-MTT, 35, 8, 710-718, 1987; J.G. Fikioris et al., IEEE-MTT, 37, 1, 21-33, 1989; K. Uchida et al. IEEE-MTT, 37, 6, 947-952, 1989; D. Homentcovschi, IEEE-MTT,38, 6, 766-769, 1990) for both, quasi-TEM and dynamic analysis. The case in which the strip is embedded in a generalized layered medium with rectangular boundary conditions can not be exactly solved, but it is possible to achieve an extremely efficient numerical analysis by proper analytical preprocessing. This is the aim of this work.

The configuration to be considered here is a microstrip line embedded in a layered configuration with arbitrary rectangular boundary conditions (electric or magnetic walls, open boundaries or periodic conditions). This problem is conveniently formulated by using the spectral domain technique and the Rayleigh-Ritz or the Galerkin method. The application of this technique leads to a system of linear equations whose entries are slowly convergent series. Although the straightforward application of the method yields results accurate enough for most practical purpouses, convergence is not satisfactory, and charge distributions can not be accurately computed. This is particularly true when the strip is near the side walls. However, the asymptotic tails of the series can be analitycally added and substracted from the original series, resulting in a drastical improvement of accuracy and CPU time. Two methods have been used to do this. The first method is based on the consideration of an asymptotic problem consisting of the same microstrip configuration embedded in an appropriate homogeneous medium. In this case, the Green's function is known in closed form in the spatial domain, and convolution integrals and inner products are almost analitically evaluated. The second one makes use of the complex variable analysis and asymptotic extraction techniques to obtain very quickly convergent expressions for the series involved in the analysis. Extremely accurate results are obtained for the characteristic parameters in just a few ms in a VAX-785 computer (these programs are then appropriate for PC computers). Charge distributions are also accurately computed in a fraction of second by using these techniques. The reliability of these computer codes has been conveniently tested with available data reported in the literature for single layer configurations.

This method has been applied to the quasi-TEM analysis of a single strip (or symmetrically coupled structures), but it can be extended to multistrip configurations and it is also useful to accelerate computations when using a dynamic model.

A FULL-WAVE SOLUTION FOR THE RCS OF A MICROSTRIP ARRAY ANTENNA

Wallace J. Bow and Adrian S. King*
Exploratory Systems Development Division I
Sandia National Laboratories, Albuquerque, NM 87185

Stealth is the term given to target signature reduction techniques. This implies the reduction of active emissions, the use of camouflage paint schemes and, most important, radar cross-section (RCS) reduction. Currently there is much interest in the analysis of the RCS of microstrip patch antenna arrays. This is because as the structural scattering of stealth platforms is reduced by the use of radar absorbing materials and platform shaping, the contribution of the microstrip patch antenna array to the total RCS becomes increasingly important.

Past numerical studies of the RCS of microstrip patch antenna arrays have been concerned with narrow frequency bands. This is due to the amount of computing time and memory required to properly analyze the RCS of microstrip patch antenna arrays. The major computational difficulties are the calculation of the coupling between the elements and the large number of current expansion modes required over a large band of frequencies.

This paper presents a computationally efficient full-wave solution to the problem of broadband plane wave scattering by an array of rectangular microstrip patches on a grounded dielectric slab. The technical approach of this investigation is to generate a spectral domain moment method solution for the scattering from an array of rectangular microstrip patches, write an efficient parallel computer program to implement the moment method solution, solve for the patch currents, and calculate the RCS. RCS data will be presented as a function of incident signal, array lattice spacing, angle of incidence, and antenna loading. Also presented are methods to reduce the RCS of microstrip patch array antennas.

Radar Cross Section **Room 2036 Salle URSI B Session 102** **Radar, surface équivalente**

Chairs/présidents: Y.M.M. ANTAR, Canada

13:30 (102.1) Resolving Components in Antenna RCS Measurements, **V.K. TRIPP**, E.E. WEAVER, B.L. SHIRLEY, *Georgia Institute of Technology, Atlanta, GA, USA*

13:50 (102.2) On Using TEM Transmission Line for RCS Measurements, **I.S. KIM**, S.R. MISHRA, *Canadian Space Agency, Ottawa, ON, Canada*

14:10 (102.3) Time and Frequency Domain Techniques for Dynamic RCS Computation, **J.S. SIDHU**, M.T. TULEY, *Georgia Institute of Technology, Atlanta, GA, USA*

14:30 (102.4) Benchmark Solutions of Radar Cross Section of Linear Antennas, **S.A. SAOUDY**, *Memorial University of Newfoundland, St. John's, NF, Canada*

14:50 (102.5) Electronically-Modulated Radar Chaff, **A. CUEVAS**, *University of Texas, Austin, TX, USA*

15:10 **COFFEE/CAFÉ**

RESOLVING COMPONENTS IN ANTENNA RCS MEASUREMENTS

V. K. Tripp,* E. E. Weaver, and B. L. Shirley
Georgia Tech Research Institute
Georgia Institute of Technology
Atlanta, Georgia 30332

The fundamental equation of antenna scattering resolves the scattered fields into a short-circuit component and the remainder. Green (1966) cast the formula into the widely used "antenna" and "structural" components, which are based on a conjugate match. Here we define a separation of components based on the transmission line match, which is more useful for our purposes. We call them "radiation" and "residual" components. (It has been shown that a similar separation can be made for any desired reference load impedance.)

Complex RCS patterns were measured on an X-Band Narda standard gain horn for the purpose of determining which component was dominant, the radiation component reflected from within the waveguide, or the structural component scattered from other horn features. At each frequency, five patterns were measured with a sliding short in the waveguide set at different arbitrary positions. At any angle, the RCS falls on a circle in the complex plane, whose center represents the structural component and whose radius represents the antenna component. In this paper, we demonstrate the resolution of the RCS components and discuss their meaning.

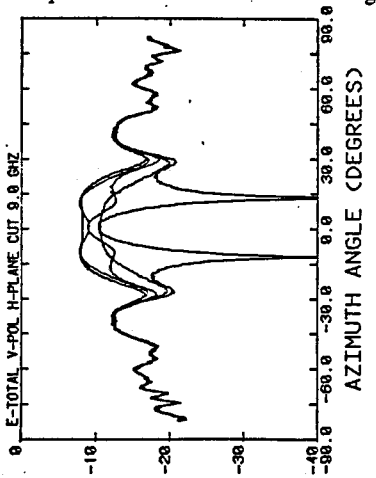

RCS measurements at 9 GHz

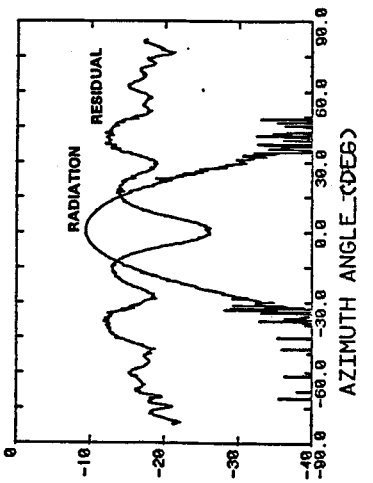

RCS components at 9 GHz

ON USING TEM TRANSMISSION LINE FOR RCS MEASUREMENTS

Ihn S. Kim* and Shantnu R. Mishra

David Florida Laboratory, Canadian Space Agency
3701 Carling Avenue, Ottawa, Ontario, K2H 8S2

The use of guided transverse electric and magnetic (TEM) propagation such as in a parallel plate transmission line has been proposed (Gans, Proc. IEEE, Vol. 53, p 1081, 1965) as a practical means of Radar Cross Section (RCS) measurements since use of radiating structures at low frequencies is not practical. Neureuther (IEEE Trans. AP, November 1971) and Gilbert (1989 IEEE AP-S) have used this technique.

Their analysis, however, does not take into account the guiding effect inherent in all types of transmission lines.

This paper reviews requirements for a range for RCS measurements and examines the suitability of TEM guided wave structures for this purpose.

Theoretical analysis substantiated by measured data will be presented to support the conclusions.

B102.3

TIME AND FREQUENCY DOMAIN TECHNIQUES FOR DYNAMIC RCS COMPUTATION

J.S.Sidhu* and M.T.Tuley
Georgia Tech Research Institute
Georgia Institute of Technology
Atlanta, GA. 30332-0800

In radar detection of targets with rotating parts, the large radar cross section (RCS) flash can be used as a detection criterion. In case of a helicopter, the time varying rotor RCS can be computed in the time or frequency domain.

In time-domain computation, the rotor can be rotated at the specified RPM and depending upon the radar frequency and the rotor size, the sampling interval is selected to meet the nyquist sampling criterion.

In frequency-domain computation, doppler contributions from each scatterer are lumped into frequency bins and then FFT is applied to the frequency spectrum to get time-domain RCS.

In this presentation, results from both these approaches will be discussed. RCS was computed for a rotor system with 200 scatterers/rotor using Georgia Tech Research Institute's TRACK program. Similar results were computed using frequency domain approach and an IMAGE post-processing algorithm to get time-domain RCS. Frequency-domain approach proved to be faster by a factor of 12. For more complex rotor designs, the advantages of frequency over time-domain approach are expected to be even better.

BENCHMARK SOLUTIONS OF RADAR CROSS SECTION OF LINEAR ANTENNAS

S.A. SAOUDY
Centre for Cold Ocean Resources Engineering
Memorial University of Newfoundland
St. John's, Newfoundland, A1B 3X5.

The bistatic radar cross sections (RCS) of a number of linear antennas are numerically calculated using the Numerical Electromagnetics Code (NEC) which is based on the moment method (G.J. Burke and A.J. Poggio, "Numerical Electromagnetics Code (NEC)-Method of Moments," Parts I and III, Tech. Document 116, Naval Ocean Syst. Cen., revised Jan. 1980, CA). Also, similar calculations will be performed using the recent AWAS package (A.R. Djordjevic et. al., " Analysis of Wire Antennas and Scatterers" Artech House, Boston 1990). Comparison with available experimental and theoretical data will be performed to establish the validity of both NEC and AWAS packages.

B102.5

ELECTRONICALLY-MODULATED RADAR CHAFF

Alfonso Cuevas
Dept. of Electrical and Computer Engineering
University of Texas at Austin
Austin, Texas 78712-1084

Electromagnetic scattering from electronically-modulated chaff elements have been theoretically investigated using a diode within the wire scattering element (R. Janaswamy and S.W. Lee, IEEE Trans., AP-36, 1649-51, Nov. 1988). New chaff elements are investigated which: (1) maintain a controllable radar cross section (RCS) backscatter response over a large frequency bandwidth; (2) have a good modulation (ON/OFF) ratio; and (3) are relatively inexpensive to produce. Further, the practical implementation of supplying diode bias is addressed.

Theoretical backscatter RCS responses using a moment-method solution are shown for several candidate elements which are suitable for diode insertion. Theoretical results for the dipole element indicate that the backscatter RCS ON/OFF ratio is on the order of: 10-20 dB using an ideal diode model; 6-10 dB using an X-band PIN diode model; and 0-10 dB using measured PIN diode characteristics in the moment-method solution.

The effects of a high-impedance parallel transmission line used to supply the diode bias at the center of the scattering element is shown. Correlation is fair between RCS theory and measurement of the element with the diode in the active state. Correlation is poor between theory and measurement of the element with the diode in the inactive state. This lack of agreement is attributed to the external scattering off the diode package and/or the impedance loading of the bias line on the scattering element. However, an acceptable modulation ratio is achieved over a narrow frequency band.

Physical-Optics Based Asymptotics | **Room 2036 Salle URSI B Session 103** | **Méthodes asymptotiques en optique physique**

Chairs/présidents: D.-S.Y. WANG, USA; K.M. MITZNER, USA

15:30 (103.1) Asymptotic Evaluation of the Physical Optics Integral for Arbitrarily Curved Surfaces, **K.R. ABEREGG**, A.F. PETERSON, *Georgia Institute of Technology, Atlanta, GA, USA*

15:50 (103.2) A Uniform Asymptotic Approach to PTD for Some Simple Shapes, **E.C. BURT**, *Massachusetts Institute of Technology, Lexington, MA, USA*

16:10 (103.3) Electromagnetic Wave Propagation Along Smooth Concave-to-Convex Boundary, **T. ISHIHARA**, S. OHTA, *National Defense Academy, Yokosuka, Japan*

16:30 (103.4) Scattering by S-Shape Surfaces, **L.C. KEMPEL**[1], J.L. VOLAKIS[1], T.B.A. SENIOR[1], S.S. LOCUS[2], [1]*University of Michigan, Ann Arbor, MI, and* [2]*Electromagnetic Engineering Company, Van Nuys, CA, USA*

16:50 (103.5) A Modified UTD Solution for Curved Surface Scattering, **E.D. CONSTANTINIDES**, R.J. MARHEFKA, *Ohio State University, Columbus, OH, USA*

B103.1

ASYMPTOTIC EVALUATION OF THE PHYSICAL OPTICS INTEGRAL FOR ARBITRARILY CURVED SURFACES

Keith R. Aberegg *
Georgia Tech Research Institute
Georgia Institute of Technology
Atlanta, GA 30332-0800

Andrew F. Peterson
School of Electrical Engineering
Georgia Institute of Technology
Atlanta, GA 30332-0250

The analysis of electrically large radar targets is typically approached using asymptotic techniques such as the Geometric Theory of Diffraction (GTD) or the physical optics (PO) radiation integrals. For realistic scatterers, one approach for evaluating the PO integral is to discretize the surface into triangular plates or other simple elements that lead to closed-form solutions. The introduction of "facet noise" and the increased computational time due to the presence of many facets are drawbacks of using this approach when modeling arbitrarily curved surfaces. An alternative approach employs a scatterer model consisting of relatively few surface elements of more arbitrary shape. For example, each of these elements might have surface shape described by a bicubic (or higher-order) polynomial function of the Cartesian variables. This approach offers a more accurate representation of the scatterer surface and should eliminate the error caused by a large number of facets, provided that the PO integral can be evaluated over the more general surface shape. A direct numerical integration is possible, but prohibitively CPU intensive.

In this presentation, a closed-form asymptotic evaluation of the PO integral will be described for surface elements having bicubic shape. Results obtained using the asymptotic evaluation exhibit excellent agreement in far-field magnitude and phase with results found by direct numerical integration, except when a specular point approaches the surface element edge. In the latter situation, a correction factor is introduced in order to account for the excess energy arising from an interior stationary phase point near an edge. The motivation and development of the correction factor will be discussed.

A UNIFORM ASYMPTOTIC APPROACH TO PTD FOR SOME SIMPLE SHAPES

E.C. Burt
Lincoln Laboratory
Massachusetts Institute of Technology

In this paper we describe an approach for predicting the RCS of complex targets described as a collection of simple shapes, such as triangular plates, cylinders, cones, and disks. The motivation for the approach is to account for mutual shadowing effects among the various components in a computationally practical manner.

A straightforward implementation of physical optics (PO) and the physical theory of diffraction (PTD) calls for performing integrals over the illuminated surfaces and edges of the target. However, for a complex target the process of determining exactly what is illuminated can be very computationally expensive, overshadowing by orders of magnitude other computational considerations. Moreover, since the shape of the area that is illuminated can be quite complicated, there is little hope for using analytical methods to evaluate the integrals.

The compromise discussed in this paper is to evaluate, for each component, the appropriate PO and PTD integrals regardless of mutual shadowing, in such a way that the result is the sum of terms associated with scattering centers. In this way shadowing can be accounted for by only including terms associated with scattering centers that are visible. This reduces the shadowing problem to determining the visibility of a collection of discrete points on the target, rather than finding all the illuminated surfaces. The major difficultly with this approach is in determining well behaved expressions for the scattering amplitudes associated with the various scattering centers.

We will show for the cases of a triangular plate, circular disk, cylinder, and cone, well behaved, analytical expressions for the contribution from the various scattering centers on these shapes. We will show that our expressions agree asymptotically with other results, e.g. the GTD solution for a cylinder and disk, but remain uniformly bounded as a function of aspect angle.

B103.3

ELECTROMAGNETIC WAVE PROPAGATION ALONG SMOOTH CONCAVE-TO-CONVEX BOUNDARY

T.Ishihara* and S.Ohta
Dept. of Electrical Engineering,
National Defense Academy,
Hashirimizu, Yokosuka, 239, Japan

High frequency asymptotic field solutions for smooth boundaries with variable radius of large curvature compared to the wavelength are of interest for a variety of applications involving propagation along, and scattering from the surface contour. When the source is located near or on the concave boundary, rays with many reflections are confined near the surface. These rays with many reflections may be treated collectively either in terms of a selected number of whispering gallery(WG) modes or in parabolic equation(PE) form. The phenomena of the field behavior for convex shapes are also well understood.

The most difficult problem is posed by a surface whose curvature changes from concave to convex. When the source is far from the boundary, the ray method can be employed to approximate the surface currents on the illuminated portion, and asymptotic treatment of the physical optics integral containing these currents can then provide information about the inflection-induced transition behavior. This does not account however, for WG modes and their conversion to radiating the beam-like wave and the creeping wave.

We examine the electromagnetic wave propagation along the variable curvature boundaries including concave-convex shapes. When the boundary is concave, with variable radius of curvature, a combination of ray shooting algorithm and PE method is applied to calculate the fields excited by the line source located near the boundary. When the boundary changes smoothly from concave to convex, the modal ray tracing technique and the PE method are applied to show conversion of an initially well-confined WG mode into the beam-like wave and the creeping wave after passing through the inflection point of the boundary. Numerical comparisons reveal the validity and utility of the various alternative field representations.

Scattering by S-Shape Surfaces

L.C. Kempel*,J.L. Volakis,T.B.A. Senior
Radiation Laboratory
Department of Electrical Engineering and Computer Science
University of Michigan
Ann Arbor, MI 48109-2122
and
S.S. Locus
Electromagnetic Engineering Co.
Van Nuys, CA 91405

When an S-shaped surface posseses no derivative discontinuities, techniques such as the Geometrical Theory of Diffraction are not applicable. However, if the radius of curvature is relatively large at every point on the surface, the physical optics approximation may be employed. In this paper, we present a Uniform Physical Optics (UPO) solution which remains valid at caustics occurring when more than one specular point coalesce at the inflection point of the S-shaped surface. It is developed by approximating the surface with a localized cubic expansion leading to exact expressions in terms of Airy integrals. In contrast to other solutions, the one given here requires only knowledge of the stationary phase points and the first two derivatives of the surface generating function at those points. A major effort is devoted to the validation of the UPO solution. This is accomplished with numerical models of the S-shaped surface. It is found that the given UPO solution is quite accurate in the specular and non-specular regions for backscatter computations and is also acceptable for bistatic computation in regions where whispering gallery modes are not present.

B103.5

A MODIFIED UTD SOLUTION FOR CURVED SURFACE SCATTERING

E. D. Constantinides* and R. J. Marhefka
The Ohio State University, ElectroScience Laboratory
Department of Electrical Engineering
Columbus, Ohio 43212

The ordinary UTD solution for curved surface scattering (*IEEE Trans. Antennas and Propag.*, Vol. AP-28, No. 5, Sep. 1980) provides an efficient means for calculating the reflected and surface diffracted fields. However, since it was originally derived from the canonical problem (circular cylinder) and then heuristically extended to a general slowly varying convex surface, it tends to fail when applied to more complex surfaces with non-slowly varying radii of curvature.

In this paper, the currents induced on a general convex surface due to plane wave illumination are derived using the UTD solution for the radiation of sources on a convex surface (*IEEE Trans. Antennas and Propag.*, Vol. AP-29, No. 4, July 1981) and the reciprocity theorem. Upon incorporating these currents in the usual radiation integral it is found that they produce excellent results for the scattered field for a variety of surfaces including ones with fast varying curvature profiles such as superelliptic cylinders.

An asymptotic reduction of the radiation integral results in a set of modified UTD reflection and transmission coefficients that introduce a curvature slope dependance to the reflected and surface diffracted fields, respectively, and also reduce to the ordinary UTD solution for slowly varying surfaces. The special functions involved in the solution are very similar to the Pekeris' Caret functions and can be tabulated for efficient field computations. Verification of the accuracy of our alternate formulation and the improvement that it provides is accomplished via comparison with moment method and ordinary UTD results for the scattering from circular, elliptic and superelliptic cylinders.

Antennas I **Room 3014 Salle URSI B Session 108** **Antennes I**

Chairs/présidents: Y. RAHMAT-SAMII, USA

13:30 (108.1) Radome/Antenna Combination RCS Using the Physical Optics Scattering Method, **G. PLIMPTON**, M. CERULLO, *Raytheon Company, Tewksbury, MA, USA*

13:50 (108.2) Application of Integral Equations to Numerical Solution of Radiation from Horns, H. MOHEB, **L. SHAFAI**, *University of Manitoba, Winnipeg, MB, Canada*

14:10 (108.3) Method of Moments Analysis of Symmetric Dual Reflectors Including the Feed, **D.C. JENN**, *Naval Postgraduate School, Monterey, CA, USA*

14:30 (108.4) A Uniform GTD Diffraction Coefficient for the Electromagnetic Scattering by Metallic Tapes on Paneled Compact Range Reflectors, **G.A. SOMERS**, P.H. PATHAK, *Ohio State University, Columbus, OH, USA*

14:50 (108.5) Environmental Effects Upon the Performance of Travelling Wave Receiving Antennas, **W.A. SHAHEEN**, L.S. NAGURNEY, [1]*University of Hartford, West Hartford, CT, USA*

15:10 **COFFEE/CAFÉ**

15:30 (108.6) Finite Arrays of Microstrip Patch Antennas: The Infinite Array Approach, **A.K. SKRIVERVIK**, J.R. MOSIG, F.E. GARDIOL, *École Polytechnique Fédérale de Lausanne, Switzerland*

15:50 (108.7) A Computationally Efficient Method of Calculating the Green's Function for an Open Microstrip Structure, **L.C. HOWARD**, J.M. DUNN, *University of Colorado, Boulder, CO, USA*

16:10 (108.8) Recursive T-Matrix Algorithms for Conducting Patches, **L. GUREL**, W.C. CHEW, *University of Illinois, Urbana, IL, USA*

16:30 (108.9) Perturbation Calculations for Parasitically Coupled S-Parameters, **J.C. MOORE**, E.F. KUESTER, *University of Colorado, Boulder, CO, USA*

16:50 (108.10) De-Embedding S-Parameters from Numerically Determined Current Distributions of Planar Junctions, **J.C. MOORE**, J.-X. ZHENG, E.F. KUESTER, D.C. CHANG, *University of Colorado, Boulder, CO, USA*

B108.1

RADOME/ANTENNA COMBINATION RCS USING THE PHYSICAL OPTICS SCATTERING METHOD

Glenn Plimpton
Michael Cerullo
Raytheon Company
Missile Systems Laboratories
Tewksbury, MA 01876

Modern missile systems often carry radar cross section (RCS) performance specifications in addition to traditional component (e.g., seeker and radome) requirements. The specific interaction of the radome and seeker antenna has been modeled in this work to predict radome/antenna combination RCS. The goal here is to determine those regions of gimbal space where the radome affects seeker antenna RCS and to quantify those effects.

A physical optics equivalent current scattering model includes the primary reflected ray species. One species is received through the radome, reflected from the seeker antenna, and retransmitted through the radome to its outer surface. The other species is reflected from the radome wall only.

Both ray bundle fields (GTD Approximation) are locally traced to the radome outer surface for each radome sub-area, or pixel, via infinite planar slab transmission coefficients. The ray fields are next superimposed and equivalent magnetic and electric surface currents formed using Love's Equivalence, in keeping with the physical optics scattering approach. These currents are then integrated over the outer surface contour to obtain the radome/antenna combination scattered field from which RCS is calculated in the standard far field limit.

Model comparison with test cases for which rigorous solutions exist are presented. For example, a perfect electric conductor antenna inside an "air" radome yields typical flat plate bistatic cross sections of the Bessel function form.

Tip and base attachment ring diffraction effects may be included using a moment method software subroutine.

Phased array seeker antenna model reflection analysis is also available for future applications. Comparisons with antenna/radome RCS measurements is discussed.

APPLICATION OF INTEGRAL EQUATIONS TO NUMERICAL SOLUTION OF RADIATION FROM HORNS

H. Moheb and L. Shafai
Department of Electrical & Computer Engineering
University of Manitoba
Winnipeg, Manitoba, Canada R3T 2N2

Horn antennas are one of the most fundamental and useful antennas, that offer numerous advantages in practice. They have simple geometry, are easy to fabricate and can handle large powers. They also have good polarization characteristics and flexible bandwidths. The most common design is the rectangular horn, which in most applications is accepted as the antenna standard.

Although a rectangular horn has the simplest shape, its finite size does not allow an exact analytic solution. Fortunately, approximate analysis, based on aperture field integration or the Geometrical Theory of Diffraction provide an accurate predication of their far field patterns. However, the former gives results that are accurate mostly around the broadside direction and the latter become complicated in attempting to include the secondary rays. Numerical methods are more general and can provide solutions to more complex shapes. Also, their application becomes more convenient for small antenna, where approximate methods lose accuracy. But, they have, so far, been used only investigating conical horns, where the geometrical symmetry is used to reduce the scattering matrix to a set of uncoupled matrix equations for each mode. Here, we have extended the method to horn antennas that have non-circular cross-sections.

In this study, the radiation field patterns of rectangular horns of finite length is obtained numerically. The electric field integral equation is formulated to relate the radiation patterns of the horn to the current distribution on its surface. These currents are determined by reducing the integral equations to a matrix equation, using the moment methods. To model the horn's surface two hybrid orthogonal unit vectors are defined. Along one, surface currents are represented by discrete overlapping triangle basis functions and along the other by entire domain Fourier modes. To enable the latter, the horn's cross-section is conformally transformed onto a unit circle. These current are then used to compute the far fields, that is the radiation patterns and cross polar fields of the rectangular waveguides or horns. The source of excitation is assumed to be an electric dipole located inside the waveguide. The behavior of the solutions and the radiation patterns are studied, to determine the mode convergence and the effect of various geometrical parameters. The method is numerically efficient and can be used for computation and optimization of the antenna configurations. It can also be used for investigation of other horn configurations with more complex shapes.

B108.3

METHOD OF MOMENTS ANALYSIS OF SYMMETRIC DUAL REFLECTORS INCLUDING THE FEED

David C. Jenn
Naval Postgraduate School
Monterey, CA 93940

The advantages and disadvantages of dual reflecting systems are well known. They have shorter focal lengths than corresponding single surface reflectors, but suffer performance degradation due to interference from the feed and subreflector. For axially symmetric reflectors the subdish must be small enough to avoid excessive aperture blocking, yet large enough to be an efficient reflector. This usually requires that the main reflector diameter be greater than 50 wavelengths for classical Cassegrain and Gregorian configurations. However, several recent applications, such as direct broadcast satellites, have been cause to re-examine the capabilities of symmetric dual reflector antennas with main dish diameters less than 50 wavelengths, and perhaps as small as 20 wavelengths. Although suited for such applications because they are compact, lightweight and simple, traditional designs have unacceptably low efficiencies. Modified versions of the standard dual reflector geometries have had efficiencies in the 40 to 50 percent range. This was accomplished by either displacing the reflector axes (W. Rotman, 1987 AP-S Intl. Symp. Digest, p. 507) or by shaping (Y. C. Chang, 1989 AP-S Intl. Symp. Digest, p. 1602).

The analysis of reflectors of this size is more complicated than that for electrically large antennas. When the subreflector is small the null-field hypothesis is not valid because the effective aperture may be significantly different than the physical aperture. In addition, the two reflectors and the feed are closely space and therefore interactions are important. In practice, the design is complicated when a directive low-spillover feed is used. It may have an aperture size comparable to the subreflector's, and consequently the subreflector may be in the near field of the feed.

The method of moments is ideal for evaluating the performance of small reflectors. When basis functions are defined on all of the antenna surfaces, including the feed, then all of the important interactions mentioned above will be included. Such a solution has been implemented for rotationally symmetric dual reflector antennas with feeds consisiting of surfaces of revolution and wires. Calculated gain and pattern data will be presented for antennas with feeds such as cavity-backed dipoles and dipole-excited rings. The MM results are compared to those based on approximate far-field focal point feed models. Several matrix relationships that can be used to significantly reduce the size of the impedance matrix that must be inverted are also discussed.

A UNIFORM GTD DIFFRACTION COEFFICIENT FOR THE ELECTROMAGNETIC SCATTERING BY METALLIC TAPES ON PANELED COMPACT RANGE REFLECTORS

G.A. Somers* and P.H. Pathak
The Ohio State University ElectroScience Laboratory
Department of Electrical Engineering
Columbus, Ohio 43212

In present day compact range systems the main reflector may be physically very large for operation over a large bandwidth necessitating the need for the reflector to be manufactured in sections. Once these paneled sections are aligned, one can use metallic tape to cover the inter-panel gaps. It is therefore of interest to study the effect of the scattering by the tape on the fields in the target zone of the range. The scattering by a metallic tape on a reflecting surface was previously examined in two dimensions (2-D) by the method of moments and an empirical study was presented to indicate the effect of the tape as a function of tape dimensions,[I.J. Gupta and W.D. Burnside, AMTA Conference, Monterey, Calif., Oct. 1989, pp. 15-35–15-39]. However, that procedure is computationally time consuming and difficult to apply to the 3-D situation.

Previously [G.A. Somers, P.H. Pathak and I.J. Gupta, 1990 URSI Radio Science Meeting, Dallas, Tx., May 1990, p. 358], an analytic solution to the tape scattering problem was presented, however, that solution was best suited for wide tapes. In this paper, the tape diffraction coefficient is formed by superimposing the fields scattered from both edges (steps) of the tape. The step diffraction is constructed from the solutions to two canonical problems; one being a well known simple 2-D parallel plate waveguide problem. The other is a Wiener-Hopf solution to a semi-infinite ground plane over an infinite ground plane. These solutions are then combined by the generalized scattering matrix technique to form the diffraction coefficient of each step which in turn forms the tape. Since the tape may be electrically narrow, multiple step diffraction terms are added to account for the coupling of the two steps. The electrical distance between the steps may be too small to ensure a ray optical illumination of the second step. Since this incident field is not ray optical, multiple diffraction effects cannot be calculated via the GTD in the usual way. To circumvent this difficulty, the fields diffracted from a given edge are given by an integral in the spectral domain where each component of the spectra is ray optical and therefore the diffraction can be calculated using standard GTD principles for each spectral component and then employing the superposition integral. A uniform asymptotic reduction of the inverse spectral integral then yields an analytical expression for the doubly diffracted fields.

The 2-D analytical solution is compared with an independent reference moment method solution of an integral equation to confirm the accuracy of the former. The analytical result for the 2-D tape scattering configuration is next extended to treat the corresponding 3-D case by using principles of ray optics.

B108.5

Environmental Effects Upon the Performance of Travelling Wave Receiving Antennas

William A. Shaheen*
College of Engineering
University of Hartford
West Hartford, CT 06117

Ladimer S. Nagurney
College of Engineering
University of Hartford
West Hartford, CT 06117

In an attempt to eliminate interference in the increasingly crowded medium-wave AM broadcast band, many users are discovering the advantages of directional receiving antennas. The effect of the environment on the computed radiation pattern and on the impedance of a single-wire travelling wave antenna is studied. In particular, variations in antenna geometry, and the effect of vegetation in contact with the antenna on performance is computed using the method of moments.

Results are compared and quantified to existing analytical information. The antennas under study are 1λ to 8λ long end-fed horizontal wires in close proximity to ground (around 0.03λ), often referred to as Beverage-type antennas. The antenna may be operated with or without a terminating resistor. Fields are numerically computed as a function of geometric deviation from the straight wire case and as a function of the shunting impedance presented by uninsulated tree supports.

FINITE ARRAYS OF MICROSTRIP PATCH ANTENNAS : THE INFINITE ARRAY APPROACH

A.K. Skrivervik*, J.R. Mosig and F.E. Gardiol
Department of Electrical Engineering
Ecole Polytechnique Fédérale de Lausanne, Switzerland

Phased arrays of printed antennas have since several years been of great interest, particularly in conjunction with the development of MMIC, where the radiators and the phase shifters can be integrated on the same substrate. Usually, finite phased arrays are studied either using an "element by element" approach if the number of radiators is not too large, or using the infinite array approximation for large arrays. The latter method takes automatically into account the mutual coupling between elements but neglects the edge effects. It is thus suitable only for the analysis of array elements located not too close to the edge.

The method presented in this paper for the analysis of finite arrays is based on the technique proposed by A. Ishimaru et al. for the case of finite arrays of dipoles (IEEE Trans. on AP, vol. AP-33, nov. 1985, pp. 1213-1220) : The active input impedance corresponding to the infinite array is convoluted with the equivalent aperture distribution of the current over the area of the array, to yield the finite array solution. In our approach, this method has been adapted to the case of finite arrays of microstrip patches by applying the convolution integral directly on the EFIE (Electric Field Integral Equation) used to solve the case of the infinite array of microstrip patches rather than on the input impedance.
As an example, the figure shows the modulus of the active reflection coefficient as a function of the scan angle for the central element of arrays of several sizes compared to the infinite case. The scan plane is the E-plane. All the arrays are formed by 60 mm x 40 mm rectangular microstrip patches and the grid is rectangular with spacings of 0.4 λ_0 in both directions. The substrate has a permittivity $\varepsilon_r = 4.32$, a thickness of 0.8 mm and a loss tangent tg $\delta = 0.02$. As expected, the active reflection coefficient converges to the infinite array case as the array grows larger.

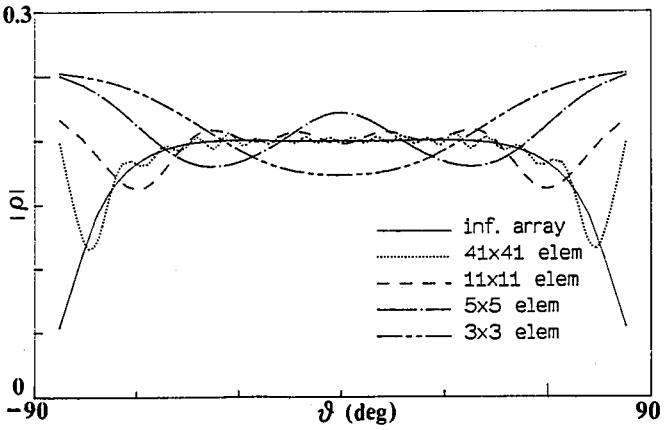

B108.7

A COMPUTATIONALLY EFFICIENT METHOD OF CALCULATING THE GREEN'S FUNCTION FOR AN OPEN MICROSTRIP STRUCTURE

Lincoln Cole Howard* and John M. Dunn
Center for Microwave and Millimeter-Wave CAD
Department of Electrical and Computer Engineering
University of Colorado at Boulder
Boulder, CO 80309-0425

Moment method analysis of microstrip structures is becoming increasingly popular because of its ability to model very general structures. One drawback is the amount of computer time required. A new, and highly efficient, approximation to the Green's function used in many formulations is presented here.

Typically, several minutes of computer time are required to analyze a single component of a circuit using a full wave analysis CAD program. The problem quickly becomes unreasonable if several data points are required at different frequencies. The time to carry out a computation consists of three parts: the evaluation of the Green's functions involved, the calculation of the individual elements of the matrix, and the solution of the matrix equation. For realistically sized problems, the filling of the matrix can take a majority of the time.

In this paper, new approximations to the Green's functions used in these programs are presented. The approximations have a number of advantages. They rely on the substrate of the circuit being electrically thin, which is a reasonable assumption in realistic circuits. There is no restriction on lateral separation between two points. If the substrate is thin enough, the approximation presented here can be used instead of having to calculate the Green's functions numerically. If the substrate is thicker, the form of the approximation can still be used; the coefficients are determined numerically at a few points by numerical evaluation of the Green's functions. Typically, only 20 points are needed as opposed to 500 for a complete numerical solution. Another advantage of this representation is that they can be used to speed up the run time of the matrix fill when several frequencies are needed. This results in substantial savings of time in the CAD program.

RECURSIVE T-MATRIX ALGORITHMS FOR CONDUCTING PATCHES

L. GUREL* AND W. C. CHEW
ELECTROMAGNETICS LABORATORY
DEPARTMENT OF ELECTRICAL AND COMPUTER ENGINEERING
UNIVERSITY OF ILLINOIS
URBANA, IL 61801

In this paper, we will discuss the applications of two recursive T-matrix algorithms[1,2] to the electromagnetic problem of scattering from geometries consisting of conducting patches[3]. (see Fig. 1) These two algorithms are shown to have complexities of $O(N^2P)$ and $O(NP^2)$, where N is the number of unknowns in the problem, and P is the number of terms that satisfies a convergence criterion in the addition theorems for the spherical wave functions. We will show that, for certain clusterings of patches, the recursive T-matrix algorithms require less than $O(N^3)$ operations. We will also outline a formulation that uses scalar—rather than vector—addition theorems for the vector-natured problem of electromagnetic scattering from patches.

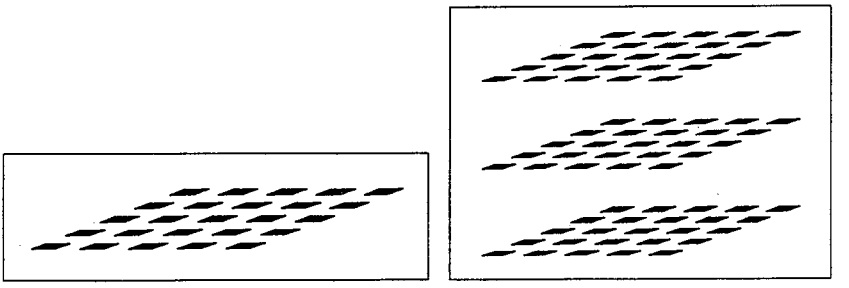

(a) (b)

Fig. 1. Canonical patch geometries, (a) the case of 2-D clustering, (b) the case of 3-D clustering.

[1] W. C. Chew, "An N^2 algorithm for the multiple scattering solution of N scatterers," *Microwave Opt. Tech. Lett.*, vol. 2, pp. 380–383, Nov. 1989.

[2] W. C. Chew and Y. M. Wang, "A fast algorithm for solution of a scattering problem using a recursive aggregate $\overline{T}$ matrix method," *Microwave Opt. Tech. Lett.*, vol. 3, pp. 164–169, May 1990.

[3] L. Gurel and W. C. Chew, "A recursive T-matrix algorithm for strips and patches," submitted for publication, Oct. 1990.

PERTURBATION CALCULATIONS FOR PARASITICALLY COUPLED S-PARAMETERS

John C. Moore* and Edward F. Kuester
Dept. of Electrical and Computer Engineering
MIMICAD CENTER: Campus Box 425
University of Colorado, Boulder 80309

Integral equation based numerical codes provide a means for accurately modeling microstrip junctions and discontinuities. These methods eventually reduce to solving a linear system of equations. Unfortunately, such a system is usually dense and can become quite large. For even moderately complicated microstrip structures, the time required to solve such a linear system by standard *matrix inversion* techniques can become prohibitively large.

In this paper an approach is developed that will produce an approximate solution to the linear system via perturbational techniques. This is accomplished by subdividing the microstrip junction into logically coherent blocks. A zeroth order current distribution is then calculated on these blocks that ignores parasitic coupling between these blocks. Perturbational techniques are then applied to these current distributions to produce currents accurate to first order. In many cases, these first order corrections are sufficient to model the parasitic coupling effects. The perturbation calculations involve matrix-vector multiplications, avoiding the computationally expensive matrix inversion calculations.

DE-EMBEDDING S-PARAMETERS FROM NUMERICALLY DETERMINED CURRENT DISTRIBUTIONS OF PLANAR JUNCTIONS

John C. Moore*, Jian-Xiong Zheng,
Edward F. Kuester and David C. Chang
Dept. of Electrical and Computer Engineering
MIMICAD CENTER: Campus Box 425
University of Colorado, Boulder 80309

Integral equation based numerical codes provide a means for accurately modeling the current distribution on microstrip junctions and discontinuities. Usually the parameter of interest is not the detailed current distribution. Instead, a network model parameterization (S-parameters, Z-parameters) may be more appropriate to characterize a given junction or discontinuity. When this is the case, a method for extracting the desired parameters from the current distribution is necessary.

In this paper two methods for extracting (*de-embedding*) S-parameters from numerically determined current distributions are presented. One method is based on the concept of fundamental mode distributions on a section of transmission line and is quite general. The second method is based on basic transmission line and network theories. Although this second method assumes a specific type of excitation in its integral equation formulation and is therefore less general, it has the advantage of providing a means of calculating the characteristic impedance of the junction ports (as well as the Z-parameters of the network) in addition to the S-parameter characterization. The two methods are then compared in terms of computational efficiency and accuracy.

Scattering III — Diffusion III

Room 3022 Salle
URSI B Session 110

Chairs/présidents: P.Y. UFIMTSEV, USA

13:30 (110.1) Isoparametric Edge Elements for 3-D Scattering Problems, **J.W. PARKER**, R.D. FERRARO, P.C. LIEWER, *California Institute of Technology, Pasadena, CA, USA*

13:50 (110.2) Electromagnetic Scattering by a Composite Body of Revolution, **H. MASSOUDI**[1], N.J. DAMASKOS[2], P.V. DONATO[2], [1]*General Electric Company, Schenectady, NY, and* [2]*Damaskos Inc., Concordville, PA, USA*

14:10 (110.3) Scattering from Conducting Bodies Coated by a Thin Layer of Magnetic Matter, **A. SADIGH**, E. ARVAS, *Syracuse University, Syracuse, NY, USA*

14:30 (110.4) Scattering by Gaps in Coated Strips, **J. MOORE**, H. LING, *University of Texas, Austin, TX, USA*

14:50 (110.5) Waves Diffraction on Screens with Dielectric Tips, **Z.T. NAZARCHÚK**, Z.M. KHMIL, *Ukrainian SSR Academy of Sciences, Lviv, USSR*

15:10 **COFFEE/CAFÉ**

15:30 (110.6) Diffraction by a Resistive Strip Attached to an Impedance Wedge, **R.G. ROJAS**, M.F. OTERO, *Ohio State University, Columbus, OH, USA*

15:50 (110.7) Diffraction by an Impedance Wedge – Resistive Sheet Junction, **J.R. NATZKE**, T.B.A. SENIOR, *University of Michigan, Ann Arbor, MI, USA*

16:10 (110.8) TE Scattering from a Conducting Wedge of Arbitrary Angle Loaded by a Slot, **J.W. SILVESTRO**, C.M. BUTLER, *Clemson University, Clemson, SC, USA*

16:30 (110.9) Electromagnetic Scattering from Lossy Corrugated Surfaces: Application to Microwave Absorbers, A.J. GASIEWSKI, **D.M. JACKSON**, A.F. PETERSON, *Georgia Institute of Technology, Atlanta, GA, USA*

16:50 (110.10) O(N) Algorithm for Vector Electromagnetic Scattering from N Scatterers, **B. HOUSHMAND**, W.C. CHEW, J. FRIEDRICH, *University of Illinois, Urbana, IL, USA*

ISOPARAMETRIC EDGE ELEMENTS FOR 3-D SCATTERING PROBLEMS

J. W. Parker, R. D. Ferraro, P. C. Liewer*

Jet Propulsion Laboratory / California Institute of Technology
4800 Oak Grove Drive
Pasadena, CA 91109

A family of high-order 3-D vector edge elements are examined, which combine tangential continuity of Whitney edge element with the flexibility of Lagrangean elements. Edge elements have been proposed for avoiding spurious modes, enforcing material boundary conditions, and reducing the density of the resulting matrix. However, elements based directly on the Whitney complex are only of zero order: they allow only piecewise constant variation of the vector field components tangent to the mesh edges. In addition to the approximation problem this implies, such elements cannot be conveniently utilized with local absorbing boundary conditions which rely on the first derivatives of these tangential field components.

In contrast, the new family of elements uses the scalar Lagrangean basis functions (of arbitrary order) both to map the element from an ideal space to the physical space, allowing curved elements, and also to weight the mapped Whitney vector-valued basis functions; thus these elements may be termed "isoparametric" by analogy to isoparametric scalar elements. Because the Whitney basis implies the tangential component is constant, the new family of basis functions has tangential components varying with the order of the Lagrangean basis functions. In order to preserve the tangential interpolation property of edge elements (i.e., the value of the unknown variable for a given basis function is the tangential component of the field at the associated node), the Whitney set is constructed in the mapped (possibly curved) space using the physical space gradients of the barycentric coordinates of the element. Such elements satisfy the boundary conditions at material interfaces and conductors in the simplest possible way: since only the tangential components are solved for, tangential continuity is automatic, while normal component conditions follow in a Galerkin sense. While the basis functions are not divergenceless, elements of the sort proposed here appear to be free of "spurious mode" type problems, at least for scattering solutions. The key may be that the function space is a subset of H_{curl} (fields with square integrable curl), rather than $(H_1)^3$ (fields for which each component is has square integrable spatial derivatives).

A quadratic tetrahedral element is implemented, with a second-order local absorbing boundary condition. Scattering from a 3-d reference object is obtained.

ELECTROMAGNETIC SCATTERING BY A COMPOSITE BODY OF REVOLUTION

Habib Massoudi*
General Electric Company
Corporate Research and Development
One River Road
Schenectady, NY 12301

N.J. Damaskos and P.V. Donato
Damaskos, Inc., PO Box 4609
Concordville, PA 19331

Electromagnetic scattering by a composite body of revolution for plane wave excitation with arbitrary angle of incidence is treated in this presentation. The scatterers of primary interest are bodies of revolution consisting of inhomogeneous cladding layers with imbedded resistive sheets.

The scattering problem is formulated as a set of coupled integral equations with induced electric and magnetic currents as unknowns. Method of moments, Galerkin's method with pulse basis functions and extended operators, is utilized to transfer the coupled integral equations into a set of linear equations for the unknown induced currents. The induced currents are solved for via matrix inversion and then the far-field data are calculated for the body of revolution problem.

Curves showing the bistatic and monostatic scattering cross-sections for some composite geometries will be presented. Numerical results for composite spherical structures will be compared with those of the exact series solutions. Some numerical aspects of the scattering problem such as the optimum mathematical cell size and criteria for converged solutions will also be discussed.

B110.3

SCATTERING FROM CONDUCTING BODIES COATED BY A THIN LAYER OF MAGNETIC MATTER

Ali Sadigh*, Ercument Arvas
Department of Electrical and Computer Engineering
Syracuse University, Syracuse, NY, 13244

A simple moment solution is given to the radar cross section of a closed perfectly conducting body coated by a thin layer of magnetic matter. The conducting body is of arbitrary shape. The method is based on the fact that the normal component of the magnetic field vanishes on the surface of a perfect conductor and is relatively small close to it. Neglecting the normal component of the magnetic field in magnetic coating which is assumed to be thin enough, enables us to approximate the effect of the coating by a magnetic surface current density **M** residing on the surface of the conductor. Furthermore it could be shown that **M** is proportional to $\mathbf{n}\times\mathbf{J}$, where **n** is the outward normal to the conducting surface and **J** is the equivalent electric surface current density induced on the conducting body. This method reduces the size of the problem to the one of scattering from a conductor alone. The surface of the conductor is approximated by triangular patches. **J** is expanded in terms of triangular current basis functions. The method of moment is used to solve for **J** and consequently **M**. Some numerical results are presented. The figure below shows the RCS of a conducting sphere when it is coated by a thin layer of magnetic matter $t(\mu_r-1)=.01-j.03$.

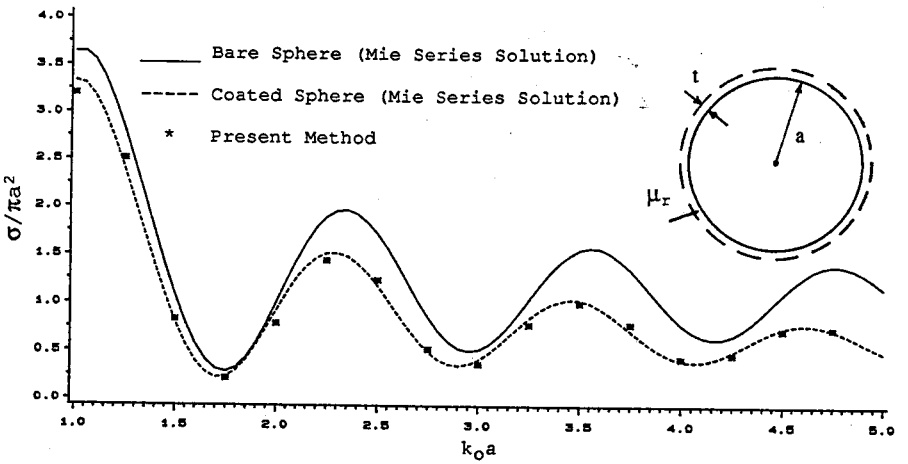

SCATTERING BY GAPS IN COATED STRIPS

John Moore* and Hao Ling
Department of Electrical and Computer Engineering
The University of Texas at Austin
Austin, TX 78712-1084

We have recently developed two numerical solutions to the problem of scattering from gaps in infinite conductor-backed material coatings. They include a boundary integral equation formulation and a spectral integral equation formulation. In the boundary integral formulation, the discretization domain of the infinite structure is reduced to a localized region near the gap by removing the specular solution and surface wave contributions from the boundary integral equation. The spectral integral formulation utilizes the Green's function for the conductor-backed coating in a volume integral equation. We obtained the isolated scattering contribution from the gap and the surface waves excited by the gap. The two solutions agree quite well with one another.

The goal of this work is to take advantage of these numerical solutions and integrate them efficiently into existing high-frequency scattering codes such that the effects of gaps in complex coated bodies can be predicted. In this paper, the scattering from a coated strip with a gap in the material coating is investigated. The approach is to systematically account for the isolated contributions and the interactions of the different scattering mechanisms. The isolated scattering mechanisms include as shown below (a) diffraction due to the gap, (b) surface waves excited by the gap, (c) diffraction at the strip edge, and (d) surface waves excited at the strip edge. The solutions to (c) and (d) are found using the technique presented by Bernard (J.-M.L. Bernard, Wave Motion 9, 543-561, 1987). We can then construct the total scattered field by systematically building up the multiple interactions.

We will show that (i) gaps in material coatings can significantly alter the scattering characteristics of the composite structure; and (ii) good results can be obtained from this "component" approach in that it compares favorably with the brute-force method of moments solution. This methodology is attractive since it allows the integration of scattering contributions from fine features such as gaps, cracks, and exposed cavities into existing high-frequency radar cross section prediction codes.

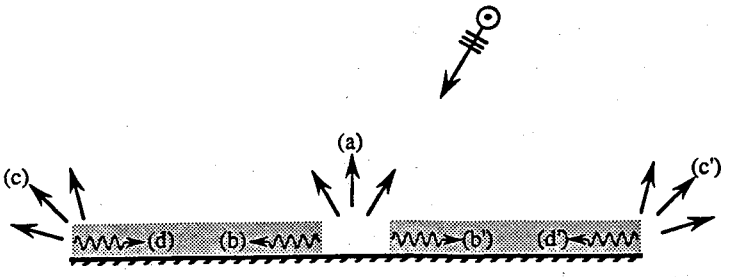

B110.5

WAVES DIFFRACTION ON SCREENS WITH DIELECTRIC TIPS

Z.T.Nazarchúk, Z.M.Khmil

On the basis of the integral equations method there is offered algorithmization of solution of the scalar problem of electromagnetic waves diffraction on cylindrical mirrors whose edges enter the dielectric bars of arbitrary cross-section. For the efficient algorithmization of the diffraction problem the initial structure is considered as an electrodynamic system of individual interacting scatterers with common edge points coinciding with geometrical and physical singularities when the screens cross dielectric solids. Its solution is reduced to the system of the second kind integral equations by the known method. Such equations have the logarithmic features, and in the case of H-polarization, besides, hypersingular integrals are singled out which are considered in the finite part sense according to Hadamard, and also are added to the stationary features. The built up integral equations are solved by the method of mechanical quadratures accounting for the behaviour of the unknown functions in the vicinity of the edge points of the integration contours. As a result of the numerical experiments the possibility of presenting the equation solution on the dielectric boundary in the class of continuous periodical functions was shown.

As an illustration we presented the calculations of the diffracted field components in the near and far zones at excitation by the E- or H-polarized wave of two parabolic screens protruding from the dielectric cylinder of the ellyptical profile, as well as the results of scattering by the screens with dielectric tips on the edges.

DIFFRACTION BY A RESISTIVE STRIP ATTACHED TO AN IMPEDANCE WEDGE

R.G. Rojas*, M.F. Otero
The Ohio State University ElectroScience Laboratory
Department of Electrical Engineering
Columbus, Ohio 43212

The high frequency electromagnetic diffraction by a resistive strip attached to an impedance wedge is considered in this paper. This problem is solved by breaking up the original geometry into simpler canonical geometries for which solutions exist or are easier to obtain. This can be done because of the local nature of high frequency diffraction. Once all the canonical problems are solved, they are then combined by means of the modified spectral ray method. The use of this latter procedure is necessary because the canonical geometries are solved assuming that the incident field is a plane wave; however, due to the close spacing of the various points of diffraction in the original geometry, the incident fields to each of these points of diffraction are not in general ray optical.

There are numerous applications where this geometry is important. The wedge is a canonical geometry that can be used to locally model a wide variety of scatterers. The purpose of adding the resistive strip is to have a greater control in the scattering characteristics of the wedge. For example, a resistive strip with a piecewise constant profile of its resistivity can be used to design a desired response in the frequency as well as in the spatial domains.

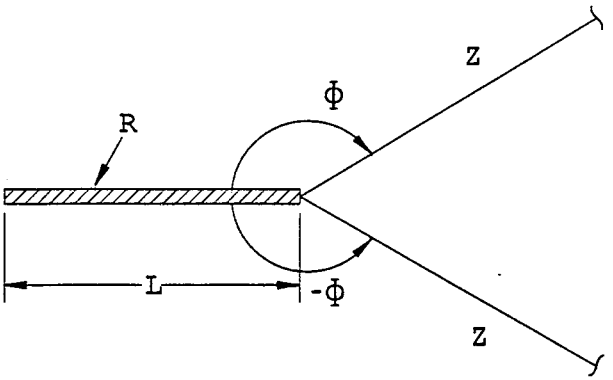

Resistive strip attached to an impedance wedge

B110.7

DIFFRACTION BY AN IMPEDANCE WEDGE - RESISTIVE SHEET JUNCTION

J. R. Natzke* and T. B. A. Senior

Radiation Laboratory
Department of Electrical Engineering and Computer Science
University of Michigan
Ann Arbor, MI 48109-2122

An exact solution is obtained for the total field of an impedance wedge and resistive half plane junction under E-polarized plane wave illumination. The spectral function of the integral expression for the total electric field is found to satisfy a second order difference equation which is reduced to pair of first order equations for solution. A diffraction coefficient for the junction is obtained and numerical data are presented, showing a significant reduction in scattering due to the vertex of the wedge.

TE SCATTERING FROM A CONDUCTING WEDGE OF ARBITRARY ANGLE LOADED BY A SLOT

John W. Silvestro*
Chalmers M. Butler
Clemson University
Clemson, SC 29634-0915

The Transverse Electric (TE) scattering from a conducting wedge of arbitrary angle, loaded by a slot, is considered. The problem is that of an infinitely long wedge with a slot or groove cut in one face which is illuminated by a plane wave TE to the wedge axis. This configuration is being studied for the purpose of determining how the slot affects the wedge scattering. An integral equation is formulated for the electric field in the slot and solved by a numerical procedure. The kernel of the integral equation is in the form of an infinite series which must be treated carefully in the numerical analysis. From knowledge of the slot electric field or equivalent magnetic current, obtained from the integral equation solution, the far-zone field scattered by the slotted wedge is computed. Numerical data will be presented, as will comparisons against published data, where available. Lastly, the possible use of the Geometrical Theory of Diffraction in place of the Green's function for a current near a wedge will be discussed.

B110.9

Electromagnetic Scattering from Lossy Corrugated Surfaces: Application to Microwave Absorbers

A.J. Gasiewski, D.M. Jackson*, and A.F. Peterson
School of Electrical Engineering
Georgia Institute of Technology
Atlanta, GA 30332

Electromagnetic scattering from a corrugated interface between two homogeneous, lossy dielectric half-spaces is analyzed using two numerical approaches: Green's function integral equation (GFIE) and coupled wave (CW) techniques. Motivation for this investigation derives from a need to analyze the performance of microwave absorbers (e.g., radiometric calibration loads and anechoic material), and to develop wideband absorber design criteria.

The GFIE approach requires the introduction of equivalent electric and magnetic surface currents located on the interface, and radiating into both regions of space. Coupled integral equations are obtained by enforcing continuity of fields at the interface. These equations are discretized into matrix form using subsectional pulse basis functions and point matching. Series acceleration techniques are used to efficiently compute the matrix entries.

In the CW approach, the corrugated interface is discretized into periodically inhomogeneous horizontal slabs (M.G. Moharam and T.K. Gaylord,J. Opt. Soc. Am., 72, 1385-1392, 1982). The fields within each slab are expressed as a sum of Floquet harmonics. By expressing the permeability and permittivity as Fourier series, and using Maxwell's curl equations, a set of coupled equations for the harmonic amplitudes is generated. A solution for the amplitudes is found using eigenanalysis and the slab boundary conditions. Conservation of energy is used to check the numerical acuracy within each slab.

The presentation will cover the implementation of these techniques, a comparison of their relative accuracies and efficiencies, and preliminary numerical results for radiometer calibration loads. Plans for experimental verification using laboratory measurements of the bistatic scattering pattern of a millimeter-wave radiometer calibration load will be discussed.

O(N) Algorithm for Vector Electromagnetic Scattering from N Scatterers

B. Houshmand*, W. C. Chew, J. Friedrich
Electrical and Computer Engineering Department
University of Illinois at Urbana - Champaign
Urbana, IL 61801

A fast recursive algorithm based on vector addition theorem is developed for vector electromagnetic scattering from many scatterers. This algorithm uses a recursive approach where the scattering from N+1 bodies is computed from the knowledge of the N scattering solution and the scattering properties of the isolated N+1st body. The scattering properties of each isolated body is given by its T (scattering) matrix (P. C. Waterman, Proc. IEEE, Vol. 53, 1965, pp. 805-811). The computation cost for the scattering solution increases linearly with N in the long wavelength limit, where N is the number of the scatterers. The algorithm development and its applications to scalar scattering from multiple and large bodies are reported elsewhere (W. C. Chew, New York: Van Nostrand Reinhold, 1990, pp. 463-469).

Here, this algorithm is applied to the problem of vector electromagnetic scattering of a plane wave from multiple spheres. The arrangement, permittivities, numbers and sizes of spheres can be chosen arbitrarily. The number of spheres considered in this paper are of the order 10, and the single sphere dimension (ka), and scatterer separation (kd) are of order 1, where k is the wave number. The scattering solution from many spheres is used to calculate the effective permittivity for various scatterer arrangements.

Antennas II

Room 2024 Salle
URSI B Session 114

Antennes II

Chairs/présidents: S. ADACHI, Japan; J. TRANQUILLA, Canada

08:30 (114.1) Effect of a Thin Dielectric Radome on the Horizontal Radiation Patterns of Transmitting TV Antennas, A. SADIGH, **E. ARVAS**, *Syracuse University, Syracuse, NY, USA*

08:50 (114.2) The Radiation Characteristics of a Loop Antenna on an Infinitely Long Dielectric Rod, **W.D. RAWLE**, *Technical University of Nova Scotia, Halifax, NS, Canada*

09:10 (114.3) The Input Admittance of the Coated Spheroidal Antenna, **J.D. KOTULSKI**, *Sandia National Laboratories, Albuquerque, NM, USA*

09:30 (114.4) Input Admittance of Multiply Fed and/or Loaded Insulated Linear Antenna in Air, **S.A. SAOUDY**, B.P. SINHA, *Memorial University of Newfoundland, St. John's, NF, Canada*

09:50 (114.5) L-Band Probe Antenna, **A. KUMAR**, *AK Electromagnetique Inc., Coteau Station, PQ, Canada*

10:10 **COFFEE/CAFÉ**

10:30 (114.6) Analysis of Strip Grating Antennas, R.R. DeLYSER, **E.F. KUESTER**, S. KOGUT, *University of Colorado, Boulder, CO, USA*

10:50 (114.7) Planar Antennas for the Millimeter and Submillimeterwave Range, **V. HANSEN**, *Ruhr-Universität Bochum, Germany*

11:10 (114.8) Scattering and Receiving Characteristics of a Narrow Slot Antenna in Tri-Layered Media, **W.J. GESANG**[1], E.J. ROTHWELL[1], K.M. CHEN[1], W.P. HANSEN[2], J.L. LIN[2], K. BURKET[2], [1] *Michigan State University, East Lansing, MI, and* [2] *Boeing Military Airplanes Division, Seattle, WA, USA*

11:30 (114.9) Equiangular Spiral Slot Antennas on a Semi-Infinite Substrate, **W.E. McKINZIE**, N.G. ALEXOPOULOS, *University of California, Los Angeles, CA, USA*

11:50 (114.10) Hybrid Mode Surface Wave Excitation by a Loop Antenna of an Infinitely Long Dielectric Circular Cylinder, **W.D. RAWLE**, *Technical University of Nova Scotia, Halifax, NS, Canada*

EFFECT OF A THIN DIELECTRIC RADOME ON THE HORIZONTAL RADIATION PATTERNS OF TRANSMITTING TV ANTENNAS

Ali Sadigh and *Ercument Arvas* *
Department of Electrical and Computer Engineering
Syracuse University, Syracuse, NY 13244

The deformation of the horizontal radiation patterns of TV transmitting antennas due to a thin dielectric radome is analysed by solving the problem using two different and simple moment solutions. In the first method, an exact equivalent problem is obtained by using the surface equivalence principle. Here, the radome is replaced by a set of equivalent surface electric and magnetic currents residing on the inner and the outer surfaces of the radome. The antennas and the other perfectly conducting supports are replaced by electric surface currents. The boundary condition on the tangential component of the electric field yields a set of coupled integral equations for the surface currents. These are solved approximately by using method of moments with pulse expansion and testing schemes. In the second method the radome is approximated by an impedance sheet and again the resulting integral equations are solved using the method of moments. Results obtained by both approaches are in excellent agreement. The figure below shows the radiation pattern with and without the radome. The cross section of the structure is shown on the left. The frequency is 600MHz and the length of the structure is more than ten wavelengths. Hence the problem was treated as a 2-D problem with TE excitation. The effect of all radial modes and the edge diffractions are automatically included in the solution.

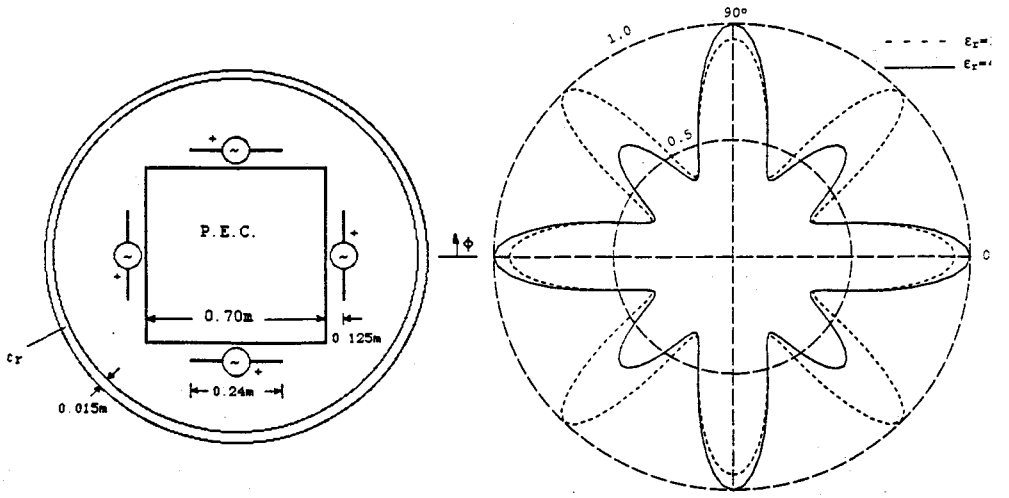

THE RADIATION CHARACTERISTICS OF A LOOP ANTENNA ON AN INFINITELY LONG DIELECTRIC ROD

W.D. Rawle
Dept. of Electrical Engineering
Technical University of Nova Scotia
P.O. Box 1000, Halifax, N.S. B3J 2X4

This paper presents an analysis of the radiation characteristics of a loop antenna which is mounted on an infinitely long dielectric circular rod. Such a structure presents an interesting model for certain classes of antenna.

The analysis is based upon a rigorous approach, employing Debye potential functions, which formulates expressions for electromagnetic field components resulting from the current distribution on the antenna. As shown in Figure 1, the antenna is positioned on the air-dielectric interface with its current exhibiting an $f(\phi)\delta(z)$ dependance at $\rho = a$. The antenna is excited with a voltage source as shown.

As reported earlier, a modal parameter approach has been employed to calculate the input impedance and current distribution on the antenna under a variety of conditions. These results, along with a steepest descent approximation to the exact expressions obtained from the initial formulation are employed to calculate the radiation characteristics of the structure. Selected numerical results are presented for antenna parameter Ω and rod dielectric constant ϵ_r. The results indicate that the dielectric constant of the rod will have significant impact upon the radiation characteristics of the antenna itself. The results are verified by comparing the special case $\epsilon_r = 1$ to other results found in the literature.

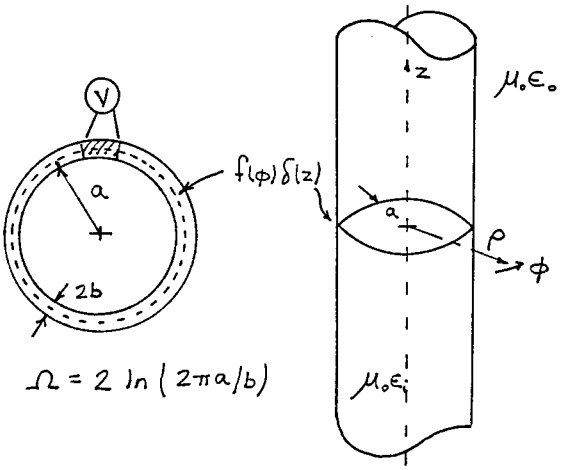

FIGURE 1

B114.3

THE INPUT ADMITTANCE OF THE COATED SPHEROIDAL ANTENNA

J. D. Kotulski
Sandia National Laboratories
Radiation and Electromagnetic Analysis, Div 9352
Albuquerque, NM 87185–5800

Antennas with a dielectric coating are present in a number of diverse applications. To help understand the effect of the coating on antenna performance it is useful to consider an antenna structure in a separable coordinate system. One such system is prolate spheroidal coordinates which allows the thin wire and the spherical antenna as limiting cases. The separation of variables technique is used to derive the input admittance of the spheroid with an assumed ϕ – independent voltage across the equatorial gap. The input admittance of the spheroidal antenna is examined for different types of coatings in a frequency region that includes the first resonance. The input admittance can be described by poles in the complex frequency plane together with the residues at the poles. The poles of this coated system will be identified and their location with respect to eccentricity and coating properties will be identified. For certain coatings for which an impedance boundary condition is valid an equivalent circuit can be generated. This can then be compared to previous results for the spherical and the thin–wire antennas with an impedance boundary condition.

INPUT ADMITTANCE OF MULTIPLY FED AND/OR LOADED INSULATED LINEAR ANTENNA IN AIR

S.A. SAOUDY
Center for Cold Ocean Resources Engineering
and
B.P. SINHA
Faculty of Engineering and Applied Science

Memorial University of Newfoundland
St. John's, Newfoundland, A1B 3X5.

In this work, analytic expressions are derived for the input admittance of a multiply fed and/or loaded dielectric coated linear antenna in air. This is done by employing the axial field discontinuity (AFD) method which is based on the Wiener-Hopf type analysis. The AFD method which does not employ superposition, was originally developed for multiply fed and/or loaded isolated antenna (S.A. Saoudy and M. Hamid, " Analysis of an Arbitrarily Excited-Loaded Dipole Antenna with a Derived Expression for the Field in the Feed Gap," Can. J. Phys., Vol.66, pp.680-691, 1988.). It treats the conducting antenna surface as a series combination of longitudinal electric field surface functions that may exist due to feeding and/or loading. Also, the analysis can handle any shape of the feed gap electric field ranging from the delta function generator across infinitesimally thin gaps to the Fourier-Bessel series field across wider feed gaps. Typical results are presented for different feed and loading arrangements.

The main advantage of this technique is the elimination of the need for a guess at a first approximation for the current and it presents the final expressions in terms of an asymptotic series which gives reasonably accurate results by using only the first term, especially when the antenna is long.

B114.5

L-BAND PROBE ANTENNA

A. Kumar
AK Electromagnetique Inc.
P. O. Box 240
30 Rue Lippee
Coteau Station
Quebec
Canada J0P

This paper describes the design, construction and test results of a circularly polarized crossed-dipole probe antenna at L-band. The antenna can be used as a probe for near field tests of large reflectors. We have used two inputs which are fed with a 3 dB quadrature hybrid, to provide circular polarization. In feeding the crossed dipole, one dipole is fed from port 1 and the other from port 4 (A. Kumar, IEE J. MOA, 2, 91-95, 1978). By changing the feeding port, the polarization can be changed from left hand circular polarization to right circular polarization. Each dipole is separately fed from a compensated balun, which is capable of broadband impedance matching (A. Kumar and H. D. Hristov, Microwave Cavity Antennas, Artech House, MA, USA, 1989).

The test range for the antenna is an indoor chamber of about 6m x 4.5m x 3.5m (AK Electromagnetique Inc.). A circularly polarized source horn is rotated for the axial ratio pattern measurements and the distance between the source horn and the test antenna is about 4m. The return loss is better than -25 dB for both ports in the frequency range of 1.530 to 1.665 GHz. The axial ratio is better than 0.5 dB on axis in the above frquency range.

A detailed description on design, measurement and applications will be given at the conference.

ANALYSIS OF STRIP GRATING ANTENNAS

Ronald R. DeLyser, Edward F. Kuester* and Sophie Kogut
Dept. of Electrical and Computer Engineering
MIMICAD Center: Campus Box 425
University of Colorado at Boulder
Boulder, CO 80309

Rectangular microstrip antennas consisting of a periodic strip grating oriented at an angle with respect to the sides of the antenna are analyzed, and the results compared to experimental data. The analysis uses the equivalent boundary conditions for an infinite periodic strip grating in the development of an integral equation which is then solved using the method of moments.

The boundary conditions are developed using the method of homogenization. The technique of multiple scales is used to expand the fields scattered from the periodic structure in a series in powers of the grating period p. This process leads to separation of the fine structured boundary layer fields from the average fields which exist at a distance from the grating. Solution of these separate problems leads to the boundary conditions for the average fields which are referred to in the literature as "equivalent" or "averaged" boundary conditions.

Analysis of the finite antenna structure in the layered microstrip geometry then proceeds in a classical manner using spectral domain techniques. The equivalent boundary conditions are applied at the interface where the antenna lies. This process results in an integral equation (containing scalar Green's functions) for the current densities on the antenna. The current is then expanded in a power series in p, resulting in a sequence of integral equations. The first is that for the zeroth order currents corresponding to a unidirectionally conducting surface, and the second for the first order currents. These equations are then solved numerically using the method of moments.

The attractiveness of this method is that only one mesh for the numerical analysis need be used for any angle of orientation, period of the grating, or strip width-to-period ratio. Also, the fine mesh needed to accurately analyze a narrow gap or strip is not necessary. These advantages are contrasted to the increased length of computation time necessary to solve two integral equations instead of just one.

B114.7

Planar antennas for the millimeter- and submillimeterwave range

Volkert Hansen
Institut für Hochfrequenztechnik
Ruhr-Universität Bochum
D-4630 Bochum, FRG

Planar antennas are well established up to some ten GHz. Because of their many advantages they are also attractive even for higher frequencies, e.g. for applications in mm-imaging systems or combined with a hemispherical lense for astronomical measurements. So far some measured results have been reported up to 1760 GHz.

The main problem of planar antennas at high frequencies is that a significant part of the power is coupled into guided modes, which substantially reduces the efficiency. One way to overcome this difficulty might be the use of suitable multilayer structures and the arrangement of the feeding network and the antenna elements in different planes and coupled by slots. However, by this the manufacturing costs increase considerably. Another way may be a planar antenna on a single layered grounded crystal quartz substrate which feeds a non-linear mixing element. Quartz is selected because it is available in thin wafers, it owns a low dielectric constant (3.83) even in the far infrared range and a low losstangent of less than 0.0001. For the non-linear load SIS elements are chosen, which show good performances at mm- and submillimeter wavelengths. However, a difficulty with this elements is the capacitive roll-off which can significantly decrease the RF coupling efficiency of the mixer. Therefore inductive elements must be used to resonate the capacidence at the signal frequency.

The development of the antenna requires a very careful design. Therefore a full-wave analysis is applied using the spectral domain approach. The SIS element can be modelled by a complex load. Therefore the spectral domain approach is extended for the analysis of circuits containing active or passive lumped loads or even finite areas with specified surface impedances. With the latter it is possible to study the performances if the whole circuit including the antenna or parts of it are operated below the critical temperature. The effect of the dielectric lense is discussed with the help of calculations for the antenna covered by dielectric superstrates.

SCATTERING AND RECEIVING CHARACTERISTICS OF A NARROW SLOT ANTENNA IN TRI-LAYERED MEDIA

W.J. Gesang*, E.J. Rothwell, and K.M. Chen
Department of Electrical Engineering
Michigan State University, East Lansing, MI 48824
William P. Hansen, J.L. Lin and Kevin Burket
Boeing Military Airplanes Division
P.O. Box 3707, Seattle, WA 98124

This paper investigates the effect of a substrate backed lossy layer on the scattering and receiving characteristics of a narrow slot antenna.

Consider a narrow slot antenna in a ground plane covered by a thin lossy sheet on top of a substrate. The slot is modeled by an equivalent magnetic current, which is proportional to the tangential electric field in the slot. A spectral domain Green's function, consisting of Sommerfeld type integrals, is derived to determined the electromagnetic field produced by a horizontal magnetic current source in the stratified media. The magnetic field integral equation derived for the slot is converted to a Hallen-type integral equation and solved using the method of moments. Conversion to the Hallen-type integral equation is found to improve convergence of the spectral integrals in matrix element calculation.

The receiving problem is decomposed into scattering and transmitting cases. In the scattering case, the structure is illuminated by a plane wave. In the transmitting case, the slot antenna is excited by a current source across the slot. The input impedance is obtained by solving the transmitting case. The backscattered field and the received power of the receiving antenna are calculated by superposition. It is found that the scattered field can be reduced substantially while reduction of received power is maintained at an acceptable level by the application of a thin lossy coating.

EQUIANGULAR SPIRAL SLOT ANTENNAS ON A SEMI-INFINITE SUBSTRATE

William E. McKinzie * and Nicolaos G. Alexopoulos
Department of Electrical Engineering
University of California, Los Angeles
Los Angeles, CA90024

The purpose of this paper is to numerically investigate the characteristics of a planar, balanced, centerfed, two-arm, spiral slot antenna located on a semi-infinte dielectric halfspace. The aperture integral equation is solved using the method of moments with triangular patches modeling the aperture electric field $\vec{E}_a$. Since the aperture is finite, both feed and termiation regions are modeled.

The triangulated spiral geometry approximates the polar curves $\rho = e^{.3063(\phi - n\frac{\pi}{2})}$, $n = 0, 1, 2, 3$ for $0.005R < \rho < R$. Each arm is truncated in a circle of radius R. An impressed 1 ampere current source bridges the $.002R$ wide slot at the origin. At each frequency 1500 unknowns (interior edges) are used to model $\vec{E}_a$.

Axial ratio and directivity are computed for cases of substrate $\epsilon_r = 1.0$, 2.2, and 13.0. It is observed that a low broadside axial ratio (< 2 dB) may be obtained over at least two octaves ($0.34 < R/\lambda < 1.7$) for all cases of ϵ_r where λ is a free space wavelength. The axial ratio at broadside is the same in both hemispheres. The directivity at broadside into the substrate increases with increasing ϵ_r with the substrate-to-air directivity ratio given by $\epsilon_r^{3/2}$. Near midband, for $\epsilon_r = 2.2$, the nominal directivity is 7 ± 0.5 dBi with a front-to-back ratio of 5.14 dB. This increases for $\epsilon_r = 13$ to a nominal directivity of 9.25 ± 0.3 dBi and a 16.71 dB front-to-back ratio ($0.34 < R/\lambda < 1.36$).

Directivity patterns reveal a single main beam without sidelobes for all cases. However, it can be seen that scalloping of the power pattern occurs at high frequencies and high dielectric constants. This is due to contributions from secondary rings of magnetic current which are widely separated in terms of the substrate wavelength.

HYBRID MODE SURFACE WAVE EXCITATION BY A LOOP ANTENNA ON AN INFINITELY LONG DIELECTRIC CIRCULAR CYLINDER

W.D. Rawle
Dept. of Electrical Engineering
Technical University of Nova Scotia
P.O. Box 1000, Halifax, N.S. B3J 2X4

This paper presents an analysis of hybrid mode surface wave excitation on an infinitely long dielectric circular cylinder by a loop antenna positioned on the air-dielectric interface. Surface wave excitation by a loop antenna serves as an interesting model for certain physical situations.

The analysis is based upon a Debye potentials formulation for the two region medium shown in Figure 1. Previous work has led to the calculation of the loop antenna's input impedance and current distribution. The present work investigates the excitation of all surface waves which may exist under the given geometries. Both electromagnetic field component amplitudes and power transfer are investigated. Numerical results are provided for ϵ_r = 2.56, 5.6, and 9.0. Verification of the present results is accomplished through comparison to experimental results published elsewhere in the literature.

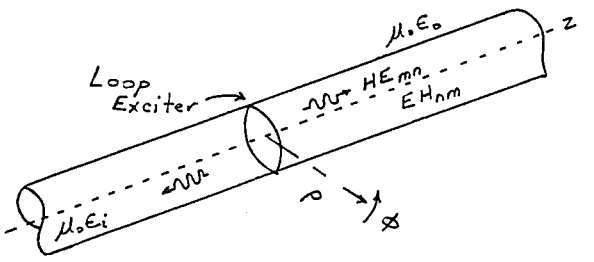

FIGURE 1

Guided Waves | Room 2028 Salle URSI B Session 115 | **Ondes guidées**

Chairs/présidents: R.E. COLLIN, USA; D.C. CHANG, USA

08:30 (115.1) Stability Analysis of Nonlinear TE_1 Guided Waves, **J.R. SOUZA**, *Pontifical Catholic University, Rio de Janeiro, Brazil*

08:50 (115.2) Electric Dipole Excitation of an Insulated Conductor, **D.A. HILL**, *National Institute of Standards and Technology, Boulder, CO, USA*

09:10 (115.3) Different Types of Bound to Leaky Mode Transitions, **M. TSUJI**[1], H. SHIGESAWA[1], A.A. OLINER[2], [1]*Doshisha University, Kyoto, Japan;* [2]*Polytechnic University, Brooklyn, NY, USA*

09:30 (115.4) Analysis of Single-Tone Excited Nonlinear Transmission Line Section Using the Harmonic Balance Method, X. WANG, **T.T.Y. WONG**, *Illinois Institute of Technology, Chicago, IL, USA*

09:50 (115.5) Transverse-Field Integral Operator Analysis of Integrated Dielectric Optical Waveguides, **J.M. GRIMM**, D.P. NYQUIST, *Michigan State University, East Lansing, MI, USA*

10:10 **COFFEE/CAFÉ**

10:30 (115.6) Determination of the Phase Constant of Closed Transmission Line Systems Using the Finite Difference and the Conjugate Gradient Method, **V. NARAYANAN**, T.K. SARKAR, *Syracuse University, Syracuse, NY, USA*

10:50 (115.7) EM Characterization of Complex Terminations Inside Electrically Large Open Cavities, **R.J. BURKHOLDER**, P.H. PATHAK, C. CHUANG, R.-C. CHOU, *Ohio State University, Columbus, OH, USA*

11:10 (115.8) Calculation of Magnetic Induction on Buried Pipeline Due to their Proximity to EHV Transmission Line, A.Y. HANNALLA[1], **M.M.A. SALAMA**[2], [1]*Ains Shams University, Cairo, Egypt;* [2]*University of Waterloo, ON, Canada*

11:30 (115.9) Wave Propagation through Regular Fractal Structures, **S.A. BULGAKOV**, V.V. KONOTOP, *Ukrainian SSR Academy of Sciences, Kharkov, USSR*

11:50 (115.10) Correct Mathematical Models of Electrodynamical Process in Open Waveguide Resonators, **I.E. POCHANINA**, N.P. YASHINA, *Ukrainian SSR Academy of Sciences, Kharkov, USSR*

B115.1

STABILITY ANALYSIS OF NONLINEAR TE_1 GUIDED WAVES

J. R. SOUZA
Center for Telecommunication Studies (CETUC)
Pontifical Catholic University of Rio de Janeiro (PUC/RIO)
Rua Marques de Sao Vicente,225 22453 Rio de Janeiro-RJ Brazil

The stability of TE_1 guided waves in a dielectric film bounded by semi-infinite, Kerr-type nonlinear substrate and cladding is investigated numerically.

The stability analysis is carried out using a variational formulation on the wave equation developed earlier (Proc. 1989 URSI Nat. Radio Sci. Meeting, p 183, Boulder, CO), which yields a standard eigenvalue problem (EVP). Initially, the stationary analytical solution available in the literature is used to provide the effective refractive index and electric field profile for a given value of the guided-wave power. Next, these data are fed into the EVP. The resulting effective index and field profile are used to update the nonlinear refractive index distribution, keeping the power level constant, and the EVP is solved again. If both the effective index and the electric field profile are not altered as the EVP is repeatedly solved, then the initial data correspond to a stable solution of the nonlinear wave equation. If either is altered, the initial data correspond to an unstable solution. The results indicate that portions of the analytical solution are not only unstable, but may follow a route to chaos through period doubling as the guided-wave power increases. The figure below shows the variation of the effective index with the number of iterations on the EVP in a waveguide with a 2.0μm thick film, whose refractive index is 1.57, bounded by nonlinear substrate and cladding, with 1.55 low power refractive indices, and nonlinear coefficients, respectively, 1.0×10^{-9} m^2/W and 2.0×10^{-9} m^2/W. The wavelength is 0.515μm, and the initial effective index is 1.56478, for a guided-wave power of 30.5987 W/m. The oscillatory character of the solution is clearly seen, showing that it is unstable. In general the results agree with those of Zabeu & Souza (Microwave and Optical Technology Letters 3, 298-302, 1990), who employed finite difference techniques in their analysis, although considerably fewer iterations are needed in the present algorithm to detect unstable solutions.Again, as in Zabeu & Souza's paper, solutions considered as stable by Ariyasu and colleagues (IEEE J. Quantum Electron. 22, 984-987, 1986), who employed the beam propagation method in their analysis, were found to be unstable and possibly chaotic.

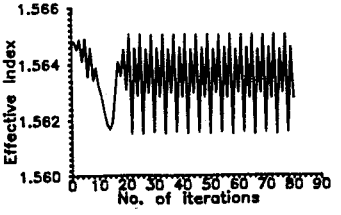

ELECTRIC DIPOLE EXCITATION OF AN INSULATED CONDUCTOR

David A. Hill
Electromagnetic Fields Division
National Institute of Standards and Technology
Boulder, CO 80303 USA

The excitation of currents on long underground conductors is important in many applications. Power lines and rails in tunnels can enhance transmission for mine communications, and electromagnetic probing of the earth can be influenced by the presence of cables or pipes (J.R. Wait and K.R. Umashankar, Pure and Appl. Geophys. 117, 711-742, 1978). Magnetic dipole excitation of infinitely long (D.A. Hill, IEEE Trans. Geosci. Rem. Sens. GE-26, 720-725, 1988) and finite length (D.A. Hill, IEEE Trans. Geosci. Rem. Sens. GE-28, 289-294, 1990) conductors in a lossy medium has been analyzed with application to detection of underground conductors.

In this paper our model consists of an infinitely long horizontal conductor in a homogeneous, lossy medium and a horizontal electric dipole source. The conductor can be either insulated or bare to model ungrounded or grounded conductors. The derivation of the conductor current follows the spatial Fourier transform method, and numerical results for the current and the scattered fields are obtained by fast Fourier transform. Insulated conductors support a quasi-TEM transmission line current that decays slowly along the conductor. At long axial distances, the fields generated by this transmission line current dominate the primary fields of the dipole source and should be detectable. Grounded conductors are also strongly excited, but the currents decay more rapidly. In either case, frequencies from about 5 to 500 kHz appear to be useful.

Excitation by an electric line source of finite length or a plane wave is also considered. An electric line source of constant current and finite length is a good model for an insulated antenna grounded at the ends. Numerical results for this source are obtained by integrating the electric dipole solution over the finite source length. Plane wave excitation is used to model a distant source, and this excitation does not excite the transmission line current.

B115.3

DIFFERENT TYPES OF BOUND TO LEAKY MODE TRANSITIONS

M. Tsuji* and H. Shigesawa
Doshisha University, Kyoto, Japan

and

A. A. Oliner
Polytechnic University, Brooklyn, New York

It has been recognized for some years that the transition region between bound-mode and leaky-mode ranges on certain open guiding structures is rather complicated even though it occurs over a narrow frequency range. Such behavior was found previously for guidance by a dielectric layer and by open periodic structures. Recently, these transition regions have been examined by us in connection with the newly found leakage phenomena on printed-circuit waveguides. In fact, we reported at the 1990 URSI Meeting in Dallas, TX, that such effects were observed on microstrip line when Epsilam 10 was used as the anisotropic substrate.

The behavior within this narrow transition region for all of the previous examined guiding structures, including the one discussed last year, forms a common pattern, which we shall call "regular" behavior. It involves a short region in which the mode is purely real but improper. In the present talk, we first summarize this behavior, and show why this intermediate stage between the bound-wave (real, proper) solution and the leaky-wave (complex, improper) solution appears to be necessary and understandable.

Recently, however, we have examined the transition region for various printed-circuit guiding structures, and we found all kinds of ***unusual and interesting behavior.*** For some structures, "regular" behavior was found, but in some of those cases the transition region is very narrow whereas in other cases it is rather wide. Even more interesting, we find several examples of very unusual, and different, behavior. For instance, microstrip line on a more-strongly anisotropic substrate offers a variety of complex behaviors, and is discussed separately in a companion paper. In this paper, results will be presented for slot line and coplanar waveguide, which may be conventional or conductor-backed, with finite or infinite width, to illustrate the various types of "regular" or "unusual" transition-region behavior. We will introduce some order into the variety, and indicate the possible physical implications of some of the more unusual solutions.

ANALYSIS OF SINGLE-TONE EXCITED NONLINEAR TRANSMISSION LINE SECTION USING THE HARMONIC BALANCE METHOD

Xiaohai Wang and Thomas T. Y. Wong *
Department of Electrical and Computer Engineering
Illinois Institute of Technology
Chicago, Illinois 60616

The harmonic balance method has proved to be highly effective in analyzing nonlinear circuits and devices ranging from subsonic to microwave frequencies (S. A. Maas, Nonlinear Microwave Circuits, Norwood, MA: Artech House, 1988.) Most of the applications have been concerned with lumped nonlinear circuit elements embedded in a linear network which may be lumped or distributed in nature. In this paper, an application of the harmonic balance method for studying wave propagation in a nonlinear transmission line is considered.

A resistively terminated lossless nonlinear transmission line excited by a sinusoidal signal is analyzed by means of the harmonic balance method. The nonlinearity is taken to be arising from a distributed nonlinear capacitance as realizable on the surface of a semiconductor substrate using planar technology for integrated circuit fabrication. After discretizing and partitioning the transmission line into linear and nonlinear subnetworks, the harmonic balance equations are formed. An FFT based iterative algorithm is implemented to obtain numerical solution to the system of equations. Techniques for enhancing convergence and reducing computation time will be discussed.

B115.5

TRANVERSE–FIELD INTEGRAL OPERATOR ANALYSIS OF INTEGRATED DIELECTRIC OPTICAL WAVEGUIDES

J. M. Grimm* and D. P. Nyquist
Department of Electrical Engineering
Michigan State University, East Lansing, MI 48824

As the number of integrated optics applications increase, analytical predictions for the theoretical behavior of the basic structures becomes vital. This problem can be solved using full–wave analysis by replacing the guiding region with equivalent polarization currents in a uniform medium and treating the waveguide as a re–radiating obstacle. This allows the construction of the following electric field integral equation based upon Hertzian potentials, namely,

$$\vec{e}(\vec{\rho}) - \left(k_c^2 + \tilde{\nabla}\tilde{\nabla}\cdot\right) \int_{CS} \frac{\delta n^2(\vec{\rho}')}{n_c^2} \tilde{g}(\vec{\rho}\,|\vec{\rho}')\cdot\vec{e}(\vec{\rho}')\, ds' = 0\,; \quad \text{all } \vec{\rho} \in CS$$

where $\delta n^2(\vec{\rho})$ is defined as $n^2(\vec{\rho}) - n_c^2$, the contrast between the arbitrarily graded guiding region of refractive index $n(\vec{\rho})$ and a cover region of refractive index n_c; CS is the cross-section of the guiding region; and $\tilde{g}(\vec{\rho}\,|\vec{\rho}')$ is the Green's dyadic for the background layered surround region.

It has long been known that a uniformly–clad dielectric waveguide can be described by using only transverse–field components. Just recently (M. Viola and D. P. Nyquist, JEWA paper to be published), it has been demonstrated that a dielectric optical waveguide in a multi–layered surround region can likewise be described using the transverse-field components. It is this new technique which is implemented for rib and strip guiding structures in this paper. A major advantage in this technique is reduced matrix size in a MoM formulation, allowing for more accuracy. Additionally, the new formulation is equivalent to a mixed–potential formulation. This has the effect of reducing the source–point singularity strength and rendering numerical evaulation of the problem more stable.

Determination of the phase constant of closed transmission line systems using The finite difference and the conjugate gradient method

Viswanathan Narayanan and Tapan K. Sarkar
Department of Electrical and Computer Engineering
Syracuse University, Syracuse, NY 13244-1240

The aim of this paper is to compute the characteristics (the phase constant β, the cutoff wave numbers and the field distributions) for the first few dominant modes of arbitarary shaped conducting and dielectric filled waveguide structures. Dispersion characteristics for the hybrid modes in inhomogenous shielded transmission line structures has been obtained.

The analysis would employ the finite difference technique. The resulting eigenvalue problem will then be solved iteratively using the conjugate gradient method.

Although transmission lines can be very simple in construction, they belong to a family of the so called inhomogenously filled waveguide structures. This implies that no TEM or waveguide type TE or TM modes exist independently, making an accurate analysis difficult.

The quasi-TEM analysis does not account for the hybrid nature of the guided modes and hence results in the inaccuracy. The dispersive nature of the structure cannot be predicted by the quasi-TEM method. Hence there is a need for a much rigorous full wave solution taking into consideration the various boundary conditions. The finite difference method proposed, involves such a full wave analysis.

For the solution of the modes in the waveguide structures, it is necessary to apply the finite difference technique to the operator equation. This results in solving an $N \times N$ matrix eigenvalue problem. This could be a limiting factor due to memory limitations in computers. However,this is overcome by observing that the system matrix is very sparse. Hence the information about an $N \times N$ system may be stored in an array of $N \times 8$ matrix with another $N \times 8$ matrix containing the column position of the elements. So one may drastically cut down on the memory requirements of the finite difference technique. Also the minimum eigenvalues of this sparse matrix are of interest because we are looking for the first few dominant modes. The conjugate gradient method takes advantage of this fact and solves iteratively for the lower few eigenvalues. Unlike the traditional methods in which all eigenvalues are found and the first few desired ones are selected, this method just finds the required eigenvalues. This results in a saving on computer time. The phase constant β can be obtained from the eigenvalues.

The eigenvectors corresponding to the desired eigenvalues for the TE, TM and hybrid mode equations give the electric and magnetic vector potentials inside the structure. Hence the various E and H field plots may be obtained from this information.

So one would have the complete solution for β of the first few dominant TE, TM and hybrid modes of arbitrary shaped conducting structures partially filled with dielectrics.

B115.7

EM CHARACTERIZATION OF COMPLEX TERMINATIONS INSIDE ELECTRICALLY LARGE OPEN CAVITIES

Robert J. Burkholder*, Prabhakar H. Pathak, Chiwei Chuang, and Ri-Chee Chou
The Ohio State University ElectroScience Laboratory
1320 Kinnear Road, Columbus, Ohio 43212

The external EM scattering by complex terminations or obstacles inside electrically large open-ended waveguide cavities has been formulated recently using a reciprocity integral (P.H. Pathak, P.H. Law, G. Crabtree & D. Foreman, *IEEE AP-S Symposium Digest*, 1710-1713, 1990). In this formulation, the external fields scattered by an interior obstacle/termination are given in terms of an integration of fields over a conveniently chosen cross sectional surface S_T located near the obstacle/termination. A significant advantage of this formulation is that it is useful for separately estimating the effect on the overall cavity-obstacle scattering which results from modifications in the cavity shape for a given type of complex obstacle, and from different types of complex obstacles for a given type of cavity shape.

It is assumed that the coupling of externally applied fields into the cavity via the open end, and the propagation of these fields down the cavity to S_T can be found, for example, using modal, ray, and beam methods (P.H. Pathak & R.J. Burkholder, *IEEE Trans. Antennas and Prop.* 37, 635-647, 1989; H. Ling, R. Chou, & S.W. Lee, *IEEE Trans. Antennas and Prop.* 37, 194-205, 1989; P.H. Pathak & R.J. Burkholder, *Radio Science* 37, Jan-Feb 1991). In this presentation, different methods will be considered for characterizing the interior fields scattered by the complex obstacle/termination beyond S_T in such a way as to easily couple to the fields arriving down the cavity to S_T via the reciprocity formulation. This involves a three step process: (1) the fields at S_T incident from the cavity side of S_T are expanded into an appropriate set of basis functions, such as waveguide modes or discrete plane waves, (2) the fields reflected back to S_T by the obstacle/termination due to each of these basis functions are found, and (3) these reflected fields are expanded in terms of the same set of basis functions to simplify the reciprocity integral using orthogonality properties of the basis set. Step (2) can be performed analytically, numerically, or experimentally, depending on the complexity of the interior obstacle/termination. Various examples will be presented to demonstrate the effect on the scattering by a complex obstacle within a relatively arbitrarily shaped cavity structure.

Calculation of Magnetic Induction on Buried Pipeline due to their Proximity to EHV Transmission Line

A. Y. Hannalla
Department of Electrical Engineering
Faculty of Engineering
Ain Shams University
Cairo, Egypt

M.M.A. Salama
Department of Electrical &
Computer Engineering
University of Waterloo
Waterloo, Ontario
Canada N2L 3G1

Shock hazards appear at some points when working personnel touch gas pipelines when they are buried in proximity to the EHV transmission line, Cairo-500 KV. Asyout pipeline is buried in the right of way to the EHV line for a distance about 250 km. Both lines are located in desert where the nature of the earth in most locations is rockets covered with sand. The pipeline is covered with nonconductive coating. Measurements have been reported. Some earthings have been done but the improvements were not as good as expected.

The objective of the paper is to present a comprehensive method for calculating the magnetic induction on buried pipeline in the desert environment, due to their proximity to EHV transmission line. The model of calculation will take into consideration the nature of the soil, the coating of the pipeline and the location and the earth electrodes resistance of the earthing electrodes used in the pipeline laying scheme.

The method is applied on a Moustored Asyout gas pipeline buried in the right of way with the 500 kV Aswan Cairo transmission line. Shock hazards are considerably reduced and conditions on the pipeline that give rise to high induced voltage are also avoided when mitigation techniques suggested in this paper as a result of the mathematical model is implemented.

B115.9

WAVE PROPAGATION THROUGH REGULAR FRACTAL STRUCTURES

S. A. Bulgakov* and V. V. Konotop
Institute for Radiophysics and Electronics,
Proscura Str. 12 , Kharkov 310085 , USSR

The wave propagation through one-dimensional fractal media with dielectric permittivity profiles described by trigonometric serieses has been studied. Two cases of principle are considered analytically and numerically. The first one is the wave transmission through uniformly limited fractals (like , in particular, Weierstrass function). To this end the approximation method is developed. It is based on the separation of the boundary (i.e. the large scale part) and fractal scattering. It is shown by numerical analysis that the method can be successfully applied to the region of wave vectors **k** and fractal length **L** where $\mathbf{a}\,\mathbf{k}\mathbf{L} < 10$ (here **a** is an amplitude of a fractal tone of a scale $2\pi/\mathbf{k}$). The boundary scattering describes resonant effects. The internal (fractal) scattering decreases as **k** rises .

The wave propagation properties have been examined in details for different values of local fractal dimension **D** . It is shown that a discrepancy arises between analytical and numerical methods only in the region of $\mathbf{D}\sim\mathbf{2}$. It can be with the fact explained that the method developed for one-dimensional systems is unsuitable for **2D** ones .

Another case under consideration is a class of "singular" fractals, i.e. described by trigonometric sets that do not have uniform asymptotics. However the singularity is assumed to be integrable so that the outcomes can be obtain analytically , for example in the Born approximation. In the above terms the internal scattering by such fractals having small width is more stronger than the boundary scattering. The above approach allows to obtain only some estimates. This case is considered in detail by numerical methods.

CORRECT MATHEMATICAL MODELS OF ELECTRODYNAMICAL PROCESS IN OPEN WAVEGUIDE RESONATORS.

Irina E.Pochanina and Natalia P.Yashina (Ph.D.)

(Institute of Radiophysics and Electronics of the Academy of Sciences of the Ukrainian SSR, Akad. Proskury st.,12,Kharkov 310085,USSR)

Open waveguide resonators (OWR) are wide range of electrodynamical objects,disigned by the set of different discontinuities in regular infinite waveguides. Varying their geometrical parameteres one may control electrodynamical characteristics of OWR. This fact open new opportunities in designing of devices using OWR: filters, couplers, linesplitters, matchings. We have developed the elements of the OWR theory, based on the correct mathematical model of spectral and diffraction boundary value problems and corresponding effective numerical algorithms. This theory provides a reliable description, explanation and prediction of physical nature of electrodynamical processes in OWR .

The axisl simmetrical resonators are considered. OWR of this type are rather good model of real microwave devices.The mathematical model of the boundary value problem (BVP) is developed on the base of partial-inversion method according to which we can obtain an algebraic equations infinite system of the second kind:

$$\{I - \mathcal{A}\}x = \mathcal{B} \tag{1}$$

The solution of this system provides us with value of scattering matrix elements. Asimptotic properties of enables us to ground the application of the reducing method for numerical solution. The fast convergence of numerical results provides its efficiency.

Extensive numerical investigations of OWR diffraction characteristics with variable geometrical parameters and frequency permit us to find and describe the most interesting and useful phenomena arising in diffraction processes.

The spectral problem consists in determining values of spectral parameter $\varkappa = \varkappa' + i\varkappa''$ in which exist nontrivial solution of the homogeneous BVP. This problem like the diffraction problem can be led to the system similar to (1) but now homogeneous:

$$\{I - \mathcal{A}(\varkappa)\}x = 0. \tag{2}$$

Due to the properties of the operator $\mathcal{A}(\varkappa)$ it can be shown that the considered OWR spectrum is discrete, finite multiplicit in $C_\varkappa$ and is determined as the roots of function:

$$\mathcal{F}(\varkappa) = \det\{I - \mathcal{A}(\varkappa)\}, \quad \varkappa \in C_\varkappa \tag{3}$$

It can be shown also that characteristic values of the operator $I - \mathcal{A}(\varkappa)$ with any required accuracy may be approximated by characteristic values of reduced operators. To obtain a 1% accuracy we should take into account equations in (3) with $N = 12\varkappa + 3$ as it has been shown by numerical investigation of convergence.

The analisis of the spectrum (1) permit us to discover and investigate the relations between resonant displays in diffraction characteristics and excitation in OWR of induced modes close to their natural ones, made possible the prediction of appearence of total reflection and transmission regimes.

Complex Media | Room 2032 Salle URSI B Session 116 | Milieux complexes

Chairs/président: I.V. LINDELL, Finland; D.L. JAGGARD, USA

08:30 (116.1) Gaussian Beam Propagation in Nonlinear Media, **R.W. ZIOLKOWSKI**, *University of Arizona, Tucson, AZ, USA*

08:50 (116.2) Fractal Electrodynamics and Diffraction by Cantor Targets, **D.L. JAGGARD**, T. SPIELMAN, X. SUN, *University of Pennsylvania, Philadelphia, PA, USA*

09:10 (116.3) Analysis of Stacked Metallic Grids in a Multilayered Substrate by Iterative/FFT Methods, **J.G. CUEVAS**, J.R. MOSIG, *École Polytechnique Fédérale de Lausanne, Switzerland*

09:30 (116.4) Dyadic Green's Functions for a Biaxially Anisotropic Medium: II. Two-Layer Case, **S. MUDALIAR**, J.K. LEE, *Syracuse University, Syracuse, NY, USA*

09:50 (116.5) Transient Response of Chiral Materials, P.G. ZABLOCKY, **N. ENGHETA**, *University of Pennsylvania, Philadelphia, PA, USA*

10:10 **COFFEE/CAFÉ**

10:30 (116.6) Novel Designs for Reciprocal Phase Shifters Using Pseudochiral or Ω Medium, M. SAADOUN, **N. ENGHETA**, *University of Pennsylvania, Philadelphia, PA, USA*

10:50 (116.7) Green Functions for Bi-Isotropic (Nonreciprocal Chiral) Media, **I.V. LINDELL**, A.J. VIITANEN, *Helsinki University of Technology, Espoo, Finland*

11:10 (116.8) The Chiral Dällenbach Absorber, **J.H. CLOETE**, A.G. SMITH, *University of Stellenbosch, South Africa*

11:30 (116.9) Surface Wave in Chiral Media, **V.E. GRIKUROV**, *USSR Academy of Sciences, Leningrad, USSR*

11:50 (116.10) Nonstationary Wave Problems for a Layered Media, **A.G. BUGROV**, M.A. GUZEV, V.I. KLYATSKIN, *Far Eastern Branch USSR Academy of Sciences, Vladivostok, USSR*

B116.1

Gaussian Beam Propagation in Nonlinear Media †

Dr. Richard W. Ziolkowski
Electromagnetics Laboratory
Department of Electrical and Computer Engineering
The University of Arizona
Building 104, Room 422E
Tucson, AZ 85721

There is a great deal of current interest in the interaction of electromagnetic beams generated by high power microwave and millimeter wave systems with materials and in the propagation of pulses along and near transmission lines in the presence of passive and active nonlinear elements. General aspects of these problems will be reviewed briefly and a generic nonlinear medium model will be derived which incorporates dispersion, inhomogeneities, and amplitude and intensity nonlinearities. A geometrical optics method that describes the propagation of a wave in such a medium will then be presented.

A particular application of this nonlinear geometrical optics method will be made to the propagation of a Gaussian beam in a medium with a quadratic (intensity) nonlinearity. A complex, distorted phase will be generated that is used to describe both the zeroth-order amplitude and the nonlinear rays along which the energy propagates. It will be demonstrated that this approach recovers standard linear geometrical optics results and the standard self-focusing and self-blooming effects in such a quadratically nonlinear medium. In the case of strong dispersion, it will be shown that the amplitude of the wave has the same form as in the linear case but with its phase modified by a term related to the nonlinearity. In the case of of weak dispersion where the dispersion is comparable to the nonlinearity, it will be shown that the method yields the expected soliton solutions.

Some generalizations of these concepts to very short pulse propagation in the generic nonlinear medium will be made. As will be discussed, this problem is of interest when ultra-wide bandwidth systems are involved.

---

† This work was supported in part by the Lawrence Livermore National Laboratory under the auspices of the U. S. Department of Energy under contract No. W-7405-ENG-48.

FRACTAL ELECTRODYNAMICS AND DIFFRACTION BY CANTOR TARGETS

D. L. Jaggard, T. Spielman and X. Sun
Complex Media Laboratory
Moore School of Electrical Engineering
University of Pennsylvania
Philadelphia, PA 19104

Fractal electrodynamics is the blend of fractal geometry with electromagnetic theory [see e.g., D. L. Jaggard, "Fractal Electrodynamics," in *Recent Advances in Electromagnetic Theory*, H. N. Kritikos and D. L. Jaggard, eds., Springer-Verlag (1990)]. Here, electromagnetic waves are used to remotely interrogate fractal structures and to determine fractal descriptors of those objects by information impressed on their scattered fields. Often, wavelength or pulse width is used as a variable-length yardstick to characterize these fractal geometries using frequency-domain or time-domain methods, respectively. These variable-length yardsticks and measurements are needed due to the multi-scale nature of fractal structures.

Here we are interested in small-angle scattering by fractal apertures and disks. While previous work in diffraction by fractal geometries has been concerned with factally corrugated aperture edges [Y. Kim, H. Grebel and D. L. Jaggard, "Diffraction by Fractally Serrated Apertures," *J. Opt. Soc Am. A8*, 20-26 (1991)], we now examine electromagnetic wave diffraction by cantor targets as a function of growth stage and fractal dimension. The variable-length yardstick used to interrogate these fractal apertures and disks is $Q\ (= |\mathbf{k}_{inc} - \mathbf{k}_{diff}|)$, the magnitude of the difference between incident and diffracted wave vectors, which plays the role of frequency. Variations in either angle or wavenumber can be used to retrieve the desired information.

The problem is investigated analytically and numerically. As one example, we show below a sample target (inset), the triadic cantor target in the third stage of growth. Also displayed below is a comparison of the far-zone diffracted fields of a circular aperture (Airy Pattern) and of this cantor target (Radial FT of Cantor Set) as a function of transverse coordinate on a log-log plot. The fundamental physics of the diffraction problem will be discussed and an examination made of a variety of Cantor targets in various stages of growth.

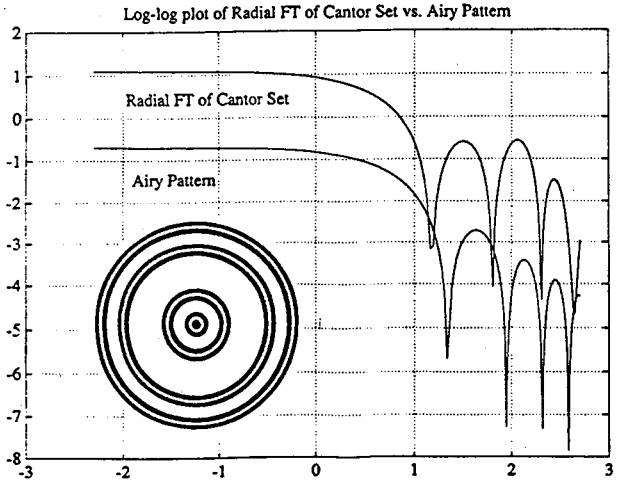

B116.3

ANALYSIS OF STACKED METALLIC GRIDS IN A MULTILAYERED SUBSTRATE BY ITERATIVE / FFT METHODS

J.G. Cuevas * and J.R. Mosig
Laboratory of Electromagnetics and Acoustics
Ecole Polytechnique Fédérale de Lausanne, CH-1015 Lausanne, Switzerland
(*) On leave from Universidad Politécnica de Madrid, Spain.

Metallic grids are currently used as dichroic or frequency selective surfaces (FSS) in reflector antennas to obtain a frequency filtering of electromagnetic waves. Usually, the design of such structures is aimed at the achievement of relatively close transmission and rejection bands. Moreover, the bands should be sufficiently wide and grating lobes for incident angles belonging to the desired directions should be avoided. These specifications can be met by using dual resonance elements in the grid (concentric patches, Jerusalem crosses) but a more flexible approach is the use of two or more stacked grids embedded in a multilayered dielectric (Cahill and Parker, Elett. Letters., 1982, pp 313-314). Such a structure is also able to modify the polarization state of the transmitted electromagnetic wave and hence, it can be used as a polarizer to obtain circular polarization from a linearly polarized transmitter.

Stacked grids have been theoretically analyzed by characterizing each grid individually and then using a Generalized Wave Matrix technique to connect all the grids (Shuley, IEE Proc., **131**, pp 129-132). A drawback of this approach is that the spatial periodicity must be the same in each grid. Also, coupling phenomena between grids are dealt with in an approximate manner. We propose an alternate approach, useful for a small number of grids, in which stratified Green's functions are used to characterize the multilayered substrate. Then, an integral equation is set up for the whole set of metallic elements. This equation is solved with an iterative / FFT technique which reduces considerably the length of computations. Subsectionnal basis functions are employed to discretize the electric current, thus yielding great flexiblility to the possible shapes of metallic elements. As an example, the figure below shows our results for a typical two-layer FFS described by Shuley in the above referenced paper.

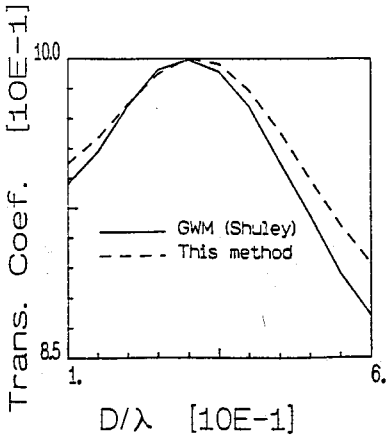

DYADIC GREEN'S FUNCTIONS FOR A BIAXIALLY ANISOTROPIC MEDIUM; II. TWO-LAYER CASE

Saba Mudaliar* and Jay K. Lee
Department of Electrical & Computer Engineering
Syracuse University
Syracuse, New York 13244-1240

This is a sequel to our earlier paper (Part I: S. Mudaliar and J. K. Lee, IEEE AP-S/URSI Symposium Digest, p. 84, May 7-11, 1990) where the dyadic Green's function (DGF) for an unbounded biaxially anisotropic medium is obtained. The geometry of our problem here consists of a planar layer of the anisotropic medium (Region 1) bounded by two isotropic media above and below (Region 0 and Region 2). An electric source is located in Region 0 above the anisotropic layer. Our objective is to find the dyadic Green's functions, $\bar{\bar{G}}_{00}$, $\bar{\bar{G}}_{10}$ and $\bar{\bar{G}}_{20}$, where the first subscript denotes the region of the field point and the second denotes the region containing the source.

Based on the result of Part I, the DGF's for the two-layer problem is formulated. The coefficients of the DGF's need to be evaluated by using the appropriate boundary conditions. The procedure of directly solving the above boundary value problem is not only tedious but also leads to very complicated results. We, therefore, follow an alternative matrix method and express the coefficients of the DGF's in terms of half-space Fresnel coefficients. Next we evaluate the various Fresnel reflection and transmission coefficients and express them in a very compact form. Using computed data some characteristics of the Fresnel coefficients are examined. Finally our DGF's are compared with those of a corresponding uniaxial problem.

TRANSIENT RESPONSE OF CHIRAL MATERIALS

Paul G. Zablocky and Nader Engheta*
Moore School of Electrical Engineering
University of Pennsylvania
Philadelphia, Pennsylvania 19104

It is known that, in the frequency regime, chiral materials can be described by the constitutive relations $\mathbf{D} = \varepsilon_c(\omega)\,\mathbf{E} + i\xi_c(\omega)\,\mathbf{B}$ and $\mathbf{H} = \mathbf{B}/\mu_c(\omega) + i\xi_c(\omega)\mathbf{E}$ where the time-harmonic $\exp(-i\omega t)$ is considered. Most of the work done in the area of electromagnetic wave interaction with chiral media has been concentrated on the time-harmonic monochromatic cases. However, for certain applications of chiral materials, it is essential to study the transient behavior of such media when they are exposed to transient pulse excitations. The motivation behind this study is the potential applications of chiral materials to radar cross-section control of chiral coated targets in an impulse radar environment, and to novel designs of antenna radomes.

In this talk, we present the analysis of transient response of isotropic homogeneous chiral materials. We study the behavior of transient radiation emitted from a localized source, such as a short dipole with a pulse excitation, in an unbounded chiral material. Since, in the frequency domain, chiral materials are expected to rotate the plane of polarization of a linearly polarized wave, it is of great interest to find out how this phenomenon is observed in the transient case. Figure 1 illustrates a sketch of transient co-polarized and cross-polarized signals radiated from a dipole excited by a pulsed current embedded in a homogeneous chiral material. In this talk, we discuss the evolution of pulses as they propagate in this medium, and show how chirality of the medium affects the generation of cross-polarized component in the time domain. The impulse response of a homogeneous chiral material is then obtained, and the role and physical significance of chirality parameter and its dispersion on such a response is discussed. Applications of the present study in the design of broadband radomes made of chiral materials are also addressed.

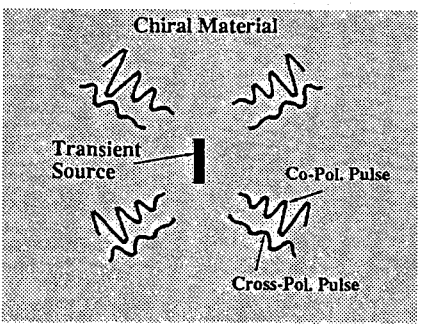

Fig. 1. Sketch of transient signals, both co-polarized and cross-polarized components, radiated from a dipole excited with a pulsed current in a chiral material.

NOVEL DESIGNS FOR RECIPROCAL PHASE SHIFTERS USING PSEUDOCHIRAL OR Ω MEDIUM

Mamdouh Saadoun and Nader Engheta*
Moore School of Electrical Engineering
University of Pennsylvania
Philadelphia, Pennsylvania 19104

Here we introduce the idea of novel designs for reciprocal phase shifters using a new type of synthetic material which we have named coupling or Ω medium. The microstructures of such an artificial dielectric have the shape of Ω, and they can be embedded in an isotropic host material. Figure 1a presents a collection of these Ω-shaped microstructures lying in the x-y plane all parallel with the y axis. Here it is assumed that the dimensions of these microstructures are much smaller than the wavelength. The constitutive relations describing this particular example of coupling medium are $\mathbf{D} = \underline{\underline{\varepsilon}} \cdot \mathbf{E} + \underline{\underline{\Omega}}_{em} \cdot \mathbf{B}$ and $\mathbf{H} = \underline{\underline{\mu}}^{-1} \cdot \mathbf{B} + \underline{\underline{\Omega}}_{me} \cdot \mathbf{E}$ where $\underline{\underline{\varepsilon}}$, $\underline{\underline{\mu}}$, $\underline{\underline{\Omega}}_{em}$, and $\underline{\underline{\Omega}}_{me}$ have the following forms: $\underline{\underline{\varepsilon}} = \varepsilon_{xx}\,\hat{x}\hat{x} + \varepsilon_{yy}\,\hat{y}\hat{y} + \varepsilon_{zz}\,\hat{z}\hat{z}$, $\underline{\underline{\mu}} = \mu_{xx}\,\hat{x}\hat{x} + \mu_{yy}\,\hat{y}\hat{y} + \mu_{zz}\,\hat{z}\hat{z}$, $\underline{\underline{\Omega}}_{em} = i\,\Omega_c\,\hat{y}\hat{z}$, and $\underline{\underline{\Omega}}_{me} = i\,\Omega_c\,\hat{z}\hat{y}$. Here the parameter Ω_c is the coupling coefficient and takes into account the coupling between electric and magnetic fields along the y and z axes, respectively. Due to the similarity in the shape of microstructures of this medium and that of the isotropic chiral medium, we can also name this material pseudochiral materials although they are not strictly chiral.

Figure 1b presents a rectangular waveguide filled partially with a slab of the material described by the above constitutive relations. In this talk, we discuss the the propagation characteristics of guided modes within this structures, and present the dispersion relations and Brillouin diagrams for this waveguide. Furthermore physical insights and interpretation for the results are provided, and the role of cross coupling terms is discussed. It is shown that this device can operate as a reciprocal phase shifter, and that the phase shift is a linear function of coupling coefficient Ω_c. Since the seeding microstructures of these media can be made planar, fabrication of these composite materials can be achieved using several techniques such as photolithography and micromechanic technology. Potential applications of these reciprocal phase shifters and other novel elements which can be designed using this new composite in microwave and millimeter-wave systems are also addressed.

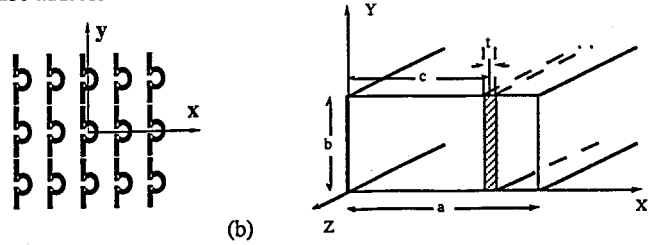

Fig. 1. (a) Anisotropic Ω medium with Ω-shaped microstructures, and (b) a reciprocal phase shifter made of Ω medium.

GREEN FUNCTIONS FOR BI-ISOTROPIC (NONRECIPROCAL CHIRAL) MEDIA

I.V. Lindell, A.J. Viitanen
Electromagnetics Laboratory
Helsinki University of Technology
Otakaari 5A, Espoo SF-02150 FINLAND

Chiral media have raised interest in recent years because of their extra parameter over the isotropic medium, allowing more freedom in the design of man-made materials for electromagnetic purposes. In fact, a whole new culture of research has arisen in just a few years upon this fact with applications emerging in antennas, wave-guiding structures and reflectionless surfaces. The chiral medium considered so far has been a reciprocal special case within the class of more general bi-isotropic media, which includes both reciprocal and nonreciprocal chiral as well as nonchiral media with general scalar medium parameters. The constitutive equations can be written in the form

$$\mathbf{D} = \epsilon\mathbf{E} + (\chi - j\kappa)\sqrt{\mu_o\epsilon_o}\mathbf{H},$$

$$\mathbf{B} = \mu\mathbf{H} + (\chi + j\kappa)\sqrt{\mu_o\epsilon_o}\mathbf{E}.$$

where all medium parameters are real for lossless media. Compared to the reciprocal chiral case, the general bi-isotropic medium contains one more parameter χ (the Tellegen parameter) to work upon, which makes it worthwile to make analytical studies although such a medium may not yet have been artificially produced. For example, nonreciprocity can be applied to produce surfaces which give totally cross-polarized reflection for linearly polarized incoming waves, an effect which cannot be produced by lossless reciprocal chiral media alone.

In the present paper, the basic Green dyadic problem is solved for the general bi-isotropic medium, based on a factorization of the dyadic Helmholtz operator. It is seen that the Green dyadic for the general bi-isotropic medium is just a little more complicated than for the reciprocal chiral medium. In addition to making nonreciprocal devices possible, the added χ parameter is seen to enhance the effect of the chirality parameter κ so that smaller values of κ are needed for the same chiral effect.

The Chiral Dällenbach Absorber

J.H. Cloete* and A.G. Smith
Department of Electrical and Electronic Engineering
University of Stellenbosch
7600 South Africa

Jaggard and Engheta (*Electronics Letters*, 25, 3, pp. 173-174, 1989 & *URSI Symposium Digest*, Dallas, p.137, 1990) have proposed the use of artificial chirality in microwave absorbing materials. To this end we considered uniform plane wave reflection by a chiral Dällenbach layer of thickness d. In other words, a lossy homogeneous chiral slab with a perfect conductor on one side, and a lossless homogeneous achiral medium, typically free space, on the other. For normal incidence we derived the following equation for the specular reflection coefficient referred to the chiral-achiral interface:

$$\rho = \frac{Z_c - \eta_a}{Z_c + \eta_a}, \tag{1}$$

with

$$Z_c = -i\eta_c tan((k_r + k_l)d/2). \tag{2}$$

The notation is similar to that of Jaggard and Engetha. Thus $\eta_c = \eta/\sqrt{1+(\xi\eta)^2}$ is the intrinsic wave impedance of the chiral medium, with $\eta \stackrel{\text{def}}{=} \sqrt{\mu/\epsilon}$, ξ the complex chirality admittance, μ the complex permeability and ϵ the complex permittivity. $k_r = +\omega\mu\xi + \sqrt{k^2 + (\omega\mu\xi)^2}$ and $k_l = -\omega\mu\xi + \sqrt{k^2 + (\omega\mu\xi)^2}$ are the wavenumbers of the right-hand and left-hand circularly polarized plane wave eigenmodes, with $k \stackrel{\text{def}}{=} \omega\sqrt{\mu\epsilon}$. The lossless achiral medium has intrinsic wave impedance $\eta_a = \sqrt{\mu_a/\epsilon_a}$ and wave number $k_a = \omega\sqrt{\mu_a\epsilon_a}$, with μ_a and ϵ_a assumed to be real, i.e. no losses. The harmonic time convention is $e^{-i\omega t}$.

Clearly eqns. (1) and (2) simplify to the well known expression for the achiral Dällenbach layer if $\xi = 0$. For electromagnetically thick lossy layers they yield, in the limit, the expression given by Jaggard and Engetha for a semi-infinite chiral slab. The condition for total absorption is $Z_c = \eta_a$. Fernandez and Valenzuela (*Electronics Letters*, 21, 1, 20-21, 1985) have solved the *achiral* Dällenbach layer problem, subject to this condition.

We have used eqns. (1) and (2) to study the effect of chirality on the absorptive properties of the Dällenbach layer. Our particular interest has been to find out if chirality can be beneficial in the sense of providing increased bandwidth, or reduced layer thickness. Results will be presented at the Symposium.

SURFACE WAVE IN CHIRAL MEDIA

V.E.Grikurov
Mathematical Inst.AS, Leningrad Branch, USSR

The goal of given paper is to demonstrate the theoretical possibility for the existence of waves concentrated in the vicinity of the interface of two contacting chiral media, alike well known Stonely and Raleigh waves in elasticity theory.

Let constitutive equations for chirality be of Born's form $\mathbf{D} = \varepsilon(\mathbf{E} + \beta \mathrm{rot}\mathbf{E})$, $\mathbf{B} = \mu(\mathbf{H} + \beta \mathrm{rot}\mathbf{H})$ and two chiral media (further denoted by subscripts 1 and 2) are separated by plane $z = 0$; time-harmonic ($\exp\{-i\omega t\}$) dependence is assumed. Maxwell equations used in conjunction with the constitutive equations allow separately in each half-space the solutions of non-uniform plane wave type, i.e. $\mathbf{E}_j = \mathbf{e}_j^0 \exp\{i\zeta x - \lambda_j(\zeta)|z|\}$ and the same for H field, with $\lambda_j(\zeta) = \lambda_j^{\pm} \equiv [\zeta^2 - (\gamma_j^{\pm})^2]^{1/2}$, $j=1,2$, where $\gamma_j^{\pm} = k_j/(1 \pm k_j\beta_j)$ are wave numbers of left and right circularly polarized plane waves. This wave hasn't any special polarization and its wave number ζ must be a solution of certain dispersive relation to satisfy the standard boundary conditions. For $\mu_1=\mu_2=1$ this dispersion relation may be written in the following form

$$(\sqrt{\varepsilon_1}A_1^- + \sqrt{\varepsilon_2}A_2^-)\,(B_1^+ + B_2^+) = (A_1^+ + A_2^+)\,(\sqrt{\varepsilon_1}B_1^- + \sqrt{\varepsilon_2}B_2^-), \quad (1)$$

where

$$A_j^{\pm}(\zeta) = \gamma_j^+/\lambda_j^- \pm \gamma_j^-/\lambda_j^+,$$

$$B_j^{\pm}(\zeta) = \sqrt{\varepsilon_j}\,[(1-2k_j\beta_j)\gamma_j^+/\lambda_j^- \mp (1+2k_j\beta_j)\gamma_j^-/\lambda_j^+].$$

The propagating surface wave exists provided equation (1) has real roots, and such a wave must be slower then any of LCP or RCP waves. Critical value of $\zeta = \max(\gamma_{1,2}^{\pm})$ being combine with equation (1) yields the critical relation for parameters of problem (for example, for frequency or chirality measure provided other parameters being fixed). No combinations of allowed values of parameters have been found out by numerical experiments to observe more then one real root of this equation.

Asymptotic generalization for non-uniform chiral media separated by weakly curved interface is also possible.

NONSTATIONARY WAVE PROBLEMS FOR A LAYERED MEDIA

A.G.Bugrov, M.A.Guzev, V.I.Klyatskin
Wave processes Lab., Pacific Oceanological Institute, Far Eastern Branch USSR Academy of Sciences, 7 Radio Str., Vladivostok, 690032, USSR.

In this paper some problems associated with the wave propagation in inhomogeneous media are considered in the time domain on the basis of imbedding method.

We considered the propagation of a wave pulse in a slab of inhomogeneous medium such as linear regular medium, nonlinear regular medium and linear random medium.

In the problem with linear regular medium we found that the wave front amplitude depends on the local values of a wave propagation speed only. Then we constructed the procedure for solving the inverse scattering problem using a single imbedding equation for the back-scattered field on a slab boundary. We found also two exact analytical solutions of this problem (for the linear and exponential time dependences of back-scattered field).

We investigated the wave front propagation in a nonlinear medium. For the wave inside the medium and the wave front amplitude the imbedding equation were obtained. We shown that in the simplest case of a wave selfaction the wave front amplitude depends on the impedance locally.

In a stochastic linear problem we obtained an expression for the average intensity of the wave field in inhomogeneous half-space and in a finite thickness slab. It is shown that the wave field jumps on the slab boundaries aren't essential in forming the wave field statistics. The accumulating effects are determinated, in particular, by the wave scattering on a random inhomogenities.

Signal Processing in Communications | **Room 3010 Salle URSI C Session 9** | **Traitement des signaux en télécommunications**

Chairs/présidents: P.H. WITTKE, Canada

08:30 (9.1) The Performance of Trellis Coded Noncoherent FSK in Noise and Jamming, **P.H. WITTKE**[1], M.J. SCHEFTER[1], Y.M. LAM[2], [1] *Queen's University, Kingston, ON, Canada;* [2] *Hong Kong Polytechnic, Hong Kong*

08:50 (9.2) Routing Algorithms for Frequency-Hopping Spread Spectrum Packet Radio Networks, **C.A. POMALAZA-RÁEZ**, *Purdue University, Fort Wayne, IN, USA*

09:10 (9.3) All-Digital Bit Synchronizers for Communication Systems, **C.A. POMALAZA-RÁEZ**, S. MAYNARD, *Purdue University, Fort Wayne, IN, USA*

09:30 (9.4) Non Linear Performance of Third Order PLL's, **J.M. RIERA**, L. MERCADER, *Universidad Politécnica de Madrid, Spain*

09:50 (9.5) New Interpolation Technique for Noisy Spectral Data, S.-F.D. LIN, **N.H. YOUNAN**, C.D. TAYLOR, *Mississippi State University, Mississippi State, MS, USA*

10:10 **COFFEE/CAFÉ**

10:30 (9.6) Super High Resolution of Intermodulation Products in a Nonlinear Environment, **A.K. GUPTA**, *SIGCOM Research, Westboro, MA, USA*

10:50 (9.7) On a Multibeam Antenna System as an Optimal Receiver, **A.K. GUPTA**, *SIGCOM Research, Westboro, MA, USA*

11:10 (9.8) A Digital Beacon Receiver for Propagation Measurements with the ACTS Program, **P. GENDRON**, W. SYLVESTER, J. McKEEMAN, *Virginia Polytechnic Institute and State University, Blacksburg, VA, USA*

11:30 (9.9) Design and Construction of a Data Acquisition System for the Olympus Propagation Experiments at Virginia Tech, **P.W. REMAKLUS**, J.C. McKEEMAN, *Virginia Polytechnic Institute and State University, Blacksburg, VA, USA*

11:50 (9.10) An Enhanced Predictive Multipulse LPC Speech Coder at 2.4 Kbits/s, **Y. QIAN**[1,2], B. JIANG[1], Q. ZHU[1], P. KABAL[2], [1] *Tsinghua University, Beijing, China;* [2] *Université du Québec, Verdun, PQ, Canada*

THE PERFORMANCE OF TRELLIS CODED NONCOHERENT FSK IN NOISE AND JAMMING

Paul H. Wittke*, Michael J. Schefter,
Dept. of Electrical Engineering, Queen's University,
Kingston, Canada
and Y.M. Lam
Hong Kong Polytechnic, Hong Kong

Abstract- The performance of trellis-coded FSK modulation with noncoherent detection is presented, as applicable to a frequency-hopped spread spectrum communication system or a conventional FSK system. Nonorthogonal tone spacing is considered as a parameter to control bandwidth expansion of the coded hopped signal and to allow an increased number of users. Soft decision decoding with a maximum metric decoder is employed. The metrics considered are the energy metric with and without ideal jammer state information as well as a self-normalizing metric that compensates for jamming or interference.

Performance analysis of the system under full and partial band noise jamming as well as multitone jamming is presented. For nonorthogonal tone spacing, the signals are correlated, and so new Chernoff bounds on the pairwise error probability for energy detectors with correlated signals are derived. Then the union Chernoff bound on bit error probability is evaluated using the transfer function bounding technique and the method of Zehavi and Wolf. To assess the tightness of the bounds, simulations have been carried out. The theoretical bounds in most cases are within 1 to 3 dB of the simulated results.

System performance is evaluated for 2, 4 and 8-state trellis codes with tone spacings of 1/3T, 1/2T, 2/3T and 1/T Hz. The use of a reduced tone spacing brings little degradation in error performance, but allows an increased number of tones and hence trellis coding without expansion of the hopped band. Jammer side information improves performance substantially. For the codes under study, improvements of 30 dB over the uncoded system can be realized. Much of this improvement can be realized with a practical self-normalized metric.

ROUTING ALGORITHMS FOR FREQUENCY-HOPPING SPREAD SPECTRUM PACKET RADIO NETWORKS

CARLOS A. POMALAZA-RÁEZ(*)
Department of Engineering, Purdue University
Fort Wayne, Indiana 46805, USA

This paper describes research in adaptive descentralized routing algorithms for frequency-hopping spread spectrum radio networks. Until recently routing algorithms adopted for this type of networks have been simple extensions of well known and tested algorithms such as the one used in the ARPA network. These algorithms do not however take into account the special nature of radio networks. The networks studied in this paper are multihop systems where a radio can not transmit directly to all of the other radios in the network, long messages are broken down into shorter "packets" of limited length and these packages are routed (switched) through the network over one or more links (hops) to their destination. The network topology is dynamic, i.e., the radio nodes are mobile, and the communication protocols designed must provide reliable and survivable communication links. Frequency-hopping (FH) spread spectrum provides multiple-access capabilities and anti-jam communications. All of these features should be taken into consideration when designing the routing algorithms.

To help in the design and analysis of the algorithms a detailed simulation model has been developed. FH signal capture characteristics, dynamic topology, node and link failure, etc. have been implemented. Several adaptive routing strategies are investigated for different conditions such as variable packet length, and variable rate of topology change.

Simulation results shows that the amount, type and frequency of information exchanged by the nodes to update their topology related databases (distance tables, routing tables, etc.) is very critical. Careful design of the nature of this information plus adaptive strategies are of paramount importance for keeping the protocol and transmission overhead within practical values. As a conclusion the paper offers guidelines for the design of efficient routing protocols taking into account packet radio network characteristics.

C9.3

ALL-DIGITAL BIT SYNCHRONIZERS FOR COMMUNICATION SYSTEMS

CARLOS A. POMALAZA-RÁEZ (*) AND SCOTT MAYNARD
Department of Engineering, Purdue University
Fort Wayne, IN 46805

Bit synchronization is traditionally accomplished using analog implementations of well known systems such as the Data-Transition Tracking Loop (DTTL), the Early-Late Gate Loop (ELGL) and nonlinear synchronizers. All-digital implementations of these and other similar systems can take advantage of processing speeds and memory densities available with current technology. Unlike analog implementations the digital loops do not have to be causal, i.e. only past and present data are used to estimate the bit timing. It is then reasonable to expect an improved estimation by using a noncausal system.

All-digital implementations of bit synchronizers such as the DTTL are proposed and investigated in this work. Both, statistical analysis and computer simulation methods are used to obtain loop characteristics such as bit error rate and bit slippage. The method of analysis is reduction of the loops to Markov chain models. The analytical results are in very close agreement with computer simulation results which are used to validate the method of analysis. All-digital implementations of the DTTL and a zero-crossing bit synchronization loop are studied in detail. The use of sequential filters for improved loop performance is also proposed and investigated.

Finally, tree search algorithms, in particular the (M,L) algorithm (J.B. Anderson and S. Mohan, IEEE Trans. Commun, vol 32, February 1984), are proposed as a way to take further advantage of the digital nature of the systems and increase the performance. This implementation can be useful in situations in which the bit duration of the received signal is varying. This variation can take place when relative motion exists between the receiver and the transmitter. In these situations, such as in deep space communications, doppler components are superimposed on the fundamental frequency of the carrier and on the baseband process. For these systems, conventional tracking and synchronization loops will not work efficiently and tree search algorithms offer a viable alternative. Numerical results give evidence of this improved performance.

NON LINEAR PERFORMANCE OF THIRD ORDER PLL'S

Jose M. Riera(*), Luis Mercader
Dpto. SSR, ETSI Telecomunicacion,28040 MADRID(Spain)

Linear analysis and characterization of third order Phase Locked Loops have been presented in a previous meeting (Riera&Mercader, URSI Nat.Meet., Boulder CO, 1990). Its performance is better than the second order one in several aspects, including its well-known ability to track a frequency ramp, and both are very similar in other aspects. It seems that the only trade-off is the increased complexity of third order design to guarantee stability.Rules for achieving unconditional stability were presented.

In this paper we present the results of a research about the non linear aspects of their performance. Third order loops are classified according to their linear characterization and parameters, and non linear analysis is then carried out to investigate its performance out of the linear range. Comparison with the well-known second order loop is always presented.

Pull-In Time and Range have been described (Russo & Verrazzani, IEEE Trans. AES-12, p.213-218, Mar.1976), for Third Order Type III loops. Richman quasistationary approach was used. We present an extension of this method to obtain results for third order type I and type II loops.

The application of third order loops for synchronization purposes in mobile systems was suggested in the first mentioned reference. The loop performance in the presence of cochannel interference must be considered. We present some results about its performance with CW interferences, comparing with the performance of second order loops with equal bandwidth.

Empirical phase distribution functions in the presence of noise are presented and related to the exact results of first order loops. The theoretical analysis of this problem requires the solution of a three-dimension vectorial non-linear and non-homogeneous differential equation. Approximation of the empirical results with the ones of first order loops is possible, and more practical for design purposes.

The performance of third order loops is understood better with the results presented in this paper. A more general approach has been preferred, even if it implies that each point can not be considered in depth. Overall performance and usefull design keys have been considered more important.

C9.5

NEW INTERPOLATION TECHNIQUE FOR NOISY SPECTRAL DATA

by

Shin-feng David Lin
Nicholas H. Younan
Clayborne D. Taylor

Department of Electrical and Computer Engineering
Mississippi State University
Mississippi State, MS 39762

Interpolation is to model the function, in between the known data points, by some plausible function form. It is therefore related to function approximation. There are some difficulties in interpolation techniques on noisy spectral data. Ideally, interpolation presumes some degree of smoothness for the function interpolated. However, this is not always the case for noisy data.

Traditional interpolation techniques such as linear interpolation, cubic spline interpolation, and Lagrange interpolation have been shown to be dependent on data type and are generally not satisfactory. Accordingly, a new interpolation technique, based on rational function interpolation that has yielded promising results, has been developed.

Owing to the measurement errors, typical data never exactly fit the model that is being used. Thus, it is necessary to have the means to assess if the model is appropriate. A fitting procedure should provide (1) an estimate of the model coefficients (2) a statistical measure of goodness-of-fit. The appropriate coefficients can be determined by three major steps: (a) setting up the simultaneous equations by least square-error method. (b) solving for the model coefficients via the singular value decomposition technique. (c) eliminating the noise-dominated coefficients by a relative magnitude test. Then, the consistency of two distributions, the original and the interpolated, is concerned. In order to show that two distributions are consistent, it is a good approach to check their means and variances. Student's t-test for consistent means and F-test for consistent variances have been used to check for consistency.

The new technique has self-tuning ability to obtain an estimate of the model order and coefficients. Results for simulated data with low signal-to-noise ratios, as low as 3 dB, are illustrated to ascertain the validity of the technique.

SUPER HIGH RESOLUTION OF INTERMODULATION PRODUCTS IN A NONLINEAR ENVIRONMENT

Ashok K Gupta
SIGCOM Research
10 Wheeler Rd.
Westboro,MA 01581

In this paper,modern space-time-frequency domain multichannel detection theory techniques(A.K. Gupta,IEEE A&P Int. Symp. and National Radio Science Mtg.,Syracuse,NY 1988) are applied to show the feasibility of resolving intermodulation products at the output of a nonlinear system, such as zero-memory nonlinear devices(ZNLD). Such situations commonly arise in areas such as communications,radar and somar(A.K. Gupta,National Radio Science Mtg,Boulder,CC.,1988 and 1990). For simplicity,two tone transmission thru a hard-limiter is considered such that the hard-limited output,for small input signal-to-noise + interference ratio and for input A $\exp(j\theta)$+ B $\exp(j\phi)$ is $\exp(j\phi)+ a_1 \exp(j\theta) - a_2 \exp(j(2\phi - \theta))$ at frequency w_0. For arbitrary signal-to-interference ratio,there may be more than three phasors(A.K. Gupta,Proc. of 1984 IEEE Globe-COM Conf.;A.K. Gupta et al., Electronics letters,vol. 18,NO. 21,1982).

The problem,therefore,consists of phasors rather than the resolution in currently utilized space-time-frequency domain (A.K. Gupta,NOVEL SUPER HIGH RESOLUTION IN SPATIAL DETECTION,GE Syracuse Research Report,March 1990). In this paper,phase-domain filtering techniques are proposed to resolve the phase ϕ, θ, $2\phi - \theta$, either fixed or adaptively, similiar to the author-proposed filters in time-frequency-space domain (A.K. Gupta,Proc. of IEEE Southeastern Symposium on System Theory,Charlottsville,NC,March 1988, A.K. Gupta et al., IEEE Trans. on ASSP,April 1986 and references therein) utilizing multichannel detection theory and author-proposed estimator-subtractor configuration.

Based upon the proposed phase-domain filtering techniques,we also show that a currently used multibeam antenna system is an optimal receiver only under the assumption of a known signal in colored noise(such as clutter,reverberation,interference). Currently used linear prediction filter models of colored noise are also generalized by this author proposed whitening filters (A.K. Gupta, IEEE Trans. on ASSP,April 1986 and references therein).

C9.7

ON A MULTIBEAM ANTENNA SYSTEM AS AN OPTIMAL RECEIVER

Ashok K Gupta
SIGCOM Research
10 Wheeler Rd.
Westboro,MA 01581

In this paper,modern multichannel detection theory principles are applied to show that a currently used multibeam antenna system in a radar, sonar and communication is an optimal receiver under the assumption of a known signal detection in colored noise. Therefore,the receiver will be suboptimum for detecting a vector Gaussian or random signal in vector colored noise,similiar to a linear phased-array receiver system(A.K. Gupta,IEEE Int. A&P Symp. and National Radio Science Mtg.,Syracuse,NY 1988;A.K. Gupta,IEEE Southeastern Symp. on System theory,Charlottsville,NC, March 1988).

For binary hypothesis,the received signal $r_i(t)=s_i(t)+n_i(t)$;and = $n_i(t)$;H_0,i=1,--,M; $T_i \leq t \leq T_f$,one can obtain the optimal receiver equation $\int_{T_1} S(t)\,dt \gtrless \gamma$.This equation can be modified for a multibeam antenna system as

$$\int R_i^T(t)\ D\ p(t) \gtrless \gamma,$$

where $R_i^T(t)=(r_i',i=1,--,M)$ is the interference-free vector received signal. Vector interference estimation is different for different signal and noise characteristics.In the author proposed estimator-subtractor configuration, for known signal case,the interference is estimated,assuming no signal present. For Gaussian signal case,the interference estimator includes the signal and noise statistics,such as in causal and noncausal Wiener and Kalman filtering under Gaussianity.S(t) can be defined as S(t)=D p(t). D and p(t) are defined similiar to in W.F. Gabriel,IEEE Trans. on A&P,vol. 17,No. 1,Jan. 1989,PP. 16 -29). By the proposed optimal equation,number of beam structures can be obtained by redefining S(t).For example,S(t)=T D p(t),where T is a matrix, which includes shading or beam transformation.A paper is in preparation on this topic.

We now show,by an example,that the above equation is the optimal receiver equation for a multibeam antenna system.Performance analysis of the receiver can be obtained similiar to a linear phased array antenna system(A.K. Gupta,National Radio Science Mtg.,Boulder,Jan. 1988). Let's consider a 4 element array and 3 sources.The detector equation can be written as

$$\left(\sum_{i=1}^{3} p_i(t) \sum_{k=1}^{4} r_k'(t)\, d_{ki}\right) dt \gtrless \gamma.$$

Since $r_k'(t)=r_k(t)-$ estimate of the correlated interference,one can write the above equation in terms of $r_k(t)$. Note that for each source i,there is a corresponding beam $\sum r_k'(t)\, d_{ki}$. d_{ki} are the weights applied to each received signal $r_k(t)$. If the number of sources are unknown,one has to span the space by predetermined number of beams,possibly orthogonal beams.A method of generating super high resolution orthogonal and spatially flexible beam is recently proposed by this author (A.K. Gupta, Novel Super High Resolution Multibeam antenna System,GE Syracuse Research Report,March 1990). This super high resolution system is applicable in new models of clutter and reverberation.The proposed new models,by this author consists of causal and noncausal optimal pole-zero filters(similiar to Wiener filtering,A.K. Gupta,IEEE Trans. on ASSP,April 1986 and references therein).

A DIGITAL BEACON RECEIVER FOR PROPAGATION MEASUREMENTS WITH THE ACTS PROGRAM

P. Gendron*, W. Sylvester and J. McKeeman

Computer Applications Research Laboratory
Bradley Department of Electrical Engineering
Virginia Polytechnic Institute and State University
Blacksburg, VA 24061
(703) 231-4141

The impending launch of NASA's ACTS satellite offers new opportunities to study propagation statistics at Ka band. To accurately gather propagation statistics at Ka band will require measurement equipment with greater sensitivity and dynamic range than those currently available. These requirements have led to the design of several specialized beacon receivers including the digital receiver discussed in this paper.

The receiver design incorporates digital signal processing techniques and exploits VLSI technology to achieve high performance and stability. Further, this design digitizes the incoming beacon signal at a greater RF than existing receiver designs. This allows the receiver to capitalize on the advantages of digital signal processing and decreases the dependence on analog components. The intent of this design is to provide a low cost, high resolution digital receiver to acquire and track the ACTS propagation beacons.

This receiver focuses on the reception of the ACTS 20 and 27 GHz beacons. Downconversion and subsequent IF stages are used to lower the beacon frequency to 10 MHz. The beacon signal is then sampled and quantized with a 12 bit analog to digital convertor. The digitized signal is then decimated, filtered and Fast Fourier Transformed (FFT). Successive FFT stages are then used to locate the carrier to within 0.23 Hz. The carrier is tracked in software using a simple filter and the power of the beacon is derived from the power spectral density of the carrier. The outputs of the receiver include the center frequency and power of the beacon.

DESIGN AND CONSTRUCTION OF A DATA ACQUISITION SYSTEM FOR THE OLYMPUS PROPAGATION EXPERIMENTS AT VIRGINIA TECH

*P.W. Remaklus and J.C. McKeeman
Computer Applications Research Laboratory
Bradley Department of Electrical Engineering
Virginia Polytechnic University and State University
Blacksburg, VA 24061-0111

Virginia Tech has designed and constructed a Data Acquisition System (DAS) for use during experiments with the OLYMPUS satellite. The DAS collects propagation, environmental and status information and automatically controls periodic calibrations. Data collection has been continuous since the DAS was brought online August 7, 1990.

OLYMPUS is a European Space Agency three-axis stabilized experimental satellite. Of the four payloads carried by OLYMPUS, the 12/20/30 GHz propagation package aids research in the higher frequency ranges. The three beacons provided by the propagation package have the property of being coherent by virtue of a common frequency source. This coherency is extremely valuable for researching the 20 GHz and 30 GHz frequency bands during periods of heavy rain.

Virginia Tech is presently collecting propagation data from colocated 12 GHz, 20 GHz and 30 GHz terminals and a 20 GHz diversity terminal located 50m from the others. Associated with each terminal is a beacon receiver and a total power radiometer. Weather conditions are monitored by recording outside air temperature, barometric pressure, wind speed, wind direction and humidity. Additionally, digital signals such as rain gauge trips and PLO lock alarms are collected.

The DAS consists of two units: a rack mounted portion and an IBM PS/2 Model 60. The interface between these units is a parallel data link connected to a custom interface card located in the PS/2. Information transfer over this link is packetized and the accuracy of the data is verified through the use of checksums. Data collection is initiated by starting a background task on the PS/2. This task first sends the current time and date to the DAS and then saves data records received from the DAS on the PS/2s hard disk. Timestamps integral to each record allow the background task to store the collected data in one hour long files. Once a day the accumulated data is archived to tape without the need to interrupt data collection.

The standalone portion of the DAS is an Intel 80286 based microprocessor which utilizes an STDBUS form factor interface bus. The control microprocessor, bus interface circuitry and interface to the PS/2 occupies two cards. Additional cards include: two I and Q detectors, digital input, digital output, analog input and radiometer interface. The I and Q detectors are dual channel 80286 based units which accept a 10 KHz IF signal and a 40 KHz sample clock from the beacon receivers. The 10 KHz signal is detected and lowpass filtered to 3 Hz. Sample points for obtaining in-phase and quadrature samples are derived from the sample clock. One thousand I/Q pairs are sampled each second and every 0.1 second an 1116 point FIR filter is applied to the most recent data. The resulting output is the observed beacon signal strength in a 3 Hz window. The digital input card interfaces to rain gauges, alarms, and various status signals. The digital output card allows automated calibration by controlling noise diodes, waveguide switches and step attenuators. Temperature controlled RF cabinets, outside temperature, barometric pressure, humidity, wind speed and wind direction are measured via the analog input card. Finally, the radiometer input card counts the number of pulses output by each radiometer's voltage to frequency converter during the last second.

An Enhanced Predictive Multipulse LPC Speech Coder at 2.4 kbits/s

*Qian Yasheng[1,2] Jiang Baocheng, Zhu Qinglin[1] Peter Kabal[2]
[1]Department of Radio-Electronics
Tsinghua University
Beijing, China
100084

[2]INRS-Telecommunications
Universite du Quebec
3 Place du Commerce
Verdun, Quebec
Canada H3E 1H6

A 2.4 kbits/s Predictve Multipulse LPC coder,which could produce better speech quality than conventional LPC-10 coder, has been proposed in the paper. A simple multipulse LPC coder can not operate with acceptable good speech quality below 6–8 kbits/s, because to transmit a minimial number of multipulses amplitudes and locations requires at least 6 kbits/s. The performance of MPLPC coder degrades rapidly below this lower bound. The quality of a CELP coder also dramatically deteriorates below 4.8 kbits/s, beccause of insufficient representation of pitch harmonics,when a Gaussian excitation codebook is used.The main features of the proposed Predictive Multipulse LPC coder are as follows: 1. Input speech frames each with 180 samples are first divided into subframes, referred to as prediction intervals. The locations and magnitudes of three multi pulses optimized by a closed-loop search in first subframe are transmitted. Multipulses in other subframes are interpolated by a linear time varying synthesis filter to trace the time-varying characteristics of the vocal tract for consecutive subframes in one frame. The first subframe length and the multipulses are jointly determined by minimizing the mean-square error (MSE) between the orignal and the synthesized speech. 2. Speech signals are classified into voicing/unvoicing categories by an analysis-by-synthesis(ABS) method. Based on a speech database, a SNR threshold has been found for the V/UV classification. A frame is defined as an unvoicing one,if the SNR is less than 1.05 dB. This novel algorithm for classification has improved SNR by about 3 dB during transition periods,compared to a pitch predictive MPLPC coder. 3. Vector quantization for LPC parameters of tree structure with branching factor of 32 is used to tailor the proposed algorithm to work at 2.4 kbits/s. The two-stage tree codebook has reduced computation load down to 1/16 with only slightly increased memory requirement. Cepstrum distance (CD) with average 2.91 dB and informal listening test of several phonetically balanced sentences have shown that the proposed algrithm of an enhanced Predictive MPLPC coder could obtain better quality than present LPC-10 vocoder.

Chiral Materials — Room 3010 Salle, URSI D Session 24 — **Matériaux chiraux**

Chairs/présidents: N. ENGHETA, USA; D.L. JAGGARD, USA

13:30 (24.1) Intrinsically Achiral Matter on the Rotating Earth: The Ultimate Challenge in Chiral Materials, **M.P. SILVERMAN**, *Trinity College, Hartford, CT, USA*

13:50 (24.2) Towards a Dictionary Between Chiral Languages: Rayleigh Mixing Formula as a Case Study, **A. SIHVOLA**, *Pennsylvania State University, University Park, PA, USA*

14:10 (24.3) Generalized Impedance/Resistive Boundary Conditions for a Planar Chiral Slab, **R.G. ROJAS**, L.M. CHOU, *Ohio State University, Columbus, OH, USA*

14:30 (24.4) Chiral Layers for RCS Control of Curved Surfaces: Spherical Case, **D.L. JAGGARD**, J.R. LIU, *University of Pennsylvania, Philadelphia, PA, USA*

14:50 (24.5) Edge Diffraction in Chiral Media and RCS Applications: Meixner Edge Condition and the Sommerfeld Half-Plane Problem in Chiral Media, **N. ENGHETA**, P. PELET, G. LI, *University of Pennsylvania, Philadelphia, PA, USA*

15:10 **COFFEE/CAFÉ**

15:30 (24.6) Theory and Applications of Chiral Multilayers, **D.L. JAGGARD**, X. SUN, *University of Pennsylvania, Philadelphia, PA, USA*

15:50 (24.7) Chiral Rectangular Directional Coupler, **K.S. CHAN**, P.L.E. USLENGHI, *University of Illinois, Chicago, IL, USA*

16:10 (24.8) Electromagnetic Properties of Finite-Length *Chirostrip* Antennas, P. PELET, **N. ENGHETA**, *University of Pennsylvania, Philadelphia, PA, USA*

16:30 (24.9) Microstrip Line on a Chiral Substrate, **M.S. KLUSKENS**, E.H. NEWMAN, *Ohio State University, Columbus, OH, USA*

D24.1

INTRINSICALLY ACHIRAL MATTER ON THE ROTATING EARTH: THE ULTIMATE CHALLENGE IN CHIRAL MATERIALS

M. P. SILVERMAN
Trinity College, Hartford, Connecticut 06106 U.S.A.

The structural unit of an intrinsically chiral material ordinarily lacks a center of symmetry and is consequently not superposable on its mirror image. Chirally asymmetric materials can interact asymmetrically with left and right circularly polarized light to manifest a variety of optical phenomena broadly classified as optical activity (e.g. optical rotation and circular dichroism). In the absence of weak nuclear interactions which give rise to small parity-violating effects, atoms have long been regarded as centro-symmetric electrodynamic systems forbidden by physical laws to manifest optical activity.

Recent studies [1] have shown that in a rotating, and hence noninertial, reference frame atoms can become circularly birefringent and display gyrotropic effects to a co-rotating observer. From the perspective of quantum mechanics the global rotation introduces into the quantum equations of motion (e.g. the Schroedinger equation) an energy term involving the coupling of the angular momentum of the bound electrons to the rotational angular velocity of the frame; this breaks the degeneracy of magnetic substates of atomic energy levels and gives rise to chirally asymmetric electronic polarizabilities. From the perspective of classical mechanics it is the differential effect of the Coriolis force on oppositely circulating electron orbits that leads to chirally asymmetric atomic polarizabilities. In both cases there results a circular birefringence linear in the frame rotation frequency that is maximum for light propagation along the axis of rotation.

The rotation of the Earth (7.3×10^{-5} rad/sec) can engender in atoms a difference in refractive indices for left and right circularly polarized light on the order of a few parts in 10^{18}. Although very weak, this circular birefringence falls within the theoretical measurement capability of large ring-laser interferometers now under development. A successful experiment, however, would need to discriminate against a number of competing effects that could either mask or mimic the sought-for rotationally-induced optical activity.

The Earth's rotation may already provide an undetected bias in the measurement of the hydrogen atom ground state hyperfine structure [2] (the 21-cm line) of importance to metrology and in tests of quantum electrodynamics.

[1] M. P. Silverman, "Effect of the Earth's Rotation on the Optical Properties of Atoms", Physics Letters A 146 (1990) 175-180

[2] M. P. Silverman, "Measurement of the Hydrogen Hyperfine Splitting as a Test of Quantum Mechanics in a Noninertial Reference Frame", Physics Letters A (1991) [To be published]

TOWARDS A DICTIONARY BETWEEN CHIRAL LANGUAGES: RAYLEIGH MIXING FORMULA AS A CASE STUDY

Ari Sihvola

The Pennsylvania State University
Department of Engineering Science and Mechanics
Center for the Engineering of Electronic and Acoustic Materials
University Park, Pennsylvania 16802, USA

In the present-day analysis of chiral media, three sets of constitutive relations are in common use. For reciprocal chiral media, three (complex) material parameters are needed to describe the chiroelectromagnetic behavior of the interaction of electric and magnetic fields with the medium. The different sets all employ permittivity and permeability, like nonchiral materials, too, but these differ in the manner how to express the chiral effect. Furthermore, the difference in this chiral parameter, a pseudoscalar, will lead to differences in the permittivity and permeability in different systems, which are, however, of the second order in the chiral effect.

In addition to comparison and translation of chiral parameters and electromagnetic quantities encountered in the research of chiral media, this presentation will foces on chiral mixtures. The Maxwell-Garnett mixing formula, derived recently for chiral/nonchiral mixtures with spherical and ellipsoidal geometries, will be shown to transform itself to the generalized Rayleigh form. This mixing rule, expressed in all three systems of chiral notation, express clearly the essential differences and characteristics of these constitutive relations.

GENERALIZED IMPEDANCE/RESISTIVE BOUNDARY CONDITIONS FOR A PLANAR CHIRAL SLAB

R.G. Rojas*, L.M. Chou
The Ohio State University ElectroScience Laboratory
Department of Electrical Engineering
Columbus, Ohio 43212

Generalized impedance boundary conditions (GIBC) are developed for a planar, homogeneous chiral slab in free space which is grounded by a perfect electric conducting plane. By taking advantage of some symmetry conditions, Generalized Resistive Boundary Conditions (GRBC) are also developed for a chiral slab without the presence of the ground plane. The procedure followed here is similar to that used in [Rojas, Al-hekail, Radio Science, Vol. 24, pp. 1-12, Jan.-Feb. 1989] for a dielectric slab. Note that the GIBC and GRBC developed here recover the **exact** Fresnel reflection and transmission coefficients.

In the analysis of the scattering of electromagnetic waves by a chiral slab or other related geometries, a planar surface which satisfies these boundary conditions can be used to replace the chiral scatterer and thus simplify the analysis because it is no longer necessary to calculate the fields inside the chiral material. These boundary conditions are specially useful in the study of high frequency diffraction by chiral objects with edges because they make possible the use of well known functional analytic techniques. To further simplify these mixed boundary value problems, the GIBC's and GRBC's can be expanded in a series accurate to $O(t^n)$ where t is the thickness of the slab. The number of terms that are kept depend on the thickness of the slab and the degree of accuracy that is expected.

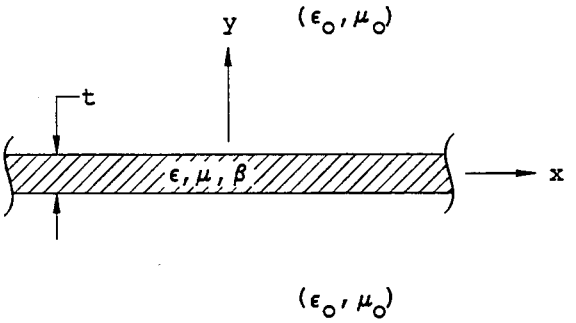

Planar chiral slab of thickness t

CHIRAL LAYERS FOR RCS CONTROL OF CURVED SURFACES: SPHERICAL CASE

D. L. Jaggard and J. R. Liu
Complex Media Laboratory
Moore School of Electrical Engineering
University of Pennsylvania
Philadelphia, PA 19104

Coatings placed on conducting or composite targets to significantly reduce reflected electromagnetic radiation over specified frequency regimes provide one of several methods of radar cross-section (RCS) management and control use . By incorporating electromagnetic chirality [D. L. Jaggard, A. R. Mickelson and C. H. Papas, "On Electromagnetic Waves in Chiral Media," *Appl. Phys. 18*, 211-216 (1979)], new screens and shields offer unique advantages, such as increased absorption in thin layers with broadband response, over their conventional counterparts. In the planar case, we have shown that chiral coatings can be used for RCS reduction through impedance matching at the front surface and increased absorption throughout the coating over a broad range of frequencies [D. L. Jaggard and N. Engheta, "*Chirosorb*™ as an Invisible Medium," *Electronics Lett. 25*, 173-174 (1989)]. Both mechanisms can be easily understood through the physical processes involving electromagnetic wave interactions with chiral structures. Here we study the canonical problem of scattering from a chiral coated conducting sphere illuminated by an electromagnetic plane wave as sketched in the figure below (left).

Chiral materials are represented by the constitutive relations, $\mathbf{D} = \varepsilon\mathbf{E} + i\xi_c\mathbf{B}$ and $\mathbf{H} = \mathbf{B}/\mu + i\xi_c\mathbf{E}$ where **D**, **E**, **B**, and **H** are the usual time-harmonic electromagnetic field vectors. In addition to the permittivity ε and the permeability μ, a quantity denoted the chirality admittance ξ_c has been introduced. The magnitude of ξ_c determines the strength of chirality and is responsible for the cross-coupling of electric and magnetic fields in the medium. Therefore, this parameter offers a new degree of freedom so that chirality can either be incorporated into existing materials for increased efficacy or it can be used in the design of new chiral composites.

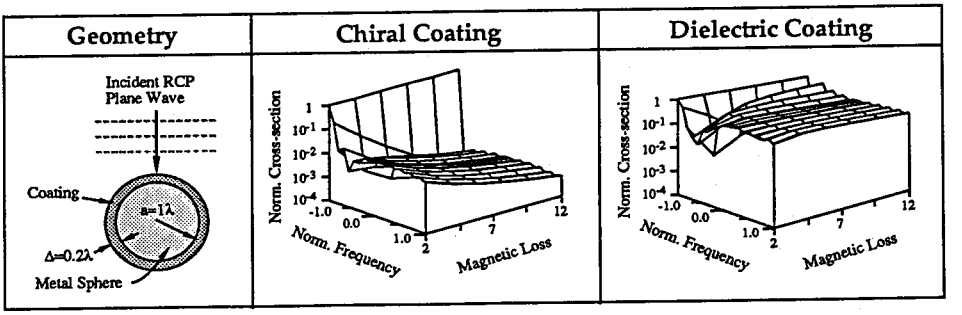

Figure. Normalized backscatter corss-section for a chiral-coated metallic sphere (middle) and its achiral counterpart (right) as a function of magnetic loss tangent and normalized frequency. Both plots are normalized to the uncoated case.

Using the planar results [D. L. Jaggard, N. Engheta and J. Liu, "*Chiroshield*™: The Salisbury/Dallenbach Shield Alternative," *Electronics Lett. 26*, 1332-1333 (1990)] as a guide, we examine several cases of reflection from conducting spheres with lossy chiral coatings and various sizes. The physical principles involved, the formulation using appropriate eigenmode expansions and the detailed results are investigated. We find that just as in the planar case, thin chiral coatings offer advantages over their achiral counterparts for specified values of chirality admittance for curved surfaces. For cases examined here, some ~20 to ~30 dB additional reduction in RCS can be achieved through the use of electromagnetic chirality.

EDGE DIFFRACTION IN CHIRAL MEDIA & RCS APPLICATIONS: MEIXNER EDGE CONDITION AND THE SOMMERFELD HALF-PLANE PROBLEM IN CHIRAL MEDIA

Nader Engheta*, Philippe Pelet, and Guangying Li
Moore School of Electrical Engineering
University of Pennsylvania
Philadelphia, Pennsylvania 19104

In recent years, chiral materials have gained revived interest and become the subject of extensive research in electromagnetics, optics and material science due to their novel applications in low-reflection coatings, radar absorbing materials and electromagnetic shielding. A variety of canonical problems on scattering and interaction of electromagnetic waves with chiral coated targets have been studied and reported in the literature. These studies reveal the notable characteristics of chiral media in reducing the radar cross-section (RCS) of targets covered with such materials. One of the fundamental scattering problems involving chiral media is diffraction of EM waves from sharp edges, corners and tips covered with chiral materials. The motivation behind this study is to investigate the role of chirality in control of RCS of targets with edges and corners.

In this talk, the behavior of electromagnetic fields near conducting edges covered with chiral materials is studied via extending the well-known Meixner edge condition to the chiral case. We present the effects of chirality on this condition and emphasize the similarities and differences of the Meixner Edge conditions for chiral and nonchiral cases. The left Figure below shows the geometry of the problem used to study edge condition. It is shown that the behavior of electric and magnetic fields in the neighborhood of such edges involving chiral layer is modified due to chirality of coatings, and therefore the induced current distributions over the conductor is affected. This current change is one of the important factors in RCS modification of such edges when chiral materials are used.

As a particular case, the Sommerfeld half-plane problem is revisited for the conducting half plane embedded in chiral materials as shown in the right Figure below. A right- or left-circularly polarized plane wave is incident on this semi-infinite conducting sheet in chiral media, and diffracted waves are studied in detail. Scattering patterns of this case are evaluated and compared with those of the nonchiral case, and the physical insights and important features are given. Applications to RCS control of chiral coated sharp-edged targets are also addressed.

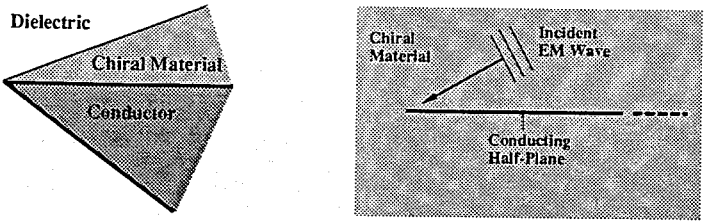

Figure. In the left is shown the geometry used to extend the Meixner edge condition to the chiral case in EM wave diffraction. In the right is shown diffraction of an incident RCP or LCP plane wave by a conducting half plane in chiral media.

THEORY AND APPLICATIONS OF CHIRAL MULTILAYERS

D. L. Jaggard and X. Sun
Complex Media Laboratory
Moore School of Electrical Engineering
University of Pennsylvania
Philadelphia, PA 19104

We investigate reflection from and transmission through chiral multilayers with discrete variations in material characteristics. The S-parameter matrix and associated co-polarized and cross-polarized reflection and transmission coefficients are derived from the chiral constitutive relations, Maxwell's equations and boundary conditions.

Electromagnetic chirality [D. L. Jaggard, A. R. Mickelson and C. H. Papas, "On Electromagnetic Waves in Chiral Media," *Appl. Phys. 18*, 211-216 (1979)], is found in materials characterized by the generalized constitutive relations $\mathbf{D} = \varepsilon\mathbf{E} + i\xi_c\mathbf{B}$ and $\mathbf{H} = \mathbf{B}/\mu + i\xi_c\mathbf{E}$ for the electromagnetic field vectors **D**, **E**, **B** and **H** where, for the time-harmonic case, ε, μ are the permittivity and permeability of the medium and ξ_c is the chirality admittance. This admittance is introduced to take into account the handedness properties of the material and its absolute value is the measure of material chirality. As a result of the presence of ξ_c, two eigenmodes of circular polarization and wavenumbers k_+ and k_- appear naturally through the blending of the generalized constitutive relations with Maxwell's equations. Thus, at any interface between two chiral materials, an incident mode of given circular polarization yields modes of both handedness in transmission and reflection.

Here we examine the reflection from and transmission through chiral multilayers for incident waves at both normal and oblique incidence. We first formulate the general interface problem between two chiral regions using a boundary-value method. This leads to the magnitude transfer matrix $\underline{\underline{M}}$, and reflection and transmission matrices at an interface. When combined with appropriate phase transfer matrices $\underline{\underline{P}}$ between interfaces, they yield the system transfer matrix or S-parameter matrix for a system of chiral multilayers through chain matrix multiplication. For a chiral multilayer system, the S-parameter matrix is given by,

$$\underline{\underline{S}} = \underline{\underline{M}}_0 \underline{\underline{P}}_1 \underline{\underline{M}}_1 \cdots \underline{\underline{P}}_n \underline{\underline{M}}_n \cdots \underline{\underline{P}}_N \underline{\underline{M}}_N \cdot$$

The S-parameter matrix may be further written in terms of the four sub-matrices $\underline{\underline{S}}_T$, $\underline{\underline{S}}_R$, $\underline{\underline{S}}'_T$ and $\underline{\underline{S}}'_R$ as,

$$\underline{\underline{S}} = \left[\begin{array}{c|c} \underline{\underline{S}}_T & \underline{\underline{S}}'_R \\ \hline \underline{\underline{S}}_R & \underline{\underline{S}}'_T \end{array}\right] .$$

All results are exact and applicable to both normal and oblique incidence. Special emphasis is given to the physical principles involved, special cases, and salient features. Special cases include conditions for single-mode transmission, total internal reflection, polarizing angles and matching conditions. The results reported here reproduce previous results [D. L. Jaggard, N. Engheta and J. Liu, "*Chiroshield*™: The Salisbury/Dallenbach Shield Alternative," *Electronics Lett. 26*, 1332-1333 (1990)] in the limiting case of normal incidence. Applications involving total internal reflection, polarizing angles and matching conditions will be discussed.

D24.7

CHIRAL RECTANGULAR DIRECTIONAL COUPLER

K.S. Chan* and P.L.E. Uslenghi
Department of Electrical Engineering and Computer Science
University of Illinois at Chicago
Box 4348, Chicago, IL 60680, USA

Chiral materials may find interesting applications in integrated optical systems. A detailed analysis of the rectangular chirowaveguide embedded in a dielectric substrate has just been completed (K.S. Chan and P.L.E. Uslenghi, PIER Symposium, Boston, MA, 1991), by extending Marcatili's approximate treatment of the rectangular dielectric waveguide to the case of a chiral guiding region.

In this work, we extend our treatment to a directional coupler consisting of two identical rectangular chirowaveguides embedded in a dielectric substrate which, for practical purposes, may be considered of infinite extent in the (x,y) cross-sectional plane of the coupler. The chirowaveguides occupy the regions ($d \le x \le d + 2a, -b \le y \le b$) and ($-d - 2a \le x \le -d, -b \le y \le b$) in the (x,y) plane, and are coupled along a length l in the z-direction. Their material is characterized by permittivity ϵ, permeability μ and chiral admittance ξ_c.

The coupling coefficient between the two rectangular chirowaveguides is determined on the basis of the weak-coupling theory of Miller and Marcatili. Our coupling formula reduces to the formula previously obtained by Marcatili (Bell Syst. Tech. J., vol. 48, pp. 2071-2102, 1969) for the particular case of nonchiral guides. Several numerical results are presented and discussed in detail, with a special emphasis on the influence exercised by chirality on the power transfer between the two guides.

Finally, our analysis is extended to the case when also the rectangular coupling region ($-d \le x \le d, -b \le y \le b$) sandwiched between the two guides is allowed to assume chiral properties. In particular, we study the modifications which chirality in the coupling region alone introduces to Marcatili's original coupler.

ELECTROMAGNETIC PROPERTIES OF FINITE-LENGTH *CHIROSTRIP* ANTENNAS

Philippe Pelet and Nader Engheta
Moore School of Electrical Engineering
University of Pennsylvania
Philadelphia, Pennsylvania 19104

Isotropic chiral materials belong to the class of biisotropic media, and are characterized by the set of constitutive relations $\mathbf{D} = \varepsilon_c \mathbf{E} + i\xi_c \mathbf{B}$ and $\mathbf{H} = \mathbf{B}/\mu_c + i\xi_c \mathbf{E}$ where $\exp(-i\omega t)$ is considered. Such materials are circular birefringent and thus exhibit two unequal characteristic wavenumbers $k_{\pm} = \pm\omega\mu\xi_c + \sqrt{\omega^2\mu\varepsilon_c + (\omega\mu\xi_c)^2}$ for right- and left-circularly polarized eigenmodes, respectively. For the isotropic chiral materials these wavenumbers are independent of the direction of propagation. These materials have recently attracted attention due to their potential applications to novel designs of microwave and millimeter-wave devices and components. Among these applications, one can mention the use of chiral materials in the design of printed-circuit antennas. This idea was first introduced in 1988 and the name *chirostrip* antenna was given to this class of radiators [N. Engheta, *Proc. 1988 IEEE AP-S/URSI*, Syracuse, New York]. These antennas consist of conventional microstrip antennas for which chiral materials are used as their substrates and/or superstrates. Several canonical problems related to *chirostrip* antennas have been studied and reported in the literature. For instance, it has been shown that for the two dimensional chirostrip antennas, chiral substrates can, under certain circumstances, provide reduction in surface wave power and enhancement in radiation efficiency [N. Engheta and P. Pelet, *Electronics Letters*, 27, 5-7, 1991]. We have also studied and analyzed radiation characteristics of planar and conformal arrays of chirostrip antennas, and have put in evidence the role of chirality of substrates in such chirostrip arrays [N. Engheta and P. Pelet, Proc. 1991 PIERS, Boston, MA].

In this talk, we address a more practical case of a center-fed finite-length chirostrip antennas as shown in Figure below. In this problem, we first review the dyadic Green's function of a printed source in a grounded chiral substrate, then find the current distribution on this antenna using the standard numerical technique. Finally, from a knowledge of the current distribution, all the relevant quantities such as radiation patterns, input impedance, surface-wave power, efficiency, and bandwidth of this antenna are determined. The role of chirality of the substrate on these parameters is emphasized and physical insights and interpretation of these results are given. Applications of these results to the novel design of conformal antennas in airborne platforms, radar, and communications are also addressed.

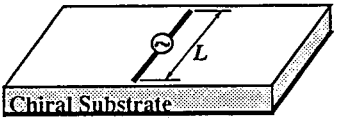

A center-fed finite-length *chirostrip* antenna with chiral substrate.

D24.9

MICROSTRIP LINE ON A CHIRAL SUBSTRATE

Michael S. Kluskens* and Edward H. Newman
Department of Electrical Engineering
The Ohio State University
ElectroScience Laboratory
Columbus, Ohio 43212

A spectral-domain solution of a microstrip transmission line on a chiral substrate is presented. The chiral substrate Green's function is obtained by expanding the fields in the substrate in terms of right and left circular vector potentials, similar to the usual magnetic and electric vector potentials. This spectral-domain Green's function is used to obtain an integral equation for the current on the microstrip line. The integral equation is solved by the method of moments (MM), and the propagation constant and current distribution on the microstrip line are determined by setting the determinant of the MM impedance matrix to zero.

On an achiral substrate the longitudinal current on a thin microstrip line is essentially the symmetric Maxwellian distribution. However, the asymmetry caused by a chiral substrate requires additional asymmetrical longitudinal current components, in addition to transverse components. Numerical results for the dispersion characteristics and currents of a chiral microstrip line are presented and compared with those of a similar achiral microstrip line.

Optical Devices and Circuits | **Room 3010 Salle URSI D Session 73** | **Circuits et dispositifs optiques**

Chairs/présidents: T. ITOH, USA

13:30 (73.1) Optical Space-Fed Beam Forming Network, **R. RAZDAN**, D. PAUL, B. PONTANO, J. EVANS, *COMSAT Laboratories, Clarksburg, MD, USA*

13:50 (73.2) Voltage Calibration of the Electrooptic Sampling Technique, **D.R. HJELME**, A.R. MICKELSON, *University of Colorado, Boulder, CO, USA*

14:10 (73.3) Propagation of Profiled Beams through a Finite Length of a Cubically Nonlinear Medium, **R.M. MISRA**, P.P. BANERJEE, *Syracuse University, Syracuse, NY, USA*

14:30 (73.4) An Inverse Scattering Approach to Designing Optical Logic Gates, **L.S. TAMIL**[1], A.K. JORDAN[2], [1] *University of Texas, Richardson, TX, and* [2] *Naval Research Laboratory, Washington, DC, USA*

14:50 (73.5) Investigation of Diffraction Efficiencies of a Thick Holographic Grating for Various Tilt Angles, S.-O. MIN, **M.R. CHATTERJEE**, *State University of New York, Binghamton, NY, USA*

15:10 **COFFEE/CAFÉ**

15:30 (73.6) FD-TD Modeling of Dispersive Media, **R. JOSEPH**, S. HAGNESS, A. TAFLOVE, *Northwestern University, Evanston, IL, USA*

15:50 (73.7) Eigenmodes and Dispersion Relations for a Topologically Dispersive Planar Optical Dielectric Waveguide, P.P. BANERJEE[1], **M.R. CHATTERJEE**[2], M.-S. OH[2], [1] *Syracuse University, Syracuse, NY, and* [2] *State University of New York, Binghamton, NY, USA*

16:10 (73.8) Coplanar Radiating Structures for Quasi-Optical Power Meters, **W.P. HAROKOPUS JR.**, P.B. KATEHI, *University of Michigan, Ann Arbor, MI, USA*

16:30 (73.9) Simple Model for Dynamic Characteristics of Multimode DCPBH Lasers, **M.C.R. CARVALHO**, *Pontifical Catholic University of Rio de Janeiro, Brazil*

16:50 (73.10) Theoretical Modelling of Inhomogeneous Buried Optical Waveguides by Field-Assisted Ion Exchange in Glass, **P.C. NOUTSIOS**, G.L. YIP, *McGill University, Montreal, PQ, Canada*

D73.1

OPTICAL SPACE-FED BEAM FORMING NETWORK

R. Razdan*, D. Paul, B. Pontano and J. Evans
COMSAT Laboratories, 22300 Comsat Drive, Clarksburg, MD 20871

Future satellite systems will feature multiple spot beams which will: increase transmission capacity by means of frequency reuse of the scarce satellite BW; provide service flexibility, especially in conjunction with on-board processing and be more energy efficient by illuminating each spot only when demand is high enough. Multibeam systems require a beam forming network (BFN) to distribute the RF power to the various phased array antenna (PAA) feed elements. Utilizing optical technology in BFNs can result in reduced size/weight and lower crosstalk. Comsat Labs. is presently designing novel optical space-fed BFNs that utilize free-space time delays to create the required phase shifts at the feed array.

Two optical space fed BFN architectures are presently being investigated: one using optical fibers as delay lines to simulate the required microwave phase shifts at the feed array elements and the other formed by reducing the microwave BFN to optical dimensions and then converting, in a 1:1 correspondence, the optical phase shifts to the microwave equivalent. The second approach requires the use of a optical-to-microwave phase converter. An optical Mach-Zehnder hetrodyne interferometer designed on a $LiNbO_3$ chip could provide this conversion by beating together on a square-law photo-detector the phase-shifted optical signal with a microwave frequency shifted optical signal (R.A.Soref, IEEE LT-3, No. 5, 992-998, Oct. 1985). The first approach is conceptually simpler and does not require optical-to-microwave phase conversion but does require the use of a large number of optical fibers.

An optical space-fed BFN, using either architecture, designed to switch 6 signals to 128 different beam positions using 169 feed elements could easily be fitted into a bundle of a few cm. in diameter. The microwave equivalent of such a BFN would have ~1 m spacing between input and output ports and a height of ~1 m. Estimates of mass and power for the optical space-fed BFN will be provided.

VOLTAGE CALIBRATION OF THE ELECTROOPTIC SAMPLING TECHNIQUE

Dag R. Hjelme* and Alan R. Mickelson
Electrical and Computer Engineering
University of Colorado, Boulder CO 80309-0425

The direct electrooptic probing technique relies on the circuit substrate as part of the measurement system. Hence, voltage calibration requires consideration of the optical properties of the substrate. In reflection mode optical probing, the circuit substrate and the ground plane or the signal line forms an Gires-Tournois etalon for the optical probe beam. In this work we will present results showing the effect of this etalon on the voltage calibration factor of the electrooptical sampling system. Simple analytical expressions for the calibration factor are derived in two limiting cases; long and short optical sampling pulses. Experimental verification of the theoretical results are presented using an electrooptic saampling system on GaAs microstrip circuits.

Depending on the length of the sampling pulse relative to the substrate transit time, the etalon will affect either the voltage calibration factor or the system bandwidth. For pulses long compared to the transit time, interference at the surface will result in a wavelength dependent storage time effect. The resulting electrooptic signal shows a resonant behavior as a function of substrate thickness or probe wavelength. In GaAs substrates this will result in a maximum signal variation of 22 dB. By using pulses short compared to the transit time, these interferometric effects can be eliminated. However, the multiple reflections will reduce the effective bandwidth of the system to a bandwidth less than that given by the transit time or samling pulse width. On a 100 μm GaAs substrate, the 3 dB bandwidth of the sampling system is reduced to about 85 GHz.

D73.3

PROPAGATION OF PROFILED BEAMS THROUGH A FINITE LENGTH OF A CUBICALLY NONLINEAR MEDIUM

Raj M. Misra* and Partha P. Banerjee
Department of Electrical Engineering
Syracuse University, Syracuse NY 13244-1240

Propagation of Gaussian beams through a cubically nonlinear medium has been extensively studied over the last three decades [for a detailed background see Marburger **Self-focusing: Theory**, Progress Quant. Electr. 4 (1975)]. For $n_2>0$ (<0), the beam initially focusses (defocusses) due to the induced lensing effect. This property has, in fact, been utilized in the so-called z-scan method to determine the nonlinear refractive index coefficient n_2 of a Kerr-type material. The sign and the magnitude of n_2 can be determined by focussing a Gaussian beam into a nonlinear sample of finite length, and thereafter monitoring the far-field beam width while changing the separation between the external focussing lens and the nonlinear sample [Sheik-bahae et al SPIE **1105** pp. 146-153 (1989)]. When the nonlinearity is of thermal origin, a Gaussian beam entering the sample with plane wavefronts gets defocussed if the parameter defining the thermal nonlinearity, viz., dn/dT, where n denotes the refractive index and T the temperature, is negative. In some cases, it is possible to define an average n_2 of this nonlinear sample in terms of dn/dT [Litvak JETP Lett. 4 pp. 230-233 (1966)].

In this paper, we investigate the propagation of other profiles through a cubically nonlinear medium. As an example, we will consider the propagation of the diffraction pattern of a one-dimensional rectangular slit, which is generated by placing the slit on the front focal plane of the external focussing lens mentioned above. Near the back focal plane of this lens, the diffraction pattern is approximately the product of a sinc function and a Gaussian. This profile propagates through the nonlinear sample and the far-field pattern is again monitored. Propagation through the sample is numerically modelled using a split-step method, which incorporates the effect of propagational diffraction in the spatial frequency domain and the nonlinearity in the spatial domain. Similarities and differences between thick and thin samples are studied. The significance of this study is that, through a slight variation of the z-scan method, it is possible to understand the nature of propagation of multiple adjacent beams through the nonlinear sample, and the behavior of the ensuing far-field pattern for various lens-sample separations. Propagation through both Kerr-type as well as thermally nonlinear media are studied, analytically and numerically. Preliminary experimental results based on a material exhibiting thermal nonlinearity are also presented.

AN INVERSE SCATTERING APPROACH TO DESIGNING OPTICAL LOGIC GATES

Lakshman S. Tamil
Erik Jonsson School of Engineering and Computer Science
and
Center for Applied Optics
The University of Texas at Dallas
Richardson, Texas 75083

A. K. Jordan
Space Science Division,
Naval Research Laboratory,
Washington, D.C. 20375

An optical logic gate is a very important photonic component for future communication, signal processing and computer systems. The design of optical logic gates have been studied by many authors and is usually based on the analysis of passive or active etalon. In this paper, we present a method for designing optical logic gates using inverse scattering method. This work draws upon our earlier use of inverse scattering theory to design wide core single mode planar optical waveguides. (Opt. Lett. **14**, 411 (1989)). Here a pair of phase-conjugate reflection coefficients characterizing the two output states (ON and OFF) of an optical logic gate are chosen such that the 'ON' state supports a propagating or a bound mode and the 'OFF' state does not. The reconstructed potentials corresponding to the reflection coefficients are related to two different refractive index profiles. A possible design for an optical AND gate is a Y shaped planar waveguide with core made up of a nonlinear material with refractive index profile corresponding to the OFF state. The two input arms combine the input light intensities. When the input is (0,0), (0,1) or (1,0), the combined light intensity is not sufficient to change the refractive index to that corresponding to ON state. However when the input is (1,1), the combined input intensity is sufficient to change the refractive index to that corresponding to the ON state so that this thin film waveguide guides a propagating mode that can be detected at the output. It is feasible to fabricate the optical logic gate described here using well known techniques such as molecular beam epitaxy.

D73.5

INVESTIGATION OF DIFFRACTION EFFICIENCIES OF A THICK HOLOGRAPHIC GRATING FOR VARIOUS TILT ANGLES

Sung-Oh Min and Monish R. Chatterjee*
Department of Electrical Engineering, SUNY at Binghamton
Binghamton, New York 13902-6000

The efficiency of the diffracted light in the Bragg domain is an important consideration in the operation of holographic optical interconnects. In general, Bragg-domain solutions are derived by assuming plane waves of incident light, and the corresponding efficiencies are calculated for different parameters such as the grating constant, the incident angle, the optical wavelength, and lumped parameters such as an effective "Q" (similar to the Klein-Cook parameter in acousto-optics) and "β" of the grating. In most cases, the orientation of the grating itself is assumed to be untilted, i.e. consisting of a 90-degree tilt angle.

In this paper, we begin with the general plane-wave grating solutions using the Kogelnik identities, and introduce arbitrary Bragg angles as well as tilt angles into the problem. Arbitrary tilt angles may be important in the recording of the holographic gratings, depending on the particular recording technique (such as dichromated gelatins, direct UV, or others), and the target angles. Diffraction efficiencies are then evaluated for varying grating constants, angles of incidence (Bragg- and twice-Bragg angles), and angles of tilt. It is found that the efficiency drops rapidly as the tilt-angle is increased. Ongoing work includes modifying the solution technique for arbitrary light profiles and general Bragg angles using a multiple plane wave scattering approach.

FD-TD MODELING OF DISPERSIVE MEDIA

R. Joseph*, S. Hagness, and A. Taflove
EECS Department, McCormick School of Engineering
Northwestern University, Evanston, IL 60208

In this paper we report a finite-difference time-domain (FD-TD) model for electromagnetic wave propagation in media having frequency-dispersive dielectric properties. Our approach relates D(t) and E(t) via an ordinary differential equation in time, rather than a convolution. This differs from the approach of Kunz *et. al.* [IEEE EMC **32**, 222 (1990)]. The new approach is computationally efficient, requiring only one additional backstore in time beyond the basic FD-TD approach for second-order dielectric relaxations, and one extra backstore for each subsequent increase in the order of the defining D(t) vs. E(t) equation.

With this method, we have demonstrated highly accurate results for the broadband reflection coefficient vs. frequency of dispersive half-spaces subjected to Gaussian pulse illuminations. We have successfully treated both first order (Debye) and second order (Lorentz) relaxations. We have further investigated the computation of Sommerfeld and Brillouin precursors from first principles (Maxwell's equations) and shown agreement with published analyses based upon asymptotic techniques [Oughstun and Sherman, J. Opt. Soc. Amer., **6**, 1394 (1989)]

Our approach has application both to electromagnetic scattering by targets coated with lossy, dispersive materials, and to propagation of optical pulses in fibers. We shall summarize our research efforts so far in these areas.

D73.7

EIGENMODES AND DISPERSION RELATIONS FOR A TOPOLOGICALLY DISPERSIVE PLANAR OPTICAL DIELECTRIC WAVEGUIDE

Partha P. Banerjee[1*], Monish R. Chatterjee[2] and Min-Seok Oh[2]

[1]Department of Electrical Engineering,
Syracuse University, Syracuse NY 13244-1240

[2]Department of Electrical Engineering,
SUNY at Binghamton, Binghamton NY 13902-6000

As a follow-up to a previous work involving a topologically dispersive optical filter using periodic serrations in a planar dielectric structure [Banerjee and Chatterjee 1990 URSI/AP-S Meeting Abstracts, Dallas, p.151], we investigate further the dispersion characteristics for a single Gaussian mode. The results indicate group velocity characteristics which undergo a rapid variation about a critical frequency, and eventually approach a saturation limit. Thus, by operating in the neighborhood of the critical frequency, one may obtain variable delays for signal processing applications by changing the carrier frequency. Additionally, the amount of the delay for a fixed frequency may be varied, for instance, by changing the thickness of the overlay.

Further, starting from the dispersion relation, we find the underlying partial differential equation (PDE) describing the propagation of the above-mentioned Gaussian mode. Next, by solving this PDE, we establish other possible eigenmodes which may be propagated in the structure. Thereafter, by applying individual possible eigenmodes to the technique mentioned in the beginning, we calculate the dispersion characteristics associated with these new modes. The resulting delays are then compared.

COPLANAR RADIATING STRUCTURES FOR QUASI-OPTICAL POWER METERS

W. P. Harokopus, Jr. * and P. B. Katehi
The Radiation Laboratory
Electrical Engineering and Computer Science Department
1301 Beal Ave.
University of Michigan, Ann Arbor MI., 48109
(313) 936-2975

A quasi-optical system can be used to measure the power generated by an oscillator at terahertz frequencies. In this approach, the oscillator output power is coupled to a monolithic antenna through an appropriate matching network and the radiated power is measured quasi-optically. In this manner, transmission line losses are circumvented, and the spectral content of the oscillator may be determined.

The planar antennas and matching circuits needed for this application are integrated on substrates which appear to be very thick electrically at the operating frequency. As a result, a large percentage of the few μ-watts of radiated power would be trapped within the dielectric in the form of surface waves, reducing radiation efficiency considerably. In order to avoid this problem, the integrated antennas and matching network are fabricated in a coplanar form on a hemispherical dielectric lens.

The lens, which is covered by a matching layer, provides a perfect match to free space at the frequency of interest and does not reflect the radiated power. Although the approach optimizes the gain of the integrated antenna, it does not eliminate parasitic radiation from the matching network which may lower the performance of the system if it is not designed carefully.

This paper presents a complete theoretical study of the high frequency performance and radiation losses of a coplanar waveguide 500 GHz oscillator matching circuit printed on an InP substrate and covered by a silicon lens. The Si lens will has a quarter wave matching teflon layer on its surface to optimize power transfer. The theoretical approach is based on the space domain integral equation method which has been successfully applied to a number of planar structures. The theoretical results will be validated by experiments to be performed on circuit models scaled to lower frequencies.

SIMPLE MODEL FOR DYNAMIC CHARACTERISTICS OF MULTIMODE DCPBH LASERS

M. CRISTINA R. CARVALHO
Center for Telecommunication Studies (CETUC)
Pontifical Catholic University of Rio de Janeiro (PUC/RIO)
Rua Marques de São Vicente, 225 22453 Rio de Janeiro-RJ BRAZIL

A simple model in described for the dynamic behaviour of DCPBH InGaAsP lasers under high speed modulation. Comparisons between modelled and measured data show good agreement.

The model includes the effects of rf current spreading in the blocking layers, gain saturation and mode-coupling. The large-signal circuit model of the active region follows directly from the multi-mode rate equations, which includes a nonlinear gain term. The net gain of mode i is taken as $G_i=G_i^L+G_i^{NL}$, where G_i^L and G_i^{NL} are the linear and nonlinear components, respectively. The form used here in for G_i^{NL} is that outlined by Agrawal (IEEE J. Quantum Electron.,1987,QE.23, p.860). The stimulated emission in each mode is modelled by the nonlinear dependent current sources G_{ij}, which represents the contribution in mode i due to the photon density in mode j. The parasitic lateral p-n junction is modelled as a distributed network, which makes a ladder of resistances (R_i) and capacitances (C_i). The values of C_i and R_i are related to the doping levels. Their influence in the modulation bandwidth of the laser depend on the width of the blocking layers.

The circuit model is illustrated here with a DCPBH laser fabricated by CPqD - Telebrás in Brazil. The theoretical results of frequency response were calculated from the model described here using the circuit analysis program SPICE2. The parameters of the active region and the dc leakage current were estimated from practical data and the expressions for threshold current and resonant frequency. The form and magnitude of the nonlinear gain were estimated from measurements of the longitudinal mode-spectra and published data (J.Appl. Phys., 1982,52,p.4631). The distributed parasitics were obtained from the reflection coefficient measurements. The initial data were then adjusted so that the modelled frequency responses matched the measured ones, under different bias levels. The figure shows the modelled and measured small-signal frequency responses, in the frequency range 0,3MHz-2.6GHz. Agreement between experimental and computed data is good, with discrespancies of less than o,5dB.

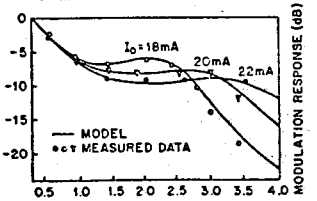

THEORETICAL MODELLING OF INHOMOGENEOUS BURIED OPTICAL WAVEGUIDES BY FIELD-ASSISTED ION EXCHANGE IN GLASS

P.C. Noutsios* and G.L. Yip
Guided Wave Optics Laboratory
McGill University
Department of Electrical Engineering
3480 University Street
Montreal, Quebec, Canada H3A 2A7

The electric field-assisted $K^+ - Na^+$ ion-exchange technique has become a promising technology for passive, low loss, single-mode optical waveguide device fabrication. This technique has also been used to fabricate active devices, such as waveguide lasers and integrated-optic sensors in glass. Recently, we reported a detailed study of the surface waveguide characteristics in soda-lime glass using this process. Here, we report on the refractive index profile characteristics of buried waveguides by theoretical modelling and experimentation with the help of scanning electron microscopy (SEM). These graded-index buried guides have led to low insertion losses with optical fiber.

The index profile characteristics can be determined directly from the dopant concentration profile which is deduced by solving the planar nonlinear ion exchange equation. This equation is solved numerically by a finite difference scheme with parameters derived from previous characterizations. Buried waveguides profiles are modelled by using appropriate initial and boundary conditions. The guide characteristics can be determined accurately as a function of the initial diffusion time t_1, the backdiffusion time t_2, and the total applied electric field, E_a^T. Furthermore, the buried K^+-ion concentration profile can be fitted and, hence, modelled by an analytical buried modified Fermi function with the fitting parameters dependent on E_a^T, t_1, and t_2. Using this analytical function greatly simplifies the design of waveguide structures.

The propagation characteristics, such as the dispersion curves, can, in general, be obtained from the solution of the Helmholtz equation. Using experimentally determined values of the maximum index change, the use of the scalar wave approximation is justified. To generate single-mode dispersion curves, the Runge-Kutta technique is used after transforming the Helmholtz equation into a first order Ricatti differential equation.

The modelling of the index profile and characterization results provide useful information in the design of low loss single-mode buried waveguide devices with improved fiber-waveguide coupling. Further details will be presented at the meeting.

Microwave Circuits and MMIC's | **Room 3010 Salle URSI D Session 90** | **Circuits micro-ondes et circuits intégrés monolithiques micro-ondes**

Chairs/présidents: L. SHAFAI, Canada; K.C. GUPTA, USA

08:30 (90.1) Design Considerations for Image-Guide Band-Reject Filters, **J.A. ENCINAR**, *Universidad Politécnica de Madrid, Spain*

08:50 (90.2) A Microstrip Antenna Configuration Suitable for Integration with Monolithic Circuits, **R.P. PARRIKAR**, K.C. GUPTA, *University of Colorado, Boulder, CO, USA*

09:10 (90.3) Influence of a Dielectric Cap Layer on Coupling Phenomena for Schottky or MIS Coplanar Lines for M.M.I.C., **P. PRIBETICH**, C. SEGUINOT, P. KENNIS, *U.S.T.L., Villeneuve d'Ascq, France*

09:30 (90.4) On the Comparison of Full Wave Approaches to Determine Microstrip Conductor Losses for MMIC Applications, E. PALECZNY, D. KINOWSKI, J.F. LEGIER, **P. PRIBETICH**, P. KENNIS, *U.S.T.L., Villeneuve d'Ascq, France*

09:50 (90.5) A Tunable Planar Grid Oscillator for Switching Operation, **T. MADER**, S. BUNDY, Z. POPOVIĆ, M. YADLOWSKI, D. HJELME, A. MICKELSON, *University of Colorado, Boulder, CO, USA*

10:10 **COFFEE/CAFÉ**

10:30 (90.6) Guided Quasi Complex Waves on Lightly Lossy Substrate Boxed Microstrip Lines, F. HURET, **P. PRIBETICH**, P. KENNIS, *U.S.T.L., Villeneuve d'Ascq, France*

10:50 (90.7) Design Methodology of Monolithic Millimeter Wave Integrated Circuits, **H. WANG**, T.H. CHEN, K.W. CHANG, G.S. DOW, *TRW, Redondo Beach, CA, USA*

11:10 (90.8) An FDTD Networking Approach to Lossy and Dispersive Transmission Lines, **G. PAN**[1], B. WANG[1], B. GILBERT[2], [1]*University of Wisconsin, Milwaukee, WI, and* [2]*Mayo Foundation, Rochester, MN, USA*

11:30 (90.9) A Quasi-Static Model for Fuss Button Interconnects, **G. PAN**[1], X. ZHU[1], B. GILBERT[2], R. EDEN[3], [1]*University of Wisconsin, Milwaukee, WI,* [2]*Mayo Foundation, Rochester, MN, and* [3]*GigaBitLogic, Newbury, CA, USA*

11:50 (90.10) Single Path Millimeter Wave Attenuation through Linearly Graded Moving Rectangular Spot Illumination Semiconductor Panel Which is Used in Millimeter Wave Image Convertor, **M.H. RAHNAVARD**, A. BAKHTAZAD, *Shiraz University, Shiraz, Iran*

D90.1

DESIGN CONSIDERATIONS FOR IMAGE-GUIDE BAND-REJECT FILTERS

Jose A. Encinar
Grupo de Electromagnetismo Aplicado y Microondas
E.T.S.I. de Telecomunicacion, Univ. Politecnica
Ciudad Universitaria, 28040 Madrid, Spain

A image guide periodically loaded with metal strips is analyzed as a band-reject filter for microwave-millimeter frequencies, and some design considerations are obtained.

To analize the structure, first the finite width loaded image guide is reduced to an infinite grounded slab with an ϵ effective, by using the Effective Dielectric Constant (EDC) method. Then, a mode matching technique is applied to compute dispersion characteristics, fields and transmitted power for the infinite width periodic structure. Transmitted power is used as a simple approach to evaluate the central frequency and bandwidth of the filter. Since the structure is assumed infinite-length, the attenuation computed by this approach is very high, theoretically infinite. The attenuation for a finite-length structure is computed by a simple monomode equivalent circuit.

Some considerations for the design of the filter are infered from the plots of transmitted power. First of all, the structure is open and radiation can occur. To minimize radiation losses, radiation region must be avoided and the first stop-band (β*period = π) must be used to obtain the band rejection. Bandwidth can be controlled primarily by changing the width of the metal strips. The attenuation in the rejected band depends on both width of the metal strips and number of periods. Also, the utilization band of the filter out of the stop-band is important, and it is determined by transmitted power. The upper limit is given by the beginning of radiation region, or if some radiation losses are permissible, these are computed as the difference of guided power between the beginning and the end of the structure. The lower limit is imposed by the amount of guided energy that is transmitted by the air. This must be a small percentage of the total guided energy, in order to avoid interference and feeding problems.

A band-reject filter can be designed for a given characteristics by changing the geometry parameters. Some numerical results will be shown in the oral presentation.

A Microstrip Antenna Configuration Suitable for Integration with Monolithic Circuits

Rajan P. Parrikar* and K. C. Gupta
Department of Electrical and Computer Engineering
University of Colorado, Boulder

A proximity fed microstrip antenna configuration suitable for integration of monolithic microwave circuits is proposed. In this configuration (shown in the figure below), the radiating patch is located on the top of the Si_3N_4 (or polyamide) passivating layer (typically 1-4 microns thick) and is fed by microstrip circuitry on the GaAs substrate (typically 100-200 microns thick) underneath.

The Multiport Network Model approach is used for analysis and design of this radiating configuration. The region underneath the patch is modeled as a cavity surrounded by magnetic walls on the sides and electric walls on the top and the bottom. Unlike in the conventional cavity model, the proposed model accounts for field variations in the vertical dimension also. The Schelkunoff Equivalence Principle is used to separate the cavity volume into a source region and a source-free region. The electromagnetic analysis of fields in the source and the source-free regions results in the formulation of two equivalent networks called the Feed Network and the Patch Network. These networks are characterized by a multiport Z-matrix and a multiport hybrid matrix respectively. The external fields (fringing, radiation etc.) are represented by an Edge-Admittance-Network which is combined with the other two networks to obtain an overall network model of the antenna. Network analysis yields equivalent magnetic currents at the edges of the antenna which are used for evaluating the radiation characteristics. Methods of analysis and typical results will be presented.

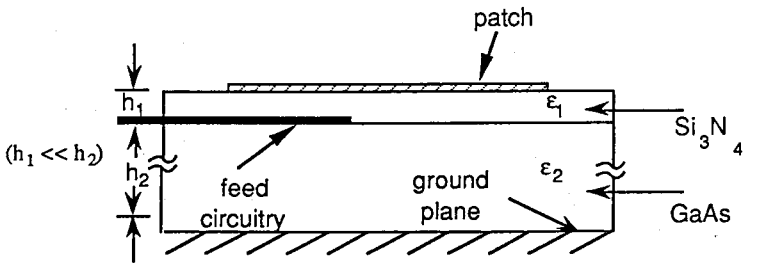

INFLUENCE OF A DIELECTRIC CAP LAYER ON COUPLING PHENOMENA FOR SCHOTTKY OR MIS COPLANAR LINES FOR M.M.I.C.

P. PRIBETICH - C. SEGUINOT - P.KENNIS.
Equipe Electromagnétisme des circuits
Centre Hyperfréquences et Semiconducteurs
U.S.T.L. Flandres et Artois BAT P 4
59655 VILLENEUVE D'ASCQ
FRANCE

Active devices represent the key components of modern microwave electronic system. The MESFET and more recently, the High Electron Mobility Transistor (HEMT) faced an impressive improvement in microwave performance during the last years thus enabling present day developments such as monolithic integrated circuits for the mm wave range. Using 0.1µm gate lengths, transit frequencies of more than 200 GHz can be obtained. In this frequency range, the question arises whether lumped theory describes the FET with sufficient accuracy or whether distributed effects have to be account. Furthermore, novel FET structures such as the so called travelling wave FET's are proposed. All these investigations require reliable qualitative and quantitative informations on the waves propagating along the electrodes in microwaves FET structures. One way to simulate these kind of structures is to employ an distributed equivalent circuit model including the propagation phenomena and the active phenomena.Several publications have shown that for this problem outlined it is favourable to treat travelling wave transistor by the coupled modes theory which considers all the important properties of wave propagation and furthermore offer significantly numerical efforts. For this communication , the study focuse namely on the propagation of waves more precisely the passive coupling between the gate source and the drain source lines(figure 1) . The aim of that study is to show the influence of a dielectric cap layer on the mode coupling for a SCHOTTKY contact or MIS coplanar lines In order to take into account the most physical parameters and effects,we have studied the structure shown on figure 2 using the mode matching technique, considering the relative complex permittivityfor each layer of the structure and the hybrid nature of the two fundamental modes.As example,we present figure 3, the evolution of the coupling capacitance Cm versus the thickness t of the metallization and for different values of permittivities of the dielectric cap layer.At the conference,we will present all the detail of the analysis and the main typical results.

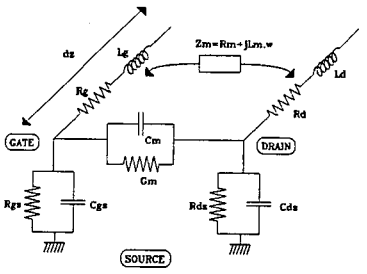

Figure 1

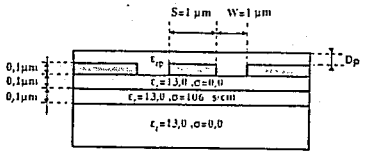

figure 2

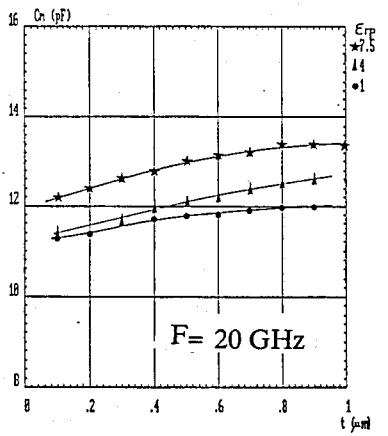

figure 3

ON THE COMPARISON OF FULL WAVE APPROACHES TO DETERMINE MICROSTRIP CONDUCTOR LOSSES FOR MMIC APPLICATIONS

E.PALECZNY, D. KINOWSKI, J.F. LEGIER, P. PRIBETICH*, P. KENNIS

Centre Hyperfréquences et Semiconducteurs
Equipe Electromagnétisme des Circuits
U.A. CNRS n° 287
USTL FLANDRES-ARTOIS
59650 VILLENEUVE D'ASCQ , FRANCE

Transmission losses in microstrip lines are usually determined by perturbation methods. This evaluation becomes questionable when the metallization thickness is about or less than the skin depth or when very small width strips are considered. In this proposition of communication, we propose a comparative study of the losses obtained by two numerical tools. The first one is based on the classical S.D.A. in which the losses are modelled through a complex resistive boundary condition. The second one is based on a full wave modelling that is to say the Mode Matching Technique where the lossy strip is seen as a rectangular complex permittivity aera (fig. 1).As example numerical simulations by the two full wave approaches are presented on fig. 2. Two strips have been considered, one with W=10μm and the other with W=30μm. The results exhibits the behaviour of the numerical simulations versus thickness t, for a given frequency of 10 GHz. The comparative study between the two theorical methods shows that for usual applications, the results obtained by the modified S.D.A. describe with enough accuracy the behaviour of the microstrip structure. However, for very narrow strip (W<10μm), the modified SDA does not yield to quite accurate numerical results, even when the metallization thickness t is greater than the skin effect depth(δ). At this step, as mode matching technique is intensive of CPU time, it would be better to define a weighting factor for the surface impedance, in order to obtain accurate numerical data, with modified S.D.A.. This weighting factor, would be obtained by fitting S.D.A. results to mode matching ones for some typical structures. At the conference, we propose to show in an engineering purpose other comparative studies between the full wave approaches in order to point out the range of validity of the less consumming CPU time method.

e=5 μm, ϵ_{r3}=13
σ of strip = 4.1 10^5 S/cm
σ of ground plane = 4.1 10^5 S/cm

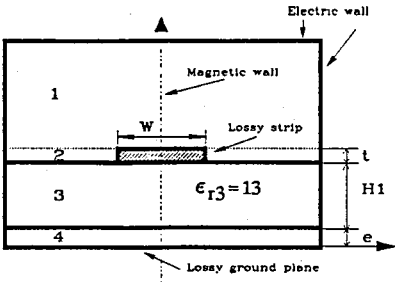

Figure 1 : Studied Structure

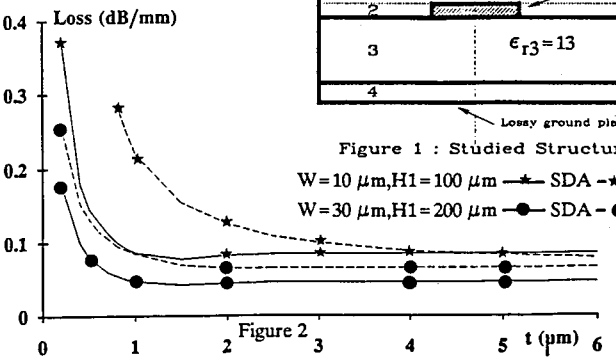

W=10 μm, H1=100 μm —★— SDA -★- MMT
W=30 μm, H1=200 μm —●— SDA -●- MMT

Figure 2

A TUNABLE PLANAR GRID OSCILLATOR FOR SWITCHING OPERATION

T. Mader, S. Bundy, Z. Popović*
M. Yadlowski, D. Hjelme, A. Mickelson
University of Colorado, Boulder, CO 80309-0425

Abstract – The planar grid oscillator (PGO) is a compact, lightweight, potentially high power device that is suitable for monolithic integration. It consists of a metal grid loaded with active solid-state devices. The device is at the same time a transmitter, receiver and antenna, and is attractive for such applications as flush mounted radar. A 100-MESFET PGO has been demonstrated as a power-combining oscillator (Popović *et al.*, IEEE-MTT, Feb. 1991), but its characteristics as a systems element, as well as its switching transients, remain to be investigated. In this work, a gate-feedback PGO, shown schematically in Fig. 1(a), will be presented. A proof of-concept 16-element gate-feedback PGO self-locks around 5 GHz, and can be frequency and power-tuned by translating the mirror behind it, and dielectric slabs in front of it, Fig. 1(b). In a systems application, it would be desirable to perform this tuning electrically, which can be done with a bias-dependant surface impedance of a grid loaded with varactor diodes. A second gate-feedback PGO will also be presented, in which the MESFETs are in chip form, and can be optically inspected and optically driven. This grid will be operated in pulsed mode, and the resulting voltage between the gate and the source monitored by an optical sampling technique, in an attempt to determine the pulsed mode characteristics of the device.

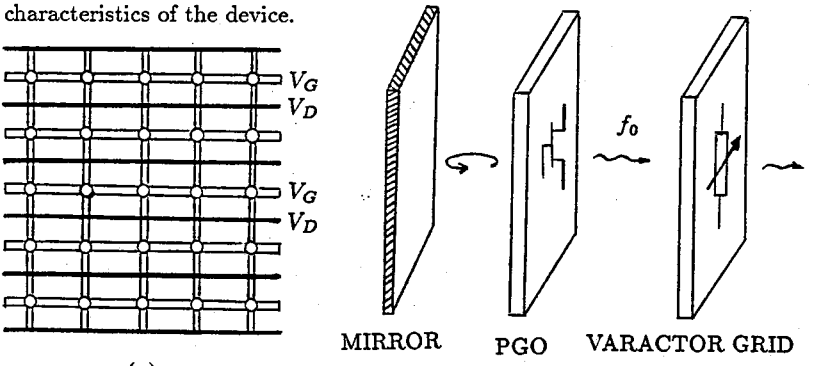

Fig. 1. The gate-feedback PGO (a) self-locks through mirror feedback (b) and can be electrically tuned with a varactor grid.

Guided Quasi Complex Waves on Lightly Lossy Substrate Boxed Microstrip Lines.

F. HURET, P. PRIBETICH*, P. KENNIS
Equipe Electromagnétisme des circuits
Centre Hyperfréquences et Semiconducteurs, U.A. CNRS N° 287
U.S.T.L. FLANDRES ARTOIS
59655 VILLENEUVE D'ASCQ FRANCE

The analysis of discontinuities between planar transmission lines, particulary for microstrip lines, has received a great interest from many years.Accurate modeling of such discontinuities is of fundamental importance for successful monolithic integrated circuit design.In fact increasing circuit complexity needs very efficient numerical techniques in order to solve electromagnetism problems.In this mind when mode matching method in the discontinuity plane is used, it is necessary to determine the set of modes with as accuracy as possible.More ever for boxed losseless structure, it has been shown that complex modes can occur, so that ignoring those modes would lead to non accurate solutions.

Up to now, most of published works concern the possibility of propagation of complex modes in lossless structure and only a few works focuse on complex and backward-wave modes in lossy waveguides.So, when shielded microstrip lines laid on semi-insulating or doped semi-conductor substrates, are considered for MMIC applications, it is necessary to investigate the evolution of complex solutions for lossless structure, under the effect of bulk losses in the substrate.

In this communication, by using spectral domain approach improved by asymptotic expansions, we show by means of coupling integral values that the notion of quasi complex modes can be introduced for lightly lossy substrates[1].The quasi complex modes are particular modes with similar behaviour than lossless structure complex modes.In this mind, and for example, we present the evolution of the two propagation constants for a pair of modes initially complex on the lossless structure versus the substrate conductivity for a frequency F= 19 Ghz.

[1] Huret F., P. Pribetich and P. Kennis, "Quasy complex modes on lossy substrate boxed microstrip lines," Microwave and Optical Technology Letters, Vol.3,N° 12,pp 439-445,Dec. 1990.

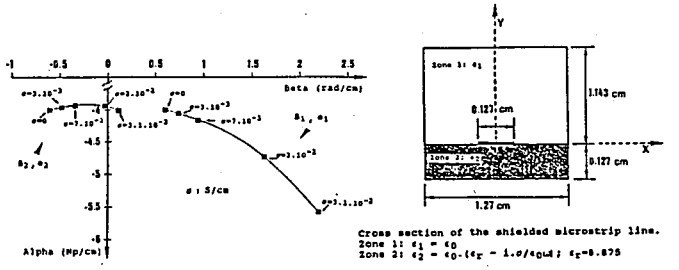

Propagation constant $\gamma = \beta + i \cdot \alpha$ of the two modes versus the conductivity for a frequency, F=19 GHz.

D90.7

Design Methodology of Monolithic Millimeter Wave Integrated Circuits

H. Wang*, T. H. Chen, K. W. Chang, and G. S. Dow

TRW
Communication Laboratory
R8/1722, One Space Park, Redondo Beach, CA 90278

Microwave and millimeter wave monolithic integrated circuits (MMICs) have the advantages of mass production, high reliability, and low cost over the conventional hybrid integrated circuits. A good design/analysis methodology is crucial for a successful monolithic design since there is no tuning flexibility after the circuits are fabricated. The importance of design/analysis methodology is more significant for millimeter wave circuits since simplified assumptions used at microwave frequencies, such as microwave circuit theory and quasi-static models are inadequate at higher frequencies. Rigorous analysis procedures have been developed and incorporated in our monolithic chips design, which include accurate active device modeling, full-wave electromagnetic (EM) analysis of passive structures, linear and non-linear circuit performance simulations. We have developed various monolithic integrated circuits ranging from 35 GHz to 94 GHz, including amplifiers, mixers, oscillators and high level integration chips such as downconverters, and achieved the first pass success by using this systematic design procedure. The analysis results and measurement data of different monolithic millimeter wave chips will be presented in the symposium.

The design procedure for millimeter wave MMICs is briefly described as follows. Accurate modeling techniques are the key issues of the design methodology. Active device linear and non-linear models can be obtained by careful curve-fit from measured small signal S-parameters and $DC-IV$ curves of existing device with same fabrication process. Critical passive components used in a particular circuit need to be identified and characterized by full-wave EM analysis before initial design. The S-parameters calculated from the full-wave EM analysis of these critical components are used to design and simulate circuit performance based on microwave circuit theory. After design is finished, the complete matching structures are simulated by EM analysis again to ensure no sever coupling effects between elements.

There are several commercially available full-wave EM analysis software for arbitrarily shaped MMIC structures. Software currently being used includes method of moment to solve integral equation based on the assumption of stratified medium in a conducting box and finite element method to solve partial different equation. The comparison between these methods along with experiment results will also be discussed.

AN FDTD NETWORKING APPROACH TO LOSSY AND DISPERSIVE TRANSMISSION LINES

G. Pan and B. Wang*
University of Wisconsin-Milwaukee
Milwaukee, WI 53201

B. Gilbert
Mayo Foundation
Rochester, MN 55905

A finite-difference time-domain (FDTD) method with improved absorbing boundary condition (ABC) has been applied to the full-wave analysis of three coupled lossy and dispersive transmission lines. The stripline or microstrip transmission lines modeled were very long in the direction of signal propagation in comparison with the width and thickness of their cross-sections.

To save computation time and computer memory, only a short portion of the transmission lines was modeled in the time domain by the FDTD. The time domain results were then converted into the frequency domain, by means of an FFT, to obtain the S-parameters. A networking formulation was then derived to utilize these S-parameters such that the frequency-dependent S-parameters for the entire length of the transmission lines could be obtained.

These circuits were fabricated on a multilayer test coupon and measured with an HP8510 network analyzer; good agreement was observed between the simulated and measured results.

A QUASI-STATIC MODEL FOR FUZZ BUTTON INTERCONNECTS

G. Pan and X. Zhu*
University of Wisconsin-Milwaukee
Milwaukee, WI 53201

B. Gilbert
Mayo Foundation
Rochester, MN 55905

R. Eden
GigaBitLogic
Newbury, CA 91320

In multilayer high speed computer circuit boards, vertical connections between different layers are needed. One method for connecting the layers is the fuzz button, a vertical interconnect with an approximate 20 mil diameter hole, filled with a long thin piece of gold alloy wire crushed into a tiny ball. The fuzz button is flexible during assembly and it has a high potential of integrating (with alternating vias) up to 50 substrate layers.

In this study of the high frequency electrical characteristics of these fuzz buttons, we first applied image theory and the magnetic current concept to obtain the electric potential equation on the surface of the conductor. We then set up a second equation, namely, the normal components of displacement vector are continuous across a dielectric-to-dielectric interface. These two equations were solved by the method of moments, so that charge and current distributions along the fuzz buttons and vias were found. Finally, these static parameters were imposed to model signal propagation along the vertical paths; in addition, waveform distortion and cross-talk were evaluated. Lastly, the time-domain waveforms were transformed into the frequency domain by means of an FFT, and the S-parameters for the fuzz button structures were obtained.

Single Path Millimeter Wave Attenuation Through Linearly Graded Moving Rectangular Spot Illumination Semiconductor Panel Which is Used In Millimeter Wave Image Convertor

M. H. Rahnavard
A. Bakhtazad
EE Dept.
School of Engineering
Shiraz University
Shiraz, Iran

Moving Spot illuminated semiconductor panels are used as millimeter wave image convertors. To determine the performance of this system, it is required to know the response of illuminated semiconductor panels. Response of moving strip and uniformly rectangular illumination semiconductor panel are studied by Rahnavard and Bakhtazad. In these cases there is a lag between the maximum of the response with the position of the illumination spot on the panel. This lag will degrade the resolusion of the system. In this paper it is shown that it is possible to compensate the lag and improve the resolusion of the system using linearly graded illumination along the moving illumination spot.

High Frequency Devices, Waveguides and Interconnections

Room 3010 Salle URSI D Session 107

Dispositifs, guides d'ondes et interconnexions hautes fréquences

Chairs/présidents: M. SHUR, USA

13:30 (107.1) P-I-P+ Buffer Structure for Submicron Gate Modfets, M. KANAMORI[1], G. JENSEN[1], **M. SHUR**[1], K. LEE[2], [1] *University of Virginia, Charlottesville, VA, USA;* [2] *KAIST, Seoul, Korea*

13:50 (107.2) InGaAs Diodes for Terahertz Mixers with Low LO Power Requirements, **R.J. MATTAUCH**, T. BRENNAN, U. BHAPKAR, *University of Virginia, Charlottesville, VA, USA*

14:10 (107.3) α-Silicon Carbide Junction Field Effect Transistors, **G. KELNER**[1], M. SHUR[2], S. BINARI[1], K. SLEGER[1], J. PALMOUR[3], [1] *Naval Research Laboratory, Washington, DC,* [2] *University of Virginia, Charlottesville, VA, and* [3] *Cree Research Inc., Durham, NC, USA*

14:30 (107.4) Analysis of Millimeter Wave Integrated Balanced Mixers, **K. SUN**[1], D.-F. LI[2], D. WU[2], [1] *Jackson State University, Jackson, MS, USA;* [2] *University of Science and Technology of China, Hefei, China*

14:50 (107.5) Analysis and Experimental Results on Multiple Gunn Diode Power Combining Oscillators, A. MORTAZAWI[1], **H. FOLTZ**[2], T. ITOH[2], [1] *University of Central Florida, Orlando, FL, and* [2] *University of Texas, Austin, TX, USA*

15:10 **COFFEE/CAFÉ**

15:30 (107.6) Unified Model for Non-Uniformly Doped Microwave GaAs MESFETS, K. KIM, M. SHUR, **T.A. FJELDLY**, *University of Virginia, Charlottesville, VA, USA*

15:50 (107.7) Analysis of Coupled Lossy Transmission Lines with Nonlinear Terminal Networks, **G. PAN**[1], G. WANG[1], B. GILBERT[2], [1] *University of Wisconsin, Milwaukee, WI, and* [2] *Mayo Foundation, Rochester, MN, USA*

16:10 (107.8) Calculation of Attenuation in Waveguides with General Cross-Sections Using the Finite-Element Method, **G.W. SLADE**, K.J. WEBB, *Purdue University, West Lafayette, IN, USA*

16:30 (107.9) Dispersion and Circuit Properties of Striplines on Anisotropic Substrates: Numerical and Experimental Results, **G.W. SLADE**[1], L. CARIN[2], K.J. WEBB[1], [1] *Purdue University, West Lafayette, IN, and* [2] *Politechnic University, Farmingdale, NY, USA*

16:50 (107.10) Study of Several Low-Pass Filter in Microstrip Line Applying Modal Analysis in the Spectral Domain, **A. CASANUEVA**, J.L. GARCÍA, *Universidad de Cantabria, Santander, Spain*

D107.1

P-I-P+ BUFFER STRUCTURE FOR SUBMICRON GATE MODFETS

Mikio Kanamori, Geir Jensen, Michael Shur*, and Kwyro Lee#
Department of Electrical Engineering, Thornton Hall, University of Virginia,
Charlottesville, VA 22903-2442, USA
#Department of Electrical Engineering, KAIST, Seoul, Korea

In order to reduce the two major problems of a limited threshold voltage controllability and short channel effects in submicron gate MODFETs, we propose to use a p-i-p+ structure in the buffer. The p-layer is adjacent to the channel and the p+-layer is located fairly far from the channel. This structure decreases the potential of the buffer under the channel, which reduces the current in this region. The p+-layer has the additional purpose of allowing to adjust the threshold voltage by changing the potential of the p+-layer externally.

The 2-d electron gas density, n_s, was calculated as a function of the gate voltage for varying p+-layer bias using a self-consistent one-dimensional procedure for 2-d electron density, subband levels, and electrostatic potential for a δ-doped AlGaAs/GaAs structure with p-i-p+ buffer. It was observed that the threshold voltage can be easily controlled by the bias applied to the p+-layer. This controllability significantly reduces the process requirements for threshold voltage uniformity. It should be noted that the maximum 2-d electron gas density, n_{smax} becomes limited when the distance between the channel and the p+-layer decreases. Moreover, the gate capacitance at gate voltages below the threshold voltage increases with a reduction in the same distance. In addition, the p-layer doping density must be restricted to approximately $1.5 \times 10^{11} cm^{-2}$ for the same reason.

Using a p-i-p+ structure optimized from the above considerations, we calculated I-V characteristics for a 0.3μm gate length δ-doped AlGaAs/GaAs MODFET with self-aligned n+ source and drain regions by ensemble Monte Carlo simulation. Fig. 1 shows the pronounced improvement in the confining nature of the potential distribution in the buffer. The net result is a reduction of the output conductance in saturation by about 80 % compared to a conventional buffer device.

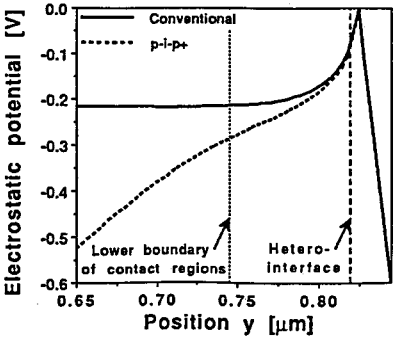

Fig.1. Electrostatic potential vs. perpendicular position y at a lateral position 0.08 μm into the device channel. The resulting improvement in electron confinement to the channel is obvious.

InGaAs DIODES FOR TERAHERTZ MIXERS WITH LOW LO POWER REQUIREMENTS

Robert J. Mattauch*, Theresa Brennan, and Udayan Bhapkar
Semiconductor Device Laboratory, Department of Electrical Engineering,
University of Virginia, Charlottesville, VA 22903-2442, USA

Sufficiency of local oscillator power for space-based heterodyne receivers operating in the submillimeter wave range is a continual problem. Sources such as carcinotrons or molecular lasers which provide ample power are massive, costly, and power intensive. Solid state sources consisting of a fundamental oscillator, such as a Gunn diode, used in conjunction with a varactor frequency multiplier chain have been shown to yield power in the sub-millimeter wave range. The output power of such a source, however, decreases monotonically with increasing frequency. Efforts are presently underway to provide greater output power from such solid-state sources.

The mixer element of choice for submillimeter wave receivers is the Schottky barrier diode which has been fabricated historically from GaAs. Such devices placed in an antiparallel configuration can be employed in a harmonic mixer. Such an arrangement will require LO power at approximately one-half the signal frequency, thus easing the high power-high frequency burden. This burden can be eased even further by reduction of the forward turn-on voltage of the antiparallel mixer diode pair. This is expected to result in a decreased LO power requirement.

Use of $In_xGa_{(1-x)}As$ in place of GaAs for fabrication of mixer elements will decrease the diode forward turn-on voltage in proportion to the indium mole fraction, x. This is accompanied however by an increase in device reverse saturation current. This paper presents a summary of a preliminary generalized barrier transport analysis resulting in a diode current-voltage relationship, the use of that relationship in a mixer analysis program similar to that of Siegel and Kerr (IEEE Trans. MTT, 28, No. 3, 275-276, March 1980), and resulting prediction of a reduction in mixer LO power needs. In addition, preliminary results will be presented on the technology necessary for fabrication of $In_xGa_{(1-x)}As$ devices along with experimentally determined electrical characteristics.

D107.3

α–SILICON CARBIDE JUNCTION FIELD EFFECT TRANSISTORS

G. Kelner*, M. Shur,S.Binari, K. Sleger, and J. Palmour*****

Naval Research Laboratory
Washington DC 20375-5000
**Department of Electrical Engineering
University of Virginia
Charlottesville, VA 22903-2442
***Cree Research, Inc., Durham, NC 27713

We report the results of the experimental study of α-SiC JFETs with high-pinch voltages (40-45 V) in the temperature range from 24 °C to 400 °C. The structure used for fabrication of these devices employs a N -doped hexagonal α-SiC layer epitaxially grown on a p-type Al-doped α-SiC film. Epitaxial layers of 6H α-SiC were grown on the Si face of unintentionally doped n-type α-SiC substrates. Fabricated devices with 4 μm gate length have a maximum transconductance (g_m) in the saturation region of 17 mS/mm and a maximum drain saturation current (I_{dss}) of 450 mA/mm at room temperature. This value of the transconductance is the highest reported for devices of similar structure. Devices are completely pinched-off at a gate voltage of -40 V. Using a "square-law" model, we extract the values of the effective electron field effect mobility and source and drain series resistances. In spite of smaller mobility in the channel (240 cm^2/Vs compared to about 500 cm^2/Vs for β–SiC JFET at room temperature), we achieved similar values of transconductances for similar device geometries. This was achieved by optimizing the device design, i.e. by using devices with smaller channel thickness and higher carrier concentration in the channel. The extracted values of the series source and drain resistances are quite high and we predict a drastic improvement in the device performance (especially for short channel devices) if the ohmic contact resistance is decreased. The device transconductance drops with temperature increase because of the decreasing electron mobility. The values of the electron mobility extracted from the measured values of the device transconductance and channel conductance are in good agreement with independently measured Hall data. Based on our experimental data, we compare the performance of α-SiC and β-Sic JFETs.

Analysis of Millimeter Wave Integrated Balanced Mixers

Kunquan Sun, Duen-fu Li*, and Duan Wu*

School of Science and Technology
Jackson State University, Jackson, MS 39217

*Department of Radio and Electronics
University of Science and Technology of China
Hefei, Anhui, The People's Republic of China

The purpose of this paper is to present a study of a simplified model for millimeter wave integrated balanced mixers. A single diode model has been developed in terms of current distributions in all sidebands, power dissipated by series resistances, and energy stored by series inductances and package capacitances. The single diode model reduces 3N+1 port network to N+1 port network, where N is the total number of sidebands used in the model. Our results show a good agreement with the published data.

This simplified model was used to analyze integrated balanced mixers at the different millimeter wave bands. The effect of non-linear junction capacitance, parasitic parameters on conversion loss, and input and output impedances were studied. It was found that the non-linear junction capacitances of millimeter wave diodes may improve the conversion loss of millimeter wave balanced mixers. Experimentally, we have developed 8mm and 6mm band integrated balanced mixers which utilized large non-linear junction diodes. The results have shown improvement of double side band noise figures compared with those using relatively small non-linear junction diodes. This might be the evidence of the above conclusion. Further experimental study is being undertaken in order to completely support the conclusion.

D107.5

ANALYSIS AND EXPERIMENTAL RESULTS ON MULTIPLE GUNN DIODE POWER COMBINING OSCILLATORS

Amir Mortazawi
Dept. of Electrical Engineering
Univ. of Central Florida, Orlando, FL 32816

Heinrich Foltz* and Tatsuo Itoh
Electrical Engineering Research Laboratory
Univ. of Texas, Austin, TX 78712

Structures consisting of negative resistance devices placed periodically along a transmission line have proven to be an efficient means for microwave power combining. The power can either be delivered to a load at one end of the transmission line, or radiated from an antenna connected to each device and combined in free space. Such circuits are planar and require no external resonators or back-reflectors, and are thus suitable for monolithic fabrication.

Design considerations for periodic power-combining oscillators will be presented, including experimental determination of large-signal device parameters, application of large-signal parameters to circuit design, selection of tuning structures, and limitations to the number of devices that can be used.

Because of the large-signal operation and the strong coupling between the devices, the usual small-injection analysis of the locking properties is not sufficient. Accurate analysis requires self-consistent nonlinear calculations. We will present results of computations using a relaxation-based solution of the harmonic balance equations. The relaxation method has been adapted to allow efficient analysis of multiple device oscillators under both free-running (self-injection locked) and externally-injection locked conditions. The results give information on power level, harmonic generation, tunability, and locking.

Data from several experiments on planar periodic power combiners will be discussed. Past experiments with X-band Gunn diodes mounted along a microstrip transmission line have resulted in power combining efficiencies in excess of 100% , with good locking and stability characteristics.

UNIFIED MODEL FOR NON-UNIFORMLY DOPED MICROWAVE GaAs MESFETS.

Kisang Kim, M. Shur, and T. A. Fjeldly *.
Department of Electrical Engineering, University of Virginia
Charlottesville VA 22903-2442 USA (804)-924-6109
*On leave from the Norwegian Institute of Technology, University of Trondheim,
Trondheim, Norway

We have developed a new model for non-uniformly doped GaAs MESFETs which describes both below and above threshold regimes of device operation using one unified expression for the effective differential channel capacitance. This capacitance is represented as a series connection of the depletion capacitance and the capacitance corresponding to the charge induced into the depletion layer at voltages below the threshold voltage. The model accounts for the series drain and source resistances, velocity saturation in the channel, finite output conductance in the saturation regime, shunt substrate resistance, and for the kink effect which is usually important in submicron devices. The model parameters, such as the effective channel mobility, threshold voltage, pinch-off voltage, saturation velocity, channel thickness, etc. are extractable from in-situ experimental data. In case of a uniform profile, the model is analytical; for a non-uniform profile, a numerical integration (with no iterations) is generally required. This makes the model very suitable for the incorporation into a circuit simulator and for the design of microwave GaAs MESFETs. We apply our new characterization procedure to several devices fabricated at different laboratories and obtain an excellent agreement with our experimental data. Based on the model, we compare the cutoff frequencies of GaAs MESFETs and pseudomorphic InGaAs/AlGaAs Heterostructure Field Effect Transistors and demonstrate advantages of thin highly doped channel devices grown on moderately doped p-type buffer layers.

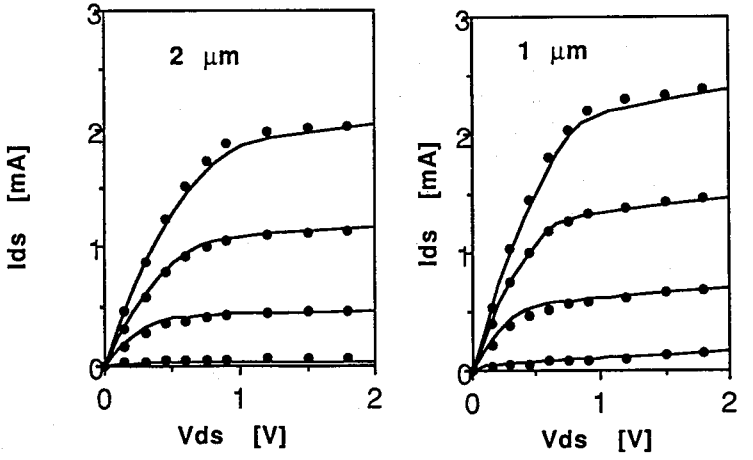

Measured (dots) and calculated (solid lines) I-V characteristics of 2 μm and 1 μm gate GaAs MESFETs. W=20 μm, top curve Vgs=0.2 V step - 0.4V. All parameters used in the calculation are extracted from our experimental data.

D107.7

ANALYSIS OF COUPLED LOSSY TRANSMISSION LINES WITH NONLINEAR TERMINAL NETWORKS

G. Pan and G. Wang*
University of Wisconsin-Milwaukee
Milwaukee, WI 53201

B. Gilbert
Mayo Foundation
Rochester, MN 55905

Multiple transmission lines with skin-effect losses and dispersive characteristics were analyzed by the Finite Difference Time Domain (FDTD) and the spectral domain methods, and the S-parameters of the transmission lines were obtained. These S-parameters were then transformed by the inverse FFT into the time-domain. The scattering matrix representation is multiplicative in nature, which leads to the time-domain formulation as a set of convolutional integrals.

Instead of attempting to solve a set of coupled convolutional integral equations by the Newton-Raphson method (which is very difficult, especially for multiple variables), we generated a set of object functions and applied a multivariable optimization technique to attain the solutions. The new method, which is quite general, reduces to the special cases derived in many previous publications. For instance, if only a single dispersive transmission line is considered, this method gives the same results as (Q. Gu et al., Journal of EM Waves and Applications, vol. 3, No. 3, 183-197, 1989 and R. Veghte & C. Balanis, IEEE MTT-34, 6, 1427-1436, Dec. 1986). Our results are also identical to those of multiple transmission lines with frequency dependent losses, but without dispersion (A. Djordjevic et al., IEEE MTT-34, 6, 660-666, June, 1986 and J. Schuti & R. Mittra, IEEE MTT-36, 3, 529-536, 1988). The new method solves the most general cases of coupled lossy transmission lines with nonlinear terminations.

CALCULATION OF ATTENUATION IN WAVEGUIDES WITH GENERAL CROSS-SECTIONS USING THE FINITE-ELEMENT METHOD

G. William Slade* and Kevin J. Webb
School of Electrical Engineering
Purdue University
West Lafayette, IN 47907

The trend toward both larger and more dense integrated circuits results in many longer thinner interconnects between devices with resulting increased losses. Such losses in electrical interconnects due to imperfect dielectrics and conductors becomes more of a concern as signaling speeds and operating frequencies increase.

A method of computing losses due to material losses in microwave transmission lines has been developed. This technique is based on a perturbational approach to loss. The novelty of this work centers on the use of the finite element method for finding the field solution for the lossless general waveguide problem (G. Slade and K. Webb, *IEEE Trans. Magnetics,* July 1989, pp. 3052-3054). A variational vector magnetic field formulation is used, from which field and equivalent transmission line parameters for each mode can be determined. Dissipation in conductors and dielectrics is then determined allowing the attenuation per unit length to be found. The conductor loss is approximated by using a skin-effect model similar to Wheeler's incremental inductance rule. Dielectric loss is given in terms of a non-zero material conductivity. In order to generate losses using this model, dielectric loss tangents and conductor surface impedances from the skin effect model are assumed to be known for the frequencies of interest. Some examples of lossy structures will be presented. In particular, lossy microstrip will be the focus of the discussion.

In addition to the perturbational loss scheme, notes and available results will be presented on a rigorous finite element formulation in which dissipation is explicitly included in the wave equation. In this case it is necessary to solve a complex eigenvalue problem or perform a time-domain iteration (D. Lynch, et al., *IEEE Trans. Antennas Propagat.,* Dec. 1990 pp. 1933-1942).

D107.9

DISPERSION AND CIRCUIT PROPERTIES OF STRIPLINES ON ANISOTROPIC SUBSTRATES: NUMERICAL AND EXPERIMENTAL RESULTS

G. William Slade*♣, Lawrence Carin♣, and Kevin J. Webb♣

♣ School of Electrical Engineering
Purdue University
West Lafayette, IN 47907

♣ Department of Electrical Engineering and Computer Science
Polytechnic University
Farmingdale, NY 11735

Numerical investigations into the dispersion and impedance characteristics of striplines on substrates exhibiting transverse uniaxial anisotropy are presented here. These parameters are generated from a finite-element solution of the enclosed microstrip problem (L. Carin, G. Slade and K. Webb, 1990 MTT-S Digest, pp. 677-680). The field solution is reduced to a circuit solution via Ampere's Law and the integration of the Poynting vector. Results will be presented illustrating the apparent "mode transitions" involving the quasi-TEM mode found in Epsilam-10 and, furthermore, information will be given on the possibility of similar mode properties in sapphire substrates. In addition to the numerical work, results of phase constant measurements performed on microstrip with an Epsilam-10 substrate will be presented.

STUDY OF SEVERAL LOW-PASS FILTER IN MICROSTRIP LINE APPLYING MODAL ANALYSIS IN THE SPECTRAL DOMAIN

A. Casanueva*, J.L. García*

* Dpto. Electrónica, Lab. Microondas. Univ. CANTABRIA - SPAIN
** This work has been supported by Spanish Government (CICYT N° PA86-0372-CO3-02)

An abrupt change in microstrip linewidth, is a discontinuity that appears frequently in MMICs, such as, stepped impedance transformers and matching networks for example. Therefore, the accurate description of these step-discontinuties is important for the computer-aided design of hybrid and monolithic MICs. It is the aim of this work to describe cascades of step discontinuities which constitute a basic configuration in the design of integrated microwave circuits.

In this paper we have applied modal analysis in the spectral domain to the analysis of simple and cascaded step discontinuities. We have studied the mode set that appears in a boxed microstrip, including complex modes, in applied to expanded the E-field at both discontinuity sides. When we have cascade discontinuities we have to characterize it in terms of the generalized scattering matrix. All microstrip modes, fundamental, higher and compex modes are included in this analysis.

The validity of our method has been checked by analyzing various low-pass filters, 8 GHz, 13 GHz and 15 GHz cut frequency, made up of cascades of microstrip discontinuties. The results theoretical for frecuency response of low-pass filters provide an excelent convergence a good agreement to the experimental ones.

Natural Impulsive and Spectral Noise and Propagation Effects

Room 3010 Salle URSI E Session 40

Bruit spectral et impulsif naturel et effets de la propagation

Chairs/présidents: D.V. GIRI, USA

08:30 (40.1) ELF/VLF Magnetospheric Noise at High Latitudes and Its Significance for Radio Communications, **A.C. FRASER-SMITH**, R.A. HELLIWELL, *Stanford University, Stanford, CA, USA*

08:50 (40.2) Terrestrial and Planetary EM Noise, **E.K. SMITH**, *University of Colorado, Boulder, CO, USA*

09:10 (40.3) Analytic Description of Wave Beams Propagation in the Waveguide Earth-Ionosphere with Asymmetric Distribution of Conductivity, **N.I. PETROV**, I.N. SISAKIAN, *USSR Academy of Sciences, Moscow, USSR*

09:30 (40.4) Diffraction of VLF Modes by the Antarctic Ice Cap – An Analytical Model, **J.R. WAIT**, *Tucson, AZ, USA*

09:50 (40.5) On the Functional Dependencies Between Parameters of Leader in Lightning, **N.I. PETROV**, G.N. PETROVA, *All-Union Electrotechnical Institute, Moscow, USSR*

10:10 **COFFEE/CAFÉ**

10:30 (40.6) Measurements of Environmental Fields Using Broadband Active Sensors, **A. THANSANDOTE**, S.S. STUCHLY, P.J. KWASNIOK, *University of Ottawa, ON, Canada*

10:50 (40.7) Preliminary Results from a Broadband EM Test of a C3 System, K. CALLAHAN[1], **M. DINALLO**[2], [1]*Los Alamos National Laboratory, Los Alamos, NM, and* [2]*Quatro Corporation, Albuquerque, NM, USA*

11:10 (40.8) Simulation of the Electromagnetic Pulse Influence on the Cylindric Objects, **L.B. VAVRIV**, N.I. ZHUK, *Ukrainian Academy of Sciences Kharkov, USSR*

11:30 (40.9) MHD-EMP Effects on Long Lines, **IR. R. MIDDELKOOP**, *TNO, The Hague, The Netherlands*

11:50 (40.10) Monitoring Man-Made Radio Emissions Below 10 GHz, **M. PRICE**, *University of New Mexico, Albuquerque, NM, USA*

E40.1

ELF/VLF MAGNETOSPHERIC NOISE AT HIGH LATITUDES AND ITS SIGNIFICANCE FOR RADIO COMMUNICATIONS

A.C. Fraser-Smith* and R.A. Helliwell
STAR Laboratory, Stanford University,
Stanford, California 94305

Radio noise in the ELF/VLF band (10 Hz - 30 kHz) at all locations on the earth's surface is characteristically produced by lightning in the lower atmosphere, and it consists predominantly of a series of impulses, or sferics. At high latitudes, however, additional strong noise signals are observed that originate in the magnetosphere. A particularly strong and commonly occurring form is polar chorus, which may be described as band-limited hiss with rising tones. It typically occurs in the frequency range 300 Hz to 2.0 kHz. The other strongly occurring ELF/VLF noise is auroral hiss. Measurements of ELF/VLF radio noise we are currently making in Greenland and in the Antarctic indicate that auroral hiss occurs less often than polar chorus, but when it does occur it can fill the entire ELF/VLF band. Both these forms of radio noise can strongly influence the conventional noise statistics we are deriving from our measurements. The 'voltage deviation' statistic, or V_d, for noise measurements in the range 300 Hz to 2.0 kHz, is characteristically strongly reduced when polar chorus occurs. At higher frequencies, the auroral hiss has to be exceptionally strong to completely mask the sferics that typically are dominant in the VLF range, and thus its influence on the noise statistics tends to be less marked than that of polar chorus in its much narrower frequency range, but it has the potential to degrade communication and navigation transmissions at high latitudes. We will present a number of examples of polar chorus and auroral hiss measurements made at our high latitude stations, and we will show the 'signatures' that the two noise forms produce in our noise statistics.

TERRESTRIAL AND PLANETARY EM NOISE

Ernest K. Smith
NASA Propagation Information Center
Electrical and Computer Engineering
University of Colorado
Boulder, Colorado 80309

This talk will describe the progress and future needs of the URSI Commission E Working Group on Terrestrial and Planetary Electromagnetic Noise. This Working Group was established at the URSI XXIII General Assembly, Prague August 28-September 5, 1990 under the chairmanship of Professor M. Hayakawa of Nagoya University and myself. The objectives of this WG as summarized in its first newsletter (December 1990), prepared by Dr. Hayakawa are:

1. The study of characteristics of terrestrial noise in the frequency range ULF through EHF (1 Hz to 300 GHz).
   (a) General characteristics of terrestrial noise of both natural and man-made origins.
   (b) The statistical description and modeling of these types of terrestrial EM noise.
   (c) The physical processes and mechanisms involved in the generation of the various types of terrestrial noise.
2. The study of planetary noise.
   (a) The general characteristics of planetary and other extraterrestrial EM noise sources at frequencies above 2 MHz.
   (b) The physical processes involved in the generation of planetary EM noise.
   (c) The comparative study of other planetary noise environments and the terrestrial one.

The author is particularly interested in the development of these objectives in terms that may be helpful to the CCIR in future revisions of its Report 720 "Radio Emission From Natural Sources Above About 50 MHz" . This talk will focus on computer representations of noise from the clear atmosphere, from rain, and from clouds.

E40.3

ANALYTIC DESCRIPTION OF WAVE BEAMS PROPAGATION IN THE WAVEGUIDE EARTH-IONOSPHERE WITH ASYMMETRIC DISTRIBUTION OF CONDUCTIVITY

N.I.Petrov, I.N.Sisakian
Central Designer's Office of Unique Instrument Building of the USSR Academy of Sciences, Butlerova str.15, 117342 Moscow, USSR

It is known that the effective method for the analysis of propagation of HF radiation in the waveguide Earth-Ionosphere turn out to be the expansion of field in the Gaussian beams. However the Gaussian beams are optimal only in the waveguides with the symmetric distribution of conductivity. But the waveguide Earth-Ionosphere has the asymmetric distribution of conductivity.

In this paper the analytical solutions of the wave equation localized around the rays trajectories propagating in the waveguide Earth-Ionosphere with asymmetric distribution of conductivity are finded. It is shown that the such solutions of the wave equation are the coherent states which well known in quantum mechanics. Coherent States have minimal possible width and diffractional angle divergence. These states allows the notion of width of geometrical ray naturally to be introduced and the connection between the wave description and geometrical optics clearly to be observed.

Analytical expressions for the width of a rays in the dependence on the longitudinal coordinate also are obtained. It is shown that the different values of divergences at the any distance in the dependence on the initial conditions of the source (angle of slope, heigth over the Earth surface) and a width of the beam may be obtained.

Such approach proves to be effective also for the calculations of more complicated fields by the summing up method. The method may be easily transfered on the case of longitudinal inhomogeneous waveguide. Note that the coherent states are the generating functions for the modes of the waveguide. The quantum mechanical methods for the calculation of energy transformation between the modes caused by the day-night height asymmetry are used. It is shown that the knowledge of experimentally obtained intensities of two first modes makes it possible to determine the displacement parameters between the day and night waveguides.

DIFFRACTION OF VLF MODES BY THE ANTARCTIC ICE CAP -AN ANALYTICAL MODEL

James R. Wait
2210 East Waverly
Tucson Arizona 85719 USA

There is mounting evidence that VLF(very low frequency) radio waves will be highly attenuated when the path traverses the Greenland or Antarctic ice caps(S.Westerlund,F. Reder, Jour. Atmos. Terr. Phys.35, 1475,1973 and F.J.Kelly, F.J.Rhoads, et al,Radio Science, 23,240, 1988). Attenuation rates 10 or 20 times normal rates of 2 dB/1000 km over sea water are not uncommon. In fact, we might say the ice caps are electromagnetically opague. Indeed, it has been observed that actually the propagation path will deviate around the edge of the ice cap(R.Barr, Jour. Atmos. Terr. Phys. 49, 1, 1987). Barr's remarkable data were taken on a flight from Christchurch to Scott Base employing VLF transmissions from La Reunion Island and from Argentina.

In the present paper, we examine an idealized theoretical model attempting to give a semi-quantitive explanation of the phenomena particulary with reference to the Antarctic paths. Our first step is to develop an effective boundary condition which characterizes the complex ratio of the vertical electric field and the magnetic field tangential to the contour of the coast line. We show this ratio has a magnitude somewhat greater than 377 ohms,the characteristic impedance of free space. Then, at least for a circularly shaped ice cap, we can develop a scattered mode expansion which becomes computationally manageable if we apply the well known Watson transform technique. Thus, while retaining the usual "vertical" modes, we obtain a creeping wave representation for the "horizontal" behavior of the diffracted fields. An interesting case arises when the geometrical great circle path just grazes the convex coast line of the ice cap. In agreement with Barr, the received signal is then of the order of 3 dB below the signal for the unobstructed path for the same over sea water conditions.

E40.5

ON THE FUNCTIONAL DEPENDENCES BETWEEN PARAMETERS OF LEADER IN LIGHTNING

N.I.Petrov, G.N.Petrova

All-Union Electrotechnical Institute, Krasnokazarmennaj str.12, 111250 Moscow, USSR

Examination of the leader discharge modelling a lightning is of interest from the practical aspects, in particularly, the lightning radiation may be used for investigation of ionosphere and earth resources. In present a series of experimental dependences between the different parameters of the leader discharge in the laboratory are known. However the extrapolation of these dependences on the case of lightning is not always justificated.

In this paper the theoretical dependences between the different parameters of leader are obtained. It is shown that the set of equations describing the leader process to the nonlinear evolution equation may be reduced. Analytical relations between the radius of the leader head and the streamer zone length are obtained. It is shown that the ratio of these values in the stability regime is preserved. The physical mechanism of the instability leading to the formation of the streamer zone is supposed. The instability has the wave nature and is caused by the self-influence effects of the space charge. The nonlinearity of the system caused by the space charge influence leads also to the chance character of the leader propagation direction and branching of lightning channel. Using a stability condition of the leader propagation a dependence of the current across the leader head on the its velocity of moving is obtained. The dependence of the streamer zone length on the gap length is obtained. It is shown that the streamer zone length is saturated with the increasing of the gap length. A correlation between the duration of the return stroke current and the streamer zone length is shown. A physical mechanism of the stepped propagation of lightning is proposed.

MEASUREMENTS OF ENVIRONMENTAL FIELDS USING BROADBAND ACTIVE SENSORS

A. Thansandote*, S.S. Stuchly and P.J. Kwasniok

Laboratory for Electromagnetics and Microwaves
Department of Electrical Engineering
University of Ottawa
161 Louis Pasteur
Ottawa, Ontario, Canada K1N 6N5

Environmental fields generated by lightning, power line surges, electromagnetic pulses and those due to high power switches have broadband spectra and can cause electromagnetic interference to communication systems and computers. Knowledge of the characteristics of these fields is important for design of telecommunication, electronic and computer equipment to achieve minimum susceptibility.

The measurement system consists of an active electric field sensor, an active magnetic field sensor, a high-speed digitizing oscilloscope (HP 54502A) and a portable microcomputer (GRID). The electric field sensor utilizes an electrically small spherical antenna directly coupled to a very high input impedance amplifier and has a flat response with sensitivity of 2.5 mV/(V/m) from 40 Hz to 300 MHz. The magnetic field sensor, consisting of an electrically small loop, a current transformer and a very low input impedance amplifier, operates with constant sensitivity of 180 mV/(A/m) from 1 kHz to 150 MHz. Environmental fields detected by the sensors at a test site are simultaneously displayed on the oscilloscope and transferred to the microcomputer for recording. The recorded data are subsequently analyzed to obtain the waveform of the measured field and its spectrum.

In this paper, the results of environmental field measurements at various transient-source test sites are presented and discussed.

E40.7

PRELIMINARY RESULTS FROM A BROADBAND EM TEST OF A C3 SYSTEM

Ken Callahan
Los Alamos National Laboratory
AT-9 MS H851
Los Alamos, NM 87545

Mike Dinallo*
Quatro Corporation
4300 San Mateo Blvd., NE
Suite B-290
Albuquerque, NM 87110

A communications system was tested from 1MHz to 1GHz using both continuous wave and pulsed environments. The purpose was to develop transfer functions for test points deep within the electronics for assessment of effects in various hypothetical EMP environments. The broadband simulated environments will be presented along with the details of probe swept frequency characterization and measurement compensation. Incident field and probe bandwidth limitations will be discussed. Pulsed and cw transfer functions will be compared and some will be shown to have significant "pass bands" at frequencies above 100MHz.

SIMULATION OF THE ELECTROMAGNETIC PULSE INFLUENCE ON THE CYLINDRIC OBJECTS.

L.B.VAVRIV,N.I.ZHUK
Research and project-design institute "MOLNIJA" under Kharkov Politechnical Institute,47 Shevchenko St.,310013 Kharkov,The Ukraine,USSR.

The paper presents the solution of the problem of the EMP dissipation on the cylindric inhomogeneities in the microstrip line.

In the thin-wire approximation the problem is reduced to the solution of integral equation relative to the spectral components of the induced current.The analytic solution of the equation is obtained by the method of sequantial approximations The compact formulae for the natural waves amplitudes have been suggested.In application to the symmetric and antisymmetric current components the direct formulae for the resonant frequencies and for the object lengths embracing the resonances both of the lower and of the higher types have been determined The regularities of shaping the induced current in the resonance and nonresonance excitation regimes have been investigated.

The systematic investigation of the dissipation of the electromagnetic pulses produced by the lightning has been carried out. The calculations results of the currents induced on the objects were compared with the results for the case of pulses dissipation on the object located in the free space.

Thus,the simulation authenticity of the lightning pulse influence on the objects having the form of cylinder or parallelepiped using the microstrip line as a field forming system has been studied.The parameters correlation of the dissipated pulse with the dimensions of the objectand the field-forming system at which the requiredsimulation authenticity is reached has been determined.

MHD-EMP EFFECTS ON LONG LINES.

Ir. R. Middelkoop
Physics and Electronics Laboratory TNO
P. O. Box 96864, NL-2509 JG Den Haag, The Netherlands

A nuclear detonation, high above the earth atmosphere causes a fast rising electromagnetic pulse (EMP) on the surface over a vast area. This pulse is followed by a much slower pulse that produces similar effects as a geomagnetic storm: the MHD-EMP (Magneto-Hydro- Dynamic EMP). An EMP couples large currents into electrical conductors and threatens the connected electronic systems. The magnitude, the direction and the time history of the produced MHD-EMP is rather complex. The amplitude differs according to the exact location. For a "reasonable worst case" analysis, however, small areas can be identified around the ground zero point of the burst over which the field strength is constant. The frequency spectrum contains only low-frequency components, typically below 1 Hz. So, the electromagnetic field will couple preferably with a system of large dimensions. The electric power system and the telephone system, both using long lines, are potential victims. Coupling of the MHD-EMP can essentially be modelled with a DC excitation on a DC resistive network.

Figure 1 shows an example for a typical part of the power grid. The large near-DC currents that are induced by MHD-EMP in above ground power lines cause problems to the connected power transformers. The extra magnetization current shifts the transformer working point which yields harmonic generation and possible insulation damage. Triangle-switched 3-phase transformers isolate the induced currents.
Long shielded underground telephone cables are relatively unaffected by MHD-EMP as long as a good ground connection is provided on both cable ends. The current on the inner wire pairs can be isolated by a signal transformer if need be.

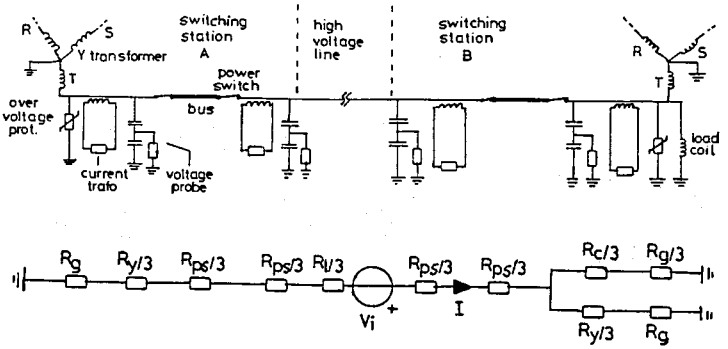

Figure 1. Quasi-static MHD-EMP model of an electric power grid.

MONITORING MAN-MADE RADIO EMISSIONS BELOW 10 GHz

Marcus Price
Department of Physics and Astronomy
University of New Mexico

With the ever increasing use of the radio spectrum it is becoming more important to understand the radio noise environment. This is especially so for incidental and non-intentional radiation from FCC Part 15 devices. Increasing numbers of consumer products are using RF and digital techniques and are potential sources of RFI, especially to passive radio services. Monitoring RF emissions has generally been an expensive research-type task requiring sophisticated equipment and personnel. However, advances in the technology of communications receivers and personal computers now make it possible to build and operate RF monitors at a fraction of the cost of previous systems. At frequencies above 2 GHz, where lower noise receiver systems are required, room temperature HEMT pre-amplifiers may provide a practical solution. Antenna systems remain a challenge and depend upon sky coverage (e.g. horizon vs. whole sky) and degree of desired accuracy in gain calibration. A proposed RF monitoring radiometer system will be described.

Manmade EM Environment (EMI/EMC/EMF) | **Room 3010 Salle URSI E Session 56** | **Environnement électromagnétique artificiel (BEM/CEM/TEM)**

Chairs/présidents: J.P. CASTILLO, USA

13:30 (56.1) Potential for a Unified Topological Protection Approach to Electromagnetic Environments (EME), G. BAKER[1], **J.P. CASTILLO**[2], [1]*Defense Nuclear Agency, Washington, DC, and* [2]*R and D Associates, Albuquerque, NM, USA*

13:50 (56.2) Trends in Wireless Communication Technologies - The Issue for Improving Spectrum Utilization, **D.J. COHEN**, *National Telecommunications and Information Administration, Annapolis, MD, USA*

14:10 (56.3) EM Scattering from a Vertical Column of Ionization in the Earth Ionosphere Waveguide, **J.R. WAIT**, *Tucson, AZ, USA*

14:30 (56.4) Lightning Location System Evaluation Techniques, **D.N. MARCH**, P. PONCA, *Montana State University, Bozeman, MT, USA*

14:50 (56.5) The Electromagnetic Environment in Hospitals, **P. BOISVERT**, T.J.F. PAVLASEK, B. SEGAL, *McGill University, Montreal, PQ, Canada*

15:10 **COFFEE/CAFÉ**

E56.1

POTENTIAL FOR A UNIFIED TOPOLOGICAL PROTECTION APPROACH TO ELECTROMAGNETIC ENVIRONMENTS (EME)

GEORGE BAKER
Defense Nuclear Agency
Washington, D.C.

J. PHILIP CASTILLO*
R and D Associates
Albuquerque, NM

This paper presents an approach to the potential unification of protection technology for a wide spectrum of electromagnetic environments (EME). Of particular interest is the development of consolidated protection practices for complex electronic systems. An electromagnetic topological approach is utilized to develop a consistent shielding protection methodology. First, applicable electromagnetic topological techniques will be presented. Next the characteristics of important EME will be described, including sources internal and external to the system. These EME include the following:

- Electromagnetic Interference (EMI/EMC)
- Lightning
- High Power Microwaves (HPM)
- Nuclear EMP (NEMP)
- Ultra-Wideband Pulse (UWB)

Existing protection practices will be discussed. Incompatibilities and suggested remedies among these practices are presented. Finally, a generalized topological protection approach will be introduced.

TRENDS IN WIRELESS COMMUNICATION TECHNOLOGIES THE ISSUES FOR IMPROVING SPECTRUM UTILIZATION

David J. Cohen
National Telecommunications and Information Administration
Annapolis, Maryland 21401

A number of new wireless communication technologies are being suggested as methods to support our growing information society. Due to the scarcity of spectrum an important requirement for these new technologies is that they utilize the spectrum effectively and efficiently. This paper, for long range spectrum planning applications, reviews these new technologies and examines how these technologies are being designed to improve spectrum utilization. Much of the improvement in spectrum utilization is a result of the continuing trend to convert from analog to digital signals and the application of computer processing to communications.

Some of these methods are based on making better use of the communications channel. These include multiple access techniques such as TDMA, FDMA, CDMA, trunking, packet technology, and dynamic frequency channel sharing methods. Other techniques to improve spectrum utilization result in more information per bandwidth (bits/sec./Hz). These include new modulation methods such as linear, constant envelope and higher order (M'ary). Additionally, improved information capacity of the channel is achieved by coding of the information. Another helpful technique is reducing transmitter power combined with smaller geographical separation between transmitters.

Presently, for many wireless communication applications, an important issue is deciding which of the competing technologies to implement. The paper closes with a description of ongoing research and tests which are underway to help make these decisions.

E56.3

EM SCATTERING FROM A VERTICAL COLUMN OF IONIZATION IN THE EARTH IONOSPHERE WAVEGUIDE

James R. Wait, Consultant
2210 East Waverly
Tucson Arizona 85719 USA

Propagation of VLF(Very Low Frequency) electromagnetic waves in the earth ionosphere wave guide is often modelled by concentric spherical surfaces(J.R.Wait,Electromagnetic Waves in Stratified Media,Pergamon, 2nd.Ed. 1970). Thus mode conversion is usually ignored although the day/night terminator has been treated as a junction between two wave guides with differing widths.Two dimensional modelling has been adequate to analyze this class of problems even where the boundary line makes an arbitrary angle with the propagation path.(J.R.Wait, Jour. Geophys. Res.73, 3537-3548,1968).More recently, it has been suggested that lightning electron precipitation produces significantly increased ionization below the reflection level(Inan and Carpenter, Jour. Geophys.Res. 92,3293-3303, 1987). In such situations,the propagation great-circle path may not intercept the disturbed region,yet,the received field is modified(Dowden and Adams Jour. Geophys. Res.93,11,543-11,550,1988). In fact it has been suggested (R.L.Dowden,personal comm.) that there may be situations where the disturbed region has limited horizontal width compared with , for example, the vertical extension. An extreme example would be a stalactite or tongue of enhanced ionization formed just below the normal reflecting layer. Clearly, as we will show,the incident waveguide propagating modes will individually scatter energy into modes of all orders.We also show that even a modest sized column of ionization will produce field perturbations which are detectable at global ranges.

LIGHTNING LOCATION SYSTEM EVALUATION TECHNIQUES

Dr. Daniel N. March*, Professor
Mr. Peter Ponca, Graduate Student
Electrical Engineering Department
Montana State University

Several unique methods to evaluate lightning location systems which use remote crossed loop direction finders have been developed. The United States Bureau of Land Management lightning location system, made by Lightning Location and Protection, Inc. of Tucson, Arizona, covers the Western part of the U.S., including Montana. Ground truth data showed that the system was missing a substantial percent of the discharges in at least some parts of its coverage area. An isodensity map of the lightning activity in Montana showed areas with low lightning activity whereas other areas showed surprisingly high activity.

An isodensity map of the peak current amplitude, as determined by the system, for the State of Montana showed an inverse relationship to the lightning activity, i.e. areas with low lightning activity had high average peak currents while areas of high lightning activity had low average peak currents. Polar plots were made of each direction finder to show the percent of discharges seen by the direction finder in a particular direction versus those seen by the system. The plots showed that most areas of reported low lightning activity were in areas of poor coverage. Further it was shown that the reported areas of highest lightning activity in Montana were being caused by the system's response to noise. The conclusion is that lightning activity isodensity maps, at least for Montana, based on the BLM data are not valid.

In August of this past summer a privately owned LL&P lightning location system became operational in Northern California using nine direction finders. All of the data from the direction finders were available to the authors. The data were analyzed not only as discussed above but also now responses of the direction finders to events not used in triangulations were available. Again polar plots were made of these signals for each direction finder where the angle was the direction the radiation came from while the magnitude was proportional to the signal amplitude received. There were significant differences in the plots made where only random noise was present and those where there was one or more distinct noise source.

Finally, correlations were made between those lightning events recorded by the private system and those recorded by the BLM system. The correlations were performed in both directions, i.e. what percent of the discharges recorded by BLM were seen by the private system and vice versa. Interesting results were found when the correlation distance and time between discharges being correlated were allowed to vary. Examples of all processed data will be given.

THE ELECTROMAGNETIC ENVIRONMENT IN HOSPITALS

Philippe Boisvert*, T.J.F. Pavlasek, Bernard Segal
Electrical and Biomedical Engineering Dept.
McGill University, Montreal, Quebec, Canada H3A 2A7

The last two decades have witnessed a highly intensifying use of the electromagnetic spectrum, as well as a growing sophistication of medical devices. The sensitivity of these instruments is increasing while patient care depends more and more on their use. The combination of all these factors leads to an increasing concern regarding the reliability of medical devices in such an electromagnetic environment. This paper reports the results of a pilot study whose purpose it was to determine the environment in which medical devices operate.

First, a theoretical prediction of the ambient r.f. electric fields was made in the range of 30 to 1000 MHz using official Department of Communications Canada (DoC) records of radiation characteristics and geographic location of all known, fixed and documented sources. The E field was computed from this data assuming free space propagation.

Next, measurements were carried out simultaneously by the DoC and by the McGill Biomedical Engineering Group on EMC. The DoC group used a laptop-computer-controlled- spectrum analyzer with a folding biconical antenna for frequencies below 300 MHz and a circuit board antenna for frequencies above 300 MHz. All non-broadcast bands from 30 to 1000 MHz were scanned over selected 10 or 100 MHz ranges with $^1/_4$% resolution. Then FM and TV transmitter signals were measured individually. The McGill group used a manually controlled spectrum analyzer with a specially designed broadband, isotropic, triaxial E field probe. Because the measurements were performed manually, only measurements of the fields of known FM and TV stations were made.

Several conclusions can be derived from this pilot investigation. Firstly, the field levels to which sensitive medical devices are subjected in an urban environment are very high, generally in the region of 105-125 dBμV/m but occasionally as high as 135 dBμV/m, and they cover a wide frequency range. Thus, any device whose failure mode makes it susceptible to broadband interference is going to be subject not to one but to several high intensity signals. To better characterize the spectral power density, the Equivalent Electric Field (EEF) was defined as the E field which would result from a single source producing as much power density as the sum of power densities from all the sources in a given band. Although simple in concept, this tool has proved a very reliable indicator of hospital locations where equipment had failed due to EMI. Secondly, predictions of field levels using free space propagation in an urban environment are inadequate. A better propagation model is needed to account for the influence of other buildings, as well as the attenuation due to the structure of the building under study. Thirdly, varying temporal and spatial distributions of signal strength make measurements difficult to repeat and therefore require more attention. Fourthly, the experiments have re-emphasized that the interpretation of the output of a sensing probe in a electromagnetically complex environment such as a hospital room merits a basic research effort. Along with this it is evident that in all cases the three dimensions of the field vector, rather than the one single component usually measured, needs to be determined in such measurements. Finally, an entirely separate investigation needs to be launched to study the mechanisms of medical device failures due to EMI.

Recording and Interpretation of ULF/ELF/VLF Signatures

Room 3028 Salle
Joint URSI E/F/H Session 15

Enregistrement et interprétation des signatures UBF/EBF/TBF

Chairs/présidents: T. WATANABE, Canada; W.M. BOERNER, USA

08:30 (15.1) Review of Research and Observation Results for Seismogenic Emissions in the Last Decade, **T. YOSHINO**, *University of Electrocommunications, Tokyo, Japan*

08:50 (15.2) Induced Piezoelectric Signals from Quartz Veins Measured with a Long-Wire Antenna, **R.D. RUSSELL**, M. MAXWELL, A.W. KEPIC, K.E. BUTLER, *University of British Columbia, Vancouver, BC, Canada*

09:10 (15.3) Observations of Seismo-Electromagnetic Earth/Sea-Quake Precursor Radiation Signatures Along Southern Californian Fault Zones: Evidence of Long Distance Precursor ULF Signals Observed Before a Moderate Southern California Earthquake Episode, J.Y. DEA[1], C.I. RICHMAN[1], **W.-M. BOERNER**[2], [1] *Naval Ocean Systems Center, San Diego, CA, and* [2] *University of Illinois, Chicago, IL, USA*

09:30 (15.4) Geomagnetically Induced Current in the Power Lines in the Northeastern Japan, T. MINAKAWA[1], T. SAITO[2], **T. TAKAHASHI**[2], J. KOBAYASHI[1], O. TAKAHASHI[1], [1] *Tohoku Electric Company Ltd., Sendai, and* [2] *Tohoku University, Sendai, Japan*

09:50 (15.5) Further Geophysical Investigations of Electromagnetic Induction Using Power Lines as the Source, **W.F. SLAWSON**, L.E. FISK, T. WATANABE, *University of British Columbia, Vancouver, BC, Canada*

10:10 (15.6) ULF Waves Excited by Mohican-Cut Type Solar Corona, **T. TAKAHASHI**[1], T. SAITO[1], A. IMASAKI[1], S. MINAMI[2], [1] *Tohoku University, Sendai, and* [2] *Osaka City University, Osaka, Japan*

10:30 (15.7) Observations of ELF Signatures Arising from Space Vehicle Disturbances of the Ionosphere, J.Y. DEA[1], W. VAN BISE[2], E. RAUSCHER[2], **W.-M. BOERNER**[3], [1] *Naval Ocean Systems Center, San Diego, CA,* [2] *Magtek Laboratory, Reno, NV, and* [3] *University of Illinois, Chicago, IL, USA*

10:50 (15.8) Solar Cycle Variation in Diurnal Frequency of Occurrence of Pi2 Pulsations, Y. KOZUKA, T. SAITO, H. TAKEUCHI, **T. TAKAHASHI**, *Tohoku University, Sendai, Japan*

11:10 (15.9) Statistical Study on Characteristics of Pc 3-4 at Synchronous Orbit, H. MATSUOKA, T. SAITO, **T. TAKAHASHI**, *Tohoku University, Sendai, Japan*

11:30 (15.10) Wave Mode of Pi2 Pulsations at Synchronous Orbit Associated with the Substorm Current Wedge, H. TAKEUCHI[1], T. SAITO[1], T. SAKURAI[2], H. MATSUOKA[1], **T. TAKAHASHI**[1], [1] *Tohoku University, Sendai, and* [2] *Tokai University, Hiratsuka, Japan*

11:50 (15.11) Generation and Propagation of the Banded Rising and Falling LF Emissions Observed in the Lower Magnetosphere by EXOS-D(Akebono) Satellite, M. KIKUCHI, H. OYA, **A. MORIOKA**, *Tohoku University, Sendai, Japan*

REVIEW OF RESEARCH AND OBSERVATION RESULTS FOR SEISMOGENIC EMISSIONS IN THE LAST DECADE

Takeo Yoshino
Sugadaira Space Radio Observatory
Applied Electronics Department
University of Electrocommunications
Chofu-shi, Tokyo, Japan

The seismogenic or seismo-electro-magnetic radiation emission monitoring, data processing, modeling and signature interpretation research was initiated by the author's research team of the S.S.R.O., Japan and in the USSR as a cooperative joint project in 1980. During the last decade, many seismo-electromagnetic or seismogenic emission signatures were truly observed and skillfully recorded at times just prior to various major earthquakes and volcano eruptions by ground-stationed and satellite-borne sensors in Japan, the USSR, Bulgaria, the Mediterranian region, the USA (Loma Prieta and Upland), and other regions.

Although, initially questioned and rejected by the conventional seismologic research community, sincere interest and intense discussions in this novel field have progressed world-wide. The international scientific community of seismo-electromagnetologists has now shifted its attention toward the physical analysis of the source mechanism of radiation emission, occurring throughout the electromagnetic non-invasive spectral region, at the source region, beginning at early stages of signal detection. In order to fully explain the rather complicated and intricate radiation source mechanisms, further detailed observations paired with laboratory model tests are required. In any event, continuous seismo-electromagnetic/seismogenic signature observations and skillful recordings from -- long before the onset to long after the radiation emissions occur -- must be intensified and the pertinent sensor technology must be rapidly advanced.

Next to providing a detailed assessment of this new transdisciplinary science of seismoelectromagnetology, also, the latest results and new discoveries will be presented and explained.

INDUCED PIEZOELECTRIC SIGNALS FROM QUARTZ VEINS MEASURED WITH A LONG-WIRE ANTENNA

R. D. Russell*, M. Maxwell, A. W. Kepic and K. E. Butler
Department of Geophysics and Astronomy
The University of British Columbia
Vancouver, BC, Canada V6T 1W5

The objective of this research is to determine the credibility of piezoelectric and related methods of geophysical exploration. Soviet publications and patents have reported that some geophysically important targets produce electromagnetic signals through conversion of seismic to electromagnetic energy, one mechanism apparently being piezoelectricity. There are further claims that such converted signals provide information about the distance to the target (from the delay of the arrival), about the thickness of the target (from the duration of the arrival) and about the mineralogy of the target (from the spectra of some of the higher frequency responses). Such achievements would be of very great importance to geophysical exploration.

We became interested in carrying out an experiment at Humboldt, Australia, when our laboratory measurements showed quartz samples with piezoelectric coefficients three to four times as large as any we had observed at Canadian sites (we have since found Canadian veins comparably active). R. D. Russell and A. S. Barker, Jr. (Geophysical Prospecting, 39: 105-118, 1991) had predicted that the electrical response is expected to be proportional to the product of the piezoelectric coefficient and the electrical resistivity of the surrounding material.

The experiment took place in April 1990. The acoustic source used was a jackhammer driven by compressed air from a remote diesel compressor. Triggering and stacking software were accomplished, with a PC-based acquisition system obtained from RC Electronics of Santa Barbara, California, to stack as many as 3000 arrivals. For detection of the electromagnetic responses we used long wire antennas similar to those described by W. X. Wu and D. V. Thiel (IEEE Trans. Geophysics and Remote Sensing, 27: 24-27, 1989). Although some of the advantages of these have been strongly disputed by J. R. Wait (*ibid*, 27: 789, 1989), it does seem reasonable that seismically-induced noise at the electrodes should be reduced by eliminating the electrodes. The signal from the long wire antenna was applied to an appropriate charge amplifier. As configured, the arrangement recorded the weighted mean of the electric potential variations in the ground beneath the antennas.

Our measurements successfully reproduced earlier positive results of Alan Boyle of CRA, Pty. Furthermore, they demonstrated simultaneity of arrival at four long-wire antennas and progressive delays as the source was moved away from the target. Responses were obtained at distances up to 20 meters from the target, and apparently could have been recorded at still greater distances.

OBSERVATIONS OF SEISMO-ELECTROMAGNETIC EARTH/SEA-QUAKE PRECURSOR RADIATION SIGNATURES ALONG SOUTHERN CALIFORNIAN FAULT ZONES:

EVIDENCE OF LONG DISTANCE PRECURSOR ULF SIGNALS OBSERVED BEFORE A MODERATE SOUTHERN CALIFORNIA EARTHQUAKE EPISODE

Jack Y. Dea, Charles I. Richman
Naval Ocean Systems Center
Code 832
San Diego, CA/USA 92152-5000

and

Wolfgang-M. Boerner*
University of Illinois at Chicago, EECS
Communications and Sensing Laboratory, M/C 154
Chicago, IL/USA 60680-4348

Although questioned for a long time, there is accumulating growing evidence for the existence of detectable seismo-electromagnetic phenomena worldwide. California is geologically as well as seismically a unique region for studying these phenomena in depth; and, in particular, the Southern California geologic province with a multitude of off-shore and inland fault zones with San Diego in its center. At the NOSC Low Frequency Noise Laboratory, San Diego, we monitor 0.1 to 10 Hz ULF and 10 to 40 Hz ELF signals using mu-metal loaded multi-turn coil sensors, as well as 10 to 100 kHz VLF signals using large one meter diameter loop antennas. We report on observations of broadband ULF signals before and during the Upland quake of April 17, 1990 (M_s = 4.6), centered 200 km north of San Diego. The signals were detected with the vertically oriented coil sensor and not with the horizontally oriented sensors, which suggests a disturbed ionosphere as the most likely source of these signals. The large pre-quake ULF activity, the rapid decay of ULF activity after the quake, and the absence of any geomagnetic storms indicate a good correlation of the ULF activity with the Upland quake. Although the exact mechanisms for coupling geologic activity to the ionosphere is not known, we cite a number of hypotheses concerning these mechanisms. Based on this succinct overview, an interpretation of our radio observation of seismic activity is presented and extented to earth/seaquake precursor or predictor studies. We are in the process of expanding this research with the building of more monitoring stations and the improvement of our measurement, data collection, formatting and data processing capabilities.

GEOMAGNETICALLY INDUCED CURRENT IN THE POWER LINES IN NORTHEASTERN JAPAN

T. Minakawa, J. Kobayashi and O. Takahashi

Tohoku Electric Co. Limited
1-Bancho, Aoba-ku, Sendai 980, Japan

and

*T. Saito and T. Takahashi,
Onagawa Magnetic Observatory & Geophysical Institute, Tohoku University
Aoba-ku, Sendai 980, Japan

Geomagnetically induced current has been continuously observed in the power line network in the northeastern region of Japan, 1989 to the present. The DC current from the point of neutral grounding of a transformer to the ground has been measured at one substation and the two generating stations; the northern end, the center, and the southwestern end of the region, respectively.

The currents are well correlated with geomagnetic variations observed at the Onagawa Magnetic Observatory depending on the period of the variations. The maximum current amounted as high as 40 ampere at the time of the storm sudden commencement that occurred on November 17 (UT), 1989, when a prominent low-latitude aurora was observed in Northern Japan. A cross-power spectrum analysis is applied to the observed data. A speculation is given to the analyzed result.

FURTHER GEOPHYSICAL INVESTIGATIONS OF ELECTROMAGNETIC INDUCTION USING POWER LINES AS THE SOURCE

W.F. Slawson, L.E. Fisk and *T. Watanabe
Department of Geophysics and Astronomy
The University of British Columbia
Vancouver, B.C., Canada V6T 1W5

As a further refinement on the use of power line harmonic fields by McCollor et. al. (J. Geomag. Geoelectr. 35, 221-244, 1983) power lines are modelled as purely inductive sources over a layered earth. For a straight line source exact solutions of conductivity structure are obtained in the form of (inverse) Fourier transforms. A bent line of current causes the computation to become extremely costly so these solutions are approximated by image theory. In all cases it is shown that survey logistics and subsequent analysis may be simplified by measuring two total magnetic field components at each survey station. Lateral inhomogeneties in electrical conductivity can be investigated best by means of laboratory analogue models. The ever present problem of nonuniqueness in potential field interpretation may be partially alleviated by collecting at each station the total field measurements at two or more harmonic frequencies of the radiated signals.

ULF WAVES EXCITED BY MOHICAN-CUT TYPE SOLAR CORONA

T. Takahashi, *T. Saito and A. Imasaki
Onagawa Magnetic Observatory & Geophysical Institute
Tohoku University, Aoba-ku, Sendai 980, Japan

and

S. Minami
Dept. of Electrical Engineering, Osaka City University
Sumiyoshi, Osaka 558, Japan

ULF waves, especially Pc3 pulsations observed at the Onagawa Magnetic Observatory show 27-day recurrence tendency depending on phase of the solar activity. It is found that the recurrence is closely affected by a distribution of the solar corona in the following processes: The polar-cap magnetic fields of the sun change their polarities during every sunspot maximum. It was already proposed that the change is associated with a rotational reversing of the equivalent centered dipole of the heliomagnetosphere. The large scale coronal streamers are found to be distributed always along the heliomagnetic equatorial plane like the mohican-cut hair. The high-speed solar winds blow out from the coronal holes, in other words, from the "magnetic" polar caps of the sun, exciting the Pc3 pulsations in the geomagnetosphere. Consequently, the recurrence of the Pc3 is closely related with the rotation of the mohican-cut type solar corona.

OBSERVATIONS OF ELF SIGNATURES ARISING FROM SPACE VEHICLE DISTRUBANCES OF THE IONOSPHERE

Jack Y. Dea
Naval Ocean Systems Center,
San Diego, CA/USA 92152-5000
Code 832

and

William Van Bise and Elizabeth Rauscher
Magtek Laboratory
7685 Hughes Drive
Reno, NV 89506

and

Wolfgang-M. Boerner*
University of Illinois at Chicago, EECS
Communications and Sensing Laboratory, M/C 154
Chicago, IL/USA 60680-4348

We report on observations of ELF signatures during exit or reentry of space vehicles through the ionosphere. The two modes regularly observed gave signals that peaked at 5.6 Hz and 11.2 Hz. The evidence points to the lower ionosphere, i.e. the D- and E-layers, as the generator of these signals. The measurements were performed using ground-based multi-turn coil sensors located in Reno and San Diego. The nature of these signals is unclear at present but it is surmised that we are detecting either the evanascent fields of hydromagnetic waves traveling in the ionosphere or the oscillating geomagnetic field associated with these hydromagnetic waves.

SOLAR CYCLE VARIATION IN DIURNAL FREQUENCY OF OCCURRENCE OF Pi2 PULSATIONS

Y. Kozuka, *T. Saito, H. Takeuchi and T. Takahashi
Geophysical Institute & Onagawa Magnetic Observatory
Tohoku University, Aoba-ku, Sendai 980, Japan

It was pointed out by Saito and Matsushita (J. Geophys. Res. 73, 267,1968) that a solar cycle variation exists in frequency of occurrence of Pi2 pulsations, that indicates the frequency of occurrence of substorms. According to their result, the local time of frequency of occurrence of individual Pi2 tends to have a clear peak at pre-midnight from declining to minimum phases, while an unclear peak around midnight in maximum phase. Their analysis was limited only during sunspot cycle 19. The purpose of this present paper is to investigate if this tendency exists or not for sunspot cycle Nos. 20, 21 and the former half of No. 22.

In order to examine the solar cycle variation for the local time of frequency of occurrence of Pi2, the times of occurrence are recorded for individual Pi2. The data are from the induction magnetograms obtained at the Onagawa Magnetic Observatory, Japan. A statistical analysis is carried out on the basis of the occurrence times of individual Pi2 pulsations. If a Pi2 wave is excited on a certain local time meridian, a peak of occurrence is expected to appear near the local time of the excitation.

According to our analyzed result, the local time of peak occurrence of Pi2 changes obviously with the solar activity through four cycles including the previous analyses.

One of the possibilities of the solar cycle variation of the peak local time of Pi2 occurrence is considered to be related to a condition of the solar wind velocity or large-scale structure of the solar wind associated with the phase of the sunspot cycle.

E/F/H15.9

STATISTICAL STUDY ON CHARACTERISTICS OF Pc 3-4 AT SYNCHRONOUS ORBIT

H. Matsuoka, *T. Saito and T. Takahashi
Geophysical Institute & Onagawa Magnetic Observatory
Tohoku University, Aoba-ku, Sendai 980, Japan

Introduction It has been considered that Pc 3-4 magnetic pulsations in the magnetosphere are due to the standing Alfven waves driven by some internal or external sources. Although many authors have studied the mechanism of the wave generation, some part is still remained unresolved. We analyzed statistically the wave mode characteristics of dayside Pc 3-4 pulsations at the synchronous orbit by obtaining the vector having the largest variation. Moreover, the correlation between the wave mode and the interplanetary magnetic field (IMF) is studied to clarify the solar wind factors controlling the occurrence probability of the waves at the synchronous orbit.

Data analysis Based on our spectral analysis, a number of wave events are found to represent the harmonic structure as was reported recently on Pc 3-4 pulsations observed near the equatorial plane in the magnetosphere. Hence, the wave with the period corresponding to each spectral peak of the harmonic structure is selected as an event. The oscillation vector having the largest variation is obtained by the minimum variance method. Then, the angle θ_1 between the oscillation vector and the ambient magnetic field is calculated together with the angle θ_2 between the oscillation vector and the east-west direction. Taking into consideration of the angles, θ_1 and θ_2, the events are classified into three modes; azimuthally transverse, radially transverse, and compressional, respectively.

Results Local time distribution of these modes implies that the azimuthally transverse waves exist widely on the dayside, and that the energy of these waves are provided by the solar wind. On the other hand, the radially transverse waves are rarely observed in the morning sector and the energy source seems not to exist in this sector. It is found that, if the IMF sector angle is denoted by ϕ, the compressional waves show a ϕ - dependent local-time variation; the waves tend to occur for $\phi \sim 330°$ at 9h LT and $\phi \sim 30°$ at 15h LT. This local time variation and a relatively small cone angle would suggest a condition of the intrusion of the upstream waves for the compressional waves.

WAVE MODE OF Pi2 PULSATIONS AT SYNCHRONOUS ORBIT ASSOCIATED WITH THE SUBSTORM CURRENT WEDGE

H. Takeuchi[1], *T. Saito[1] , T. Sakurai[2], H. Matsuoka[1] and T. Takahashi[1]

1. Geophysical Institute & Onagawa Magnetic Observatory, Tohoku University, Aoba-ku, Sendai 980, Japan
2. Department of Aeronautics and Astronautics, School of Engineering, Tokai University, Hiratsuka, 259-12, Japan

Observation Wave mode of Pi2 pulsations observed by the two geosynchronous satellites, GOES 5 (76° W) and GOES 6 (108° W), during April 1986 are analyzed by means of the minimum variance method. The observed results are as follows:
(1) The azimuthally transverse mode is dominant, and the radially transverse mode is not observed so frequently. The compressional mode is detected more frequently than the radially transverse mode, but less than the azimuthally transverse mode.
(2) The azimuthally transverse mode shows two occurrence peaks, near 21h LT and 01h LT, respectively. The compressional mode tends to occur at 23h LT.
(3) Occurrence of the compressional mode is similar to the total occurrence of Pi2 pulsations, that is, it shows an occurrence peak around 23h LT.
(4) Different wave modes appear at one satellite from the other, even if the two satellites observe pulsations simultaneously.

Conclusion The compressional mode is expected to be observed between a pair of field-aligned currents. The azimuthally transverse mode and the radially transverse mode should be observed near the field-aligned current meridian. The position of the current wedge is inferred from the simultaneous observation by the two satellites.

E/F/H15.11

GENERATION AND PROPAGATION OF "BANDED RISING AND FALLING LF EMISSIONS" OBSERVED IN THE LOWER MAGNETOSPHERE BY EXOS-D (AKEBONO) SATELLITE

H.Oya, A.Morioka* and M.Kikuchi
Geophysical Institute, Tohoku University
Sendai, 980 Japan

Plasma waves and sounder experiment (PWS) onboard the EXOS-D (Akebono) satellite has detected the new type of whistler mode emissions in the plasmasphere. The emission shows the banded structure in the frequency range from 20 kHz to 300 kHz. Some of dynamic spectra of the banded emission show the maximum of its frequency near the magnetic equator, forming the rising frequency structure as the satellite moves toward the magnetic equator and falling structure as it moves away from the equator. These phenomena are named as Banded Rising and Falling LF Emission (BRIFLE).

The statistical analyses of the BRIFLE phenomena indicated that the emissions are not the in-situ waves but the propagating whistler mode waves because they have no relation with the local plasma frequency and local electron cyclotron frequency, and have no positive correlation with the angle between the ambient magnetic field and the antenna plane.

The results of the ray tracing using the plasma density model base on the in-situ plasma observation showed that rays started from both hemispheres with the range of L= 1.2 to 1.6 and altitudes of 1000 to 2000 km give suitable interpretation for observed BRIFLE.

The generation mechanism of the BRIFLE is discussed that the precipitating energetic electrons with the energy from 500 kev to 2 Mev from the radiation belt interact with the whistler mode waves through the incoherent anomalous electron cyclotron resonance.

Mobile and Indoor Radio Channel Modelling

Room 3024 Salle URSI F Session 13

Modélisation des canaux de radio communications mobiles et intérieures

Chairs/présidents: R.J.C BULTITUDE, Canada

08:50 (13.1) An Indoor Propagation Analysis Using Delay Profiles Measured by the Superresolution Pulse-Compression Method, **H. TAKAI**, T. MANABE, *ATR Optical and Radio Communications Research Laboratories, Kyoto, Japan*

09:10 (13.2) An Evaluation Study of the Prediction Models for Mobile Radio, **Y.K. LI**[1], R. VALLET[1], E. ZINOVIEFF[2], [1]*École Nationale Supérieure des Télécommunications, Paris, and* [2]*Service des Télécommunications avec les Mobiles, Paris, France*

09:30 (13.3) A UTD Wave Propagation Model for Urban Areas Considering Multipath Effects, **M. LEBHERZ**[1], W. WIESBECK[1], W. KRANK[2], [1]*Universität Karlsruhe, and* [2]*Südwestfunk Baden-Baden, Germany*

09:50 (13.4) Scattered Lateral Wave Model for UHF Propagation in Forest, **R. CAMPBELL**, H. WANG, *Michigan Technological University, Houghton, MI, USA*

10:10 **COFFEE/CAFÉ**

10:30 (13.5) Derivation of Channel Impulse Response Via Ray Tracing, **M. KAHRS**, *Rutgers University, Piscataway, NJ, USA*

10:50 (13.6) Duration of Fades Due to Shadowing in LMSS, **A. BENARROCH**, L. MERCADER, *Universidad Politécnica de Madrid, Spain*

11:10 (13.7) Measured Characteristics of Indoor Radio Channels at 950 MHz, **R.J.C. BULTITUDE**, P. MELANCON, R.F. HAHN, *Communications Canada, Ottawa, ON, Canada*

11:30 (13.8) Approche théorique et expérimentale de la propagation des ondes électromagnétiques haute fréquence en milieu confiné, P. MARIAGE, M. LIÉNARD, **P. DEGAUQUE**, *Université de Lille I, Villeneuve d'Ascq, France*

An Indoor Propagation Analysis Using Delay Profiles Measured by the Superresolution Pulse-Compression Method

Hitoshi TAKAI* and Takeshi MANABE
ATR Optical and Radio Communications Research Laboratories
Seika-cho, Soraku-gun, Kyoto 619-02, Japan

To analyze indoor propagation, high-resolution delay profile measurement is necessary. In general, the time resolution of the delay profile measured by the pulse-compression method using correlation of a pseudonoise (PN) code is limited to the chip interval T_c of the PN code.

A new method based on an eigen-value analysis (SPM: Superresolution Pulse-Compression Method) can remarkably improve the resolving power of the pulse-compression method. It is verified that it can resolve two waves with a delay difference of a few tenths of the chip interval T_c by an experiment using coaxial delay lines.

Applying the method to analyze the propagation inside an office room at 240MHz, 910MHz and 2.3GHz, it is found that waves travel back and forth between facing walls. Figure 1 shows an SPM delay profile, which has remarkably higher resolution, as compared with the corresponding delay profile measured by the conventional pulse-compression method. The periodic structure found in the SPM profile suggests the existence of multiple reflections between a pair of facing walls. Although many multiple-reflection routes are considered to exist, the simplest model which considers the one dominant route above is sufficient to explain our results.

This model is also supported by the fact that the averaged power delay profiles exponentially decay with a decay constant independent of the location of the receiving antenna within the room (Fig.2). This result also indicates that the room can be modeled as a one-dimensional cavity. The Q-factor of the cavity or the decay constant is an important parameter in characterizing the indoor multipath environment.

SPM is found to be a powerful method for analyzing indoor propagation. In this measurement, the propagation inside a room can be modeled as a one-dimensional cavity in which multiple reflections occur between a pair of facing walls.

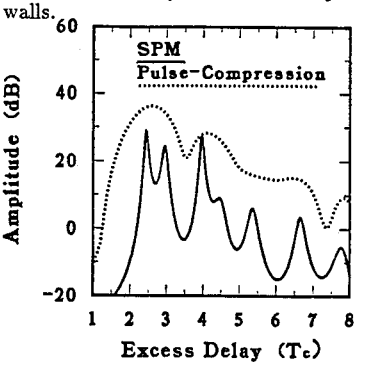

Fig.1 Delay profiles measured at 910MHz
T_c:33ns (30Mchips/s)

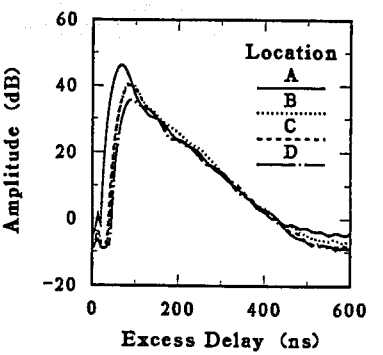

Fig.2 Averaged power delay profiles measured at different locations in a room at 2.3GHz

AN EVALUATION STUDY OF THE PREDICTION MODELS FOR MOBILE RADIO

Y. K. LI* R. VALLET* E. ZINOVIEFF**

* Ecole Nationale Supérieure des Télécommunications
** Service des Télécommunications avec les Mobiles

The frequency planning and the mobile radiocommunication engineering utilize more and more the radiowave propagation models, a lot of propagation prediction models have been developed, among them, it can be very difficult to choose a suitable model for a particular case. So, the development of the mobile radio systems and the frequency planning require an examination of the numerous prediction models.

For the purpose of an evaluation of the propagation models, at first, we have made a census of the published propagation prediction models in the scientific literature, more than thirty models have been found, they are classified in three parts: (1) for narrow bandwidth; (2) for wide bandwidth; (3) for indoor. Due to the complexity of the propagation environment, there are very few pure theoretical models, most of them are empirical or semi-empirical, presented in different forms (curves, formula or software), we give each model a brief description, the conditions of validation and some comments. The second step of the evaluation is concerned a comparison between the measuremental data gathered by France-Telecom and the prediction results obtained with several existing propagation models including the CCIR model, in several typical regions including urban, suburban and rural areas at frequencies in the VHF and UHF bands .

F13.3

A UTD Wave Propagation Model For Urban Areas Considering Multipath Effects

*M. Lebherz^, W. Wiesbeck^, W. Krank^^

^ Institut für Höchstfrequenztechnik und Elektronik (IHE)
Universität Karlsruhe, Kaiserstr. 12
D-7500 Karlsruhe, FRG
(Telephone: 49-721/608-2522 Telefax 49-721/691865)

^^ Südwestfunk Baden-Baden (SWF)
Haus der Technik
D-7570 Baden-Baden, FRG

The system planning methods for the new services in individual communication (mobile radio, PCN) requires coverage prediction mainly in urban areas. Characteristic for the wave propagation in these areas are multipath effects due to multiple reflection and diffraction between buildings. Since the mutual coupling between surface elements (building walls) is more significant in urban areas than in natural terrain, an approach as given by Lebherz et al in recent papers (IEEE Proc. AP-Symp., Dallas, 1990 and RTM, 33, 6, 284-291,1989), neglecting mutual coupling effects between surface elements, is not sufficient. Thus a new model for urban areas has been developed and will be introduced in this paper.

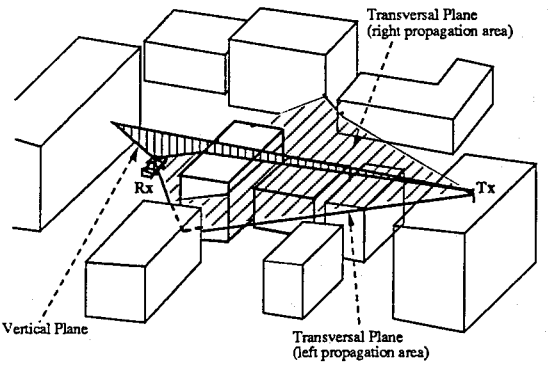

The basic data for the modelling of buildings are supplied by a database that contains the height values of the urban area in reasonable resolution. Each height value can be surrounded by an elementary rectangular cylinder, so that the sides of the elementary rectangular cylinder are parallel to the grid of the database. Buildings can be composed of several elementary rectangular cylinders, like in a unit construction system. They must be considered as 3D-diffracting obstacles, i. e. structures with limited dimensions in all directions so that, diffracted waves must be calculated not only for the edges on the top of a building, but also for the edges on the side. Since for the considered frequency range (>700MHz) the typical dimensions of buildings are large compared to the wavelength, a ray optical approach for wave propagation modelling is appropriate. The calculation of diffraction loss for each obstacle (wedge, double wedge) is performed by UTD using the results of Tiberio et al (IEEE Trans. AP-37, 9, 1172-1180, 1989) and Kouyoumijan et al (Proc. IEEE, Nov. 1974, 1448-1461).

The mutual coupling of the bulding walls and the extension to 3D-diffracting obstacles leads to a ray tracing problem that can only be solved with further assumptions. In this work the propagating rays are assumed to be restricted to a vertical and a transversal plane as shown in the figure above. The complete propagation model for urban areas is given by the combination of a vertical plane model and a transversal plane model.

First calculations in an urban area will be presented and the dominance of different multipath contributions will be discussed.

SCATTERED LATERAL WAVE MODEL FOR UHF PROPAGATION IN FOREST

Richard Campbell* and Huailiang Wang
Department of Electrical Engineering
Michigan Technological University
Houghton, MI 49931

The direct wave attenuates very rapidly in a forest due to the lossy foliage. Recent measurements by Vogel and Goldhirsch at 900 and 1500 MHz show a direct wave attenuation on the order of 1 dB/m. Many studies of received signal intensity versus distance in forest environments indicate that the attenuated direct wave model applies at distances up to tens of meters, but that loss is much less than 1 dB/m at greater distances. Tamir proposed a lateral wave model for propagation through forests at longer wavelengths. The textbook lateral wave model is not physically reasonable for UHF propagation because the forest is a poor approximation to a smooth, lossy dielectric slab at decimeter wavelengths.

We propose a scattered lateral wave model, illustrated in figure 1.

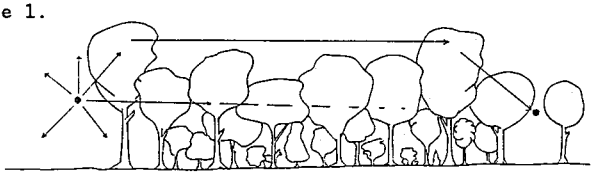

Scattered Lateral Wave Figure 1

The transmitted signal is radiated in all directions. Some travels toward the receiver and is attenuated by the intervening foliage. Some of the transmitted signal travels up to treetop level, where it is scattered by the tallest trees. Near the receiver, these scattered lateral waves once again encounter tall treetops and are scattered down toward the receiver. Our measurements of scattering from roadside trees indicate that about 1% of the transmitted signal is scattered by treetops near the transmitter and about 1% of the signal incident on treetops near the receiver arrives at the receiver. Thus, "launching" and "catching" the scattered lateral wave each involve about 20 dB loss. Figure 2 compares attenuation versus distance for free space, attenuated direct with 1 dB/m loss and scattered lateral wave with 0.1 dB/m loss and 20 dB scattering loss at each end of the path.

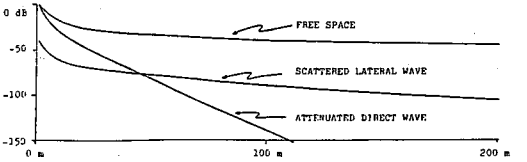

Attenuation Versus Distance Figure 2

F13.5

DERIVATION OF CHANNEL IMPULSE RESPONSE VIA RAY TRACING

Mark Kahrs
Wireless Information Networks Laboratory
Rutgers University
P.O. Box 909
Piscataway, NJ 08855-0909

Optimal placement of transmitters for a wireless network in an office interior is fundamentally a hard problem because the interior of a building offers many reflective paths for a radio transmitter. These "multipath" delays significantly effect receiver performance. Presently, the only approach to multipath measurement is to experimentally fix a transmitter in the environment and then move a receiver around taking measurements. This approach is not only time consuming, but is also prone to error and variability depending on the particular environment. What is needed is a simulation based approach that delivers repeatability as well as a fair prediction of the physical behavior.

Impulse Response Ray Tracing promises to change this by making the entire process one of simulation, not experimentation. The process begins with an architect's drawing. Assuming the drawing has been entered into a Computer Aided Design (CAD) system, then the output of the system can be used as input by the ray tracer. Note that the office interior (desks, equipment and so forth) must also be described to give the ray tracer an accurate idea of reflective surfaces. The ray tracer attempts to simulate the effects of radio transmissions within the building by emitting rays from a transmitter placement. The intended receiver location "measures" the time delay and attenuation of each ray. Multiple transmitters can also be simulated. The output of the simulator is an impulse response approximation. This impulse response can then be used by a channel simulator to demonstrate the effect of transmitter placement on various receiver locations. Note that with this process, it is possible to simulate the radio environment well before actual construction of the building or interior.

Ray tracing in Computer Graphics is a well developed and well known technique. The difference between this form of ray tracing and graphics ray tracing is that in graphics, rays are traced from the eye into the scene; in this method, rays are traced from the transmitter(s) to the receiver. This is equivalent to tracing from light source(s) to the eye.

For this problem the time distance must be measured from the transmitter to the receiver. Each object in the interior must also be represented by the CAD system. IGES (the Initial Graphics Engineering Standard) offers both edge representations as well as Computational Solid Geometry (CSG) representations. This system uses CSG because it is easier to computer object intersections. Because of the long time taken by simulation, initial computational overhead for data structure construction is acceptable if it makes the ray intersection calculations cheaper.

The simulation program, called "DIRT" (Direct Impulse response via Ray Tracing) has 3 parts: first, the building data is read in and interior data structures constructed. Second, rays are emitted from transmitter locations and traced until they are below the receiver threshold. If the ray crosses a receiver "cell", then the signal strength is computed as well as the path length. These results are saved in a file. Lastly, these results can be displayed on a graphics screen.

DURATION OF FADES DUE TO SHADOWING IN LMSS

A. Benarroch* and L. Mercader.
ETSI Telecomunicación, UPM.
28040 Madrid, Spain.

A LMSS propagation experiment at 1.5 GHz using the MARECS satellite has been carried out in Europe in the framework of ESA's PROSAT (phase II) program (A. Benarroch and L. Mercader, Signal statistics from a LMSS propagation experiment in Europe, ITS-IEEE Proc., Rio de Janeiro, Brazil, 1990). The mobile satellite systems planned for the near future will have low link margins and will be impaired mainly by shadowing, as it has been derived from most LMSS experiments. The fade duration statistics obtained from this experiment include average and maximum fade durations, and fade duration distributions (see the example below) and time share of fades.

Fade durations were calculated after averaging the original samples, so that the minimum duration considered is of 0.1 seconds. Therefore only shadowing effects are taken into account. The distributions shown below correspond to rural environments in Spain, France (the area of woods also belongs to France) and Sweden , the elevation angles being 39^{o}, 26^{o} and 13^{o}, respectively. Fade durations increase both for lower elevation angles and with the amount of vegetation.

Fade duration statistics for rural, suburban and urban areas in Spain, France and Sweden, and also for the railways environment in Spain, will be presented.

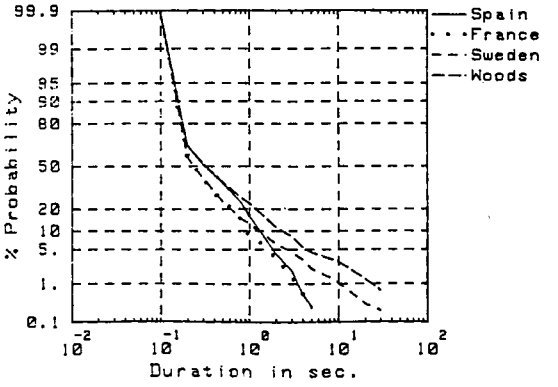

F13.7

MEASURED CHARACTERISTICS OF INDOOR RADIO CHANNELS AT 950 MHZ

By
R.J.C. Bultitude*, P. Melancon, and R.F. Hahn
Canadian Communications Research Centre
Ottawa, Canada

This presentation gives results of measurements that were performed in order to investigate propagation characteristics of indoor radio channels that are considered to be of importance in the design of indoor wireless communication systems. First, descriptions of the measurement system, the principle of its operation, and typical experimental configurations are given. Measurement and modelling results follow. These include: Information pertinent to propagation loss between transmit and receive locations in line-of-sight and non-line-of-sight environments in furnished as well as unfurnished buildings; propagation loss along corridors and between floors of a building; Multipath and rms delay spreads and their relationship to transmit/receive antenna separation, building geometry and polarization; reciprocity (which has been reported by some as possibly not applicable on indoor channels); and the results of investigations concerning spatial and temporal changes in wideband characteristics as a result of motion within the communications environment. The latter will include a brief discussion of the validity of Bello's Gaussian-wide-sense-stationary-uncorrelated-scattering model on indoor channels between stationary and portable terminals. The presentation may also include a discussion of applications for the results.

APPROCHE THEORIQUE ET EXPERIMENTALE DE LA PROPAGATION DES ONDES ELECTROMAGNETIQUES HAUTE FREQUENCE EN MILIEU CONFINE

P. Mariage, M. Liénard et P. Degauque*

Université de Lille 1, Dept. Electronique,
59655 Villeneuve d'Ascq Cédex, France

Il existe une demande de plus en plus importante pour l'établissement de radiocommunication et de transmission de données entre un point fixe et un mobile se déplaçant dans un milieu confiné tel qu'une galerie souterraine ou un tunnel. A titre d'exemple, on peut citer la liaison entre une rame de métro automatique et un poste de commande. Si la fréquence de l'onde est suffisamment élevée, supérieure ou égale au gigahertz, les ondes électromagnétiques pourront se propager librement dans le tunnel qui se comporte comme un guide d'ondes surdimensionné à pertes, les parois étant caractérisées par leur conductivité σ et leur permittivité ε. Si, en première approximation, la section droite de ce guide peut être supposée rectangulaire, des changements importants de section se produiront lors d'un rétrécissement. Dans le cas d'un tunnel de métro, cela correspond soit au passage d'un tunnel 2 voies à deux tunnels 1 voie, soit à la présence d'une rame qui obstrue le tunnel sur une certaine longueur. L'objet de cet article est de présenter une analyse théorique et expérimentale de l'effet de ces changements de section sur l'amplitude du champ en tout point. Les obstacles et les arêtes ayant des dimensions grandes par rapport à la longueur d'onde, la théorie des rayons associée à la théorie uniforme de la diffraction a été utilisée. Ces résultats théoriques sont comparés à ceux obtenus expérimentalement pour deux fréquences : 950 MHz et 10 GHz. A titre d'exemple, la Figure ci-dessous montre l'influence d'un rétrécissement très important du tunnel.

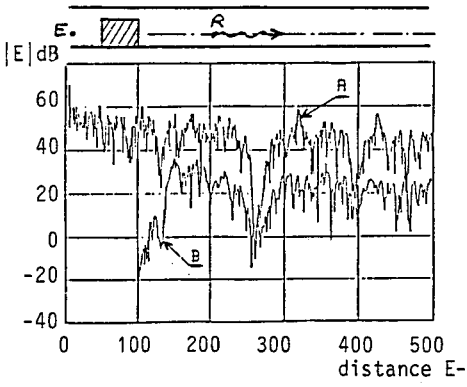

A : sans obstacle
B : avec obstacle

tunnel :
6m20 x 4m

obstacle :
5m70 x 4m x 50m

F = 10 GHz (V)
epsr = 10
sigma = 0.01 S/m

Microwave Propagation

Room 3024 Salle
URSI F Session 28

Propagation des micro-ondes

Chairs/présidents: J. RICHTER, USA

13:30 (28.1) Radar Detection of Low-Altitude Targets Over the Ocean, **K.D. ANDERSON**, *Naval Ocean Systems Center, San Diego, CA, USA*

13:50 (28.2) Fade Prediction and Simulation for a Low Elevation Angle Ku-Band Satellite Link, **C.E. MAYER**[1], E. LOPEZ-TELLO[1], W.J. VOGEL[2], [1] *University of Alaska, Fairbanks, AK, and* [2] *University of Texas, Austin, TX, USA*

14:10 (28.3) Angle-of-Arrival Measurements at 2GHz, **I.J. DILWORTH**, A.N. KENT, *University of Essex, Colchester, UK*

14:30 (28.4) New Techniques for Predicting the Multipath Fading Distribution on Terrestrial Line-of-Sight Links in the VHF/UHF/SHF Bands in Canada, **R.L. OLSEN**, B. SEGAL, *Communications Canada, Ottawa, ON, Canada*

14:50 (28.5) Representation of Multipath Transfer Function Notch by Means of the Normalized Two-Ray Model, Y.K. LI, **M. SYLVAIN**, *C.R.P.E., Issy les Moulineaux, France*

15:10 **COFFEE/CAFÉ**

15:30 (28.6) Some Experimental Results Relating to Diversity Systems on Line-of-Sight Microwave Links, **A.R. WEBSTER**, *University of Western Ontario, London, ON, Canada*

15:50 (28.7) Multipath Depolarization on Terrestrial Line-of-Sight Links: A New Ray Theory, **R.L. OLSEN**, *Communications Canada, Ottawa, ON, Canada*

16:10 (28.8) Contribution of Ground Reflection to Multipath Selectivity, **H.N. KHEIRALLAH**, A.A. EL SHAFEY, H.M. RASHWAN, *Alexandria University, Alexandria, Egypt*

16:30 (28.9) Some Aspects of Attenuation Frequency Scaling, **G. ORTGIES**, F. RÜCKER, F. DINTELMANN, *Deutsche Bundespost Telekom, Darmstadt, Germany*

16:50 (28.10) Effect of Sea Water and Fresh Water on Wave Propagation – Exact Analysis, **G.S.N. RAJU**, K.R. GOTTUMUKKALA,, N.S. KASIBHATLA, B.V. APPA RAO, K.R. RAJESWARI, *Andhra University, Visakhapatnam, India*

F28.1

RADAR DETECTION OF LOW-ALTITUDE TARGETS OVER THE OCEAN

Kenneth D. Anderson
Ocean and Atmospheric Sciences Division
Naval Ocean Systems Center
San Diego, CA 92152-5000

In recent years there have been numerous instances where maximum radar detection ranges of low-altitude, over-water targets have been less than expected. These instances of less-than-normal detection ranges are associated with the presence of ducting, particularly evaporation ducting. Wave-propagation models predict defocusing effects on both the direct and sea-reflected paths that can (1) move the location of the last optical interference null (Lloyds mirror effect) outward in range, (2) decrease the signal return at the peak of the last interference maximum by as much as 6 dB, and (3) decrease the slope of the signal falloff with respect to range at ranges beyond the last interference maximum. For typical radar systems, the predicted decreased return at or near the horizon range can be the difference between detection and non-detection of a small radar-cross-section target.

Results from an analytical and experimental effort to assess low-altitude, short-range propagation effects over the ocean are presented. On the experimental side, an X-band radar has been installed at NOSC to measure signal return from a set of calibrated targets which are carried on a high-speed ocean-going boat. In addition, surface and upper air meteorological sensors are used to measure the ducting conditions. On the analytical side, the NOSC Radio Parabolic Equation (RPE) model is used to predict the transmission loss for the measured ducting conditions for comparison to the measured transmission loss. Although the measurement program is in its early phases, the modeled and measured transmission characteristics obtained so far are in excellent agreement.

FADE PREDICTION AND SIMULATION FOR A LOW ELEVATION ANGLE Ku-BAND SATELLITE LINK

C. E. Mayer*
and
E. Lopez-Tello
Electrical Engineering Department
University of Alaska Fairbanks
Fairbanks, Alaska 99775-0660

W. J. Vogel
Electrical Engineering Research Lab
The University of Texas at Austin
Austin, Texas 78758-4497

Low elevation angle scintillation data were studied to address the issues of fade prediction and fade simulation. Weather indicators were measured at the site to be correlated with the fade measurements. The indicators were air temperature, relative humidity, wind speed, wind direction, all measured with ground based meteorlogical instrumentation, and sky temperature measured with a radiometer. The source was Intelsat V-F10 transmitting at 11.2 GHz. The geosynchronous satellite is positioned at 335.5° East Longitude, which resulted in an elevation angle of 5.8° from Austin, Texas, the site of the measurements.

Two days of scintillation data were analyzed. One day contained the passage of a cold frontal system, which triggered rain. The scintillation level was small before the event, but rapidly increased to large levels with passage of the front. The second day was a day of clear sky. The scintillation level gradually increased to large levels during the day.

F28.3

ANGLE-OF-ARRIVAL MEASUREMENTS AT 2GHZ

I.J. Dilworth * and **A.N. Kent**†
University of Essex, Department of Electronic Systems Engineering, Colchester, Essex. CO4 3SQ. UK.* and the Home Office, UK †

SYNOPSIS

This paper reports some recent results from a 93km, 2GHz transhorizon link set up to represent a typical 'interference' path for a working system. The experimental set up is designed to measure received signal magnitude and angle-of-arrival so that the validity of theoretical model (s) can be investigated.

Background

In the United Kingdom the very limited spectrum available in the 2GHz fixed link bands used by UK Police and Fire services requires 'spectrum managers' to optimise frequency re-use and thus take due account of the interference potential of low-loss transhorizon propagation which can occur for small percentages of time under anomalous tropospheric conditions. This type of propagation can be modelled by various methods (CCIR Report 569-3, Vol. V, 1986, p460. and Levy, M.F., 1990, Elec. Letters, Vol.26, No. 15, pp1153-1155, 19th July.)
One method which is currently receiving renewed interest is reflection from elevated atmospheric layers having strong negative refractivity gradients (Rue, O., 1987, IEE Conference Publication 274, Part 2, pp343-346, 30 March-2 April).

Received signal level and angle-of-arrival measurements are being recorded on a 93km, 2GHz experimental transhorizon link on an overland path in East Anglia, UK. Significant periods of signal enhancement have been observed, associated with stable atmospheric conditions. The link and experimental system is described. Of note is that in addition to the usual signal level measurements a diversity system is employed to accurately measure the angle of arrival of the incoming 2GHz signals over the transhorizon path. Preliminary results are analysed primarily with reference to a relatively simple reflecting-layer propagation model and also some example events are considered using a 'parabolic equation method.

NEW TECHNIQUES FOR PREDICTING THE MULTIPATH FADING DISTRIBUTION ON TERRESTRIAL LINE-OF-SIGHT LINKS IN THE VHF/UHF/SHF BANDS IN CANADA

R.L. Olsen* and B. Segal, Communications Research Centre, Department of Communications, P.O. Box 11490, Station H, Ottawa, Ontario, Canada K2H 8S2

For over fifteen years, designers of terrestrial microwave line-of-sight links in Canada have almost universally used the techniques of Barnett and Vigants developed in the USA for predicting the deep fading range of the multipath fading distribution for individual hops. More recently, on the basis of a fairly extensive set of measurements, link designers in British Columbia have used the technique of Morita developed in Japan. Although the forms of the empirical equations are very similar, the "geoclimatic factor" model for Japan results in the prediction of significantly less severe fading in the average worst month than does that for the USA. However, neither of these techniques have been satisfactory in accounting for the terrain and climatic variability actually present on links in Canada. For the the planning and design of line-of-sight hops in the VHF/UHF bands, even less satisfactory prediction approaches have been applied. The best of these have been again the Barnett-Vigants technique for the upper UHF band and the curves of Bullington for both the VHF and the UHF bands. The Barnett-Vigants technique, however, was based on data for the SHF band and there has been no experimental or theoretical justification for its use at UHF. The Bullington curves were based on few observational data, with no allowance for geoclimatic variability. In the prediction of the shallow fade depth range of the clear-air fading distribution for the average worst month, there has been no technique available for any band that allowed for geoclimatic variability.

In this paper, new methods are presented for predicting the signal fading distribution due to multipath propagation for the average worst month on VHF/UHF/SHF terrestrial line-of-sight links in Canada. One method for the deep fading range does not require detailed path profile information and is suitable for preliminary planning or licensing purposes. A second method which does employ the path profile is intended for more detailed design purposes. A third method, complementary to the other two, is available for predicting the distribution in the shallow fading range. All three methods have been presented in step-by-step form elsewhere (R. Olsen and B. Segal, submitted to Canadian Electrical and Computer Engineering Journal, 1990) for ease of application. Worldwide versions have been adopted by the CCIR in Report 338-6. The current paper focuses on the detailed bases of the Canadian methods, particularly the estimation of geoclimatic variability though refractivity gradient statistics and the extension to include the upper VHF and UHF range of the spectrum. These methods are the first to employ refractivity gradient statistics in the predictions and to cover the upper VHF and UHF bands in addition to the SHF band.

REPRESENTATION OF MULTIPATH TRANSFER FUNCTION NOTCH BY MEANS OF THE NORMALIZED TWO-RAY MODEL

Y.K. LI and M. SYLVAIN*- CRPE (CNET-CNRS)
Issy les Moulineaux - France

A propagation experiment aimed at studying multipath propagation was performed in the summer of 1986. It consisted mainly in measurements of the atmospheric transfer function (TF) by means of a Microwave Link Analyzer on a 1 GHz wide bandwidth around 11.2 GHz, at a sweeping rate of 15 Hz, and of associated meteorological measurements. Three multipath events, corresponding to different meteorological situations, have been selected for a detailed analysis. To describe the shape of the TF notch, we characterize it, as a first approximation, by three parameters:its frequency F_n, its level A_n (dB) relative to normal propagation level, and its width $\Delta f(A_n,s)$ given by the interval between the two frequencies surrounding F_n at which the level is s dB higher than A_n.

In the following, we present the results of a statistical analysis of the notch width. It appears that it is narrower when the notch level is lower. For a given value of s, the dependence of Δf with A_n can be empirically fitted by the relation

$$\Delta f_s(A_n) = \alpha \exp(\beta A_n) \qquad (1)$$

where α and β depend on s and on the event.

The relationship between Δf, s and A_n can also be obtained theoretically, representing the TF around the notch by a normalized two-ray model which writes

$$H(f)=1-b \exp\{j(2\pi f\tau+\phi)\} \qquad (2)$$

and by computing the statistical average value of $\Delta f(A_n,s)$, for giving A_n and s, on the distribution of the model parameters. We thus find again, as a first approximation, the $\exp(\beta A_n)$ dependence with now a fixed value β=0.05. We also checked that the theoretical dependence of the averaged (on all notch levels) notch width on s was verified by experimental data, once a multiplicative factor had been estimated.

These results show that the normalized two-ray model, which was known to represent correctly multipath TF on bandwidth of less than 100 MHz, can be used to describe the frequency notch on wider frequency ranges (extending here up to 500 MHz).

Some Experimental Results Relating to Diversity Systems on Line-of-Sight Microwave Links.

A. R. Webster,
Dept. of Electrical Engineering,
The University of Western Ontario
London, Ontario, Canada. N6A 5B9.

A vertical wide aperture receiving array has been operated for a number of fading seasons on three separate microwave links in southern Ontario. At the receiving end, a total of 16 horn antennas span a vertical range of 666 wavelengths at 16.65 GHz, the operating frequency. As a result, samples of the complex amplitude across this height range are available for periods of signal fading which, in addition to the direct assessment of the presence of multiple ray paths, allow the simulation of the effects of different combinations of antennas. Such diversity systems are of particular interest as a means to counter the effects of multipath propagation on such line-of-sight microwave communications systems.

Space diversity, using close-spaced antennas, is directly accessible from these experimental data and results are presented which support the contention that as antenna separation is increased, the improvement obtained rapidly reaches a maximum and (more or less) constant value. Results from all three links show strong similarities in broad features but significant differences in the details.

Angle diversity is an alternative which has many attractions and results are presented for simulated combinations of antenna beamwidths and pointing angle. These preliminary results indicate that as a minimum, similar improvement factors are to be expected to those obtained with the above space diversity.

F28.7

MULTIPATH DEPOLARIZATION ON TERRESTRIAL LINE-OF-SIGHT LINKS: A NEW RAY THEORY

R.L. Olsen, Communications Research Centre, Department of Communications, P.O. Box 11490, Station H, Ottawa, Ontario, Canada K2H 8S2

Because of the limitation in the extent to which the capacity of terrestrial microwave digital radio systems can be increased by increasing the number of modulation states, manufacturers are again looking at dual polarization frequency reuse as a possible solution. It is fairly well recognized that, at least in temperate climates, multipath depolarization is the major depolarization phenomenon that must be accounted for in microwave systems operating below about 12 GHz. However, efficient design of dual polarization systems has been handicapped by the lack of a widely agreed interpretation of the main cause of multipath depolarization and the lack of suitable link design procedures that can be used to ameliorate it and to estimate its magnitude.

In this paper, a new ray theory of multipath depolarization is presented that appears to explain the available data. Statistical equations relating the cross-polarization isolation to the co-polarized fade depth are given for the two most likely causes of the severe clear-air depolarization observed (see R.L. Olsen, Radio Sci., 2, 631-647, 1981): (a) defocussing (i.e., beam spreading) of the direct wave plus ground reflection, and (b) atmospheric multipath with or without surface reflection. Sample calculations are given for each mechanism. The results suggest that the first mechanism is the dominant one causing the depolarization on virtually all the links for which data are available. They also suggest that atmospheric multipath is the more severe source of depolarization when it occurs. Although the theory does not yet provide a complete prediction technique for individual hops, it does indicate antenna and link design procedures that can be followed in principle to minimize the effects of multipath depolarization.

CONTRIBUTION OF GROUND REFLECTION TO MULTIPATH SELECTIVITY

HN Kheirallah*, AA El Shafey, HM Rashwan
Dept. of Elec. Eng., Fac. of Eng., Alexandria Univ.
Alexandria, Egypt

Recently it has been recognized that ground reflections can play a role in degrading the performance of terrestrial LOS links. This role has long been neglected due to the belief that the amplitude of the reflected ray is quite small compared to that of the direct ray. However, in cases where the direct ray amplitude is largely reduced due to either interference from refractive multipath rays or due to defocussing, the contribution of the reflected ray may become appreciable. In the multipath ray tracing model [Kheirallah, Rashwan and Aboul Saoud, IEE Proc., 136, Pt.H, 2, 175-178, April 1989] a specular reflected component from a dry sand surface is added. Results indicate that the shape of the fade level versus either frequency or received height is altered if ground reflection is taken into consideration. Furthermore, the pattern of the antenna is a highly important parameter discriminating against ground reflections.

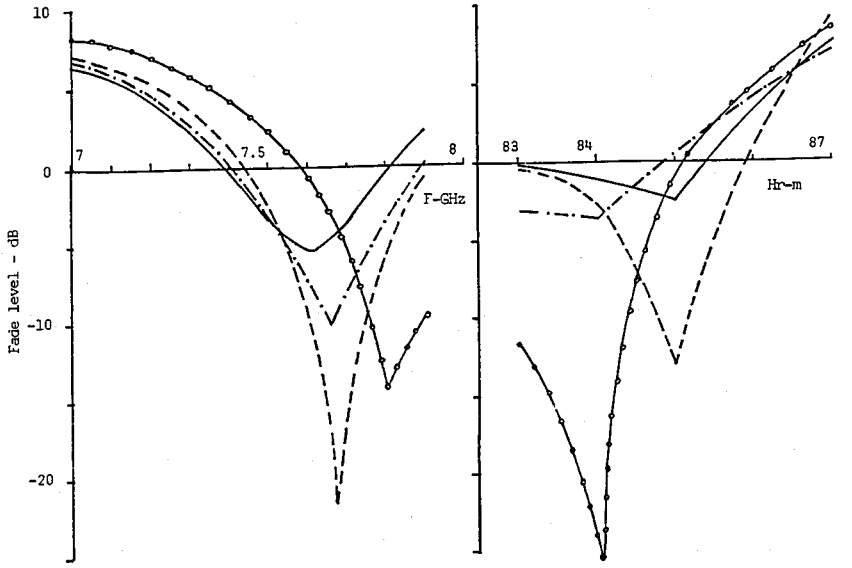

Fade level versus frequency F and received height Hr.
——— no reflection, with antenna gain
– – – – – no reflection, no antenna gain
—·—·— with reflection, with antenna gain
—o—o— with reflection, no antenna gain

F28.9

SOME ASPECTS OF ATTENUATION FREQUENCY SCALING

Gerd Ortgies*, Friedrich Rücker, Fritz Dintelmann
Forschungsinstitut der Deutschen Bundespost Telekom
D6100 Darmstadt, Federal Republic of Germany

Scaling of attenuation in frequency is a technique which system planners often use if data for a particular frequency are not available but are for another. The scaling techniques applied in this context are normally referred to as long-term frequency scaling. In open-loop up-link power control, the situation is different from the above where an estimate of the quasi-instantaneous attenuation at some frequency is sought which is based on the attenuation measured at another frequency.

It is well known that the various attenuation effects show different frequency dependencies and, therefore, they should be separated at least at higher frequencies where gaseous and cloud attenuations cannot be neglected. Turbulent scattering in the atmosphere is another effect which is often ignored. It manifests itself as fluctuations superimposed on the signal. Although the mean scintillation amplitude is zero, its excursions from the mean may significantly deteriorate instantaneous frequency scaling.

Power density spectra of beacon signals for various propagation conditions reveal three distinct signal frequency ranges: The first one extending from zero to about 0.03 Hz, the second from 0.03 to roughly 0.1 Hz depending on wind velocity and the third one above this frequency. The energy density in the second and third part of the spectrum is mainly due to scatter while the slowly varying phenomena such as gaseous, cloud and rain attenuation give rise to the spectral power density below about 0.03 Hz. Since scintillations are not well correlated on the up and down path of a satellite link and in order to not wrongly scale their amplitudes, it is necessary to remove the fast fluctuations by low-pass filtering of the signal. The attenuation derived from the filtered signal can then be scaled conventionally while scintillations can be described only in statistical terms.

By way of example, this contribution shows the effect of various software filters. It appears from our analysis that averaging of the signal over about 30 s greatly reduces the effect of scintillations on frequency scaling while retaining the basic properties of the other effects. One of the interesting observations is that a hysteresis is found when moving from low to high attenuation and back again. This has some significant bearing on instantaneous scaling and deserves further investigations.

EFFECT OF SEA WATER AND FRESH WATER ON WAVE PROPAGATION - EXACT ANALYSIS

G.S.N. Raju*, K.R. Gottumukkala, N.S. Kasibhatla, B.V. Appa Rao, K.R. Rajeswari, A.U. College of Engineering, Visakhapatnam 530 003, INDIA.

The conducting properties of different media depend upon the primary constants of the media and frequency of operation. As a wave propagates in a particular medium, it is attenuated and hence it can travel only a certain distance before the wave amplitude reduces to an acceptable level. For the design of a communication system to be used in ships and submarines, the information on the variation of exact penetration of the waves in different waters is essential. To provide this vital data, computations are carried out from the derived exact formulae, for the evaluation of the variationof the distance of propagation with frequency for sea and fresh water and results are presented in Fig.1.

From the data presented, it is found that there is a major difference between the results of two media. As a natural consequence, the design of a required communication system needs to be altered for each media. The results presented in this paper are very accurate and are extremely useful for the selection of exact operating frequency.

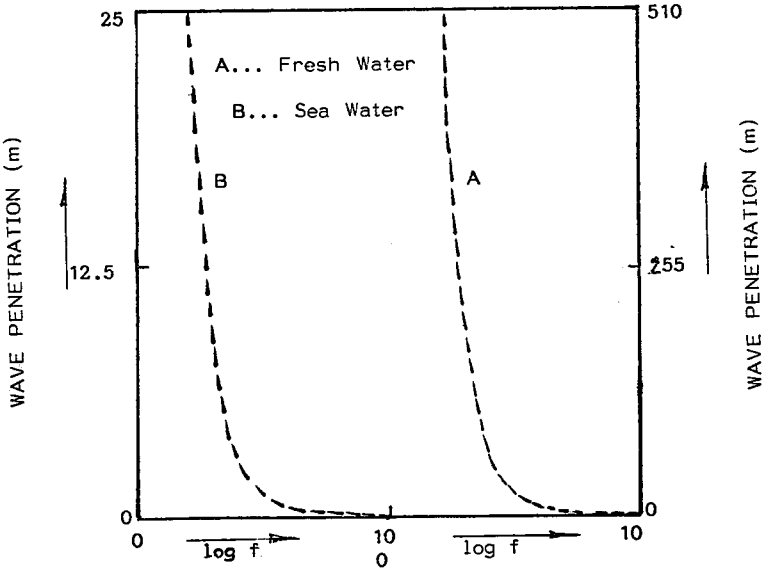

Fig. 1

Rain Effects on Propagation | **Room 3024 Salle URSI F Session 44** | **Effets de la pluie sur la propagation**

Chairs/présidents: J. GOLDHIRSCH, USA

08:30 (44.1) Rain Sidescatter Interference in the Satellite Links of the 1990's, **F. HAIDARA**, C.W. BOSTIAN, *Virginia Polytechnic Institute and State University, Blacksburg, VA, USA*

08:50 (44.2) Analysis of 20-GHZ Crosspolar Events, **F. DINTELMANN**, F. RÜCKER, G. ORTGIES, *Deutsche Bundespost Telekom, Darmstadt, Germany*

09:10 (44.3) Olympus Precipitation Attenuation and Depolarization Measurements Correlated with 9.6-GHz Dual-Polarized Radar Measurements, **D.V. ROGERS**, R.L. OLSEN, D. MAKRAKIS, R. BÉRUBÉ, *Communications Canada, Ottawa, ON, Canada*

09:30 (44.4) Olympus Beacon Rain Fade Measurements at 12, 20, and 30 GHz, **W. STUTZMAN**, J. McKEEMAN, T. PRATT, A. SAFAAI-JAZI, *Virginia Polytechnic Institute and State University, Blacksburg, VA, USA*

09:50 (44.5) Scattering Angle and Frequency Dependent Properties of Precipitation Scattered Signals, **J. RACZEK**, *Deutsche Bundespost Telekom, Darmstadt, Germany*

10:10 **COFFEE/CAFÉ**

10:30 (44.6) Measurements of Rain Induced Interference at 23 GHz, K.C. ALLEN, **P.B. PAPAZIAN**, R.O. DeBOLT, *National Telecommunication and Information Administration, Boulder, CO, USA*

10:50 (44.7) Slant-Path Rain Attenuation Prediction for Tropical and Equatorial Regions, **M.S. PONTES**, R.S.L. SOUZA, L.A.R. SILVA MELLO, *Pontificia Universidade Católica do Rio de Janeiro, Brazil*

11:10 (44.8) Application of Propagation Theory in Adaptive Cancellation of Cross Polarisation, **A. GHORBANI**[1], N.J. McEWAN[2], [1]*Amirkabir University of Technology, Tehran, Iran;* [2]*University of Bradford, UK*

11:30 (44.9) The Observations of Typhoon Precipitation by Using Chung-Li VHF Radar, **Y.-H. CHU**[1], L.-P. CHIAN[1], C.-H. LIU[2], [1]*National Central University, Taiwan, China;* [2]*University of Illinois, Urbana, IL, USA*

11:50 (44.10) Investigation of Electromagnetic Wave Attenuation by a Distribution of Dielectric Spheres with a Shell in Application to Models of Hail and Rain, **E.A. SKIRTA**, *Ukrainian SSR Academy of Sciences, Kharkov, USSR*

F44.1

RAIN SIDESCATTER INTERFERENCE IN THE SATELLITE LINKS OF THE 1990'S

Fatim Haidara * and Charles W. Bostian
Satellite Communications Group
Bradley Department of Electrical Engineering
Virginia Polytechnic & State University
Blacksburg, Virginia 24061-0111

The problem of rain scatter interference involving satellite links was investigated widely in the early 1970's, and it has had relatively little attention since then. This paper establishes the severity of the interference problem that might be expected for the satellite systems of the 1990's, particularly, for the rapidly growing number of low fade margin Ku-band systems using inexpensive very small aperture terminals (VSATs). The larger beamwidth of these systems makes them more sensitive to intersystem interference. Also, the current 2 degree orbital spacing now allowed by FCC regulations increases the potential for side-scatter interference from what it was in the 1970's.

The particular cases treated here involve (1) the interference created by an earth terminal illuminating a satellite in the orbital slot adjacent to the intended satellite via scattering of the uplink signal by rain and (2) the inverse situation. Note that the probability of harmful interference would be enhanced if an earth station increased its uplink power to compensate for attenuation due to rain.

Our purpose is to predict the interfering signal both qualitatively (coherent vs. incoherent) and quantitatively for frequencies above 10 GHz. This involves a close study of the single and multiple scattering processes in the random rain media, taking into account both the rain parameters and the system parameters. We will present two approaches to the problem; the first uses the bistatic radar equation (BRE) with first order multiple scattering to compute the average power scattered by the rain. We compare this results with those from a closely related method developed by Chu [T.S. Chu, *IEEE Trans. Ant. and Prop.*, Vol. AP-25, 287-288, March 1977]. The second employs the vector radiative transfer equation (VRTE) and multiple scattering to evaluate the incoherent scattered intensity. To our knowledge this is the first published application of the VRTE to the VSAT problem.

ANALYSIS OF 20-GHZ CROSSPOLAR EVENTS

Fritz Dintelmann*, Friedrich Rücker, Gerd Ortgies
Forschungsinstitut der Deutschen Bundespost Telekom
D6100 Darmstadt, Federal Republic of Germany

The 20-GHz beacon signal emitted from the propagation package of the Olympus satellite is switched between horizontal and vertical polarisations at a rate which is much faster than decorrelation time constants in the troposphere. Thus, with quasi-simultaneous beacon measurements at orthogonal polarisations, the complete transfer matrix of the propagation medium can be determined.

In a very simple approach, the medium can be described by two perpendicular principal planes which are rotated by a canting angle ϕ with respect to the polarisation plane of the incident electromagnetic wave and which are characterised by different propagation constants.

Using this approach, propagation events exhibiting attenuation and depolarisation are presented. Independently measured quantities are copolar and crosspolar levels at horizontal and vertical polarisations as well as the phase differences between the copolar signals and between the respective co- and crosspolar channels. In one event, considerable differential attenuation and differential phase shift between the vertically and horizontally polarised signals were measured. This event is assumed to be caused mainly by oblate rain drops. For another event, differential phase shift was the major effect together with considerable attenuation. Hence, this event is considered to be due to ice depolarisation (differential phase) and rain attenuation from nearly spherical rain drops.

From the measured differential attenuation, differential phase shift and crosspolar discrimination, the canting angle can be estimated while from the anisotropy elements (differential attenuation, differential phase) of the transfer matrix and the canting angle, the phase difference between the copolar and the crosspolar signal is calculated. A comparison of the calculated with the measured phase shows good agreement which indicates that the simple model is applicable for pure rain events as well as for combined events, i.e. ice depolarisation and rain attenuation, if rain drops are nearly spherical.

The analysis of more complex cases, e.g. ice depolarisation caused by differential phase followed by rain depolarisation (differential phase, differential attenuation, canting angle of rain drops different from the canting angle of ice crystals) deserves further investigations.

showed only selected events

use cross cancellation getting 60dB XPOL
used software 11

F44.3

OLYMPUS PRECIPITATION ATTENUATION AND DEPOLARIZATION MEASUREMENTS CORRELATED WITH 9.6-GHz DUAL-POLARIZED RADAR MEASUREMENTS

D.V. Rogers*, R.L. Olsen, D. Makrakis and R. Bérubé
Communications Research Centre, Department of Communications, Ottawa, Canada K2H 8S2

The melting layer, a region of melting snow and ice that exists above the rain regime in many rain structures, is poorly understood. Its contribution to path attenuation and precipitation-scatter interference is unclear, and the corresponding frequency-scaling behavior is unknown.

Path attenuation and depolarization measurements at multiple frequencies, in conjunction with concurrent dual-polarized radar data, provide a powerful method to investigate the propagation path. An experiment of this type has been implemented by the Communications Research Centre on the grounds of the National Research Council of Canada in Ottawa. Receivers are used to monitor beacon signals from the Olympus satellite at 12.5, 19.8, and 29.7 GHz at a path elevation angle of 14.3°. Both attenuation and depolarization statistics are obtained at each frequency. Adjacent sky noise radiometers operating in the same frequency bands provide additional propagation information.

A colocated dual-polarized 9.6-GHz radar is used to probe the state of the precipitation particles along the path, including identification of the melting layer. The radar polarization is switchable between circular and linear; both are used in the experiment. Collection of radar data is initiated and concluded automatically by sensing the path conditions with the radiometric and beacon data.

By correlating the radar data with the beacon and sky noise data, information on the propagation effects encountered on the path can be deduced. A specific goal of the measurement program is to investigate the propagation characteristics of the melting layer. The experiment and analysis procedures will be described and results to date discussed.

OLYMPUS BEACON RAIN FADE MEASUREMENTS AT 12, 20, AND 30 GHz

W. Stutzman, J. McKeeman
T. Pratt, and A. Safaai-Jazi

Satellite Communications Group
Bradley Department of Electrical Engineering
Virginia Polytechnic Institute & State University
Blacksburg, Virginia 24061-0111

The European Space Agency launched the OLYMPUS satellite in July 1989. In addition to communications experiment packages in Ku- and Ka-bands, OLYMPUS has frequency coherent propagation beacons at 12.5, 19.77 and 29.66 GHz. These beacons are visible from Blacksburg at an elevation angle of 14°. Virginia Tech has four receivers, one at each frequency plus a second portable terminal at 20 GHz for short-baseline diversity measurements.

The receiving system was constructed to take advantage of the frequency coherent beacons. A frequency locked loop derives frequency tracking information from the 12 GHz receiver which experiences smaller fading than that at 20 and 30 GHz. This permits accurate fade measurements of the relatively frequently occurring deep rain fades (25 dB or more) on 20 and 30 GHz. The 12 GHz derived FLL also permits rapid reacquisition after loss of lock.

Measurements at Virginia Tech began in August 1990 and will run for one year. Statistical results are currently being processed. These include; fade, fade rate, and fade duration for rain and scintillation events. Frequency scaling results are especially valuable due to the common elevation angle and location of the receivers. Initial results confirm the somewhat less than frequency squared scaling law. For a diversity separation of 50 m for the two 20 GHz receivers, no improvement during rain fading is experienced, while decorrelation for scintillation events is common.

F44.5

SCATTERING ANGLE AND FREQUENCY DEPENDENT PROPERTIES OF PRECIPITATION SCATTERED SIGNALS

Johannes Raczek
Forschungsinstitut der DBP Telekom
D-6100 Darmstadt, Federal Republic of Germany

The Research Institute of the DBP Telekom is currently involved in an extensive research programme, whose primary objective is the investigation of scattering by hydrometeors at frequencies above 10 GHz. In this presentation some results on the scattering angle and frequency dependence of the measured signal fluctuations will be reported.

The measurements are performed on bistatic 30-GHz short-path links using - inter alia - four fixed identical antennas transmitting beams at elevation angles between 3.8° and 15°. Signals are received with two fixed identical antennas under elevation angles of 27° and 153°.
In addition, a 12-GHz link is used, where the elevation angles of the transmit and receive antennas are chosen to be identical to one of the 30-GHz links yielding nearly identical scattering volumes (e.g. identical positions).
Data are collected simultaneously with a sampling rate of some kHz for each individual scattering angle.

Because of the high sampling rate it is possible to analyse the fine structure of the measured scatter signals and to establish their characteristics; these are directly related to static and dynamic quantities describing the scattering particle state. In the analysis, it is necessary to account for and to eliminate a variety of disturbing effects, which are superimposed on the scattering signal.

The discussion is mainly restricted to the interpretation of the width of the Wiener spectra and the dynamic range of the measured signals, both terms of scattering angle and transmitting frequency. Thereby, different types of hydrometeors (e.g. rain, snow) are considered separately.
For example, the investigation for a fixed height of the scattering volume shows that for 30 GHz the width of the measured Wiener spectra for rain is the broader (up to some kHz) the larger the scattering angle. Furthermore, for a given fixed scattering angle the Wiener spectra at 12 GHz are considerably narrower than those at 30 GHz. First interpretations of these and other properties of Wiener spectra yield good agreement of the measured results with our theoretical estimations, which are related to meteorological quantities.
The investigations of the angular dependence of the dynamic range of the measured scattering signals are relatively complex. For example, for snow unexpected angular dependencies of the dynamic range for the co- and x-polar components are often observed. The reasons for these and other effects will be discussed.

MEASUREMENTS OF RAIN INDUCED INTERFERENCE AT 23 GHZ

K.C. Allen, P.B. Papazian*, and R.O. DeBolt
National Telecommunication and Information Administration
Institute for Telecommunication Sciences
Boulder, CO 80303

Guidelines to prevent interference between communication links are based on the principle of providing an interference protection margin separating the level of the undesired signal from the desired signal. The interference threshold is the difference in desired signal level and the undesired signal level at which interference becomes harmful. The interference protection margin should be chosen so that the desired signal can fade a reasonable amount and still have a margin greater than the interference threshold so that no harmful interference occurs. Thus, the interference protection margin is the sum of a fade allowance and the interference threshold. Interference would still be expected on occasion, but only when the differential fading between the desired and undesired signal exceeded the fade allowance. In order to determine the amount of time that interference will occur, it is necessary to know something about the differential fading that occurs on paths due to rain, multipath, etc. Measurements of the differential attenuation in the 23 GHz band due to rain are described below.

Two transmitters at 23 GHz were located about 12 km from their common receiver in Hilo, Hawaii. At the receiver, the apparent angle separating the transmitters was about one degree. This geometry was chosen to simulate a terrestrial link together with an earth-space link in which the satellite is just above the horizon. Because the actual earth-space path would extend beyond the 12 km terrestrial path, the simulation geometry gives the worst case for the satellite interfering with the terrestrial link. On the other hand, the geometry is overly optimistic for determining the interference of the terrestrial link with the earth-space link.

The frequencies of the transmitters differed by 5 MHz and resulted in IFs of about 1 and 6 MHz at the receiver. A PC data acquisition system was used to digitize the IF and record the amplitude of each signal.

The rain attenuation was modeled as log-normally distributed so that the logs of the attenuation on each path are jointly normally distributed. The correlation coefficient for the log of the attenuation is expected to be a function of the angle between the paths. The log-normal-model prediction of the cumulative distribution of the differential attenuation is compared with the measured data.

F44.7

SLANT-PATH RAIN ATTENUATION PREDICTION FOR TROPICAL AND EQUATORIAL REGIONS

M.S. Pontes* R.S.L. Souza L.A.R. Silva Mello
Center for Telecommunication Studies - CETUC
R. Mqs. S.Vicente 225-Rio de Janeiro-22453-BRAZIL

Several methods have been proposed to predict the cumulative distribution of attenuation due to rain in earth-space links. Most of them, including the currently recommended by the CCIR (Report 564-3, XVIIth Plenary Assembly, Düsseldorf, 1990), are empirical or semi-empirical methods, derived using rainfall rate and rain attenuation data measured in temperate climates. When applied to sites in tropical and equatorial regions, the resulting predictions usually show poor agreement with the measured distributions.

The CCIR method is based on the estimation of the attenuation exceeded at 0.01% of the time ($A_{0.01}$), from the measured point rainfall rate exceeded at the same time percentage ($R_{0.01}$). An empirical formula is used for scaling to other time percentages, in order to produce the complete distribution.

For tropical and equatorial climates, it seems that the estimates of $A_{0.01}$ lack accuracy mainly because the values for rain height used in the method are too low. Also, the expression for time percentage scaling does not produce the proper slope for the distribution.

In this work, a modified method to be applied for sites in these regions is proposed, which uses the 0° isotherm height as rain height to calculate the attenuation exceeded at a particular time percentage. This height is determined as a function of the site latitude, using a regression formula obtained from radiosonde measured data. The problem of time percentage scaling is also addressed. The attenuation predictions obtained with this modified method and the current CCIR method are compared with measured distributions available for tropical and equatorial regions.

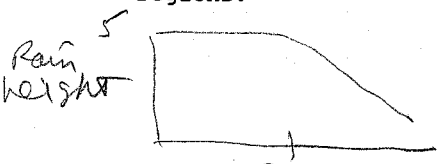

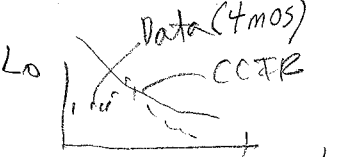

No Show

F44.8

APPLICATION OF PROPAGATION THEORY IN ADAPTIVE CANCELLATION OF CROSS POLARISATION.

A. GHORBANI N.J. McEWAN
N.J. McEWAN is with the school of studies in Information Systems Engineering. University of Bradford, Bradford BD7 1DP, U.K.
A. GHORBANI *, is with the school of Electronic Eng. Amirkabir University of Technology (Tehran Polytechnic), Hafez Ave., No.424 , Tehran,Iran
Tel: 61390 , Telex: 214269

This paper will attempt to complete the exposition of all the ways in which propagation theory impacts on the structure and control of adaptive networks designed to cancel hydrometeor-induced cross-polarisation in microwave communication links. When adaptive cross-coupling networks are realized at radio frequency as variable waveguide polarisers, desirable simplifications are to make them lossless devices with at most two free parameters. Performance calculations for such simplified forms are fully reviewed.

The remainder of this paper attempted to set out all the significant applications of propagation ideas to the cancellation control. It disscussed the possiblity of using a single pilot tone to provide information for driving cross-coupling cancellers in both channels. Three methods were considered, all based on a knowledge of the mathematical structure of the medium transmission matrix . The simplest method simply sets the two coupling co-efficients equal, and the most complex computes the differential propagation from the single complex XPD measured. Predicted performance is encouraging even for the simplest method, (A.Ghorbani and N.J. McEwan, Int.,J.,of Satellite Comm., Vol. 6, pp 41-52 , 1988)

Next the idea of control based on single correlator was investigated. It was concluded that a single correlator could be used for cancellers dealing with in-phase cross-polar components, e.g. for rain around 30 - 40 GHz. The hardware saving might be rather marginal and the method is unsuitable for ice effects.

Attention was then given to control strategies for cancellation which would not be possible at all using the purely systems approach. Two general areas of interest were investigated. The first was the case of inferring the cross-polar parameters simply from the co-polar attenuation. This method has some promise , especially in partial re-use where neither a second receiver channel nor a pilot tone in the unwanted channel is available.

The second and final extension of the arguments covered the case of up-link pre-distortion control based on a down-link beacon. This is strictly impossible if no assumptions are made about propagation. The first assumption made was that the propagation is reciprocal in the network sense, a seemingly safe assumption since hydrometeors are simple dielectrics. A previously unstated result is that control is nominally perfect if the beacon has the same frequency as the up-link and the orthogonal polarisation. More detailed propagation modelling allows frequency scaling to be included, with the orthogonally polarised beacon remaining a superior case.

F44.9

THE OBSERVATIONS OF TYPHOON PRECIPITATION BY USING CHUNG-LI VHF RADAR

Yen-Hsyang Chu, Lee-Po Chian
Institute of Atmospheric Physics, NCU, Taiwan, CHINA

and

Chao-Han Liu
Department of Electrical Computer Engineering, University of Illinois at Urbana/Champaign, IL 61801

In this paper, the results of precipitation observed by Chung-Li VHF radar during the passage of typhoon Susan through Taiwan area on June 2, 1988, are presented. We find that the terminal velocity of ice particles and rain drops are 1 m/s and 6-8 m/s, respectively, consistent with those observed by the conventional meteorological radar. The echo power due to precipitation is generallly far smaller than that due to atmospheric refractivity fluctuations. However it is enhanced strikingly at the height of melting layer (about 5 km in Taiwan area), and its value can be greater than that due to refractivity fluctuations by about 5 dB. The echo power profiles of the vertical and oblique beams (with zenith angle 17o) are also examined. They indicate that there is no aspect sensitivity for the echoes scattered from the atmospheric refractivity fluctuations. Suprisingly, however, for the echo power of precipitation the feature of aspect sensitivity does exist above the melting layer, and disappears below this altitude. The correlation between the horizontal wind speed and the Doppler spectral width of precipitation is found to be fairly heigh, with a correlation coefficient of 0.86. This suggests that the beam broadening effect due to the irregularities drifted by the horizontal wind through the radar volume can not be ignored if the distribution of the rain drop size is to be deduced from the Doppler spectral width of precipitation.

F44.10

INVESTIGATION OF ELECTROMAGNETIC WAVE ATTENUATION BY A DISTRIBUTION OF DIELECTRIC SPHERES WITH A SHELL IN APPLICATION TO MODELS OF HAIL AND RAIN

Dr.E.A.Skirta
Institute of Radiophysics & Electronics, Ukrainian SSR Academy of Sciences, Kharkov 310085, USSR

Accuracy of integral attenuation characteristics computation can be determined by virtue of finding the total scattering cross section and by the functions of particle size distribution according to the percipitation models (e.g. rain, snow, hail, or fog) being investigated. Hail particles, being ice kernels covered with a shell of water, ice, or wet snow are the most complicated from the viewpoint of both the physical structure and formulation of mathematical models. The worst studied are also size distribution functions of these particles, in contrast to raindrops for which there are a series of recommended standard functions.

In this paper a realized calculation algorithm is presented for coefficients of a series of scattering by dielectric spheres with shells, for the scattering cross-section, and inverse and total scattering cross sections. On the basis of the obtained results we calculate an effective cross-section of radio location scattering per unit area and attenuation coefficients for a few size distribution functions of raindrops and hailstones. The rain model, being a particular case of the general problem stated as the kernel radius tends to zero, is investigated for the Marshall and Palmer distribution and lognormal distribution. Parameters of the latter approximated by a three-parameter function were obtained on the basis of measurements at middle lattitudes and presented by M.V.Zaharyan, L.N.Kornilov & V.N.Pozhidaev, Radiotekhnika i Elektronika, 10, 2017-2022, 1989. The comparison is drawn between the obtained results and results for the lognormal raindrop size distribution in the tropics from G.O.Ajayi & R.L.Olsen, Radio Sci., 20, 2, 193-202, 1985. Due to the strong dependence of Mee functions on the size of scatterers, the integration range in calculating the decay coefficients should be chosen so as to take into account the function oscillation structure. We discuss an impact on the calculation results of the choice of particle distribution boundaries in rain of different kinds: drizzle, steady rain, thunderstorm, and in hail. The hail model is based on the particle size gamma distribution. An analysis has been made for model experiment results at different rain rates and hydrometeor shells in the wavelength range 1 to 8 mm, and comparison with known measurements is also given.

Rain Effects on Propagation and Observations of the Atmosphere

Room 3024 Salle URSI F Session 61

Effets de la pluie sur la propagation et l'observation de l'atmosphère

Chairs/présidents: D.V. ROGERS, Canada

13:30 (61.1) The Dynamics of Rain-Induced Fades, **D.G. SWEENEY**, C.W. BOSTIAN, *Virginia Polytechnic Institute and State University, Blacksburg, VA, USA*

13:50 (61.2) Dynamic Behaviour of Rainfall and Slant-Path Rain Attenuation in Tropical and Equatorial Regions, **L.A.R. SILVA MELLO**, M.R.B.P. JIMENEZ, M.S. PONTES, *Pontificia Universidade Católica do Rio de Janeiro, Brazil*

14:10 (61.3) Low Angle Earth-Satellite Beacon Fades and Scintillation at 11 GHz, **W.J. VOGEL**, G.W. TORRENCE, *University of Texas, Austin, TX, USA*

14:30 (61.4) Measured and Predicted Multipath Fading Distributions from 8 Line-of-Sight Links in Brazil, **L.A.R. SILVA MELLO**, G.L. SIQUEIRA, N.R. DHEIN, C.M. EINLOFT, *Pontificia Universidade Católica do Rio de Janeiro, Brazil*

14:50 (61.5) Global Estimates of Oceanic Rain from SSM/I Measurements, **T.T. WILHEIT**[1], A.T.C. CHANG[2], L.S. CHIU[3], [1]*Texas A&M University, College Station, TX,* [2]*NASA Goddard Space Flight Center, Greenbelt, MD, and* [3]*General Sciences Corporation, Laurel, MD, USA*

15:10 **COFFEE/CAFÉ**

15:30 (61.6) Detection and Measurement of Atmospheric Wave Structure Using a Scanning 118-GHz Spectrometer, **P.G. BONANNI**, D.H. STAELIN, *Massachusetts Institute of Technology, Cambridge, MA, USA*

15:50 (61.7) Measurements of the 60-GHz O_2 Spectrum of Air, **H.J. LIEBE**, G.A. HUFFORD, R.O. DeBOLT, *U.S. Department of Commerce, Boulder, CO, USA*

16:10 (61.8) Calculation of Optical Properties of Impure Cloud Drops Using FDTD and Realistic Modeling of Scavenging of Carbonaceous Particles, **M.F. ISKANDER**[1], P.C. CHERRY[1], H.Y. CHEN[1], J.E. PENNER[2], [1]*University of Utah, Salt Lake City, UT, and* [2]*Lawrence Livermore National Laboratory, Livermore, CA, USA*

16:30 (61.9) A Matrix Doubling Formulation of Internal Layer Emission with Irregular Boundaries, **H.J. EOM**, *Korea Advanced Institute of Science and Technology, Taejon, Korea*

F61.1

THE DYNAMICS OF RAIN-INDUCED FADES

Dennis G. Sweeney* and Charles W. Bostian
Satellite Communications Group
Bradley Department of Electrical Engineering
Virginia Polytechnic Institute & State University
Blacksburg, VA 24061-0111

This paper examines the dynamics of rain induced fades on radio links by evaluating the rate at which the first Fresnel zone volume fills with rain. The amount of water in this volume determines the fade depth, and the rate at which it fills establishes the fade slope. A compact expression for fade slope on a terrestrial path is derived. This expression shows that once the rain rate is specified, fade slope is very sensitive to differences in rain velocity. Thus there is no unique relationship between fade slope and rain rate.

DYNAMIC BEHAVIOUR OF RAINFALL AND SLANT-PATH RAIN ATTENUATION IN TROPICAL AND EQUATORIAL REGIONS

L.A.R. Silva Mello M.R.B.P.Jimenez M.S. Pontes
Center for Telecommunication Studies - CETUC
R. Marques S. Vicente 225-Rio de Janeiro-22453-BRAZIL

Long term cumulative distributions of point rainfall rate and slant-path rain attenuation have been extensively investigated in the past. A large amount of measured data has been obtained, particularly in temperate climate regions. Although not entirely satisfactory for use in a global basis, several methods for rain attenuation prediction have been developed.

On the other hand, the dynamic behaviour of rain attenuation, which is particularly important for the design of low availability systems, is not well known. The subject raised the interest of several authors in recent years. A detailed analysis of fade durations using SIRIO satellite measurements has been reported by Matricciani et al (Alta Frequenza LVI, N. 1-2, 33-46, 1987). Vilar et al (IEEE Trans. Comm. 36, N. 6, 650-661, 1988) performed comprehensive analysis and modeling of point rainfall rate dynamic characteristics, based on a data bank of 49-years measurements in Barcelona.

The problem is addressed in this paper using 6 year-station data from 4 sites in Brazil. Concurrent measurements of rainfall rate and radiometric attenuation were made at 3 sites in equatorial climate (Amazon region) and one site in tropical region (Rio de Janeiro). Histograms of number and the total time of durations, of both fade level and rainfall rate exceedances are obtained, as well as the corresponding cumulative distributions. Parameters of log-normal functions fitting the distributions for each region are calculated. Statistics of return time to a given fade or rainfall rate level are computed. The relation between average fade durations and average point rainfall rate durations is also investigated.

CD of fade duration
Conditional fade dur.: conditioned on exceeding a given level

F61.3

LOW ANGLE EARTH-SATELLITE BEACON FADES AND SCINTILLATION AT 11 GHZ

W. J. Vogel*
and
G. W. Torrence
Electrical Engineering Research Lab
The University of Texas at Austin
Austin, Texas 78758-4497

A low elevation angle (5.8°) satellite propagation experiment at 11 GHz has been carried out in Austin, Texas for three years. The link performance is characterized by scintillation and rain attenuation. As both processes can occur simultaneously, an effort has been made to quantify the scintillations during rain fade events separately, with the objective of providing modelers with uncoupled statistics.

MEASURED AND PREDICTED MULTIPATH FADING DISTRIBUTIONS FROM 8 LINE-OF-SIGHT LINKS IN BRAZIL

L.A.R. Silva Mello* G.L. Siqueira
N.R. Dhein C.M. Einloft
Center for Telecommunication Studies - CETUC
R. Mqs. S.Vicente 225-Rio de Janeiro-22453-BRAZIL

Multipath fading is one of the most important propagation effects to be considered in the design of line-of-sight microwave links. It has been observed that cumulative distributions of measured attenuation show, in the deep fades region, the slope of a Rayleigh distribution. The probability that a fading depth A(dB) is exceeded, can, thus, be expressed as $P(A) = r.10^{-A/10}$.

The multipath fading occurrence factor r is a function of operation frequency, path geometry and geoclimatic characteristics of the link region. Over the years, several semi-empirical methods have been proposed in different countries to estimate r. The CCIR (Report 338-5, XVIIth Plenary Assembly, Düsseldorf, 1990) recently adopted a method to be used in a global basis. Nevertheless, due to the lack of measured data, particularly from tropical and equatorial regions, this method provides only a rough estimate of the geoclimatic parameter included in the calculation of the multipath occurrence factor r.

A multipath fading measurements program is currently being developed in Brazil. One-year measurements have been concluded in 8 links and are under way in other 6 links. This work presents cumulative distributions of fade depth obtained from the measured data. The measured distributions are compared with those predicted by the CCIR and other prediction methods. The geoclimatic factors for the links sites are derived.

For two of the links, statistics of fade duration for several attenuation thresholds have also been obtained. These statistics are important to allow the distinction between availability and reliability times in systems design.

F61.5

Global Estimates of Oceanic Rain from SSM/I Measurements

T. T. Wilheit *(Department of Meteorology, Texas A&M University, College Station, TX, 77843)
A. T. C. Chang (Hydrological Sciences Branch (974), NASA Goddard Space Flight Center, Greenbelt MD, 20771)
and L. S. Chiu (General Sciences Corp., Laurel MD, 20707)

An algorithm has been developed for the retrieval of monthly rain totals over ocean areas using the data from the SSM/I microwave radiometer on the DMSP satellite. The algorithm is based on histograms of the frequency of occurrence of brightness temperatures and linear combinations of brightness temperatures over 5° cells for one month intervals. The linear combination 2·T19V-T22V is used to reduce the impact of variability in the atmospheric water vapor content. A comparison of the T19V and T22V histograms is used to estimate the freezing level and rain layer thickness.

The algorithm assumes a Log-Normal (L-N) distribution of rain rates and calculates a predicted histogram which is compared with the observed histogram. The parameters of the L-N distribution are adjusted to achieve satisfactory agreement between the computed and observed histograms. The L-N parameters determine the monthly rain total for the cell.

More than 2 years of SSM/I data have been processed. Comparisons with climatology and other data indicate that the results are quite reasonable. The expected features can easily be seen in monthly and annual averages. The derived freezing levels also compare well with the observed freezing levels.

The only completely arbitrary parameters are the minimum detectable rain rate and the liquid water content of the non-raining cloud component. Uncertainties in these parameters do not appear to have an excessively large impact on the retrievals. The results are corrected for beam-filling by extrapolating the results of previous studies.

Detection and Measurement of Atmospheric Wave Structure Using a Scanning 118-GHz Spectrometer

P. G. Bonanni and D. H. Staelin
Research Laboratory of Electronics
Massachusetts Institute of Technology
Cambridge, Massachusetts 02139

Imaging of horizontal structure in the atmosphere at millimeter wavelengths can be accomplished with a nadir- or zenith-viewing instrument by scanning a narrow antenna beam through a sequence of angular positions; the scanning results in a set of viewing directions that can be chosen to lie within a plane perpendicular to the atmosphere's relative motion. The physics associated with observations of atmospheric buoyancy wave structure under these conditions gives rise to signatures that exhibit unique structural features. Assuming the scan angles are separated by constant angular increments and are symmetrically placed with respect to a strictly vertical viewing direction (total excursion $\pm 45^{\circ}$), the features characteristic of horizontally-traveling plane waves include an altitude-dependent distortion of the planar wavefronts and a viewing-angle-dependent amplitude attenuation that resembles a Bartlett apodization applied along one image dimension.

These signal distortions have direct consequences with respect to the detection and measurement of atmospheric waves: (1) the distortions permit discrimination of periodicities due to interference signals from those due to observed wave structure, and (2) the physics of the observation process enables an improved ability to infer the vertical amplitude and phase structure of the wave perturbation. In particular, vertical resolution and accuracy of retrieved wave-amplitude profiles are better than for the static profile retrieval problem (which relies on the altitude-slicing properties of coincident multispectral measurements); using a maximum-likelihood-based retrieval operator, vertical wave-amplitude profile accuracies of 0.1 K at 4-km resolution can be achieved for a 10-km wavelength disturbance without the use of *a priori* profile measurements. (The results apply for 10-minute observations of wave fields that include 100 consecutive 14-spot scans with an 8-channel instrument operating near 118 GHz; the assumed single-spot brightness accuracy is 0.5 K.)

In this paper, wave detection and parameter estimation methods, together with heuristic and model-based methods for interference discrimination, are applied to an extensive database of 118-GHz imagery gathered with an 8-channel scanning spectrometer. The database consists of atmospheric observations from both aircraft- and ground-based platforms. A statistical survey of aircraft-based data obtained on the high-altitude ER-2 during the Genesis of Atlantic Lows Experiment (January-February 1986) and the Cooperative Huntsville Meteorological Experiment (June-July 1986) elicits fewer than 14 wave candidates in a 33-hour statistical sample, and no evidence of wave activity above 0.17 K amplitude. Ground-based imagery from the New Hampshire White Mountains region reveals an abundance of ~5–10 K periodic brightness structure which is demonstrated to be consistent with 2–10 km-wavelength modulations in either relative humidity or cloud liquid density. Vertical wave-amplitude retrievals for the latter case are performed despite an inability to discriminate such structure on the basis of multispectral measurements alone.

F61.7

MEASUREMENTS OF THE 60-GHz O_2 SPECTRUM OF AIR

Hans J. Liebe*, George A. Hufford, and Robert O. DeBolt

Institute for Telecommunication Sciences
National Telecommunications and Information Administration
U.S. Department of Commerce
NTIA/ITS.S1, 325 Broadway, Boulder, CO 80303, USA

Molecular oxygen dominates throughout V-band (50-75 GHz) the attenuation and delay properties of dry air. The complex refractivity spectrum N displays with increasing altitude a pattern that changes from an unstructured band to isolated line behavior. For atmospheric conditions of pressure equivalent to heights between sea level and 30 km (100-1 kPa), this behavior for the most part has never been confirmed by experiment.

We studied the O_2-spectrum of dry air with a resonance spectrometer under controlled laboratory conditions. Key parts of the instrumentation were an automatic network analyzer operating as a reflectometer, and a one-port Fabry-Pérot resonator with Q values on the order of 300,000. Introducing gas into the resonator changes the resonance response. The changes were deduced from measured scattering parameters S_{11} by means of a nonlinear least squares method and expressed as complex refractivity N. All operations were controlled by a microcomputer, including reference level calibrations at multiple (up to 15×) fundamental resonance frequencies separated by about 0.7 MHz, and control of the pressure steps.

So far, analysis of data has been focussed on the loss part of N, expressed as attenuation rate α in dB/km. Over 4×10^6 S_{11} parameters were reduced to about 8,000 attenuation values. Measurements were made at frequencies between 49.3 and 67.2 GHz in 0.1 GHz increments for eleven pressure steps (1-100 kPa) and three different temperatures (7-30-53°C). Measurement uncertainties of α-values between 0.2 and 18 dB/km were estimated to be typically the worse of $\pm$0.05 dB/km or 2 percent. The collective spectral behavior of 38 pressure-broadened O_2 lines is described by a model named MPM89 (Liebe, Int. J. IR & MM Waves 10, 631-650, 1989). A first comparison of the experimental absorption results with MPM89 predictions reveals systematic differences which range, for example, at 60 GHz (30-100 kPa) from -2% (7°C) to -8% (53°C). The discrepancies correlate with O_2 line width and overlap parameters and their determination is central to describing the atmospheric O_2 spectrum. An interpretation of the new, extensive data set with Rosenkranz's overlap theory [JQSRT 39(4), 287-297, 1988] needs to be undertaken.

Calculation of Optical Properties of Impure Cloud Drops using FDTD and Realistic Modeling of Scavenging of Carbonaceous Particles

M. F. Iskander, P. C. Cherry, H. Y. Chen
Electrical Engineering Department
University of Utah

and

J. E. Penner
Lawrence Livermore National Laboratory

In determining the radioactive properties of clouds, it is important to consider the scavenging of carbonaceous particles of cloud drops. Previous efforts have treated the absorbing carbon nucleus as a core surrounded by a shell of pure water (Danielson, et. al. 1969) or using mixing rules to calculate an effective index of refraction for a cloud drop with soot particles distributed randomly throughout the volume of the drop (Chylek, et. al. 1984). Our initial efforts to calculate the optical properties based on accurate numerical modeling using the method of moments were limited because of difficulties in modeling electrically large water drop in the visible frequency range.

In this paper we present the results of using FDTD to accurately model and calculate optical absorption of impure cloud drops. The sizes, locations, and index of refraction of soot impurities within a cloud drop are included in the model. Initial results indicate significant enhancement in the absorption of carbon aerosols as a result of cloud condensation. Typical absorption values are 15 to 30 m^2/gm which are much larger than 8 to 10 m^2/gm absorption of carbon aerosols in air. Very high absorption cross-section values based on a shell-like model (multi-layer spherical model) particularly at a small volume fraction (10^{-6} to 10^{-7}) of carbonaceous particles, however, seems to be questionable.

R. E. Danielson, D. R. Moore, and H. C. Van de Hulst, "The Transfer of Visible Radiation through Clouds," *J. Atmos. Sci.*, Vol. 26, pp. 1078-1087, 1969.

P. Chylek, V. Ramaswamy, and R. J. Cheng, "Effect of Graphitic Carbon on the Albedo of Clouds," *J. Atmos. Sci.*, vol. 41, pp. 3076-3084, 1984.

F61.9

A Matrix Doubling Formulation of Internal Layer Emission with Irregular Boundaries

Hyo J. Eom

Department of Electrical Engineering
Korea Advanced Institute of Science and Technology
400, Kusung-dong, Yusung-gu, Taejon, Korea
Phone (042)-829-5525
Fax (042)-861-5635,6
e-mail hjeom@convex.kaist.ac.kr

A formulation for internal emission from a thermal scattering layered medium with irregular boundaries is developed. The matrix doubling method is utilized to obtain the emissivity expression which represents the up and downward thermal intensities inside the scattering layer. The scattering layer is assumed to be a random slab which is imbedded with thermal scattering particles, so that the intensity scattering approach is used with the radiative transfer formulation. The layer top and bottom boundaries are assumed to be random rough surfaces where a surface scattering process takes place. The developed emission model may be useful for the understanding of the internal emission problem where a radiometer is located inside an emitting medium with irregular rough boundaries. This type of problems is often encountered in the atmospheric temperature measurements with airborne or spaceborne remote sensing devices at optical and microwave regimes.

Microwave Scattering Signatures for Remote Sensing | Room 3024 Salle URSI F Session 78 | Signatures de diffusion micro-ondes en télédétection

Chairs/présidents: R.L. OLSEN, Canada

13:30 (78.1) Azimuthal Scattering Signatures of Various Tree Species at X-Band, **R.M. NARAYANAN**, S.E. NELSON, J.P. DALTON, *University of Nebraska, Lincoln, NE, USA*

13:50 (78.2) Sensitivity of Tree Canopy Backscatter to Variations in Open Canopy Parameters, **K.C. McDONALD**, F.T. ULABY, *University of Michigan, Ann Arbor, MI, USA*

14:10 (78.3) Millimeter Wave Scattering from Needle Arrays, **R.H. LANG**, O. KAVAKLIOGLU, *George Washington University, Washington, DC, USA*

14:30 (78.4) Techniques for Calibrated Measurement of Polarization of Scattered Echoes from Terrain, **K.V.N. RAO**, W.G. STEVENS, *Rome Air Development Center, Hanscom AFB, MA, USA*

14:50 (78.5) Bistatic Scattering Statistics of Echoes Scattered Out of the Plane of Incidence, W.G. STEVENS, **K.V.N. RAO**, *Rome Air Development Center, Hanscom AFB, MA, USA*

15:10 **COFFEE/CAFÉ**

15:30 (78.6) An Efficient Method of Computing the Phase Matrix and the Extinction Matrix for Arbitrary Rayleigh Particles, **M.W. WHITT**, F.T. ULABY, *University of Michigan, Ann Arbor, MI, USA*

15:50 (78.7) Effects of Rain and Wind on Satellite Measured Ocean Cross Section, **L. BLIVEN**[1], P. SOBIESKI[2], J.-P. GIOVANANGELI[3], H. BRANGER[3], [1]*NASA/GSFC, Wallops Island, VA, USA;* [2]*Université Catholique de Louvain, Louvain-la-Neuve, Belgium;* [3]*I.M.S.T., Marseille, France*

16:10 (78.8) Ocean Surface Radar Backscatter Measured with a Nadir-Looking 5.3/13.6 GHz Airborne Scatterometer, **L.G. HEVIZI**[1], R.E. McINTOSH[1], D.J. McLAUGHLIN[2], [1]*University of Massachusetts, Amherst, MA, and* [2]*Northeastern University, Boston, MA, USA*

16:30 (78.9) Calibrated Measurements of NRCS of the Ocean Surface at Ka-Band, **I. POPSTEFANIJA**, P. FERRARO, R.E. McINTOSH, *University of Massachusetts, Amherst, MA, USA*

16:50 (78.10) Automatic Ocean Surface Elevation Retrieval Using Passive Optical Remote Sensing Techniques, **H. SCHULTZ**, *University of Massachusetts, Amherst, MA, USA*

F78.1

AZIMUTHAL SCATTERING SIGNATURES OF VARIOUS TREE SPECIES AT X-BAND

Ram M. Narayanan*, Scott E. Nelson and Jon P. Dalton
University of Nebraska
Lincoln, NE 68588-0511

The azimuthal scattering characteristics of a variety of trees were measured in the field using a short range X-Band bistatic radar system operating at 9 GHz. The system consisted of a HP 8720B Network Analyzer, whose power output was amplified to 1 Watt in a Varian VTX 6180S1 TWT Amplifier. The receiver front end consisted of a 3.5-dB NF Miteq AMF-3B-8012-30 low noise amplifier. Standard gain horn antennas of 20 degree beamwidth were used. Calibration was performed for the backscatter measurement using a 7.08-cm (18-inch) corner reflector. Azimuthal measurements were made for both VV and VH polarizations over a 180 degree angle between the transmitter and receiver antennas at 10-degree azimuthal intervals. Data were collected at transmit and receive ranges of approximately 5 meters, and the beam impinged horizontally on the trees.

The trees investigated were fully foliated during our measurements. However, they represented wide variability in leaf cover characteristics, and included needleleaf as well as small and large leaf deciduous trees. The azimuthal polar power pattern, normalized to the co-polarized backscattered power, showed a peak in the forward scattering direction (azimuth angle of 180 degrees) due to direct coherent transmission, whose magnitude was seen to depend on the leaf area index. We also observed that the broadleaf trees have a more uniform diffuse scattering pattern as compared to the needleleaf trees, which showed more pronounced peaks and troughs. In addition, needleleaf trees were found to depolarize the incident energy more than the broadleaf trees with depolarization ratios averaging -5 dB and -10 dB respectively.

SENSITIVITY OF TREE CANOPY BACKSCATTER TO VARIATIONS IN OPEN CANOPY PARAMETERS

K. C. McDonald* and F. T. Ulaby

The Radiation Laboratory
Department of Electrical Engineering and Computer Science
The University of Michigan
Ann Arbor, MI 48109-2122, U.S.A.
Phone: (313) 764-0501
FAX: (313)763-1503

A first-order radiative transfer model for predicting backscatter from tree canopies at microwave frequencies has been developed at The University of Michigan Radiation Laboratory. This model, known as the Michigan Microwave Canopy Scattering (MIMICS) model, is fully polarimetric and operates over a wide range of incidence angles and canopy architectures. The first version of the model, MIMICS I, was developed for application to canopies with continuous (closed) crown layer geometries. Although MIMICS I has proven to be an effective tool for analyzing canopy backscatter in several studies, it does not adequately model backscatter for sparsely populated canopies in which the crown layer is discontinuous (open). Therefore, development of a second generation model, MIMICS II, that accounts for open crown geometries was undertaken.

MIMICS II models open canopies by accounting for the location, size and shape of the individual tree crowns. By treating these parameters as random variables, a statistical approach is taken in determining the solution to the radiative transfer equations. The canopy backscattering coefficients may then be determined by introducing statistics derived from the individual crown parameters into the radiative transfer solution.

This paper discusses development and applications of MIMICS II. The radiative transfer equations as applied to open canopies are reviewed and a solution to these equations is derived. The application of random variables that define open crown layer geometries and the incorporation of these random variables into the radiative transfer solution is presented. The sensitivity of canopy backscatter to variations in the open canopy architecture is discussed. Effects of the shape and spatial distribution of the individual tree crowns are considered. A comparison of these results to closed crown model results is made.

F78.3

MILLIMETER WAVE SCATTERING FROM NEEDLE ARRAYS

Roger H. Lang* & Omer Kavaklioglu
Department of Electrical Engineering & Computer Science
The George Washington University
Washington, DC 20052 USA

The needles of many conifers are arranged in a semi-random fashion along small stem-like structures. The question addressed in this paper is: "Does the spatial correlation that exists between the needles on each stem have substantial influence on the backscattering properties of the whole canopy?". To address this issue the backscattering characteristics from a half space of randomly oriented needles will be contrasted with the backscattering from a half space of randomly oriented arrays of needles.

Individual needles will be modeled by finite lossy dielectric cylinders whose diameter is small compared to a wavelength. By using quasi-static techniques the internal field in the needle can be estimated and from this field the dyadic scattering amplitude of a needle can be computed. In the simplest approximation the internal field in each needle of an array can be estimated as though the needle is isolated. The scattering amplitude of the array can then be computed.

Once the scattering amplitudes are known, the distorted Born approximation can be employed to compute the backscatter from a half space of independent needles and a half space of arrays of needles. The results show that as the wavelength becomes comparable to the needle array size the scattering effects of independent needles and arrays of needles differ.

TECHNIQUES FOR CALIBRATED MEASUREMENT OF POLARIZATION OF SCATTERED ECHOES FROM TERRAIN

K. V. N. Rao
William G. Stevens
Rome Air Development Center
Hanscom AFB, MA 01731

In this paper we discuss the relative merits of the techniques used to calibrate the clutter measurement sensors in both monostatic and bistatic geometrical configurations. Particular emphasis is placed on the techniques used for calibrated measurement of the polarization state of the scattered echoes from terrain. A brief review of the conventional techniques used for calibrating monostatic clutter sensors will be given. Bistatic measurements introduce additional complications. We describe two bistatic calibration techniques used in our measurement program to establish the dependence of bistatic clutter on signal polarization. Discussion of the errors involved will be presented.

One monostatic technique consists of using targets such as spheres, dihedrals, etc. whose backscatter cross sections can be calculated. A second option is to inject various level calibrated signals from the transmitter into the receiver. A third option is measuring the response of active transponders. Improper alignment of the receiver and the calibrating target, imprecise knowledge of the beam registrations, and polarization characteristics of the targets are some of the dominant sources of errors. The impact of these errors on the measurement of the normalized clutter cross section will be discussed.

A different method is required to calibrate the polarization dependence of bistatic clutter measured by our short-range bistatic sensor. A portion of the signal from the transmitter is coupled via a directional coupler into the calibration antenna whose polarization state can be matched with that of the receiver antenna. The coupling of the radiated power from the calibrated antenna into the receiver depends on both the antenna patterns. These antenna patterns are measured in a free-space range. The calibration technique consists of rotating the calibration antenna and the receiver antenna in synchronism so that their polarization states match. The received power was measured at ten degree increments of polarization angle and time-averaged. The spatial average of these power measurements was then taken as a reference. The observed power at any polarization angle deviated from the average by plus or minus one dB. A slight modification of this technique, which avoids rotation of the antennas is to use dual-polarized feeds in both the antennas. The polarization state of the calibrating antenna is switched rapidly between the orthogonal polarization states. The switching times have to be faster than the correlation time of the expected echoes from the desired clutter patch. At the receiver site, the amplitudes and phases of both orthogonal polarizations are measured and recorded simultaneously. This information combined with the echo signals from any range-azimuth resolvable cell yields the necessary parameters associated with the polarization statistics of the bistatic clutter. A discussion of the errors associated with deriving the normalized bistatic clutter cross section will be given.

F78.5

BISTATIC SCATTERING STATISTICS OF ECHOES SCATTERED OUT OF THE PLANE OF INCIDENCE

W. G. Stevens
K. V. N. Rao
Rome Air Development Center
Hanscom AFB, MA 01731

The primary object of the experiment described in this paper was to determine the temporal statistics, including the mean and standard deviation, of an illuminated clutter patch as a function of the receiver polarization state. The second objective was to compare measurements with analytically predicted (minima in) scattered power. A 3.2 GHz, 200 MHz bandwidth microwave measurement system was used to measure the temporal distributions of the power scattered by deciduous trees. The 4.5 square meter surface area of terrain was illuminated with either vertical or horizontal transmit polarization at an incident elevation angle of 76 degrees and the scattered elevation angle of 84 degrees. The bistatic scattering from the terrain was observed with a 6 foot parabolic antenna of variable polarization at an azimuthal scattering angle of 105 degrees.

The measured probability density functions of the scattered power from different range bins for both incident polarizations will be described. The coefficient of variation, defined as the ratio of the standard deviation to the mean of the scattered power was found to depend both on the polarization state of the receiver and the location of the particular resolution cell. These experiments indicate that the spread of the diffuse power scattered out of the plane of incidence is dependent both on the polarization angle and the mean scattered power. Results indicate that the measurement of mean scattered power is not sufficient to describe the behavior of the bistatic clutter.

Reasonable agreement was observed between the measured location of the linearly polarized minima and maxima and those predicted by analytical models. Experiments are currently being conducted to measure the relative magnitudes and the time phase angle between the orthogonal components of the elliptically polarized scattered wave.

AN EFFICIENT METHOD OF COMPUTING THE PHASE MATRIX AND THE EXTINCTION MATRIX FOR ARBITRARY RAYLEIGH PARTICLES

M. W. Whitt* and F. T. Ulaby

Radiation Laboratory
Department of Electrical Engineering and Computer Science
The University of Michigan
Ann Arbor, MI 48109-2122
Phone: 313-764-0501
FAX: 313-763-1503
Telex: 432-0815 UOFM-UI

A technique for efficient computation of the extinction matrix and the phase matrix for arbitrary Rayleigh particles is presented. In the standard computation of these matrices for general particles, the integration over orientation uses the Eulerian angles of rotation, and hence it is three-dimensional. It must also be recomputed, in general, for each combination of incident and scattered directions. By representing the scattering in terms of the polarizability tensor of the Rayleigh particles, the three-dimensional integration can be reduced to a finite number of one-dimensional integrations, independent of the incident and scattered directions. Therefore, they are computed only once for a given orientation distribution.

The general formulation for the polarizability tensor representation is given, and then used to derive expressions for the phase matrix and the extinction matrix of a restricted set of Rayleigh particles, namely axisymmetric particles. The standard method of computing the extinction matrix and the phase matrix is also reviewed for a comparison of the two techniques. Finally, the resulting integrals are evaluated for some common orientation distribution functions used in the literature.

F78.7

EFFECTS OF RAIN AND WIND ON SATELLITE MEASURED OCEAN CROSS SECTION

L Bliven*
NASA/GSFC
Wallops Island
VA 23337 USA

J-P Giovanangeli
IMST
12 General Leclerc
13003 Marseille FR

P Sobieski
U Catholique de Louvain
1348 Louvain-la-Neuve
Belgium

H Branger
IMST
12 General Leclerc
13003 Marseille FR

Microwave backscatter measurements of the sea surface are made by satellite-borne instruments such as altimeters, scatterometers, and synthetic aperture radars. Wind is nearly ubiquitous and it generates sea-surface roughness. So techniques were first developed to infer wind conditions from the backscatter cross sections because wind fields are needed for meteorological and ocean circulation studies. Recent efforts to improve some of these algorithms by considering various physical factors are recapitulated.

Rain also generates sea-surface roughness, but its effect on wind speed algorithms is not well understood. We review case studies of anomalous wind estimates due to rain. A discussion of various air-sea interaction processes that are altered by rain is presented and then we discuss how these changes may effect wind speed algorithms. Recent research concerning the effects of rain and wind on scatterometer measurements is summarized.

Condensation of water vapor releases heat into the Earth's atmosphere and this is a major forcing function in the troposphere. The Tropical Rainfall Measuring Mission (TRMM) and the Tropical System Energy Budget (BEST) are being planned to make rain measurements over the oceans. Active microwave systems are being considered for this purpose because they have the potential to measure rainfall profiles. Sea-surface cross sections are used in the mirror-image algorithm to obtain rainfall profiles. We briefly discuss possible effects of wind and rain generated sea-surface roughness on system operation. Research needs are examined.

OCEAN SURFACE RADAR BACKSCATTER MEASURED WITH A NADIR-LOOKING 5.3/13.6 GHz AIRBORNE SCATTEROMETER

Laszlo Gy. Hevizi, Robert E. McIntosh
Department of Electrical and Computer Engineering
University of Massachusetts
Amherst, MA 01003, USA
Telephone: (413)-545-4579 FAX: (413)-545-0724

and

David J. McLaughlin
Department of Electrical and Computer Engineering
Northeastern University
Boston, MA 02115, USA

An airborne scatterometer system of the University of Massachusetts (UMASS), participating in the Electromagnetic Bias Experiment of the National Aeronautics and Space Administration (NASA), simultaneously measured the relative normalized radar cross section of the ocean surface at 5.3 and 13.6 GHz. These are the operating frequencies of a satellite altimeter, which is scheduled for launch in 1992 as part of the joint United States and French Ocean Topography Experiment.

A series of flights, with the objectives of electromagnetic bias characterization, was accomplished by the Oceanographic Research Branch of NASA at Wallops Island, Virginia, between February and April in 1989. The UMASS scatterometer was installed on a NASA P-3 aircraft along with the NASA Oceanographic Lidar and Surface Contour Radar. Eleven hours of data was collected over the Atlantic Ocean during various sea conditions in 9 flights. The footprint illuminated by the UMASS scatterometer was small compared to the dominant length of the ocean waves, thus the measured normalized radar cross section combined with accurate target range from the other two instruments allowed us to relate ocean surface backscatter to surface elevation, and to wave height. A decrease in ocean surface normalized radar cross section with increasing wave height was measured at both operating frequencies, though the decrease was more significant at 5.3 GHz than at 13.6 GHz. A 6 dB variation was observed at both frequencies as significant wave height ranged from 0.5 to 4.5 m. The ocean normalized radar cross section has not changed at 5.3 GHz for waves higher than 2.5 m, and at 13.6 GHz for waves higher than 3 m.

F78.9

CALIBRATED MEASUREMENTS OF NRCS OF THE OCEAN SURFACE AT Ka-BAND

Ivan Popstefanija*, Paul Ferraro and Robert E. McIntosh
Department of Electrical and Computer Engineering
University of Massachusetts
Amherst, MA 01003, USA
Telephone: (413)-545-0779, FAX: (413)-545-0724

Determining the limits of widely used theories that predict radar backscatter from the ocean surface (e.g., specular and composite Brag scattering theories) is of great importance, especially when applied to SAR imagery of the ocean. For the purpose of studying these limits, the University of Massachusetts has fabricated a Ka-band Stepped Frequency Scatterometer. Important characteristics of this sensor are: short-range (17 - 64 m), high resolution (.5 m), fully coherent, fast sampling (10 ms) and mechanically switchable to all four linear polarization combinations.

Large sets of data were collected at two test sites. One site was the Chesapeake Light Tower during the SAXON-CLT experiment and the other was a pier in Duck, N.C., which is a part of the U.S. Army's Coastal Engineering Center. In our paper we will present analysis of the dependance of radar backscatter on a wide range of environmental parameters for different incidence angles (0° - 60°) and different polarization combinations (e.g. VV, HH and HV). Typical results of our analysis are shown in Figure 1 .

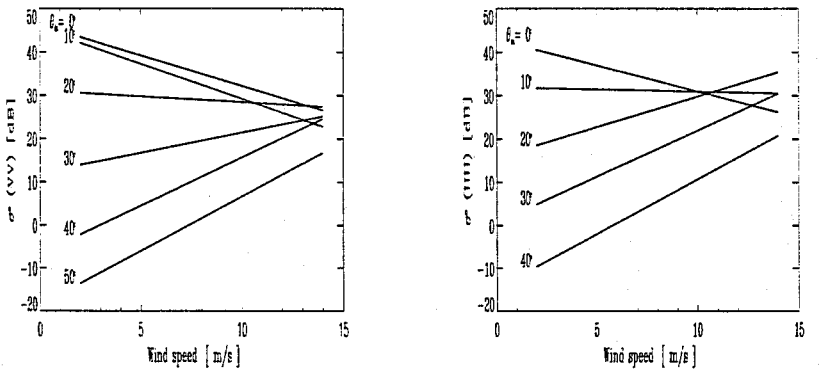

Figure 1: Radar-cross section dependance for up- and down-wind of the ocean at Ka-band

AUTOMATIC OCEAN SURFACE ELEVATION RETRIEVAL USING PASSIVE OPTICAL REMOTE SENSING TECHNIQUES

Howard Schultz
Microwave Remote Sensing Laboratory
University of Massachusetts, Amherst
Amherst, Massachusetts 01003

A method is presented for retrieving the small scale spatial and temporal structure of the ocean surface, which is especially valuable for radar remote sensing studies where linear approximations and classical theories fail to predict the radar return from the ocean surface. For example, the interpretation of radar images of the ocean surface depends on the modulation of centimeter surface waves by several environmental parameters including the wind and long period waves. Because of the complexity of these interactions, the best method of studying radar imaging mechanisms is to make simultaneous radar and optical observations of the water surface, which enables direct comparisons between the radar return, the small scale structure of the surface, and environmental parameters.

In the vicinity of wave breaking, in patches of foam, or along sharp wave crests, the optical characteristics of the ocean surface is best described by a Lambertian model. For smooth areas of the ocean surface, however, a specular model best describes the optical characteristics of the surface. The surface reconstruction system utilized two types of retrieval algorithms, one for Lambertian type surfaces and the other for specular type surfaces. The Lambertian retrieval algorithms are based on existing stereoscopic reconstruction theory with modifications to improve processing speed and accuracy. For Lambertian surfaces, two views of a surface provide sufficient information for retrieving the surface shape. For specular type surfaces, however, at least three views of a surface are required for surface reconstruction. Because of the qualitative differences between images of Lambertian and specular surfaces, a new set of specular surface retrieval algorithms were derived based on the question: For three or more cameras viewing a water surface, what is the surface shape that will result in the observed set of images?

To demonstrate these retrieval algorithms, several test cases were run on a simulated water surface. In the examples, a simulated ocean surface was used as input to a ray tracing program which produced simulated images assuming a Lambertian or specular surface reflection model. The simulated images were then processed by the retrieval algorithms. The performance of the retrieval algorithms was evaluated by comparing the retrieved elevation maps to the original simulated surfaces.

Remote Sensing
Concepts and Instruments
for Telesonde

Room 3024 Salle
URSI F Session 94

Concepts en télédétection
et instruments
pour télésonde

Chairs/présidents: E.R. WESTWATER, USA

08:30 (94.1) TELESONDE: An Integrated Remote-Sensing System, **S.F. CLIFFORD**, E.R. WESTWATER, *National Oceanic and Atmospheric Administration, Boulder, CO, USA*

08:50 (94.2) Measurement of Water Vapor Profiles Using Raman Lidar, **S.H. MELFI**[1], D. WHITEMAN[1], R. FERRARE[1,2], [1]*NASA Goddard Space Flight Center, Greenbelt, MD, and* [2]*Universities Space Research Associates, Greenbelt, MD, USA*

09:10 (94.3) Remote Sensing of Temperature Profiles by the Radio Acoustic Sounding System (RASS), **D.B. WUERTZ**, B.L. WEBER, R.G. STRAUCH, K.P. MORAN, D.A. MERRITT, *National Oceanic and Atmospheric Administration, Boulder, CO, USA*

09:30 (94.4) Remote Sensing of Temperature and Water Vapor Profiles by a Combination of Surface- and Satellite-Based Remote Sensors, **L.S. FEDOR**, J.A. SCHROEDER, E.R. WESTWATER, B.L. WEBER, B.B. STANKOV, *National Oceanic and Atmospheric Administration, Boulder, CO, USA*

09:50 (94.5) Remote Sensing of Water Vapor Profiles with an Autocorrelation Radiometer, **P. GAISER**, C. SWIFT, *University of Massachusetts, Amherst, MA, USA*

10:10 **COFFEE/CAFÉ**

10:30 (94.6) Implementation of the NOAA Wind Profiler Demonstration Network, **D. BERAN**, M. ACKLEY, R. CHADWICK, M. BARTH, D. LAW, D. COTE, *National Oceanic and Atmospheric Administration, Boulder, CO, USA*

10:50 (94.7) Retrieval of Water Vapor Profiles from a Network of Surface-Based Remote Sensors, Y.-H. KUO[1], J.A. SCHROEDER[2], **E.R. WESTWATER**[2], [1]*National Center for Atmospheric Research, Boulder, CO, and* [2]*National Oceanic and Atmospheric Administration, Boulder, CO, USA*

11:10 (94.8) Clear-Air Temperature Profile Retrievals Using Passive 118-GHz O_2 Spectra, **A.J. GASIEWSKI**, J.T. JOHNSON, *Georgia Institute of Technology, Atlanta, GA, USA*

11:30 (94.9) Determination of the Atmosphere Refraction Index by Satellite Radio Signals, **B.M. SHEVTSOV**, *Pacific Oceanological Institute, Vladivostok, USSR*

11:50 (94.10) A Study of Frequency Domain Interferometry Made with Chung-Li VHF Radar, **Y.-H. CHU**, *National Central University, Taiwan, China*

F94.1

TELESONDE: AN INTEGRATED REMOTE-SENSING SYSTEM

Steven F. Clifford* and Ed R. Westwater
NOAA/ERL/Wave Propagation Laboratory
Boulder, Colorado 80303

Recent developments in remote-sounding technology and in data assimilation techniques give the promise that hourly or better radiosonde quality profiles of winds, temperature, and moisture can be derived by an integrated sounding system. Such an integrated system consists of three components:

(1) Surface-based remote sounders. Starting from Wind Profilers and their deployment into a national demonstration network, additional instruments are available to complete the thermodynamic sounding requirements. Such technologies include Radio Acoustic Sounding Systems, microwave and infrared radiometers, and Raman and DIAL lidars.

(2) Satellite-based remote sounders. Data from both polar-orbiting and geostationary satellites can be blended with soundings from a network of surface-based remote sounders.

(3) A data assimilation and forecast model. Such a model can optimally integrate data from the satellite- and surface-based observing systems. This model will also be fully capable of integrating high volume in situ data that will be available in the 1990's.

This presentation will discuss requirements of modern weather forecasting models and how these requirements may be met by the proposed integrated sounding system called TELESONDE.

MEASUREMENT OF WATER VAPOR PROFILES USING RAMAN LIDAR

S. H. Melfi* and David Whiteman
NASA/Goddard Space Flight Center
Greenbelt, MD 20771

Richard Ferrare
NASA/Goddard Space Flight Center
and
Universities Space Research Associates
Greenbelt, MD 20771

Water vapor is one of the variables which define the state of the atmosphere. It is an important source of heat which drives atmospheric circulation and it has a large impact on radiative transfer through the direct absorption/emission of infrared radiation and also through its role in cloud formation. Atmospheric moisture figures prominently in the earth/atmosphere hydrological cycle as an important storage term giving rise to precipitation. The variation of moisture with altitude is a prime factor in convective stability and as such, is a determinant in the outbreak of deep convective storm systems. In addition, when moisture is expressed as a mixing ratio, it is a conserved parameter under all meteorological processes except condensation and evaporation, and thus serves as an excellent tracer to visualize dynamic atmospheric processes.

The lidar discussed in this paper is described by Melfi, Whiteman, and Ferrare (*J. Appl. Meteor.*, **28,** 789-806, 1989). It consists of a vertically pointed Nd:YAG laser operating at the tripled wavelength of 355 nm whose optical axis is aligned parallel with a 30-inch diameter Dall-Kirkham telescope. The laser radiation backscattered by the atmosphere is collected by the telescope and divided by beam splitters onto three photomultipliers, one sensitive to Raman scattering by water vapor (408 mm), a second to Raman scattering by nitrogen (387 nm), and the third to scattering by aerosols and molecules at the laser wavelength (355 nm).

It has been shown by Melfi (*Appl. Opt.* **11**, 1605-1610, 1972) that the ratio of Raman scattering by water vapor to that from nitrogen is proportional, to a good approximation, to water vapor mixing ratio. Lidar data of water vapor mixing ratio have been acquired during a number of field campaigns. During each operational period, the lidar system acquires accumulated backscatter data for a 2-minute period, records that data, and cycles again. Observations using the Raman lidar have been made during times when interesting atmospheric changes have taken place. The changes that have been observed include cold and warm frontal passages, gravity waves moving overhead, and the development of clouds. Several examples of the time-height displays will be shown and explained during the presentation.

F94.3

REMOTE SENSING OF TEMPERATURE PROFILES BY THE RADIO ACOUSTIC SOUNDING SYSTEM (RASS)

David B. Wuertz*, Bob L. Weber, Richard G. Strauch,
Kenneth P. Moran, and David A. Merritt
NOAA/ERL/Wave Propagation Laboratory
Boulder, Colorado 80303

Vertical profiles of virtual temperature in the lower troposphere can be measured with radiosonde-type accuracy using the Radio Acoustic Sounding System (RASS) technique. Temperature data are obtained with the same height and time resolution as that obtained with wind profiling, and extend from about 200 m above the surface to several km. An overview of how RASS works and the factors that affect its performance are discussed. Examples show how RASS can improve the observation of significant weather events (see figure).

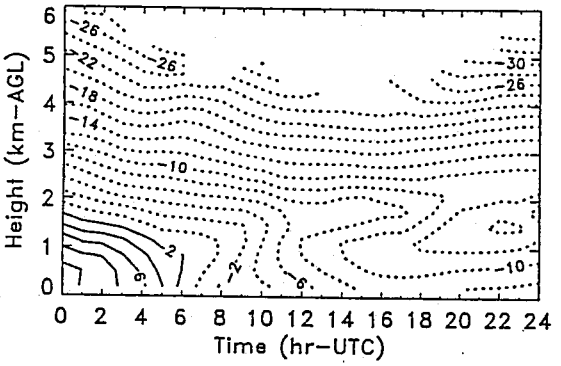

Fig. RASS temperature measurements (°C) showing the passage of a cold front on 13-Feb-90. Data from three radar sites (at Denver, Platteville, and Erie, Colorado) are combined here.

Comparisons of RASS and radiosonde temperature measurements over a two-month period of continuous operation show very good agreement. These results demonstrate that RASS promises to be a powerful tool for meteorological studies and an important instrument in the TELESONDE project.

Remote Sensing of Temperature and Water Vapor Profiles by a Combination of Surface- and Satellite-Based Remote Sensors

by

L.S. Fedor*, J.A. Schroeder, E.R. Westwater, B.L. Weber, and B.B. Stankov
NOAA/Wave Propagation Laboratory
325 Broadway
Boulder, CO 80303

Temperature profiles derived from the Tiros-N Operational Vertical Sounder (TOVS) on board the NOAA polar orbiting satellites are reasonably well-determined above 500 mb. Ground-based remote sensing systems such as the Radio-Acoustic Sounding System (RASS) provide accurate but altitude-limited temperature profiles. Several papers have discussed combining surface- and satellite-based remote sensing measurements to determine more accurate temperature profiles; a recent paper contains references to earlier works and also gives results of combining RASS and TOVS soundings (Schroeder et al; J. Ocean. Atmos. Tech., in press). The Wave Propagation Laboratory operates a 915 MHz RASS and a six-channel microwave radiometer located at Stapleton airport (Denver, Colorado), a 406 MHz RASS located at Erie, Colorado, and a 50 MHz RASS and a dual-channel microwave radiometer at Platteville, Colorado. Each of these systems provides a temperature profile covering a different altitude range; the radiometers provide integrated amounts of water vapor and cloud liquid. A low-altitude combined temperature profile derived from the 915 MHz RASS and blended with the most recent National Weather Service radiosonde release to provide a first guess for a TOVS temperature retrieval. The subsequent profiles are compared with data from specially launched radiosondes. We also discuss the possibilities of combining data from the Wind Profiler Demonstration Network with both polar-orbiter and geostationary satellite soundings. Examples are also given of combining microwave radiometric soundings of water vapor with soundings from the VAS instrument on GOES.

F94.5

REMOTE SENSING OF WATER VAPOR PROFILES WITH AN AUTOCORRELATION RADIOMETER

Peter Gaiser* and Calvin Swift
University of Massachusetts at Amherst

Water vapor is one of the most dynamic variables in the atmosphere. Determining the amount and distribution of tropospheric water vapor presents an important problem in atmospheric sciences. Microwave radiometery offers a technique that can provide highly repeatable measurements of the water vapor profile, averaged over a controlled volume.

The Microwave Remote Sensing Laboratory at the University of Massachusetts has developed a K-Band Autocorrelation Radiometer (CORRAD). CORRAD measures the autocorrelation function of the downwelling thermal emission across a wide bandwidth (20.5 to 23.5 GHz) centered near the 22.235 GHz water vapor absorption line. These measurements are Fourier transformed in software to produce samples of the brightness temperature spectrum across the band with 100 MHz resolution. The high number of samples serve to better constrain the inversion process from brightness temperatures to water vapor profiles. Furthermore, the individual autocorrelation measurements have a higher signal-to-noise ratio than standard direct measurements of brightness temperature because of the much larger bandwidth used in the CORRAD.

CORRAD receives downwelling atmospheric radiation through an offset parabolic reflector antenna. The input signal is split into two channels and downconverted to C-band (4.5 to 7.5 Ghz). One of the channels passes through a variable length of non-dispersive transmission line to generate the necessary time delays. The two signals are then cross-multiplied and averaged, producing an autocorrelation function.

Water vapor profiles are retrieved using a minimum squared error technique. This inversion process involves a linear perturbation of the water vapor profile about some a priori estimate. Profiles have been produced with spatial resolutions ranging from .2 km in the lower troposphere to 3 km in the upper troposphere. These profiles agree to within ten percent of profiles from radiosondes.

The material to be presented will include a detailed description of the CORRAD hardware and methods used in calibration. The inversion process will also be addressed along with water vapor profiles that have been measured. In addition, plans for replacing the serial delay lines with parallel delays will be discussed.

Implementation of The NOAA Wind Profiler Demonstration Network

D. Beran, M. Ackley, R. Chadwick,
M. Barth, D. Law, and D. Cote

Profiler Program Office
R/E/FS3, 325 Broadway
Boulder CO, 80303

The NOAA Wind Profiler Demonstration Network (WPDN) is an array of 30 profilers covering the central region of the United States. Its primary purpose is to demonstrate the impact of this new technology on atmospheric research, meteorological analyses, and operational weather forecasts. A secondary objective is to evaluate engineering aspects of wind profilers and the logistics required to operate an array of remote sensors linked to a common data collection and control center. This demonstration is a precursor to larger national networks.

A discussion of the design of the network and its major components (wind profilers, data collection and control center, and communications) is followed by a description of the system logistics and operation. Early results from an analysis of system reliability and critical component failures is related to overall system performance. Examples of the meteorological assessment of the network data and special studies, such as clear air turbulence detection are discussed.

The paper concludes with a discussion of critical issues for the future of remote profiling technology, such as operational frequency allocations, and the role of the demonstration network in assessing temperature and moisture profiling concepts.

F94.7

RETRIEVAL OF WATER VAPOR PROFILES FROM A NETWORK OF SURFACE-BASED REMOTE SENSORS

Ying-Hwa Kuo
National Center for Atmospheric Research
P.O. Box 3000, Boulder, CO 80307

Judith A. Schroeder and Ed R. Westwater*
Wave Propagation Laboratory/NOAA
325 Broadway, Boulder, CO 80303 3328

Over the past 10 years, there has been significant progress in the development of remote sensing instruments for wind and temperature profiling (e.g., the VHF and UHF wind profiler and the radio acoustic sounding systems--RASS). However, the development of remote sensing instruments for water vapor has been slow. Even with the most advanced technology (such as the high-resolution interferometer sounding system), the vertical resolution of water vapor profiling is on the order of 200-mb. This is inadequate for initialization of operational numerical weather prediction models, and for mesoscale observational studies.

In this paper we develop a methodology to retrieve vertical profiles of water vapor by assimilating observations from a network of surface-based remote sensors into a mesoscale meteorological model. We assume that a network of wind profilers, RASS, and dual-channel microwave radiometers are available. The basic idea is to couple the vertical profilers of relative humidity provided by the model and the remote sensing measurements in a time-continuous manner. Although the radiometers can only provide the vertically integrated water vapor, this type of measurement is highly accurate. We tested this methodology with the 3-h special rawinsonde data collected during the 1979 SESAME experiment. The results showed that by assimilating the vertically-integrated water vapor measurements into the model, we can retrieve the vertical profiles of water vapor with significant accuracy. This method is considerably superior to other methods based on climatology or statistical approaches.

Clear-air Temperature Profile Retrievals Using Passive 118-GHz O_2 Spectra

A.J. Gasiewski* and J.T. Johnson
School of Electrical Engineering
Georgia Institute of Technology
Atlanta, GA 30332

The retrieval of atmospheric vertical temperature profiles in clear air using passive 118-GHz O_2 emissions is demonstrated using nadiral aircraft-based brightness observations made during the Cooperative Huntsville Meteorological Experiment (COHMEX, 1986). The spectra were measured using the Massachusetts Institute of Technology's Millimeter-wave Temperature Sounder (MTS) instrument on the NASA ER-2 high-altitude aircraft. The MTS is a Dicke-switched imaging radiometer with eight double sideband channels located from 450 to 2100 MHz around the 118-GHz oxygen (1^- line) resonance.

A linear-statistical minimum mean-square-error (LSMMSE) estimator was derived from 100 non-independent coincident pairs of radiosonde observations and 118-GHz spectra. Temporal and spatial colocation was typically better than ~50 minutes and ~100 kilometers. Both day and night observations were included in the ensemble. A statistical (rather then physical) retrieval operator was chosen to remove the effects of any biases in the radoisonde or MTS measurements and any radiative transfer model uncertainties.

The ensemble of temperature profile retrieval errors are shown in Figure 1; statistics for this ensemble are shown in Figure 2 (●). These errors are significantly smaller than the a-priori variation of atmospheric temperature observed either within the ensemble (△) or throughout COHMEX (□). The results suggest that clear-air 118-GHz retrieval errors of ~0.5-1 K can be expected for the troposphere during summer-midlatitude conditions using satellite radiometers.

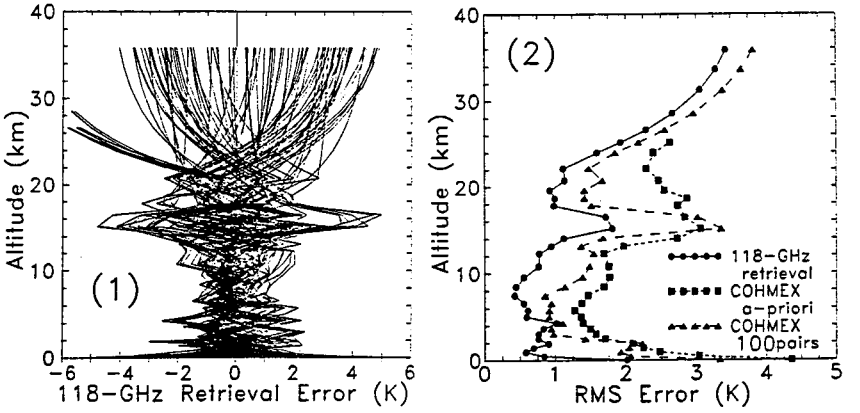

F94.9

DETERMINATION OF THE ATMOSPHERE REFRACTION INDEX BY SATELLITE RADIO SIGNALS

B.M.Shevtsov, Pacific Oceanological Institute,
7 Radio St., Vladivostok,USSR,690032

During observations of radio signals from satellites of the navigation system TRANSIT (150 and 400 MHz) over the sea surface not far from the horizon one notes enough frequently signal oscillations more fast than usual interference beats. By contact measurements of the atmosphere radio characteristics there was found the relationship of these oscillations with raised inversion layers. It is possible to show by the solution of the direct problem that fast oscillation are the result of the multipath interferation of the radiation, reflected from the inversion layer. The frequency of fast oscillations is defined by the altitude of the layer bedding,and the amplitude - by the layer reflection factor. This allows to estimate parameters of the inversion layer according to the character of beats (A.N.Bogaturov et.al., DAN AN SSSR, in print, in Russian).

It is possible to solve the inverse problem in the rigorous statement, i.e. to restore the altitude dependence of the atmosphere refraction index by satellite radio observations using the differential method (Shur-algorythm).

Because of the big remoteness of satellites, their radio signals can be regarded as monochromatic plane waves, incident an angle upon the nearsurface inhomogeneous atmosphere layer. Radio signals which pass through the atmosphere inhomogeneitics, are received near the Earth surface. It is possible to show, that synchronized amplitude - phase measurements of radio signals over two polarization in dependence on the incidence angle, give the initial data which are necessary for the inverse problem solution by the differential algorythm. However, random influences (the noustability of the satellite transmitter, deposit of ionosphere and atmosphere turbulence) lead to fluctuation of receiving data and put restrictions on the resolution of the restoration method.

A STUDY OF FREQUENCY DOMAIN INTERFEROMETRY MADE WITH CHUNG-LI VHF RADAR

Yen-Hsyang Chu
Institute of Atmospheric Physics, NCU, Taiwan,. CHINA

In the past few years, the technique of Frequency Domain Interferometry(FDI) has been developed on VHF radar. By using this technique, the characteristics of a very thin atmospheric layer structure, which is embedded in the radar volume and can't be solved by the conventional VHF radar with only one operational frequency, can be determined through the calculation of the coherence and the phase from the two echo signals with different operational frequency. The layer thickness can be deduced from the former, while the position of the layer in the radar volume can be calculated from the latter. According to the FDI theory, the coherence will be approached to zero if the layer thickness is fairly greater than the radar volume. However, in this study, it will be shown that if the pulse radar is applied and the atmospheric refractivity irregularities are distributed uniformly in the radar volume, that is , there is no narrow layer structure existed in the scattering volume, the coherence of two signals with different operational frequencies is still high and its behavior can be described by the equation $C \propto \mathrm{Sinc}(\Delta k\, \Delta r)/(1+N/S)$, where C is the coherence, Δk is the wave number difference between two carrier frequencies, Δr is the spatial resolution of radar pulse, N/S is the noise-to-signal power ratio. This feature can be interpreted physically by the finite volume filtering effect on the turbulent wavenumber spectrum. This theoretical prediction has been compared with the FDI experiments carried out by Chung-Li VHF radar, and the results are quite consistent. Thus, it is suggested that when the FDI technique is applied to estimate the thickness and the position of a thin layer, the finite volume filtering effect should be tahen into account.

HF and Microwave Radar for Observations of Land and Sea

Room 3024 Salle URSI F Session 111

Systèmes radar HF et micro-ondes pour observations terrestres et maritimes

Chairs/présidents: J. GOWER, Canada

13:30 (111.1) Land Backscatter Coefficients at HF, **S.J. ANDERSON**, *Defence Science and Technology Organisation, Salisbury, Australia*

13:50 (111.2) On the Ground Wave Propagation Over a Cliff with Finite Ground Parameters, H. WANG, **S.A. SAOUDY**, J. WALSH, *Memorial University of Newfoundland, St. John's, NF, Canada*

14:10 (111.3) VLF Radiowave Reflection from Distant Mountain Ranges, **J.R. WAIT**, *University of Arizona, Tucson, AZ USA*

14:30 (111.4) Bridged Knife Edges – A Model for Terrain Diffraction, **J.H. WHITTEKER**, *Communications Canada, Ottawa, ON, Canada*

14:50 (111.5) Measurement Technique of the Hardware Phase Shifters of an HF Linear Phased Array, **S.A. SAOUDY**, R. KHAN, *Memorial University of Newfoundland, St. John's, NF, Canada*

15:10 **COFFEE/CAFÉ**

15:30 (111.6) Environmental Effects on Ocean Current Measurement Using Multifrequency Radar, **I. POPSTEFANIJA**, R.E. McINTOSH, *University of Massachusetts, Amherst, MA, USA*

15:30 (111.7) Active Reduction Ground Penetrating Radar Antenna, **L. PETERS JR.**, M. BARNES, M. POIRIER, E. NASSER, *Ohio State University, Columbus, OH, USA*

16:10 (111.8) Focused Array Radar Subsurface Imaging, **W.J. GRAHAM**, *Graham Research Corporation, Bensalem, PA, USA*

16:30 (111.9) RF Electronics Subsystem for the Spaceborne Imaging Radar-C, **B.L. HUNEYCUTT**, *California Institute of Technology, Pasadena, CA, USA*

16:50 (111.10) A Correction Method for Range Effects in Scheduling Reflector Antenna Footprints for Low-Earth-Orbit Satellites, **F. FOK**[1], B. EATOCK[2], [1]*Atlantis Scientific Systems Group Inc., Ottawa, ON, and* [2]*Defence Research Establishment, Ottawa, ON, Canada*

F111.1

LAND BACKSCATTER COEFFICIENTS AT HF

S.J.Anderson
Surveillance Research Laboratory
Defence Science and Technology Organisation
SALISBURY SOUTH AUSTRALIA 5108

The variability of the sea surface under different wind conditions yields a corresponding diversity of radar signatures, especially in the Doppler domain. HF skywave radars have long exploited this variability to estimate sea state parameters from the measured Doppler spectrum of radio signals backscattered from the distant ocean surface. Echoes from land are of much less intrinsic interest, since the time-independent surface imposes no Doppler shift on the reflected radio waves, assuming of course that the radar is at rest relative to the land being illuminated. (Here we shall consider only land-based skywave radars operating in a quasi-monostatic mode.) Nevertheless, there are several ways in which a knowledge of the radar cross section per unit area, or 'backscatter coefficient' can be used to advantage.

First, the problem of coordinate registration which arises with skywave radars because of the unkown ionospheric reflection height can be solved if there are recognisable features in the radar returns. While beacons and coastlines are the best known features used in this role, echoes from both discrete and extended land formations have been shown to afford useful references for coordinate transformation. Second, knowledge of the backscatter coefficient affords a means of calibrating the radar echoes in amplitude, thereby enabling estimation of the RCS of other echo sources in the field of view. A related benefit is the ability to determine ionospheric propagation losses. Third, it is well known that the electrical properties of the ground change with moisture content. It is not unreasonable to speculate that there may be some remote sensing potential in monitoring seasonal variations in the HF backscatter coefficient.

As part of the remote sensing program undertaken during the 1980's with the JINDALEE skywave radar, extensive measurements of both land and sea clutter were recorded over the Northern Australia region. Transponders, a commandable beacon and other reference scatterers were employed to provide calibration sources. Results emerging from the analysis of this data show that (i) spatial variations exceeding 15 dB are not uncommon, (ii) some individual prominences can be identified, (iii) seasonal variations are detectable, and (iv) some dependence on elevation angle is evident.

ON THE GROUND WAVE PROPAGATION OVER A CLIFF WITH FINITE GROUND PARAMETERS

H.Wang, S.A. Saoudy** and J. Walsh**
**Faculty of Engineering and Applied Science*
***Centre for Cold Ocean Resources Engineering*
Memorial University of Newfoundland
St. John's, Newfoundland, A1B 3X5.

The characteristics of ground-wave propagation over a cliff will be investigated using both the compensation method and the residue method. Presently, a prototype bistatic radar system which uses ground wave propagation for over the horizon target detection is being built on a cliff at Cape Race, Newfoundland. The radar has a log periodic antenna as the transmitter and a phased linear array as a receiver. The charcteristics which include the cliff gain, the attenuation coefficient and the site gain for the ground wave propagation will be used in determining the portion of radio wave scattered towards the ionoshpere while transmitting and the received signal level across the linear array on the nonuniform coastline. The difference between the assumptions of the two methods will be identified and comparison of the relevant results will be illustrated. The compensation method has been developed by Wait who employed the surface impedance technique (J. Wait, " Recent Analytical Investigations of Electromagnetic Ground Wave Propagation over Inhomogeneous Earth Models," Proc. IEEE, Vol. 62, pp.1061-1072, 1974). The residue method has been developed by Furutsu who employed the Green function (K. Furutsu, "A Systematic Theory of Wave Propagation over Irregular Terrain," Radio Science, Vol 17, pp. 1037-1050, 1982).

F111.3

VLF RADIOWAVE REFLECTION FROM DISTANT MOUNTAIN RANGES

James R. Wait, (Univ.of AZ)
2210 East Waverly
Tucson Arizona 85719 USA

It has been demonstrated by Thomson(Jour. Atmos. Terr.Phys. 51, 339,1989) that there is convincing evidence electromagnetic waves will be "reflected" from distant topography. In fact Thomson has shown that such may be the case even if the ridges are well displaced from the great circle path between transmitter and receiver. Here we propose an analytical model to provide a possible explanation for the observations.

The formulation is an extension of mixed path ground wave theory as summarized recently by Wait(Chap.7,Electromagnetic Wave Theory,Wiley,1988). Here we allow implicitly for the presence of the ionosphere and the analysis deals with modes in the earth ionosphere waveguide.

The topographical region, considered as the target,extends over a rectangular area which is characterized by anisotropic surface impedances to allow for elongated and parallel type features. Then, by an application of the Compensation Theorem, an expression,for the modification of the mutual impedance of transmitting and receiving antennas caused by the target, can be deduced.

Employing the above results, we consider explicitly several models for the terrain profiles. In particular we show that a possible resonance may occur,for a bistatic configuration, in the scattered signal,when the spatial terrain harmonic coincides with half the effective radio wavelength. Other scattering and focussing mechanisms also exist and we will try to justify their relevance to Thomson's observations and related suggestions by Barr and Helm(Jour. Atmos. Terr. Phys. 44, 967, 1982) which bear on the question.

BRIDGED KNIFE EDGES — A MODEL FOR TERRAIN DIFFRACTION

James H. Whitteker
Department of Communications
Communications Research Centre
P.O. Box 11490, Station H
Ottawa, Canada K2H 8S2

A solution to the problem of calculating the attenuation due to diffraction over multiple knife edges has been found by Vogler [Radio Sci., 17, 1541-1547, 1982]. The attenuation is found as the sum of an infinite series, each term of which is the sum of a finite series. Vogler's work starts from rigorous diffraction theory, but the same result can be obtained from Fresnel-Kirchhoff theory [Whitteker, Radio Sci., 25, 837-851, 1990]. From the Fresnel-Kirchhoff point of view, the integrals may be interpreted as a superposition of all possible paths from the source at O to the point P at which the field is to be found.

If the knife edges are now bridged over with perfectly reflecting plane surfaces, the resulting obstruction is a solid object. The terrain profile along the propagation path is composed of line segments. To find the diffraction attenuation, the same method can be used as for knife edges, except that the possible paths from O to P now include reflected paths. Whereas in the knife-edge problem, there was only one mode of propagation, the mode with no reflections, now there are 2^{N+1} modes, where N is the number of knife edges, and $N+1$ is the number of reflecting surfaces. Because of the 2^{N+1} modes, one would expect a much larger number of terms. However, many terms are identical, and in some cases the solution is not much more complicated than the corresponding knife-edge solution.

For two bridged knife edges, the method described here gives results identical to an analagous method described by Whitteker [IEE Proc., 137, Pt. H, 113-116, 1990]. The attenuation due a round hill, known from rigorous diffraction theory, may be reproduced approximately by representing the hill by a few straight-line segments. The advantages of the method are that (a) path profiles of arbitrary shape can be modelled, (b) the solution is in the form of a series, so that its numerical accuracy can be assessed, and (c) the calculated fields are free of shadow-boundary discontinuities. The disadvantages are that (a) the number of terms increases exponentially with the number of knife edges, and (b) the assumption of perfectly reflecting ground will sometimes be unrealistic.

F111.5

MEASUREMENT TECHNIQUE OF THE HARDWARE PHASE SHIFTERS OF AN HF LINEAR PHASED ARRAY

S.A. Saoudy and R. Khan
Centre for Cold Ocean Resources Engineering
Memorial University of Newfoundland
St. John's, Newfoundland, A1B 3X5

A prototype radar system which uses ground wave propagation for over the horizon target detection is being built on a coastal site at Cape Race, Newfoundland. The radar has a log periodic antenna as a transmitter and a phased linear array as a receiver. The steering of the main beam of the receiver array is done by software and hardware phase shifting arrangement. The linear array is divided into N identical subarrays where each is composed of M elements. the software steering is applied to the elements within each subarray. The hardware steering within each subarray is achieved by switching in up to 45 appropriate lumped phase shift elements using relays. Due to such a large number of lumped elements, the need arises for performance check of all N phase shifters without dismantling. In this work, we will describe an experimental technique is to be used to perform such a task which involves erecting a transmitter antenna (a monopole) and measuring the relative received signal on each of the subarrays. Comparison with theoretical data will determine the status of every one of the N hardware phase shifters.

ENVIRONMENTAL EFFECTS ON OCEAN CURRENT MEASUREMENT USING MULTIFREQUENCY RADAR

Ivan Popstefanija* and Robert E. McIntosh
Department of Electrical and Computer Engineering
University of Massachusetts
Amherst,MA 01003, USA
Telephone: (413)-545-0779 FAX: (413)-545-0724

University of Massachusetts has build a multifrequency radar to investigate the feasibility of measuring ocean surface currents using microwave frequencies. A radar technique called ΔK is implemented. Special emphasis was given in the design of the real time data processor, so that a large volume of data could be collected.

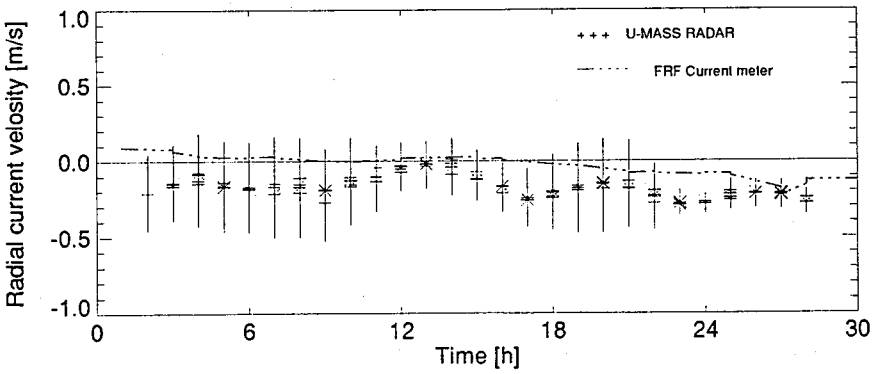

Figure 1: Ocean current measurements

In this paper we will present an analysis of the quality of ocean surface current measurements using this technique. Simultaneously with radar data a wide range of environmental data were gathered, including the ocean wave spectra. A comparison of ocean current estimates collected with the radar sensor and an in-situ current meter is shown in Figure 1. Error bars on the radar data represent the standard deviation of the current estimate. Results show that the standard deviation of the measurement is highly correlated with the ratio of the energy in the resonant wave and the total ocean wave energy.

F111.7

Active Reduction Ground Penetrating Radar Antenna

L. Peters, Jr., M. Barnes, M. Poirier and E. Nasser

Ground Penetrating Radar systems usually use a band limited impulse excitation. The major difficulty with these radars is to reduce the level of the direct coupled (from transmit to receive systems) signals to a level so that the weak signal reflected from a buried scatterer can be detected. A previous paper discussed the use of separate transmit and receive dipoles mounted on a resistive sheet. This bistatic antenna has been improved by the introduction of graded absorber and metallic shielding. These improvements are to be briefly reviewed. A major innovative advance shows great promise. This is the use of active reduction. Two separate transmit dipoles are activated by impulsive sources of opposite polarity. The receive antenna is positioned on the planar resistive sheet so that these two transmitted pulse signals are received at the same time. Their relative amplitudes are adjusted so that they are equal as seen by the receiver. To the degree that symmetry has been preserved, the direct coupled signal is cancelled. In practice, this has resulted in an increase of signal to clutter levels of up to 30 dB where the target is a buried four inch diameter pipe. Various configurations of this antenna are included and measured results are to be discussed.

FOCUSED ARRAY RADAR SUBSURFACE IMAGING

William J. Graham
Graham Research Corporation
2137 Galloway Rd.
Bensalem, PA 19020

The theoretical background and system concept is presented for a focused array radar for the detection and imaging of buried objects. The concept utilizes a bistatic radar propagation geometry with transmit and receive antennas directed obliquely at the ground at the Brewster angle for the soil medium. An experimental system has been developed using this geometry which significantly reduces ground surface reflections when vertical polarization is used. The system uses a focused horizontal line array receive antenna at 3.5 GHz to detect and generate two-dimensional (horizontal-depth) images of buried metal and plastic targets, and natural objects. The system yields resolution of 7.5 cm so that several resolution cells were obtained on each object. The resulting images allowed identification and accurate localization of the objects.

Ground penetrating radar has been considered for many years for the detection of buried objects such as pipes, land mines, and natural objects. There are several operational systems at low frequencies using short pulses which can detect deep buried objects. Shallow buried objects however present a more difficult problem since the ground surface reflection cannot generally be separated from the object reflection because they are usually in the same pulse return. Low frequencies cannot be used to make images of the objects since the wavelength is often on the order of the size of the object and resolution is low as a consequence.

A concept which has been developed to reduce or eliminate ground surface reflections and to yield higher resolution images is the use of a bistatic radar system operating at 3.5 GHz and using a focused horizontal line array as a receive antenna. A wide beam transmit antenna illuminates the ground at an oblique angle of incidence, while the receiver antenna is located at the angle of reflection. With polarization in the plane of incidence at the Brewster angle for the medium, the ground surface reflections will be significantly reduced and the incident wave will be mostly transmitted into the medium. Upon geometrical optics reflection from a buried object, ideally the wave will be totally transmitted back into free space and will continue at the angle of reflection to the receiving array.

A frequency as high as 3.5 GHz is possible if the objects are shallow (less than about 15 cm). At this frequency, attenuation is still reasonably low even for moist soil. The proximity of the focused array to the ground yields a free-space horizontal resolution of 7.5 cm and a free-space depth resolution of 28 cm.

F111.9

RF ELECTRONICS SUBSYSTEM FOR THE SPACEBORNE IMAGING RADAR-C

Bryan L. Huneycutt
SIR-C Instrument Manager

Jet Propulsion Laboratory
California Institute of Technology
4800 Oak Grove Drive, Pasadena, California 91109

The Spaceborne Imaging Radar-C (SIR-C) is designed to operate from a platform in the payload bay of the Space Shuttle Orbiter. SIR-C is the next critical step in the series of spaceborne radar experiments that began with Seasat in 1978 and continued with SIR-A in 1981 and SIR-B in 1984. SIR-C is the next step in the imaging radar series, eventually leading to the Earth Observing System imaging radar.

The previous imaging radars in the series were single frequency, single polarization, and conventional single source radars. SIR-C is a multifrequency radar and a distributed phased array radar. The transmit/receive modules and phase shifters located on the antenna panels are fed the chirp signals at RF frequencies from the RF electronics subsystem located below on the Shuttle pallet carrier. The SIR-C instrument is designed to demonstrate innovative engineering techniques such as (1) digital frequency step chirp generation to allow multiparameter selection and (2) interferometry.

The SIR-C RF electronics subsystem (RFES) generates the multifrequency RF signals to drive the antenna distributed array high power amplifiers and receives the return echoes from the antenna distributed array low noise amplifiers. The RF signals are down-converted to offset video, and steered into the digital electronics subsystem. The RFES generates calibration tones into the antenna to provide built-in-test capability. The crucial timing signal, from which the entire instrument derives its RF signals and timing, is produced via a stable local oscillator within the RFES.

The SIR-C RF electronics subsystem (RFES) is designed to allow flexibility in the selection of radar parameters such as range bandwidth to improve resolution, and pulsewidth to reduce dc power usage. This provides the experimenter tradeoffs among image quality parameters such as resolution, image SNR, and swath width. Understanding the various techniques employed by the SIR-C instrument during the in-flight capturing of raw SAR data will better equip the scientists and other users of the SIR-C data to interpret their data.

A Correction Method for Range Effects in Scheduling Reflector Antenna Footprints for Low-Earth-Orbit Satellites

Fredric Fok*
Atlantis Scientific Systems Group Inc.
1827 Woodward Drive
Ottawa Ontario
Canada K2C-0P9

Brian Eatock
Defence Research Establishment Ottawa
Ottawa Ontario
Canada K1A-0Z4

A rapid method for calculating the position of the earth footprint from a reflector antenna of a low-earth-orbit satellite is desired. Because the range to the earth varies over the footprint, the actual 3dB footprint differs from the footprint obtained by calculating the intersection of the 3dB beam contour with the ground. This effect is important for a low-earth-orbit satellite, especially when scanning close to the horizon. However, the effect can be reduced with narrow beamwidth antennas. In this paper, a rapid beam-scheduling method to compensate for this error is described.

Equations describing the earth coverage of a narrow beamwidth reflector antenna are derived in the satellite-centred coordinate system. The 3dB beam shape is invariant on a spherical surface in this system as the antenna is mechanically scanned. The 3dB coverage contours with and without range effects are compared. The results show that the 3dB coverage without range effect approximates well the 3dB coverage contour with range effect in size and orientation, but not in location. The 3dB coverage contour with range effect is displaced inward as the antenna scans outward towards the horizon. The error as measured by the overlap of the footprints with and without range effect can be as large as 20%.

The problem is rotationally symmetric about the vertical axis; hence, the positional error is only necessary to be corrected by re-positioning the center of the footprint in the elevation direction. Simulations have shown that the resultant coverage improves to 95%. This correction can be included in a beam-scheduling algorithm using a look-up table that is calculated once for a satellite altitude.

High Latitude F and E Region Observations

Room 3026 Salle URSI G Session 45

Observations des régions E et F aux hautes latitudes

Chairs/présidents: S. BASU, USA; J.-P. ST-MAURICE, Canada

08:30 (45.1) Spectral Plasma Line Measurements at Sondrestrom, **R. SHOWEN**, C. HEINSELMAN, D. WESTOVER, J. VICKREY, *SRI International, Menlo Park, CA, USA*

08:50 (45.2) Results on the Occurrence of Irregularities and Plasma Convection in the High Latitude F Region Obtained with HF Coherent Scatter Radars, **J.M. RUOHONIEMI**, R.A. GREENWALD, *Johns Hopkins University, Laurel, MD, USA*

09:10 (45.3) Scintillation Patch Structure in High Midlatitudes, **J.W. MacDOUGALL**, A. CHAMSEDDINE, *University of Western Ontario, London, ON, Canada*

09:30 (45.4) The Effects of High Frequency Ionospheric Scintillations on Displaced Phase Centre Antennas for Space Based Radar, **E.H. BULLER**[1], J.K.E. TUNALEY[1], R.H. MARTIN[2], [1]*London Research and Development Corporation, London, ON, and* [2]*Defence Research Establishment, Ottawa, ON, Canada*

09:50 (45.5) Characteristics of the Mid-Latitude Trough as Observed by Digisonde 256 Observations, **J.L. SCALI**[1], B.W. REINISCH[1], J. BUCHAU[2], G. CROWLEY[1], [1]*University of Lowell, MA, and* [2]*Phillips Laboratory (AFSC), Hanscom AFB, MA, USA*

10:10 **COFFEE/CAFÉ**

10:30 (45.6) A Study of the Mid-Latitude Ionospheric Trough Poleward of Australia Using the Differential Phase Technique, M. MALLIS, **E.A. ESSEX**, *La Trobe University, Bundoora, Australia*

10:50 (45.7) HF Coherent Radar Findings on Irregularity Occurrence and Plasma Instability in the High-Latitude E Region, **R.A. GREENWALD**, *Johns Hopkins University, Laurel, MD, USA*

11:10 (45.8) Observational Characteristics of Type 3 Echoes of VHF Radar Aurora, **C. HALDOUPIS**, *University of Crete, Iraklion, Greece*

11:30 (45.9) Type 4 Echoes from the Disturbed Polar Cap, **M. McKIBBEN**, G. SOFKO, P. PRIKRYL, J.A. KOEHLER, *University of Saskatchewan, SK, Canada*

G45.1

SPECTRAL PLASMA LINE MEASUREMENTS AT SONDRESTROM

R. Showen,* C. Heinselman, D. Westover, and J. Vickrey
SRI International
Acoustics and Radar Technology Laboratory
Menlo Park, California 94025 USA

Observations of the plasma line component of the incoherent scatter spectrum are presented from the radar at Sondrestrom, Greenland. Spectral measurements with 3 kHz frequency resolution show strong F-region cutoffs corresponding to the f_oF_2 critical frequency. These highly accurate daytime peak density determinations show in detail structure of the variable auroral ionosphere during stationery or beam swinging experiments. An apparent discrepancy between f_oF_2 values determined from plasma lines and from a vertical ionospheric sounder will be discussed. Measured values of the up- and down-shifted plasma lines resonance frequencies should allow an estimate of the radial electron velocities.

Results on the Occurrence of Irregularities and Plasma Convection in the High Latitude F Region Obtained with HF Coherent Scatter Radars

J. Michael Ruohoniemi and Raymond A. Greenwald

(JHU/Applied Physics Laboratory)

By operating in an HF range of frequencies (8 - 20 MHz) radars of the Goose Bay type are able to observe irregularities in the high latitude F region using coherent backscatter. The nearly continuous records of backscatter extend over half a decade for the Goose Bay radar and over three years for the Halley Bay radar. These indicate that irregularities are prevalent in the F region and can often be associated with specific ionospheric domains. We review findings on the occurrence of irregularities and examine the characteristics of the polar cusp and terminator zones in particular as source regions. An important plasma parameter that can often be derived is the convective drift of the ambient plasma. We illustrate with both case studies of local convection and statistical results on global convection patterns. We also describe observations of gravity waves that appear to have been launched by high latitude electrojet enhancements mapped out by irregularity scatter.

G45.3

SCINTILLATION PATCH STRUCTURE IN HIGH MIDLATITUDES

*John W. MacDougall and A. Chamseddine
Department of Electrical Engineering
University of Western Ontario
London, Ontario N6A 5B9

Spaced receiver measurements of scintillations from two sites are used to map the location of scintillation causing irregularities. From this mapping the structure of patches may be determined. The radio sources used are the 150 MHz NNSS satellites. The two sites used are London, Ontario (43N, 81W) and Kingston, Ontario (44N, 76W). The west-east spacing between these sites is approximately 360 km. From these two sites the structure of patches in the west-east direction can be much better determined than with just a single site. An overview of observed structures will be presented. Attention will then focus on a persistent discrete structure observed on 4 November 1990.

THE EFFECTS OF HIGH FREQUENCY IONOSPHERIC SCINTILLATIONS ON DISPLACED PHASE CENTRE ANTENNAS FOR SPACE BASED RADAR

E.H. Buller* [1], J.K.E. Tunaley[1] and R.H. Martin[2]

[1] London Research and Development Corporation, London, Ont.
[2] Defence Research Establishment Ottawa, Ottawa, Ont.

Space based radar (SBR) will be used for surveillance of the earth's surface to detect moving targets against the stationary background clutter. For a space based platform, looking downwards, the clutter signal is very much larger than that of the target. One technique that has been considered is a clutter cancellation scheme known as displaced phase centre antenna (DPCA). With this technique, the platform motion is effectively arrested by combining complex signals so that the return from the stationary clutter is cancelled, while the phase shift caused by target motion leads to signals which are not cancelled. The method is sensitive to varying phase errors which are equivalent to clutter motion and cause incomplete clutter cancellation.

The DPCA system uses the full antenna aperture for pulse transmission but, on reception, the antenna is divided into two apertures. The signal on the trailing aperture is delayed and paired with the signal received on the leading aperture one PRI earlier. The pairing allows the motion of the platform to be arrested since two equivalent monostatic phase centres will occupy the same position at different times.

After the cancellation process, the residual clutter signal can be shown to be proportional to the square of the phase difference between the two signals. In the Doppler domain, the fractional error is proportional to the power spectrum of the phase errors.

The cancellation can be done in the time domain, before Doppler processing, or in the frequency domain. These two approaches are compared using the usual power spectrum model of ionospheric irregularities. Spectral indices of 2 and 3 are compared. The time domain approach gives cancellation ratios of 59 dB for a spectral index of 2 and 75 dB when the spectral index is 3. A complete digital implementation of the cancellation process gives cancellation ratios of 65 dB and 78 dB for spectral indices of 2 and 3 respectively. The improved performance of the digital approach arises from the fact that simple time domain approach is not optimal; it neglects information in higher order terms.

Clutter cancellation ratios of 35 dB will be required to reduce the clutter signal enough to make targets detectable. High latitude ionospheric irregularities will not usually create enough phase noise to make this cancellation ratio unobtainable. Some benefit is possible by doing Doppler processing before the clutter cancellation.

G45.5

CHARACTERISTICS OF THE MID-LATITUDE TROUGH AS OBSERVED BY DIGISONDE 256 OBSERVATIONS.

J.L. Scali*[1], B.W. Reinisch[1], J. Buchau[2], and G. Crowley[1]

1. University of Lowell Center of Atmospheric Research, Lowell, MA. 01854
2. Phillips Laboratory (AFSC), Geophysics Directorate, Hanscom AFB, MA. 01731

The two most promising theories to explain the formation of the mid-latitude F-layer trough are the so called "stagnation " and "enhanced recombination" theories. The stagnation theory takes into account the competing effects of the rotation of the earth and the auroral electric field induced by convection (Kundsen et. al., J. Geophys. Res. 82, 4784-4792, 1977). Electric field induced plasma drifts enhance the recombination rates (Schunk et. al., J. Geophys. Res. 80, 3121-3130, 1975). Hence it becomes extremely important to measure the convection pattern in and around the trough region in order to determine which process is dominating in the formation of troughs.

In this paper a network of Digisonde 256 stations are used to access the characteristics of the mid-latitude trough. Since the Digisonde provides ionospheric parameters (such as foF2 and hmF2) and measures the drift velocities, it offers the unique opportunity to observe the relation between convection patterns and the trough development from different stations.

Observations from Goose Bay (53N, 299E), Argentia (47N,306E), and Millstone Hill (42N, 288E) will be discussed. It will be shown that the onset of a trough is generally associated with an increase in the convection motion, which tends to occur quite rapidly. These motions will be discussed in terms of trough formation theories. The study also outlines the quiet day diurnal variations of the ionospheric behavior, and makes comparisons with days when Kp is high and troughs are observed over the stations.

A Study of the Mid-latitude Ionospheric Trough Poleward of Australia Using the Differential Phase Technique

M Mallis and E A Essex (Both at: Department of Physics, La Trobe University, Bundoora, Victoria, Australia 3083)

A differential phase technique for determining the ionospheric total electron content (TEC) was used on the 150 and 400 MHz signals of the polar orbiting TRANSIT (NNSS) satellites from December 1987 to March 1989. Receiving stations were established at Macquarie Island (64.5S inv. lat.) and at Beveridge (48.4S inv. lat.). The aim of this experiment was to study the mid-latitude ionospheric trough poleward of Australia. Results will be presented showing seasonal and diurnal variations of the location, structure and magnetic activity response of the trough. Of particular interest is the unexpected high incidence of daytime and summer troughs and the relative low incidence of troughs for the winter and autumnal equinox. The summer season troughs are often preceded by a daytime prominent TEC enhancement poleward of Macquarie Island and a minimum TEC located equatorward of Macquare island and poleward of Beveridge. This feature is less prominent during the equinoxes and almost non-existent for the winter season.

G45.7

HF Coherent Radar Findings on Irregularity Occurrence and Plasma Instability in the High-Latitude E region

Raymond A. Greenwald

(JHU/Applied Physics Laboratory)

The coherent HF radars operating out of Goose Bay, Schefferville, and Halley Bay observe backscatter from small-scale (7.5 - 20 m) irregularities in the high latitude ionosphere. Although the HF backscatter technique was devised for observations in the F region in particular, it is also useful as a diagnostic of the E region, extending the coherent radar studies to a wavelength regime where the fluid approximation of instability processes is more valid. In this presentation, we describe sample observations of E region activity and present an overview of statistical results. We also discuss the types of irregularities encountered and the evidence for the excitation of electrostatic ion cyclotron waves and ion acoustic waves by field aligned current flows. We outline the application of the theory of plasma instability to the interpretation of the radar results and compare with UHF/VHF results.

Observational Characteristics of Type 3 Echoes of VHF Radar Aurora

Christos Haldoupis
Physics Department, University of Crete, Iraklion 714 09, Crete, Greece

Type 3 echoes of radar aurora relate to strong backscatter signals with very narrow power spectra peaking below ion acoustic Doppler speeds in the 100 to 300 m/s range and preferentially close to 200 m/s. The first observations were made at 50 MHz where the prominent Doppler speeds of type 3 echoes correspond approximately to the cyclotron frequencies, or their 1st harmonic, of the main ionic species in the E region plasma. This suggested that type 3 echoes may be due to electrostatic ion cyclotron (EIC) plasma waves generated at altitudes well above the electrojet where ions become magnetized. More recent evidence, however, from multifrequency studies and observations at 140 MHz, supported the idea of a preferential phase velocity and not that of a characteristic angular frequency which would fit the ion cyclotron wave mechanism. This, plus theoretical difficulties, plus altitude interferometry measurements which showed type 3 echoes to originate from within the electrojet where ions are strongly collisional, put the EIC interpretation in geopardy. Today, type 3 echoes remain a mystery to radar auroral researchers and an outstanding problem in ionospheric plasma physics. The main purpose of this presentation is to identify and outline the most prominent and undisputed observational properties of type 3 echoes by considering published information as well as cross beam observations of type 3 echoes at 140 MHz obtained with the Stare radars. We believe, such a clarification is useful particularly to theorists interested on the problem. Furthermore, we consider the assumption that type 3 echoes are due to type 1 waves originating in narrow sporadic E layers located at lower electrojet altitudes and investigate the effect of both an enhanced mean ionic mass (because of predominance in metallic ions) and a large destabilizing electron density gradient, on lowering the phase velocity well below typical ion acoustic speed values.

G45.9

TYPE 4 ECHOES FROM THE DISTURBED POLAR CAP

M. McKibben, G. Sofko, P. Prikryl and J. Koehler

Institute of Space and Atmospheric Studies
University of Saskatchewan, Saskatoon, Sk. S7N 0W0

In 1982, two 50 MHz bistatic CW Doppler radar links were used to view a common region above Sachs Harbour, NWT ($\Lambda \approx 77°$). One of these links had a bisector almost exactly along a magnetic north-south line. On that link, very dynamic polar cap echoes were received on the magnetically disturbed morning of July 16. The echoes were typically narrow in spectral width and occurred at Doppler velocities well above the nominal ion acoustic velocity. These echoes showed a preference for fixed frequencies, sometimes with several peaks occurring simultaneously. Possible instabilities responsible for these echoes will be discussed, with emphasis on the electrostatic ion-cyclotron instability.

High Latitude and Low Latitude E & F Region Observations

Room 3026 Salle URSI G Session 62

Observation des régions E et F aux hautes et aux basses latitudes

Chairs/président: D.R. MOORCROFT, Canada

13:30 (62.1) Unusual VHF Auroral Doppler Spectra with Multilink and Dual Frequency CW Bistatic Radars, **G. SOFKO**, D. DANSKIN, J.A. KOEHLER, *University of Saskatchewan, Saskatoon, SK, Canada*

13:50 (62.2) Aspect Angle Dependencies of 34 CM *E* Region Coherent Echoes Observed at Millstone Hill, **J.C. FOSTER**[1], D. TETENBAUM[1], C.F. DEL POZO[1], J.-P. ST. MAURICE[2], D.R. MOORCROFT[2], [1]*Massachusetts Institute of Technology, Westford, MA, USA;* [2]*University of Western Ontario, London, ON, Canada*

14:10 (62.3) 50 MHz Coherent Radar Aspect Sensitivity, **J.A. KOEHLER**, G.J. SOFKO, P. PRIKRYL, D. ANDRE, *University of Saskatchewan, Saskatoon, SK, Canada*

14:30 (62.4) Refraction of Radar Beams in Curved Ionospheric Layers, **D. ANDRE**[1], M. USPENSKY[2], A. KUSTOV[2], G.F. SOFKO[1], J.A. KOEHLER[1], [1]*University of Saskatchewan, Saskatoon, SK, Canada;* [2]*Polar Geophysical Institute, Murmansk, USSR*

14:50 (62.5) A Quantitative Study of Magnetic Aspect Angle Effects in Radar Aurora at 50 MHz Taking into Account the Effects of Refraction, **G.E. HALL**, D.R. MOORCROFT, *University of Western Ontario, London, ON, Canada*

15:10 **COFFEE/CAFÉ**

15:30 (62.6) Statistical Analysis of the Spatial Relationship Between the Radio and Optical Aurora: Further Evidence for Refraction, **P. PRIKRYL**, *University of Saskatchewan, Saskatoon, SK, Canada*

15:50 (62.7) A New Type of Pulsation Detected by Radar Probing of the Ionosphere, **I.F. GRANT**, D.R. McDIARMID, A.G. McNAMARA, *National Research Council Canada, Ottawa, ON, Canada*

16:10 (62.8) Effect of Geomagnetic Activity on Variations of TEC at Low Latitude, M. MUKUND RAO[1], M. JAYARANI MALLIGA[2], **R. SETHURAMAN**[3], V. ALAMELU[4], [1]*Indian Institute of Technology, Madras,* [2]*Anna Adersha College for Women, Madras,* [3]*Hindustan College of Engineering, Madras, and* [4]*SDNB Vaishnava College for Women, Madras, India*

16:30 (62.9) Measurements of Spatial and Frequency Coherence of an Equatorial HF Path During Spread-F, **T.J. FITZGERALD**, P.A. ARGO, R.C. CARLOS, *Los Alamos National Laboratory, Los Alamos, NM, USA*

G62.1

UNUSUAL VHF AURORAL DOPPLER SPECTRA WITH MULTILINK AND DUAL FREQUENCY CW BISTATIC RADARS

G. Sofko, D. Danskin, and J. Koehler

Insitute of Space and Atmospheric Studies
University of Saskatchewan, Saskatoon, Sk. S7N 0W0

Two spectral sequences will be discussed. The first is a sequence in which four bistatic links were operated simultaneously, with a common auroral zone target area over Southend, Sk. Although the two transmitters and the two receivers were working well, strong signals were received on only three of the links, while the fourth had virtually no signal at all. The effects of refraction and Faraday rotation will be invoked to explain how such an unusual occurrence might arise. In the second sequence, Type 4 echoes were received at both 50 and 144 MHz using a geometry which differed only slightly from that for backscatter. There was a very different signature at the two frequencies, with the 50 MHz echoes showing the usual behaviour observed with the Univ. of Sask. radars, namely a type 4 peak at about double the Doppler shift of the accompanying Type 1 peak. The simultaneous 144 MHz echoes showed a different behaviour; they were broader than the 50 MHz echoes, and occurred at Doppler velocities between the two frequencies observed at 50 MHz.

ASPECT ANGLE DEPENDENCIES OF 34 CM *E* REGION COHERENT ECHOES OBSERVED AT MILLSTONE HILL

J. C. Foster, D. Tetenbaum, C. F. del Pozo, Atmospheric Sciences Group, M.I.T. Haystack Observatory, Westford, MA 01886, U.S.A.
J.-P. St. Maurice and D. R. Moorcroft, University of Western Ontario, London, Ont.

The sensitivity of the Millstone 440 MHz radar system is such that coherent echoes from *E* region irregularities can be observed over a 90 dB dynamic range above the incoherent scatter background. At antenna elevation angles between 4° and 20°, aspect angles between 0° and 10° (from perpendicularity with the magnetic field) are viewed at *E* region heights at invariant latitudes between 61°Λ and 57°Λ. During disturbed conditions, when convection electric fields in excess of 15 mV/m and *E* region irregularities span this range of latitudes, antenna scanning experiments have been performed to determine the aspect angle sensitivity with high precision. We find that the 440 MHz aspect sensitivity is -15dB deg^{-1} for aspect angles between 0° and 3°, -10dB deg^{-1} for aspect angles between 3° and 6°, and -7dB deg^{-1} for aspect angles between 6° and 9° (see figure). The magnitude of the phase velocity is at an approximate ion acoustic level (350 m/s) for aspect angles <2° and decreases to <200 m/s as the aspect angle increases to >3°. There is a tendency for the altitude of the most intense return to decrease by ~5 km as the aspect angle increases beyond 2°. For highly disturbed conditions, the magnitude of the velocity can increase to > 700 m/s for aspect angles <2°.

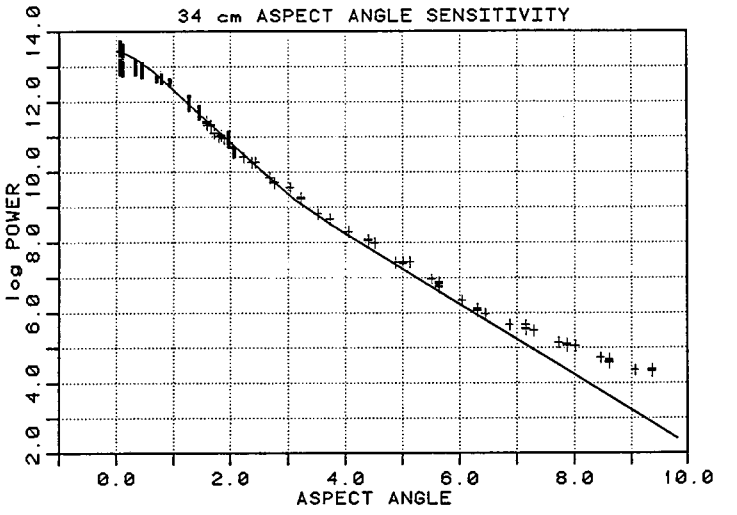

G62.3

50 MHz COHERENT RADAR ASPECT SENSITIVITY

J.A. Koehler, G.J. Sofko, P. Prikryl, D. Andre'

Institute of Space and Atmospheric Studies,
University of Saskatchewan, Saskatoon, Sask., Canada S7N 0W0

A suite of coherent radar data particularly suitable for aspect angle studies was collected by the U of S radar group in the summer of 1981. This paper will deal with a subset of the data which was carefully selected for uniformity. The main study reported here is that of the aspect angle dependence of Doppler shift and backscatter cross-section. These observations are particularly relevant in light of recent theories for decreased aspect angle dependence due to refraction and this topic will be discussed.

REFRACTION OF RADAR BEAMS IN CURVED IONOSPHERIC LAYERS

Dieter Andre(1), Mikhail Uspensky(2), A. Kustov(2),
G. Sofko(1) and J. Koehler (1)

(1) - Institute of Space and Atmospheric Studies
University of Saskatchewan
Saskatoon, Canada S7N 0W0

(2) - Polar Geophysical Institute
183023 Murmansk, USSR

It has been shown that tilted plane ionospheric layers can cause considerable refraction of 6 m wavelength radar beams. In this paper, we demonstrate that curved layers are even more effective in producing refraction. A simple theoretical model will be discussed, and ray tracing examples for several curved geometries will be presented. It will be shown that moderate electron densities and gradients are sufficient to cause large amounts of refraction. This mechanism is discussed with respect to VHF auroral radar experiments in which scatter signals have been received under very unfavourable conditions of magnetic aspect angle geometry.

G62.5

A QUANTITATIVE STUDY OF MAGNETIC ASPECT ANGLE EFFECTS IN RADAR AURORA AT 50 MHZ, TAKING INTO ACCOUNT THE EFFECTS OF REFRACTION

G. E. Hall* and D. R. Moorcroft
Department of Physics
University of Western Ontario
London, Ontario, Canada N6A 3K7

Although there have been many previous studies of magnetic aspect angle effects in auroral E region backscatter at VHF, few if any have dealt adequately with the effects of refraction, which can markedly alter the interpretation of such observations. In this study we have analyzed 48.5 MHz backscatter observations obtained with the Bistatic Auroral Radar System (BARS). By concentrating on spatially and temporally uniform, daytime events, and by making use of the results of other studies on the effects of refraction in BARS data, we have been able to obtain some of the first reliable estimates of aspect angles and their effects at VHF.

Because the study is restricted to widespread, steady, daytime events, it is possible to narrow very considerably the possible range of E region electron densities, and the corresponding refractive effect on VHF backscatter. After correcting for these refractive effects we have observed auroral backscatter at magnetic aspect angles exceeding 6°. At an aspect angle of ~ 4° the aspect sensitivity is found to be about -5 dB/deg, and to decrease with increasing aspect angle; the values and trend are very similar to values found in other experiments made at UHF. Doppler velocities for these periods were also studied. Velocity estimates from other instruments were not available, but modelling of the observations from the two radars suggests that the Doppler velocity is proportional to the line-of-sight component of the convection drift velocity, but that the constant of proportionality at 5° - 6° is approximately one half of what it is at 2° - 3°.

STATISTICAL ANALYSIS OF THE SPATIAL RELATIONSHIP BETWEEN THE RADIO AND OPTICAL AURORA: FURTHER EVIDENCE FOR REFRACTION

Paul Prikryl

Institute of Space and Atmospheric Studies,
University of Saskatchewan, Saskatoon, Sask., Canada S7N 0W0

Recent studies have produced strong evidence that ionospheric refraction can explain some of the large aspect angle VHF radio aurora observations. The spatial relationship between such observations made with the Bistatic Auroral Radar System (BARS) and simultaneous 557.7 nm emissions detected by an all-sky imager (ASI) has been found consistent with the above idea [Hall et al., 1990]. In this paper, results of a cross-correlation analysis of the BARS and ASI intensities are presented. Two dimensional cross-correlation functions are computed for a large statistical sample of several months of data.

Hall, G. et al., J. Geophys. Res., 95, 15281, 1990.

G62.7

A NEW TYPE OF PULSATION DETECTED BY RADAR PROBING OF THE IONOSPHERE

I.F. Grant*, D.R. McDiarmid and A.G. McNamara
Herzberg Institute of Astrophysics
National Research Council of Canada
Ottawa, K1A 0R6, Canada

Because the ionosphere is a boundary of the magnetosphere, radio wave probing of the former can reveal consequences of magnetospheric physics as well as ionospheric. In this paper we describe the discovery, through radar observation, of the ionospheric signature of a new type of geomagnetic pulsation. These pulsations have periods in the 200 to 400 s range and also have a large spatial phase variation. They occur in the afternoon local time sector. Similar pulsations have previously been detected by radar. Their spatial phase variation corresponds to a westward phase velocity whereas that of the new pulsation is southwestward. The polarization ellipse of the previously reported pulsations is approximately linear and oriented in the magnetospheric radial direction. That of the new pulsation is more definitively linear but is oriented between the radial and azimuthal directions in the magnetosphere, indicating mode coupling. Details of the ionospheric signature of the new pulsation will be presented and discussed in terms of possible source mechanisms.

Effect of Geomagnetic Activity on Variations of TEC at Low Latitude

M. Mukund Rao[1], M. Jayarani Malliga[2], R. Sethuraman[3] *, and V. Alamelu[4]
1 Aeronomy Laboratory, Indian Institute of Technology, Madras 600 036, India.
2 Anna Adersha College for Women, Madras, India.
3 Hindustan College of Engineering, Madras 603 103, India.
4 SDNB Vaishnava College for Women, Madras 600 044, India.

The total electron content of the ionosphere (TEC) is known to be subject to considerable day to day variations. Attempts have been made to correlate these variations with geomagnetic A_p index but without success, probably due to the fact that the index represents the average effect over the period of time while TEC variations are instantaneous.

This paper examines a parameter suggested by Mukund Rao *et al.*[N.Mukund Rao, R.Sethuraman, & V.Alamelu, Indian Journal of Radio and Space Physics, 13, 71, 1984] as a possible indication of the geomagnetic field on TEC variations. This index, designated Δ HST, is given by the quantity Δ HST = ($H_{equator}$ - $H_{low\ latitude}$) disturbed day - (H_{eqator} - $H_{low\ latitude}$) mean IQ values. This index has been previously shown to correlate well with certain features of the equatorial electrojet like the extension of its periodic behavior of the change in the electrojet parameters with a period of one day for one or two successive days, the lowering and some times the disappearance of equatorial sporadic E (indicative of weakening or the reversal of the electric field of the electrojet rejoin, during such periods) and the behavior with changes in the latitude of the polar cusp region [V.Alamelu, R.Sethuraman, & N.Mukund Rao, Advances in Space Physics, 10, 1990].

The present work relates this parameter to the variation of TEC measured at a low latitude station (Waltair) in India with Δ HST in the region. The changes in the TEC correlate well with Δ HST oı the three chosen occasions with a small time lag. The f_pE_s at the corresponding sub-ionospheric point and f_pE_s also show correlation showing that this parameter is a sensitive indicator of the influence of geomagnetic variations on the ionosphere during disturbed periods.

G62.9

MEASUREMENTS OF SPATIAL AND FREQUENCY COHERENCE OF AN EQUATORIAL HF PATH DURING SPREAD-F

T. J. Fitzgerald*, P. A. Argo, and R. C. Carlos
Atmospheric Sciences Group, MS D466
Los Alamos National Laboratory
Los Alamos, New Mexico 87545

In conjunction with the NASA sponsored equatorial rocket campaign conducted in August, 1990, at the Kwajelein Missile Range, we set up an hf (10.2 MHz) path between Maloelap Atoll and Bikini Atoll. The path, which had a range of 700 km, reflected in the ionosphere approximately 100 km north of the Altair radar location. Transmitters at Maloelap broadcasted four cw tones within a bandwidth of 10 kHz to be used to determine frequency coherence and also a phase-coded psuedo random sequence with a bandwidth of 60 kHz (channel probe) to be used to determine time delay spread. A spatial array of seven antennas was deployed at Bikini to measure spatial coherence and angle of arrival using the cw broadcasts. Receivers also monitored the multiple frequency cw broadcasts and the channel probe transmission. The system was run in the post-sunset time period over two weeks during which almost every night showed significant degradation due to spread F resulting in rapid fading, decreased spatial and frequency coherence, and increased time delay spread. We will present the results of these measurements and compare them to model calculations of the effect on the hf path of electron density fluctuations estimated from the Altair radar data.

Ionosonde Results and Atmospheric Gravity Waves

Room 3026 Salle URSI G Session 79

Résultats des ionosondes et ondes de gravité atmosphérique

Chairs/présidents: H. SOICHER, USA

13:30 (79.1) Correlation Analysis of Ionospheric Parameters at Midlatitudes, **H. SOICHER**, F.J. GORMAN, *U.S. Army Communications-Electronics Command, Fort Monmouth, NJ, USA*

13:50 (79.2) Observations of Small-Scale Ionospheric Tilts, **L.F. McNAMARA**, *Andrew Government Systems, Dallas, TX, USA*

14:10 (79.3) Analytic Ray Tracing Including the Effects of Absorption and the Earth's Magnetic Field, **P.L. DYSON**[1], J. CHEN[1], J.A. BENNETT[2], [1]*La Trobe University, Bundoora, and* [2]*Monash University, Clayton, Australia*

14:30 (79.4) Techniques of Backscatter Ionogram Synthesis and Inversion, **P.L. DYSON**[1], J.A. BENNETT[2], C.Y. ONG[2], [1]*La Trobe University, Bundoora, and* [2]*Monash University, Clayton, Australia*

14:50 (79.5) Next Generation Portable Digital Ionosonde, **D.M. HAINES**, B.W. REINISCH, *University of Lowell, MA, USA*

15:10 **COFFEE/CAFÉ**

15:30 (79.6) A Simplified Procedure for Calculating and Displaying the Maximum Usable Frequency, **G.L. WIEMANN**, N.C. GERSON, *Laboratory for Physical Sciences, College Park, MD, USA*

15:50 (79.7) Response of the High Latitude Ionosphere to Atmospheric Gravity Waves, G. KIRSCHENGAST[1], **R. LEITINGER**[1], K. SCHLEGEL[2], [1]*Universität Graz, Austria;* [2]*Max-Planck-Institut für Aeronomie, Katlenburg-Lindau, Germany*

16:10 (79.8) Gravitywave Study with a Chain of Digisondes, **Z. ZHANG**, W. WAN, B.W. REINISCH, *University of Lowell, MA, USA*

16:30 (79.9) Some First Results from the SuperWAGS Campaign: Gravity Wave and TIDs During the Period 10-24 November 1990, R.D. HUNSUCKER[1], **K.C. YEH**[2], C.-H. LIU, [1]*University of Alaaska, Fairbanks, AK, and* [2]*University of Illinois, Urbana, IL, USA*

16:50 (79.10) Preliminary Results from the SuperWAGS Campaign: Sondrestrøm, Greenland to Arecibo, Puerto Rico, **R.D. HUNSUCKER**, N. JING, *University of Alaska, Fairbanks, AK, USA*

G79.1

CORRELATION ANALYSIS OF IONOSPHERIC PARAMETERS AT MIDLATITUDES

H. Soicher* and F.J. Gorman
U.S. Army Communications-Electronics Command
CECOM Center for C^3 Systems
Fort Monmouth, NJ 07703

Communications among mobile as well as fixed HF nodes along short, medium and long range paths require propagation assessment which would be facilitated through the determination of circuit reliability within an extended geographic area based on the monitoring of the vertical ionosphere at a central location. To this end a network of ionospheric sounder facilities were established in Western Europe in order to establish a regionalized data base with the aim of determining ionospheric correlation distances.

While data gathering is still in progress, preliminary correlation analysis using hourly vertical modes has been performed for a number of sites separated by ~1000 km distances. Various ionospheric parameters have been correlated during periods which span different seasons during the increasing phase of the solar cycle.

Future plans call for the extension of the data base to oblique HF modes and to perform vertical/oblique correlation studies.

OBSERVATIONS OF SMALL-SCALE IONOSPHERIC TILTS

Leo F McNamara

Andrew Government Systems
2916 National Drive
Dallas, Texas 75041

Multi-frequency tilt measurements have been made in north Texas using a vertical incidence ionosonde, and tilts have been derived from angle of arrival measurements of signals from transmitters at known locations. These tilts will be used to illustrate the highly dynamic state of the ionosphere on a small scale, with special emphasis on TIDs, and some of the more unusual observations will be discussed in detail, since they offer interesting interpretations.

Ionospheric tilts play a major role in setting the accuracy with which the location of a short-range HF transmitter may be determined, using a Single Station Location (SSL) system. Several case studies will therefore be used to illustrate the potential for taking the tilts into account when attempting to determine the locations of HF transmitters at short ranges.

G79.3

ANALYTIC RAY TRACING INCLUDING THE EFFECTS OF ABSORPTION AND THE EARTH'S MAGNETIC FIELD

P.L. Dyson*, J. Chen
Department of Physics
La Trobe University
Bundoora, Victoria, Australia 3083

and

J.A. Bennett
Department of Electrical and Computer Systems Engineering
Monash University
Clayton, Victoria, Australia 3168

To radio waves, the ionosphere is an inhomogeneous and anisotropic medium, the properties of which are affected by the earth's magnetic field. There is no analytical solution for the rays describing radio propagation in general, realistic ionospheres. Numerical ray tracing can be used to predict propagation conditions, but usually requires significant amounts of computer time, making it slow in many practical cases.

The vertical structure of the ionosphere can be described in detail using Quasi-Parabolic Segments (QPS) making it possible to develop analytical expressions for many ray parameters in oblique radio wave propagation when the Earth's magnetic field is ignored. While valid only under more restricted circumstances than general numerical ray tracing, the speed with which the analytic calculations can be carried out makes them preferable in many cases. The range of validity of analytical ray tracing can be extended by using suitable approximations. In particular the effects of the Earth's magnetic field and absorption due to collisions can be included. Both effects can be treated in a similar way be determining 'effective' frequencies to take account of the magnetic field and absorption effects so that ray parameters can be calculated for not just the ordinary mode, but also for the extraordinary mode.

The methods will be discussed and results presented, including comparison with full numerical ray tracing to illustrate the conditions under which the methods are valid. The application of the methods to oblique and backscatter ionogram synthesis and Single Station Location, will also be discussed and results presented.

TECHNIQUES OF BACKSCATTER IONOGRAM SYNTHESIS AND INVERSION

P.L. Dyson*
Department of Physics
La Trobe University
Bundoora, Victoria, Australia 3083

and

J.A. Bennett and C.Y. Ong
Department of Electrical and Computer Systems Engineering
Monash University
Clayton, Victoria, Australia 3083

Ionograms obtained from backscatter sounder systems provide comprehensive information about HF propagation paths from the sounder site. However, in order to fully utilize the information available for, say, real-time applications, it is necessary to either invert the backscatter ionogram to obtain a description of the ionosphere or to synthesize the ionogram using an ionospheric model. Synthesis involves tracing thousands of rays through an ionospheric model and this limits the usefulness of numerical ray tracing because of the amount of computer time required. Inversion presents problems primarily because of the difficulty of taking account of the three dimensional structure of the ionosphere.

Techniques for backscatter ionogram synthesis have been developed using both analytical and numerical ray tracing, and each has particular advantages. Results will be presented comparing synthesized ionograms with actual ionograms obtained by the backscatter sounder system operated as part of the Jindalee over-the-horizon radar.

Inversion of backscatter ionograms has been investigated using two methods: inversion of the leading edge and inversion using all the frequency-group path-echo power information contained in the backscatter ionogram. The leading edge technique is based on fitting the leading edge to different 'families' of quasi-parabolic layers to obtain 'equivalent' ionospheres which reproduce propagation characteristics quite well, even if they do not accurately represent the real ionosphere. The more complete inversion technique describes the ionosphere in terms of a tilted electron density profile. Results obtained using the two methods applied to test data and real ionograms will be presented and discussed.

G79.5

NEXT GENERATION PORTABLE DIGITAL IONOSONDE

D. Mark Haines* and Bodo W. Reinisch
University of Lowell Center for Atmospheric Research,
Lowell, MA 01854

The University of Lowell Center for Atmospheric Research has developed a next generation programmable Digisonde dubbed the Digisonde Portable Sounder, or DPS. The new system relies on advanced coherent signal processing to compensate for a 10 dB reduction in peak transmitter power from 6KW of the previous generation systems to 500W.

Large signal processing memory and high speed processors provide complex Doppler spectra at all ranges (heights) simultaneously. Furthermore, up to four parallel receivers in the same system provide simultaneous phase and Doppler measurements on up to four antennas for Drift studies in high Doppler environments. This four-receiver system is especially designed for plasma drift and wave studies in the polar ionosphere. With Doppler ranges up to ±50 Hz, plasma drifts up to about 2km/sec can be measured without experiencing aliasing effects. This suffices to monitor and measure the high velocity drifts occasionally observed by incoherent scatter radar and satellite techniques. The advantage of the low cost portable Digisondes is that they can continuously monitor the polar cap plasma convection at many points and map the instantaneous convection pattern.

Simultaneous high resolution Doppler (0.012 Hz), high resolution echo range (0.5km), and high resolution angle of arrival (1degree) measurements at all frequencies and ranges are a new tool to measure waves in the drifting plasma. Description of measurement capabilities and processing and analysis techniques will be presented together with observational results.

A Simplified Procedure for Calculating and Displaying the Maximum Usable Frequency

G.L. Wiemann* and N.C. Gerson

Laboratory for Physical Sciences
4928 College Avenue
College Park, MD 20740

A method is described for providing global maps of the footprint of the Maximum Usable Frequency (MUF) with a simplified, user-friendly procedure requiring the entry of only the transmitter location and time (hour, month and sunspot number).

G79.7

RESPONSE OF THE HIGH LATITUDE IONOSPHERE TO ATMOSPHERIC GRAVITY WAVES

G Kirchengast and R Leitinger*
(Both at: Institut für Meteorologie und Geophysik,
Universität Graz, Halbärthgasse 1, A-8010 Graz, Austria
K Schlegel
(Max-Planck-Institut für Aeronomie, D-3411 Katlenburg-Lindau, FRG)

The equations of continuity and momentum for the electrons were used to construct a numerical model particularly adequate for the F layer of the high latitude ionosphere. It yields the spatial and temporal evolution of the plasma parameters *electron density*, n_e, and *magnetic field parallel ion velocity*, $v_{||}$, respectively.

The model is flux tube oriented, includes all relevant field aligned transport processes, and the contribution of perpendicular convection due to electric fields and neutral winds is fully taken into account, too (cf. *Schunk, PAGEOPH 127*, 255-303, Birkhäuser Verlag, Basel, 1988.). No linearization procedure is adopted to the basic equation set, altough the particular problem of interest is the plasma response to neutral atmosphere disturbances, especially atmospheric gravity waves. The utilization of the full continuity equation is considerably more adequate and flexible.

To satisfy the necessary inputs to close the equation set (i.e. plasma temperatures, temperature and composition of the neutral atmosphere, neutral wind, electron production, magnetic and electric field etc.) we use the at present "best available and realistic" models in an at first purely theoretical access.

The model is set up in a way, that measurement volumes or complete raypaths of the EISCAT (European Incoherent Scatter Facility located in Northern Scandinavia) common programmes (CPs) 1 and 2 can be simulated. EISCAT-CP1 and 2 observe just our model parameters n_e and $v_{||}$ in ~20 km height and ~5 min time resolution in F region heights, which allows us direct comparison. Supplementary, further observed quantities (ion and electron temperature, T_i and T_e, and tristatic measurement of the electric field vector) let deduce real models to reduce the theoretical input necessities.

We introduce main properties and capabilities of our model and present results of the simulation of the response of the high latitude ionosphere to model large scale atmospheric gravity waves (LSTIDs) which are overlaid upon the neutral atmosphere as disturbances in the presence of varying electric fields. Several important features of the observed LSTIDs are discussed in some detail. First results of comparison with EISCAT data are presented and future aims are mentioned.

GRAVITYWAVE STUDY WITH A CHAIN OF DIGISONDES

Zhaoming Zhang*, Weixing Wan[1] and Bodo W. Reinisch
University of Lowell Center For Atmospheric Research
Lowell, MA 01854 USA

1. On Leave from Wuhan Institute of Physics, Wuhan, PRC

During the November 1990 WAGS campaign Digisondes at Qaanaaq (87° CGLAT), Sondrestrom (77°), Goose Bay (65°), Argentia (57°), Millstone Hill (55°), and Wallops Island (49°) collected ionogram, skymap and drift data every 5min from November 10 to 24. From the automatically obtained vertical electron density profiles isodensity contours (as function of time) are generated for each sounding station. Travelling Ionospheric Disturbances associated with atmospheric gravitywaves can be identified on these contour plots. High resolution Doppler and incidence angle measurements of the reflected HF waves are analyzed in new ways to determine the structure and velocity of the TID from single station observations. The multi-station observations are used to verify the new single station analysis technique.

G79.9

Some First Results from the SuperWAGS Campaign: Gravity Wave and TIDs during the period 10–24 November 1990

R. D. Hunsucker
Geophysical Institute
University of Alaska
Fairbanks, AK 99775-0800

K. C. Yeh and C.-H. Liu
ECE Dept
University of Illinois
Urbana, IL 61801-2991

A worldwide atmospheric gravity wave campaign called "SuperWAGS" was carried out from 10–24 November 1990, with over 50 globally distributed observatories participating. The observing interval in November was characterized as geomagnetically "quiet-to-moderately disturbed" with a maximum daily $\sum K_p$ of 28 on 16 and 17 November. One might expect mainly medium-scale TIDs to be generated by the geomagnetic activity observed, with the possibility of large-scale TIDs from $\sim$ 15–19 November. We present a summary of the global observations a some tentative identification at AGWs and sources.

Preliminary Results from the SuperWAGS Campaign: Sondrestrøm, Greenland to Arecibo, Puerto Rico

R. D. Hunsucker and Ning Jing
Geophysical Institute, University of Alaska-Fairbanks
Fairbanks, Alaska 99775-0800

A global campaign "SuperWAGS" was conducted from 10–24 November 1990 to study Atmospheric Gravity Wave (AGW) sources and the resulting Traveling-Ionospheric-Disturbances (TIDs). The Incoherent Scatter Radars (ISRs) at Sondrestrøm, Greenland and at Arecibo, Puerto Rico were operated in an "AGW-mode-of-operation" for part of the observation period. Preliminary results will be discussed.

Recent Advances in Ionospheric Tomography I

Room 3026 Salle
URSI G Session 95

Progrès récents en tomographie ionosphérique I

Chairs/présidents: J.A. KLOBUCHAR, USA

08:30 (95.1) The Promise and the Potential Perils of Ionospheric Tomography, **J.A. KLOBUCHAR**[1], P.F. FOUGERE[1], P.H. DOHERTY[2], [1]*Geophysics Laboratory, Hanscom AFB, MA, and* [2]*Boston College, Newton, MA, USA*

08:50 (95.2) How Well Can We Image Ionospheric Structures by Tomography, **K.C. YEH**, T.D. RAYMUND, *University of Illinois, Urbana, IL, USA*

09:10 (95.3) Reconstruction Techniques and Resolution Limit of Tomographic Imaging of Electron Density Profiles in the Ionosphere, **H. NA**, H. LEE, *University of California, Santa Barbara, CA, USA*

09:30 (95.4) A Two Dimensional Fourier View of the Nonideal Ionospheric Tomographic Geometry, **T.D. RAYMUND**, K.C. YEH, *University of Illinois, Urbana, IL, USA*

09:50 (95.5) Background Resolving Capabilities of Ionospheric Computerized Tomography, **J.R. AUSTEN**[1], C.-H. LIU[2], S.J. FRANKE[2], *Tennessee Technological University, Cookeville, TN, and* [2]*University of Illinois, Urbana, IL, USA*

10:10 **COFFEE/CAFÉ**

10:30 (95.6) Application of a Stochastic Inverse Technique to Ionospheric Tomography, **E.J. FREMOUW**, J.A. SECAN, *Northwest Research Associates Inc., Bellevue, WA, USA*

10:50 (95.7) Methods to Estimate the Initial Value of Differential Doppler Data, **R. LEITINGER**, *Universität Graz, Austria*

11:10 (95.8) An Experimental Demonstration of Ionospheric Tomography, **S.E. PRYSE**, L. KERSLEY, *University College of Wales, Aberystwyth, UK*

11:30 (95.9) The Phase-Difference Ionospheric Tomography, E.S. ANDREEVA[1], **V.E. KUNITSYN**[1], YU.A. MELNICHENKO[2], E.D. TERESHCHENKO[2], [1]*Moscow University, Moscow, and* [2]*Polar Geophysical Institute, Murmansk, USSR*

11:50 (95.10) Radiotomography of Scattering Ionosphere Irregularities, V.E. KUNITSYN[1], **E.D. TERESHCHENKO**[2], [1]*Moscow University, Moscow, and* [2]*Polar Geophysical Institute, Murmansk, USSR*

G95.1

THE PROMISE AND THE POTENTIAL PERILS OF IONOSPHERIC TOMOGRAPHY

J. A. Klobuchar* and P. F. Fougere
Ionospheric Physics Division
Geophysics Laboratory
Hanscom AFB, MA 01731

P. H. Doherty
Institute for Space Research
Boston College
Newton, MA 02159

It has been shown that the application of tomographical techniques to simulated experimental total electron content (TEC) data from a number of stations allows reconstruction of certain features of ionospheric electron density profile information, (Austen, et. al., RADIO SCIENCE 25, 299, 1988, Raymund, et. al. RADIO SCIENCE, 27, 771, 1990). The potential spatial resolution of an ionospheric tomography system, (ITS), is limited, on the small scale, by diffraction, to a size greater than a few kilometers, and, on the large scale, by the total number and spacing of the receiving stations. Since the experimentally measured quantity is TEC, the reconstructed vertical electron density profile is limited by the TEC measurement accuracy to a few scale heights either side of the region of the peak electron density. Within these limitations, however, an ITS has potential for use in near-real-time determinations of ionospheric F region features which are important in many practical areas, such as in improving communications, and in providing ionospheric corrections for radio navigation systems, radio astronomy, and precise time transfer via satellite radio link. The relatively inexpensive projected capital and operating costs of a real-time ionospheric tomography system could make it ideal for long term studies of large-scale features of the F region for improving our understanding of the physics of this highly variable, economically important, part of the earth's ionosphere.

The issues which must be addressed in implementing an ITS include: 1) continued availability of suitable satellites of opportunity to measure TEC; 2) optimum number and spacing of stations; 3) best method of determining absolute TEC from relative differential phase measurements; 4) removing phase scintillation effects; 5) data transmission from remote sites; 6) use of other ionospheric data, such as vertical incidence ionosoundings; 7) the most efficient tomographic reconstruction algorithm; and 8) the potential funding source for such a system.

HOW WELL CAN WE IMAGE IONOSPHERIC STRUCTURES BY TOMOGRAPHY?

K. C. Yeh and T. D. Raymund
Wave Propagation Laboratory
Department of Electrical and Computer Engineering
University of Illinois at Urbana-Champaign

The advent of orbiting artificial satellites marked the beginning of the radio beacon technique era. This technique has been used to probe the ionospheric structures ever since. One of the quantities that can be measured using the radio beacon technique is the integrated electron density or the total electron content (TEC) along the satellite to ground receiver path. As the satellite moves along its orbit, this path to a given receiver sweeps through the ionosphere. A localized structure in the ionosphere is therefore viewed with changing view angles and has the potential of being imaged by using the tomographic inversion technique. In the idealized two dimensional plane geometry with ground receivers of infinite density extending to $\pm \infty$, a localized structure can be imaged uniquely with no loss of fidelity if the TEC data is available for all the view angles and for all the infinite receivers. If the view angles are limited, or the receivers are discretely spaced over a finite aperture, or the geometry is circular, the fidelity of the reconstructed image in general will suffer deterioration. This paper is concerned with an investigation of how well these ionospheric structures can be imaged when such imperfect data are used.

G95.3

RECONSTRUCTION TECHNIQUES AND RESOLUTION LIMIT OF TOMOGRAPHIC IMAGING OF ELECTRON DENSITY PROFILES IN THE IONOSPHERE

Helen Na* and Hua Lee
Center for Information Processing Research
Department of Electrical and Computer Engineering
University of California, Santa Barbara
Santa Barbara, California 93106

Estimating the electron density profile in the ionosphere is a challenging research topic of increasing importance. One potential approach is to apply tomographic techniques to perform image reconstruction of the electron density distribution. The data acquisition of this task can be achieved by using an orbiting satellite as a scanning transmitter, and the receiving aperture can be formed by an array of ground stations or a low-altitude orbiting satellite.

The path defined by each pair of transmission-receiving positions gives an index in terms of the relative angle. Then, we compile the data samples according to the angular index. As a result, the data samples are grouped into various *projections* and each projection contains data with identical angular index. After this re-indexing step, the data acquisition system is in a form similar to the one in classical X-ray tomography. By using this modeling approach, we are able to perform resolution analysis and sensitivity study with respect to the tomographic reconstruction process. Subsequently, we can identify key parameters associated with the resolving capability of the system.

In this paper, we present the tomographic modeling approach and outline various versions of the image reconstruction algorithms. In addition, we perform the resolution analysis of the electron density profile estimation process and illustrate the degradation parameters such as limited spatial-frequency bandwidth, limited aperture size, accuracy of spectral estimation due to limited data samples in each projection, non-uniform sample spacing, and angular quantization error during the re-indexing procedure.

A TWO DIMENSIONAL FOURIER VIEW OF THE NONIDEAL IONOSPHERIC TOMOGRAPHIC GEOMETRY

T. D. Raymund* and K. C. Yeh
Wave Propagation Laboratory
Department of Electrical and Computer Engineering
University of Illinois at Urbana-Champaign

Recent discussions of ionospheric tomography have purposed using total electron content measurements to compute vertical slice images of ionospheric electron density. Limitations in receiver location, spacing and number (defined as the measurement geometry) cause the total electron content data to be incomplete. Using the projection slice theorem, the measurement geometry has been mapped to the two dimensional Fourier domain, showing where in the spatial frequency domain information is missing. Common ionospheric features have also been transformed to the two dimensional Fourier domain, and plotted against the missing regions, showing the relationship between missing information and the measurement geometry. Transform reconstructions using only measured data have been computed numerically, showing the impact of the nonideal geometry and yielding information about the minimum geometry required to resolve particular features. Methods to improve the results by obtaining mathematically consistent and physically reasonable extensions to the data are discussed.

G95.5

BACKGROUND RESOLVING CAPABILITIES OF IONOSPHERIC COMPUTERIZED TOMOGRAPHY

J. R. Austen*
Tennessee Technological University
Box 5004
Cookeville TN 38505

C. H. Liu and S. J. Franke
University of Illinois at Urbana-Champaign
1406 W. Green St.
Urbana IL 61801

Computerized tomography (CT) techniques can be used to produce a two-dimensional image of the electron density in the ionosphere (Austen et al., *Radio Sci.*, *23*(3), 299–307, 1988; Raymund et al., *Radio Sci.*, *25*(5), 771–789, 1990). The necessary data are transionospheric satellite beacon total electron content (TEC) data recorded simultaneously at multiple ground stations.

The ionospheric imaging case presents a difficult problem due to large amounts of missing data. This is a consequence of the locations of the transmitter (in orbit) and receivers (ground-based) and causes the reconstruction algorithm to fail to correctly reconstruct the background density profile. When a reasonable background profile is assumed, ionospheric irregularities and some characteristics of the profile are successfully reconstructed; however, the background of the reconstruction still retains several characteristics of the assumed profile.

Computer simulation of the entire data collection and image reconstruction process is used to demonstrate the characteristics of the background profiles that can and cannot be reconstructed when using a geometry consisting of one satellite and several ground stations. To overcome this problem it is noted that in addition to TEC data, the algorithms used for ionospheric CT have the ability to utilize data obtained from other sources. By using data which contains information on the background profile it may be possible to reconstruct an image which contains the true background profile. This additional data may be obtained from sources such as a second orbiting satellite or a ground-based ionosonde.

APPLICATION OF A STOCHASTIC INVERSE TECHNIQUE TO IONOSPHERIC TOMOGRAPHY

E.J. Fremouw and J.A. Secan
Northwest Research Associates, Inc.
Bellevue, WA 98009

Stochastic techniques have been developed from inverse theory for producing tomographic images of geophysical structures using a judiciously weighted combination of path-integral data and *a priori* information, and they have been applied to a fluid medium in ocean acoustic tomography. We have reviewed those techniques and applied one of them --- the "weighted, damped, least-squares" technique --- to realistic plasma-density structures in the ionosphere, using simulated measurements of total electron content (TEC) as input data. We successfully employed simulated measurements of our own and such measurements sent to us "blind" by an independent party. From tradeoff calculations employing a series of parameter sets, including different numbers of receivers and different TEC sample rates at each receiver, we have found that inversion of TEC data from as few as five receivers can produce tenable images of structures containing scales down to a few tens of km. The horizontal resolution is set, not primarily by the number of receivers, but rather by the sample rate and computational resolution. Thus, scales down to the Fresnel diffraction limit (about a km at VHF) could be imaged cost-effectively, without further theoretical development. The number of receivers influences primarily one's ability to resolve the orientation of anisotropic structures. From this work, we conclude that stochastic inversion of TEC data is a potentially powerful and relatively inexpensive technique for developing images of plasma-density structures in ionospheric physics.

G95.7

METHODS TO ESTIMATE THE INITIAL VALUE OF DIFFERENTIAL DOPPLER DATA

R Leitinger
(Institut für Meteorologie und Geophysik,
Universität Graz, Halbärthgasse 1, A-8010 Graz, Austria)

Differential Doppler (carrier phase difference) observations on the signals of polar orbiting navigation satellites are presently used to derive the latitude dependence of ionospheric electron content. An other important application is ionospheric tomography.
Both applications need estimates of the initial value of the phase difference data. The observations give relative phase differences only and additional information is necessary to carry out initial value estimates.
The following possibilities are discussed and compared using the large European data base of Differential Doppler values collected and stored at the University of Graz:
1) Calibration by means of electron content from the Faraday effect on the VHF signals of geostationary satellites.
2) Two stations method (combined evaluation of Diff. Doppler from two stations in nearly the same geogr. longitude and with latitude differences between about 3 and 15 degrees).
3) Assumptions about the latitudinal structure of the ionosphere.
4) Information from other sources: ionosonde data combined with empirical models.
5) Rough estimates using plausibility considerations.
The experiences gained over many years of observation and evaluation are presented. Advantages and disadvantages of the different methods are discussed throughly. Sample results are presented including unusual magnetic storm effects.

AN EXPERIMENTAL DEMONSTRATION OF IONOSPHERIC TOMOGRAPHY

S. E. Pryse and L. Kersley
University College of Wales,
Aberystwyth, UK.

An experimental campaign to obtain tomographic images of ionospheric electron density is described. Simultaneous observations of transmissions from NNSS satellites were made at four stations covering an 8 degree range in latitude in the vicinity of the trough region. Measurements of ionospheric total electron content were made by means of the differential carrier phase method for some 25 satellite passes over a two-day period. A tomographic reconstruction algorithm has been used to obtain two-dimensional images of electron density as a function of latitude and height. The development of the ionosphere during the period of campaign is discussed to illustrate the potential of ionospheric tomography.

G95.9

THE PHASE-DIFFERENCE IONOSPHERIC TOMOGRAPHY

E.S.Andreeva, V.E.Kunitsyn*
Physics Dept., Moscow Univ., Moscow,119899,USSR
Yu.A.Melnichenko, E.D.Tereshchenko
Polar Geophys. Inst., Murmansk, 183023, USSR

There are different variants of the ionospheric tomography based on measurements of group delay, total electron concentration or phase. Such methods correspond to the case of the classical tomography using linear integrals. The theoretical analysis and mathematical simulation show essential limitation of these methods. In particular, the absolute phase is measured with great errors in the case of irregular ionosphere.

So we suggest a new method of phase-difference radiotomography (RT) or tomography based on the difference of linear integrals. The difference system is transformed to large sparse system of linear equations. The approximation of higher orders is necessary. The numerical simulation shows the opportunity of global structure reconstruction with the resolution about dozens kilometers. We worked out the software for simulation of the ionospheric RT,which permits to vary parameters of receiving systems and to process experimental data. The RT experiments for the reconstruction of the main ionospheric trough were carried out in spring and autumn 1990 (Andreeva E.S.et al.,JETP Lett. (Sov.) 52, 783-785,1990). For the first time 2D cross-sections of main ionospheric trough were obtained by methods of satellite RT. In the most cases we observed the regular smooth cross-sections of the ionosphere. The ionospheric trough was observed at night and it often had a complicated structure with many additional extrema. The example of reconstruction of ionospheric trough in isolines in units 10^6el/cm^3 is presented in Fig., h- the ionosphere height, τ - the distance along Earth's surface.

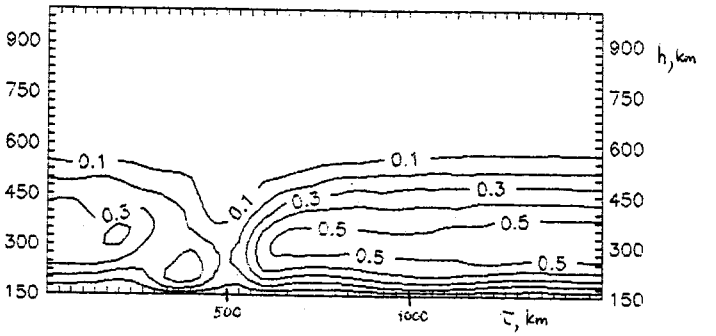

RADIOTOMOGRAPHY OF SCATTERING IONOSPHERE IRREGULARITIES

V.E.Kunitsyn, E.D.Tereshchenko*
Physics Dept., Moscow Univ., Moscow, 119899, USSR
Polar Geophys. Inst., Murmansk, 183023, USSR

The reconstruction problems of scattering irregularities structure are related to diffractional tomography problems. The satellite radiotomography(RT) can be divided into determinate and statistical problems. The determinate RT problems can be reduced to inverse scattering problems (ISP). We obtain the solution of ISP in the case of weak and strong scatterers using the small-angle scattering data. This solution permits to reconstruct the integral electron density and collision frequency along the direction of radioprobing wave propagation. An experimental complex for reconstruction of the inhomogeneities two-dimensional (2D) structure by using probing source of metre-range on the board of the navigational satellite was built. We discuss the experimental results of reconstruction of isolated irregularities 2D structure.

In the of case strong disturbed ionosphere layers with inhomogeneities it is necessary to use a statistical approach to RT. We derive an integral equation connecting the second coherence function of the field measured with the correlation function cross-section of scattering inhomogeneities. In the case of statistical homogeneous medium it is possible to determine a layer's height and a set of correlation function projections by means of one receiver, which registrates the satellite probing radiation passed through the layer under different angles. Fig. shows the 2D normalized spectrum of electron density fluctuations, reconstructed by experimental data, as a function of polar angle θ $(-\pi/2<\theta<\pi/2)$ and spectral variable $\varkappa$ $(0,1<\varkappa<2,5 km^{-1})$. We develop the method in the case of arbitrary inhomogeneities clusters. The method allows to reconstruct the spatial intensity distribution, correlation coefficient's structure of electron density fluctuations.

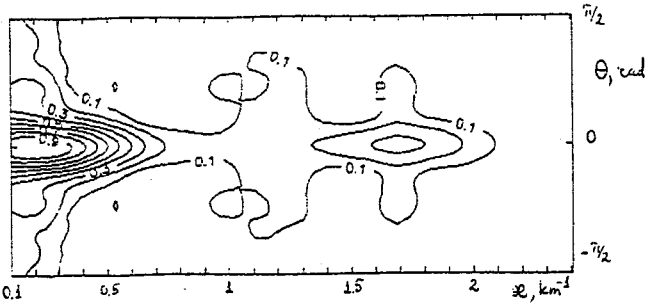

Recent Advances in Ionospheric Tomography II | **Room 3026 Salle URSI G Session 112** | **Progrès récents en tomographie ionosphérique II**

Chairs/présidents: S.J. FRANKE, USA

13:30 (112.1) The Possibility of 3-D Ionospheric Tomography with GPS, **G.A. HAJJ**, T.P. YUNCK, *California Institute of Technology, Pasadena, CA, USA*

13:50 (112.2) Simulation of Space-Based Ionospheric Tomography, **Y.T. CHIU**, R.M. ROBINSON, G.T. DAVIDSON, R.A. RINALDI, *Lockheed Missiles & Space Company Inc., Palo Alto, CA, USA*

14:10 (112.3) WITHDRAWN/ANNULÉ,

14:30 (112.4) Broad Area Mapping of Electron Density Profiles, X. HUANG[1], **G.S. SALES**[1], B.W. REINISCH[1], J. WOYTAL[2], [1] *University of Lowell, MA, and* [2] *Staff Meteorology, Hanscom AFB, MA, USA*

14:50 (112.5) Potential Coverage and Interference Areas of HF Radar, **N.C. GERSON**, G.L. WIEMANN, *Laboratory for Physical Sciences, College Park, MD, USA*

15:10 **COFFEE/CAFÉ**

15:30 (112.6) A New Superresolution Cepstral Technique for Multipath Propagation Analysis, **R.L. JOHNSON**, *Southwest Research Institute, San Antonio, TX, USA*

THE POSSIBILITY OF 3-D IONOSPHERIC TOMOGRAPHY WITH GPS

George A. Hajj* and Thomas P. Yunck
Jet Propulsion Laboratory
California Institute of Technology, Pasadena, California

The Global Positioning System (GPS) will consist of 24 satellites equally spaced in six orbit planes at about 20,000 km altitude. With the high precisions and low cost of GPS receivers, hundreds of them are expected to be distributed around the globe within a few years. With a simple linear combination of dual frequency GPS data we can continuously measure the total electron content (TEC) along all GPS-to-receiver raypaths. Pseudorange smoothed against precise carrier phase will give absolute TEC with an accuracy of about 10^{15} e/m^2, about 0.1% of the daytime zenith peak. Carrier phase measurements will give TEC change with a precision of better than 10^{14} e/m^2. TEC measurements taken along many raypaths can be used to construct maps of electron distribution in 2 or 3 dimensions.

With each ground receiver seeing an average of 7 GPS satellites instantaneously, a dense mesh of global/regional ground receivers will provide an immensely rich data set for global/regional ionospheric tomography. The additional information of TEC along links between GPS and one or more low earth orbiters will enhance the ground data by providing cuts that are mostly horizontal in the region of interest. We study the feasibility and performance of 3-D tomography in a rectangular box lying inside the ionosphere with dimensions of 5000x5000 Km^2 in the horizontal and 500 Km in the vertical . Dividing this region into N voxels of equal size, numbered from 1 to N, we define $f_i(r)=1$ if r is in voxel i and 0 otherwise. The horizontal and vertical dimensions of each voxel define the resolution of the recovered electron density. Writing f(r), the electron density distribution, in terms of $f_i(r)$ we have

$$f(r) \approx \sum_{i=1}^{N} x_i f_i(r)$$

where x_j represents the average electron density in voxel i. The N unknown x_j form the vector X. TEC_j is the integral of f(r) along a specific path P_j. With M TEC measurements we form the vector Y. Y and X are then related through $Y = D X + E$, where E includes measurements and discretization errors. The minimum distance solution to this equation is

$$X = \sum_{i=1}^{L} \frac{U_i . Y}{\lambda_i} V_i$$

where λ_i^2 (i=1,L) are the non-zero eigenvalues of DD^T and U_j, V_j are the eigen vectors of DD^T and D^TD respectively. The closer VV^T is to a unit matrix, the closer our solution is to the exact one. The Dirichlet spread function = $\| VV^T - I \|^2$ is a measure of the goodness of the solution. We will examine the dependence of the Dirichlet spread function on the horizontal and vertical resolution for several cases of ground receiver distributions, and the additional benefit of having TEC data from one or more low earth orbiters. Such an examination will tell us about the faithfulness of the recovered density and the spatial and temporal resolution that we can expect, and will set the stage for developing a set of system requirements to enable us to do 3-D tomography.

SIMULATION OF SPACE-BASED IONOSPHERIC TOMOGRAPHY

*Y.T. Chiu, R.M. Robinson, G.T. Davidson, and R.A. Rinaldi
Lockheed Palo Alto Research Laboratory
3251 Hanover Street, Palo Alto, California 94304

In order to monitor the dynamics of the ionosphere, it is not sufficient to determine its one- or two-dimensional behavior over some limited regions of the globe. Ionospheric responses to dynamics of the magnetosphere and thermosphere require monitoring on a global scale. Among various global monitoring schemes, the one closest to realization is that of deriving multi-directional total electron contents from coherently-phased Global Positioning System signals, since the GPS constellation is nearing completion. If appropriate GPS receivers were carried on board low-altitude satellites in polar-orbit constellations, such as that of the Defense Meteorological Satellite Program, the multi-directional TEC's gathered by the GPS receivers in a single orbit of two satellites will be sufficient to perform ionospheric tomography. If the ionosphere is assumed to be static during the 100-minute orbit, the multi-directional TEC's will cross-cover the global ionosphere sufficiently to yield tomography in the true sense of the word. Since each contact between a DMSP and a GPS satellite allows the TEC measurements to perform a scan of the ionsophere for about 2 minutes, additional information on ionospheric structure can be derived from the data. We have performed an end-to-end computer simulation of such an ionosphere monitoring system using the Chiu model as a surrogate to specify the ionosphere for calculation of the multi-directional TEC's. The entire TEC data set, with the DMSP and GPS constellations, is then subjected to a non-linear tomography algorithm. We show that a 3-dimensional reconstruction of the ionosphere density distribution can be obtained in terms of a user-specified model. A simple demonstration of this method of tomographic reconstruction with a refresh time of 100 minutes will be given. We also show that an accurate retrieval of the original vertical profile at any given location of the globe can be obtained from the global TEC data base.

G112.4

BROAD AREA MAPPING OF ELECTRON DENSITY PROFILES

X. Huang[1], G. S. Sales*[1], B. W. Reinisch[1], and J. Woytal[2]

1. University of Lowell Center for Atmospheric Research
450 Aiken Street, Lowell MA., 01701

2. Staff Meteorology
Hanscom AFB, MA., 01731

Electron density profiles from an areal network of Digisonde 256 sounders are used to map the three dimensional electron density distribution in a region of about 2000 km in diameter. The Digisondes are located at Goose Bay, Labrador, Argentina, Newfounland, Millstone Hill, Massachussets Wallops Island, Virginia and Bermuda. The Digisonde profiles are represented as a sum of Chebyshev Polynomials for each of the ionospheric layers E, F1 and F2. A new sets of coefficients representing the combined F1 and F2-region profile at each site is generated first. Then, the total set of these profiles is treated as a spatially sampled set of time series. After Fourier analyzing the profile coefficients at each station, the Fourier representation of the coefficients for an arbitrary location within the area is obtained by surface interpolation techniques. In a different approach the coefficients for an arbitrary point within the area are obtained from measured correlation coefficients between pairs of these stations. The results from the Fourier and correlation techniques are compared.

Potential Coverage and Interference Areas of HF Radar

N.C. Gerson* and G.L. Wiemann

Laboratory for Physical Sciences
4928 College Avenue
College Park, MD 20740

The coverage and interference areas of high power HF radar are of concern to communicators, ionosphericists, and radar operators. This paper depicts those areas for a typical radar, located near Bangor, Maine. The change in footprint with time of day, time of year and sunspot cycle is depicted. The results show that even on this statistically smoothed climatological basis the ionosphere comprises a dynamic region. Much greater changes are to be expected on a minute to minute basis. The results are depicted as footprints of the Maximum Usable Frequency (TOPOMUF) for a standardized transmitting antenna. Similar results can be obtained for any other high power transmitter, radar or broadcast.

A NEW SUPERRESOLUTION CEPSTRAL TECHNIQUE FOR MULTIPATH PROPAGATION ANALYSIS

Richard L. Johnson
Electromagnetics Division
Southwest Research Institute
San Antonio, TX, USA 78228

The problem of analyzing echoes or reverberations which result from multipath propagation occurs in many areas of signal processing. This paper describes a new technique for the estimation of echo delay time using the framework of cepstral analysis combined with more recently developed methods of superresolution spectrum estimation. In particular we develop a normalized eigen-based cepstrum and present experimental results obtained using the technique to analyze ionospheric multipath. The proposed eigen cepstrum is shown to be a more robust delay time estimator than the conventional cepstral technique for (a) narrow bandwidth signals, (b) low SNR and (c) signal formats having unevenly spaced spectral components.

The complex cepstrum is conventionally defined as the inverse z-transform of the complex logarithm of the z-transform of the function x. In cepstral analysis, the function given by log[X(z)] exhibits a periodicity which contains the echo time delay information. In our approach, we solve the problem in the Fourier domain by substituting the normalized cross-power spectrum for the logarithmic function. The MUSIC superresolution spectrum estimator is then applied instead of the inverse z-transform. The resulting normalized MUSIC cepstrum provides a robust estimate of the propagation delay time between sensors for the original signal as well as for each echo present. It also estimates the relative propagation time delay between each multipath component from transmitter to receiver.

A proof-of-concept experiment was conducted using an HF transmitted FSK signal which propagated to the receiving site via a groundwave and an ionospherically reflected skywave. A pair of crossed-loop antennas were used to sense the received signal. The normalized MUSIC cepstrum was applied to estimate intermode delay time as well as angle-of-arrival for each component using inter-sensor delay times. The results indicate that the proposed technique was successful in resolving echo delay time.

Extremely High Latitude Observatories and Observations I

Room 3026 Salle URSI G&H Session 14

Observatoires et observations aux latitudes extrêmement hautes I

Chairs/présidents: R. BEHNKE, USA

08:30 (14.1) A Polar Cap Observatory: Conception Rationale, **M.C. KELLEY**, *Cornell University, Ithaca, NY, USA*

08:50 (14.2) Polar Cap Incoherent Scatter Radar Observatory, **J.D. KELLY**, *SRI International, Menlo Park, CA, USA*

09:10 (14.3) Implications of Neutral Wind Dynamo on Ion Convection at High Latitudes, **J.P. THAYER**, J.F. VICKREY, *SRI International, Menlo Park, CA, USA*

09:30 (14.4) Plasma Structuring in the Polar Cap: The Role of the Polar Cap Observatory, **Su. BASU**[1], Sa. BASU[2], [1]*Boston College, Newton Center, MA, and* [2]*Geophysics Laboratory, Hanscom AFB, MA, USA*

09:50 (14.5) Optical Measurements in the Central Polar Cap Region, **J.W. MERIWETHER**, *Geophysics Laboratory, Hanscom AFB, MA, USA*

10:10 **COFFEE/CAFÉ**

10:30 (14.6) Ground-Based Optical Measurements from Within the Geomagnetic Polar Cap at Thule, Greenland (Λ=186°), **T.L. KILLEEN**, R.J. NICIEJEWSKI, Y. WON, G.S.N. MURTY, *University of Michigan, Ann Arbor, MI, USA*

10:50 (14.7) Characterizing Ne Variations in the Polar Cap F Region, **J. BUCHAU**[1], B.W. REINISCH[2], [1]*Phillips Laboratory (AFSC), Hanscom AFB, MA, and* [2]*University of Lowell, MA, USA*

11:10 (14.8) Observations of Polar Cap Total Electron Content During Solar Maximum, **G.J. BISHOP**[1], J.A. KLOBUCHAR[1], P.H. DOHERTY[2], [1]*Geophysics Laboratory, Hanscom AFB, MA, and* [2]*Boston College, Newton, MA, USA*

A Polar Cap Observatory: Conception Rationale

M C Kelley (School of Electrical Engineering, Cornell University, Ithaca, NY, 14853)

A radar and optical observatory located in the Earth's northern polar cap is essential for continued progress in understanding the Sun's influence on the structure and dynamics of our planet's atmosphere. Studies conducted during the past 5 years by the international community of atmospheric scientists have all indicated the crucial importance of the electrodynamics on the polar cap region and the key role that this region plays in coupling the solar wind with the Earth's magnetosphere, ionosphere and thermosphere. The existing observatories and those planned elsewhere do not extend into the polar cap, so that unfortunately there exists a paucity of observations in this region. This represents the most conspicuous gap in our understanding of the Earth's upper atmosphere--a gap that can be eliminated by the implementation of a polar cap observatory. Measurements that are critically needed include the electric field convection pattern across the polar cap and the response of the atmosphere to the varied forms of high-latitude energy input. The former quantified the interaction of the solar wind with the Earth's plasma environment, and the latter is of particular significance during geomagnetically disturbed conditions. Both need to be measured with high time and spatial resolution. The availability of an observational capability at these extremely high latitudes would also provide an opportunity to investigate important topics in atmospheric science, such as polar mesospheric clouds, and would allow timely monitoring of global change effects in the middle and lower atmosphere.

POLAR CAP INCOHERENT SCATTER RADAR OBSERVATORY

John D. Kelly
SRI International
333 Ravenswood Avenue
Menlo Park, California 94025 USA

The coupling of energy from the Sun to the Earth depends strongly on the processes that take place in the Earth's polar regions. Studies conducted during the past five years by the National Science Foundation's chain of combined radar and optical observatories in the American sector, global modeling efforts at the National Center for Atmospheric Research, and investigations carried out by the international community of atmospheric scientists have all indicated the key role that the polar caps play in coupling energy from the solar wind with the Earth's magnetosphere, ionosphere, and thermosphere. An extremely high-latitude location of the proposed polar cap observatory will extend observations into the central polar cap and complete an existing chain of upper atmosphere observatories, which currently range from the magnetic equator to the auroral zone. To realize its scientific potential, the polar cap observatory (PCO) will consist of an unprecedented assemblage of state-of-the-art instrumentation for aeronomic applications. A key element of the facility is an incoherent scatter radar capable of simultaneously measuring the ion drift velocity vector as well as other ionospheric plasma parameters. Essential to the success of a polar cap incoherent scatter radar will be the ability to measure atmospheric and ionospheric properties from the middle atmosphere to altitudes greater than 1,000 km. This requirement drives several radar parameters that will be discussed. In addition, a proper location for the polar cap observatory is vital. The location must be such that it is suitable not only in terms of geomagnetic location, but also in terms of providing the necessary logistic capabilities.

G&H14.3

IMPLICATIONS OF NEUTRAL WIND DYNAMO ON ION CONVECTION AT HIGH LATITUDES

J. P. Thayer* and J. F. Vickrey
SRI International
333 Ravenswood Avenue
Menlo Park, California 94025 USA

The importance of the neutral wind dynamo in generating electric fields which in turn drive F region plasma convection has been well established at middle and low latitudes. However, at high latitudes, this effect has been largely ignored as it has been assumed that the solar wind-magnetospheric dynamo is the dominant electrical energy source. It must be recognized that the electric field, under which the F region plasma drift in an $\mathbf{E} \times \mathbf{B}$ direction, is the result of both dynamo sources. Therefore, the resultant ion drift observed by spacecraft or ground-based instruments implicitly contains the neutral wind contribution as well as the solar wind contribution. In this study we demonstrate the significance of the neutral wind dynamo in establishing ion motion in the high-latitude F region. We find that the neutral wind contribution to ion motion can dominate over the solar wind dynamo, particularly in areas where the plasma convection reversal would otherwise occur. Thus, such convection signatures should not necessarily be attributed to magnetospheric boundaries. In order to relate observations of F region ion drift motion to solar wind-magnetosphere interactions unambiguously, knowledge of the neutral wind profile is required.

PLASMA STRUCTURING IN THE POLAR CAP: THE ROLE OF THE POLAR CAP OBSERVATORY

Sunanda Basu*
Institute for Space Research
Boston College
885 Centre Street
Newton Center, MA 02159 USA

Santimay Basu
Geophysics Laboratory (LIS)
Hanscom AFB, MA 01731 USA

Propagation experiments providing scintillation, total electron content and drift data in the field of view of an all-sky imager near the magnetic pole in Greenland have provided information regarding the manner in which ionospheric plasma becomes structured within the polar cap. Under IMF B_z southward conditions, the structuring is assumed to occur through the $\vec{E} \times \vec{B}$ gradient drift instability process which operates through an interaction between the antisunward plasma convection in the neutral rest frame and large scale plasma density gradients that exist at the edges of the ionization patches which convect into the polar cap probably through the dayside cusp. On the other hand, under IMF B_z northward conditions, the plasma structuring is found to occur around polar cap arcs in the presence of sheared plasma flows. While this broad framework exists, many important questions remain regarding the structuring process, much of it related to the nature of convection in the dark polar cap when the observed structuring is the most intense. The major contribution of the proposed Polar Cap Observatory (PCO), with an incoherent scatter radar as its centerpiece, will be its ability to provide continuous measurements of this convection pattern with high time and spatial resolution in a region where the interaction of the solar wind with the earth's plasma environment controls plasma structuring in a fundamental way. The talk will try to focus on the role of the PCO in answering outstanding questions on plasma structuring such as the role of the IMF and solar wind pressure on creating discrete plasma structures, the nature of the inhomogeneous electric field and density gradients near polar cap arcs, and the effects of E-region coupling on F-region structures.

OPTICAL MEASUREMENTS IN THE CENTRAL POLAR CAP REGION

J. W. Meriwether, Geophysics Laboratory, Ionospheric Effects Branch
Ionospheric Physics Division, Hanscom AFB, 01731-5000

A cluster of optical instruments of Class I CEDAR quality and located at the Polar Cap Observatory (PCO) at Resolute promises to be a valuable and productive attribute in many ways. While optical measurements at a central polar cap site would be of considerable interest in their own right, correlative comparisons with the measurements from the radio science instruments considered for PCO would greatly enhance the scientific usefulness of the optical results. A representative list of optical instruments viewed to be important for this observatory includes a total of 9 instruments. Among these would be 4 grating spectrophotometers configured to span simultaneously the entire spectral region from the UV to the IR. These instruments would provide the capability of monitoring spectral intensities of the airglow or auroral emissions simultaneously regardless of wavelength, which is important for the quantification of energetics of airglow and auroral processes. Also included would be two Fabry-Perot interferometers to achieve simultaneously low and high spectral resolutions for possible doppler and spectral intensity applications. These instruments would be primarily used to study the dynamics of the mesosphere, thermosphere, and exosphere regions with simultaneous doppler shift measurements. Two imaging systems are envisioned as well, one fitted with multiple filters for general purpose application, and the other for specific goals such as spatial distribution of the OH rotational temperature. We would anticipate that a Rayleigh/sodium resonance lidar would be included to provide temperature measurements for the entire range from 10 km to 100 km. The science issues that could be examined with such an optical facility combined with radio science instruments are numerous. They cover the wide variety of aeronomy and magnetospheric physics questions relating to the dynamics and chemistry of neutral and ionospheric phenomena in the central polar cap for atmospheric regions ranging from the lower stratosphere to the geocorona.

GROUND-BASED OPTICAL MEASUREMENTS FROM WITHIN THE GEOMAGNETIC POLAR CAP AT THULE, GREENLAND (Λ=86°)

T. L. Killeen*, R. J. Niciejewski, Y. Won,
and G. S. N. Murty
Space Physics Research Laboratory
Department of Atmospheric, Oceanic, and Space Sciences
The University of Michigan
Ann Arbor, Michigan 48109-2143

Observations of the dynamics and thermodynamics of the polar cap thermosphere have been obtained routinely since the winter of 1984 with an automated optical observatory located at Thule, Greenland (Λ=86°). The instrumentation at the observatory includes a Fabry-Perot interferometer (FPI), a half-meter Ebert-Fastie spectrophotometer (EFS), and a digital all-sky camera (ASC) system. The FPI has a 10 cm etalon coated for operation between 5577-Å and 7320-Å and an image plane detector similar to that flown on the Dynamics Explorer spacecraft. The FPI and EFS instruments are controlled automatically throughout each 8-month winter observing season (September - April) with an LSI 11/23 computer system and CAMAC interface cards. The ACS is operated on a campaign basis. The thermospheric neutral winds and temperatures measured with the FPI in the years 1985-1991 show strong dependencies on the solar cycle, local time, geomagnetic activity level and interplanetary magnetic field orientation. The EFS has been used to observe various nightglow emissions including NI (5200-Å), OI(5577-Å), OI(6300-Å), Balmer H_α(6563-Å), OII(7320-30-Å), and the OH (8-3) vibrational band. The ACS has been used in conjunction with the FPI to correlate sun-aligned polar cap arcs and thermospheric dynamics. This paper will describe the current status and plans for the automated optical observatory at Thule and will discuss several of the more significant scientific findings made over the past several years.

G&H14.7

CHARACTERIZING Ne VARIATIONS IN THE POLAR CAP F REGION

Jurgen Buchau*[1] and Bodo W. Reinisch[2]
1.Phillips Laboratory (AFSC), Geophysics Directorate, Hanscom AFB, MA. 01731
2.University of Lowell Center for Atmospheric Research, Lowell MA. 01854

A Digisonde 256 ionosonde has monitored the polar cap ionosphere at Qaanaaq, Greenland (87° CGLAT) since the solar minimum in 1986 through the current solar maximum. This paper analyzes solar cycle, seasonal and geomagnetic effects on the diurnal variations of Nmax, the peak electron density in the F layer. Combining Digisonde and All-Sky Imaging Photometer data has brought some order to the irregular plasma density variations. During Bz north conditions the polar cap is populated with sun-aligned F layer arcs with week plasma density enhancements above the background. Large ionization patches dominate during Bz south conditions (Buchau et al., 1983, Radio Sci., 18, 6, 995); these patches have up to tenfold plasma density enhancements and move fast antisunward across the polar cap.

The Digisonde's capability to measure O and X wave polarizations, Doppler frequencies, and incidence angles makes it possible to accurately determine the critical frequency foF2, i. e. Nmax, from the generally very disturbed ionograms and the plasma drift velocity from the drift observations. From these measurements a median patch size of 850 km was deduced for the solar max period, and a median amplitude of 3MHz. Modeling the patches as plasma transported from the sub-cusp solar produced ionosphere into the cap by the polar cap convection shows differences between solar maximum and minimum with likely source regions at 65° CGL for the maximum and 73° for the minimum.

OBSERVATIONS OF POLAR CAP TOTAL ELECTRON CONTENT DURING SOLAR MAXIMUM

G. J. Bishop* and J. A. Klobuchar
Ionospheric Physics Division
Geophysics Laboratory (AFSC)
Hanscom AFB, MA 01731

P. H. Doherty
Institute for Space Research
Boston College
Newton, MA 02159

Ionospheric absolute total electron content (TEC) was first measured in the northern polar cap in 1984 (E. J. Weber et al, JGR 91, 121-12, 129, 1986). These near-solar-minimum observations, made using signals from satellites at 20,000 km altitude, revealed the existence of a fundamental diurnal TEC cycle, with large TEC enhancements occurring preferentially in the 1200-2400 UT period and often more than doubling background values in less than ten minutes.

Recent polar cap observations during the 1989-90 winter (solar maximum), using the same technique, show that both the diurnal TEC cycle and enhancements' occurrence persist, but both are typically larger by a factor of three than in the same month of 1984. Background values are still seen to be more than doubled in less than ten minutes at solar maximum, implying that significantly greater spatial TEC gradients occur. Comparison of polar cap observations from October 1989 with February 1990 data suggests that at solar maximum there continues to be an annual variation in magnitude and occurrence of TEC enhancements that parallels the variation in magnitude and occurrence of amplitude scintillation, (Bishop et al, Vol 8, SPI Conference Proc, Scientific Publishers Inc, 1989).

Results will be presented from polar cap diurnal TEC observations, as well as near-auroral and mid-latitude data from the same general time periods. Available data from 1,000 km altitude satellite signal observations will be included to give insight to the spatial uniformity of TEC during the period of the diurnal observations.

Extremely High Latitude Observatories and Observations II

Room 3026 Salle URSI G&H Session 29

Observatoires et observations aux latitudes extrêmement hautes II

Chairs/présidents: J. KOEHLER, Canada;

13:30 (29.1) Coordinated Radar and Optical Measurements of Stable Auroral Arcs at the Polar Cap Boundary, **J.F. VICKREY**[1], E.J. WEBER[2], [1]*SRI International, Menlo Park, CA, and* [2]*Geophysics Laboratory, Hanscom AFB, MA, USA*

13:50 (29.2) Scanning Radar Observations of Ionospheric Convection at the Auroral Oval - Polar Cap Boundary, **J.C. FOSTER**, *Massachusetts Institute of Technology Haystack Observatory, Westford, MA, USA*

14:10 (29.3) The Sapphire Data Collection System, **D. ANDRE**, J.A. KOEHLER, G.J. SOFKO, *University of Saskatchewan, Saskatoon, SK, Canada*

14:30 (29.4) Constraints on Satellite Communication Links Operating in the Polar Environment, **Sa. BASU**[1], Su. BASU[2], A.L. JOHNSON[3], E.J. WEBER[1], [1]*Geophysics Laboratory, Hanscom AFB, MA,* [2]*Boston College, Newton Center, MA, and* [3]*Wright Research Development Center, Wright-Patterson AFB, OH, USA*

14:50 (29.5) The Downward Mapping of the Polar Electrojet Current During Disturbed Conditions, **D.H. WERNER**[1], A.J. FERRARO[2], [1]*Pennsylvania State University, State College, PA, and* [2]*Pennsylvania State University, University Park, PA, USA*

15:10 **COFFEE/CAFÉ**

15:30 (29.6) Detection of Signal Propagation from a Heated Polar Ionosphere, R.J. LUNNEN JR.[1], D.H. WERNER[1], **T.W. COLLINS**[2], A.J. FERRARO[2], [1]*Pennsylvania State University, State College, PA, and* [2]*Pennsylvania State University, University Park, PA, USA*

15:50 (29.7) Measurement and Interpretation of Ionospheric Effects Produced by a Large Ground-Based Explosion, **S.J. ANDERSON**, *Defence Science and Technology Organisation, Salisbury, Australia*

16:10 (29.8) A Study of the Slab Thickness of the Ionosphere, **K. DAVIES**, *NOAA/ERL/Space Environment Laboratory, Boulder, CO, USA*

G&H29.1

COORDINATED RADAR AND OPTICAL MEASUREMENTS OF STABLE AURORAL ARCS AT THE POLAR CAP BOUNDARY

James F. Vickrey*
SRI International
Geoscience and Engineering Center
Menlo Park, California USA 94025

Edward J. Weber
Geophysics Laboratory
Hanscom Air Force Base
Bedford, Massachusetts USA 01731

A specialized incoherent radar scanning mode has been developed for use in conjunction with simultaneous real-time all-sky images. These complementary diagnostics are used to examine the aeronomy and electrodynamics of stable auroral arcs that delineate the boundary between the polar cap and the auroral oval. The first arc discussed, observed at 2000 MLT, represents the boundary between anti-sunward plasma flow in the polar caps, and sunward return flow equatorward of the arc. The arc defined an equipotential in the high latitude convection pattern in that no plasma flowed across the arc. The radar line-of-sight velocity measurements also indicate that this arc is consistent with a convergent electric field and an associated weak upward field aligned current.

The second arc was observed at 2330 MLT and was associated with a nightside gap, or reconnection region. Strong antisunward flow was observed directly across the arc, although a velocity shear was superposed on this steady flow along the poleward edge of the arc.

Detailed plasma density, temperature, and line-of-sight velocity measurements from the radar are presented for both arcs to define the electric field, horizontal and field-aligned currents, and thermal plasma parameters associated with these arcs.

SCANNING RADAR OBSERVATIONS OF IONOSPHERIC CONVECTION AT THE AURORAL OVAL - POLAR CAP BOUNDARY

John C. Foster, Atmospheric Sciences Group, M.I.T. Haystack Observatory, Westford, MA 01886, U.S.A.

Azimuth scanning experiments at low elevation angle with the monostatic Millstone Hill and Sondrestrom incoherent scatter radars provide two-dimensional maps of *F* region plasma convection near the dayside cusp and in the vicinity of the auroral oval - polar cap boundary. The spatial and temporal resolution which can be achieved with this technique are set by the pulse length and antenna scan rate which, in turn, must be chosen in light of the conditions which determine the accuracy of Doppler drift measurements within the field of view of interest (range, density, spatial scale size of structure). During disturbed conditions, the northward-directed field of view of the Millstone Hill UHF radar at 4° elevation angle observes a 5-hour local time span of the large-scale convection pattern at the polar cap boundary with 20 min temporal resolution (see figure). The Sondrestrom radar, at a closer range to the boundary phenomena, can investigate meso- and small-scale phenomena with a temporal resolution determined by integration and antenna motion times. The strengths and limitations of monostatic scanning experiments for monitoring ionospheric convection at extreme high latitudes are discussed.

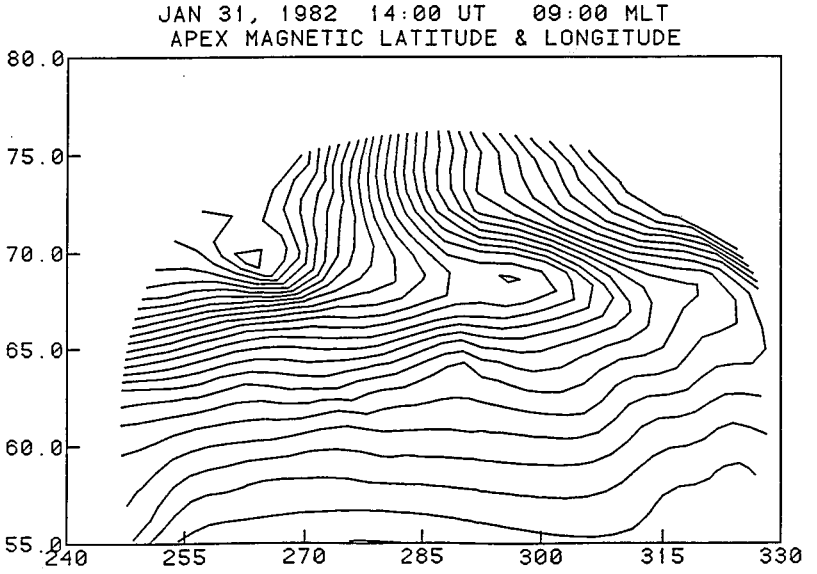

G&H29.3

THE SAPPHIRE DATA COLLECTION SYSTEM

Dieter Andre, J. A Koehler and G. J. Sofko

Institute of Space and Atmospheric Studies
University of Saskatchewan, Saskatoon, Canada S7N 0W0

In its final version, the University of Saskatchewan SAPPHIRE CW radar system will receive backscatter from 32 transmitter-receiver antenna beam intersections, resulting in a maximum of 160,000 data samples per second. This is more than ten times the data rate used during earlier campaigns, usually of a few weeks duration, in which data were recorded in analog form and analyzed off-line. An identical approach for the SAPPHIRE system (which will run continuously) would be almost impossible in terms of time and labour. We are therefore implementing a parallel processing system that does all the standard analysis tasks on line. This system and the tasks performed by it are described, along with actual operating experiences.

CONSTRAINTS ON SATELLITE COMMUNICATION LINKS OPERATING IN THE POLAR ENVIRONMENT

S. Basu*
Geophysics Laboratory (LIS)
Hanscom AFB, MA 01731 USA

Sunanda Basu
Institute for Space Research
Boston College
Newton Center, MA 02159 USA

A.L. Johnson
Wright Research Development Center
Wright-Patterson AFB, OH 45433 USA

E.J. Weber
Geophysics Laboratory (LIS)
Hanscom AFB, MA 01731 USA

A special propagation experiment was planned at Sondrestrom, Greenland in October, 1990 to determine message errors in satellite communication links operating through structured plasma in auroral and polar regions. Messages were transmitted on a satellite link at 250 MHz and simultaneously a CW signal was received on an adjacent channel. The CW channel was utilized to determine phase and amplitude scintillations and to perform spaced receiver drift measurements. With the help of supporting observations by the incoherent scatter radar and all-sky imaging photometer at Sondrestrom, it was found that the number of error-free messages over a given interval is greatly dependent on the type of plasma structure and associated convection. It particular, when ionization patches were detected, the CW channel suffered fast fadings and the message link recorded individual bit errors whereas polar cap arcs caused slow deep fades and losses of entire messages of several seconds duration. Drift measurements indicate that patches are associated with large uniform drifts whereas arcs occur in conjunction with velocity shears providing a regime of slow velocities prior to flow reversal.

THE DOWNWARD MAPPING OF THE POLAR ELECTROJET CURRENT DURING DISTURBED CONDITIONS

D. H. Werner
The Applied Research Laboratory
The Pennsylvania State University
P. O. Box 30
State College, PA 16804

A. J. Ferraro
Electrical and Computer Engineering
The Pennsylvania State University
University Park, PA 16802

An investigation is made of how the polar electrojet currents and associated electric fields map down from the E region, through the D region and to the ground. The electrojet current is represented by a simple Cowling model in which the geomagnetic field is vertical. A finite difference technique is used to obtain a numerical solution to the boundary value problem which characterizes the electrojet mapping behavior. This model is employed to study the downward mapping of the polar electrojet current during intense magnetic storms occurring under sunspot maximum daytime conditions. Results have also been obtained for the downward mapping of the electrojet currents and electric fields in the presence of ionospheric D region conductivity irregularities. A possible application of electrojet mapping theory to the interpretation of high-latitude ionospheric modification data taken during polar electrojet events is discussed.

DETECTION OF SIGNAL PROPAGATION FROM A HEATED POLAR IONOSPHERE

R. J. Lunnen, Jr., D. H. Werner
The Applied Research Laboratory
The Pennsylvania State University
P. O. Box 30
State College, PA 16804

T. W. Collins*
Electronic Design Services
The Pennsylvania State University
115 Engineering Services Building
University Park, PA 16802

A. J. Ferraro
Electrical and Computer Engineering
The Pennsylvania State University
University Park, PA 16802

During August of 1989, The Pennsylvania State University investigated signal propagation from a heated polar ionosphere using the High Power Auroral Stimulation (HIPAS) heating facility located approximately 47 kilometers east of Fairbanks, Alaska. The high frequency (HF) transmitter at HIPAS consisted of a circular array of eight crossed dipole antennas tuned to 2.85 MHz. The transmitter carrier frequency was modulated by Quadrature Phase Shift Keying (QPSK) for a portion of the testing. Another method of modulating the signal amplitude and phase was accomplished using conical scan by rotating the HF beam in a circular path tilted 30 degrees from vertical. A single channel ELF/VLF receiving system was assembled in a 26 foot mobile van with ferrite core and air core loop antennas. A two channel recorder with a bandwidth of 60 Hz - 60 KHz, was provided by The Johns Hopkins University Applied Physics Laboratory for continuous recording of the testing signal and noise environment. Remote locations from 130 to 387 miles from the heater were selected and propagated signal amplitude and phase were recorded. Communications between the mobile van and the transmitter coordination and control facility was via an amateur VHF digital link using packet radio. This paper will discuss the results of these tests and compare the findings to earlier results obtained by researchers using the HF heater at Ramfjordmoen near Tromso, Norway.

G&H29.7

MEASUREMENT AND INTERPRETATION OF IONOSPHERIC EFFECTS PRODUCED BY A LARGE GROUND-BASED EXPLOSION

S.J.Anderson
Surveillance Research Laboratory
Defence Science and Technology Organisation
SALISBURY SOUTH AUSTRALIA 5108

In May 1990 a ground-level detonation of 7500 kg of high explosive took place near Woomera, South Australia. Although the purpose of the test was to measure blast effects in the immediate vicinity of the explosion, the event provided an opportunity to look for delayed acoustic disturbances in the ionosphere.

To detect the passage of the pulse through the ionosphere above the explosion, an oblique radio sounding system was deployed. This consisted of a portable transmitting facility of 25W mean power, radiating a linear FMCW waveform of 15 kHz bandwidth at a WRF of 15 Hz, together with the fixed receiver system of the JINDALEE skywave radar located near Alice Springs. Part of the JINDALEE receiving array was phased to look backwards towards Woomera and the portable transmitter was installed at Mt Gambier so that the midpoint of the oblique path lay directly above the explosion.

This sounding system was operated as a channel scattering function monitor, with Doppler shift and group delay measured directly from the deramped waveform Doppler spectrum. In addition, a number of ionosondes, magnetometers and other instruments were deployed within 1000 km of the blast. The JINDALEE Miniradar was operated as a second channel scattering function monitor over the path from Alice Springs to Darwin, in the opposite direction to the blast, in the hope of observing travelling ionospheric disturbances excited by the explosion.

Analysis of the data collected from the Mt Gambier - Alice Springs path shows evidence of a weak Doppler shift which persisted for several minutes after the pulse reached the lower F-region. To explain the unusual form of this signature, a mathematical model of the effects of a travelling density wave on the phase path of an obliquely-propagating radio signal has been developed. On the basis of this model, the connection between the electron density profile, the acoustic pulse parameters and the Doppler shift has been established.

A Study of the Slab Thickness of the Ionosphere

By

Kenneth Davies
NOAA/ERL/Space Environment Laboratory
325 Broadway
Boulder, Colorado 80303

Satellite radio beacons have been used to measure the total electron content of the ionosphere since the launch of Sputnik I in 1957. Measurements of Faraday rotation and time of flight give information on the topside and on the protonosphere. Morphological studies show that the slab thickness of the ionosphere depends on the solar index but is approximately independent of geographical location. The total electron content can be obtained from a knowledge of the slab thickness and the maximum electron density that can be estimated from ionospheric models (e.g., IONCAP).

Ionospheric Heating and Modification | **Room 3028 Salle URSI H Session 46** | **Chauffage et modifications ionosphériques**

Chairs/présidents: D.B. MULDREW, Canada

08:30 (46.1) Observations of HF-Enhanced Plasmalines by Chirped ISR, **T. HAGFORS**, B. ISHAM, *Cornell University, Ithaca, NY, USA*

08:50 (46.2) High Resolution Measurements of the HF Enhanced Plasma Line at Arecibo and Tromsø, **M.P. SULZER**[1], F.T. DJUTH[2], J.A. FEJER[3], H. KOHL[4], P. STUBBE[4], M.T. RIETVELD[5], [1]*Arecibo Observatory, Arecibo, PR,* [2]*The Aerospace Corporation, Los Angeles, CA, and* [3]*University of California at San Diego, La Jolla, CA, USA;* [4]*Max-Planck-Institut für Aeronomie, Katlenburg-Lindau, Germany;* [5]*E.I.S.C.A.T, Ramfjordbotn, Norway*

09:30 (46.3) Space and Time Dependence of Strong Langmuir Turbulence Excited by HF Modification of the Ionosphere, **D.F. DuBOIS**[1], H.A. ROSE[1], D. RUSSELL[2], [1]*Los Alamos National Laboratory, Los Alamos, NM, and* [2]*Lodestar Research Corporation, Boulder, CO, USA*

10:10 **COFFEE/CAFÉ**

10:30 (46.4) Observations and Theories of HF-Induced Langmuir Turbulence, **J.A. FEJER**, *University of California at San Diego, La Jolla, CA, USA*

10:50 (46.5) Duct-Model Explanation of the Broad Component of the Plasma-Line Spectrum Observed at Arecibo, **D.B. MULDREW**, *Communications Canada, Ottawa, ON, Canada*

11:10 (46.6) Oblique Ionospheric Heating by HF Waves, D. HINKEL-LIPSKER[1], **M. SHOUCRI**[1], T. SMITH[1], T. WAGNER[1], J. HANSEN[2], G. MORALES[2], [1]*TRW Space and Technology Group, Redondo Beach, CA, and* [2]*University of California, Los Angeles, CA, USA*

11:30 (46.7) Nonlinear Refraction of O-Mode Waves in the Ionosphere, **J.D. HANSEN**, G.J. MORALES, J.E. MAGGS, *University of California, Los Angeles, CA, USA*

11:50 (46.8) Excitation of Airglow by High Power Radio Waves from the "SURA" Ionospheric Heating Facility, **P.A. BERNHARDT**[1], W.A. SCALES[1], D.S. KOTIK[2], S.M. GRACH[2], A.N. KEROSHTIN[2], [1]*Naval Research Laboratory, Washington, DC, USA;* [2]*Radiophysical Research Institute, Gorky, USSR*

H46.1

OBSERVATIONS OF HF-ENHANCED PLASMALINES BY CHIRPED ISR

T. Hagfors and B. Isham
National Astronomy and Ionosphere Center
Cornell University
Ithaca, NY 14853-6801

Most of the chirped ISR observations of the enhanced plasma line reported so far have been taken during the day-time. The reason for this choice has been the desire for simultaneous observation of the heater-enhanced line and the natural plasma line in order to place the two in spatial relation. In these experiments the frequency shift of some 100 kHz between the natural and the heater-enhanced chirped plasma lines, interpreted as small scale density depletions near the critical level, is seen quite regularly. Some times, however, a few seconds after the HF turn-on, a second scattering layer develops about 2 km below the initial level, often corresponding to the height of the natural plasma line. In our observations, the return from the higher level often disappears when this happens. In some of the observations there is spreading and reformation of the natural plasma line on a time scale of 30 sec, when a 30 sec on 30 sec off HF time sequence is used. This spreading of the natural plasma line is thought to be due to small scale field-aligned striations with relative density fluctuations of 1 to 2 %. The heater-enhanced plasma line still appears primarily to come from a very thin layer near the critical level.

Recent night-time observations of the same type have revealed qualitatively different results. In these observations it is not possible to observe the natural plasma line and place the heater-enhanced plasma line in relation to it. The latter is no longer confined to a narrow height range as in the day-time observations, but often extends over a height range as large as 4 km. There is some evidence that the extent of the height spreading depends strongly on the power level of the HF-heater.

A number of examples of the observations are shown, and the possible reasons for the different behavior of the heater-enhanced plasma line between day-time and night-time observations are discussed.

HIGH RESOLUTION MEASUREMENTS OF THE HF ENHANCED PLASMA LINE AT ARECIBO AND TROMSØ

M. P. Sulzer*
Arecibo Observatory, Arecibo, Puerto Rico
F. T. Djuth
The Aerospace Corporation, Los Angeles, Ca.
J. A. Fejer
University of California at San Diego, La Jolla, Ca.
H. Kohl and P. Stubbe
The Max-Plank-Institut für Aeronomie, 3411 Katlenburg-Lindau, FRG
M. T. Rietveld
EISCAT, Ramfjordbotn, Norway

An extensive set of high resolution measurements of the response of the HF enhanced plasma line in the region near HF reflection has been carried out. Responses in both the time and altitude domains have been optimized within certain existing system constraints using innovative data-recording and pulse coding techniques. Measurements of total power versus altitude and spectral power density versus frequency and range are presented. Measurements are shown from the Arecibo facility, made in the last two years, with mid-latitude B field configuration using the 430 MHz radar, and from the MPI Tromsø facility, made in November, 1990, with a high-latitude B field configuration using the EISCAT 224 MHZ and 930 MHZ radars.

The scatter from the plasma is found to be highly structured in all of the measured domains. Some aspects of the behavior are highly repeatable for a given cycling of the HF modifier, but there are random aspects of the response as well. Reapeatable behavior is the rule near the beginning of a cold start cycle, in which the HF modifier has been off for several minutes and for certain pulsing sequences. There are substantial differences in the dynamic behavior of the plasma line at Arecibo and at Tromsø. The significance of the observations in terms of the various theories regarding how the plasma instabilities are generated is discussed.

H46.3

SPACE AND TIME DEPENDENCE OF STRONG LANGMUIR TURBULENCE EXCITED BY HF MODIFICATION OF THE IONOSPHERE

D. F. DuBois,[a]* Harvey A. Rose[a] and David Russell[b]
[a]Los Alamos National Laboratory, Los Alamos, NM 87545
[b]Lodestar Research Corp., 2400 Central Avenue, Boulder, CO 80301

Recent experiments (Djuth, Sulzer and Elder and Fejer, Sulzer and Djuth, 1990) have revealed the space-time structure of the Langmuir turbulence excited by HF heating of the ionosphere at Arecibo, with spatial (temporal) resolution of about 100 m (~10 ms). At early times ($\lesssim$100 ms) following HF turn-on, the turbulence resides in a narrow layer near the reflection height and produces a plasma line power spectrum which is consistent with strong Langmuir turbulence (SLT) predictions but not with the conventional approximation known as weak turbulence theory (WTT). At later times the turbulence unevenly fills a layer 1 to 2 km thick below the reflection height and produces a spectrum *qualitatively* similar to some WTT predictions. Our recent work, based on numerical simulations of the complete nonlinear equations describing the turbulence, shows that caviton collapse, a basic SLT phenomenon, and parametric decay cascades can coexist at densities (altitudes) below critical density. Significant *quantitative* differences are found from WTT predictions: a truncation of the number of cascade steps, and most dramatically a different level, $\underline{k}$-space distribution, and power spectrum of ion density fluctuations which arise primarily from caviton collapse. For the observed spectra, to be consistent with decay of free Langmuir waves, some modification of the ionospheric electron density profile must be invoked. One mechanism, which can be effective on the 100 ms time scale, is the density depletion in the observed narrow layers of turbulence due to the *averaged* ponderomotive force of the HF-induced turbulent electric fields. With this modification the SLT predictions appear to agree with the observed time dependence of various spectral features, including the free mode line, following HF turn-on (in a 'cold start') and HF turn-off. A theoretical description of the up-down asymmetry of the free-mode line observed by Cheung et al. (1990) will also be discussed.

OBSERVATIONS AND THEORIES OF HF-INDUCED LANGMUIR TURBULENCE

Jules A. Fejer, Department of Electrical and Computer Engineering, University of California at San Diego, La Jolla, CA 92093

The first interpretations of 430 MHz radar backscatter spectra from HF-induced Langmuir turbulence in the ionosphere above Arecibo were in terms of a cascade of those parametrically excited Langmuir waves that were generated at the so called matching height. That height is defined by the condition that Langmuir waves in the ambient plasma could there simultaneously satisfy both, the Pines and Bohm dispersion relation and the Bragg backscatter condition for the 430 MHz radar at Arecibo. The unstable Langmuir waves were predicted to form very small angles with the geomagnetic field and were therefore not directly detectable by the Arecibo radar. Only the detection of the relatively weak Langmuir waves resulting from the scatter of the HF pump and of the unstable Langmuir waves by the thermal ion acoustic waves was predicted; the observed weak backscatter was predicted to come from the matching height, roughly a kilometer below the reflection height of the pump wave.

Observations over the last decade showed conclusively that the backscatter was strong rather than weak and came from a range of heights which could extend from the matching height up to the reflection height rather than from only the matching height.

The above first interpretation, based on the weak turbulence approximation, has also been questioned on theoretical grounds. It has been asserted that the correct theoretical approach is in terms of strong Langmuir turbulence of collapsing cavitons, described by the Zakharov equations, rather than in terms of the weak turbulence approximation.

The purpose of the present work is twofold. First it will be shown that recent numerical simulations based on the Zakharov equations lead under certain conditions to a cascade of Langmuir waves that is very similar to the one predicted by the weak turbulence approximation.

Secondly the nature of the limited agreement of recently observed radar backscatter spectra with existing theoretical predictions will be examined. Based on the results of that examination suggestions for future experimental and theoretical investigations will be made.

H46.5

DUCT-MODEL EXPLANATION OF THE BROAD COMPONENT OF THE PLASMA-LINE SPECTRUM OBSERVED AT ARECIBO

D. B. Muldrew
Communications Research Centre, Department of Communications
P.O. Box 11490, Station 'H', Ottawa, Ontario K2H 8S2, CANADA

The plasma-line spectrum observed during on-off cycling of the HF heater at Arecibo contains one or more decay lines and a 'broad component' (BC), sometimes called the 'broad bump', which can have a maximum in intensity and can extend for tens of kilohertz (Showen and Kim, J. Geophys. Res., 83, 623, 1978). The heater wave decays parametrically into Langmuir (L) waves and ion-acoustic waves. Some of the L waves cross the duct axis (parallel to the magnetic field) at an angle of 45° or more and are responsible for the first parametric-decay line. The frequency offset of this line from the HF, and the frequency asymmetry between the upshifted and downshifted components, can be calculated from the duct model using reasonable parameters. For the power levels used in the early experiments of Showen and Kim, the growth time for this line is a few milliseconds.

L waves which propagate almost along the axis of the duct (and thus have their electric field almost parallel to the electric field of the heater wave) have a growth time of about 1 ms. Their frequency offset can be considerably greater than that of the observed first decay line. These axial L waves can then decay parametrically into secondary L waves. For a given axial L wave there are two decay schemes that produce secondary L waves which are observed by the radar. The offset frequencies of these secondary waves differ by a few to several kilohertz and can vary from about three times the offset of the first decay line to considerably greater than this. The maximum intensity of the BC occurs near these two frequencies. The primary axial L waves can cross the duct axis over a range of angles. This results in a range of frequencies which smoothes out the BC. Axial L waves also decay into secondary axial L waves and these secondary waves then decay into L waves which are observed by the radar. Only one or two additional decays of this type are necessary to generate the 50-kHz width of the BC. Hence, the BC can be observed a few milliseconds after the heater is turned on.

There is another possible parametric instability which may contribute to the BC. L waves crossing the duct axis at intermediate angles (e.g. near 45°) can decay into ion-acoustic and Bernstein waves. Bernstein waves propagate almost perpendicular to the magnetic field and have negligible Landau damping. These grow and propagate in the duct with very little refraction. They can then decay into ion-acoustic waves and into L waves which are observed by the radar.

OBLIQUE IONOSPHERIC HEATING BY HF WAVES

D. Hinkel-Lipsker, M. Shoucri, T. Smith*
and T. Wagner
TRW, Space and Technology Group
Redondo Beach, CA 90278
J. Hansen and G. Morales
Physics Dept., UCLA, Los Angeles, CA 90024

Oblique propagation of high power high frequency (HF) waves produces heating in the ionosphere which in turn causes nonlinear deformation of the incident HF beam. An advanced ray tracing code is coupled to an ionospheric transport code in order to model the self-consistent deformation of the beam by the heated ionospheric volume. Results showing the unique capabilities of the wave ray tracing code have been previously presented. In the current effort, we show the upgrade work done on the transport code as well as the coupling of both codes. We also present preliminary results on the feedback effect the heating has on the HF beam.

H46.7

NONLINEAR REFRACTION OF O-MODE WAVES IN THE IONOSPHERE

J. D. Hansen*, G. J. Morales, and J. E. Maggs
Department of Physics, University of California Los Angeles,
Los Angeles, CA 90024

Nonlinear refraction is the self-consistent bending of an O-mode electromagnetic beam by heating-induced density modifications in a strongly magnetized plasma in which the ambient density gradient makes an angle relative to the magnetic field, as is common in ionospheric heating experiments. Power absorbed in the initially horizontal reflection region creates a large field aligned density depletion. This reorients the reflection surface parallel to the magnetic field and causes intense heating along a narrow flux tube. The region of depleted density increases the extent of the resonant interaction region along the magnetic field and provides a favorable geometry for the occurrence of nonlinear effects and upper-hybrid phenomena. A transport model including nonlinear refraction has successfully explained the formation of large scale ionospheric modifications in experiments performed at Arecibo (J. D. Hansen, et. al., Phys. Rev. Lett. 65, 3285, 1990). The observations also include preliminary evidence supporting the occurrence of upper-hybrid phenomena after nonlinear refraction sets in.

EXCITATION OF AIRGLOW BY HIGH POWER RADIO WAVES FROM THE "SURA" IONOSPHERIC HEATING FACILITY

P. A. Bernhardt and Wayne A. Scales
Space Physics Branch, Code 4780
Plasma Physics Division
Naval Research Laboratory
Washington, DC 20375-5000 USA

D. S. Kotik, S. M. Grach, and A. N. Keroshtin
Radiophysical Research Institute
N. Novgorod (Gorky) 603600 USSR

The SURA system for generation of high power radio waves is located near the village of Vasil'sursk, USSR. There, a 300 x 300 m^2 transmitting antenna is fed by three 250 kW transmitters operating between 4.5 and 9.0 MHz. The maximum ERP of this system is 300 MW. Optical measurements were made at SURA during August 1990. Images of enhanced red-line (630 nm) and green-line (557.7 nm) emissions were recorded during radio wave transmissions at 4.785, 5.455, 5.828, and 7.815 MHz. Field-aligned structures with scale sizes on the order of 1-10 km were observed. The airglow clouds drifted across the night sky, disappeared, and reformed at the zenith of the antenna array. This has been previously interpreted in terms of radio beam refraction in drifting plasma irregularities and "snap-back" when the beam can no longer be entrained by density cavities [Bernhardt et al., J. Geophys. Res., 94, 9071, 1989]. Energetic electrons are accelerated out of the interaction regions by the electrostatic waves. Ambient oxygen atoms are collisionally excited by these suprathermal electrons to yield enhanced airglow. From the intensities of the airglow emissions, one can estimate the distribution of suprathermal electrons streaming out of the radio wave interaction regions in the ionosphere. Electron fluxes and effective temperatures will be estimated for variations in transmitter frequencies and power densities. We were able to make reliable airglow measurements at SURA every time the high power transmissions occurred at frequencies below the F-layer critical frequency. Subject to clear skies, the low-light-level-imaging technique is a reliable method to study large scale irregularities and electron acceleration with HF transmitting facilities having effective radiated power of 250 MW or greater.

Waves in Laboratory and Ionospheric Plasmas | **Room 3028 Salle URSI H Session 63** | **Ondes dans les plasmas en laboratoire et dans l'ionosphère**

Chairs/présidents: K.G. BALMAIN, Canada

13:30 (63.1) Ball Lightning, **D.B. MULDREW**, *Communications Canada, Ottawa, ON, Canada*

13:50 (63.2) Ionospheric Emissions Stimulated by *In Situ* High Power High Frequency Wave Injection, **R.F. BENSON**, V.A. OSHEROVICH, *NASA/Goddard Space Flight Center, Greenbelt, MD, USA*

14:10 (63.3) Diffuse Resonance Below the Electron Gyrofrequency – The Case of a Mistaken Identity? **V.A. OSHEROVICH**, R.F. BENSON, *NASA/Goddard Space Flight Center, Greenbelt, MD, USA*

14:30 (63.4) Heating and Ionization of the Lower Ionosphere by Lightning Discharges, **U.S. INAN**, T.F. BELL, J.V. RODRIGUEZ, *Stanford University, Stanford, CA, USA*

14:50 (63.5) VLF Remote Sensing of Thunderstorm and Radiation Belt Coupling to the Lower Ionosphere, **U.S. INAN**, *Stanford University, Stanford, CA, USA*

15:10 **COFFEE/CAFÉ**

15:30 (63.6) Bistatic RF Investigations in the Oedipus-A Tether Experiment, **H.G. JAMES**[1], A.E. HAMMOND[1], M.L. LAUZON[1], G.W. HULBERT[2], [1]*Communications Research Centre, Ottawa, ON, and* [2]*York University, Downsview, ON, Canada*

15:50 (63.7) Z-Mode Propagation in Ionospheric Density Irregularities Observed on Oedipus A, **H.G. JAMES**, *Communications Research Centre, Ottawa, ON, Canada*

16:10 (63.8) RF Signal Transmission Along a Tether in the Ionosphere, **C.C. BANTIN**[1], K.G. BALMAIN[1], H.G. JAMES[2], G. HULBERT[3], [1]*University of Toronto, ON,* [2]*Communications Canada, Ottawa, ON, and* [3]*York University, Downsview, ON, Canada*

16:30 (63.9) Application de la spectroscopie dans le domaine du temps à l'étude des résonances de gaine, **P.-R. RENAUD**, M. NACHMAN, *École Polytechnique de Montréal, PQ, Canada*

16:50 (63.10) Experimental Study and Modelling of Magnetoplasmas Sustained by Electromagnetic Guided Waves, **J. MARGOT**, M. MOISAN, *Université de Montréal, PQ, Canada*

BALL LIGHTNING

D. B. Muldrew
Communications Research Centre, Department of Communications
P.O. Box 11490, Station 'H', Ottawa, Ontario K2H 8S2, CANADA

A few rather poor photographs of ball lightning and a very large number of surprisingly consistent eye-witness observations have been reported in the literature. The observations have been reduced to a set of reliable characteristics. These have been used to develop a model of ball lightning which is presented here. In this model electromagnetic-wave propagation, guided by a spherical plasma shell, is an essential component.

Ball lightning is assumed to have a solid, positively charged, core at its centre. The large amount of energy often associated with ball lightning is mainly due to the electrostatic energy of the charge on the core. The upper energy limit is determined by the size and strength of the core and this energy can be orders of magnitude greater than the energy which can be confined by atmospheric pressure alone. A pure electron layer and a plasma layer surround the core. The charge of the electron layer is equal in magnitude to that of the core. An electromagnetic field is completely trapped by the electron and plasma layers. The electron temperature is sufficiently high that absorption by electron-ion collisions is small, enabling the ball to have a lifetime of seconds or more. The ponderomotive force (radiation pressure) of the trapped electromagnetic field balances the electrostatic force of the electrons toward the core plus the force of atmospheric pressure.

IONOSPHERIC EMISSIONS STIMULATED BY IN SITU HIGH POWER HIGH FREQUENCY WAVE INJECTION

R.F. Benson* and V.A. Osherovich
NASA/Goddard Space Flight Center, Code 692
Laboratory for Extraterrestrial Physics
Greenbelt, MD 20771

Powerful topside sounders perturb the ionosphere to the point where stimulated emissions are routinely observed. These stimulated emissions were first identified by Nelms and Lockwood [Space Res., 7, 604, 1966] who introduced the name diffuse resonances because of their appearance on topside sounder ionograms. They can usually be easily distinguished from the principal resonances observed at the electron plasma frequency f_N, the harmonics of the electron cyclotron frequency f_H and the upper hybrid frequency $f_T = (f_N^2 + f_H^2)^{1/2}$ which are well explained in terms of the reception of echoing sounder-generated electrostatic waves. These diffuse resonances appear as a sequence of resonances between the harmonics of f_H and below f_N. The sequence nature was first recognized by Oya [J. Geophys. Res., 75, 4279, 1970]. The recent observations of Shuiskaya et al. [Planet. Space Sci., 38, 173, 1990] provide evidence for a close relationship between sounder-accelerated electrons and the spectrum of sounder-stimulated diffuse resonances.

Several theories have been proposed to explain the diffuse resonance phenomena. Oya [Phys. Fluids, 14, 2487, 1971] attributed the waves to a Harris instability initiated by a sounder-stimulated electron temperature anisotropy and maintained by a three-wave coupling process. Kiwamoto and Benson [J. Geophys. Res., 84, 4165, 1979] replaced the three-wave coupling process by an nonlinear Landau damping process. Both of these mechanisms were based on weak turbulence theory. Pullinets and Selegey [J. Atm. and Terr. Phys., 48, 149, 1986] proposed a mechanism based on strong turbulence. Osherovich [J. Geophys. Res., 92, 316, 1987] applied a macroscopic theory of force-free electromagnetic oscillations to predict the spectrum of frequencies of various bounded states that were interpreted as members of the sequence of diffuse resonances.

The present paper will summarize and consolidate the diffuse resonance observations with the inclusion of new observations that extend the diffuse resonance sequence, review the various theoretical approaches and compare predictions with observations, outline the major problems to be solved and discuss planned laboratory and space experiments including the Space Shuttle/Spartan flight of the Waves in Space Plasmas/High Frequency (WISP/HF) instrumentation scheduled for 1995.

DIFFUSE RESONANCE BELOW THE ELECTRON GYROFREQUENCY — THE CASE OF A MISTAKEN IDENTITY?

V.A. Osherovich* and R.F. Benson
NASA/Goddard Space Flight Center, Code 693
Greenbelt, MD 20771

Oya [Phys. Fluids, 14, 2487, 1971] interpreted the sequence of diffuse plasma resonances D_n in terms of a wave-particle nonlinear interaction in a weakly turbulent plasma. He suggested the frequency relation

$$f_{Dn} = f_{Qn+2} - 2f_H$$

for n = 1,2,3 and 4, where Q_n are the Bernstein modes and f_H is the electron gyrofrequency.

Recently, using antarctic rocket observations in the auroral ionosphere, Morioka et al [J. Geomag. Geoelectr., 40, 923, 1988] extended this relation to the case of n = 0, i.e.,

$$f_{Do} = f_{Q2} - 2f_H.$$

We have analyzed their passive rocket data and concluded that the above formula does not agree with their observations. In our presentation we will discuss an alternative interpretation.

HEATING AND IONIZATION OF THE LOWER IONOSPHERE BY LIGHTNING DISCHARGES

U. S. Inan*, T. F. Bell, and J. V. Rodriguez
STAR Laboratory, Stanford University,
Stanford, California 94305

It is suggested that ionospheric electrons at 90 km altitude can be strongly heated during the upward passage of short (<100 μs) pulses of intense electromagnetic radiation from lightning discharges. Using observed electric field intensities of 5-20 V/m normalized to 100 km distance from cloud-to-ground discharges, and a pulse of duration 50 μs, the temperature of the ambient electrons at 90-95 km altitude in the nighttime ionosphere can be increased by factors of up to 100-500. These energized electrons in turn produce secondary ionization, leading to local density enhancements in a single ionization cycle (~ 3 μs) of up to 400 el cm^{-3} at ~ 95 km altitude. The relative effects of both elastic and inelastic collisions are considered in determining the heating levels. The time constant of the heating is of the order of 10 μs, so that steady state can be reached and a number of ionization cycles could occur during a 50 μs radiation pulse, leading to even higher density enhancements. This effect can account for most of the previously reported observations suggesting direct upward coupling of lightning energy to the lower ionosphere as manifested in 'early' or 'fast' subionospheric VLF perturbations following within $<$ 50 ms of radio atmospherics or lightning and exhibiting unusually rapid ($<$50 ms) signal changes. The heating and ionization due to radiation from lightning is compared with that due to high power VLF transmitters.

H63.5

VLF REMOTE SENSING OF THUNDERSTORM AND RADIATION BELT COUPLING TO THE LOWER IONOSPHERE

U. S. Inan
STAR Laboratory, Stanford University,
Stanford, California 94305

Very Low Frequency (VLF) waves propagating in the earth-ionosphere waveguide are used to measure transient and localized disturbances of the nighttime lower ionosphere that occur in association with lightning discharges. Upward/downward coupling between the troposphere and the ionosphere occurs in lightning-induced electron precipitation events in which localized density enhancements in the D-region are produced by energetic (>40 keV) electrons precipitated by whistlers. Using observations at distributed sites and over many collinear VLF great circle paths, and by comparing with the predictions of a new three dimensional theoretical model of earth-ionosphere waveguide propagation, new information on the location and transverse extent of the ionospheric disturbances can be extracted. In some cases, especially on relatively short (<1500 km) paths, the VLF event signatures exhibit sensitive dependences on the altitude profile of the electron density, indicating that energy spectrum of precipitating electrons may also be measurable with this technique. New examples of direct upward coupling of lightning energy to the lower ionosphere are also revealed in the course of such measurements as unusually rapid VLF signal changes. These signatures are believed to be due to localized heating of the lower ionosphere by intense radiation from lightning discharges that also leads to ionization enhancements. In this paper, recent examples of both kinds of coupling effects observed on multiple collinear VLF paths will be discussed.

BISTATIC RF INVESTIGATIONS IN THE OEDIPUS-A TETHER EXPERIMENT

H.G. James*, A.E. Hammond and M.L. Lauzon
Communications Research Centre
Ottawa, Ontario K2H 8S2

G.W. Hulbert
Institute for Space and Terrestrial Science
York University
Downsview, Ontario M3J 1P3

The tethered OEDIPUS-A payload was launched on a sounding rocket from Andøya, Norway during an active auroral display on 30 January 1989. The tether separation subsystem extended the electrically conducting wire between the two approximately equal subpayloads to a length of 958 m near apogee (512 km). Active and passive radio experiments in the 0-5 MHz range were carried out using a transmitter (HEX) on one subpayload and a companion receiver (REX) on the other subpayload. These instruments were programmed to operate in a sequence of modes that repeated every 6 s throughout the flight. During each 6-s major frame, the HEX output was connected either to a dedicated 4-m dipole or between the tether wire and the payload body. At certain points in the major frame, the HEX power was off. Correspondingly, the REX at its end of the tether was connected either to a 5-m dipole or between the tether and the payload body. The HEX and REX together executed one of three different frequency sweeps, one in the range 0 to 5 MHz ('SH1'), one in 20 to 10000 Hz ('SH2'), and one in 1.138 to 1.363 MHz ('Fn'). These modes were designed to address a number of scientific questions about plasma waves and rf electrostatic probes.

Examples of data from different HEX/REX modes are given. SH1 results contain a variety of novel phenomena in the areas of sheath waves and electrostatic waves. Some of these are described in other papers at this meeting. The SH1-mode data are found to provide a direct measurement of local plasma frequency f_p which lay between 2 and 4 MHz for most of the flight. The history of f_p across the flight scaled from the REX data is very similar in shape to that determined from the onboard Langmuir probe. There are some differences in magnitude, especially when the payload descends through the densest part of the ionosphere at a height of 130 km where the electron density is about 3×10^5 cm^{-3}.

In its SH2 mode, the HEX applied to the tether a series of 8 consecutive sinusoidal voltage waveforms at frequencies logarithmically spaced between 20 and 10000 Hz. The current waveforms observed with REX are compared with predictions based on the theoretical response of the large double Langmuir probe formed by the tethered double payload. During the Fn frequency mode, 50-μs pulses were emitted by HEX at frequencies in the vicinity of the electron gyrofrequency. The decay time constant of these short pulses measured by REX is about 50 μs and exhibits a frequency dependence similar to the resonance effects observed in the SH1 mode.

Z-MODE PROPAGATION IN IONOSPHERIC DENSITY IRREGULARITIES OBSERVED ON OEDIPUS A

H. G. James
Communications Research Centre
3701 Carling Avenue
Ottawa, Ontario K2H 8S2

The tethered sounding rocket payload OEDIPUS A was used to conduct bistatic propagation experiments on plasma waves in the auroral ionosphere. The tether was aligned to within about 10° of the magnetic field direction throughout the flight. Synchronized sweeps of the frequency range 0 - 5 MHz by the 2-W transmitter HEX on the upper end of the tether and its associated receiver REX on the lower end have produced signatures of quasi-electrostatic waves in the slow Z mode guided along field-aligned depletions of ambient density. These waves have signal delays of about 1 ms over the transmitter-receiver separation which varies up to 960 m during the flight. The Z mode identification is based on payload measurements of the local plasma frequency . The transmitted pulses typically appear inside a frequency bandwidth of about 100 kHz just above the plasma frequency, but occasionally occupy most of the available bandwidth between the plasma frequency and the upper hybrid resonance frequency (BW $\simeq$ 300 kHz). The observed delays and the stretching by a factor of 3 of the transmitted 300-μs pulses are accounted for with two-dimensional ray tracing using a complete electromagnetic solution of the hot-plasma dispersion relation.

RF SIGNAL TRANSMISSION ALONG A TETHER IN THE IONOSPHERE

C.C Bantin* and K.G. Balmain, University of Toronto, Toronto
H.G. James, Communications Research Centre, Ottawa
G. Hulbert, York University, Toronto

In January 1989 a rocket-borne tether experiment called OEDIPUS-A was launched from Andoya, Norway. During the flight the nose-cone and tail sections of the rocket separated and moved apart to a distance of about 1km while connected by a thin insulated conducting wire. The wire was oriented essentially parallel to the magnetic field. An RF transmission system was carried on board in which a stepped-frequency series of pulses was applied to the tether at the nose-cone and received at the tail. This scheme provided an excellent opportunity to characterize the transmission of signals on a tether in a plasma and to observe for the first time the propagation of sheath waves along a tether in the ionosphere. The RF signals were applied to the tether as a series of short pulses which were stepped in frequency from 50 kHz to 5 MHz. The results of successive frequency sweeps during the flight are presented in the form of grey scale plots of received signal levels over the entire post-separation flight.

The RF experiment operated in two modes which alternated throughout the flight. In one mode the pulses were applied at 50 volts and received by a low impedance load. In the other mode the pulses were applied at 1 volt and received by a high impedance load. In addition, for each mode there was a low level residual signal transmitted between pulses. This provided an opportunity to observe the transmission of signals at different levels. Results are shown that demonstrate both linear and non-linear behaviour.

Resonances are observed in the received signals at low frequencies. These resonances depend on the length of the tether and are attributed to sheath waves propagating along the tether and reflecting off the ends. Estimate are made of the propagation constant for these waves. These results show an improvement over the initial estimates and a more accurate dispersion curve is deduced from the resonant frequencies displayed in each frequency sweep up to the mid-point of the flight. The observed results are shown to be in excellent agreement with computations done using an improved method-of-moments simulation of the rocket/tether system.

The results of the OEDIPUS-A RF tether transmission experiment show that significant RF coupling occurs along a thin wire tether in the ionosphere. Coupling is especially strong at low frequencies due to sheath waves. This demonstrates that, although the surrounding plasma is essentially cut-off from propagation, significant signal coupling can occur along conducting structures at low frequencies.

H63.9

APPLICATION DE LA SPECTROSCOPIE DANS LE DOMAINE DU TEMPS À L'ÉTUDE DES RÉSONANCES DE GAINE

Pierre-Richard RENAUD * et Manfred NACHMAN
Département de génie électrique et informatique
École Polytechnique de Montréal
Montréal (Québec), Canada

La spectroscopie dans le domaine du temps (**SDT**) est une méthode de mesure du coefficient de réflexion complexe (Γ) sur une large bande de fréquences. Elle fait appel à la réflectométrie temporelle qui, combinée aux techniques de traitement numérique des signaux et de transformée de Fourier rapide (**TFR**), en fait une excellente alternative à la méthode plus traditionnelle de la réflectométrie dans le domaine des fréquences (**RDF**) basée sur l'utilisation de l'analyseur de réseaux. Le principal avantage de la **SDT** sur la **RDF** est le fait qu'elle offre la possibilité d'obtenir des résultats sur une large bande de fréquences par le biais d'une seule mesure, normalisée par rapport à un signal de référence (par ex. le signal réfléchi par un court-circuit de précision). Par contre, la **SDT** implique un traitement mathématique beaucoup plus long et une moindre résolution fréquentielle que la **RDF** (J.R. Andrews, Proc. IEEE 66, 414-423, 1978).

Le but de ce travail est d'évaluer la possibilité d'appliquer la **SDT** à l'étude des caractéristiques des antennes immergées dans un plasma et, plus particulièrement, à l'observation des résonances associées aux ondes de gaine. Comme on le sait, tout conducteur dont le potentiel est flottant ou négatif par rapport au plasma où il est plongé, se trouve entouré d'une couche appauvrie en électrons, la gaine ionique. Or, la présence de cette gaine permet, sous certaines conditions, la propagation d'ondes de surface lentes - les ondes de gaine - le long d'une sonde cylindrique dans un plasma. Des résonances associées à ces ondes sont observées dans la réponse fréquentielle de la sonde.

Les expériences ont lieu dans un plasma d'argon de basse pression (0.4 *mtorr*) et de densité électronique de (0.5 à 8) $\times\ 10^9/cm^3$, en l'absence ou en présence d'un champ magnétique (maximum 0.012 *T*) orienté parallèlement à la sonde. La sonde cylindrique (longueur: 5 *cm*, rayon: 0.24 *cm*) est constituée par le conducteur interne d'une ligne coaxiale semi-rigide dénudée sur une courte section (M. Nachman, M. LeBlanc & N.P. Linh, IEEE Trans. Plasma Sci. 16, 333-341, 1988). L'épaisseur de la gaine ionique est controlée par l'application d'une tension dc à la sonde par le biais d'une unité de polarisation.

Une impulsion de type échelon est envoyée vers la sonde dans le plasma. Le signal de retour est traité numériquement après échantillonnage et quantification. On lui applique, par la suite, la **TFR**. Le signal de référence, provenant d'un court-circuit remplaçant la sonde, est soumis à un traitement identique. Puis, par comparaison des spectres des deux signaux, on dérive la réponse en fréquence du Γ de la sonde. Il est à noter que, pour fin de vérification de la méthode **SDT**, les mesures sont répétées par la **RDF**.

Des graphiques représentant la phase et l'amplitude du coefficient de réflexion de la sonde en fonction de la fréquence, obtenues par les deux méthodes, **SDT** et **RDF**, ont été tracés pour différentes conditions d'expérimentation. Les résultats recueillis démontrent une très bonne concordance entre les deux méthodes dans le domaine de fréquences investigué (0 à 1000 MHz), la **SDT** pouvant être appliquée de façon efficace à l'étude des résonances de gaine.

EXPERIMENTAL STUDY AND MODELLING OF MAGNETOPLASMAS SUSTAINED BY ELECTROMAGNETIC GUIDED WAVES

J. Margot* and M. Moisan
Département de Physique, Université de Montréal, CP 6128 Succ. A, Montréal H3C 3J7

This communication deals with the investigation of electromagnetic waves guided by a cylindrical plasma column, in the presence of a static magnetic field B_0 oriented axially to the plasma column. These waves are solutions of Maxwell's equations coupled to linearised hydrodynamic cold plasma equations, with appropriate boundary conditions. For a given azimuthal field configuration defined by the integer m in the factor $\exp(im\phi)$ of the field amplitude, we obtain: 1) one solution for $\omega<\omega_e$ (ω and ω_e are the wave and electron cyclotron angular frequency, respectively) that tends toward a surface wave when B_0 -> 0 2) an infinite number of solutions for $\omega>\omega_e$. All these waves are hybrid modes (combination of TM and TE waves). Our objective is to determine among these waves those that can be used to sustain a plasma column. This requires examining the dispersion and attenuation of these various modes as well as the stability of the wave-plasma power balance, as a function of electron density, plasma radius, ω and ω_e. The influence of the polarisation of the wave electric field is also considered. Such a subject is important when achieving low-pressure (i.e. large ion mean free path) high density plasma columns.

The problem of selectively launching these waves is also examined both theoretically and experimentally. In particular, it is shown how to obtain large (with respect to wavelength in free space) diameter plasma column sustained in a given m mode.

Experimental results are presented for 915 MHz and 2.45 GHz discharges sustained in tube diameters between 30 and 300 mm, in argon, at pressures ranging from 10^{-4} Torr to 1 Torr. A particular attention is paid to 1) operation at $\omega=\omega_e$ in collisionless (resonant absorption) and collisional regime 2) radial homogeneity of the plasma density and temperature.

Waves in Plasmas: Applications

Room 3028 Salle URSI H Session 80

Ondes dans les plasmas: applications

Chairs/présidents: J.A. KONG, USA

13:30 (80.1) On Three-Dimensional Propagation and Dispersion of Wave Packets Described by Spatial Moments, **B. DONG**, K.C. YEH, *University of Illinois, Urbana, IL, USA*

13:50 (80.2) SEDS/DELTA II Long-Wire Vertical Antenna in Earth Orbit for E.M. Wave Radiation Experiments in the Band ULF-to-VLF, **M.D. GROSSI**, *Harvard-Smithsonian Center for Astrophysics, Cambridge, MA, USA*

14:10 (80.3) Spectral Broadening of VLF Signals on Aircraft and Spacecraft Antennas, **F.J. KELLY**, *Naval Research Laboratory, Washington, DC, USA*

14:30 (80.4) Measurement of Electron Plasma Densities Developed During Space Vehicle Atmospheric Re-entry Using a Stepped Double Side-Band Suppressed Carrier Millimeter Wave Radar System, **G.A. YBARRA**[1], S.H. ARDALAN[1], R.E. MARSHALL[2], R.T. NEECE[3], [1]*North Carolina State University, Raleigh, NC,* [2]*Research Triangle Institute, Research Triangle Park, NC, and* [3]*NASA Langley Research Center, Hampton, VA, USA*

14:50 (80.5) Estimation of Plasma Sheath Boundary Layer Characteristics from the Admittance of Circular Apertures, **R.W. LAWRENCE**, *NASA Langley Research Center, Hampton, VA, USA*

15:10 **COFFEE/CAFÉ**

15:30 (80.6) A Space Shuttle Deployed Four Frequency Millimeter Wave Radar for Measuring Electron Density Profiles in Geosynchronous Reentry Plasma, **R.T. NEECE**[1], R.E. MARSHALL[2], [1]*NASA Langley Research Center, Hampton, VA, and* [2]*Research Triangle Institute, Newport News, VA, USA*

15:50 (80.7) Plasma Ringing Driven by Electrodes Stepped to Large Positive and Negative Potentials, **G.W. HULBERT**[1], J.G. LAFRAMBOISE[1], A.C. CALDER[2], [1]*York University, North York, ON, Canada;* [2]*Computer Sciences Corporation, Lanham-Seabrook, MD, USA*

16:10 (80.8) Transient Analysis of Magnetoactive Plasma Using the Finite-Difference Time-Domain Method, **F. HUNSBERGER**, R. LUEBBERS, K. KUNZ, *Pennsylvania State University, University Park, PA, USA*

16:30 (80.9) Interference Minima of Low-Frequency Electromagnetic Fields Produced by a Horizontal Electric Dipole, **A.S. INAN**, *University of Portland, OR, USA*

16:50 (80.10) Artificial Ionospheric Mirrors for Radar Applications, R. SHORT[1], **C. STEWART**[2], [1]*ARCO Power Technologies Inc., Washington, DC, and* [2]*George Mason University, Fairfax, VA, USA*

H80.1

ON THREE-DIMENSIONAL PROPAGATION AND DISPERSION OF WAVE PACKETS DESCRIBED BY SPATIAL MOMENTS

B. Dong* and K. C. Yeh
Wave Propagation Laboratory
University of Illinois at Urbana-Champaign
Urbana, Illinois 61801-2991

In this paper we study the three-dimensional propagation of a vector wave packet in a lossless, homogeneous but anisotropic medium. By using the superposition principle and Fourier transform theory a general formulation of wave packet propagation theory is developed. We prove that the square magnitude of the complex amplitude of the wave packet over the whole space integrates to a constant. The conservation of this integral merely reflects the lossless nature of the medium. This integral can be considered as the zeroth spatial moment. Upon this foundation the first and second spatial moments are introduced. The first moment determines the position vector of the centroid of a wave packet. It is a linear function of time, showing the motion of the centroid at a spectrum weighted average of the gradient of frequency in wave number space. Thus the concept of group velocity is extended to the wide banded wave packets. The second moment of the wave packet describes the property of dispersion. It reflects the anisotropic nature of the propagating medium and reveals the fact that the length of the wave packet expands with time in the form of time squared.

* On leave from Chengdu Institute of Meteorology, China

SEDS/DELTA II LONG-WIRE VERTICAL ANTENNA IN EARTH ORBIT FOR E.M. WAVE RADIATION EXPERIMENTS IN THE BAND ULF-to-VLF

by

MARIO D. GROSSI
Harvard-Smithsonian Center for Astrophysics
Cambridge, Massachusetts 02138

An experiment has been recently designed by our Observatory to perform feasibility tests in Earth orbit on the generation and radiation of e.m. waves by a long, vertical wire-antenna (a dipole with tip-to-tip length of 8 Km), in a frequency band that extends from a fraction of 1 Hz (at the lower end of the ULF band) up to 30 KHz (the upper end of the VLF band).

The long antenna (a conducting wire coated with dielectric)consists of two SEDS tethers/deployers, mounted on a Delta II/GPS platform (SEDS stands for Small Expendable Deployment System). One tether, 4 Km long, is deployed upwards and the other, of the same length, downwards.

When experimenting at ULF, the antenna operates in a self-powered, drag-compensated mode, with a total electromotive force (generated by the $\underline{V} \times \underline{B} \cdot \underline{l}$ mechanism) of about 1 KiloVolt, and a tether current of about 18 Ampere. At 0.25 Hz, Signal-to-Noise ratios of about + 6 dB are expected at receivers on the Earth surface, in a bandwidth of 10^{-2}Hz.

When experimenting at VLF, a battery-operated on-board transmitter will feed at mid-point the dipole.

The results of these experiments, expected to be carried out possibly in 1993 at an orbital altitude of about 400 Km or higher, could provide the scientific foundation on which to base the system design of spaceborne strategic communications.

H80.3

SPECTRAL BROADENING OF VLF SIGNALS ON AIRCRAFT AND SPACECRAFT ANTENNAS

Francis. J. Kelly
Ionospheric Effects Branch, Space Sciences Division
E. O. Hulburt Center for Space Research
Naval Research Laboratory, Washington, DC 20375-5000

Experiments on the Naval Research Laboratory P-3 aircraft in 1986 show that the spectra of very low frequency transmissions received on electric field antennas were artificially broadened when the aircraft experienced "precipitation static" while flying through rainclouds. This phenomena is very similar to the "spectral broadening" observed by vlf receivers flying on satellites through the auroral zone in the ionosphere. Relations between these phenomena will be discussed . Their possible common origin in the charging and discharging of the vehicles as they fly through ionized media will be described.

MEASUREMENT OF ELECTRON PLASMA DENSITIES DEVELOPED DURING SPACE VEHICLE ATMOSPHERIC RE-ENTRY USING A STEPPED DOUBLE SIDE-BAND SUPPRESSED CARRIER MILLIMETER WAVE RADAR SYSTEM

G.A. Ybarra*, S.H. Ardalan*, R.E. Marshall**, and R.T. Neece***

*North Carolina State University, Dept. of Electrical and Computer Engineering, Box 7911 Raleigh, NC 27695 USA

**Research Triangle Institute, Research Triangle Park, NC 27709 USA

***NASA Langley Research Center, Hampton, VA 23665 USA

A technique for measuring the density profile of a non-uniform electron plasma that develops next to the heat tiles of a space vehicle as it passes through the earth's atmosphere is derived and simulated. On August 25, 1994, the NASA space shuttle *Discovery* will deploy a 1/6 scale version of the prospective Mars Mission return vehicle in the upper atmosphere of the earth. The purpose of this experiment, called the Aeroassist Flight Experiment (AFE), is to determine the feasibility of using the atmosphere as an aerobrake. The Mars return vehicle will achieve extremely high velocities and must be slowed in order to achieve a lower atmosphere orbit without the use of retro-rockets since the weight of the fuel required for retro-rocket braking is prohibitive. As the AFE vehicle passes through the atmosphere, a non-uniform electron plasma will develop near the thermal protection system heat tiles. It is this plasma that is responsible for the aerodynamic friction creating the aerobrake. Hence, characterization of the dynamically changing plasma during the aeropass is of critical importance. The plasma is characterized by its density profile as a function of distance from the heat tile outer surface. In order to measure the plasma profile, a millimeterwave radar system, called the Microwave Reflectometer Ionization Sensor (MRIS), will be mounted directly behind the heat tiles. The MRIS device is to provide profile measurements from 0-15 cm from the tile surface with 0.5 cm accuracy. Measurement is facilitated by transmitting microwave energy through the heat tiles into the plasma and detecting the energy reflected by the plasma. Associated with a given frequency is a critical electron density. When energy at a given frequency is transmitted by the MRIS device and encounters its associated critical density, the energy is reflected at that point, called the *turning point*, and will return for detection. The MRIS receiver is to convert the detected echo into an estimate of the *standoff distance* which is defined to be the distance from the tile outer surface to the turning point. The dynamically changing plasma that develops is non-uniform in density and reflects microwave energy from different range locations depending on the density and microwave frequency. Therefore, the "target" range is different for different frequencies. In this application, high resolution range estimation cannot be obtained from conventional high bandwidth pulsed radar. Complicating the measurement is the physical constraint of mounting the microwave horns behind the heat tiles which are coated on the outside with a thin, high dielectric, Reaction Cured Glass (RCG) which reflects much of the energy before it ever enters the plasma, thus creating an interfering reflection.

This paper presents both analytical and simulation results obtained at NCSU for one of the primary candidate MRIS systems called the stepped double sideband (DSB) system. These simulations were performed using a hierarchical block diagram communications system simulator. One of the primary original contributions this paper presents is the implementation of a unique and accurate inhomogeneous plasma model. Another original contribution is our approach which uses the *a priori* knowledge of the glass coating range as a reference while performing a time series analysis on the DSB response data. Simulation results are presented which show remarkable accuracy obtainable from applying high resolution spectral estimation techniques to the data produced by the short-range, minimal bandwidth, stepped DSB radar system.

H80.5

ESTIMATION OF PLASMA SHEATH BOUNDARY LAYER CHARACTERISTICS FROM THE ADMITTANCE OF CIRCULAR APERTURES

Roland W. Lawrence
NASA Langley Research Center
Hampton, Virginia 23665-5225

NASA is currently planning a test flight which will include a suite of instruments to study the plasma sheath developed around the vehicle during reentry. One of the instruments which will be included on this spacecraft is a microwave reflectometer known as the Microwave Reflectometer Ionization Sensor (MRIS) which is to estimate the electron density variation in the plasma sheath surrounding the spacecraft. This measurement is greatly complicated by the presence of the Thermal Protection Tiles over the MRIS apertures. The MRIS will use multiple frequency, multiple aperture measurements, and sophisticated processing to enhance the N_e profile estimate. However, this approach is not expected to produce reliable measurements within 1.0 cm of the vehicle. While this will meet the primary science requirement, there is interest in obtaining plasma characteristics within 1.0 cm of the spacecraft. This paper will describe an approach to improve the retrieval of plasma characteristics within this region.

The theory of the input admittance of a plasma covered aperture is well known. Techniques to estimate electron density for assumed profile shapes from admittance measurements have also been studied. This paper describes an extension of these approaches to include the effects of dielectric layers over the aperture. In addition, the admittance for various frequencies is used to minimize the a priori assumptions that are required and improve the estimate of N_e. This inverse scattering problem and some difficulties encountered are discussed. Finally, several approaches to the inverse scattering problem and modeled results are presented.

A SPACE SHUTTLE DEPLOYED FOUR FREQUENCY MILLIMETER WAVE RADAR FOR MEASURING ELECTRON DENSITY PROFILES IN GEOSYNCHRONOUS REENTRY PLASMA

Robert T. Neece *, NASA Langley Research Center, Hampton, VA 23665

Robert E. Marshall, Research Triangle Institute, Newport News, VA 23606

The Microwave Reflectometer Ionization Sensor (MRIS) is being developed by the NASA Langley Research Center for the purpose of measuring the electron density profile from the surface of the Aeroassist Flight Experiment (AFE) spacecraft during a simulated earth atmosphere reentry from geosynchronous orbit. In the spring of 1995 the AFE will be deployed from the cargo bay of a space shuttle in low earth orbit. A solid rocket motor will accelerate the AFE to 33,800 feet per second simulating the reentry velocity from geosynchronous orbit. The AFE will then perform an aerobraking maneuver, or aeropass, through the upper atmosphere and return to low earth orbit where it will be retrieved by the space shuttle. During the aeropass, the MRIS will collect data for terrestrial processing which will determine the spatial and temporal profile of the reentry plasma electron density. The MRIS conical horn antennas will be located in the stagnation region of the AFE just behind the thermal protection system (TPS) tile above which the flow is predicted to be laminar. The TPS is constructed of approximately one inch of fibrous tile with a dielectric constant of 1.2 covered with approximately 10 mils of reaction cured glass (RCG). The RCG has a dielectric constant of 4.8 and presents a significant interfering target to the MRIS.

For any frequency, as the electron density increases toward the critical value, the dielectric constant approaches zero and the plasma becomes reflective. Four critical electron densities will be detected by four stepped frequency radars centered at 20, 44, 95, and 140 GHz corresponding to critical electron densities of $4.96X10^{12}$, $2.40X10^{13}$, $1.12X10^{14}$, and $2.43X10^{14}$ electrons per cm^3 respectively. Each radar will be sequenced through 64 steps separated by 64 MHz for a 4.096 GHz bandwidth. The returned signals for each frequency step will be coherently detected and processed by a fast Fourier Transform resulting in a range resolution of approximately 4 cm and an accuracy of approximately 1 cm. Electron densities will be detected from 0 to 15 cm above the TPS using a monostatic mode at 20 GHz, and a bistatic mode at 44, 95, and 140 GHz.

This paper will present the final system design, predicted signal to interference and noise ratios, 600 second data acquisition schedule, and preliminary results from a simulated plasma model.

H80.7

PLASMA RINGING DRIVEN BY ELECTRODES STEPPED TO LARGE POSITIVE AND NEGATIVE POTENTIALS

G.W. Hulbert* and J.G. Laframboise

Department of Physics
York University
North York, Ontario, Canada M3J 1P3

A.C. Calder

Computer Sciences Corporation, Greentec 2
10110 Aerospace Road
Lanham-Seabrook, Maryland, U.S.A. 20706

The details of nonlinear mechanisms behind dynamics of plasma ringing will be presented. Plasma ringing, *i.e.* driven oscillations at the plasma frequency (J.E. Borovsky, *Phys. Fluids* **31**(10),1074–1100,1988; A.C. Calder and J.G. Laframboise, *Phys. Fluids B* **2**(3), 655–666,1990), is seen in the time-dependent behaviour of a plasma sheath, studied by us via a radially symmetric PIC simulation of a collisionless, isotropic plasma surrounding an electrode, which is either a sphere or an infinite cylinder. Stepping the electrode voltage to a large DC amplitude sets up a "breathing" mode of the sheath at a frequency which is some geometry-dependent fraction of the plasma frequency. For positive potentials, the ringing is driven to large amplitude by coupling to the ion-electron two-stream instability. For negative potentials the breathing mode nonlinearly drives plasma ringing. In both cases coupling to ion-acoustic waves is observed and damps the breathing mode.

TRANSIENT ANALYSIS OF MAGNETOACTIVE PLASMA USING THE FINITE-DIFFERENCE TIME-DOMAIN METHOD

F. Hunsberger*, R. Luebbers, and K. Kunz

Communications and Space Sciences Laboratory
Department of Electrical and Computer Engineering
The Pennsylvania State University
316 Electrical Engineering East
University Park, PA 16802

A cold plasma is suitably described by a dispersive complex electrical susceptibility and a constant magnetic susceptibility. A consequence of these constitutive parameters is the inability of electromagnetic waves to propagate in the plasma if their frequency is below that of the plasma frequency, where the frequency-domain permittivity is negative. This phenomena, as well as the prediction of wave behavior when the plasma permittivity is zero, has been accurately described using a finite-difference time-domain (FDTD) algorithm which incorporates the proper time domain susceptibility functions for the plasma.

When a plasma is subjected to a static magnetic field (such as in the Earth's ionosphere) it becomes anisotropic and the permittivity of the plasma must be represented by a tensor rather than a scalar quantity. Among the phenomena which can be shown for magnetoactive plasmas is the occurrence of Faraday rotation, which occurs when a linearly-polarized wave traverses the plasma parallel to the biasing magnetic field.

The presence of anisotropy alone increases the complexity of any FDTD algorithm. It is the incorporation of dispersive anisotropy into FDTD which is the significant advancement presented here. It will be shown how the rather unique time-domain susceptibilities must be handled and how the FDTD algorithm must be modified for this class of gyrotropic media.

H80.9

INTERFERENCE MINIMA OF LOW-FREQUENCY ELECTROMAGNETIC FIELDS PRODUCED BY A HORIZONTAL ELECTRIC DIPOLE

Aziz S. Inan
Electrical Engineering Department
The University of Portland
Multnomah School of Engineering
5000 North Willamente Boulevard
Portland, Oregon 97203-5798

New analytical expressions have been derived for the quasi-static electromagnetic fields produced along the air-earth interface by a horizantal electric dipole (HED) buried inside the earth. The expressions are eaxct and usable at all distances from the source and over the frequency range for which the quasi-static condition holds. In addition, the expressions allow for explicit identification of the direct and lateral wave components of the electromagnetic fields. Numerical data is presented in graphical form for all the field components and reveals strong interference of direct and lateral wave fields for some of the components. The results are compared with other numerical data available in the literature. Comparisons are also made with fields produced by other types of dipole source configurations.

ARTIFICIAL IONOSPHERIC MIRRORS FOR RADAR APPLICATIONS

Robert Short
ARCO Power Technologies, Inc.
Washington, DC 20037

Clayton Stewart*
George Mason University
Fairfax, VA 22030-4444

Skywave OTH radars detect airborne targets by reflecting high frequency (HF) waves off the ionosphere to the target, and receiving the energy backscatter after a second reflection, at target ranges that extend beyond 3,000 kilometers. Because skywave OTH radar utilizes the naturally occurring ionosphere, it is subject to a number of uncontrollable factors that limit the performance:1)degradation of coverage by natural phenomena, e.g. aurora and sun spot activity, 2)night-time thinning and elevation of the ionosphere, necessitating use of low frequencies which can't detect small targets and are subject to natural and man-made interference at great distances, 3)random Faraday rotation, preventing polarization control, important for reducing clutter and detecting low observables (LO) targets, and 4)grazing incidence off the ionosphere, leaving a skip zone into which skywave OTH radar cannot penetrate.

Recognition of the performance limitations associated with the natural ionosphere has led a number of investigators to propose the creation of an Artificial Ionospheric Mirror (AIM) in the upper atmosphere and using it to reflect radar signals for OTH surveillance. The AIM is produced by beaming sufficient radio-frequency (RF) power to the lower ionosphere (around 70 km) to enhance the in situ ionization level to 10^7 electrons/cm^3. ARCO Power Technologies Inc. (APTI) has been under contract with AFGL and DARPA/MICOM to study the phenomenology involved in the creation of an AIM, its utility as a radar reflector, and the resulting system performance relative to air defense surveillance. Results from this study indicate that a system using this concept would both complement and enhance the performance of the existing skywave OTH radar.

The performance of the conventional OTH radar system can be enhanced by providing an additional AIM sector, which has sustained operation in the 20-30 MHz regime independent of time of day, latitude, look angle, and ionospheric state. The introduction of an AIM, located at the appropriate altitude, will create a reliable and predictable reflection of the HF energy between the radar site and the area of interest. An AIM adjunct to a conventional HF skywave radar can offer substantially improved performance with regard to: 1) filling in the range hole that exists out to about 1000 km due to minimum HF hop distance, 2) mitigation of auroral effects in polar directed surveillance sectors, 3) sustained operation through periods of increased sunspot activity and other ionospheric degradations, 4) availability of the upper end of the HF spectrum during the diurnal ionospheric cycle, and 5) improved detection of LO targets through frequency selection and positive polarization control. In addition, an AIM based system is not restricted to the HF band, but can operate in the lower VHF band, which has several advantages over HF.

Radio Techniques for Geodesy | **Room 2020 Salle URSI J Session 1** | **Techniques radios pour la géodésie**

Chairs/présidents: J. MORAN, USA

08:30 (1.1) Measurement of Crustal Motions with VLBI: Results from NASA's Crustal Dynamics Project, **J.R. RAY**, *Interferometrics Inc./NASA Goddard Space Flight Center, Greenbelt, MD, USA*

08:50 (1.2) Geodetic VLBI: Monitoring Global Change, **W.E. CARTER**, D.S. ROBERTSON, *National Oceanic and Atmospheric Administration, Rockville, MD, USA*

09:10 (1.3) Astronomical and Satellite Radio Techniques in Geodesy and Geodynamics, **J. KOUBA**[1], W.T. PETRACHENKO[1], D. DELIKARAOGLOU[2], J. POPELAR[2], [1]*Geological Survey of Canada, Ottawa, ON, and* [2]*S.M.R.S., Ottawa, ON, Canada*

09:30 (1.4) Global Positioning System Measurements of Vertical Deformation Using the California Permanent GPS Geodetic Array, **J.F. ZUMBERGE**, U.J. LINDQWISTER, G. BLEWITT, F.H. WEBB, *California Institute of Technology, Pasadena, CA, USA*

09:50 (1.5) Studies of High Frequency Earth Rotation Variations Using Very Long Baseline Interferometry, **T.A. HERRING**, *Massachusetts Institute of Technology, Cambridge, MA, USA*

10:10 **COFFEE/CAFÉ**

10:30 (1.6) Estimating Vertical Deformation Using Very Long Baseline Interferometry and the Global Positioning System, **J.L. DAVIS**, *Harvard-Smithsonian Center for Astrophysics, Cambridge, MA, USA*

10:50 (1.7) Atmosphere Correction for Radio Geodesy, **A.E. NIELL**, *Haystack Observatory, Westford, MA, USA*

11:10 (1.8) An Investigation of the Impact of the Auroral Ionosphere on the Performance of Global Positioning System Receivers, **R.B. LANGLEY**[1], K. DOUCET[1], A. KLEUSBERG[1], D. SCOTT[2], [1]*University of New Brunswick, Fredericton, NB, and* [2]*Canada Centre for Surveying, Ottawa, ON, Canada*

11:30 (1.9) Theoretical and Experimental Evaluation of the Performance of Single-Frequency GPS Carrier Beat Phase Measurements During Precipitation Periods, **J.M. TRANQUILLA**, H.M. AL-RIZZO, *University of New Brunswick, Fredericton, NB, Canada*

J1.1

MEASUREMENT OF CRUSTAL MOTIONS WITH VLBI: RESULTS FROM NASA'S CRUSTAL DYNAMICS PROJECT

J.R. Ray for the NASA CDP VLBI Group
Interferometrics Inc./Goddard Space Flight Center
Greenbelt, Maryland 20771

NASA's Crustal Dynamics Project (CDP) routinely conducts 24-hour geodetic VLBI measurement sessions to determine the relative positions of stations separated by nearly arbitrary distances. The estimated accuracies of these determinations are roughly 20 mm for the local vertical and a few mm for the local horizontal components. For the highest quality fixed-station networks, measurement accuracies may be better by a factor of about two. A comparison of global VLBI station coordinates with an independent determination using satellite laser ranging (SLR) shows weighted rms differences of 15-22 mm per component, after allowing for adjustments of offsets in origin, orientation, and scale. Much of the residual difference in geocentric coordinates may be due to errors in the local ties required to compare the separated VLBI and SLR reference points.

Repeated VLBI measurements over a few-year period permit tectonic motions to be directly observed at a significant level. Using the full span of Mark III VLBI data, horizontal velocities are estimated with typical formal uncertainties of 1 mm/yr or better. This compares with inter-site tectonic velocities of several tens of mm/yr in some cases, especially for baselines crossing plate boundaries.

The CDP has organized a variety of networks which are remeasured periodically to monitor crustal motions of three general types: large-scale motions of tectonic plates relative to one another, internal stability of nominally rigid plates, and deformation near plate margins associated with plate interactions. VLBI results to date, which measure contemporary tectonic rates, generally confirm the large-scale plate motions inferred from geological data, which average rates over the past million years. Thus, the implication is that the relative motions between stable plate interiors are smooth rather than jerky. The combination of about 10 years of VLBI data with conventional million-year geologic rates is being used to refine global tectonic models.

Tectonic motions near plate boundaries can be complex. For example, VLBI results from California show that Pacific/North American plate interaction causes a broad zone of deformation extending at least 200 km inland from the San Andreas fault. In Alaska, where the Pacific plate is being subducted beneath the North American plate, a broad zone of compression is observed along the southern coast. In addition, two instances of episodic motion, associated with earthquake events in California (Loma Prieta in 1989) and in Alaska (two large quakes in the Gulf of Alaska in 1987-88), have been detected using VLBI.

The world-wide grid of geodetic VLBI stations forms a network of fiducial reference points for denser regional measurements using GPS, GLONASS, and potentially Geobeacons.

A prime goal of current research activity is the improvement of VLBI vertical accuracy. The aim is to support determinations of vertical crustal motions (such as those expected due to post-glacial rebound) and to monitor changes in global sea level.

GEODETIC VLBI:MONITORING GLOBAL CHANGE

W. E. Carter and D. S. Robertson
National Ocean Service, N/CG 114
NOAA, Rockville, MD 20859

For more than a decade the National Ocean Service (NOS) has been working cooperatively with organizations in several nations to develop a global network of geodetic Very Long Baseline Interferometry (VLBI) observatories. The purposes of the network include the regular monitoring of Earth orientation (precession, nutation, polar motion, and Universal Time) and the measurement of contemporary plate motion and glacial rebound, to learn the structure and dynamics of the Earth.

Recent concerns about the effects of global warming have raised questions about the current rate of rise of sea level and the possibility of the rate increasing. Geodetic VLBI observations can contribute to monitoring global sea level by providing a terrestrial reference frame accurate to the sub-centimeter level to which the positions of tide gauges can be referred, by accurately mapping glacial rebound and other vertical crustal motions, by placing bounds on the building or destruction of the Greenland and Antarctic ice caps by monitoring secular the polar motion, and by providing the fundamental reference for generating accurate orbits of a variety of satellites, including the Global Positioning System (GPS) and altimetric satellites. The current status of the VLBI network, initial results, and future plans will be presented.

J1.3

Astronomical and Satellite Radio Techniques in Geodesy and Geodynamics

J. Kouba*, W.T. Petrachenko*, D. Delikaraoglou**, J. Popelar**
* Geophysics Division GSC, Ottawa
** Geodetic Survey Division SMRS, Ottawa

Radio techniques have made a major impact in geodesy and geodynamics over the past tree decades. VLBI, satellite positioning and altimetry have provided high precision measurements on the global scale and facilitated unification of geodetic control networks into a truly global world geodetic system (WGS). Repeated high precision geodetic observations continue to provide data for studies of time varying components reflecting dynamic processes which take part within the solid earth and its interaction with the oceans and the atmosphere. Radio astronomical VLBI using S/X band observations of quasars from terrestrial stations represents a kinematical system directly connected to the best realization of the inertial reference frame providing state of the art precision and long term stability to geodetic networks. Satellite positioning systems using L and S band beacons or spread spectrum signals from spacecraft in the earth orbit represent dynamical systems which determine the center of gravity to define the origin of modern geodetic systems. Satellite C and K band radar altimeters provide high precision measurements of sea surface topography, the mean sea level and related geopotential for studies of the earth's figure and its gravity field. The geodetic radio techniques use dual frequency measurements to correct for propagation effects and in some experiments also deploy water vapor radiometers for water vapor path length corrections. All geodetic radio systems have the advantage of day and night all weather operation and, in case of satellite based navigation provide real-time output using compact receiver and antenna configurations. The geodynamic applications are particularly demanding with regard to analysis of error sources and systematic effects over long time periods. Current status, typical geodetic results and possibilities for future improvements will be discussed.

GLOBAL POSITIONING SYSTEM MEASUREMENTS OF VERTICAL DEFORMATION USING THE CALIFORNIA PERMANENT GPS GEODETIC ARRAY

J. F. Zumberge, U. J. Lindqwister, G. Blewitt, and F. H. Webb
Jet Propulsion Laboratory, California Institute of Technology
4800 Oak Grove Drive, MS 238-625
Pasadena, California 91109

The Global Positioning System (GPS) is a U.S. Department of Defense Navigational system consisting of a number of earth-orbiting satellites at ~20,000-km altitude. These satellites continuously transmit radio signals toward earth at carrier frequencies of 1.57542 and 1.22760 GHz. The carriers are modulated by a signal structure that permits ground-based receivers to measure the range to each transmitting satellite. By simultaneously measuring a sufficient number of such ranges, the three-dimensional position of the receiver may be determined, provided that the satellite positions are known.

A continuously monitored array of three GPS receivers has been operating in southern California since the spring of 1990. Operated jointly by the Jet Propulsion Laboratory (JPL) in Pasadena and Scripps Institution of Oceanography in La Jolla, the California Permanent GPS Geodetic Array (PGGA) has Rogue receivers stationed at JPL, Scripps, and Pinyon Flats, approximately 172 km ESE of JPL.

GPS shares with other space geodetic techniques some inherent difficulties in measurements of vertical motion, including observational geometry (lines-of-sight are limited to above the horizon) and variable delay of the received signal due to fluctuations in tropospheric moisture content. Variations of antenna phase center with satellite elevation angle and multipath errors are additional effects which contribute to errors in GPS measurements of the vertical.

Despite these difficulties, however, the increasing number of GPS satellites, as well as advances in receiver technology, have recently resulted in ~5-mm short-term precision in measurements of vertical motion between stations separated by 100-200 km. We will present in this paper current measurements of vertical (and horizontal) baseline components from the California PGGA. Few-millimeter daily repeatability has been achieved for all components, including the vertical. Initial indications are that the long-term ($\gtrsim$ months) repeatability in the vertical is at the ~1-cm level.

J1.5

STUDIES OF HIGH FREQUENCY EARTH ROTATION VARIATIONS USING VERY LONG BASELINE INTERFEROMETRY

T. A. Herring
Massachusetts Institute of Technology,
Cambridge, MA 02139

During the last decade the determination of Earth rotation parameters from very–long–baseline interferometry (VLBI) has improved dramatically—24 hour sessions now yield estimates of the position of the Earth's rotation axis in space and with respect to the crust with precisions of between 0.2 and 0.5 milliarcseconds (mas) [6–15 mm displacements of the pole at the surface of the Earth]. The coefficients of the temporally coherent part of the rotation variations (*i.e.*, nutations) are determined with precisions of better than 0.05 mas [1.5 mm]. Twenty-four hour VLBI observing sessions allow the detection of signals in Earth Rotation Parameters (ERP) at high frequencies. We have analyzed about 10 years of VLBI data to resolve variations of ERP in the diurnal and semidiurnal bands. The preliminary results indicate that the amplitudes of coherent UT1 signals in the diurnal and semidiurnal bands are determined with one sigma errors of 0.01 and 0.02 mas. The most significant signal detected in UT1 has an amplitude of 0.39±0.01 mas at the M2 frequency. Significant (>3 sigma) results are also seen at the K1, P1, O1, M2 and S2 tidal frequencies. We discuss several mechanisms which could produce the diurnal and semidiurnal ERP variations. The incompleteness of current solid earth tide and ocean tide loading models used in VLBI processing has been considered and corrections are estimated along with the ERP variations. The amplitudes of the ocean tide contributions to diurnal and semidiurnal ERP variation are at the same level as the observed signals. The triaxiality of the Earth generates UT1 fluctuations which exceed the current estimated error level and therefore should be considered in VLBI data processing. Atmospheric angular momentum variation is also possible source mechanisms.

Estimating Vertical Deformation Using Very Long Baseline Interferometry and the Global Positioning System

J. L. Davis
Harvard-Smithsonian Center for Astrophysics
60 Garden St., MS 42
Cambridge, Massachusetts 02138

Very Long Baseline Interferometry (VLBI) and the Global Positioning System (GPS) are both radio-interferometric techniques for high-precision terrestrial relative positioning. As such, these techniques share two inherent features which prevent the vertical coordinate of site position to be determined as accurately as the horizontal coordinates. Because all radio signals are received from a direction above the horizon, the vertical direction suffers from an asymmetry which the horizontal directions generally do not. Furthermore, these radio signals are received after they have passed through the earth's neutral atmosphere, which refracts and delays those signals by an amount that is difficult to predict. Other possible sources of error affecting primarily the vertical for VLBI include antenna deformation, and, for GPS, multipath propagation and the variation of the antenna's electrical phase center with received direction.

Given accurate enough vertical determinations, there are many geophysical applications for which these space-geodetic techniques could be useful, including sea-level measurements for studies of global change; solid earth tide, ocean loading, and postglacial rebound determinations for studies of lithospheric dynamics; separation of geoid and terrain variations for gravity studies; detection of transient vertical processes for studies of subsidence and motions associated with seismicity; and measurements of vertical tectonic processes.

In this paper, we will review the current state of estimating vertical deformation using VLBI and GPS. We will present examples of space-geodetic determinations of continuous vertical deformation as well as vertical deformation associated with earthquakes. We will also discuss methods which have been used to improve vertical determinations, and prospects for future improvement.

J1.7

ATMOSPHERE CORRECTION FOR RADIO GEODESY

A. E. Niell
Haystack Observatory
Westford, Massachusetts 01886

The use of low elevation observations (3 to 10 degrees) with precise delay measurements (<30 psec) has required improvement in models of the atmosphere for correction of geodetic VLBI data. The CfA2.2 mapping function of Davis et al. (Radio Sci. 20,1593-1601, 1985) made significant improvement for observations down to 5 degrees. The Lanyi mapping function should give comparable results when used without an isothermal layer since the two functions agree well for the same surface meteorological input.

Rawinsonde data from the vicinity of a VLBI site can provide information about the state of the atmosphere other than at the surface, and should improve correction for the tropospheric path delay. For the eighteen ATD (high precision geodetic VLBI) experiments of 1987-88 temperature and relative humidity profiles from rawinsondes were used at all stations to calculate both the propagation delays through the neutral atmosphere and the partial derivatives for estimating a correction to the wet delay. Comparison with the same analysis using CfA2.2 shows that, when an analytic mapping function is used without making allowance for the near-surface effects, the winter inversion layer at Gilcreek, Alaska introduces an annual variation in baseline length of 6 mm (due to a vertical variation of about 20 mm). Observations at Gilcreek were made down to 6 degrees except where limited by antenna restrictions or the horizon.

AN INVESTIGATION OF THE IMPACT OF THE AURORAL IONOSPHERE ON THE PERFORMANCE OF GLOBAL POSITIONING SYSTEM RECEIVERS

Richard B. Langley*, Ken Doucet, Alfred Kleusberg
Geodetic Research Laboratory
Department of Surveying Engineering
University of New Brunswick
Fredericton, N.B. E3B 5A3

Doug Scott
Geodetic Survey Division
Canada Centre for Surveying
Ottawa, Ont. K1A 0E9

The Navstar Global Positioning System (GPS) is a satellite-based system which will provide precise, all-weather, three-dimensional navigation and positioning anywhere on or near the earth's surface, 24 hours a day. Scheduled to be fully operational by 1993, GPS is already in wide-spread use by navigators, surveyors, geodesists, and others. As of January, 1991, there were 15 functioning satellites providing nearly continuous two-dimensional positioning capability and three-dimensional positioning for a large fraction of the day.

One of the biases affecting GPS-derived positions is the signal delay due to propagation through the ionosphere. If simultaneous measurements are made on the two frequencies transmitted by the satellites, then knowledge of the dispersive nature of the ionosphere can be used to remove almost all of the ionosphere's effect from the measured ranges. However, if the state of the ionosphere is disturbed, the tracking loops of a GPS receiver may have trouble following the associated rapid variations in the ionospheric delay. Loss of lock might result, leading to cycle slips in the recorded data. Repair of those cycle slips in the presence of large, rapid phase variations is difficult and if not totally successful will result in reduced position accuracies.

To test the performance of GPS receivers under disturbed ionospheric conditions, the Canada Centre for Surveying contracted the University of New Brunswick to carry out a series of observations near Yellowknife ($\phi \approx 62°$ N, $\lambda \approx 115°$ W) in the Northwest Territories of Canada. Over a period of three days in June 1990, we recorded data at three sites with inter-site distances of about 50 and 100 km. At each site we used three different commercially-available GPS receivers: an Ashtech LD-XII, a Trimble Navigation 4000SST or STD, and a Wild-Magnavox WM102. Two observing sessions were held each day: one during which each receiver was fed by its own antenna, and one during which the three receivers at each site shared a common antenna through a signal splitter. In this paper we will report on the performance of the different receivers during the test, discuss the difficulties encountered in processing the data, and assess the impact of the state of the local ionosphere and geomagnetic field on the quality of the recorded data and the derived positions of the receivers.

J1.9

THEORETICAL AND EXPERIMENTAL EVALUATION OF THE PERFORMANCE OF SINGLE-FREQUENCY GPS CARRIER BEAT PHASE MEASUREMENTS DURING PRECIPITATION PERIODS

J. M. Tranquilla*
H. M Al-Rizzo
Radiating Systems Research Laboratory
Department of Electrical Engineering
University of New Brunswick
Fredericton, Canada
(506) 453-4561

In this paper, a theoretical model will be presented to predict the excess range error caused by ice clouds, melting layer, and rainfall combined with the non-ideal polarization patterns of satellite and receiver antennas. Results obtained from a GPS campaign conducted during November 1990, using two single-frequency receivers, showed some discrepancies in the adjusted baseline height component. Theoretical results showed that the effects of precipitation even under the worst assumed conditions are negligible in comparison with the unmodelled ionospheric effects. The observed discrepancies are attributed to the mismodelling of the relative tropospheric range error and possibly differential precipitation effects.

VLBI and Aperture Synthesis Techniques

Room 2020 Salle URSI J Sesssion 16

Méthodes à ouverture synthétique et VLBI

Chairs/présidents: J.R. FISHER, USA

13:30 (16.1) Measurement of Crustal Motions with VLBI: Technology Developments in Geodetic VLBI, **T.A. CLARK**, *NASA Goddard Space Flight Center, Greenbelt, MD, USA*

13:50 (16.2) The VLBA and Its Applications to Space VLBI, **J.D. ROMNEY**, *National Radio Astronomy Observatory, Charlottesville, VA, USA*

14:10 (16.3) The S-2 VLBI Digital Data Recorder and Playback System, D. BAER, **W.H. CANNON**, G. FEIL, P. LEONE, P. NEWBY, H. TAN, R. WIETFELDT, *York University, Toronto, ON, Canada*

14:30 (16.4) A New Correlator System for Space and Ground-Based VLBI, Part of the Canadian Contribution to the RadioAstron Project, **B. CARLSON**[1], D. WELLBORN[1], T. BURGESS[2], R. CASORSO[2], P. DEWDNEY[2], [1] *University of Victoria, BC, and* [2] *National Research Council Canada, Penticton, BC, Canada*

14:50 (16.5) Space VLBI Simulation Software, **D.W. MURPHY**, *Jet Propulsion Laboratory, Pasadena, CA, USA*

15:10 **COFFEE/CAFÉ**

15:30 (16.6) Low Frequency VLBI from Lunar Orbit, **J.O. BURNS**, *New Mexico State University, Las Cruces, NM, USA*

15:50 (16.7) Passive Imaging with Elliptical Boundary Arrays and Coarray Synthesis, **R.J. KOZICK**, S.A. KASSAM, *University of Pennsylvania, Philadelphia, PA, USA*

16:10 (16.8) Interferometric Aperture Synthesis in Earth Remote Sensing: The Electrically Scanned Thinned Array Radiometer (ESTAR), **A. GRIFFIS**, C. SWIFT, D. LEVINE, *University of Massachusetts, Amherst, MA, USA*

J16.1

MEASUREMENT OF CRUSTAL MOTIONS WITH VLBI: TECHNOLOGY DEVELOPMENTS IN GEODETIC VLBI

Thomas A. Clark for the NASA CDP VLBI Team
NASA Goddard Space Flight Center
Greenbelt, Maryland 20771

For more than two decades, the NASA/Haystack/MIT VLBI group has been developing the VLBI technique for high accuracy geodetic and astrometric measurements. In the mid-1970's, under the aegis of the NASA Crustal Dynamics Project (CDP), we undertook the development of the Mark-III VLBI system as the instrument for geodetic measurements in the 1980's. Our activities have used differential group delay (obtained by bandwidth synthesis) as the fundamental observable (although some measurements of baselines < 250 km have used differential phase delay). Geodetic VLBI measurements have used dual-frequency techniques at X-band (8.1 - 8.5 GHz) and S-band (2.2 - 2.3 GHz) to remove biases due to the ionosphere. Typical measurements taken during the 1980's have used eight 2 MHz bandwidth channels spanning 360 MHz at X-band plus six at S-band spanning 80 MHz, yielding a total recorded data rate of 56 Mb/s.

Although geodetic VLBI was born out of the astronomical community, it became obvious by 1980 that long-term geodetic measurement programs required dedicated geodetic VLBI stations. In the USA and other countries, new VLBI observatories were created using both existing and new antennas. Through the ensuing decade, the geodetic community amassed over 500,000 individual group delay observations, each representing from 1 to 13 minutes of data from a single baseline in networks consisting of these dedicated stations plus stations owned by the astronomy community and satellite tracking facilities. These stations were equipped with compatible GaAsFET or HEMT cryogenic receivers, Mark-III VLBI data systems (later retrofitted to the high density Mark-IIIA) , hydrogen maser frequency standards, and "Field System" automatic computer control. In parallel, Mark-III correlators were constructed at Haystack, USNO, Bonn and Kashima, and data analysis systems were implemented at a number of institutions. As measurement hardware, observing and analysis techniques and theoretical models have evolved, geodetic VLBI has demonstrated an improvement in accuracy at $\approx$ 10-fold per decade rate.

In the late 1980's, a series of improvements were begun to achieve even greater accuracy. Observing and data analysis techniques involving observations at low elevations and stochastic estimation of atmosphere and clock parameters were very successful. These techniques required coordination of measurements at a rapid rate (as many as 300/station/day) with heavily subnetted observing schedules on high sensitivity stations with fast telescope slew speeds. Instrumental sensitivity was improved by using HEMT receivers, doubling the individual channel IF bandwidth to 4 MHz, and by increasing the spanned bandwidth at X-band (to 720 MHz) and S-band (to 120 MHz). All of these improvements culminated in a two-week experiment in late 1989 which we named ERDE (Extended R&D Experiment) involving 5 stations (Fairbanks, Mojave, Pie Town, Westford and Haystack). ERDE produced the highest quality geodetic VLBI data obtained to date, with internal consistency at levels of $\approx 5 \times 10^{-10}$ in station positions.

ERDE required the use of fairly large telescopes (12 - 37 m) to achieve this performance. We have already begun the development of the Mark-IV system which will allow the use of smaller antennas by increasing the recording rate to $\approx$ 1Gb/s by retrofitting the existing Mark-III hardware; this also results in greater compatibility between the Mark-III and VLBA data acquisition systems. To complement the improved Mark-IV sensitivity, a new small (5-10 m) transportable, high-efficiency antenna is being planned. A new correlator capable of handling this data rate is being designed. The "Field System" control software will be ported to an inexpensive computer (IBM-PC compatible) and will support Mark-III, Mark-IV and VLBA data acquisition terminals.

THE VLBA AND ITS APPLICATIONS TO SPACE VLBI

Jonathan D. Romney
National Radio Astronomy Observatory
Charlottesville, Virginia

The Very Long Baseline Array (VLBA), the world's first large-scale dedicated VLBI facility, is currently under construction by the NRAO and is expected to become fully operational in 1993. Its capabilities will be outlined and the current status of the construction project reviewed.

Although the VLBA has been designed principally to support a broad range of ground-based VLBI research, it is anticipated that the array will be an essential complement to the orbiting interferometer elements in many space-VLBI observations. Thus, aspects of the VLBA design and implementation of special relevance to space VLBI will be discussed. These include the array configuration and frequency coverage, and the channelization, sampling, and wideband recording subsystems. Elements of the VLBA correlator such as wavefront model computation, integration of the cross-spectral visibility, and real-time control will be emphasized.

J16.3

THE S-2 VLBI DIGITAL DATA RECORDER AND PLAYBACK SYSTEM

Baer, D., Cannon, W.H., Feil, G., Leone, P., Newby, P.,
Tan, H., and Wietfeldt, R.

Space Geodynamics Laboratory
Institute For Space And Terrestrial Science
York University, Toronto, Ontario

The S–2 wide band VLBI digital data recorder and playback system presently under development at the Space Geodynamics Laboratory (SGL) of the Institute For Space And Terrestrial Science (ISTS) at York University is a descendant of the earlier S–1 VLBI digital data recording and playback system presently being used in Canada for geodesy and geodynamics. The S–2 VLBI recording and playback system consists of a tape transport array module containing an array of 8 "industrial" grade VHS video tape transports operated in the standard Long Play (LP) mode and a data signal and control module resident in a standard VME cage. The S–2 VLBI recording system will record up to 16 input channels of digital data at total bandwidths varying from 16 to 128 Mb/s in increments of 16 Mb/s. The unattended operation time of the S–2 VLBI recorder varies with the user bandwidth, ranging from 32 hours at the minimum bandwidth of 16 Mb/s to 4 hours at the maximum bandwidth of 128 Mb/s. The S–2 VLBI recorder will be assessed for the possibility of using the Super Long Play (SLP) mode of the VHS recorders to extend these time intervals to 48 hours and 6 hours respectively. In the LP mode the raw bit error rate (without error correction coding) for the S–2 VLBI recorder ranges between 1×10^{-5} and 3×10^{-5}.

The data signal and control module of the S–2 system has a data distributor, resident on a separate user interface card, which distributes the input data onto the recorder array in a manner which is transparent to the user. The data distributor can be customed designed to serve any user needs which allows for flexibility of application. For VLBI applications the S–2 system will have both MkIII/MkIIIA and a K–4 compatible outputs so that it will be possible to use the S–2 recorder to record VLBI data for playback at a MkIII/MkIIIA or a K–4 VLBI correlator facility. The S–2 VLBI data recorder and playback system will be provided by the Canadian Space Agency via a contract to ISTS/SGL, to the Astro Space Center of the P.N. Lebedev Physical Institute in Moscow for use in the Soviet led RadioAstron orbital VLBI mission.

A New Correlator System for Space and Ground–Based VLBI, Part of the Canadian Contribution to the RadioAstron Project

B. Carlson, Dale Wellborn (Electrical Engineering Department, University of Victoria), T. Burgess, R. Casorso, P. Dewdney (Dominion Radio Astrophysical Observatory, National Research Council of Canada)

The Dominion Radio Astrophysical Observatory is designing and building a new correlator system for Very Long Baseline Interferometry (VLBI) with funding from the Canadian Space Agency. The system will be designed to handle data from a mixture of orbiting and ground–based antennas, and will be used to correlate data for the RadioAstron project. RadioAstron is a Soviet space project to launch a 10 m antenna into a highly elliptical earth orbit with a 70000 km apogee. It will operate in four wavelength bands ranging from $\lambda 1.4$ cm to $\lambda 1$ m. The VLBI telescope system will be a flexible one consisting of the orbiter operating in conjunction with several large antennas on the ground. Its main scientific objective is to detect brightness temperatures in excess of 10^{12} K in the cores of quasars, the theoretical limit according to some models.

The design of the correlator is still at an early stage. Present plans are to build an XF type of correlator in which cross–multiplication and integration of signals between antennas is done, followed by Fourier transformation. (The alternative order, FX, is also used). The correlator will contain at least 24000 multiplier–accumulators (MAM's) which can be deployed for high resolution in spectral line modes, or for wide bandwidth in continuum modes. An implementation is currently being explored which is based on a backbone consisting of a wide–bandwidth, serial data–distribution system, conferring considerable extensibility. The correlator will interface to and be compatible with the Canadian VLBI recording/playback system which is currently being developed at the Institute for Space and Terrestrial Science. Interfaces to other recorder/playback systems will also be contemplated.

J16.5

Space VLBI Simulation Software

D. W. Murphy
Jet Propulsion Laboratory
4800 Oak Grove Drive
Pasadena Ca 91109

Space VLBI simulation software developed at the Jet Propulsion Laboratory is described. This software is the only software that can simulate the on-board spacecraft constraints of both the Japanese VSOP and the Soviet RADIOASTRON spacecraft. These constraints are described and their impact on the science return of these missions is discussed. The use of this software as a vital aid to spacecraft design, mission design and mission operations is emphasized and examples of the use of the software are presented.

LOW FREQUENCY VLBI FROM LUNAR ORBIT

Jack O. Burns
Department of Astronomy
Box 30001/Dept. 4500
New Mexico State University
Las Cruces, NM 88003

The Radio Astronomy Explorer satellite verified that the far-side of the Moon is well shielded from manmade and natural Earth-based interference at frequencies below 30 MHz. Above a few MHz, most of the interference is produced from ionospheric breakthrough of manmade communication signals and over-the-horizon radar. Below about 1 MHz, the Earth's magnetosphere is a powerful source of Auroral Kilometric Radiation. Thus, the lunar far-side is the only location in the Earth-Moon environment where the noise level reaches the expected Galactic Background at low frequencies.

The recent Presidential Space Exploration Initiative advocates the establishment of a permanently manned lunar outpost in the first part of the next century. In preparation for and in support of this outpost, a number of satellites will be placed into orbit about the Moon. One such program for the late 1990's is the Lunar Observer which is designed to image the Moon at high resolution and to map its gravitational field. We are proposing to place relatively simple phased arrays of dipoles on individual lunar satellites and perform interferometry between the spacecraft. The dipole arrays will be deployed as inflatible structures. In the VLBI mode, the experiment will function at 13 and 26 MHz. For a scenario in which two spacecraft are in perpendicular lunar polar orbits at altitudes of 100 km, the useful physical baselines will range from about 1 km to about 1500 km. The maximum useful baseline is limited by phase incoherency produced by interplanetary scintillation. With a mission lifetime of one year, the two element interferometer will produce excellent u-v plane coverage thus permitting synthetic aperture imaging with a resolution of about 2 arcsec. This resolution is comparable to the VLA at 20-cm and is more than 100 times better than the best previous ground-based mapping at 38 MHz. The RMS sensitivity for a 10^6 sec integration is about 2 Jy. Our computer simulations indicate that a number of 3C sources could be mapped with this lunar VLBI experiment.

Our proposed lunar interferometer has the advantages of being relatively simple, inexpensive, opportunistic relative to current national space initiatives, ground-breaking in terms of resolution, and astronomically productive. Among the scientific programs will be imaging of Type III solar flare events, observations of bursts from Jupiter and Saturn, investigations of the low energy population of relativistic electrons in extended extragalactic radio sources, and studies of in-situ particle acceleration in supernovae and radio galaxies.

This work has been supported by NASA grant NAG9-396.

J16.7

PASSIVE IMAGING WITH ELLIPTICAL BOUNDARY ARRAYS AND COARRAY SYNTHESIS

Richard J. Kozick* Saleem A. Kassam

Department of Electrical Engineering
University of Pennsylvania
Philadelphia, Pennsylvania 19104

Two-dimensional sensor arrays are commonly used in radio astronomy to form narrowband images of spatially incoherent radiation sources. The *difference coarray* [R.T. Hoctor & S.A. Kassam, *Proc. IEEE 78*, 735-752, 1990] of the aperture characterizes the linear imaging techniques based on beamforming, and we exploit the difference coarray to explain and generalize some previous results. The difference coarray is the set of all vector differences between sensor locations in the aperture, and the inverse Fourier transform of the system's beampattern has support on the difference coarray. Hence the aperture synthesis problem of producing some desired beampattern with a given aperture is equivalent to the problem of synthesizing a desired weighting function on the difference coarray.

The J^2-*synthesis* technique [J. P. Wild, *Proc. Roy. Soc. Lon., Ser. A 286*, 449-509, 1965] uses a *circular boundary aperture* to synthesize a desired *circularly symmetric* beampattern as a sum of squared Bessel functions. This synthesis is achieved with *phase-only* apodizations on the aperture. From the coarray viewpoint, J^2-synthesis is equivalent to an expansion of the desired *circularly symmetric* coarray weight function as a series of Chebychev polynomials in the radial variable. Several generalizations of Wild's J^2-synthesis become straightforward in the coarray domain. The phase-only aperture apodizations of J^2-synthesis can be modified slightly to allow synthesis of *non*-circularly symmetric coarray weight functions. The new aperture apodizations remain phase-only, but they allow *angular* variations in the desired coarray weighting to be synthesized using complex exponential basis functions. The coarray point of view also makes it clear that these particular basis functions are only one of many possible choices. For example, eigenfunctions of the desired coarray weighting may be used as the aperture weights. Interestingly, the phase-only aperture weights of J^2-synthesis are eigenfunctions of *every* circularly symmetric coarray weight function, which implies that J^2-synthesis has a least-squared-error approximation property. It is easy to show that all of these results for circular boundary apertures also apply to *elliptical* boundary apertures.

The coarray synthesis problem may also be considered for *discrete arrays* of sensors arranged on the boundary of an ellipse. Then the difference coarray weight function is representable as a matrix, and appropriate array apodization weights may be obtained from the singular value decomposition (SVD) of the matrix. If the desired coarray weighting is elliptically symmetric, then the SVD yields phase-only array weights which are sampled versions of the J^2-synthesis weights. We note that very similar coarray arguments allow extension of these results for *passive* imaging of spatially *incoherent* sources to *active* imaging of spatially *coherent* objects.

INTERFEROMETRIC APERTURE SYNTHESIS IN EARTH REMOTE SENSING : THE ELECTRICALLY SCANNED THINNED ARRAY RADIOMETER (ESTAR)

Andrew Griffis*, Calvin Swift and David Levine
The University of Massachusetts at Amherst

For nearly 100 years, radio astronomers have been using interferometry to resolve stellar objects and subsequently determine their size. More recently, the application of Fourier methods to interferometry has yielded mappings, or images, of the radio brightness of distant sources.

At the University of Massachusetts, these well established radio astronomy techniques have been used in a prototype airborne sensor to produce regional maps of soil moisture in a variety of soil and hydrological settings. This sensor, the Electrically Scanned Thinned Array Radiometer (ESTAR), operates over a 27 MHz bandwidth about 1413.5 MHz, and uses five eight-element linear arrays as a thinned array to obtain 15 samples of the visibility function. To date, maps of the Delmarva Peninsula, Rappahannock River Delta and Wye Island have been obtained, in addition to the images obtained in the MAC-HYDRO experiments of 1990.

The material to be presented will focus on the basic structure of ESTAR (including its analog processing), the techniques used in its calibration and the methods employed in performing the inversion needed to form images from the visibility samples measured. Some attention will also be given to the sensitivity limitations inherent in a thinned array imager. In particular, the fundamental difference between imaging a point source (or restricted distributed source) and imaging a source which encompasses the entire field of view will be brought out. A short segment of time will be devoted to the presentation of color maps of imaged regions and the utility of such maps in studying regional soil moisture characteristics.

Millimetre and Sub-Millimetre Instrumentation | Room 2020 Salle URSI J Session 31 | Instrumentation millimétrique et sub-millimétrique

Chairs/présidents: T.L. LANDECKER, Canada

08:50 (31.1) Receiver Development at the Herzberg Institute of Astrophysics, **C.T. CUNNINGHAM**[1], R.H. HAYWARD[1], J.D. WADE[1], S.R. DAVIES[2], [1] *National Research Council Canada, Ottawa, ON, Canada;* [2] *University of Kent, Canterbury, UK*

09:10 (31.2) Harmonic Effects in Superconducting Tunnel Junction Mixers, **L.M. CHERNIN**[1], R. BLUNDELL[1], C.Y.-E. TONG[2], [1] *Harvard-Smithsonian Center for Astrophysics, Cambridge, MA, USA;* [2] *Communications Research Laboratory, Tokyo, Japan*

09:30 (31.3) Self-Aligned Tunnel Junction Fabrication for Focal Plane Array Receivers, M.J. BRETT, D. ROUTLEDGE, **J.F. VANELDIK**, B.G. VEIDT, K.L. WESTRA, *University of Alberta, Edmonton, AB, Canada*

09:50 (31.4) Hybrid Antenna Structures for SIS Receivers at Submillimeter Wavelength, **T.H. BÜTTGENBACH**[1], R.E. MILLER[2], T.G. PHILLIPS[1], [1] *California Institute of Technology, Pasadena, CA, and* [2] *AT&T Bell Laboratory, Murray Hill, NJ, USA*

10:10 **COFFEE/CAFÉ**

10:30 (31.5) Wideband Spectrometers for Spaceborne Submillimeter Radiometers, **W.J. WILSON**, K. CHANDRA, *California Institute of Technology, Pasadena, CA, USA*

10:50 (31.6) Photo-Etched Focal Plane Arrays for Sub-millimetre Wavelengths, **T.H. LEGG**, *National Research Council Canada, Ottawa, ON, Canada*

11:10 (31.7) QUARRY: A 15 Element Focal Plane Array System at 3 Millimeter Wavelength, N.R. ERICKSON, R.B. ERICKSON, P.F. GOLDSMITH, R.M. GROSSLEIN, G.A. NOVAK, **C.R. PREDMORE**, F.P. SCHLOERB, P.J. VISCUSO, *University of Massachusetts, Amherst, MA, USA*

11:30 (31.8) The 8-Feed System at the National Radio Astronomy Observatory 12-Meter Telescope, **D.T. EMERSON**, *National Radio Astronomy Observatory, Tucson, AZ, USA*

J31.1

Receiver Development at the Herzberg Institute of Astrophysics,
C.T. Cunningham, R.H. Hayward, J.D. Wade National Research Council
S.R. Davies University of Kent at Canterbury

We report on SIS receiver development for the James Clerk Maxwell Telescope currently underway at the Herzberg Institute of Astrophysics in Ottawa in collaboration with the University of Kent and the Rutherford-Appleton Laboratory. The Kent/RAL 245 GHz receiver, which was successfully tested on the JCMT in May 1989, has been upgraded by fitting a new SIS mixer designed for 345 GHz operation and a new "hybrid" cryostat providing a longer hold time. This receiver is known as the Interim 345 GHz SIS Receiver and it has a tuning range of 310-380 GHz using a solid-state phase-locked local oscillator built at the HIA. We discuss the design of this receiver and its performance during recent commissioning tests on the JCMT.

HARMONIC EFFECTS IN SUPERCONDUCTING TUNNEL JUNCTION MIXERS

L.M. Chernin*, R. Blundell
Harvard-Smithsonian Center for Astrophysics, Cambridge, MA 02138
and
C.Y.- E. Tong
Communications Research Laboratory, Tokyo, Japan

We have performed five-port model simulations of a superconducting tunnel junction receiver based on quantum mixer theory (J. Tucker, Quant. Elec., 15,1234,1979). Two separate computer codes have been used to determine the large-signal currents and voltages across the junction; one based on the harmonic Newton technique and the other on the harmonic balance method. Although the harmonic Newton method is more complicated to implement, it does allow a simple extension to include higher order harmonics and is 10-100 times faster than the harmonic balance method.

Contrary to previous simulations, we find the mixer gain does not decrease as the ωCR product decreases. On the other hand, we find that the fraction of the Smith chart that is covered by unity gain or higher, is greatest if a small value of ωCR is used. Thus tuning the mixer is easiest with a small value of ωCR. However, harmonic downconversion ($2f_{LO} \pm f_{IF}$ to f_{IF}) is more significant at small ωCR, but nevertheless remains much weaker than the fundamental conversion.

J31.3

SELF-ALIGNED TUNNEL JUNCTION FABRICATION FOR FOCAL PLANE ARRAY RECEIVERS

M.J. Brett, D. Routledge, J.F. Vaneldik*, B.G. Veidt, K.L. Westra
Department of Electrical Engineering, University of Alberta,
Edmonton, Alberta

The National Research Council of Canada and the Electrical Engineering Department of the University of Alberta are engaged in a joint project to develop SIS planar array receiver prototypes for the James Clerk Maxwell Telescope. Such receivers would greatly enhance the speed and efficiency of the telescope. The proposed receivers will use superconductor/insulator/superconductor (SIS) quantum effect mixers with niobium nitride as the superconductor and magnesium oxide as the insulator. NbN has a relatively high critical temperature of 16K and consequently a high upper frequency of operation. A planar antenna structure, an SIS mixer and a stage of intermediate frequency amplification will be combined into one superconducting stripline circuit. Successful circuits will be readily assembled into dense arrays.

This paper describes details of the fabrication and properties of NbN/MgO/NbN superconductor tunnel junction devices produced at an intermediate stage in the development of 345 GHz receiver prototypes. Initial 10 μm x 10 μm and 5 μm x 5μm devices were produced using a batch-process, self-aligning technique. NbN deposition by reactive planar magnetron sputtering was optimized by study of the target voltage - nitrogen flow hysteresis curve. Intrinsic roughness of the NbN films increases the effective junction area to 1.3 times the nominal planar junction area. These junctions exhibit a gap voltage of 4.1 mV, and critical current densities between 600 and 1000 A/cm^2. Extension of the fabrication technique to junctions of much smaller areas is also described.

HYBRID ANTENNA STRUCTURES FOR SIS RECEIVERS AT SUBMILLIMETER WAVELENGTH

***Thomas H. Büttgenbach[1], R. E. Miller[2], and T. G. Phillips[1]**

[1]California Institute of Technology, MS 320-47, Pasadena, CA. 91125
[2]AT & T Bell Laboratory, ID 220, Murray Hill, N.J. 07974

We have developed a hybrid antenna using a dielectric antenna with a planar logarithmic spiral for the feed. Beam pattern and efficiency measurements from 100 to 760 GHz were performed in a two dimensional antenna range using room temperature bolometers. The same setup with a Superconductor Insulator Superconductor (SIS) detector was successfully tested at 345 and 492 GHz at the Caltech Submillimeter Observatory. The coupling efficiency between the telescope and the receiver was compared to a waveguide receiver and found to be similar. The very compact size of this antenna is promising for the development of array receivers.

J31.5

WIDEBAND SPECTROMETERS FOR SPACEBORNE SUBMILLIMETER RADIOMETERS

William J. Wilson* and Kumar Chandra
Jet Propulsion Laboratory
California Institute of Technology
Pasadena, California 91109

There are three main types of spectrometers in use with radiometer systems today: filterbanks, acousto-optic, and digital autocorrelators. Filterbanks are used in the Microwave Limb Sounder (MLS) for the Upper Atmospheric Research Satellite, and for the Middle Atmospheric Sounder shuttle instrument. In these instruments, the channel filter bandwidths are matched to the expected line shape, to reduce the number of channels. However, the large size, mass and power requirements of filterbanks make them undesirable for space applications. Acousto Optic Spectrometers (AOS) are planned for the Submillimeter-Wave Astronomy Satellite (SWAS), the Earth Observing System Microwave Limb Sounder (Eos/MLS), and the astrophysics Sub-Millimeter Moderate Mission (SMMM). The advantages of AOS's are their capability to analyze wideband signals (to 1200 MHz) with up to 1200 frequency resolution channels, and with low DC power requirements. Digital AutoCorrelator (DAC) spectrometers offer the advantages of better stability, smaller size, reliability and lower cost. However, the DAC's have bandwidths <200 MHz, and large DC power requirements of >100 mW/ delay channel. Thus, digital technology will require a significant increase in speed and reduction in power to meet the goals for spaceborne spectrometers. Design details and performance tests of the AOS's and the DAC's being developed for the Eos/MLS and the SMMM radiometers will be presented.

PHOTO-ETCHED FOCAL PLANE ARRAYS FOR SUB-MILLIMETRE WAVELENGTHS.

T.H. Legg, Herzberg Institute of Astrophysics, National Research Council, Ottawa

Part of the Canadian contribution to the instrumentation of the James Clerk Maxwell sub-millimetre wavelength telescope is the development of SIS focal plane arrays. The work is being done in a collaborative program in which Niobium Nitride SIS junctions are developed at the Electrical Engineering Department, University of Alberta, while the antenna structures are developed at the Herzberg Institute of Astrophysics, N.R.C., Ottawa. The aim is to eventually incorporate the antenna construction into the SIS fabrication process. The type of antenna that has been adopted is a new one which makes use of photo-etched patterns on the centre conductor of a strip transmission line.

The centre conductor patterns, which resemble two-dimensional electromagnetic horns, are arranged in an end-fire structure in which an incoming wave is guided as directly as possible onto a strip transmission line terminated at one end by an SIS junction. The field distribution on the strip line determines the antenna pattern in the H-plane, while the ground planes, which also act as heat conductors, have a flare at one end to control the pattern in the E-plane. The incoming radiation is coupled to the strip line through a mode converter which changes an initially parallel electric field distribution to one which is antiparallel on either side of the centre conductor. A practical advantage of the end fire arrangement is that the structure can extend as far as necessary in an axial direction (i.e. perpendicular to the focal plane) to give ample space for I.F. circuitry. A patent application has been made to cover possible commercial applications of the arrangement.

Several means have been investigated for controlling the amplitude and phase of the field on the strip line. For example, lenses have been made by photo-etching patterns of holes in the centre conductor, and curved edges of several wavelengths dimension have been photo-etched on the centre conductor and used to focus a beam within the strip line region.

To form a two-dimensional array, a number of strip line patterns are placed side by side between substrates and the metal ground planes, then several of these complete structures are stacked in the orthogonal direction. Individual antenna apertures are made 3 or more wavelengths on a side to keep off-axis aberrations small. The instantaneous bandwidth of the antennas with a simple mode converter is sufficient to cover any one of the sub-millimetre wavelength atmospheric windows and wider bandwidths appear possible. The talk will describe the present state of development of this type of array.

J31.7

QUARRY: A 15 Element Focal Plane Array System at 3 Millimeter Wavelength

N.R. Erickson, R.B. Erickson, P.F. Goldsmith, R.M. Grosslein, G.A. Novak, C.R. Predmore*, F.P. Schloerb and P.J. Viscuso
Five College Radio Astronomy Observatory
Department of Physics and Astronomy
University of Massachusetts
Amherst, Massachusetts 01003

A 15 element focal plane array system has been developed for the FCRAO 14 m millimeter telescope over the 86 to 115 GHz range. This system provides a rapid spectral line mapping capability for both galactic and extra-galactic objects.

The compact array has three rows of five elements which are spaced one beamwidth apart. The rows are spaced two beamwidths apart. The 15 Schottky mixers with integrated HEMT/FET amplifiers as well as the single sideband (SSB) filter and image termination are cooled to 20 K. The cooled optics provide SSB operation and polarization interleaving to space the elements within a row only one beamwidth apart. A local computer controls all receiver functions such as receiver noise temperature optimization, filter tuning and rotation of the receiver to track in parallactic angle. Average receiver noise temperatures are 250 to 350 K SSB depending on frequency.

For each pixel three different filter banks are available and an autocorrelator is under development. The bandwidth and resolution of these spectrometers is summarized in the following table. The velocity resolution is calculated for the CO (1-0) line at 115.3 GHz.

Type	Channels	Total Bandwidth		Resolution	
		MHz	(Km/s)	KHz	(Km/s)
Filter Bank	32	8	(21)	250	(.65)
Filter Bank	32	32	(83)	1000	(2.60)
Filter Bank	64	320	(832)	5000	(13.0)
Autocorrelator	1024	10	(26)	9.8	(.03)
Autocorrelator	1024	20	(52)	19.5	(.05)
Autocorrelator	512	40	(104)	78.1	(.20)
Autocorrelator	256	80	(208)	312.5	(.81)

Implementation of the QUARRY receiver required changes to most of the computer software that has been in use at the FCRAO. One of the major reasons for these changes has been the adoption of a new philosophy for control of instrument subsystems in which control needs are offloaded from the observatory's ModComp computer onto dedicated PC's like the one used control the QUARRY reciever itself. A second area of software development has been the adaptation of the existing telescope and data reduction software to the three dimensional data type presented by observations with a spectral line array.

THE 8-FEED SYSTEM AT THE NATIONAL RADIO ASTRONOMY OBSERVATORY 12-METER TELESCOPE

D. T. Emerson
National Radio Astronomy Observatory
949 North Cherry Avenue
Campus Building 65
Tucson, Arizona 85721

Multiple-beam systems are coming into operation at several millimeter- and centimeter-wave radio telescopes, both for continuum observations and for spectral line work. This new generation of receiver systems opens up possibilities of novel observing techniques that are not accessible with single-beam systems. The increased quantity of data produced by such systems puts greater demands on the data processing capabilities of current telescopes, but there are opportunities for more sophisticated data processing algorithms. The different temporal, spatial and spectral characteristics of image defects should permit significant enhancements in image quality to be made.

An 8-beam spectral line system has been in routine operation at the 12-Meter telescope. The system has already proved itself to be extremely powerful. This system is described, and potential future developments in observing technique and data processing are discussed.

New Radio Telescopes and Signal Processing

Room 2020 Salle URSI J Session 47

Nouveaux radiotélescopes et traitement des signaux

Chairs/présidents: J.F. VANELDIK, Canada

13:30 (47.1) The Green Bank Telescope, **G.A. SEIELSTAD**, *National Radio Astronomy Observatory, Green Bank, WV, USA*

13:50 (47.2) Active Surface for the Green Bank Telescope, **J.M. PAYNE**, *National Radio Astronomy Observatory, Green Bank, WV, USA*

14:10 (47.3) Beam Scan Performance of an Offset Gregorian Antenna, **R.D. NORROD**[1], S. SRIKANTH[2], [1] *National Radio Astronomy Observatory, Green Bank, WV, and* [2] *National Radio Astronomy Observatory, Charlottesville, VA, USA*

14:30 (47.4) The Synthesis Telescope at the Dominion Radio Astrophysical Observatory, **T.L. LANDECKER**, P.E. DEWDNEY, L.A. HIGGS, G.J. HOVEY, J.D. LACEY, C.R. PURTON, R.S. ROGER, A.G. WILLIS, W. WYSLOUZIL, *National Research Council Canada, Penticton, BC, Canada*

14:50 (47.5) The Proposed Radio Schmidt Telescope: The Technical Challenges, **P. DEWDNEY**, T.L. LANDECKER, *National Research Council Canada, Penticton, BC, Canada*

15:10 **COFFEE/CAFÉ**

15:30 (47.6) A Wide-Band Continuum Correlator Using 14 Level Quantization, **G.J. HOVEY**[1], D. KARPA[2], T. BURGESS[1], T.L. LANDECKER[1], P.E. DEWDNEY[1], D. ROUTLEDGE[2], J.F. VANELDIK[2], [1] *National Research Council Canada, Penticton, BC, and* [2] *University of Alberta, Edmonton, AB, Canada*

15:50 (47.7) Correlation Through Optical Interferometric Intensity Modulation, **N.R. PRICE**, K. IIZUKA, *University of Toronto, ON, Canada*

16:10 (47.8) Data Display and Computer Control Problems Associated with the Green Bank Spectral Processor, **J.R. FISHER**, *National Radio Astronomy Observatory, Green Bank, WV, USA*

16:30 (47.9) A Finite Impulse Response Integrated Circuit for Pulsar Signal Recovery, **A.A. KAPADIA**, J.M. RABAEY, D.C. BACKER, *University of California, Berkeley, CA, USA*

J47.1

THE GREEN BANK TELESCOPE

George A. Seielstad
National Radio Astronomy Observatory
P. O. Box 2
Green Bank, West Virginia 24944

A new radio telescope is under construction at the National Radio Astronomy Observatory in Green Bank, West Virginia. The telescope will be fully steerable over the entire sky visible 5° above Green Bank's horizon. Its primary reflecting surface measures 100m x 110m, presenting an aperture 100m in diameter on the plane normal to the electrical axis. Since this aperture is completely unblocked, it has the largest effective collecting area of any fully steerable radio telescope. The primary surface of the Green Bank Telescope will be adjustable, thereby compensating for gravitational deformations and permitting operation at higher frequencies than those other comparably sized telescopes can utilize. Operation at both prime focus and Gregorian secondary focus will be possible. One receiver at a time can be installed at prime focus, but seven simultaneously can be installed on a "receiver turntable" at the secondary focus. Rapid switching among all eight receivers will exploit favorable environmental and scientific opportunities with maximum efficiency. A laser distance-ranging system will survey the shape of the main reflector via triangulation. The orientation of the laser surveying platform will be referenced to retroreflectors fixed on the ground. This latter reference frame permits the pointing precision necessary for high-frequency operation. Construction of the Green Bank Telescope will begin in 1991. Astronomical observations will begin in 1995.

ACTIVE SURFACE FOR THE GREEN BANK TELESCOPE

J. M. Payne
National Radio Astronomy Observatory
Green Bank, West Virginia 24944

The proposed active surface system for use with the Green Bank telescope will be presented.

The proposed system uses a metrology system to both measure the surface and to refer the measured surface to fixed points on the ground. In this way the surface may be set to a high precision and precision pointing information obtained.

Results obtained with a prototype metrology system that has both the required speed and precision will be presented.

J47.3

BEAM SCAN PERFORMANCE OF AN OFFSET GREGORIAN ANTENNA

R. D. Norrod *
National Radio Astronomy Observatory†
P.O. Box 2
Green Bank, WV 24944

S. Srikanth
National Radio Astronomy Observatory†
2015 Ivy Road
Charlottesville, VA 22903

Physical optics, uniform geometric theory of diffraction, and geometrical optics techniques have been utilized to study the beam scanning performance of a 100-meter, fully offset, gregorian antenna, for feeds laterally offset from the focus. Gain loss as a function of wavelength and feed displacement has been tabulated, and the relative contributions of aperture phase errors and main reflector spillover to the gain loss studied. At longer wavelengths where the size of individual apertures in feed arrays require relatively large feed displacements, increased main reflector spillover, rather than phase errors, can dominate the gain loss. The magnitude of the increased spillover for a given beam deflection is dependent on the reflector geometry.

The results of these studies will be presented for wavelengths selected between 21 cm and 3 mm. The main reflector spillover effect and its dependence on reflector geometry will be discussed. As examples, conceptual feed arrays for 6 cm and 7 mm wavelengths will be described.

---

†The National Radio Astronomy Observatory is operated by Associated Universities, Inc. under cooperative agreement with the National Science Foundation.

The Synthesis Telescope at the Dominion Radio Astrophysical Observatory

T.L. Landecker, P.E. Dewdney, L.A. Higgs, G.J. Hovey, J.D. Lacey, C.R. Purton, R.S. Roger, A.G. Willis, and W. Wyslouzil, (Dominion Radio Astrophysical Observatory, National Research Council of Canada)

The Synthesis Telescope at DRAO has recently been expanded to seven antennas. This paper presents a technical description of the telescope and outlines its capabilities.

The Synthesis Telescope is a wide-field instrument which operates simultaneously in continuum bands at 408 MHz and 1420 MHz and in the 21-cm HI line. At 1420 MHz the images have angular resolution of 1 arcmin within a field of diameter ~2.5° ; at 408 MHz these numbers are 3.5 arcmin and 8° . (Synthesized beams are elongated by a factor cosec(declination) in the north-south direction). Continuum sensitivities are 0.3 and 3.3 mJy/beam area r.m.s. at the field centre at 1420 and 408 MHz respectively.

Seven 9-m antennas are placed on a 600-m east-west baseline. Four are fixed and three move on a precision rail to stations spaced at intervals of 4.3 m. This provides a u-v plane fully sampled between baselines of 13 and 604 m with twelve moves (*i.e.* in twelve twelve-hour observations). 13 m is the smallest separation possible between two antennas. Use of baselines as short as this gives excellent sensitivity to extended emission. Furthermore, information on the broadest structures, corresponding to baselines between 13 and 0 m, is routinely provided from single-antenna data. The fine and regular sampling of baselines leads to an excellent synthesized beam, even without image processing, and places the grating responses well outside the field of view. Both are important for HI observations.

Image processing algorithms exploit the redundancy designed into the telescope configuration and also apply self-calibration to the data.

The correlator for the 1420 MHz continuum channel has 30 MHz bandwidth and employs 4-bit quantization. A 2-bit correlation spectrometer in the HI channel can operate at bandwidths of 0.125, 0.25, 0.5, 1, 2 and 4 MHz with 128 channels.

The Synthesis Telescope finds application in both galactic and extragalactic studies. The continuum channels offer excellent sensitivity to extended emission of low surface brightness. The spectral line facility is providing a view of the distribution and dynamics of interstellar atomic hydrogen with arcminute resolution.

J47.5

THE PROPOSED RADIO SCHMIDT TELESCOPE: THE TECHNICAL CHALLENGES

P. Dewdney and T.L. Landecker (Dominion Radio Astrophysical Observatory, National Research Council of Canada)

The concept of the Radio Schmidt Telescope is designed to fill a scientific requirement for a radio telescope which is very sensitive to diffuse, extended emission, but has much higher resolution than single-antenna telescopes. Studies of extended HI emission, low–brightness continuum emission, distributed spectral–line emission, solar studies and other problems all require sensitivity to extended emission and/or rapid imaging capability and would benefit crucially from an increase in angular resolution. The aperture synthesis technique remains the only method available to us to deliver the required combination of resolution and sensitivity at cm and m wavelengths. The Very Large Array (VLA) in its most compact configuration is the current best approximation. Nevertheless, there is a gap between what is possible with the VLA, and what is required. The Radio Schmidt telescope undertakes to utilize a new region of "parameter space" in the aperture synthesis technique.

The salient characteristics of a telescope which is well suited for such applications are: a wavelength range from about 1 m to 1 cm; a large collecting area arranged in an array configuration which is optimum for the scientific requirements (a 2–dimensional array configuration which is fairly compact in wavelengths); a comparatively wide (instantaneous) field–of–view; sufficient speed for high fidelity imaging of large areas of sky containing complex structure (areas much larger than the instantaneous field–of–view); spectral line capability sufficient to handle all known lines in the cm–to–m range of wavelengths.

In this presentation we will outline a telescope which implements this concept in a reasonable way. We will further discuss the inevitable compromises which must be made in order to balance its cost and performance. The emphasis will be on a process leading to the best implementation of the concept at reasonable cost while satisfying all the scientific objectives.

A Wide-band Continuum Correlator Using 14 Level Quantization

G.J. Hovey (Dominion Radio Astrophysical Observatory, National Research Council of Canada), D. Karpa (Electrical Engineering Department, University of Alberta), T. Burgess, T.L. Landecker, P.E. Dewdney (DRAO/NRC), D. Routledge, and J.F. Vaneldik (University of Alberta)

This paper describes a continuum correlator with high sensitivity due to its 30 MHz bandwidth and 14 levels of quantization. Low cost four bit flash A/D converters have made it feasible to lower quantization noise to near zero. In order to avoid de-correlation due to fringe washing, the 30 MHz band is split into four 7.5 MHz wide sub-bands and correlated by four independent correlator racks. A correlator rack consists of four types of components, 1) A/D converters, 2) correlation modules, 3) correlator interfaces, and 4) a micro-processor controller.

The correlator architecture is extensible and systolic, as correlation modules may be incrementally chained to form half of an n by n matrix of correlator modules. In order to minimize signal paths, data and control signals are distributed along the same path. System timing is maintained between modules by re-timing the signals at each module's output. To facilitate testing of the correlator during manufacturing and in service repair, self test circuitry is build into the correlator. Auto-correlator channels are also provided to permit system calibration along the entire RF and backend input signal path.

A/D converter performance was measured using synchronous sampling techniques. This technique permits measuring A/D performance at frequencies higher than the sampling frequency of the A/D. A/D cross-talk between channels was also reduced to about 2 parts per million by making use of EMI grounding and filtering practices.

Each correlation module contains eight cross-correlators which compute all four complex cross-polarization products for a pair of input signals. The readout logic uses a token passing method in order to eliminate the need for addressing logic in the modules.

A correlator interface for each channel interconnects the A/D converters and a micro-processor based controller to the correlator modules. It also contains test circuitry which may store A/D input data or provide arbitrary stimulus for correlator modules. The interface functions are high level in nature, implemented in programmable logic, and provide a simple flexible interface to the micro-processor controller.

A 68008 STD-Bus based micro-processor (uP) is used to control each of the four correlator racks. This uP provides the ability to perform free-standing diagnostic tests and also interfaces a rack, via the IEEE-488 bus, to a host uVAX computer. The host is used to provide a high level user interface and file services, while the uP performs real time and offline test functions. The uP software is written in the C language and operates under the VRTX multi-tasking kernel.

J47.7

CORRELATION THROUGH OPTICAL INTERFEROMETRIC INTENSITY MODULATION

N. R. Price* and K. Iizuka, Department of Electrical Engineering
University of Toronto

The technique of millimetre-wave interferometry presents requirements in frequency bandwidth which cannot be met with high frequency digital circuits, or state of the art acousto-optic devices. Therefore, the development of an optical correlator with a bandwidth limited by that of an optical detector has been undertaken.

The diagram below shows the arrangement of components in the correlator. The first process involved in this correlator is the conversion of the signal voltage amplitudes $V_0x(t)$ and $V_0y(t)$ produced from two radio telescopes to a modulation of laser beam intensity. This conversion is achieved through two $LiNbO_3$ integrated optic Mach-Zehnder interferometers with electrodes arranged in a push-pull configuration. Hence there are produced two coherent laser beams with intensities proportional to $E_0^2[1 + x(t)]$ at **1**, and $E_0^2[1 + y(t)]$ at **2**. Through destructive interference via two Mach-Zehnder interferometers each incorporating an intensity modulated signal in one arm, the amplitudes exiting these two interferometers become $E_0x(t)/2$ at **3**, and $E_0y(t)/2$ at **4**, for x(t), y(t) << 1. The subsequent constructive and destructive interference of these two coherent beams produces intensities at the detectors proportional to $E_0^2[x(t) + y(t)]^2$ and $E_0^2[x(t) - y(t)]^2$. Voltage outputs from the detectors are then subtracted to produce the signal voltage proportional to $4x(t)y(t)$.

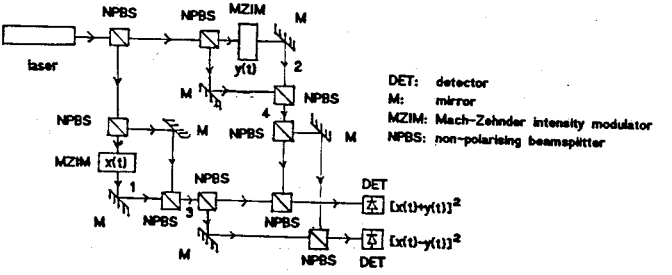

Diagram of Correlator

The device is being developed as a prototype for a completely integrated optic device.

The authors are grateful to Prof. T. Nakamura of Gifu University for his suggestions. We also want to thank Profs. P. Kronberg and E. Seaquist of the Department of Astronomy, University of Toronto.

DATA DISPLAY AND COMPUTER CONTROL PROBLEMS ASSOCIATED WITH THE GREEN BANK SPECTRAL PROCESSOR

J. R. Fisher
National Radio Astronomy Observatory
Green Bank, West Virginia 24944

Our Fourier-transform spectrometer designed for pulsar and spectral line observations presents some data display problems that are well suited to image processing techniques used in optical aperture synthesis astronomy. This paper presents a few results from experiments with gray-scale and TV animation displays in connection with pulsar dedispersion and timing, interference excision, and interstellar scintillation display.

The complexity of this spectrometer has presented a fairly difficult software problem in the translation of user setup parameters into hardware settings because of the interdependencies of many of the parameters. This is much the same problem faced by designers of telescope control systems. We present a design using object-oriented software techniques, particularly C++, that may have general application to hardware state control.

J47.9

A FINITE IMPULSE RESPONSE INTEGRATED CIRCUIT FOR PULSAR SIGNAL RECOVERY

Amar A Kapadia and Jan M. Rabaey*

Department of Electrical Engineering and Computer Science, University of California at Berkeley

Donald C. Backer

Department of Astronomy, University of California at Berkeley

Pulsars are rotating, highly magnetized neutron stars which emit pulse signals with strikingly regular periods. Pulsar timing, a field using the high stability of the pulsar signal frequency, has numerous applications in astrophysics. However, during its propagation to Earth, the signal undergoes considerable dispersion due to the presence of interstellar medium. For accurate pulsar timing, this dispersion has to be removed. The coherent dispersion removal technique implements the inverse interstellar medium transfer function through a complex arithmetic FIR filter. This paper describes the design of the finite impulse response (FIR) filter application specific integrated circuit (ASIC) with a maximum of 1024 taps which would remove dispersion for up to 4 MHz of the signal bandwidth (The product of bandwidth and taps is limited to 1024 taps x MHz). The chip uses a partially parallel and pipelined approach to implement the 7.2 Giga Operations per second computational requirement of the filter. The operational speed is up to 32 MHz and there are five levels of pipelining. Furthermore, there is 10 Kbits of on-chip memory for data and coefficient storage. The datapath consists of 32 complex multipliers and a binary adder-tree followed by accumulators which sums up the 1024 products to produce the convolution result. This chip has been designed using the LagerIV silicon assembler and will be fabricated in the MOSIS 2.0 micron process. The estimated die size is 10mm x 10mm and the estimated pin count is 64.

Magellan Mission to Venus | **Room 3022 Salle URSI J Session 76** | **Mission de Magellan vers Vénus**

Chairs/présidents: G.H. PETTENGILL, USA

13:30 (76.1) Magellan Mission Overview, A.J. SPEAR, J.F. SCOTT, R.J. PIERESON, M.J. STEWART, R.B. MORRIS, J.M. GUNN, **T.W. THOMPSON**, *California Institute of Technology, Pasadena, CA, USA*

13:50 (76.2) Radar System Design for the Magellan Imaging Radar Mission to Venus, **W.T.K. JOHNSON**, *California Institute of Technology, Pasadena, CA, USA*

14:10 (76.3) Venus: Geological Overview from Magellan Data, **G.E. McGILL**, *University of Massachusetts, Amherst, MA, USA*

14:30 (76.4) The Magellan Altimetry and Radiometry Experiment, **P.G. FORD**, G.H. PETTENGILL, *Massachusetts Institute of Technology, Cambridge, MA, USA*

14:50 (76.5) The Magellan Mission to Venus: Measurements of the Electrical and Physical Properties of the Surface, **D.B. CAMPBELL**[1], P.G. FORD[2], G.H. PETTENGILL[2], R.A. SIMPSON[3], G.L. TYLER[3], N.S. STACY[1], [1]*Cornell University, Ithaca, NY,* [2]*Massachusetts Institute of Technology, Cambridge, MA, and* [3]*Stanford University, Stanford, CA, USA*

15:10 **COFFEE/CAFÉ**

J76.1

MAGELLAN MISSION OVERVIEW

A. J. Spear, J. F. Scott, R. J. Piereson, M. J. Stewart,
R. B. Morris, J. M. Gunn, and T. W. Thompson*
Jet Propulsion Laboratory
California Institute of Technology
Pasadena, CA 91109

The Magellan Project extends and expands upon the knowledge of Venus that was provided by the Pioneer Venus Orbiter operated in the late 1970's and Soviet Venera spacecraft operated in the early 1980's. Since Venus is covered by a thick, dense layer of clouds, only radio and radar observations can provide a global picture of the Venusian surface.

The Magellan spacecraft was launched from Cape Kennedy onboard the shuttle Atlantis on May 4, 1989, and went into orbit abound the planet Venus on August 10, 1990. The collection of radar and radiometry data commenced on September 15, 1990. This data acquisition continues on a daily, orbit-by-orbit basis, interrupted only by superior conjunction period of eleven days in late October and early November 1990. The first cycle of data collection, once around the planet, will be completed in mid-May 1991. Radar data collection will likely continue for several years.

The Magellan spacecraft carries a single instrument, a radar sensor. This instrument produces a radar image of the surface using Synthetic Aperture Radar (SAR) techniques, measures surface altitude using pulse compression techniques, and detects surface temperatures via radiometry by sharing various components and modes of the radar sensor. Magellan will also refine the gravitation field of Venus via precise tracking of the spacecraft.

The Magellan spacecraft orbits Venus once every 3.27 hours with a periapsis altitude of 295 km and an apoapsis altitude of 8,472 km. Radar data is acquired and stored onboard during a 50 minute period centered on periapsis. This data is played back to Earth during a two hour period centered on apoapsis and recorded at the Deep Space Network (DSN) stations in California, Spain and Australia. This data is processed at the Jet Propulsion Laboratory (JPL) in California and the Massachusetts Institute of Technology (MIT) to produce radar imagery, altimetry, and radiometry of the surface.

RADAR SYSTEM DESIGN FOR THE MAGELLAN IMAGING RADAR MISSION TO VENUS

William T. K. Johnson*, Jet Propulsion Laboratory, California Institute of Technology, Pasadena, CA 91109

The design of the Magellan radar system reflects the mission's scientific objectives, which require the imaging of more than 70 percent of the surface of Venus at a resolution of better than 360 m, and a determination of a corresponding portion of the planet's topography with a height resolution commensurate with the imaging waveform. In fact, the radar system as implemented can image about 90 percent of the surface during the first eight months of the mission, with more than half of that at a resolution of better than 130 m. It should eventually be able to map the entire planetary surface, using data obtained in additional mapping cycles extending beyond the first eight months of operation .

Operating from a highly elliptical orbit, the Magellan radar must adapt to rapidly changing parameter requirements as its altitude varies. Furthermore, the design has had to surmount severe restrictions placed on the telemetered rate of returned data by the large interplanetary distances involved. As an all-digital system, the radar presents several novel approaches to synthetic aperture radar design, of which block-adaptive quantization is perhaps the most significant. This paper briefly describes the overall radar system and its philosophy, and shows a few examples of the SAR images obtained.

J76.3

VENUS: GEOLOGICAL OVERVIEW FROM MAGELLAN DATA

George E. McGill*, University of Massachusetts, Amherst, MA 01003

The surface of Venus is dominantly radar-dark plains, most of which appear areally uniform on Magellan SAR images. Volcanic landforms, such as lobate lava flows, dome-like structures, small cones, and large central volcanoes are abundant. Plains areas generally are hundreds of km across, and are characterized by remarkably coherent patterns of narrow, radar-bright fractures and lineaments, with spacings of one to many tens of km. Transecting the plains are radar-bright linear belts of ridges and closely spaced fractures. Ridge belts commonly are 50-100 km wide and up to many hundreds of km long. They stand a few hundred meters above the adjacent radar-dark plains, often appearing related to other local relief and areas of intense fracturing. Ridge belts are believed to result from compressional shortening with minor crustal thickening. The plains also include scattered circular to oval features up to about a thousand km in diameter, referred to as "coronae," which apparently are unique to Venus. Both volcanic activity and deformation of older plains lavas are associated with coronae; nevertheless, their origin is somewhat enigmatic, but probably related to deep-seated upwelling of hot material in the venusian mantle. The total population of impact craters on the plains indicates that the surface is relatively young – averaging a few hundred million years, with some local areas apparently even younger.

Large elevated plateaus and mountainous regions occupy a minor but significant fraction of the venusian surface. These highland regions have experienced significant shortening and crustal thickening, and include several types of terrain: 1) Much of Ishtar Terra is a radar-dark, lava covered plateau (Lakshmi Planum), that includes two large and spectacular volcanic calderas. 2) Other large areas consist of radar-bright, intricately deformed terrain dubbed "tessera" by Soviet scientists because of its resemblance to cross-lineated floor tiles. Tessera terrains probably contain the oldest materials now exposed at the surface of Venus. 3) Flanking Lakshmi Planum are major linear mountain belts consisting of long, narrow, parallel ridges of probable compressive origin. Magellan SAR images reveal dramatic evidence for lateral extension and gravitational collapse of these mountain belts. Furthermore, slopes are so steep in some localities, that mountain-building activity there must be geologically recent.

Magellan radar images suggest that Venus has experienced a complex history of volcanism and deformation, some of which must be geologically recent. Venus thus appears to be an active planet, more like the earth than the moon or Mars. Nevertheless, no evidence has yet been found in the Magellan data to suggest that the lithosphere of Venus is broken into laterally mobile, rigid plates, as is the case for the earth.

THE MAGELLAN ALTIMETRY AND RADIOMETRY EXPERIMENT

Peter G. Ford* and Gordon.H. Pettengill, Center for Space Research,
Massachusetts Institute of Technology, Cambridge, MA 02139

The Magellan Venus orbiter comprises a single scientific instrument: a 12.6-cm-wavelength radar system, shared among three data-taking modes. In addition to the primary (SAR) imaging mode, described earlier, an altimetric mode enables relative terrain height-measurement accuracies approaching 5 m, depending on the roughness of the surface below, although orbital uncertainties generally raise the absolute uncertainty to about 50 m. It also provides information on the roughness and reflectivity of the nadir region. In order to estimate these various quantities in an optimum manner, the altimetric echo is resolved in doppler frequency, and data taken over an interval of many seconds, that nevertheless originate from a given small element of the surface, are combined in two quite different ways. In one, estimation of the distance to the surface is stressed; in the other, the scattering properties are emphasized.

When used as a thermal emission radiometer, the radar receiving system can resolve surface brightness temperatures differing by as little as 2K, and can determine their absolute values to about 15K. By combining the surface brightness observations, corrected for atmospheric absorption, with knowledge of the surface physical temperatures (which on Venus are solely a function of altitude), the intrinsic surface emissivity may be calculated with an absolute accuracy of about 0.02.. These data, when combined with the radar reflectivity, provide an excellent estimate of the intrinsic dielectric permittivity of the surface material.

J77.1

Measurements of Atmospheric Phase Delays with a Radio Interferometer

Colin R. Masson
Harvard-Smithsonian Center for Astrophysics

As part of the preparation for the building of the SAO submillimeter array, an interferometric phase monitor has been constructed. This instrument has been used to measure the quality of the radio seeing at Mauna Kea in Hawaii, the first time that this quantity has been measured in advance of the construction of an interferometer.

The phase monitor consists of a pair of small satellite antennas, connected as an interferometer, receiving signals from a geosynchronous satellite at 11.712 GHz. The antennas are spaced 100 m apart and the system noise level is approximately 0.07°, corresponding to a path length of 5 μm, in an integration time of 1 second.

The results show that the radio seeing at Mauna Kea has the same range as that reported for other sites. A more quantitative comparison is not possible because the other measurements reported in the literature do not give an accurate distribution of conditions. The peak phases are extremely large, nearly 100° at 11.712 GHz on our 100 m baseline. This corresponds to a wedge of 100% humid air above the phase monitor, with an angle of nearly 45 °.

The phase data have been compared in various ways with measurements from the nearby NRAO 225 GHz radiometer. There is little correlation between the mean precipitable water vapor (PWV), as measured by the radiometer, and the rms phase, except that at very low values of PWV (< 1mm) the rms phase is reduced. There is a good correlation, however, between the opacity fluctuations and the phase fluctuations, as expected theoretically.

The power spectrum of the phase fluctuations gives information about phase on baselines longer and shorter than 100 m. The rms phase increases as approximately the 0.65 power of baseline, much less than the value predicted for Kolmogorov turbulence.

Sources of Ground Noise in Radio Telescopes Using Paraboloidal Antennas

T.L. Landecker (Dominion Radio Astrophysical Observatory, National Research Council of Canada), M.D. Anderson, D. Routledge, R.J. Smegal, P. Trikha, and J.F. Vaneldik (Electrical Engineering Department, University of Alberta

Ground radiation contributes to the system noise of radio telescopes at all microwave frequencies. In systems which use cryogenically cooled receivers, ground noise can be the dominant source of system noise at some frequencies. Antenna sidelobes which can intercept ground radiation are those due to spillover past the reflector rim, diffraction at the rim, leakage through the reflector, and scattering from the struts which support the feed (or subreflector). Ground radiation scattered from the struts into the feed can contribute up to 5 K. A simple method of estimating this contribution has been developed. The antenna temperature at 1.4 GHz of a 9 m paraboloid has been accurately measured, and the contribution from strut scattering has been isolated. Triangular struts can be used to reduce the contribution of strut scattering to antenna noise, without degrading polarization performance. On antennas where three struts are used, the optimum configuration of the tripod is the upright Y. This configuration gives lower ground noise at all elevation angles of the antenna beam, with both circular and triangular struts.

J77.3

WIDE-BANDWIDTH RECEIVERS AND INTERFERENCE: DESIGN FOR MINIMUM SUSCEPTIBILITY

William D. Brundage* and Paul Lilie
National Radio Astronomy Observatory
Socorro, New Mexico, USA

The trend toward wider bandwidths at centimeter and millimeter wavelengths for radio astronomy receiver front ends presents a design challenge to minimize susceptibility to radio interference.

Astronomers' desire for maximum sensitivity and well calibrated polarization measurements push receiver front ends toward large instantaneous bandwidths. Spectral line observers want sensitive receivers covering almost the entire radio spectrum. Therefore radio telescopes must function far outside the few protected frequency allocations. Astronomers must frequently contend with data contaminated at some level which ranges from nuisance to disaster. Interference becomes harmful when it causes significant errors in the data which cannot be adequately excised or calibrated out.

We discuss harmful levels for certain observations related to the principal sources and mechanisms of interference. Interference originates both outside the telescope and from within the receiver electronics. Harmful interference outside the detected passband occurs mainly through gain compression or intermodulation or both. We discuss the sources and mechanisms in some detail.

How can we design receivers to minimize susceptibility through these mechanisms? We discuss some rules of thumb for such design with reference to gain, bandwidth, noise, and intercept parameters. Unfortunately, these rules often require tradeoffs, which often cause less than adequate immunity to specific interferences. Design should provide for easy retrofitting to respond to future changes in the interference environment. We discuss some methods.

Case histories can be instructive. We discuss several experiences from the Very Large Array and the Very Long Base Line Array. Finally, we point out some spectral segments which could become future problems for radio astronomy.

ELECTROMAGNETIC INTERFERENCE FROM PERSONAL COMPUTERS AND WORKSTATIONS AT DRAO

W.Wyslouzil, National Research Council of Canada, Herzberg Institute of Astrophysics, Dominion Radio Astrophysical Observatory, Penticton, British Columbia.

The principal observing instrument at DRAO (Dominion Radio Astrophysical Observatory) is an aperture synthesis telescope comprising seven 8.5 meter parabolic antennas on a 600 meter baseline, making simultaneous observations at 408 and 1420 MHz. The array comes to within about 80 meters of the main observatory building containing laboratories and offices where the recent proliferation of personal computers and workstations has raised concerns about the possibility of EM interference with astronomical observations.

In addition, the DRAO 26 meter telescope, used primarily for observations at or near 1420 MHz (interstellar hydrogen emission) and 1660 MHz (OH absorption lines), is situated immediately adjacent to the main building, making it even more susceptible to low level interference.

It was therefore decided to measure the emission from a number of typical personal computers (PCs) and workstations at the frequencies of interest and relate these measurements to signal levels required to cause interference.

Measurements were performed in a small anechoic chamber with a simple receiving antenna connected to a low noise preamplifier and Spectrum Analyzer. The results were related to signals of known power transmitted from quarter wavelength monopoles positioned at the test location.

Indications are that interference with the synthesis array is highly unlikely at frequencies above 1 GHz, but interference at 408 MHz is a theoretical possibility. The results of the measurements and considerations leading to these conclusions will be discussed.

On the other hand, interference from a workstation with OH line observations using the 26 meter telescope has actually been demonstrated and some of the offending equipment has been relegated to a screened enclosure - not a preferred solution.

Consequently methods for suppressing EM emissions from PCs at frequencies below 3 GHz are being actively investigated. The most promising approach is to build a shielding enclosure for the computer proper, with signals to the monitor, keyboard, printer and other peripherals passing through low pass line filters. Construction details and the performance of various experimental configurations will be described.

Polarimetric Metrology

Room 3018 Salle
Joint URSI/AP-S Session 42

Métrologie polarimétrique

Chairs/présidents: Y.M.M. ANTAR, Canada; G. WANIELIK, Germany

08:30 (42.1) Polarimetric Study of Complex Targets at Millimetric Wavelengths, **V. SAMPATH**, G.Y. DELISLE, *Laval University, Quebec, PQ, Canada*

08:50 (42.2) Broadband Scattering Matrix Measurements and their Modelling, **G. WANIELIK**[1], D.J.R. STOCK[2], [1]*Daimler-Benz Research, Ulm, and* [2]*TST/DASA, Ulm, Germany* (APS)

09:10 (42.3) Polarimetric and Synthetic Aperture FM-CW Radar, **Y. YAMAGUCHI**[1], M. MITSUMOTO[1], M. SENGOKU[1], T. ABE[1], W.-M. BOERNER[2], [1]*Niigata University, Niigata, Japan;* [2]*University of Illinois, Chicago, IL, USA*

09:30 (42.4) Measured Monostatic Radar Cross Section of Metallic Cubes, **S.R. MISHRA**[1], J. MANTZ[2], [1]*Canadian Space Agency, Ottawa, ON, and* [2]*Concordia University, Montreal, PQ, Canada* (APS)

09:50 (42.5) A Dihedral Corner Reflector Model for Full Polarization Calibration of RCS Measurements, **K.W. SORENSEN**, *Sandia National Laboratories, Albuquerque, NM, USA* (APS)

10:10 **COFFEE/CAFÉ**

10:30 (42.6) Polarimetric Observations of Trees at 35 and 94 GHz, **A. NASHASHIBI**, Y. KUGA, F.T. ULABY, *University of Michigan, Ann Arbor, MI, USA* (APS)

10:50 (42.7) Polarimetric Scattering from Natural Surfaces at 225 GHz, **J. MEAD**, P. LANGLOIS, P. CHANG, R. McINTOSH, *University of Massachusetts, Amherst, MA, USA* (APS)

11:10 (42.8) Ku-Band Polarization Characteristics of Wheat, Barley, Canola and Fallow, **G. SOFKO**, M. HINDS, M. McKIBBEN, J.A. KOEHLER, A. WACKER, *University of Saskatchewan, Saskatoon, SK, Canada*

11:30 (42.9) Performance of a Polarization Isolation Enhancement Method in the Presence of Errors, **B.C. BROCK**, *Sandia National Laboratories, Albuquerque, NM, USA* (APS)

11:50 (42.10) A New Calibration Algorithm of Wideband Polarimetric Measurement System, T.-J. CHEN, **T.-H. CHU**, F.-C. CHEN, *National Taiwan University, Taipei, Taiwan, China* (APS)

POLARIMETRIC STUDY OF COMPLEX TARGETS AT MILLIMETRIC WAVELENGTHS

V. Sampath*, G.Y. Delisle

Electrical Engineering Department
Faculty of Sciences and Engineering
Laval University, Quebec City
Canada G1K 7P4

In the past few years, interest in the polarimetric aspects of radar target behavior appears to have revived to a considerable extent. Since most targets can be fully characterised by their scattering matrices and no scattering matrix is complete without polarization dependence included, polarimetry is, indeed, becoming extremely important.

Two types of scattering matrices exist:

- Complex voltage scattering matrix (VSM)
- Real power scattering matrix (PSM)

From the PSM, power spectra, consisting of the polarization signatures (PS) as well as the dispersive polarization signatures (DPS) can be found. The PS and the DPS are themselves of three basic types:

- Co-polarized - *i.e.* when the receiver is polarized in identical fashion to the transmitter
- Cross-polarized - *i.e.* when the receiver is polarized perpendicular to the transmitter
- Random-polarized - *i.e.* when the receiver polarization can be varied so as to capture the maximum amount of power reflected by the target.

Power scattering matrices are extremely useful in modelling partially polarized electromagnetic waves. However, the problem is that information on the phase is lost as the coefficients of the PSM are all real. Thus, from the point of view of relative phase spectra, it is the VSM that is required. But the most important role that the VSM could play is in the study of the depolarization produced by an object. This phenomenon is supposedly a function of the parameters S_{11}, S_{12} and S_{22}. Further, the material of which each target is made may influence the polarization.

The present work is therefore aimed at formulating a backscattering model that would include not only depolarization characteristics but also the nature (*i.e.* the permittivity and/or permeability) of the various objects under consideration. Numerical and experimental results will be reported using different angle of observations of the targets. They will be compared with those obtained experimentally.

POLARIMETRIC AND SYNTHETIC APERTURE FM-CW RADAR

Yoshio Yamaguchi*, Masashi Mitsumoto,
Masakazu Sengoku, and Takeo Abe
Department of Information Engineering
Faculty of Engineering, Niigata University
Ikarashi 2-8050, Niigata-shi 950-21
Japan

and

Wolfgang-Martin Boerner
Communications and Sensing Laboratory (M/C 154)
Department of Electrical Engineering and Computer Science
University of Illinois at Chicago
Chicago, IL/USA 60680

This paper presents the principle and detection results of a novel Polarimetric and Synthetic Aperture Frequency Modulated Continuous Wave Radar (FM-CW POL-SAR) System. First, the synthetic aperture technique is applied to the conventional FM-CW radar, with emphasis placed on showing that the Fourier transformed beat signal obtained by the FM-CW radar is equivalent to one kind of Fresnel holograms, which leads us to the implementation of the SAR technique. Then, polarimetric measurements for object detection are combined with the SAR mode leading to the realization of a fully polarimetric imaging radar system. Next, the resulting instrumentation testbed radar system, operative in the microwave X-band, is calibrated, tested and applied to the detection of a metallic plate of different orientations, demonstrating its usefulness in polarimetric imaging and the high resolution detection along the azimuthal direction by satisfying the Fresnel region operating conditions.

Ku-BAND POLARIZATION CHARACTERISTICS OF WHEAT, BARLEY, CANOLA AND FALLOW

G. Sofko (1), M. Hinds (2), M. McKibben (1), J. Koehler (1) and A. Wacker (2*)

(1) Institute of Space and Atmospheric Studies
University of Saskatchewan, Saskatoon, Sk. S7N 0W0
(2) Electrical Engineering Department,
Univ. of Saskatchewan, Saskatoon, Sk. S7N 0W0
(2*) deceased

A standard microwave Ku-band FM-CW ground-based scatterometer, measuring HH, HV, VH, and VV polarization states, was modified into a full polarimeter for crop and soil measurements during the growing seasons of 1987 and 1989. For each of the transmitted polarizations (H and V), received signal was measured in H, V, X, Y, L and R modes, where X and Y are linear components at 45 and 135 degrees to the horizontal, and L and R are the left and right circular components. The results show that, for all targets, the average received elliptically polarized state has the same shape (linear) as the transmitted state, so there is no depolarization. However, there s a substantial unpolarized component. The received elliptically polarized power varies significantly with incidence angle and time (i.e. crop maturity). Furthermore, the elliptically polarized power is different for the H and V transmit states, whereas the unpolarized power is about the same for both transmit states; as a consequence, the received polarization ratio m for the two transmit states is different. The most important conclusion is that the standard scatterometer measurements (HH, HV, VH and VV) contain essentially all of the polarization information. The like-polarized states HH and VV contain all the elliptically polarized power plus half the unpolarized power, while the cross-polarized states HV and VH contain the other half of the unpolarized power.

Polarimetric Imaging Radars | **Room 3018 Salle Joint AP-S URSI Session 59** | **Imagerie par radars polarimétriques**

Chairs/présidents: E. WALTON, USA

13:30 (59.1) High Resolution Imaging of Radar Targets Using Narrow Band Data, **E. WALTON**, A. MOGHADDAR, *Ohio State University, Columbus, OH, USA* (APS)

13:50 (59.2) Basic Equations of Radar Polarimetry and Its Solutions, **W.-M. BOERNER**[1], W.-L. YAN[1], A.-Q. XI[1], Y. YAMAGUCHI[2], [1] *University of Illinois, Chicago, and* [2] *Niigata University, Niigata, Japan*

14:10 (59.3) Determination of the Characteristic Polarization States of the Target Scattering Matrix $[S(AB)]$ for the Coherent Monostatic and Reciprocal Propagation Space, A.-Q. XI, **W.-M. BOERNER**, *University of Illinois, Chicago, IL, USA*

14:30 (59.4) Optimal Polarization States Determination of the Stokes Reflection Matrices $[\bar{M}_p]$ for the Coherent Case, and of the Mueller Matrix $[M]$ for the Partially Polarized Case, W.-L. YAN, **W.-M. BOERNER**, *University of Illinois, Chicago, IL, USA*

14:50 (59.5) Reconstruction of Evaporation Duct Profile from Spatial Structure of the Radar Backscatter from the Sea Surface, **A.V. VOLKOV**, K.V. LATYSHEV, K.V. KOSHEL, L.A. SLAVUTSKY, B.M. SHEVTSOV, A.A. SHISHKAREV, *Pacific Oceanological Institute, Vladivostok, USSR* (APS)

15:10 **COFFEE/CAFÉ**

15:30 (59.6) Propagation Research on 20 GHz Earth-Satellite Paths with the DLR Station, **A. HORNBOSTEL**, A. SCHROTH, *DLR Oberpfaffenhofen, Wessling, Germany* (APS)

15:50 (59.7) Adaptive Communications Polarimetry, **Y. YAMAGUCHI**[1], H.J. EOM[2], W.-M. BOERNER[3], [1] *Niigata University, Niigata, Japan;* [2] *Korea Institute of Technology, Tae-Jon, Korea;* [3] *University of Illinois, Chicago, IL, USA*

16:10 (59.8) An ISAR Simulator for Ships, **K.R. SHILLINGTON**, P.A. JAHANS, E.H. BULLER, J.K.E. TUNALEY, *London Research and Development Corporation, London, ON, Canada* (APS)

16:30 (59.9) A New Filter Method for Speckle Reduction in Synthetic Aperture Radar (SAR) Images, G.H. ABDELHAMID, **H.A. ASSAL**, M.N. FAHMY, *Cairo University, Giza, Egypt* (APS)

BASIC EQUATIONS OF RADAR POLARIMETRY AND ITS SOLUTIONS

Wolfgang-Martin Boerner, Wei-Ling Yan, An-Qing Xi
Communications and Sensing Laboratory (M/C 154)
Department of Electrical Engineering and Computer Science
University of Illinois at Chicago
Chicago, IL/USA 60680

and

Yoshio Yamaguchi
Department of Information Engineering
Faculty of Engineering, Niigata University
Ikarashi 2-8050, Niigata-shi 950-21
Japan

Basic principles of radar polarimetry are introduced. The target characteristic polarization state theory is developed first for the coherent case using the three step, the basis transformation, and the power (Mueller) matrix optimization procedures. Kennaugh's and Huynen's theories of radar target polarimetry are verified for the monostatic reciprocal case. It is shown that there exist in total five unique paris of characteristic polarization states for the symmetric scattering matrix of which the two pairs, the cross-polarization null and co-polarization max pairs are identical; whereas, the cross-pol max and the cross-pol saddlepoint pairs are distinct. These three pairs of orthogonal characteristic states are also mutually orthogonal on the polarization sphere. The fifth pair, the co-pol null pair lies in the plane spanned by the co-pol max/-cross-pol null and the cross-pol max pairs which determines the target characteristic circle on the polarization sphere reestablishing Huynen's "polarization fork" concept. The theory is verified by an example for which next to the polarization fork also the co-polarized and cross-polarized power density plots are presented. In a next step, the partially polarized case for completely polarized wave incidence is presented and compared with the results for the coherent and the partially coherent cases, the latter still being unresolved.

DETERMINATION OF THE CHARACTERISTIC POLARIZATION STATES OF THE TARGET SCATTERING MATRIX [S(AB)] FOR THE COHERENT MONOSTATIC AND RECIPROCAL PROPAGATION SPACE

An-Qing Xi and Wolfgang-Martin Boerner
Communications and Sensing Laboratory (M/C 154)
Department of Electrical Engineering and Computer Science
University of Illinois at Chicago
Chicago, IL/USA 60680

A problem originating in radar polarimetry is considered for which the radar target is to be characterized by its coherent polarization state properties, given complete coherent backscattering scattering matrix data sets at one frequency and for one target aspect angle. First the Jones vector formalism for the coherent monostatic case, together with Sinclair's backscattering matrix [S(AB)] for the general polarization basis (AB) are introduced. Using the unitary change of polarization state transformation, the concept of the characteristic polarization states of a scatterer, first introduced by Kennaugh and Huynen, is presented. For emphasizing the unique properties of the interrelation among the existing characteristic polarization states the generalized unitary transformation matrix formulation under the change of basis transformation, expressed in terms of the polarization ratio ρ, is developed. For the monostatic reciprocal case ($S_{AB} = S_{BA}$), treated here, it is shown that there exist in total five pairs of characteristic polarization states: orthogonal cross-polarization null and co-polarization maximum state pairs, being identical and sharing one main circle with the co-polarization and the orthogonal cross-polarization maximum state pairs, the latter being at right angles with the cross-polarized null pairs; and, a newly identified pair: the orthogonal cross-polarization saddle point extrema which are normal to the plane (main circle) spanned by the other four pairs on the polarization sphere. With this complete and unique mathematical description of Huynen's polarization fork concept, it is now possible to study the polarimetric radar target optimization problem more rigorously. Various examples are provided and interpreted by comparing the unique result with previous incomplete analyses.

OPTIMAL POLARIZATION STATES DETERMINATION OF THE STOKES REFLECTION MATRICES [$\bar{M}_p$] FOR THE COHERENT CASE, AND OF THE MUELLER MATRIX [M] FOR THE PARTIALLY POLARIZED CASE

Wei-Ling Yan and Wolfgang-Martin Boerner
Communications and Sensing Laboratory (M/C 154)
Department of Electrical Engineering and Computer Science
University of Illinois at Chicago
Chicago, IL/USA 60680

A problem originating in radar polarimetry is considered for which the radar target is to be characterized by its 4x4 Mueller matrix [M] properties in terms of partially polarized wave treatment for the monostatic reciprocal and non-reciprocal cases. In order to compare our results with previous coherent treatments of optimizing the corresponding 2x2 Sinclair matrix [S], first the vector formalism for the coherent case is introduced. The coherent formulation is then extended via the coherency matrix (vector) approach to the partially polarized case with the aid of the Kronecker expansion matrix and the Stokes vector formalism. Distinction of the Stokes Reflection Matrices is made between the one-antenna and the two-antenna cases. For the one-antenna case, the reception of the optimal energy densities and powers is accomplished separately for the co-polarized and the cross-polarized channels which is a natural approach in radar polarimetry. For the two-antenna case, the reception of the optimal power is accomplished by adjusting the polarization state of the receiving antenna to match or mismatch the polarization state of the scattered wave. The "degenerate Mueller matrix case" for purely coherent wave reception is analyzed first to facilitate comparison with previous methods of optimizing the corresponding Sinclair matrix [S]. Here, the Lagrangian multiplier method is used for determining the characteristic optimal polarization states subject to the constraint that the incident wave is purely polarized.

It is then shown that for the more general partially polarized scattered wave case, there exist next to the total energy density, three specific types of energy densities: (i) the adjustable purely polarized intensity, (ii) the noise-like unpolarized intensity, and (iii) the receivable polarized intensity; for which separate optimization methods are developed. Whereas, for the first category, a factorized solution may be found; for the second two criteria numerical solutions must be used. The paper is concluded with a comparison of the various results obtained here with those obatined by other methods.

ADAPTIVE COMMUNICATIONS POLARIMETRY

Yoshio Yamaguchi[(1)*], Hyo Joon Eom[(2)] and Wolfgang-M. Boerner[(3)]

(1) NIIGATA UNIVERSITY, Faculty of Electronics
NIIGATA-SHI, 〒 950-21 Japan

(2) KOREA INSTITUTE OF TECHNOLOGY
KIT/KAIST-EE/WSL, 23 Ku Song Dong
YUSUNG GU, TAE-JON-Shi, 〒 300-31 South Korea

(3) UNIVERSITY OF ILLINOIS AT CHICAGO
UIC-EECS/CSL, M/C 154, 840 W. Taylor Str.
UIC-607-4210, CHICAGO, IL/USA 60607

Commonly in radio communications fixed antenna polarization states are in use also for dual orthogonal polarization channel frequency-reuse operations. The most commonly used antenna polarizations are fixed linear "horizontal/vertical" or circular "left/right-handed" polarization states. However, the communications signal will, in general, suffer from polarization state transformation and depolarization effects caused by scattering, refraction, diffraction, etc., in a complex propagation medium. The polarization state degradation includes all obstructing objects affecting the propagation space, i.e., topology, man-induced structures, vegetation and atmospheric scatter, e.g., fog, rain, hail, etc. In addition, in a multi-path propagation environment such as in cellular communications, time-delayed multiple vector waves of different polarization states simultaneously arrive at the receiver, completely changing the polarization state of the initially transmitted wave. Therefore, the common use of (any) fixed antenna polarizations is certainly far from optimal. Thus, the aim of this paper is to develop an agile polarization state adaptive communication systems approach. This is achieved by designing the received antenna system with completely free, arbitrarily adaptive polarization state, providing the following advantages:

1) Maintain matched polarization state conditions resulting in increased steady systems performance;

2) Reject undesired signals by adaptively switching receiver antenna state to a polarization state orthogonal to that of the undesired signal;

3) Apply polarimetric matched signal filter techniques with space filtering by use of adaptive polarization array antennas, so that the desired signal can be selected within the "main beam".

In view of the rapid advances currently being made in miniature compact electro-optical signal processing device technology, the relatively large and complex adaptive antenna polarization state control and polarimetric matched signal filter systems can soon be miniaturized and realized, elevating "radar polarimetry" to an indespensible tool also in cellular communications technology.

Inverse Methods — Méthodes inverses

Room 3018 Salle
Joint AP-S & URSI B Session 75

Chairs/présidents: L.A. WEGROWICZ, Canada

13:30 (75.1) Inverse Problem Approach to Array Diagnostics, **L.A. WEGROWICZ**, R. POKULS, *McGill University, Montreal, PQ, Canada* (APS)

13:50 (75.2) One-Dimensional Imaging of Dielectric Bodies of Revolution Based on Rayleigh Approximation, **T. UNO**, Y. MIKI, S. ADACHI, *Tohoku University, Sendai, Japan* (APS)

14:10 (75.3) Iterative Methods for an Inverse Scattering Problem of a Three-Dimensional Flaw in Anisotropic Slab, **S. BARKESHLI**, R.G. LAUTZENHEIZER, L.D. SABBAGH, H.A. SABBAGH, *Sabbagh Associates Inc., Bloomington, IN, USA* (APS)

14:30 (75.4) On the Time Domain Inverse Scattering for the Bistatic Case, **S.-M. LIN**, *Northwestern Polytechnical University, Xi'an, China* (APS)

14:50 (75.5) Solution of Inverse Problems by the General Maximum Entropy Method, X. CHEN, **W.X. ZHANG**, *Southeast University, Nanjing, China* (APS)

15:10 **COFFEE/CAFÉ**

15:30 (75.6) Electromagnetic Imaging Method for Line Sources Buried in a Dielectric Half-Space, **T. UNO**, Y. HE, S. ADACHI, *Tohoku University, Sendai, Japan*

15:50 (75.7) An Inversion Approach for the Simultaneous Reconstruction of Two-Dimensional Permittivity and Conductivity Profiles, **T.M. HABASHY**[1], M.L. ORISTAGLIO[1], A.T. DE HOOP[2], [1]*Schlumberger-Doll Research, Ridgefield, CT, USA;* [2]*Delft University of Technology, Delft, The Netherlands*

16:10 (75.8) Accelerated Iterative Algorithms for the Solution of Nonlinear Inverse Scattering Problems, **Y.M. WANG**, W.C. CHEW, *University of Illinois, Urbana, IL, USA*

16:30 (75.9) High Resolution Microwave Imaging, **H.-J. LI**, *National Taiwan University, Taipei, Taiwan, China*

16:50 (75.10) An Electromagnetic Inverse Problem in Determination of Certain 2D Source Distributions, **Z.A. DELECKI**, *National Research Council Canada, Winnipeg, MB, Canada* (APS)

ELECTROMAGNETIC IMAGING METHOD FOR LINE SOURCES BURIED IN A DIELECTRIC HALF-SPACE

Toru Uno*, Yiwei He, and Saburo Adachi
Department of Electrical Engineering
Tohoku University, Sendai, 980 Japan

Many types of subsurface radar have been developed for detecting the buried objects in the ground such as water pipes, electric communication lines, etc.. The most widely used imaging method is a synthetic aperture technique in which only the direct wave between a transmitting antenna and the buried object is adopted as an electromagnetic scattering mechanism. However, this imaging method is still insufficient, because the exact scattered field can be interpreted as the sum of the direct wave, the sub-surface wave propagating along the interface and the combination of these two waves (T.Suzuki, et al., ISAP, 735-738, 1989, T.Uno, et al. IEEE AP-S Int. Symp. 898-901, 1990). Furthermore, it has been shown that these waves may be possible to have the same amplitude in some cases.

As a first step to establish the three dimensional imaging method of the buried objects, this paper studies a reconstruction method to detect the line current sources buried in a homogeneous dielectric half-space. The dielectric constant is assumes as a known constant. The line current source is the most simple model of the secondary current on the buried metallic cylinder. The radiated electric field $E(x,z)$ above the ground surface due to the radiating line source current is expressed by an integral form. Using this relation, we can obtain

$$p\Big((s-\mathbf{r}\cdot\hat{s})\frac{n}{c}\Big)=\frac{\lambda_1+\lambda_2}{\mu_0 c}\int_{-\infty}^{\infty}E(x,z,\frac{ns-\lambda_1 z-\lambda x}{c})dx$$

$$\lambda_1=\sqrt{1-\lambda^2},\quad \lambda_2=\sqrt{n^2-\lambda^2},\quad \hat{s}=(\lambda/n,\lambda_2/n)$$

where n is a refractive index, c is a light velocity, (x,z) is an observation point and $-1<\lambda<1$ is an arbitrary constant. p is the amplitude of the current source projected onto the plane determined by $\hat{s}$ and is referred to as an image function in this paper. The location of the line source is reconstructed by synthesizing the image function p for λ. The validity of this method is tested by numerical simulation.

AN INVERSION APPROACH FOR THE SIMULTANEOUS RECONSTRUCTION OF TWO-DIMENSIONAL PERMITTIVITY AND CONDUCTIVITY PROFILES

T.M. Habashy*, M.L. Oristaglio*, and A.T. de Hoop+

* Schlumberger-Doll Research
Old Quarry Road, Ridgefield, CT 06877-4108

+ Laboratory of Electromagnetic Research
Delft University of Technology
P.O. Box 5031, 2600 GA Delft, The Netherlands

In this paper we present a new inversion algorithm for the reconstruction of two-dimensional permittivity and conductivity profiles. The execution of this algorithm can be summarized in the following three steps: ***Step* 1** (The Inverse Source Problem): From the known data on the surface of the probed medium, the currents induced inside the medium are solved for from either the electric or the magnetic field source-type integral equation. ***Step* 2** (The Forward Problem): Knowing the currents induced inside the slab (obtained from step 1), the electric field can be calculated everywhere (inside as well as outside the probed medium) from the electric field equation. ***Step* 3** (The Inversion): From the knowledge of the currents induced inside the slab (obtained from step 1) and the electric field inside the slab (computed from step 2), the unknown difference variation of the complex permittivity is obtained from the constitutive relation which relates the induced currents to the internal electric field.

This method recasts the inversion, which is nonlinear in nature, in terms of the solution of a set of linear equations. The objective is to explore the possibility of developing an inversion algorithm which does not rely on an iterative approach. In this paper, we will discuss how to deal with the nonuniqueness issue associated with the implementation of the inverse source problem of step 1. We will also explore various ways of implementing the inverse source problem and study their effect on the performance of the inversion. Moreover, we will look at various ways to accommodate multiple measurement with the goal of narrowing down the class of solutions.

The inversion scheme is demonstrated for the case where the exciting source is of the dipole type that generates only TE polarized waves. The data required for inversion are the tangential component of the electric and/or the magnetic field at various frequencies and various locations on the surface of the probed medium.

Accelerated Iterative Algorithms for the Solution of Nonlinear Inverse Scattering Problems

Y. M. Wang* and W. C. Chew
Electromagnetics Laboratory
Department of Electrical Engineering
University of Illinois
Urbana, IL 61801

One problem of the iterative algorithms for the solution of nonlinear inverse scattering problems is the intensive computation time involved. For any iterative nonlinear inverse scattering algorithm, both the direct and inverse solutions in the iteration procedure are needed (Y. M. Wang & W. C. Chew, *Int. J. Imaging Syst. Technol.*, vol. 1, no. 1, pp. 100-108, 1989; W. C. Chew & Y. M. Wang, *IEEE Trans. Medical Imag.*, vol. 9, no. 2, pp. 218-225, 1990). Thus, matrix inversions are required. By using the standard Gaussian elimination algorithm, computational time for the matrix inversion is proportional to N^3. Therefore, the computational complexity of iterative nonlinear inverse scattering algorithms usually is N^3, where N is the number of meshes in the object.

One way to reduce the computational complexity of the algorithms is to apply the conjugate gradient method to both the direct and inverse solutions of the algorithms. However, the conjugate gradient method provides a solution for only one incident wave at a time. If M, the number of the incident fields (or transmitters) is large, overall computation time, which is proportional to MN^2, can be quite computationally intensive for a large object.

In order to significantly accelerate the algorithm, we have applied the fast recursive operator algorithm (Y. M. Wang & W. C. Chew, *Micro. Opt. Tech. Lett.*, vol. 3, no. 3, pp. 102-106, 1990; W. C. Chew & Y. M. Wang, *Micro. Opt. Tech. Lett.*, vol. 3, no. 5, pp. 164-169, 1990) to the solution of the direct scattering problem in each iteration step. Since the fast algorithm gives a full solution of the direct scattering problem, the computational time will be independent of the number of the transmitters (or incident fields) in the experimental configuration of the inverse scattering problem. The computational complexity of the fast algorithm is N^2 in high frequency cases. Therefore, if the conjugate gradient method is applied to the inversion part of the algorithm, overall computational time will be roughly proportional to N^2. This represents a significant reduction of the computational time.

HIGH RESOLUTION MICROWAVE IMAGING

Hsueh–Jyh Li

Department of Electrical Engineering

National Taiwan University

Taipei, Taiwan, China

In this paper we develop and analyze algorithms for extrapolating the scattered field along the frequency direction and the azimuthal direction and discuss their effects on the image resolution for polar format processing and rectangular format processing. Simulation and experimental results show that extrapolation along the frequency direction is a meaningful process. The reason is that at high frequency the scattered field of a complex–shaped object can be approximated by a superposition of the fields scattered by discrete scattering centers. In other words, the field is a superposition of discrete sinusoidal sources. It is well known that the linear prediction method is especially suited for this type of problem. Extrapolation in the azimuthal direction is also meaningful for small angle imaging using rectangular format processing. However, it does not improve image resolution of complex–shaped objects for wide angle imaging. A promising application of the above observations is in the imaging of moving targets. By applying the extrapolation algorithms described in this paper, we may obtain an image with acceptable resolution using signals with narrower bandwidth (or longer pulses) and a smaller angular interval than those required when processed by the conventional Fourier transform range–Doppler method.

Direct and Inverse Theories in Electromagnetic Imaging – Memorial Session in Honour of R.H.T. Bates I

Room 3018 Salle
Joint URSI/AP-S Session 92

Théorie directe et inverse de l'imagerie en électromagnétisme Séance en mémoire de R.H.T. Bates I

Chairs/présidents: P. NAPIER, USA; I.J. LAHAIE, USA

08:30 () **OPENING REMARKS**

08:50 (92.1) From Linearized to Quantitative Electromagnetic Inverse Scattering, K.J. LANGENBERG[1], **D.G. DUDLEY**[2], D. HUO[1], [1]*University of Kassel, Germany;* [2]*University of Arizona, Tucson, AZ, USA*

09:10 (92.2) Nonlinear Two-Dimensional Velocity Profile Inversion in the Time Domain, **M. MOGHADDAM**, W.C. CHEW, *University of Illinois, Urbana, USA* (APS)

09:30 (92.3) Simultaneous Reconstruction of the Permittivity and Conductivity of an Inhomogeneous Slab from Transient Scattered Fields Due to a Point Source, S. HE, **S. STRÖM**, *Royal Institute of Technology, Stockholm, Sweden* (APS)

09:50 (92.4) Reconstruction of Complex Permittivity in Two Dimensions, **S. BERNTSEN**, J.B. ANDERSEN, *Aalborg University, Aalborg, Denmark*

10:10 **COFFEE/CAFÉ**

10:30 (92.5) Integral Equations and Wave Propagation in an Inhomogeneous Medium, **D.J.N. WALL**, *University of Canterbury, Christchurch, New Zealand*

10:50 (92.6) Effect of View Angle Variations in Vector Diffraction Tomography, **W.-M. BOERNER**[1], Y. YAMAGUCHI[2], M. MOCHIDA[2], T. ABE[2], [1]*University of Illinois, Chicago, and* [2]*Niigata University, Niigata, Japan*

11:10 (92.7) Imaging from Scattered Electromagnetic Field and Intensity Data, **M.A. FIDDY**, *University of Lowell, MA, USA*

11:30 (92.8) Review of the Inverse Source Problem for Quasihomogeneous, Partially Coherent Sources, **I.J. LaHAIE**, *Environmental Research Institute of Michigan, Ann Arbor, MI, USA*

11:50 (92.9) Inversion of 10 GHz Scattered Field Data from Strong Scatterers, **R.V. McGAHAN**[2], F.C. LIN[1], M.A. FIDDY[1], [1]*University of Lowell, MA, and* [2]*Rome Laboratory, Hanscom AFB, MA, USA* (APS)

FROM LINEARIZED TO QUANTITATIVE ELECTROMAGNETIC INVERSE SCATTERING

K.J. Langenberg*, D.G. Dudley+, D. Huo
Dept. El. Engineering
University of Kassel
D-3500 Kassel, FRG

+ Dept. El. Engineering
University of Arizona
Tucson, AZ, USA

Electromagnetic inverse scattering plays an important role in radar target identification, medical diagnostics, and nondestructive testing of materials. Recently, it was emphasized that the full polarimetric information of the scattered field should be utilized.

Starting with a linearization of the scattered field representation in terms of either the Born or the Kirchhoff approximation of the equivalent sources a common framework of electromagnetic inverse scattering is available via either frequency or illumination angle integration of the polarimetric Porter-Bojarski integral equation. Numerical results with relevance to nondestructive testing of ceramics prove the superiority of polarimetric versus scalar algorithms.

Extensions of the above diffraction tomographic concept of electromagnetic inverse scattering are discussed for those cases where linearizations cannot be tolerated any more. Their basis is either a simultaneous TE- and TM-electromagnetic inverse profiling concept as well as a modification of the Porter-Bojarski equation.

Reconstruction of Complex Permittivity in Two Dimensions

Svend Berntsen* and Jørgen Bach Andersen.

Institute ot Electronic Systems, Aalborg University,
Fr.Bajersvej 7,DK 9000, Aalborg, Denmark.

The present work is motivated by the need for an accurate algorithm in reconstructing permittivity data in biological applications such as following the development of the temperature distribution noninvasively during a hyperthermia treatment.

Previously the reconstruction problem using quasi-static boundary data was investigated by the authors. For a circular cylinder a very simple mapping from the boundary data onto the conductivity was found. However that reconstruction problem is an ill conditioned one which works well only for a smoothly varying conductivity.

The obvious way to improve the reconstructions will be to choose a larger space of boundary data,i.e. a set of boundary electric and magnetic fields will be measured for time harmonic excitations. The basic problem will then be to find the mapping from these boundary fields onto the complex permittivity.

The paper treats the problem of reconstruction of the permittivity of an inhomogeneous medium from measurements of the boundary field. It is shown that the complex permittivity satisfies a set of nonlinear projection equations. In the nearly homogeneous case these equations reduce to linear ones. For an appropriately chosen set of boundary experiments these equations determine the permittivity uniquely. For electric or magnetic excitation of a circular cylinder the projection equations may explicitly be solved. That is the permittivity is directly expressed in terms of the boundary electric and magnetic field. However we need the boundary experiments for all frequencies. It is proved that the mapping from the set of boundary experiments onto the permittivity is continuous. That is the inverse problem is a well posed one. As an example a specified permittivity for which the exact solution of the Maxwell equations is known is treated. In that case we show that the approximately reconstructed permittivity is indeed very close to the given one.

INTEGRAL EQUATIONS AND WAVE PROPAGATION IN AN INHOMOGENEOUS MEDIUM

David J N Wall
Department of Mathematics, University of Canterbury,
Christchurch, New Zealand.

Central to the solution of the inverse scattering problem for wave propagation involving inhomogeneous media is the solution of the associated direct scattering problem. We present results on various integral equation systems, for solution of the direct problem.

It has long been known that many integral equation formulations for the scattering of waves from impenetrable obstacles suffer from lack of uniqueness at certain values of the wave number of the incident wave; although the scattering problem itself possesses a unique solution. We extend these ideas in this presentation to examine existence and uniqueness of systems of integral equations that arise from wave scattering from compactly supported inhomogeneous media with spatially varying wave properties, embedded within the homogeneous full space.

This problem can be described mathematically as requiring the solution of the Helmholtz equation and this equation is to be solved subject to the solution satisfying transmission boundary conditions across the interface between the inhomogeneous and homogeneous regions. It is these transmission boundary conditions which provide the *coupling* between the exterior and the interior Helmholtz equations; the resulting problem is called a transmission problem. If the transmission boundary conditions are such that the wave field and its normal derivative are continuous across the interface a single Fredholm integral equation for the field within the inhomogeneous region can be derived. Such formulations are called volume (or polarisation-source) formulations and have been extensively investigated in the engineering science literature both for computational and perturbation solutions. However when the transmission boundary conditions do not satisfy this condition, a system of integral equations must be studied. If the medium is homogeneous the system need only involve surface integral operators. This is not the case when the medium is inhomogeneous, unless an appropriate Green's function is available — this occurs rarely for the Helmholtz equation — and so the system also involves volume integral operators. We study the properties of such systems in this paper. We show that the integral equation systems can have uniqueness problems and illustrate how this may be overcome. Existence and convergence results for some of these integral equation systems is given.

EFFECT OF VIEW ANGLE VARIATIONS IN VECTOR DIFFRACTION TOMOGRAPHY

Wolfgang-Martin Boerner*
Communications and Sensing Laboratory (M/C 154)
Department of Electrical Engineering and Computer Science
University of Illinois at Chicago
Chicago, IL/USA 60680

and

Yoshio Yamaguchi, Masahisa Mochida, and Takeo Abe
Faculty of Engineering, Niigata University
Ikarashi 2-8050, Niigata-shi, 950-21
Japan

Under the Born/Rytov approximations, the effect of view angle variations on image reconstruction in vector diffraction tomography is investigated. This paper deals with internal image reconstructions of infinitely long, lossless and lossy dielectric cylinders placed in free space and/or in a weakly diffracting, slightly lossy medium. Emphasis is placed on showing how both the co-polarized and the cross-polarized diffracted terms vary with incident angle in the image reconstruction because any oblique incidence on a curved surface always produces repolarization (polarization state transformation). The cross-polarized component was found to contain very crucial object information on edges, i.e., the boundary position of the cylinder even under rather noisy background conditions can be clearly identified. It is demonstrated that the extension of scalar to vector diffraction microwave tomography will play an important role in precise image reconstruction in high resolution microwave imaging and sounding.

This research was initiated during the tenure (1976 January-July)* of the author as a visiting professor with the Department of Electrical Engineering, Ilam Campus of the University of Canterbury at Christchurch, N.Z. within a foremost research invigorating atmosphere created by the dynamic host. Therefore, it is with great indebtedness that this paper is dedicated to Richard H.T. Bates, a great teacher, a relentless fighter for the advancement of imaging sciences, and a true scholar:

> "It will always be with great joy that we - all of his many international guests from far away - recall these truly rewarding interactions with Richard and his lively flock of talented students."

*G.R. Dunlop, W-M. Boerner, R.H.T. Bates, "On an extended Rytov approximation and its significance for remote sensing and inverse scattering", Opt. Comm., Vol. 18(4), 1976, pp.421-423.

IMAGING FROM SCATTERED ELECTROMAGNETIC FIELD AND INTENSITY DATA

M. A. Fiddy
Department of Electrical Engineering, University of Lowell,
Lowell, MA 01854, USA

Richard Bates made many contributions to the subject of image reconstruction for remote sensing and inverse scattering (e.g. R.H.T. Bates and M.J. McDonnell, "Image Restoration and Reconstruction", Clarendon Press, 1986). Quantitative imaging by inverting (experimental) scattered field data remains a challenging problem. The most numercially tractable inverse scattering algorithms currently rely on linearizing approximations, such as the Born or Rytov approximation. These approximations, while invalid for most scattering situations of interest, have had modifications made to them (e.g. R.H.T. Bates, W.M. Boerner and G.R. Dunlop, "An extended Rytov approximation and its significance for remote sensing", Opt. Comm., 18, (1976), 421; R.H.T. Bates, "JWKB/Rayleigh-Gans (Born) inverse scattering approximation and reconstruction algorithm", Inverse Problems, 4, (1988), L29; F.C. Lin and M.A. Fiddy, Image estimation from scattered field data", Int. J. Imaging Systems and Tech., Dec 1990). Despite the limited applicability of even these modified techniques, such methods lead to a Fourier relation between the so-called induced source distribution and the distribution of the scattered far-field.

This Fourier relation is the key to many largely unexploited analytical contraints that exist between the real and imaginary parts of the scattered field and its magnitude and phase (R.H.T. Bates, B.K. Quek and C.R. Parker, "Some implications of zero sheets for blind deconvolution and phase retrieval", J.O.S.A.A7, (1990), 468.; R.H.T. Bates, H. Jiang and B.L.K. Davey, "Multidimensional system idenification through blind deconvolution", Multidimensional Systems and Signal Processing, 1, (1990), 127.; M.S. Scivier and M.A. Fiddy, "Phase ambiguities and the zeros of multidimensional band-limited functions", J.O.S.A. A2, (1985), 693.). In this talk, the importance of the intrinsic analytic properties of the scattered field (and its intensity), for successful application of inversion techniques (such as the Rytov approximation and homomorphic filtering-based approach), will be discussed. Considerable insight is available, as a result, on the range of validity of these methods for quantitative high resolution imaging from real data as well as directions for further improvement.

REVIEW OF THE INVERSE SOURCE PROBLEM FOR QUASIHOMOGENEOUS, PARTIALLY COHERENT SOURCES

Ivan J. LaHaie
Enviornmental Research Institute of Michigan
Microwave Science Laboratory
Advanced Concepts Division
P.O. Box 8618, Ann Arbor, Michigan 48107

The inverse source problem for quasihomogeneous, partially coherent sources (LaHaie, J. Opt. Soc. Am., 3A, 1073-1079, 1986) is reviewed. Comparisons are made between the formulations for two-dimensional and three-dimensional source distributions. A unified approach is presented herein by considering the two-dimensional source distribution as a three-dimensional distribution with delta-function support in one dimension. It is shown that measurements of the cross-spectral density of the field on a surface enclosing the source are sufficient to reconstruct the unknown source cross-spectral density for two-dimensional sources, while they are insufficient for three-dimensional sources. The use of a priori information and its effect on the uniqueness of the three-dimensional inverse source problem is discussed. In particular, a set of supplemental data and associated inversion algorithm is described which guarantees uniqueness of the three-dimensional inverse and which is less restrictive than that previously identified (A.J. Devaney, J. Math. Phys., 20, 1687-1691, 1980).

Direct and Inverse Theories in Electromagnetic Imaging – Memorial Session in Honour of R.H.T. Bates II

Room 3018 Salle Joint URSI/AP-S Session 109

Théorie directe et inverse de l'imagerie en électromagnétisme Séance en mémoire de R.H.T. Bates II

Chairs/présidents: R.P. MILLANE, USA; D.J.N. WALL, New Zealand

13:30 (109.1) Numerical Implementation of the Surface Radiation Condition, **R.D. MURCH**, *The University, Dundee, UK*

13:50 (109.2) Imaging Problems in High Resolution Radio Astronomy, **P.J. NAPIER**, *National Radio Astronomy Observatory, Socorro, NM, USA*

14:10 (109.3) High Spatial Resolution Astronomical Imaging with Shift-and-Add Analysis, **J.C. CHRISTOU**, *National Optical Astronomy Observatories, Tucson, AZ, USA*

14:30 (109.4) Image Reconstruction in X-Ray Crystallography, **R.P. MILLANE**, *Purdue University, West Lafayette, IN, USA*

14:50 (109.5) From Radio-Astronomy to Medical Imaging, **T.M. PETERS**, *McGill University, Montreal, PQ, Canada*

15:10 **COFFEE/CAFÉ**

15:30 (109.6) Regularized Iterative Deblurring of a Point Spread Variant Blur, **J.H.T. BATES**, B.L.K. DAVEY, *McGill University, Montreal, PQ, Canada*

15:50 (109.7) The Bates Algorithm: Fishing for Images in Speech, **H.J. JELINEK**, *Electronic Design Associates, Costa Mesa, CA, USA*

16:10 (109.8) WITHDRAWN/ANNULÉ,

16:30 (109.9) Two-Dimensional Profile Reconstruction, **R.E. KLEINMAN**[1], P.M. VAN DEN BERG[2], [1] *University of Delaware, Newark, DE, USA;* [2] *Delft University of Technology, Delft, The Netherlands* (APS)

NUMERICAL IMPLEMENTATION OF THE SURFACE RADIATION CONDITION

Dr R.D. Murch
Department of Mathematics and Computer Science, The University,
Dundee DD1 4HN, Scotland, UK.

The surface radiation condition (SRC) is a recently developed technique for approximately obtaining the solution of wave scattering from obstacles. Application of SRC has produced results which are usefully accurate over a wide range of frequencies. In many of the results reported SRC has performed significantly better than physical optics and may become accepted as a viable alternative to it.

The range of obstacles on which SRC has been applied however has been restricted. The obstacles have generally been limited to those whose surface curvature is either constant or piecewise constant. This is largely because the solution of scattering by invoking SRC from these obstacles can be obtained without resorting to numerical analysis. The usefulness of any approximate technique such as SRC however rests on being able to apply it to obstacles whose surfaces are arbitrary. It appears that non-numerical solutions of scattering by invoking SRC on obstacles whose surfaces are arbitrary is highly unlikely. Consequently it is desirable that a numerical method is developed for obtaining approximate solutions of scattering by invoking SRC.

SRC also has a variety of equations which have been proposed for its implementation. The salient differences between these equations are that there are differing terms which incorporate the effects of the surface curvature of the obstacle. It has been shown approximately that when the curvature varies "slowly" over the obstacles surface the various SRC equations perform similarly. Whether these extra curvature terms are significant for "quickly" varying curvatures is still in some debate. Consequently it would also be desirable to investigate which of these SRC equations performs best for such surfaces. Because such an investigation rests largely on being able to invoke SRC on surfaces which have varying curvatures a numerical means for obtaining SRC solutions is also necessary.

In this presentation a numerical method suitable for determining solutions of scattering by invoking SRC from surfaces of revolution is given. Surfaces of revolution encompass obstacles whose surface curvature is not constant such as the prolate and oblate spheroids. Furthermore, the numerical method maybe used in conjunction with any of the proposed SRC equations. This allows both an increased range range of obstacles for which SRC can be employed and also a full investigation of the varying effect of the curvature terms in the various SRC equations.

The computational advantages of invoking surfaces of revolution over completely arbitrary three-dimensional surfaces are two fold. The separation of variables technique can be employed on the SRC equations when the obstacles are invoked on surfaces of revolution. It transpires that the SRC equations can be separated into two ordinary differential equations so that one can be solved analytically. This allows the numerical method to be reduced to solving a single ordinary differential equation. The other advantage of invoking SRC on surfaces of revolution is that the boundary conditions can be straightforwardly applied.

The numerical method is demonstrated by invoking scalar waves with Neumann or sound hard boundary conditions on spheres and prolate spheroids. Validation of the numerical method is performed by comparing its solution with the analytic SRC solution of scattering from spheres. Also, for the prolate spheroid the various SRC equations are invoked in order to demonstrate the effectiveness of each equation.

IMAGING PROBLEMS IN HIGH RESOLUTION RADIO ASTRONOMY

Peter J. Napier
National Radio Astronomy Observatory
Socorro, NM 87801, USA

In a synthesis radio telescope an array of antennas is used to measure the two-dimensional spatial coherence function of the field radiated by an astronomical object. The two dimensional brightness distribution (a "radio image") of the object is then computed as the Fourier Transform of the measured spatial coherence function. The technique of Very Long Baseline Interferometry (VLBI) uses this synthesis principle to obtain radio images of astronomical objects with resolutions of a few milli-arcseconds or better. In VLBI the signals received from an astronomical object by antennas separated by hundreds or thousands of kilometers are recorded on broadband tape recorders using a hydrogen maser clock as a time standard. After the observation the tapes are brought together and the recorded signals are correlated to provide the measurement of the spatial coherence function. The quality of VLBI images made in this way are degraded by two problems: the sparseness of the antenna array results in the spatial coherence function being significantly undersampled and there are phase errors in the coherence function measurements caused by atmospheric pathlength variations and clock instabilities. In this paper we review the techniques that radio astronomers have developed to solve these problems with the goal of indicating their possible usefulness in other imaging fields where observations must be made with sparse arrays or through unstable propagation media.

The problem of an undersampled spatial coherence function is essentially a deconvolution problem in which one wishes to remove from the image the effects of a point spread function contaminated by the undersampling. A subtractive deconvolution procedure known as "CLEAN" and a maximum entropy deconvolution algorithm have proven effective for this purpose. Another technique which is now coming into use is "multifrequency synthesis" in which the coherence function is measured at several frequencies across a band that is a few tens of percent in bandwidth. This increases the amount of coherence information available to form the image but the fact that the image varies somewhat over the observing band must be accounted for in the imaging algorithm. The problem of phase errors has been successfully attacked using an algorithm called "self-calibration". The basis for this technique is the fact that phase errors due to the clock, electronics or atmosphere associated with a particular antenna occur identically in all coherence measurements made using that antenna. In most cases, where there is sufficient signal-to-noise ratio, there is enough information in the coherence measurements to determine the phase errors and to remove their effects from the image.

HIGH SPATIAL RESOLUTION ASTRONOMICAL IMAGING WITH SHIFT-AND-ADD ANALYSIS

Julian C. Christou
Kitt Peak National Observatory
National Optical Astronomy Observatories[1]
Tucson, AZ 85726-6732, USA

Atmospheric turbulence severely degrades the angular resolution achievable with ground-based telescopes by factors $\sim 10\times$ worse than their theoretical diffraction-limits at visible and infrared wavelengths. Over the past two decades a number of techniques have been developed to recover the high-spatial frequencies lost in conventional astronomical imaging. These consist of taking short exposure images typically $\sim$ 10–50 ms which "freeze" the effects of the atmospheric turbulence. These images have a speckle structure where each speckle has the size of the diffraction-limited image. Post-processing techniques of sets of these images obtained for the target object and a point souce reference generally consist of computing ensemble average second or third order Fourier spectra.

By comparison, the shift-and-add method (SAA) (Bates, *Opt.Commun.*, **19**, 240, 1976), stacks each image on the pixel with the maximum signal, i.e. the brightest speckle, without the requirement of Fourier analysis. Several variants of the technique have also been proposed (see Hege, in "Diffraction-limited Imaging with Very Large Telescopes", ed. Alloin & Mariotti, 1989). SAA analysis yields a diffraction-limited component sitting atop a background "fog" caused by the random addition of the remaining speckles in each image. The relative strengths of these two components is dependent upon the quality of the seeing, as characterised by the Fried parameter or atmospheric coherence length r_0, with greater strength in the diffraction-limited component under better seeing conditions.

With the advent of 2D infrared detectors high-spatial resolution imaging at infrared wavelengths is possible. This is more advantageous than at visible wavelengths because the atmospheric degradation improves, $r_0 \propto \lambda^{6/5}$. For such observations SAA analysis becomes a powerful technique. By tracking the individual short exposure images on the brightest speckle a significant gain in image quality is obtained as seen in NOAO 4m and MMT 6.8m data. This technique allows a "quick look" at the data and with careful calibration yields results commensurate with the higher-order analysis.

Active removal of the wavefront tilt at the aperture yields significantly improved image quality for good seeing conditions. Tracking the brightest speckle improves upon this and real time operation could be implemented with a rapid steering mirror. Results obtained from simulated and real data for different apertures and seeing coditions illustrate the benefits of passive SAA imaging and the potential for active correction.

[1]Operated by the Association of Universities for Research in Astronomy Inc. (AURA) under cooperative agreement with the National Science Foundation.

IMAGE RECONSTRUCTION IN X-RAY CRYSTALLOGRAPHY

R. P. Millane
Whistler Center for Carbohydrate Research, Smith Hall,
Purdue University, West Lafayette, Indiana 47907, U.S.A.

X-ray crystallography is an inverse scattering problem that involves reconstructing the three-dimensional electron density in the unit cell of a crystal, from measurements of diffracted x-rays. Analysis of the electron density distribution reveals the structure (positions of the atoms) of the molecule under study. The scattering is weak, so that the diffracted complex amplitude is the Fourier transform of the electron density. The reconstruction is complicated by two experimental constraints: (1) Only the intensities of the diffracted x-rays are detected, and (2) the crystalline (periodic) nature of the scatterer restricts diffraction to discrete directions. The first constraint means that inverting the scattering data involves solution of a three-dimensional phase problem. The second constraint leads to a sub-Nyquist sampling of the Fourier intensity. Multi-dimensional phase problems almost always have unique solutions (R.G. Lane, W.R. Fright & R.H.T. Bates, *IEEE Trans.*, ASSP-35, 520-525, 1987). However, this is based on analytic properties of the transform, that depend on it being defined continuously in Fourier space. Sub-Nyquist sampling therefore leads to non-uniqueness in general. This is in contrast to usual imaging problems. A unique solution requires additional information in the form of *a priori* constraints or independent measurements. The additional information utilized depends on the type of molecule under study.

For small molecules ($< \sim 200$ atoms), diffraction data is available at high spatial frequencies, and the impulsive nature of the image (significant electron density is confined to small regions surrounding the atomic nuclei) allows probabilistic relationships between the phases of the diffraction signals to be derived. These are reminissent of phase closure and triple correlation relationships used in radio, and optical, astronomical imaging (R.P. Millane, *J. Opt. Soc. Am. A*, 7, 394-411, 1990). Phases can usually be reliably estimated using these relationships. The variance of the phase estimates increases with an increasing number of atoms in the molecule however, so that this method is unsuitable for large molecules. For larger molecules, a unique solution relies on either structural redundancy in the molecule, or on making additional diffraction measurements on appropriately modified crystals, or both. The former situation results effectively in a denser sampling the transform intensity, and the later can be likened to holographic processing. For polymeric molecules, the diffraction data is cylindrically averaged, and the solution involves separating the angular Fourier terms, as well as phasing them.

Image reconstruction in x-ray crystallography will be reviewed in the context of general imaging problems, and the implications of redundancy, dimensionality and sampling, on uniqueness and stability, will be discussed.

From Radio-astronomy to Medical Imaging

Terry M Peters PhD FCCPM
NeuroImaging Laboratory
McConnell Brain Imaging Centre
Montreal Neurological Institute
McGill University.
Montreal QC, Canada.

A common thread in much of the medical imaging that has developed over the past 20 years has been the Fourier transform. It was Richard Bates' interest in radio-interferometry, as well as his fascination with problems of medical imaging that prompted an initial interest in applying Fourier techniques to medical imaging in general and to Computed Tomography in particular. This resulted 20 years ago in one of the earliest technical papers advocating Fourier techniques for reconstructing cross-sections from radiographic projections (Bates and Peters, NZ J Science 14:883-896, 1971). Since those early days, medical imaging has exploded into a multi-billion dollar industry. The CT scanner has become the workhorse imaging modality in the radiology department, while its more recent relative, the MR scanner, is rapidly gaining ground as a technique of even greater importance.

With the enormous amount of data being generated by these imaging devices, (eg 25 MB for an MRI study) at a quality unforeseen at the time of the early experiments, 3D techniques were soon applied to the visualization of these images.

This presentation chronicles the development of some of these techniques, from the late 1960s when the author was a graduate student of Professor Bates, to the present time where 3D imaging is used routinely in radiology and surgery. Some of the earliest CT work performed in Bates' laboratory, which at that time was still primarily concerned with problems in electromagnetics and radioastronomy, is discussed. At that time the excitement that we felt on producing our first reconstructions was not even shared with any particular enthusiasm by our medical colleagues!

The CT age, along with the ready availability of computers capable of handling the enormous computational task of reconstructing images, heralded the arrival of the age of electronic imaging in medicine. The author continues to be a part of this revolution, having been involved in the early experience with MRI in Canada, and presently with the clinical application of these modalities, including 3D imaging, in a neurological environment.

REGULARIZED ITERATIVE DEBLURRING OF A POINT SPREAD VARIANT BLUR

Jason H.T. BATES* and Bruce L.K. DAVEY, Meakins-Christie Labs. and Biomed. Eng. Dept., McGill Univ., Montreal, Quebec, CANADA.

The blurring of a signal $x(t)$ by a point spread invariant blurring function $h(t)$ is described by the convolution integral

$$y(t) = \int_0^t x(\tau)h(t - \tau)d\tau + n(t) \qquad (1)$$

where $n(t)$ is the ubiquitous measurement noise. Deblurring $y(t)$ to get an estimate $\hat{x}(t)$ of $x(t)$ is known as deconvolution, the classical approach to which is to invoke the convolution theorem for Fourier transforms and employ the Wiener filter thus:

$$\hat{X}(s) = Y(s)W(s)/H(s) \qquad (2)$$

where $\hat{X}(s)$, $Y(s)$ and $H(s)$ are the Fourier transforms of $\hat{x}(t)$, $y(t)$ and $h(t)$, respectively, and $W(s)$ is a window in the frequency (s) domain designed to attenuate those frequencies in $\hat{x}(t)$ dominated by $n(t)$ while leaving unaffected those dominated by the signals of interest. Although the Wiener filter is supposed to be optimal in the least squares sense, its practical realization usually amounts to a "rationalized" low-pass filter.

Another approach to deconvolution, suitable for large sparse images characterized by isolated point sources, is that known as CLEAN which proceeds as follows. Denoting the blurred image as $y_0(t)$ and an initial reconstuction (the CLEAN map) $\hat{x}_0(t)$ equal to zero. CLEAN iterates on $y_i(t)$ and $\hat{x}_i(t)$ thus:

$$y_{i+1}(t) = y_i(t) - \alpha y_i(t_k)h(t - t_k)/h(0) \qquad (3)$$

$$\hat{x}_{i+1}(t) = \hat{x}_i(t) + \alpha y_i(t_k)\delta(t - t_k)/h(0) \qquad (4)$$

where α is the loop-gain ($0 \leq \alpha \leq 1$), $\delta(t)$ is the Dirac delta-function and t_k is the position of the maximum in $y_i(t)$. Bates *et al.* (Mon. Not. R. Astr. Soc. 211, 1-14, 1984) showed that CLEAN performs an iterative Wiener filter if $h(t-t_k)$ in Eq. 3 is replaced by the inverse Fourier transform of $H(s)/W(s)$.

The point spread variant blurring problem is described by replacing $h(\tau - t)$ in Eq. 1 with $h(\tau, \tau - t)$. Its solution is sensitive to noise in $y(t)$ in the same way that conventional deconvolution is, but Fourier transform methods cannot be used because the convolution theorem no longer applies. However, CLEAN can be used to deblur a signal contaminated by a point spread variant blurring function if $h(t - t_k)$ in Eq. 3 is replaced with $h(t_k, t - t_k)$ plus $\beta\delta(t - t_k)$ for some $\beta > 1.0$. The addition of the β-scaled δ-function regularizes the solution and produces a smooth deblurred function $\hat{x}(t)$.

THE BATES ALGORITHM: FISHING FOR IMAGES IN SPEECH

H.J. Jelinek
Electronic Design Associates
3184-H Airway Avenue - Costa Mesa, CA 92626

The algorithm invented by R.H.T. Bates for image enhancement is referred to in his work as the "shift and add" algorithm. I propose to refer to the algorithm as the Bates Algorithm. The principles behind the algorithm that were used by Bates for image processing have been applied successfully to other problems. In this paper, a particular application of the algorithm to one dimensional speech signal processing will be discussed.

Voiced speech is generated by periodic expulsion of air through the glottis into the vocal tract. These puffs of air excite the vocal cavity, and resulting resonances produce an acoustical signal that exits through the mouth and nose. The acoustical signal that we hear may be thought of as the convolution of the glottal pulse with the vocal tract.

It is very difficult to directly measure the glottal pulse. Consequently, Bates and some of his students developed a method for deconvolving the glottal pulse from the measured acoustical signal. The technique is an interesting variant of the Bates Algorithm and provides an estimation of the glottal pulse signal that has potential applications in diagnosing voice disorders, in speaker identification and in low bit rate speech. Using the principles described in this paper, some clever engineer may find a way to apply the approach to other problems such as detection of low level signals in noise. For this reason, the method -- and some recent developments -- are described in this paper.

AUTHOR INDEX/INDEX DES AUTEURS

1992 JOINT SYMPOSIA

- **IEEE-APS INTERNATIONAL SYMPOSIUM**
- **URSI RADIO SCIENCE MEETING**
- **NUCLEAR EMP MEETING**

Hyatt Regency Chicago Hotel
Chicago, Illinois, USA

July 18–25, 1992

The 1992 IEEE-APS International Symposium sponsored by the IEEE Antennas and Propagation Society, the URSI Radio Science Meeting sponsored by USNC Commissions A, B, D, E and K of the International Union of Radio Science, and the Nuclear EMP Meeting sponsored by the Permanent NEM Committee will be held at the Hyatt Regency Chicago Hotel from July 18 through 25, 1992. The technical sessions will cover the five-day period July 20–24, 1992, and will be coordinated among the three symposia to provide a comprehensive, well-balanced program. The APS will offer Short Courses and Workshops, and will conduct Student Paper Contests.

Information about the 1992 Joint Symposia may be obtained from:

Prof. P.L.E. Uslenghi, Symposia Chair
Dept. of EECS (M/C 154)
University of Illinois at Chicago
Box 4348, Chicago IL. 60680, U.S.A.
Ph. 312-996-5487
Fax 312-413-0024

Social Science Building
U.W.O.

Floor Plan (partial).